# BENCHMARK WORKSHOP 2 ON DEVELOPMENT OF MSY ADVICE USING SPiCT (WKBMSYSPiCT2)

VOLUME 5 | ISSUE 65

ICES SCIENTIFIC REPORTS

RAPPORTS
SCIENTIFIQUES DU CIEM

**ICES** INTERNATIONAL COUNCIL FOR THE EXPLORATION OF THE SEA
**CIEM** CONSEIL INTERNATIONAL POUR L'EXPLORATION DE LA MER

International Council for the Exploration of the Sea
Conseil International pour l'Exploration de la Mer

H.C. Andersens Boulevard 44-46
DK-1553 Copenhagen V
Denmark
Telephone (+45) 33 38 67 00
Telefax (+45) 33 93 42 15
www.ices.dk
info@ices.dk

ISSN number: 2618-1371



ICES Scientific Reports

Volume 5 | Issue 65

# BENCHMARK WORKSHOP 2 ON DEVELOPMENT OF MSY ADVICE USING SPICT (WKBMSYSPICT2)

## Recommended format for purpose of citation:

ICES. 2023. Benchmark workshop 2 on development of MSY advice using SPiCT (WKBMSYSPiCT2). ICES Scientific Reports. 5:65. 472 pp. https://doi.org/10.17895/ices.pub.23372990

## Editors

Massimiliano Cardinale • Henning Winker

## Reviewers

Casper Berg • Alexandros Kokkalis • Tobias Mildenberger

## Authors

Loïc Baulier • Casper Berg • Paul Bouch • Andrew Campbell • Massimiliano Cardinale
Mickael Drogou • Roxanne Duncan • Edward Farrell • Raphaël Girardin • Alexandros Kokkalis
Wendell Medeiros-Leal • Tobias Mildenberger • Fanny Ouzoulias • Cristina Rodríguez-Cabello
Paz Sampedro • Klaas Sys • Bart Vanelslander • Lies Vansteenbrugge • Youen Vermard
Damien Villagra Villanueva • Henning Winker

ICES International Council for the Exploration of the Sea
CIEM Conseil International pour l'Exploration de la Mer

# Contents


i Executive summary ..... v
ii Expert group information ..... vi
1 Introduction ..... 1
1.1 Terms of reference ..... 1
1.2 Conduct of benchmark ..... 2
1.3 Reference points ..... 3
1.4 Catch forecast in SPiCT ..... 4
1.5 Recommendations (ToR 6) ..... 5
1.5.1 Model diagnostics ..... 5
1.5.2 Model parameterization ..... 6
1.5.3 Standardization of commercial CPUE ..... 7
1.5.4 Generation of probability distributions ..... 8
1.6 References ..... 8
2 Brill in the North Sea, Skagerrak, Kattegat, and the English Channel ..... 10
2.1 Introduction ..... 10
2.2 Input data for stock assessment ..... 10
2.2.1 Landings data ..... 10
2.2.2 Indices of abundance ..... 12
2.3 Stock assessment ..... 15
2.3.1 Exploratory assessments ..... 15
2.3.2 Final assessment ..... 25
2.4 Future considerations/recommendations ..... 35
2.5 Reviewers report ..... 35
2.6 Conclusions ..... 36
2.7 References ..... 36
2.8 Working documents for brill in North Sea, Skagerrak, Kattegat, and the English Channel (bll.27.3a47de) ..... 37
2.8.1 WD Annex 1: Preparation of catch data for brill (*Scophthalmus rhombus)* in areas 27.3a47de (Greater North Sea) ..... 37
2.8.2 WD Annex 2: Development and revision of survey indices for brill in the North Sea, Skagerrak, Kattegat and English Channel (ICES divisions 27.4a-c, 27.3a and 27.7d-e) ..... 45
2.8.3 WD Annex 3: Life-history parameters for brill (*Scophthalmus rhombus*) in areas 27.3a47de (Greater North Sea) ..... 103
2.8.4 WD Annex 4: Catch statistics for brill (*Scophthalmus rhombus*) in areas 27.3a47de (Greater North Sea) ..... 118
2.8.5 WD Annex 5: Prior options and testing for North Sea brill ..... 122
3 Boarfish in Celtic Seas, English Channel, and Bay of Biscay ..... 146
3.1 Introduction ..... 146
3.1.1 Fishery information ..... 146
3.1.2 Current assessment and advice ..... 146
3.2 Input data for stock assessment ..... 148
3.2.1 Landings and discards ..... 148
3.2.2 Acoustic Surveys ..... 150
3.2.3 Groundfish Surveys ..... 153
3.2.5 Life-history Parameters ..... 161
3.3 Stock assessment ..... 167
3.3.1 Run 1 (catch and acoustic Survey) ..... 168
3.3.2 Run 2 (Catch and Groundfish Survey Index) ..... 173
3.3.3 Run 3 - Catch, acoustic survey and groundfish survey index ..... 175

3.3.4 Final assessment ..... 185
3.4 Future considerations/recommendations ..... 185
3.5 Reviewer report ..... 186
3.5.1 Conclusions ..... 186
3.6 References ..... 187
3.7 Working documents ..... 189
4 Striped red mullet in the North Sea, eastern English Channel, Skagerrak, and Kattegat ..... 245
4.1 Introduction ..... 245
4.1.1 Fishery information ..... 245
4.1.2 Current assessment and advice ..... 246
4.2 Input data for stock assessment ..... 246
4.2.1 Landings and discards ..... 246
4.2.2 Length frequency data ..... 250
4.2.3 Biomass index ..... 251
4.2.4 Life-history traits ..... 261
4.2.5 Summary of data available ..... 262
4.3 Stock assessment ..... 263
4.3.1 Priors distributions ..... 263
4.3.2 Exploratory assessments ..... 263
4.4 Future considerations/recommendations ..... 266
4.5 Reviewer report ..... 266
4.6 Conclusions ..... 267
4.7 References ..... 267
4.8 Working document for striped red mullet: updated growth patterns ..... 268
5 Bay of Biscay and Atlantic Iberian waters plaice ..... 277
5.1 Introduction ..... 277
5.1.1 Fishery information ..... 277
5.1.2 Current assessment and advice ..... 277
5.2 Input data for stock assessment ..... 277
5.2.1 Landings and discards ..... 277
5.2.2 Biomass index ..... 280
5.2.3 Prior distributions ..... 283
5.2.4 Exploratory assessments ..... 284
5.3 Future considerations/recommendations ..... 285
5.4 Reviewer report ..... 285
5.4.1 Conclusions ..... 286
5.5 References ..... 286
6 Celtic Seas and the English Channel pollack ..... 287
6.1 Introduction ..... 287
6.1.1 Fishery information ..... 287
6.1.2 Current assessment and advice ..... 287
6.2 Input data for stock assessment ..... 288
6.2.1 Landings and discards ..... 288
6.2.2 Recreational fisheries ..... 293
6.2.3 Survey data ..... 293
6.2.4 VAST index ..... 302
6.2.5 Commercial LPUE ..... 304
6.3 Stock assessment ..... 304
6.3.1 Exploratory assessments ..... 304
6.3.2 Out-of-the-box SPiCT assessment ..... 305
6.3.3 Fixing the surplus production curve ..... 306
6.3.4 Final assessment ..... 313
6.4 Future considerations/recommendations ..... 318

6.4.1 Issues with the assessment ..... 318
6.5 Recommendations ..... 322
6.6 Reviewer report ..... 323
6.7 Conclusions ..... 323
6.8 References ..... 324
7 Pollack in Bay of Biscay and Atlantic Iberian waters ..... 325
7.1 Introduction ..... 325
7.1.1 Fishery information ..... 325
7.1.2 Current assessment and advice ..... 325
7.2 Input data for stock assessment ..... 326
7.2.1 Landings and discards ..... 326
7.2.2 Scientific surveys ..... 328
7.2.3 Standardized commercial abundance index ..... 329
7.2.4 Length composition of landings ..... 334
7.2.5 Life-history parameters ..... 335
7.2.6 Estimated priors for used in the assessment ..... 336
7.3 Stock assessment ..... 337
7.4 Input data ..... 337
7.5 Exploratory assessments ..... 338
7.5.1 Final assessment ..... 340
7.6 Future considerations/recommendations ..... 340
7.7 Reviewer report ..... 340
7.7.1 Conclusions ..... 341
7.8 References ..... 341
7.9 Working document for pollack ..... 342
8 Thornback ray in the Cantabrian Sea ..... 348
8.1 Introduction ..... 348
8.1.1 Fishery information ..... 348
8.1.2 Current assessment and advice ..... 348
8.2 Input data for stock assessment ..... 348
8.2.1 Landings and discards (e.g.) ..... 348
8.2.2 Biomass index ..... 350
8.2.3 Life-history information ..... 353
8.3 Stock assessment ..... 354
8.3.1 Exploratory assessments ..... 355
8.3.2 Final assessment ..... 361
8.4 Future considerations/recommendations ..... 371
8.5 Reviewer report ..... 371
8.5.1 Conclusions ..... 373
8.6 References ..... 373
8.7 Working document for thornback ray in the Cantabrian Sea (Division 8.c; rjc.27.8c) ..... 374
8.7.1 WD Annex 1: Age-structured rebuilding simulation evaluation for Thornback Ray with SPiCT ..... 374
9 Bay of Biscay and Atlantic Iberian waters whiting ..... 404
9.1 Introduction ..... 404
9.2 Input data for stock assessment ..... 404
9.2.1 Commercial catches and discards ..... 404
9.2.2 Length structure ..... 406
9.2.3 Scientific survey ..... 407
9.2.4 Standardized commercial abundance index ..... 408
9.3 Stock assessment ..... 415
9.3.1 Exploratory assessments ..... 418

9.4 Final assessment ..... 424
9.5 Future considerations/recommendations ..... 424
9.6 Reviewers report ..... 424
9.7 Conclusions ..... 425
9.8 References ..... 425
Annex 1: List of participants ..... 426
Annex 2: Resolutions ..... 427
Annex 3: Other working documents ..... 429
Annex 4: Stock Annex updates ..... 472

# i Executive summary

Benchmark workshop 2 on development of MSY advice using SPiCT (WKBMSYSPiCT2) is the second effort to provide MSY advice for stocks previously assessed as category 3 stocks, which also incorporated model learning sessions, with model developers and stock assessors, carried out prior to the data workshop. Ten stocks, including nine demersal fish stocks and one elasmobranch, pertaining to five ICES Assessment Working Groups (WGNSSK, WGWIDE, WGCSE, WGEF, and WGBIE), were selected based on the availability of appropriate data and network capacity. Stock assessments using the stochastic Surplus Production in Continuous Time (SPiCT) model were successful for two demersal finfish stocks, brill (*Scophthalmus rhombus*) in Subarea 4 and divisions 3.a and 7.d–e (bll.27.3a47de) and pollack (*Pollachius pollachius*) in Subareas 6–7 (pol.27.67); and one elasmobranch thornback ray (*Raja clavata*) in Division 8.c (rjc.27.8c). Plaice (*Pleuronectes platessa*) in divisions 7.f and 7.g (ple.27.7fg) and whiting (*Merlangius merlangus*) in Division 3.a (whg.27.3a) were ultimately not presented during the benchmark. For Whiting (*Merlangius merlangus*) in Subarea 8 and Division 9.a (whg.27.89a), the analysis was limited to evaluating the available input data for the application of category 3 methods during the benchmark. WKBMSYSPiCT2 considered that those stocks with an accepted SPiCT assessment model, the current category could be upgraded since the methodology is appropriate to determine stock status and a short-term catch forecast. Several model configurations were applied for the remaining stocks under assessments, but the available data did not allow distinguishing between very different, yet equally plausible stock status states and/or the models failed to produce acceptable diagnostics tests. The extensive exploration of input data and model configurations carried out during the workshop resulted in several recommendations regarding the standardization of commercial CPUE, including approaches accounting for spatial, target and technological creep effects and SPiCT model settings. Finally, for stocks where it was not possible to develop a SPiCT model, the use of integrated models could be explored as an alternative in future to account for the good amount of length and biological information available for these stocks.

**Table 1. Summary of the stocks dealt by WKBMSYSPiCT2, whether the SPICT assessment was accepted or not, and which model was proposed for providing advice.**

| Species | Area | Assessment | Advice |
|---|---|---|---|
| Brill | Subarea 4 and divisions 3.a and 7.d–e | Accepted | SPICT |
| Striped red mullet | Subarea 4 and divisions 7.d and 3.a | Rejected | Advice based on category 3 |
| Plaice | Divisions 7.f and 7.g | Not presented | Not evaluated |
| Pollack | Subareas 6–7 | Accepted | SPICT |
| Pollack | Subarea 8 and Division 9.a | Rejected | Advice based on category 3 |
| Thornback raj | Division 8.c | Accepted | SPICT |
| Boarfish | Subareas 6–8 | Rejected | Advice based on category 3 |
| Whiting | Subarea 8 and Division 9.a | Not presented | Advice based on category 3 |
| Whiting | Division 3.a | Not presented | Not evaluated |
| Plaice | Subarea 8 and Division 9.a | Rejected | Not evaluated |

# ii Expert group information

| | |
|---|---|
| **Expert group name** | Benchmark workshop 2 on development of MSY advice using SPiCT (WKBMSYSPiCT2) |
| **Expert group cycle** | Annual |
| **Year cycle started** | 2022 |
| **Reporting year in cycle** | 1/1 |
| **Chairs** | Massimiliano Cardinale, SLU |
| | Henning Winker, JRC |
| **Reviewers** | Casper Berg, DTU Aqua |
| | Alexandros Kokkalis, DTU Aqua |
| | Tobias Mildenberger, DTU Aqua |
| **Meeting venue and dates** | Data workshop: 11–13 October 2022 and 9 November 2022, online (22 participants) |
| | Benchmark workshop: 9–13 January 2023, online (22 participants) |

# 1 Introduction

## Benchmark workshop 2 on development of MSY advice using SPiCT

## 1.1 Terms of reference

2022/WK/FRSG52

The **Benchmark workshop 2 on development of MSY advice using SPiCT** (WKBMSYSPiCT3), chaired by Massimiliano Cardinale, Sweden, and Henning Winker, FAO-GFCM, and attended by invited external experts Casper Berg, Denmark, Alexandros Kokkalis, Denmark, and Tobias Mildenberger, Denmark, will be established and meet online for two days in September 2022 (7–8 September) for model learning sessions with SPiCT developers; 11–13 October 2022 for a data workshop; and 9–13 January 2023 for the final assessment workshop. WKMSYSPiCT2 will evaluate the appropriateness of data and the use of the Surplus Production in Continuous Time (SPiCT) to provide MSY advice for selected stocks. The specific ToRs for this benchmark workshop are:

a) Collate necessary data and information for the application of SPiCT for the stocks listed in Annex 1 before the data workshop;
b) Review the available data and make recommendations on the most appropriate series to be used for SPiCT and potential improvements to eliminate biases;
c) Apply the SPiCT methodology and determine the appropriateness of the data and the methodology to determine stock status for each of the stocks listed using the guidance developed following WKLIFEVII, WKLIFEVIII, WKLIFEIX, and ICES 2022[1];
d) For stocks where the methodology is appropriate, determine the methods to derive the parameters for the catch forecast using the harvest control rule for providing MSY advice using SPiCT;
e) Prepare the Stock Annex for those stocks where SPiCT is considered appropriate for providing MSY advice;
f) Provide recommendations for improving the guidance and training for the application of SPiCT and for deriving MSY advice.

WKBMSYSPiCT2 will report by 20 January 2023 for the attention of ACOM.

**Supporting information**

| | |
|---|---|
| Priority | Very high. ICES provides advice on more than 260 stocks and more than 60% of these stocks are in categories 3–6 where currently MSY advice is not provided. With the development of approaches to provide MSY advice for category 3–4, these approaches must be implemented as soon as possible. |
| Scientific justification and relation to action plan | Following on a request from the European Commission through DG MARE, to improve the scientific assessment of some category 3–6 stocks, ICES has held a series of workshops (WKLIFE) to develop methodologies that would allow to provide MSY advice (see WKLIFEIX). |

[1] ICES. 2022. ICES technical guidance for harvest control rules and stock assessments for stocks in categories 2 and 3. In Report of ICES Advisory Committee, 2022. ICES Advice 2022, Section 16.4.11. https://doi.org/10.17895/ices.advice.19801564

| | |
|---|---|
| | Currently, ICES provides advice for category 3–6 stocks with the precautionary approach. To provide MSY advice for many of these stocks, ICES through WKLIFEVII, WKLIFEVIII and WKLIFEIX has developed a coherent framework for category 3–4 stocks where available data would permit the use of SPiCT .<br>The purpose of the workshop is to conduct a benchmark peer review of the application of the SPiCT approach to provide MSY advice for selected stocks. The selected stocks to be considered in this benchmark was determined based on the availability of appropriate data and capacity.<br>In addition to producing the Stock Annex for stocks where the method is appropriate, the workshop will serve to provide recommendations to improve the guidance for the method as well as potential training. |

**List of ICES stocks to be examined during WKBMSYSPICT2.**

| | |
|---|---|
| bll.27.3a47de | Brill (*Scophthalmus rhombus*) in Subarea 4 and divisions 3.a and 7.d-e (North Sea, Skagerrak and Kattegat, English Channel) |
| boc.27.6-8 | Boarfish *(Capros aper)* in subareas 6-8 (Celtic Seas, English Channel, and Bay of Biscay) |
| bll.27.3a47de | Striped red mullet (*Mullus surmuletus*) in Subarea 4 and divisions 7.d and 3.a (North Sea, eastern English Channel, Skagerrak and Kattegat) |
| ple.27.89a | Plaice (*Pleuronectes platessa*) in Subarea 8 and Division 9.a (Bay of Biscay and Atlantic Iberian waters) |
| pol.27.67 | Pollack (*Pollachius pollachius*) in subareas 6-7 (Celtic Seas and the English Channel) |
| pol.27.89a | Pollack (*Pollachius pollachius*) in Subarea 8 and Division 9.a (Bay of Biscay and Atlantic Iberian waters) |
| rjc.27.8c | Thornback ray (*Raja clavata*) in Division 8.c (Cantabrian Sea) |
| whg.27.3a | Whiting (*Merlangius merlangus*) in Division 3.a (Skagerrak and Kattegat) |
| whg.27.89 | Whiting (*Merlangius merlangus*) in Subarea 8 and Division 9.a (Bay of Biscay and Atlantic Iberian waters) |

## 1.2 Conduct of benchmark

The list of participants and the agendas for the data workshop and the assessment benchmark workshop meetings are presented in Annex 1 and Annex 2, respectively.

To ensure credibility, salience, legitimacy, transparency, and accountability in ICES work all contributors to ICES work are required to abide by the ICES Code of Ethics and Professional Conduct[2]. This was brought to the attention of participants at the workshop and no conflict of interest was reported.

A unique feature of the WKBMSYSPiCT2 workshop were the learning sessions provided on the stochastic Surplus Production in Continuous Time (SPiCT; Pedersen and Berg, 2017) during the mornings of 7 and 8 September 2022. The learning sessions were led by Casper Berg, Tobias Mildenberger, and Alexandros Kokkalis (i.e. DTU Aqua Team). The DTU Aqua Team presented the model properties and equations, main assumptions, and data requirements, along with new developments and features in SPiCT. The DTU Aqua Team also presented and summarized

[2] https://ices-library.figshare.com/articles/report/Code_of_Ethics_and_Professional_Conduct/21647825

discussion and recommendations gleaned from WKMSYSPiCT[3]. A recommendation was made to always download the most recent version of SPiCT[4] prior to any SPiCT assessment trial run. Additionally, during the benchmark meeting, Henning Winker did a presentation on a novel age-structured simulation testing framework that can be used to explore potential bias in production models. Henning Winker also provided participants a working document and a script for the standardization of commercial CPUE data via the ICES SharePoint

Input data for SPiCT assessment runs were presented during the data workshop (11–13 October 2022) for each of the stocks listed above. Input data included landings/catch, survey and CPUE time-series. Preliminary SPiCT assessment runs were also presented and discussed.

The following ten stocks were considered for the assessment benchmark meeting (9–13 January 2023):

- bll.27.3a47de **Brill** (*Scophthalmus rhombus*) in Subarea 4 and divisions 3.a and 7.d-e (North Sea, Skagerrak and Kattegat, English Channel)
- boc.27.6-8 **Boarfish** (*Capros aper*) in subareas 6-8 (Celtic Seas, English Channel, and Bay of Biscay)
- mur.27.3a47d **Striped red mullet** (*Mullus surmuletus*) in Subarea 4 and divisions 7.d and 3.a (North Sea, eastern English Channel, Skagerrak and Kattegat)
- ple.27.89a **Plaice** (*Pleuronectes platessa*) in Subarea 8 and Division 9.a (Bay of Biscay and Atlantic Iberian waters)
- pol.27.67 **Pollack** (*Pollachius pollachius*) in subareas 6-7 (Celtic Seas and the English Channel)
- pol.27.89a **Pollack** (*Pollachius pollachius*) in Subarea 8 and Division 9.a (Bay of Biscay and Atlantic Iberian waters)
- rjc.27.8c **Thornback ray** (*Raja clavata*) in Division 8.c (Cantabrian Sea)
- whg.27.3a **Whiting** (*Merlangius merlangus*) in Division 3.a (Skagerrak and Kattegat)
- whg.27.89a **Whiting** (*Merlangius merlangus*) in Subarea 8 and Division 9.a (Bay of Biscay and Atlantic Iberian waters)

On a very positive note, the stock assessors followed the recommendations gleaned from the first WKMSYSPiCT to great detail, and made use of the additional methodologies provided by the Henning Winker for the standardization of the commercial CPUE. The presentations of the benchmark results were of high quality and special care was given to the evaluation of the input data.

## 1.3 Reference points

The workshop followed the ICES guidelines for fisheries management reference points for stocks assessed with biomass dynamic models (ICES, 2017). In a surplus production model stock status evaluation and stock catch forecast options should be based on relative reference points. This is because the use of ratios reduces the variance in the estimated quantities of interest (QoI) and are thus likely to be much more stable when new data points are added compared to absolute estimates. In other words, if $F_{MSY}$ is overestimated then F is likely to be equally overestimated, but this bias cancels out when using the ratios.

[3] ICES. 2021. Benchmark Workshop on the development of MSY advice for category 3 stocks using Surplus Production Model in Continuous Time; SPiCT (WKMSYSPiCT). ICES Scientific Reports. 3:20. 317 pp. https://doi.org/10.17895/ices.pub.7919

[4] Code repository at: https://github.com/DTUAqua/spict

In addition, the reference points are re-estimated every time the model is applied as opposed to many other assessments, where the reference points remain fixed until next benchmark, so it would make little sense to report these values.

The following reference points were used in the benchmark:

- $F_{fy}/F_{MSY}$: where $F_{fy}$ is the estimated F in the final assessment year and $F_{MSY}$ is the F that maximizes the equilibrium curve of yield vs. F;
- $B_{fy}/B_{MSY}$: where $B_{fy}$ is the estimated exploitable biomass in the final assessment year and $B_{MSY}$ is the exploitable biomass corresponding to MSY in the equilibrium curve of yield vs. stock biomass;
- $B_{fy}/B_{trigger}$: where $B_{trigger}$ is $0.5*B_{MSY}$;
- $B_{fy}/B_{lim}$: where $B_{lim}$ is $0.3*B_{MSY}$.

It is noted that $B_{lim} = 0.3*B_{MSY}$ is adopted based on the rationale that, under the Schaefer production (shape parameter n = 2), the biomass corresponding to 50% of MSY is obtained at 30% of $B_{MSY}$. Although the stocks with approved SPiCT assessments in the benchmark are mainly characterized by a Schaefer production curve, WKBMSYSPiCT2 reiterates previous recommendation that ICES should investigate and discuss the rationale to derive $B_{lim}$ for other production models (e.g. Fox).

## 1.4 Catch forecast in SPiCT

SPiCT can run a short-term forecast for a set of management scenarios. Currently, there are eight predefined scenarios in SPiCT and additional functions for user-defined scenarios. These functions allow for different intermediate year assumptions and forecast options. Therefore, a wide range of harvest control rules can be defined and used. During WKBMSYSPiCT2, four different scenarios were selected as the most relevant options for the short-term catch forecast:

1. No fishing mortality ($F = 0$);
2. Status quo fishing mortality ($F = F_{sq}$);
3. Hockey-stick MSY rule: $F = F_{MSY}$ when biomass is higher than $B_{trigger}$ ( $= 0.5\ B_{MSY}$), but F is reduced linearly to zero when the biomass is less than $B_{trigger}$;
4. Hockey-stick MSY rule with the catch fractile: in order to take into account the estimated uncertainties, the 35th percentile of the catch distribution is used instead of the median (50th percentile). The fishing mortality assumption is the same as in 3.

The ICES MSY advice rule evaluates the biomass at the beginning of the management period as in the basis for advice on fishing opportunities (ICES, 2021).

For most stocks, the assessment is done using data for the prior year and do a short-term forecast to the end of the following year. This leaves a gap of data during the intermediate year. Due to lack of data in that period, some assumptions need to be made. Two plausible assumptions were discussed during WKBMSYSPiCT2 and it was left for the assessors and the corresponding assessment groups to decide the most appropriate:

1. Status quo fishing mortality during the intermediate year;
2. A given catch is taken during the intermediate year. The catch could be, for example, the last agreed TAC for the stock.

An example SPiCT script implementing the above was provided to the participants during the benchmark meeting.

## 1.5 Recommendations (ToR 6)

The following summary recommendations are made by WKBMSYSPiCT2, further elaborated below:

- Historical catches should be considered, and ideally include the start of the fishery; In particular, the peak fishing period can hold information about carrying capacity.
- For data that lack historical catches and show limited contrast in the abundance index, it is recommended to fix or use an informative prior for the 'n' parameter and to use informative priors for 'r' (e.g. Thorson, 2020).
- When a prior on the initial depletion level (b/k ratio) is needed to achieve convergence, it is recommended to evaluate the fits, retrospective pattern and ideally the prediction skill (see below) of additional sensitivity runs (e.g. b/k = 0.3, 0.5, 0.8).
  Consider replacing the default 'alpha' and 'beta' priors with informative priors on observation variances ('logsdi' and 'logsdc'). The information for these priors should be case specific and could for logsdi for example be based on the estimated CV (or s.d. on log scale) of the abundance index / CPUE calculation. The process error in surplus production 'logsdb' is another candidate for a more informative prior (almost perfect production curves or production curves with highly negative values are unlikely).
- Recommendations regarding abundance indices ('obsI'):
  - Compare the length distribution and spatial distribution of the survey(s) with commercial fleet and catches (what and where is the exploited part of the population?).
  - Avoid generating indices for small subareas (e.g. one nation), as these may not be representative of the stock. Indices for subareas should instead be combined into a single index.
  - However, do not combine several independent representative indices.
- Recommendations regarding CPUE indices (survey and commercial):
  - Standardize CPUE: The standardization of (commercial) CPUE should include a spatial-time interaction factor, zeroes, and different assumptions of technological creep (the latter specifically in the case of commercial CPUE). Different assumptions regarding the targeting, error distribution, and model formula in general should be explored.
  - Do not smooth the year effect over time as the CPUE index observations are then no longer independent.
- Future versions of SPiCT should also include for instance MCMC to check the Laplace approximation.

### 1.5.1 Model diagnostics

SPiCT provides comprehensive model diagnostics to evaluate the goodness-of-fit to the data and retrospective analysis to evaluate model consistency. In particular, the functions to run and evaluate retrospective patterns have been substantially improved in the latest SPiCT version that was readily available for the benchmark assessment. In addition, hindcasting cross-validation to evaluate prediction skill (Kell *et al*., 2016; Kell *et al*., 2021), process residual diagnostics and a comparison plot for exploring model sensitivity to alternative configurations were added to the already extensive diagnostic toolbox of SPiCT as recommended by WKMSYSPiCT (c.f. Carvalho *et al*., 2021).

### 1.5.2 Model parameterization

For data that lack historical catches and show limited contrast in the abundance index, it is recommended to reduce the variance for the shape parameter n or fix it. To further increase model stability, formulating informative priors for r (e.g. Thorson, 2020) may be warranted[5]. In general, the reviewers found it very helpful to see "control" Schaefer model scenarios with an informative r prior for comparison against a less constraint model. This is especially important when estimated r is very different from the r prior. It is important to note that r values from other models might not corresponds exactly to r values from SPiCT. Retrospective pattern is often related to uncertainty about the shape n parameter and fixing it or constraining it using prior, can reduce the retrospective pattern and contribute model stability and convergence during future updates to new data.

Another important aspect that was highlighted during WKBMSYSPICT2 is to adequately propagate the interannual precision estimates of abundance indices into the SPiCT model. The observation error in SPiCT are configured based on a two-step approach, which can be parameterized by specifying the: (1) *stdevfacI* vector for interannual variability scaled to 1 and a (2) *logsdi* prior for the expected observation error scale that can be informed by mean observation error for the index time-series.

It was noted that the precision estimates for indices were not always estimated consistently, which can lead to biased precision estimates being propagated into the SPiCT assessment model. The importance of correctly integrating the uncertainty across spatial area grid into the observation error for annual index was emphasized, and well tested platforms such as 'surveyIndex' (Berg, 2016) or `VAST` (Thorson, 2019) are generally recommended for model based survey index standardization. Design-based and some model based approaches (e.g. SAS) may provide estimates of uncertainty in the form of standard deviation for untransformed index. However, for assessment models, observation error is conventionally specified on for log of the index (here *logsdi*), not the untransformed index on normal scale. A quick and widely accepted approximation of the required *log.sd* is the coefficient of variation CV = sdev/mean, where sdev denotes the standard deviation and mean the arithmetic mean. A statistically more more exact approximation is to first compute the CV and then approximate the the standard deviation on log-scale such that: *logsdi* = sqrt(log(CV^2 + 1)). This is in particular relevant in cases where the CV > 0.4, while at lower values the CV provides a close approximation of the logsdi.

Similarly, unconstrained estimation of the standard deviation of *logsdc* can be confounded with process error and F deviations, in particular if the catch series exceeds the observation horizon of the index of abundance. In such case, uncertainty about catch can still be admitted but the precision about this uncertainty may have to be constrained to effectively use the historical catch information in the model by specifying a more informative *logsdc* prior for the catch observation error.

In cases where the catch time-series lacks contrast further constraining the process error within plausible ranges may be warranted through formulation of an informative prior for *logsdb*. The expected range of process error is biologically linked to the inertia of the population biomass (natural fluctuation), and thus expected to be higher (0.15–0.25) for fast growing, short-lived species with fast generation time turn over, intermediate (0.07–0.15) for many commercial species (cods, hakes, flatfish, herring) and low (0.03–0.1) for very slow growing , long lived with late maturation and long generation times (e.g. porbeagle shark; Winker, 2018)[6]. However, since

[5] See also: github.com/henning-winker/SPMpriors

[6] https://bit.ly/3v965SY

surplus production model represent a simplification of the age-structured population dynamics, additional process error can to some extent account for latent processes, such age-structured lag effects and time-varying productivity.

### 1.5.3 Standardization of commercial CPUE

The standardization of catch-per-unit-effort (CPUE) is now widely regarded as a prerequisite for the use of CPUE as abundance index in stock assessment models (Maunder and Punt, 2004). The nominal CPUE index, derived from yearly means of the raw CPUE data, can be severely biased due to non-random allocation of fishing effort over time (Winker *et al*., 2014).

When commercial CPUE time-series are used in the stock assessment in general, specific consideration should be dedicated to the standardization procedure. In general, CPUE standardization analysis should be designed to account for spatial and targeting effects (fishing behaviour). Spatial effect may be dealt with using area and time interactions (random effect), GAMs (Gruss *et al*., 2019) or geostatistical approaches, such as INLA or VAST (Thorson, 2019). Spatio-temporal differences in abundance linked to environmental changes and/or depletion implies that the use of spatio-temporal models for standardizing fisheries-dependent CPUE data will be increasingly necessary in future (Gruss *et al*., 2019).

In general, the standardization procedure should include observations (e.g. hauls or trips) with zeroes, using appropriate error models, and vessels effect should be typically accounted for by way of random effects or through covariates for vessel characteristics. The year-effect should be modelled as a factor and not as a smoother when the commercial CPUE time-series is used in the assessment.

Given that commercial fishing operations do not select their fishing grounds at random, but typically seek to maximize their catch and profits through adjusting their fishing tactics, it is important to consider targeting effects in the CPUE standardization model before the CPUE can be considered in the assessment, especially when the species under assessment is not the primary target species of the fishery. There are number of approaches that are based on the catch composition to derive covariates in the form of fishing tactic clusters (He *et al*., 1997), principle components (Winker *et al*., 2014), spatial dynamic factor analysis (Thorson *et al*., 2016). We advise, however, against targeting factors that are based on catch proportions of the species under assessment because this is likely to result in removing abundance signal of interest (e.g. Hoyle *et al*., 2014).

The approaches commonly employed for standardizing of CPUE indices within ICES differ notably from international good practices, which has posed challenges for direct comparisons and the communication of the results in the past. A document was prepared prior to the meeting by the chairs with the aim to provide initial guidance towards developing a more harmonized protocol for fisheries-dependent CPUE standardization, which included a simulation experiment of the several contemporary standardization approaches (Winker and Cardinale, 2023)[7]. For sensitivity analysis, it was recommended to potentially explore several standardized indices based on different standardization treatments and evaluate those by use of the extensive SPiCT model diagnostics tools. For long time-series of commercial CPUE, the possible existence of technological creep should be taken into and additional analysis to address this particular issue should be carried out to evaluate assumptions of technological creep (see Palomares and Pauly, 2019; Scherrer and Galbraith, 2020) and its effect on the stock status.

[7] https://bit.ly/3H0aOsX

### 1.5.4 Generation of probability distributions

The generation of probability distributions in future version of SPiCT should also include, for instance, MCMC to check the Laplace approximation.

## 1.6 References

Berg, C. W., 2016. surveyIndex: Calculate survey indices by age from DATRAS exchange data.R package version 1.09.

Bouch, P., Minto, C., Reid, D.G.. 2021. Comparative performance of data-poor CMSY and data-moderate SPiCT stock assessment methods when applied to data-rich, real-world stocks. ICES Journal of Marine Science, fsaa220, https://doi.org/10.1093/icesjms/fsaa220.Carvalho F., Winker H., Courtney D., Kapur M., Kell L., Cardinale M., Schirripa M. et al. 2021. A cookbook for using model diagnostics in integrated stock assessments. Fisheries Research, 240: 105959.

Gruss, A., Walter, J. F., Babcock, E. A., Forrestal, F. C., Thorson, J. T., Lauretta, M. V., Schirripa, M. J. 2019. Evaluation of the impacts of different treatments of spatio-temporal variation in catch-per-unit-effort standardization models. Fisheries Research, 213: 75–93.

He, X., Bigelow, K. A. and Boggs, C. H. 1997. Cluster analysis of longline sets and fishing strategies within the Hawaii-based fishery. Fisheries Research, 31: 147–158.

Hoyle, S. D., Langley, A. D., and Campbell, R. A. 2014. Recommended approaches for standardizing CPUE data from pelagic fisheries. Western and Central Pacific Fisheries Commission, Scientific Committee Tenth Regular Session. Majuro, Republic of the Marshall Islands. WCPFC-SC10-2014/SA-IP-10. 21 pp.

ICES. 2017. ICES fisheries management reference points for category 1 and 2 stocks. ICES advice technical guidelines. 20 January 2017. doi: 10.17895/ices.pub.3036.

ICES. 2021. Advice on fishing opportunities. In Report of the ICES Advisory Committee, 2021. ICES Advice 2021, Section 1.1.1. https://doi.org/10.17895/ices.advice.7720

Kell, L. T., Kimoto, A., Kitakado, T. 2016. Evaluation of the prediction skill of stock assessment using hindcasting. Fisheries Research, 183: 119–127.

Kell L. T., Sharma R., Kitakado T., Winker H., Mosqueira I., Cardinale M., Fu D. 2021. Validation of stock assessment methods: is it me or my model talking?. ICES Journal of Marine Science, 78: 2244–2255.

Palomares, M. L. D. and Pauly, D. 2019. On the creeping increase of vessels' fishing power. Ecology and Society 24(3):31. https://doi.org/10.5751/ES-11136-240331

Pedersen, M. W., and Berg, C. W. 2017. A stochastic surplus production model in continuous time. Fish and Fisheries, 18: 226–243. doi: 10.1111/faf.12174.

Scherrer, K. J. N. and Galbraith, E. D. 2020. The risk of underestimating long-term fisheries creep. Ecology and Society 25(1):18. https://doi.org/10.5751/ES-11389-250118

Thorson, J. T., Scheuerell, M. D., Shelton, A. O., See, K. E., Skaug, H. J., Kristensen, K. 2015. Spatial factor analysis: a new tool for estimating joint species distributions and correlations in species range. Methods in Ecology and Evolution, 6: 627–637. doi: 10.1111/2041-210X.12359.

Thorson, J.T., Fonner, R., Haltuch, M.A., Ono, K., Winker, H. 2016. Accounting for spatio-temporal variation and fisher targeting when estimating abundance from multispecies fishery data. Can. J. Fish. Aquat. Sci. 74. https://doi.org/10.1139/cjfas-2015-0598.

Thorson, J.T. 2019. Guidance for decisions using the Vector Autoregressive Spatio-Temporal (VAST) package in stock, ecosystem, habitat and climate assessments. Fisheries Research, 210: 143-161.

Thorson, J. T., Munch, S. B., Cope, J. M., Gao, J. 2017. Predicting life history parameters for all fishes worldwide. Ecological Applications. 27(8): 2262–2276. doi/10.1002/eap.1606/full.

Thorson, J. 2020. Predicting recruitment density dependence and intrinsic growth rate for all fishes worldwide using a data-integrated life-history model. Fish and Fisheries, 21: 237–251. doi.org/10.1111/faf.12427.

Winker, H., Kerwath, S. E., Attwood, C. G. 2014. Proof of concept for a novel procedure to standardize multispecies catch and effort data. Fisheries Research, 155: 149–159.

Winker, H. 2018. Investigation into the process error in biomass dynamics of fishes. International Fisheries Stock Assessment Review Workshop, Cape Town, South Africa. MARAM/IWS/2018/Linefish/P3, 1–30.

# 2 Brill in the North Sea, Skagerrak, Kattegat, and the English Channel

## bll.27.3a47de – *Scophthalmus rhombus* in Subarea 4 and divisions 3.a and 7.d–e

## 2.1 Introduction

Brill (*Scophthalmus rhombus*) has been assessed by the Working Group on the Assessment of Demersal Stocks in the North Sea and Skagerrak (WGNSSK) since 2013. Because only official landings and survey data were available, brill in Subarea 27.4 and divisions 27.3.a and 27.7.d–e was defined as a category 3 stock and advice was given using the 2 over 3 rule applied to the Dutch commercial beam trawl LPUE index (vessels > 221 kW). From 2017–2021, this advice was complemented with a SPiCT assessment (surplus production model in continuous time; Pedersen and Berg, 2017) to evaluate the stock status against proxy reference points and the need to apply a precautionary buffer (ICES, 2017). In 2022, the WKLIFE X methods were applied and advice was given using the *chr* rule on the Dutch commercial LPUE index (ICES, 2022). However, the calculation method for the Dutch LPUE index was questioned. The current benchmark allowed for reconsidering input data and a thorough investigation of SPiCT as assessment and forecast method for this stock.

## 2.2 Input data for stock assessment

### 2.2.1 Landings data

#### 2.2.1.1 Historical landings

Historical landings were compiled from the ICES Catch Statistics website[1]. Historical nominal catches from 1950–2010 and official nominal catches from 2006–2021 were merged and analysed. In the period 1984–1989, Dutch landings were missing in Subarea 4. These data were filled by Dutch data available from the brill advice sheet. For the overlapping period 2006–2010, we chose to use the most recent time-series. Differences for those years between time-series were negligible (max. 3 tonnes difference).

Landings were below 1000 tonnes in the period 1950–1970 but steadily increased in the 1970s to around 2000 tonnes over the period 1980–2021 (Figure 2.1). A total of nine countries fished on this stock over the course of the time-series: Belgium, Denmark, France, Germany, Ireland, The Netherlands, Norway, Sweden and the UK (including the Channel Islands Guernsey and Jersey). Especially the increase in landings of the Dutch fleet has led to the increase in landings of the stock. Throughout the time-series, most of the landings originated from Subarea 4. Landings in Division 3.a have slightly decreased and landings in divisions 7.d–e have increased over the course of the time-series (note 7.d and 7.e were combined in the earlier part of the time-series).

[1] https://www.ices.dk/data/dataset-collections/Pages/Fish-catch-and-stock-assessment.aspx

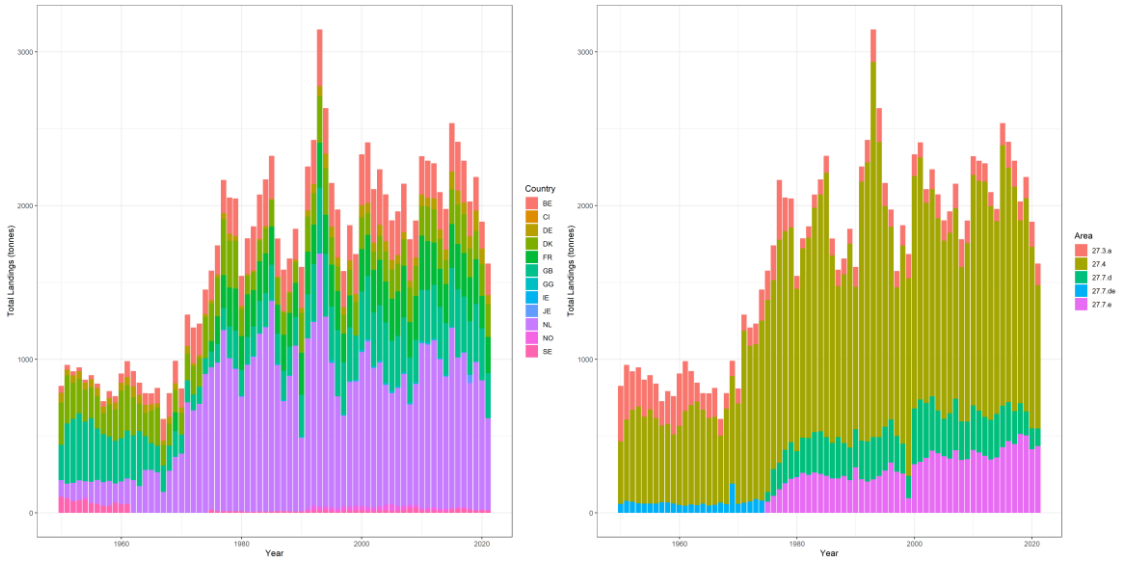


**Figure 2.1. Brill in Subarea 4 and divisions 3.a and 7.d–e. Official landings by country (left) and by area (right) over the period 1950–2021.**

### 2.2.1.2 ICES InterCatch landings

Historical landings from 2014–2021 were replaced by InterCatch landings. Countries fishing on this stock were not requested to submit/update their brill time-series, due to the absence of a data call. Nevertheless, data from 2014–2021 are considered complete. In Annex 1, the working document on InterCatch explains how discards were raised and lengths were allocated. Table 2.1 summarizes the landings that serve as input to the model, with InterCatch landings indicated in blue.

**Table 2.1. Brill in Subarea 4 and divisions 3.a and 7. d–e. Overview of the landings data that serve as input for the assessment, with InterCatch landings indicated in blue.**

| Year | Landings (tonnes) | Year | Landings (tonnes) |
|---|---|---|---|
| 1950 | 827 | 1986 | 1786 |
| 1951 | 963 | 1987 | 1583 |
| 1952 | 922 | 1988 | 1656 |
| 1953 | 947 | 1989 | 1849 |
| 1954 | 867 | 1990 | 1601 |
| 1955 | 896 | 1991 | 2255 |
| 1956 | 842 | 1992 | 2427 |
| 1957 | 727 | 1993 | 3147 |
| 1958 | 793 | 1994 | 2634 |
| 1959 | 760 | 1995 | 2147 |
| 1960 | 907 | 1996 | 1974 |
| 1961 | 987 | 1997 | 1574 |

| Year | Landings (tonnes) | Year | Landings (tonnes) |
|---|---|---|---|
| 1962 | 923 | 1998 | 1872 |
| 1963 | 847 | 1999 | 1685 |
| 1964 | 780 | 2000 | 2334 |
| 1965 | 778 | 2001 | 2411 |
| 1966 | 813 | 2002 | 2107 |
| 1967 | 611 | 2003 | 2236 |
| 1968 | 779 | 2004 | 2073 |
| 1969 | 990 | 2005 | 1904 |
| 1970 | 810 | 2006 | 1962 |
| 1971 | 1291 | 2007 | 2142 |
| 1972 | 1207 | 2008 | 1781 |
| 1973 | 1232 | 2009 | 1902 |
| 1974 | 1454 | 2010 | 2321 |
| 1975 | 1576 | 2011 | 2292 |
| 1976 | 1741 | 2012 | 2276 |
| 1977 | 2167 | 2013 | 2088 |
| 1978 | 2053 | 2014 | 1920 |
| 1979 | 2046 | 2015 | 2470 |
| 1980 | 1542 | 2016 | 2444 |
| 1981 | 1787 | 2017 | 2207 |
| 1982 | 1865 | 2018 | 1956 |
| 1983 | 2072 | 2019 | 2147 |
| 1984 | 2171 | 2020 | 1872 |
| 1985 | 2324 | 2021 | 1547 |

### 2.2.2 Indices of abundance

A standardized survey index was derived for brill in Subarea 4 and divisions 3.a and 7.d–e (North Sea, Skagerrak and Kattegat, English Channel; bll.27.3a47de) from all available DATRAS surveys in the stock area as prepared during WKFISHDIS2 (SEAwise consortium, 2022). The main objective was to obtain an exploitable biomass index for the entire stock area and move away from a spatially-limited index based on national fleets or single surveys (more information in Annex 2 WD Survey Index).

The compiled dataset was filtered to the stock's area and included six surveys (BITS, BTS, DYFS, FR-CGFS, NS-IBTS and SNS) executed by eight countries (Belgium, Denmark, France, Germany, Great-Brittain, the Netherlands, Norway and Sweden). The survey dataset spanned the period 1971–2021 and 3 quarters (1, 3, and 4). Three different gears were used by 42 different vessels: BT used in BTS, DYFS and SNS (beam trawls); GOV_CL used in FR-CGFS and NS-IBTS (Demersal trawl (bottom trawl) with clean gear and high headline net: herring bottom trawls, GOV with groundgear A) and TV used in BITS (TV-3 trawls). Night hauls were removed to avoid considering different catch rates related to different activity regimes during night-time. Weights are calculated for all length samples using a length-weight key combining all available information. Length-weight information is available from the late 1990s.

After data exploration, it became clear that sampling has not been consistent over the years. Additionally, there is substantial variation in terms of gears, quarters and areas sampled (more details in Annex 2 WD Survey index). Furthermore, on average only 7% of the hauls caught brill, but this varied again by year, gear, quarter and area. Biomass is concentrated in the southern North Sea, but rectangles with high catches per unit of effort occur in 3a.21, 7.d and 7.e.

One GAM model was used to estimate 3 indices (see Annex 2 WD Survey Index). As input for the model to calculate the survey index, only brill equal to or larger than 25 cm were retained to allow estimating the exploitable biomass necessary for SPiCT. The model contained a fixed spatial effect (2 dimensional smoother), a temporal trend (1 dimensional smoother), a spatio-temporal effect (3 dimensional smoother), a depth effect (1 dimensional smoother), a fixed gear effect, a random ship effect, a linear offset on the swept-area and the observation error was assumed to follow a Tweedie distribution.

To calculate the first index (Table 2.2), data were filtered to 1983–1998 and contained only data on quarter 1 and from areas 3.a and 4 (no sampling in English Channel). Only data collected by the GOV_CL gear remained. The gear effect was therefore removed from the model as well as the seasonal effect. The second and third index (Table 2.3) were generated with the GAM model using data filtered to the period 1999–2021 (see Annex 2 WD Survey Index). This corresponds to when most of the stock area was sampled and when there was consistent coverage in terms of gears, quarter and area. All indices and their coefficient of variation (standardized to the mean) were included in the final SPiCT assessment.

**Table 2.2. Brill in Subarea 4 and divisions 3.a and 7.d-e. Survey exploitable biomass index for quarter 1 and the coefficient of variation (CV; standardized to the mean) for the period 1983–1998.**

| Year | Biomass index | CV |
|---|---|---|
| 1983 | 513044.00 | 1.07 |
| 1984 | 560278.70 | 0.99 |
| 1985 | 430801.40 | 0.92 |
| 1986 | 424467.80 | 0.94 |
| 1987 | 725130.20 | 0.79 |
| 1988 | 353976.00 | 1.07 |
| 1989 | 271308.30 | 1.22 |
| 1990 | 520670.20 | 1.06 |
| 1991 | 1283269.60 | 0.92 |

| Year | Biomass index | CV |
|---|---|---|
| 1992 | 1120779.10 | 0.99 |
| 1993 | 969545.50 | 0.88 |
| 1994 | 667242.50 | 0.93 |
| 1995 | 487818.60 | 1.02 |
| 1996 | 952653.60 | 0.83 |
| 1997 | 146659.90 | 1.43 |
| 1998 | 680382.20 | 0.95 |

**Table 2.3. Brill in Subarea 4 and divisions 3.a and 7.d–e. Survey exploitable biomass index for semester 1 (quarter 1) and semester 2 (quarter 3 and 4) and their respective coefficient of variation (CV; standardized to the mean) for the period 1999–2021.**

| Year | Semester 1 | | Semester 2 | |
|---|---|---|---|---|
| | Biomass index | CV | Biomass index | CV |
| 1999 | 4119947.00 | 1.40 | 5224303.88 | 1.14 |
| 2000 | 4768626.61 | 1.24 | 7524136.06 | 1.22 |
| 2001 | 6038475.27 | 1.19 | 4583504.71 | 1.31 |
| 2002 | 7388700.74 | 1.25 | 5310228.10 | 1.38 |
| 2003 | 7483428.53 | 1.28 | 6030671.81 | 1.63 |
| 2004 | 9405230.73 | 1.18 | 7369403.91 | 1.32 |
| 2005 | 6317122.47 | 1.11 | 6492799.49 | 1.14 |
| 2006 | 6326257.69 | 0.95 | 8272215.05 | 1.14 |
| 2007 | 10698701.71 | 0.89 | 12458714.50 | 1.04 |
| 2008 | 9074655.77 | 0.90 | 11018555.63 | 0.81 |
| 2009 | 10290884.50 | 0.91 | 8530177.05 | 0.82 |
| 2010 | 10011845.99 | 0.91 | 11640032.20 | 0.81 |
| 2011 | 8666371.90 | 0.97 | 14727206.83 | 0.84 |
| 2012 | 12515604.55 | 0.89 | 11392919.56 | 0.78 |
| 2013 | 11473037.68 | 0.97 | 9303350.28 | 0.74 |
| 2014 | 9395805.14 | 0.92 | 11820331.73 | 0.77 |
| 2015 | 10787385.89 | 0.80 | 12003910.77 | 0.71 |
| 2016 | 13692123.22 | 0.83 | 10224801.64 | 0.77 |

| Year | Semester 1 | | Semester 2 | |
|---|---|---|---|---|
| | Biomass index | CV | Biomass index | CV |
| 2017 | 14873886.90 | 0.80 | 8155838.59 | 0.84 |
| 2018 | 8721901.74 | 0.91 | 6475362.73 | 0.82 |
| 2019 | 7788911.16 | 0.89 | 11236719.37 | 1.14 |
| 2020 | 9026989.02 | 0.91 | 12403566.66 | 1.02 |
| 2021 | 11203586.95 | 0.90 | 5811349.64 | 0.82 |

## 2.3 Stock assessment

### 2.3.1 Exploratory assessments

Several sensitivity runs were performed to analyse the robustness of the assessment to the inclusion of different catch and biomass index time-series, and to different priors on the intrinsic growth rate (r), the state of the stock biomass at the beginning of the catch time-series (bkfrac) and on the indices' observation noise (sdi). Details on these runs are presented in each of the specific sections below.

#### 2.3.1.1 Sensitivity to catch series trimming

The sensitivity to trimming the catch time-series was tested by comparing runs including the full catch time-series (1950–2021) and three alternatives trimmed versions (1960–2021, 1970–2021 and 1980–2021; Figure 2.2). In each of the four runs, the uncertainty around the catch data (stdevfacC) before 1999 was set to double of the uncertainty for data from 1999 to 2021, following the assumption that catch data were less accurate in the earlier part of the time-series. The n prior was forced to a Schaefer production curve (Log(n)~N(log(2),0.01^2)) and the prior on r was based on the species life-history traits (van der Hammen *et al*., 2013; Log(r)~N(log(0.647), 0.322^2); see Annex 3 WD Life History).

The run using the catch time-series between 1960 and 2021 did not converge and is therefore not considered as a viable option. Trimming the time-series to 1970 and 1980 resulted in a different starting point for the estimation of the absolute and relative biomass and fishing mortality compared to the other two runs. This is caused by the exclusion of the lower catches reported between 1950–1970. Around the year 1999, all four runs gave similar estimates for biomass and fishing mortality, which coincides with the beginning of the biannual biomass index time-series (1999–2021). It was decided to move forward with the run including the full catch time-series (1950–2021), because high biomass is assumed in the period after the second world war due to limited fishing during the war.

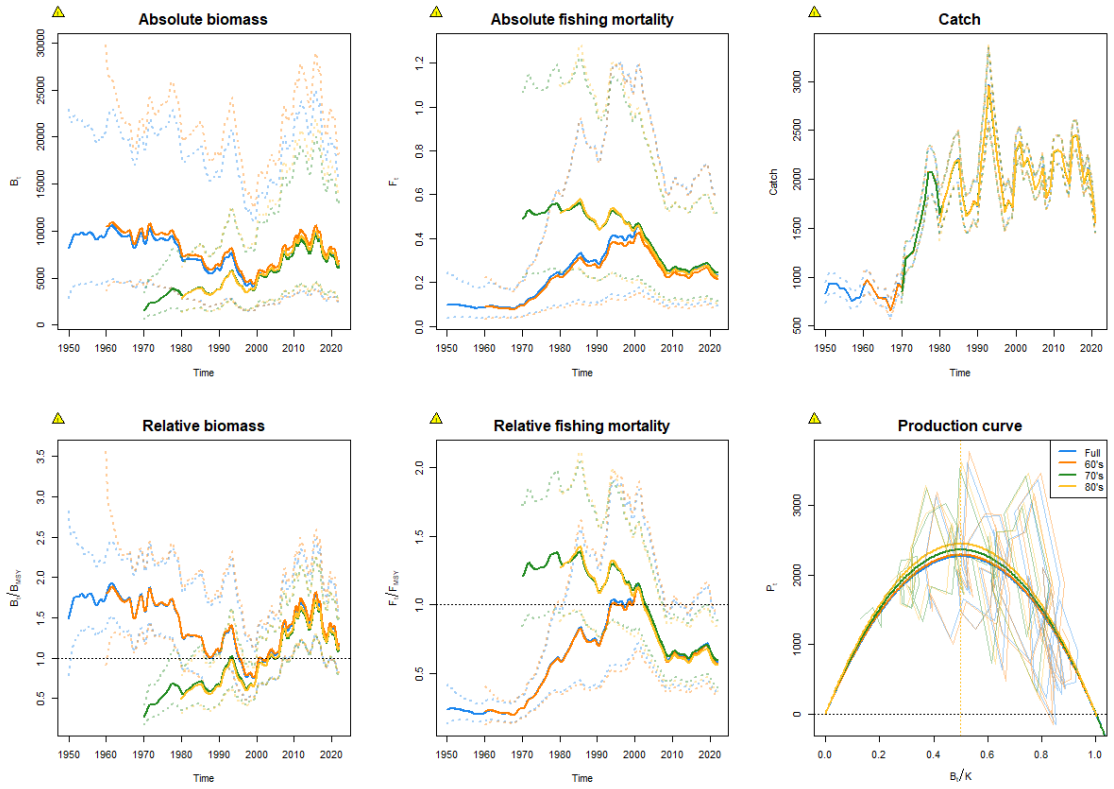


**Figure 2.2. Brill in Subarea 4 and divisions 3.a and 7.d–e. Plot comparing the output of the assessment with the full and three trimmed versions of the catch data: 1950–2021 in blue, 1960–2021 in orange, 1970–2021 in green and 1980–2021 in yellow.**

### 2.3.1.2 Sensitivity to inclusion/exclusion of biomass indices

Three exploitable biomass indices were developed for Brill in Subarea 4 and divisions 3.a and 7.d–e, including: (1) a historical index from 1983–1998 for the 1st semester in the North Sea, Skagerrak and Kattegat area, and (2) and (3) one biannual index (Semester 1 and 2) covering the entire stock area from 1999–2021 (see Annex 2 WD Survey Index). The sensitivity to the inclusion of these indices was tested by comparing the assessment output using one, two or three indices. The priors on n (Log(n)~N(log(2),0.01^2)) and r (Log(r)~N(log(0.647), 0.322^2)) were the same as used in §2.3.1.1 and the full catch time-series was included (1950–2021, with stdevfacC = 2 for 1950–1998 and stdevfacC = 1 for 1999–2021).

No clear differences were present between the runs including only the first semester of the biannual index (blue), both semesters (orange) or both semesters and the historical index for the 1st semester (green; Figure 2.3). There is therefore no reason to exclude any of the indices from the assessment.

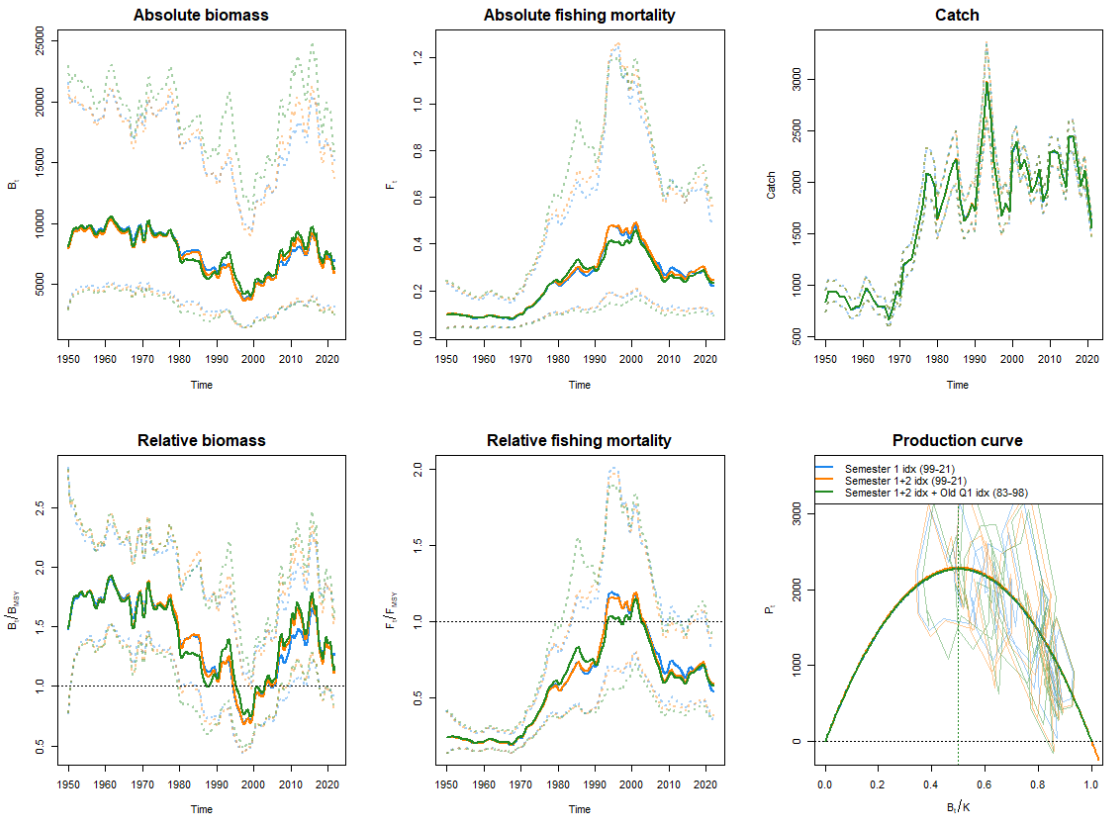


**Figure 2.3. Brill in Subarea 4 and divisions 3.a and 7.d–e. Plot comparing the output of the assessment with one (Semester 1 1999–2021, blue), two (Semester 1 and 2: 1999–2021, orange) or three (Semester 1 and 2: 1999–2021 + Semester 1: 1983–1998) exploitable biomass indices.**

High catch rates were observed in the surveys especially in Division 3.a (see Annex 2 WD Survey Index), while commercial catches originated mainly from Area 4. To evaluate the impact of this discrepancy, the biannual survey index for semester 1 and 2 (from 1999–2021) was calculated excluding observations in Division 3.a. These adjusted indices were included in the model (blue in Figure 2.4) and compared to a similar run with the semester 1 and 2 indices including Division 3.a (orange line in Figure 2.3 and 2.4). Estimates from both models were similar, with the exception of a higher relative biomass and lower relative fishing mortality around the year 2000 and a lower relative biomass and higher relative fishing mortality around 2010 in the model using the index without Division 3.a, but all within confidence bounds of models.

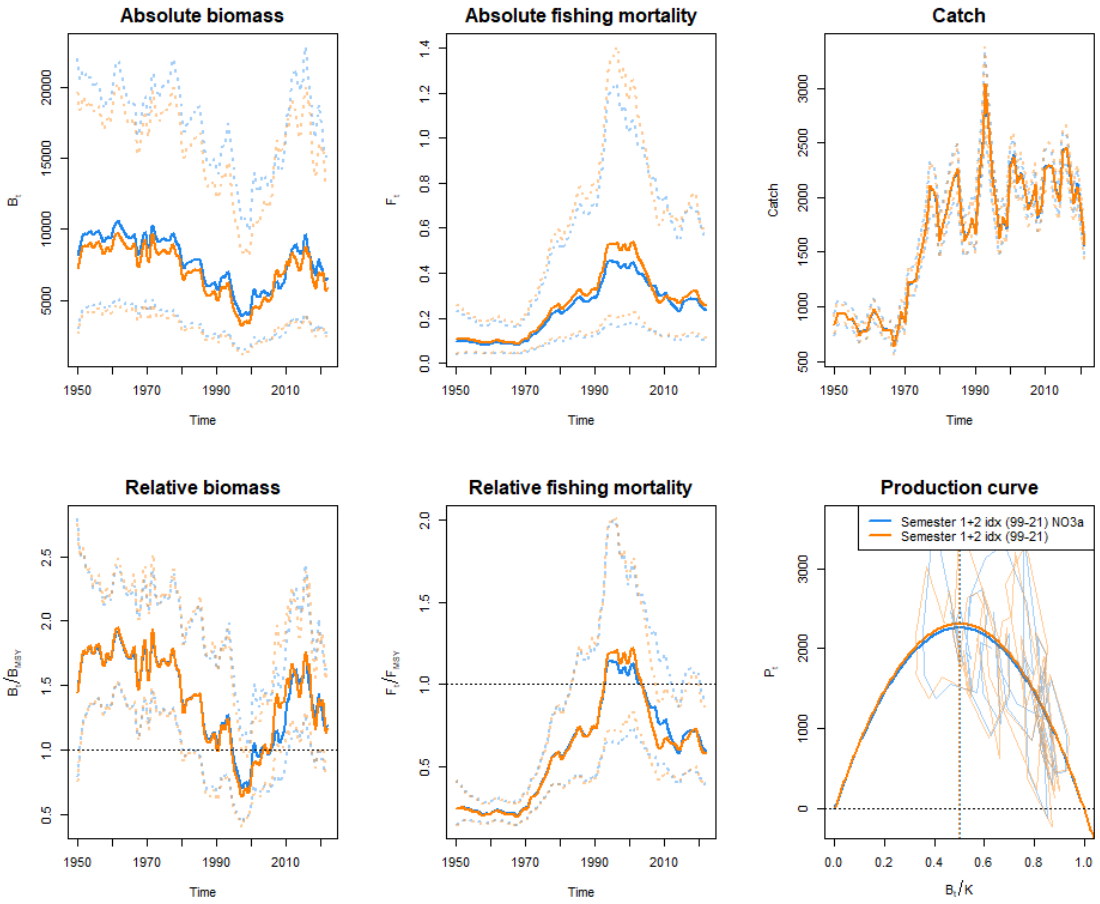


**Figure 2.4. Brill in Subarea 4 and divisions 3.a and 7.d–e. Plot comparing the output of the assessment with two exploitable biomass indices (Semester 1 and 2: 1999–2021) excluding (blue) and including (orange) Division 3.a in the calculation.**

### 2.3.1.3 Sensitivity to prior on the intrinsic growth rate (r)

The previous sensitivity runs showed that the model estimated a relatively high intrinsic growth rate (r = 0.6–0.8). Although this corresponds to the range of values estimated from the species life-history analyses (see Annex 3 WD Life History), sensitivity to different priors was investigated. Four scenarios for r priors were tested: (1) the estimated value using the stock's life history (van der Hammen *et al.*, 2013; Log(r)~N(log(0.647), 0.322^2)), (2) a strict prior on r at 0.4 (Log(r)~N(log(0.4), 0.1^2), (3) a loose prior on r around 0.5 (Log(r)~N(log(0.5), 0.5^2)) and (4) a prior on r at 0.5 with slightly more narrow CV (Log(r)~N(log(0.5), 0.3^2); Figure 2.5). All four runs included the three survey indices (§2.3.1.2) and full catch dataseries (1950–2021, with stdevfacC = 2 for 1950–1998 and stdevfacC = 1 for 1999–2021), while forcing the production curve to Schaefer (Log(n)~N(log(2),0.01^2)).

The second run (r = 0.4, orange) showed a different outcome compared to the rest of the runs, with a very low initial biomass and high fishing mortality. This implies that the stock is overexploited at the beginning of the time-series, which is very unlikely, taking into account low fishing pressure during the second world war. Although the other three runs give opposite estimates of biomass and fishing mortality at the beginning of the time-series, all four runs give similar estimates for relative biomass and fishing mortality in the most recent part of the time-series.

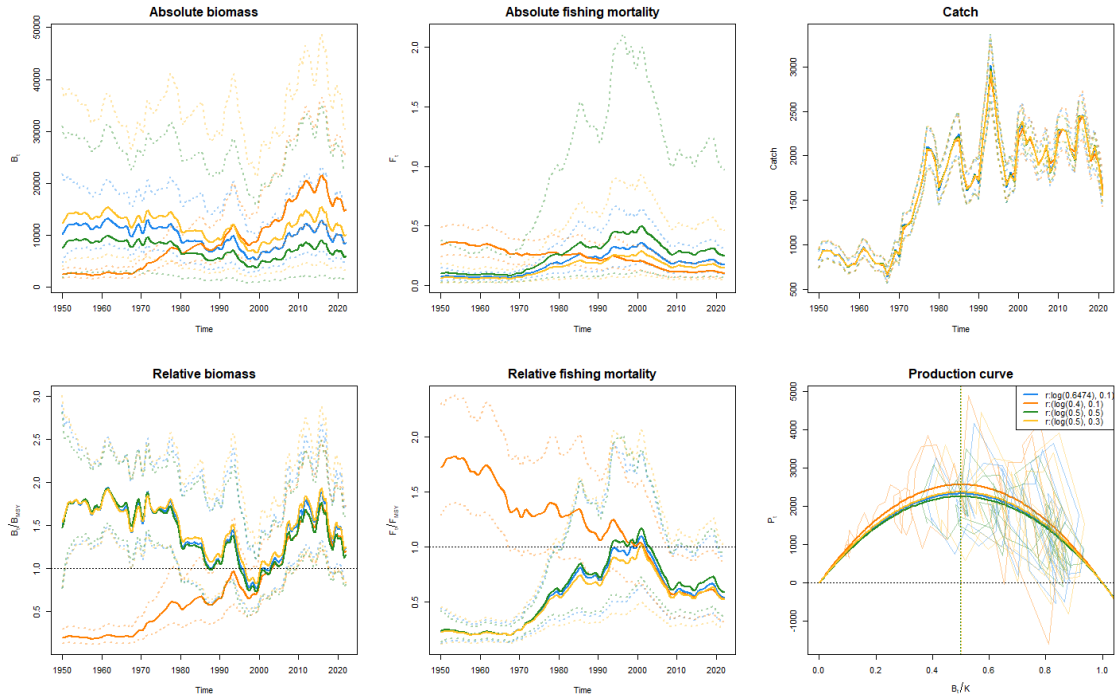


**Figure 2.5. Brill in Subarea 4 and divisions 3.a and 7.d–e. Plot comparing the output of the assessment with priors on the intrinsic growth rate: (1) blue: Log(r)~N(log(0.647), 0.322^2), (2) orange: Log(r)~N(log(0.4), 0.1^2), (3) green: Log(r)~N(log(0.5), 0.5^2) and (4) yellow: Log(r)~N(log(0.5), 0.3^2).**

Using a loose prior on r around 0.5 (run 3, green in Figure 2.5) was preferred, as this allowed the model more flexibility when new data are added. However, this run presented some issues with model diagnostics, specifically with its sensitivity to initial parameters (Table 2.4). The differences were especially present in the estimated carrying capacity of the stock (K) varying between 10 465 and 15 312 tonnes. It was therefore recommended to add a prior on the initial depletion of the stock (bkfrac).

**Table 2.4. Brill in Subarea 4 and divisions 3.a and 7.d–e. Results of the sensitivity analysis to initial parameters for the run using a loose prior on r (Log(r)~N(log(0.5), 0.5^2)).**

fit$check.ini$resmat

| | Distance | m | K | q | q | q | n | sdb | sdf | sdi | sdi | sdi | sdc |
|---|---|---|---|---|---|---|---|---|---|---|---|---|---|
| Basevec | 0.00 | 2258.81 | 10465.33 | 1372.26 | 1327.29 | 108.35 | 2 | 0.16 | 0.12 | 0.16 | 0.20 | 0.49 | 0.03 |
| Trial 1 | 4881.14 | 2411.51 | 15312.24 | 972.99 | 939.59 | 111.49 | 2 | 0.13 | 0.08 | 0.16 | 0.21 | 0.44 | 0.04 |
| Trial 2 | 4881.16 | 2411.51 | 15312.25 | 972.99 | 939.59 | 111.49 | 2 | 0.13 | 0.08 | 0.16 | 0.21 | 0.44 | 0.04 |
| Trial 3 | 4881.32 | 2411.52 | 15312.41 | 972.98 | 939.58 | 111.49 | 2 | 0.13 | 0.08 | 0.16 | 0.21 | 0.44 | 0.04 |
| Trial 4 | 0.00 | 2258.81 | 10465.33 | 1372.26 | 1327.29 | 108.35 | 2 | 0.16 | 0.12 | 0.16 | 0.20 | 0.49 | 0.03 |
| Trial 5 | 4881.14 | 2411.51 | 15312.24 | 972.99 | 939.59 | 111.49 | 2 | 0.13 | 0.08 | 0.16 | 0.21 | 0.44 | 0.04 |
| Trial 6 | 0.00 | 2258.81 | 10465.33 | 1372.26 | 1327.29 | 108.35 | 2 | 0.16 | 0.12 | 0.16 | 0.20 | 0.49 | 0.03 |
| Trial 7 | 4881.17 | 2411.51 | 15312.26 | 972.99 | 939.59 | 111.49 | 2 | 0.13 | 0.08 | 0.16 | 0.21 | 0.44 | 0.04 |
| Trial 8 | 4881.14 | 2411.51 | 15312.24 | 972.99 | 939.59 | 111.49 | 2 | 0.13 | 0.08 | 0.16 | 0.21 | 0.44 | 0.04 |
| Trial 9 | 4881.14 | 2411.51 | 15312.24 | 972.99 | 939.59 | 111.49 | 2 | 0.13 | 0.08 | 0.16 | 0.21 | 0.44 | 0.04 |
| Trial 10 | 4881.16 | 2411.51 | 15312.25 | 972.99 | 939.59 | 111.49 | 2 | 0.13 | 0.08 | 0.16 | 0.21 | 0.44 | 0.04 |
| Trial 11 | 0.00 | 2258.81 | 10465.33 | 1372.26 | 1327.29 | 108.35 | 2 | 0.16 | 0.12 | 0.16 | 0.20 | 0.49 | 0.03 |
| Trial 12 | 0.00 | 2258.81 | 10465.33 | 1372.26 | 1327.29 | 108.35 | 2 | 0.16 | 0.12 | 0.16 | 0.20 | 0.49 | 0.03 |
| Trial 13 | 4881.14 | 2411.51 | 15312.23 | 972.99 | 939.59 | 111.49 | 2 | 0.13 | 0.08 | 0.16 | 0.21 | 0.44 | 0.04 |
| Trial 14 | 4881.14 | 2411.51 | 15312.24 | 972.99 | 939.59 | 111.49 | 2 | 0.13 | 0.08 | 0.16 | 0.21 | 0.44 | 0.04 |
| Trial 15 | 0.00 | 2258.81 | 10465.33 | 1372.26 | 1327.29 | 108.35 | 2 | 0.16 | 0.12 | 0.16 | 0.20 | 0.49 | 0.03 |
| Trial 16 | 4881.13 | 2411.51 | 15312.23 | 972.99 | 939.59 | 111.49 | 2 | 0.13 | 0.08 | 0.16 | 0.21 | 0.44 | 0.04 |
| Trial 17 | 0.00 | NA | NA | NA | NA | NA | NA | NA | NA | NA | NA | NA | NA |
| Trial 18 | 4881.14 | 2411.51 | 15312.24 | 972.99 | 939.59 | 111.49 | 2 | 0.13 | 0.08 | 0.16 | 0.21 | 0.44 | 0.04 |
| Trial 19 | 4881.14 | 2411.51 | 15312.24 | 972.99 | 939.59 | 111.49 | 2 | 0.13 | 0.08 | 0.16 | 0.21 | 0.44 | 0.04 |
| Trial 20 | 4881.20 | 2411.51 | 15312.30 | 972.99 | 939.59 | 111.49 | 2 | 0.13 | 0.08 | 0.16 | 0.21 | 0.44 | 0.04 |
| Trial 21 | 4881.14 | 2411.51 | 15312.24 | 972.99 | 939.59 | 111.49 | 2 | 0.13 | 0.08 | 0.16 | 0.21 | 0.44 | 0.04 |
| Trial 22 | 4881.14 | 2411.51 | 15312.24 | 972.99 | 939.59 | 111.49 | 2 | 0.13 | 0.08 | 0.16 | 0.21 | 0.44 | 0.04 |
| Trial 23 | 4881.14 | 2411.51 | 15312.24 | 972.99 | 939.59 | 111.49 | 2 | 0.13 | 0.08 | 0.16 | 0.21 | 0.44 | 0.04 |
| Trial 24 | 0.00 | 2258.81 | 10465.33 | 1372.26 | 1327.29 | 108.35 | 2 | 0.16 | 0.12 | 0.16 | 0.20 | 0.49 | 0.03 |
| Trial 25 | 4881.12 | 2411.51 | 15312.21 | 972.99 | 939.59 | 111.49 | 2 | 0.13 | 0.08 | 0.16 | 0.21 | 0.44 | 0.04 |
| Trial 26 | 0.00 | 2258.81 | 10465.33 | 1372.26 | 1327.29 | 108.35 | 2 | 0.16 | 0.12 | 0.16 | 0.20 | 0.49 | 0.03 |
| Trial 27 | 0.05 | 2258.81 | 10465.38 | 1372.25 | 1327.28 | 108.35 | 2 | 0.16 | 0.12 | 0.16 | 0.20 | 0.49 | 0.03 |
| Trial 28 | 4881.14 | 2411.51 | 15312.24 | 972.99 | 939.59 | 111.49 | 2 | 0.13 | 0.08 | 0.16 | 0.21 | 0.44 | 0.04 |
| Trial 29 | 0.00 | 2258.81 | 10465.33 | 1372.26 | 1327.29 | 108.35 | 2 | 0.16 | 0.12 | 0.16 | 0.20 | 0.49 | 0.03 |
| Trial 30 | 4881.14 | 2411.51 | 15312.24 | 972.99 | 939.59 | 111.49 | 2 | 0.13 | 0.08 | 0.16 | 0.21 | 0.44 | 0.04 |

#### 2.3.1.4 Sensitivity to prior on the initial depletion of the stock (bkfrac)

Different priors on the initial depletion of the stock (bkfrac) were tested in an attempt solving the issues with sensitivity to initial parameters. Four runs were tested playing around with levels of bkfrac and the uncertainty around that value: (1) log(bkfrac)~N(log(0.8), 0.5^2), (2) log(bkfrac)~N(log(0.8), 0.3^2), (3) log(bkfrac)~N(log(0.5), 0.5^2), (4) log(bkfrac)~N(log(0.5), 0.3^2).

All four runs showed a fairly identical trend for both absolute and relative estimates of biomass and fishing mortality (Figure 2.6). However, runs 1 and 3, which allowed for a broader uncertainty around the bkfrac value, continued to have issues for sensitivity to initial parameters. Runs 2 and 4 did not show any issues concerning diagnostics. Run 2 having a high value on bkfrac (0.8) was preferred as it is more in line with the higher biomass we expect at the beginning of the time-series.

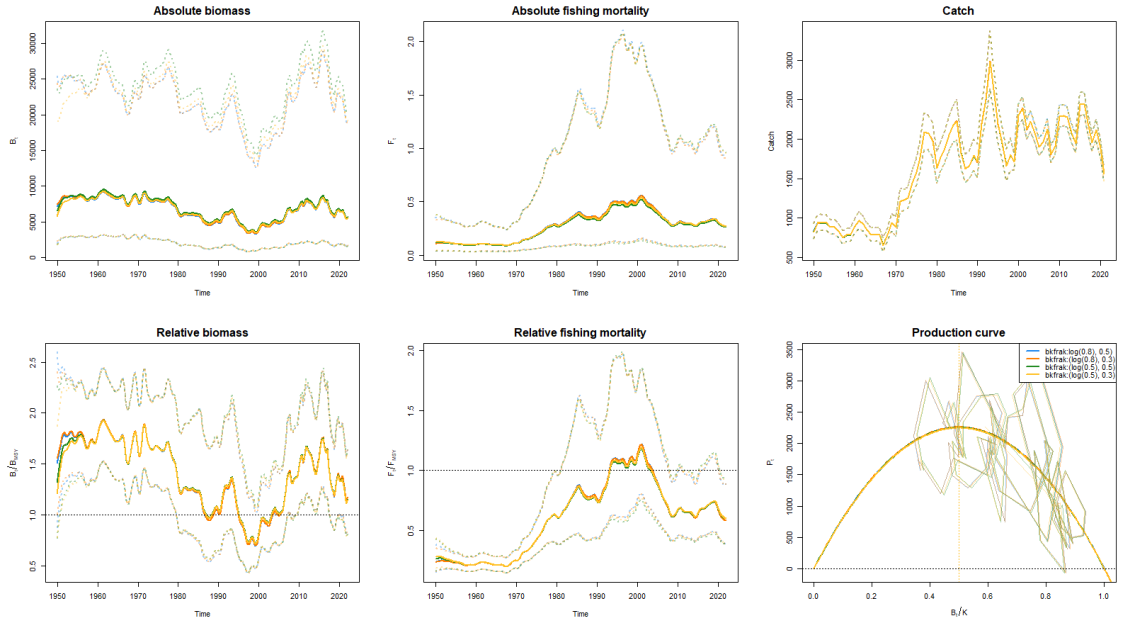


**Figure 2.6. Brill in Subarea 4 and divisions 3.a and 7.d–e. Plot comparing the output of the assessment with priors on the initial depletion of the stock: (1) blue: log(bkfrac)~N(log(0.8), 0.5^2), (2) orange: log(bkfrac)~N(log(0.8), 0.3^2), (3) green: log(bkfrac)~N(log(0.5), 0.5^2), (4) yellow: log(bkfrac)~N(log(0.5), 0.3^2).**

#### 2.3.1.5 Sensitivity to prior on observational error of the indices (sdi)

From the previous model runs, it was noted that the model gives a similar estimate of uncertainty for the first and second semester of the biannual index (sdi1 for first semester and sdi2 for second semester, Table 2.5). However, the index for the second semester (1999–2021) shows higher uncertainty around its estimates compared to the first semester (see Annex 2 WD Survey Index). A prior was therefore included on the observational error of these two indices (sdi) informing the model to follow the trend of the first semester more closely.

**Table 2.5. Brill in Subarea 4 and divisions 3.a and 7.d–e. Summary of the run as described in §2.3.1.4 with log(bkfrac)~N(log(0.8), 0.3^2) and no prior on sdi.**

```
Convergence: 0  MSG: both X-convergence and relative convergence (5)
Objective function at optimum: -8.0417508
Euler time step (years):  1/16 or 0.0625
Nobs C: 72,  Nobs I1: 23,  Nobs I2: 23,  Nobs I3: 16

Priors
      logn  ~  dnorm[log(2), 0.01^2]
      logr  ~  dnorm[log(0.5), 0.5^2]
 logbkfrac  ~  dnorm[log(0.8), 0.3^2]

Model parameter estimates w 95% CI
            estimate        cilow        ciupp    log.est
 alpha1    0.9524843    0.4441205 2.042748e+00 -0.0486817
 alpha2    1.2189315    0.6030285 2.463887e+00  0.1979746
 alpha3    2.9249713    1.5796656 5.415993e+00  1.0732847
 beta      0.2506338    0.1027115 6.115898e-01 -1.3837622
 r         0.9247296    0.3396333 2.517788e+00 -0.0782539
 rc        0.9248601    0.3396057 2.518704e+00 -0.0781128
 rold      0.9249907    0.3394479 2.520587e+00 -0.0779716
 m      2261.4155516 1921.1959474 2.661884e+03  7.7237462
 K      9781.1067602 3414.3880687 2.801968e+04  9.1882079
 q1     1480.7712067  429.6985571 5.102841e+03  7.3003183
 q2     1398.4427571  405.3737818 4.824294e+03  7.2431146
 q3      116.8703483   32.2969593 4.229091e+02  4.7610652
 n         1.9997177    1.9609093 2.039294e+00  0.6930060
 sdb       0.1660571    0.1038810 2.654476e-01 -1.7954234
 sdf       0.1222337    0.0845246 1.767661e-01 -2.1018203
 sdi1      0.1581668    0.1001013 2.499143e-01 -1.8441051
 sdi2      0.2024123    0.1363104 3.005693e-01 -1.5974488
 sdi3      0.4857123    0.3287742 7.175639e-01 -0.7221388
 sdc       0.0306359    0.0149509 6.277630e-02 -3.4855825

Deterministic reference points (Drp)
           estimate        cilow        ciupp   log.est
 Bmsyd 4890.2866947 1706.8626567 14011.030039  8.495006
 Fmsyd    0.4624301    0.1698028     1.259352 -0.771260
 MSYd  2261.4155516 1921.1959474  2661.883763  7.723746
Stochastic reference points (Srp)
           estimate        cilow        ciupp    log.est rel.diff.Drp
 Bmsys 4766.9463404 1658.5302096 13701.153757  8.4694612  -0.02587408
 Fmsys    0.4561616    0.1658666     1.254523 -0.7849081  -0.01374174
 MSYs  2173.7249260 1861.1728279  2538.764795  7.6841975  -0.04034118

States w 95% CI (inp$msytype: s)
                    estimate        cilow        ciupp    log.est
 B_2021.94      5575.6880976 1643.7582752 1.891294e+04  8.6261710
 F_2021.94         0.2648074    0.0772805 9.073821e-01 -1.3287526
 B_2021.94/Bmsy    1.1696561    0.8387895 1.631036e+00  0.1567098
 F_2021.94/Fmsy    0.5805121    0.3810833 8.843063e-01 -0.5438446

Predictions w 95% CI (inp$msytype: s)
                  prediction        cilow        ciupp    log.est
 B_2024.00      6459.2257962 2084.1245200 2.001876e+04  8.7732647
 F_2024.00         0.2648078    0.0737210 9.511969e-01 -1.3287511
 B_2024.00/Bmsy    1.3550028    0.9445300 1.943859e+00  0.3038035
 F_2024.00/Fmsy    0.5805130    0.3370689 9.997819e-01 -0.5438430
 Catch_2023.00  1670.0470914 1130.1130504 2.467945e+03  7.4206071
 E(B_inf)       6646.2003049           NA           NA  8.8018006
```

The model as shown in Table 2.5 including the full catch time-series, three survey indices, forcing the production curve to a Schaefer model, a prior on r (Log(r)~N(log(0.5),0.5^2)) and a prior on bkfrac (log(bkfrac)~N(log(0.8), 0.3^2)) was compared to its equivalent including a prior on sdi1 (Log(sdi1)~N(log(0.25), 0.3^2) on sdi2 (Log(sdi2)~N(log(0.5), 0.3^2) and deactivate the priors on sdi3 (Figure 2.7). Both model outputs were similar to small deviations in the period 1985–2005 showing higher relative biomass and lower relative fishing mortality in the model including the priors on observational error. Although the sdi estimated values changed slightly toward the given priors, they continue to be relatively close to each other compared to the sdi of the 1983–1998 index (Table 2.6).


**Figure 2.7. Brill in Subarea 4 and divisions 3.a and 7.d–e. Plot comparing the output of the assessment with priors on observational error for the exploitable biomass indices (sdi1 and sdi2).**

**Table 2.6. Brill in Subarea 4 and divisions 3.a and 7.d–e. Summary of the run with priors on sdi (Log(sdi1)~N(log(0.25), 0.3^2), (Log(sdi2)~N(log(0.5), 0.3^2) and Log(sdi3) deactivated).**

```
Convergence: 0  MSG: relative convergence (4)
Objective function at optimum: -6.12047
Euler time step (years):  1/16 or 0.0625
Nobs C: 72,  Nobs I1: 23,  Nobs I2: 23,  Nobs I3: 16

Priors
      logn  ~  dnorm[log(2), 0.01^2]
      logr  ~  dnorm[log(0.5), 0.5^2]
 logbkfrac  ~  dnorm[log(0.8), 0.3^2]
   logsdi1  ~  dnorm[log(0.25), 0.3^2]
   logsdi2  ~  dnorm[log(0.5), 0.3^2]

Model parameter estimates w 95% CI
            estimate        cilow        ciupp    log.est
 alpha1 1.329183e+00    0.7133778 2.476567e+00  0.2845647
 alpha2 1.842917e+00    1.0101848 3.362102e+00  0.6113499
 alpha3 3.373703e+00    1.8429903 6.175765e+00  1.2160111
 beta   2.918378e-01    0.1367134 6.229770e-01 -1.2315570
 r      7.769399e-01    0.2813350 2.145611e+00 -0.2523923
 rc     7.770029e-01    0.2813049 2.146189e+00 -0.2523112
 rold   7.770660e-01    0.2811686 2.147578e+00 -0.2522300
 m      2.254794e+03 1828.5554539 2.780390e+03  7.7208140
 K      1.160801e+04 3800.7994475 3.545200e+04  9.3594509
 q1     1.234520e+03  314.0281461 4.853196e+03  7.1184377
 q2     1.193470e+03  304.0643734 4.684440e+03  7.0846205
 q3     9.483538e+01   23.2567703 3.867153e+02  4.5521425
 n      1.999838e+00    1.9610267 2.039417e+00  0.6930660
 sdb    1.436143e-01    0.0908616 2.269945e-01 -1.9406237
 sdf    1.179877e-01    0.0783103 1.777686e-01 -2.1371746
 sdi1   1.908898e-01    0.1355183 2.688856e-01 -1.6560591
 sdi2   2.646694e-01    0.1890488 3.705387e-01 -1.3292739
 sdi3   4.845122e-01    0.3300434 7.112763e-01 -0.7246127
 sdc    3.443330e-02    0.0198926 5.960280e-02 -3.3687317

Deterministic reference points (Drp)
          estimate        cilow        ciupp    log.est
 Bmsyd 5803.8242811 1900.1119636 17727.574444  8.6662723
 Fmsyd    0.3885015    0.1406525     1.073095 -0.9454583
 MSYd  2254.7942452 1828.5554539  2780.389885  7.7208140
Stochastic reference points (Srp)
          estimate        cilow        ciupp    log.est rel.diff.Drp
 Bmsys 5685.1808495 1868.6078294 17296.984838  8.6456182  -0.02086889
 Fmsys    0.3836457    0.1374991     1.070436 -0.9580359  -0.01265690
 MSYs  2180.5188936 1790.3947973  2655.650392  7.6873182  -0.03406315

States w 95% CI (inp$msytype: s)
                  estimate        cilow        ciupp    log.est
 B_2021.94      6788.2285091 1809.3504909 2.546773e+04  8.8229453
 F_2021.94         0.2216588    0.0578744 8.489533e-01 -1.5066158
 B_2021.94/Bmsy    1.1940216    0.8322773 1.712996e+00  0.1773271
 F_2021.94/Fmsy    0.5777697    0.3467342 9.627486e-01 -0.5485799

Predictions w 95% CI (inp$msytype: s)
                prediction        cilow        ciupp    log.est
 B_2024.00      7654.7204262 2220.5082928 2.638799e+04  8.9430778
 F_2024.00         0.2216592    0.0555798 8.840047e-01 -1.5066140
 B_2024.00/Bmsy    1.3464339    0.9353677 1.938152e+00  0.2974596
 F_2024.00/Fmsy    0.5777707    0.3142092 1.062410e+00 -0.5485781
 Catch_2023.00  1661.2771411 1142.7699819 2.415046e+03  7.4153419
 E(B_inf)       7942.4324195           NA           NA  8.9799749
```

The run including the sdi priors was selected for the final assessment. Detailed information on the input data, priors, outputs and diagnostics are described below.

### 2.3.2 Final assessment

The input data for the stock were 1) a landings series from 1950–2021 with the first part of the time-series from the historical official landings and the most recent part (2014–2021) from ICES InterCatch landings; 2) three survey indices: one for semester 1 from 1983–1998, one for semester 1 from 1999–2021 and one for semester 2 from 1999–2021. The survey time-series were trimmed to include only brill equal to or larger than 25 cm in order to obtain a better proxy for the exploitable biomass, which is a prerequisite for a production model.

The final assessment settings and priors for the model parameters are described in Table 2.7.

**Table 2.7. Brill in Subarea 4 and divisions 3.a and 7.d–e. SPiCT settings and input data.**

| Setting/Data | Values/Source |
|---|---|
| Catch time-series | Historical landings 1950–2013<br>InterCatch landings data 2014–2021 |
| Combined survey index semester 1 | 1999–2021, ≥ 25 cm |
| Combined survey index semester 2 | 1999–2021, ≥ 25 cm |
| Combined survey index semester 1 | 1983–1998, ≥ 25 cm |
| SPiCT settings | |
| • Standard deviation on the catch (observation) (stdevfacC) | From 1950–1998 stdevfacC = 2;<br>From 1999–2021 stdevfacC = 1 |
| • Standard deviation on the indices (observation) (sdi) | Log(sdi1)~N(log(0.25),0.3^2)<br>Log(sdi2)~N(log(0.5), 0.3^2)<br>Log(sdi3) -> deactivated |
| • Uncertainty ratio of index (observation) to biomass process (alpha) | Deactivated |
| • Uncertainty ratio of catch (observation) to fishing mortality process (beta) | Deactivated |
| • Shape parameter (n) | Schaefer model, Log(n)~N(log(2),0.01^2) |
| • Intrinsic growth rate (r) | Log(r)~N(log(0.5),0.5^2) |
| • Initial depletion (bkfrac) | log(bkfrac)~N(log(0.8), 0.3^2) |
| Discretion time-step (dteuler) | 1/16 year (default) |

In the SPiCT settings, variation was increased on the catch data for the early part of the time-series (from 1950–1998) to account for the larger uncertainty around the data in that period. This gave better results in the sensitivity analysis (check.ini). Similarly, the variation on the survey indices was made narrower for the 1999–2021 index for semester 1 compared to the 1999–2021 index for semester 2. This allowed the model to give more weight to the semester 1 index, because it was noted that the estimates from the semester 1 survey index were less uncertain (see

Annex 2 WD Survey Index). This required to remove the priors for the ratios of process to observation errors (alpha and beta) and allowed the model to estimate them.

The shape parameter of the production curve was fixed to 2 (with limited variation), imposing a Schaefer production model. The shape of the production curve depends on life history (recruitment, natural mortality, growth) and exploitation patterns (selectivity). By fixing it to the Schaefer model, the complexity in the model is reduced. This results in a more robust assessment with less uncertainty, however, with a chance of getting a slightly biased stock status (usually more precautionary).

Life-history parameters were compiled and investigated (Annex 3 WD Life History). Using 3 different sources (van der Hammen *et al*., 2013, von Bertalanffy and FishLife), the growth rate for females was estimated at around 0.65 (CV = 0.32). Trial SPiCT runs revealed good fits (§2.3.1.3) with this prior, but for the final model, the prior was set to 0.5 (CV = 0.5). This gave the model more flexibility and allowed some buffer for when new data comes in. Finally, the sexual dimorphism is pronounced in this species, with males maturing earlier than females and females reaching larger body sizes than males. Having a looser r prior also takes this into account.

Because the model switched to a lower biomass when the r prior was set too low (§2.3.1.3), we implemented an initial depletion prior allowing for high biomass at the beginning of the time-series. Immediately after the second world war, when fishing effort was low, biomass was estimated to be close to carrying capacity (expert knowledge).

The output of the model is shown in Figure 2.8 and Table 2.8. Convergence was obtained. The absolute biomass fluctuates around 10000 tonnes at the beginning of the time-series but decreases in the 1980s likely as a result of higher fishing pressure. Fishing pressure increases to unsustainable levels around the year 2000. This causes the biomass to decrease below sustainable levels. However, when fishing pressure decreases, biomass increases again. Catches are rather constant from the 1980s onwards and fluctuate around 2000 tonnes. The phase plot shows that the development of biomass and fishing mortality has been largely sustainable. The production curve (fitted to Schaefer model) was considered more realistic compared to the rejected SPiCT run as executed during WGNSSK 2022 (using default priors and the Dutch commercial beam trawl index and a shorter catch time-series; Figure 2.9).

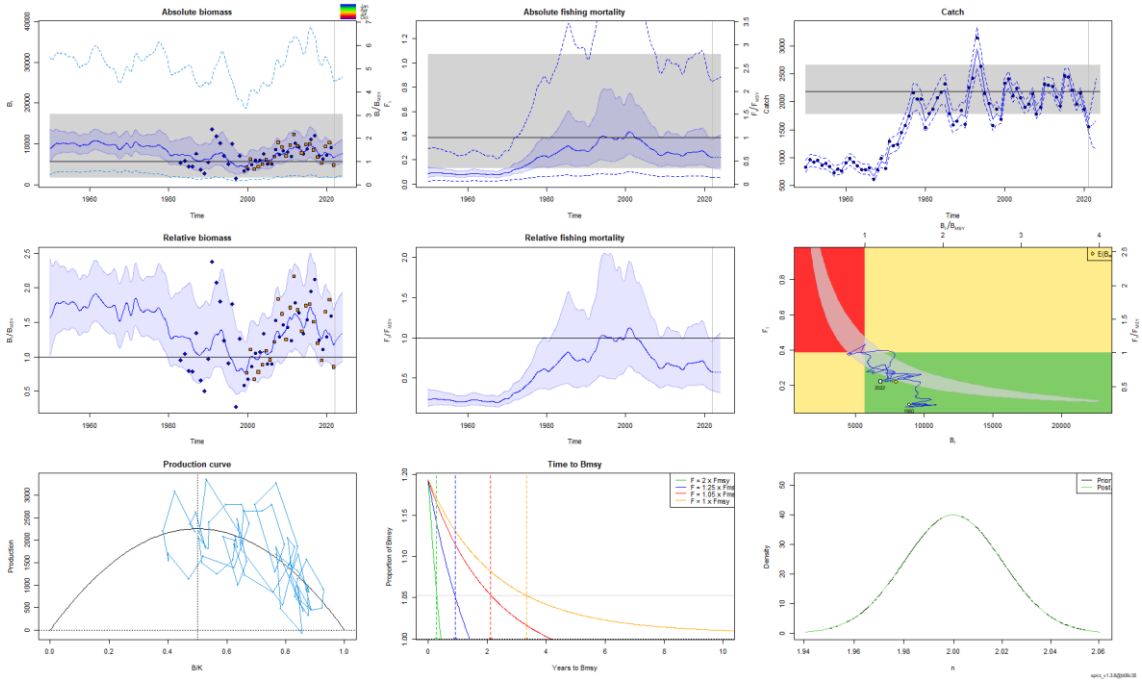


**Figure 2.8. Brill in Subarea 4 and divisions 3.a and 7.d–e. Output plot of the final SPiCT assessment.**


**Figure 2.9. Brill in Subarea 4 and divisions 3.a and 7.d–e. Plot comparing the final assessment from this benchmark (orange, final fit) with the rejected SPiCT run during WGNSSK 2022.**

**Table 2.8. Brill in Subarea 4 and divisions 3.a and 7.d–e. Summary of the final SPiCT assessment.**

```
Convergence: 0  MSG: relative convergence (4)
Objective function at optimum: -6.12047
Euler time step (years):  1/16 or 0.0625
Nobs C: 72,  Nobs I1: 23,  Nobs I2: 23,  Nobs I3: 16

Priors
      logn  ~  dnorm[log(2), 0.01^2]
      logr  ~  dnorm[log(0.5), 0.5^2]
 logbkfrac  ~  dnorm[log(0.8), 0.3^2]
   logsdi1  ~  dnorm[log(0.25), 0.3^2]
   logsdi2  ~  dnorm[log(0.5), 0.3^2]

Model parameter estimates w 95% CI
            estimate        cilow        ciupp    log.est
 alpha1 1.329183e+00    0.7133778 2.476567e+00  0.2845647
 alpha2 1.842917e+00    1.0101848 3.362102e+00  0.6113499
 alpha3 3.373703e+00    1.8429903 6.175765e+00  1.2160111
 beta   2.918378e-01    0.1367134 6.229770e-01 -1.2315570
 r      7.769399e-01    0.2813350 2.145611e+00 -0.2523923
 rc     7.770029e-01    0.2813049 2.146189e+00 -0.2523112
 rold   7.770660e-01    0.2811686 2.147578e+00 -0.2522300
 m      2.254794e+03 1828.5554539 2.780390e+03  7.7208140
 K      1.160801e+04 3800.7994475 3.545200e+04  9.3594509
 q1     1.234520e+03  314.0281461 4.853196e+03  7.1184377
 q2     1.193470e+03  304.0643734 4.684440e+03  7.0846205
 q3     9.483538e+01   23.2567703 3.867153e+02  4.5521425
 n      1.999838e+00    1.9610267 2.039417e+00  0.6930660
 sdb    1.436143e-01    0.0908616 2.269945e-01 -1.9406237
 sdf    1.179877e-01    0.0783103 1.777686e-01 -2.1371746
 sdi1   1.908898e-01    0.1355183 2.688856e-01 -1.6560591
 sdi2   2.646694e-01    0.1890488 3.705387e-01 -1.3292739
 sdi3   4.845122e-01    0.3300434 7.112763e-01 -0.7246127
 sdc    3.443330e-02    0.0198926 5.960280e-02 -3.3687317

Deterministic reference points (Drp)
           estimate        cilow        ciupp    log.est
 Bmsyd 5803.8242811 1900.1119636 17727.574444  8.6662723
 Fmsyd    0.3885015    0.1406525     1.073095 -0.9454583
 MSYd  2254.7942452 1828.5554539  2780.389885  7.7208140
Stochastic reference points (Srp)
           estimate        cilow        ciupp    log.est rel.diff.Drp
 Bmsys 5685.1808495 1868.6078294 17296.984838  8.6456182  -0.02086889
 Fmsys    0.3836457    0.1374991     1.070436 -0.9580359  -0.01265690
 MSYs  2180.5188936 1790.3947973  2655.650392  7.6873182  -0.03406315

States w 95% CI (inp$msytype: s)
                    estimate        cilow        ciupp    log.est
 B_2021.94      6788.2285091 1809.3504909 2.546773e+04  8.8229453
 F_2021.94         0.2216588    0.0578744 8.489533e-01 -1.5066158
 B_2021.94/Bmsy    1.1940216    0.8322773 1.712996e+00  0.1773271
 F_2021.94/Fmsy    0.5777697    0.3467342 9.627486e-01 -0.5485799

Predictions w 95% CI (inp$msytype: s)
                  prediction        cilow        ciupp    log.est
 B_2024.00      7654.7204262 2220.5082928 2.638799e+04  8.9430778
 F_2024.00         0.2216592    0.0555798 8.840047e-01 -1.5066140
 B_2024.00/Bmsy    1.3464339    0.9353677 1.938152e+00  0.2974596
 F_2024.00/Fmsy    0.5777707    0.3142092 1.062410e+00 -0.5485781
 Catch_2023.00  1661.2771411 1142.7699819 2.415046e+03  7.4153419
 E(B_inf)       7942.4324195           NA           NA  8.9799749
```

The diagnostics of the model indicate that there was no violation of the model assumptions based on the one-step-ahead residuals and process residuals (Figure 2.10 and Figure 2.11 respectively; bias, autocorrelation (L-box), normality (Shapiro)). P-values are not significant (>0.05). Furthermore, all variance parameters of the model parameters are finite.

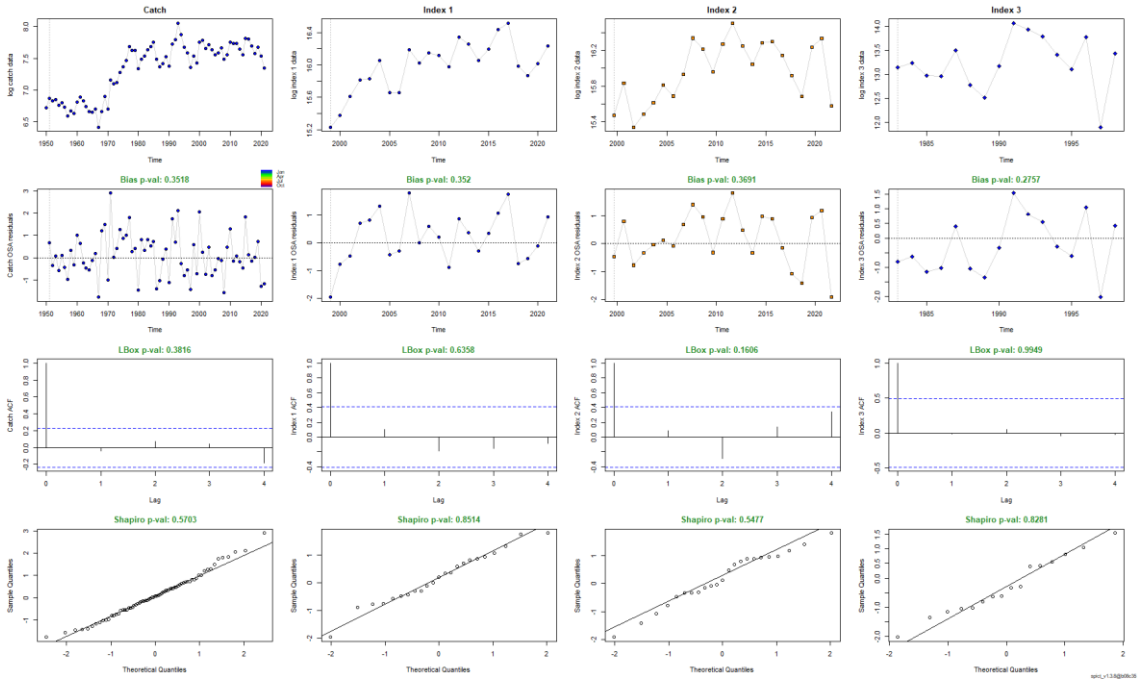


**Figure 2.10. Brill in Subarea 4 and divisions 3.a and 7.d–e. Residual plot of the final SPiCT assessment.**

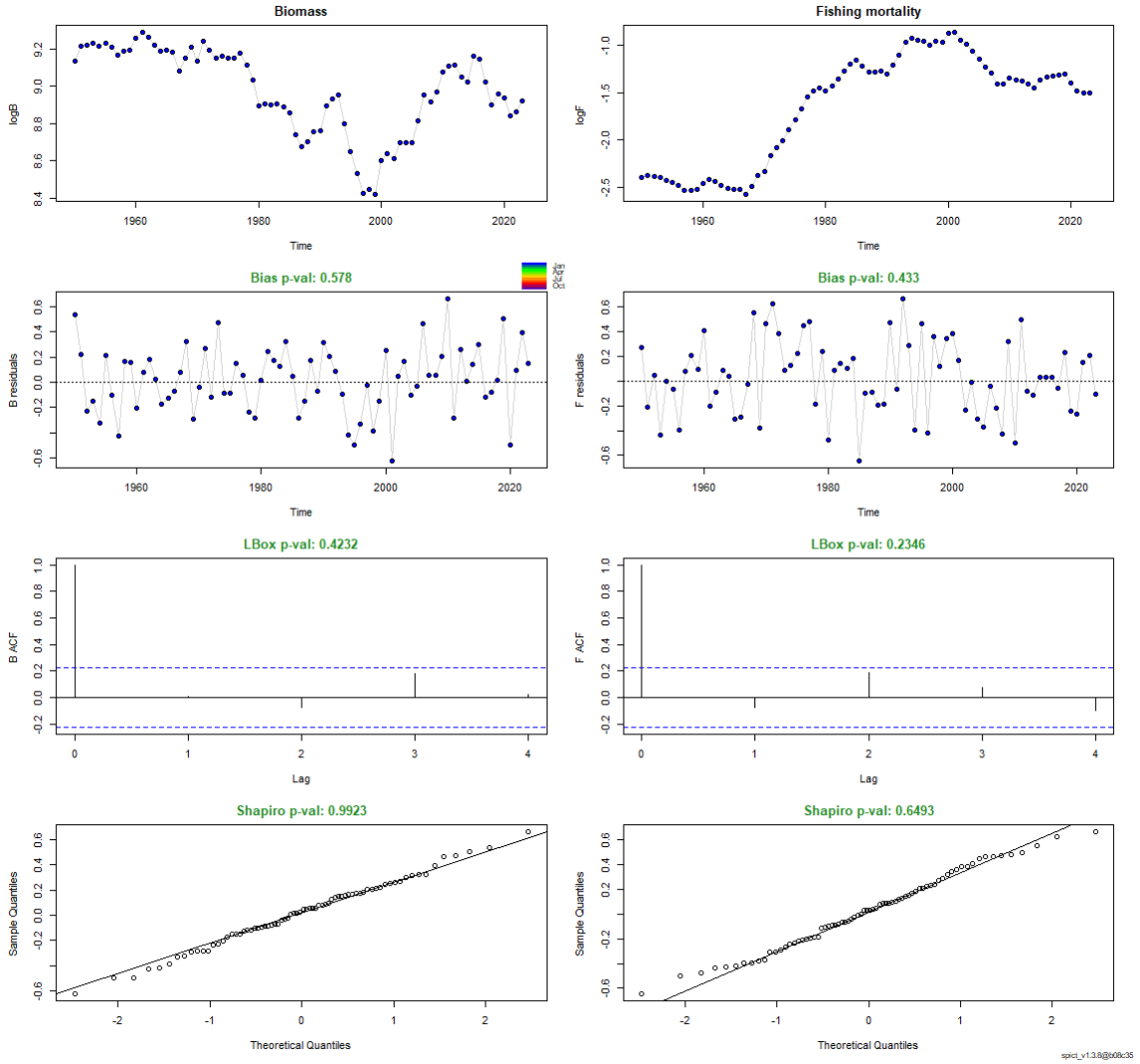


**Figure 2.11. Brill in Subarea 4 and divisions 3.a and 7.d–e. Process residual plot of the final SPiCT assessment.**

The priors and the posterior estimates are shown in Figure 2.12.

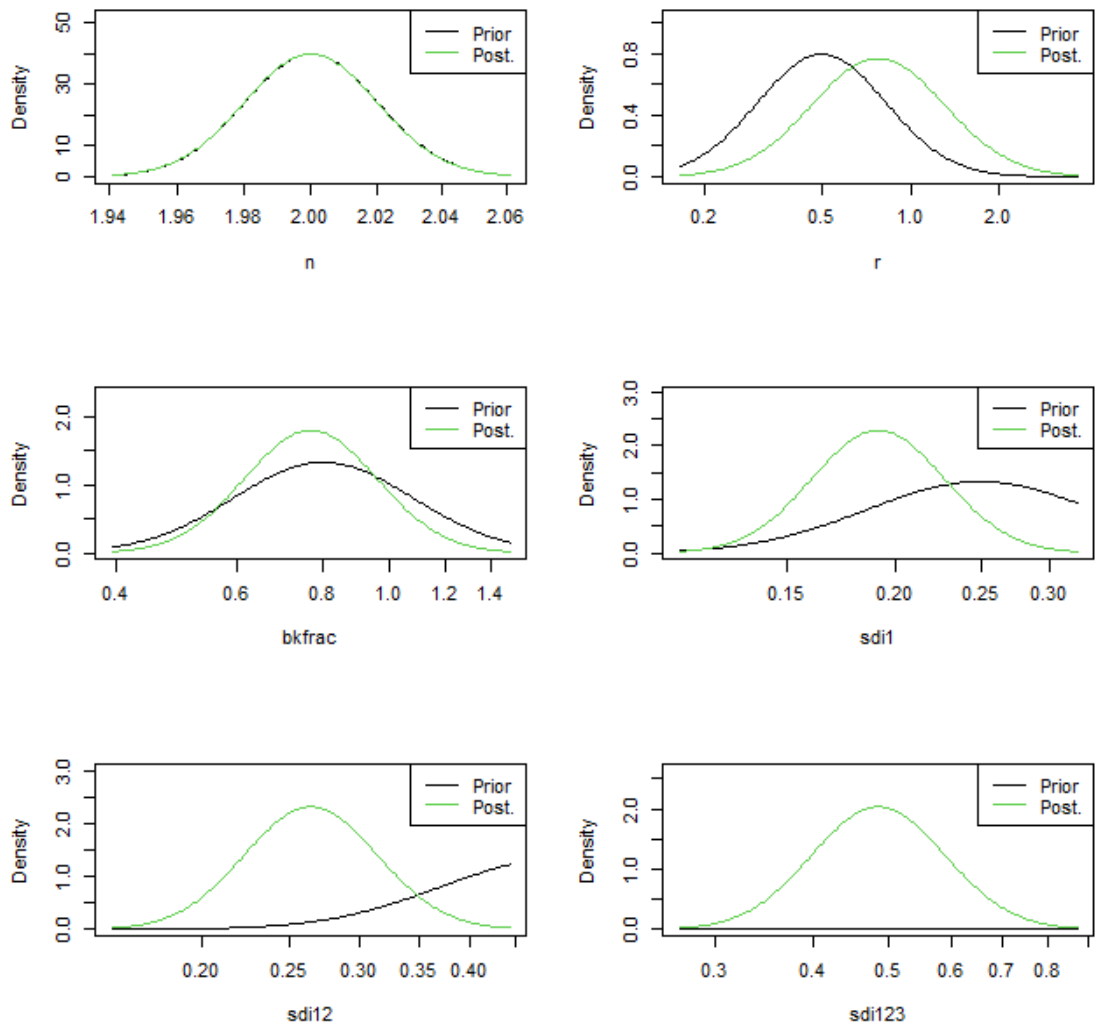


**Figure 2.12. Brill in Subarea 4 and divisions 3.a and 7.d–e. Process residual plot of the final SPiCT assessment.**

To evaluate the robustness of the model fit to the introduction of new data, a retrospective analysis using five peels was performed (Figure 2.13). Although confidence intervals are large for the absolute biomass and absolute fishing mortality, there is no consistent pattern comparing the different peels. No consistent over- or underestimation of relative fishing mortality and biomass is present, which is supported by the Mohn's rho values.

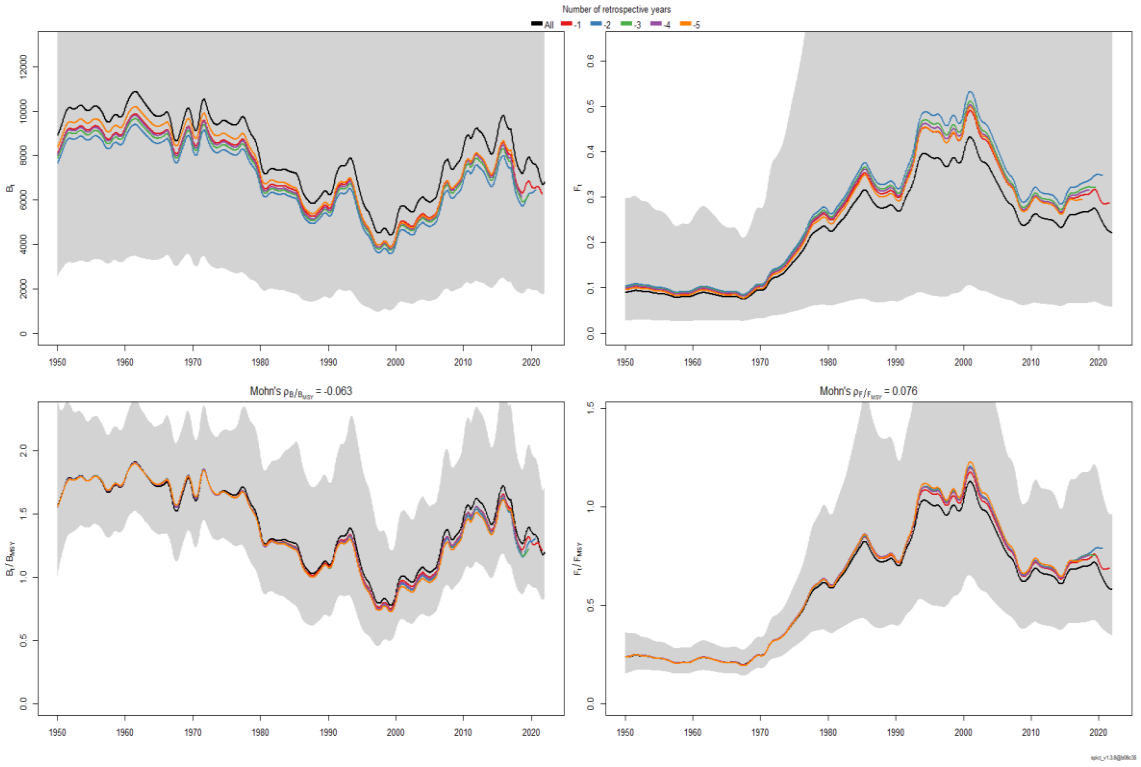


**Figure 2.13. Brill in Subarea 4 and divisions 3.a and 7.d–e. Retrospective plot of the final SPiCT assessment with Mohn's Rho values.**

A hindcast analysis was carried out to check the ability of the SPiCT model to predict the index by removing a data point and keeping the catch information (Figure 2.14). The MASE predictor was calculated and was for both indices below 1, which is considered good.

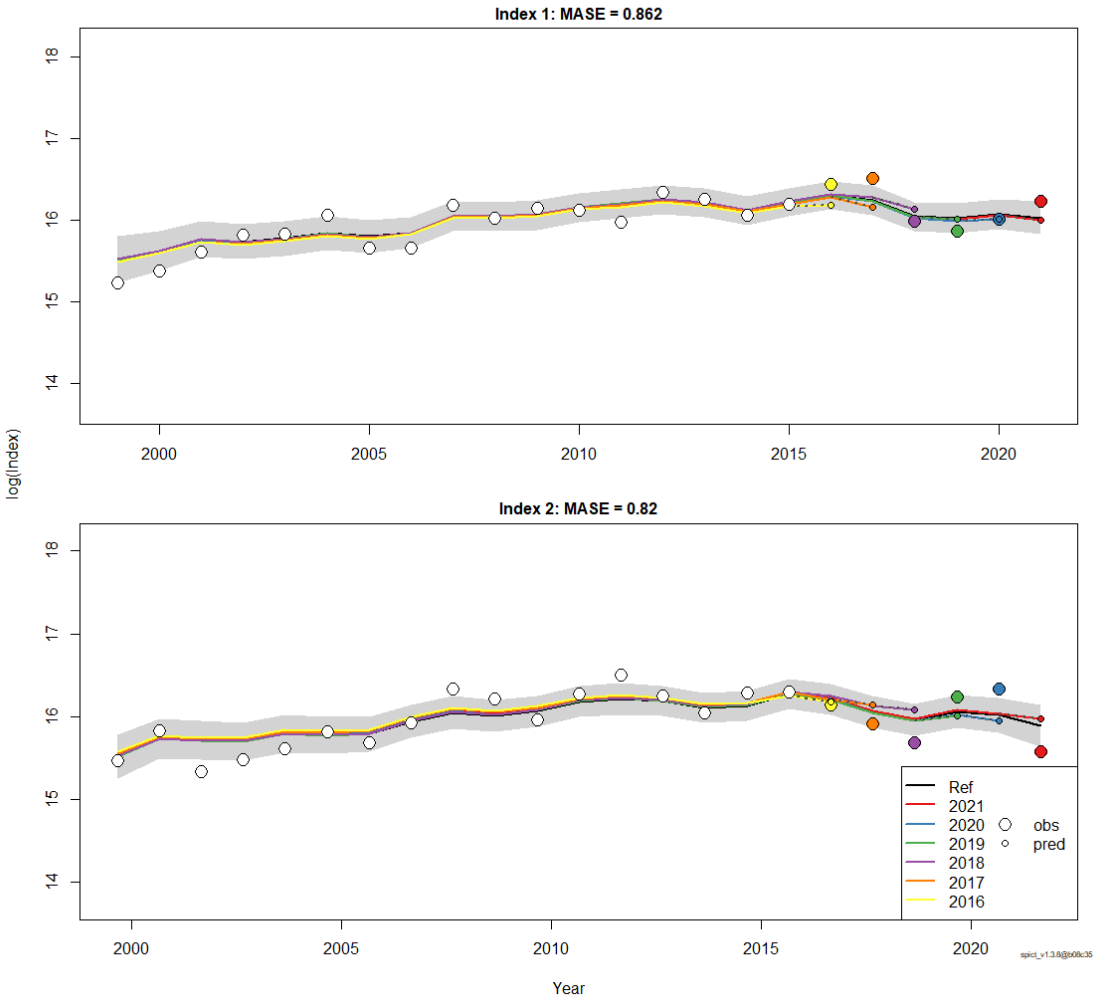


**Figure 2.14. Brill in Subarea 4 and divisions 3.a and 7.d–e. Hindcast plot of the final SPiCT assessment with MASE predictor.**

Finally, the robustness of the model was verified by checking whether the initial values influenced the parameter estimates (Table 2.9). Thirty trials were run. All converged and the difference in distance was minimal.

**Table 2.9. Brill in Subarea 4 and divisions 3.a and 7.d–e. Output of the sensitivity analyses concerning the initial parameter values (check.ini).**

| | Distance | m | K | q | q | n | sdb | sdf | sdi | sdi | sdc |
|---|---|---|---|---|---|---|---|---|---|---|---|
| Basevec | 0.00 | 2265.4 | 10885.06 | 1366.52 | 1319.04 | 2 | 0.14 | 0.12 | 0.19 | 0.26 | 0.03 |
| Trial 1 | 0.00 | 2265.4 | 10885.06 | 1366.52 | 1319.04 | 2 | 0.14 | 0.12 | 0.19 | 0.26 | 0.03 |
| Trial 2 | 0.00 | 2265.4 | 10885.06 | 1366.52 | 1319.04 | 2 | 0.14 | 0.12 | 0.19 | 0.26 | 0.03 |
| Trial 3 | 0.00 | 2265.4 | 10885.06 | 1366.52 | 1319.04 | 2 | 0.14 | 0.12 | 0.19 | 0.26 | 0.03 |
| Trial 4 | 0.17 | 2265.4 | 10885.23 | 1366.50 | 1319.02 | 2 | 0.14 | 0.12 | 0.19 | 0.26 | 0.03 |
| Trial 5 | 0.00 | 2265.4 | 10885.05 | 1366.52 | 1319.04 | 2 | 0.14 | 0.12 | 0.19 | 0.26 | 0.03 |
| Trial 6 | 0.00 | 2265.4 | 10885.06 | 1366.52 | 1319.04 | 2 | 0.14 | 0.12 | 0.19 | 0.26 | 0.03 |
| Trial 7 | 0.01 | 2265.4 | 10885.06 | 1366.52 | 1319.04 | 2 | 0.14 | 0.12 | 0.19 | 0.26 | 0.03 |
| Trial 8 | 0.00 | 2265.4 | 10885.05 | 1366.52 | 1319.04 | 2 | 0.14 | 0.12 | 0.19 | 0.26 | 0.03 |
| Trial 9 | 0.00 | 2265.4 | 10885.06 | 1366.52 | 1319.04 | 2 | 0.14 | 0.12 | 0.19 | 0.26 | 0.03 |
| Trial 10 | 0.09 | 2265.4 | 10884.97 | 1366.54 | 1319.06 | 2 | 0.14 | 0.12 | 0.19 | 0.26 | 0.03 |
| Trial 11 | 0.00 | 2265.4 | 10885.05 | 1366.52 | 1319.04 | 2 | 0.14 | 0.12 | 0.19 | 0.26 | 0.03 |
| Trial 12 | 0.00 | 2265.4 | 10885.06 | 1366.52 | 1319.04 | 2 | 0.14 | 0.12 | 0.19 | 0.26 | 0.03 |
| Trial 13 | 0.00 | 2265.4 | 10885.05 | 1366.52 | 1319.04 | 2 | 0.14 | 0.12 | 0.19 | 0.26 | 0.03 |
| Trial 14 | 0.01 | 2265.4 | 10885.07 | 1366.52 | 1319.04 | 2 | 0.14 | 0.12 | 0.19 | 0.26 | 0.03 |
| Trial 15 | 0.12 | 2265.4 | 10884.94 | 1366.54 | 1319.06 | 2 | 0.14 | 0.12 | 0.19 | 0.26 | 0.03 |
| Trial 16 | 0.21 | 2265.4 | 10885.26 | 1366.49 | 1319.01 | 2 | 0.14 | 0.12 | 0.19 | 0.26 | 0.03 |
| Trial 17 | 0.00 | 2265.4 | 10885.05 | 1366.52 | 1319.04 | 2 | 0.14 | 0.12 | 0.19 | 0.26 | 0.03 |
| Trial 18 | 0.00 | 2265.4 | 10885.05 | 1366.52 | 1319.04 | 2 | 0.14 | 0.12 | 0.19 | 0.26 | 0.03 |
| Trial 19 | 0.00 | 2265.4 | 10885.05 | 1366.52 | 1319.04 | 2 | 0.14 | 0.12 | 0.19 | 0.26 | 0.03 |
| Trial 20 | 0.00 | 2265.4 | 10885.05 | 1366.52 | 1319.04 | 2 | 0.14 | 0.12 | 0.19 | 0.26 | 0.03 |
| Trial 21 | 0.01 | 2265.4 | 10885.04 | 1366.53 | 1319.04 | 2 | 0.14 | 0.12 | 0.19 | 0.26 | 0.03 |
| Trial 22 | 0.00 | 2265.4 | 10885.05 | 1366.52 | 1319.04 | 2 | 0.14 | 0.12 | 0.19 | 0.26 | 0.03 |
| Trial 23 | 0.00 | 2265.4 | 10885.05 | 1366.52 | 1319.04 | 2 | 0.14 | 0.12 | 0.19 | 0.26 | 0.03 |
| Trial 24 | 0.00 | 2265.4 | 10885.06 | 1366.52 | 1319.04 | 2 | 0.14 | 0.12 | 0.19 | 0.26 | 0.03 |
| Trial 25 | 0.00 | 2265.4 | 10885.05 | 1366.52 | 1319.04 | 2 | 0.14 | 0.12 | 0.19 | 0.26 | 0.03 |
| Trial 26 | 0.04 | 2265.4 | 10885.02 | 1366.53 | 1319.05 | 2 | 0.14 | 0.12 | 0.19 | 0.26 | 0.03 |
| Trial 27 | 0.01 | 2265.4 | 10885.06 | 1366.52 | 1319.04 | 2 | 0.14 | 0.12 | 0.19 | 0.26 | 0.03 |
| Trial 28 | 0.00 | 2265.4 | 10885.05 | 1366.52 | 1319.04 | 2 | 0.14 | 0.12 | 0.19 | 0.26 | 0.03 |
| Trial 29 | 0.00 | 2265.4 | 10885.06 | 1366.52 | 1319.04 | 2 | 0.14 | 0.12 | 0.19 | 0.26 | 0.03 |
| Trial 30 | 0.08 | 2265.4 | 10885.14 | 1366.51 | 1319.03 | 2 | 0.14 | 0.12 | 0.19 | 0.26 | 0.03 |

## 2.4 Future considerations/recommendations

Management of brill and turbot under a combined species TAC prevents effective control of the single-species exploitation rates and could lead to the overexploitation of either species. ICES advises that management should be implemented at the species level in the entire stock distribution area (Subarea 4 and divisions 3.a and 7.d–e). In contrast to the previous assessment, this revised assessments uses survey indices that cover the whole stock area. Landings advice for this stock as output of the forecast should therefore be applied to the entire stock area (Subarea 4 and divisions 3.a and 7.d–e) and not only on the TAC area (i.e. Subarea 4 and 2.a).

Due to the absence of a dedicated data call for this benchmark, the ICES time-series was not updated and no discard data were available prior to 2014.

In 2018, Dutch fishers' association, VisNed, together with Wageningen Marine Research initiated an industry survey to monitor turbot and brill in the North Sea. The numbers of brill caught during this industry survey were approximately 10 times higher than caught during the BTS (ISI/TRI Q3) survey (Schram *et al.*, 2021). This index could serve as a potential candidate to include in the brill assessment when a sufficient time-series is built.

## 2.5 Reviewers report

Of all the benchmarked stocks, the brill stock gave the most consistent and well-performing assessments. This can be attributed to quite long time-series of data (catches from 1950 and two new survey data time-series where one goes back to 1983) that contain substantial contrast (varying fishing pressure and abundance over time). The replacement of the commercial LPUE index with independent survey time-series that covers the whole stock is a major improvement of the input data to this assessment compared to the last benchmark. The exploitation history is typical —relatively low catches in 1950 which increase substantially until a peak around 1990s followed by a slight decrease. The decrease in fishing pressure in the later period explains the observed increase in abundance observed from around 2000–2015. Some runs showed divergent results regarding the stock status in the early years before the survey index starts, however this is not unexpected nor of concern, since the estimated stock status in years after the introduction of the survey index was quite stable.

Thorough investigations of model settings including prior specifications were made, and the results were not very sensitive indicating that the signal from the data are quite strong. All diagnostics (residuals, retrospective analysis, hindcast) looked good.

Two concerns however should be highlighted. The first concern is a mismatch between the ratio of estimated survey biomass in Subarea 3.a and the North Sea, and the corresponding ratio for landings. The survey shows a large proportion of the total abundance is in Area 3.a, whereas landings are very small in 3.a compared to the North Sea. There is thus a risk that local depletion could happen in the North Sea, which might not be detected in the assessment if the abundance in 3.a is stable or increasing at the same time. While sensitivity runs showed that the assessment with an abundance index that excluded Area 3.a gave similar results, the reviewers recommend continued monitoring of the index trends in subareas such that local depletion does not go undetected. Stock ID was not discussed at the benchmark, but some genetic studies for other fish stocks indicate that Area 3.a is a mixing area between genetically distinct substocks in the Baltic and the North Sea. Future benchmarks may therefore consider whether 3.a or parts of it should be considered as part of the North Sea population or not. The second concern is about management. The management of Brill and Turbot under a combined TAC carries the risk of overexploitation of either species. Species-specific TACs would thus be preferable.

## 2.6 Conclusions

SPiCT assessment model was accepted as the basis for providing advice for brill in the North Sea[2].

## 2.7 References

ICES. 2017. Working Group on the Assessment of Demersal Stocks in the North Sea and Skagerrak (2017). 26 April–5 May 2017, ICES HQ. ICES CM 2017/ACOM:21. 1248 pp. https://doi.org/10.17895/ices.pub.5323

ICES. 2022. Working Group on the Assessment of Demersal Stocks in the North Sea and Skagerrak (WGNSSK). ICES Scientific Reports. 4:43. http://doi.org/10.17895/ices.pub.19786285

Pedersen, M.W. and Berg, C.W., 2017. A stochastic surplus production model in continuous time. Fish and Fisheries, 18: 226–243. doi: 10.1111/faf.12174.

Schram, E., Hintzen, N., Batsleer, J., Wilkes, T., Bleeker, K., Amelot, M., van Broekhoven, W., Ras, D., de Boer, E., Trapman, B., Steins, N.A., 2021. Industry survey turbot and brill in the North Sea. Wageningen University and Research report C037/21. https://doi.org/10.18174/544588

SeaWise consortium, 2022. Deliverable 5.2: Report on historic and future spatial distribution of fished stocks. https://github.com/tokami/fishdish

Van der Hammen, T., Poos, J.J., van Overzee, H.M.J., Heessen, H.J.L., Magnusson, A., Rijnsdorp, A.D., 2013. Population ecology of turbot and brill: What can we learn from two rare flatfish species? Journal of Sea Research 84, 96–108.

[2] Also see: Stock Annex: Brill (*Scophthalmus rhombus*) in Subarea 4 and divisions 3.a and 7.d–e (North Sea, Skagerrak and Kattegat, English Channel). ICES Stock Annexes. 15 pp. https://doi.org/10.17895/ices.pub.24913293

# 2.8 Working documents for brill in North Sea, Skagerrak, Kattegat, and the English Channel (bll.27.3a47de)

## 2.8.1 WD Annex 1: Preparation of catch data for brill (*Scophthalmus rhombus)* in areas 27.3a47de (Greater North Sea)

*Author: Lies Vansteenbrugge (ILVO, Belgium)*

### 1. Introduction

Brill in the greater North Sea was last revised in 2013 during WGNEW, but has never been benchmarked. InterCatch procedures were therefore never thoroughly investigated. This working document provides an overview of the currently available data in InterCatch and how discards were raised and lengths were allocated. Note that there has not been a data call for this stock prior to the WKBMSYSPiCT2 2023 benchmark to request countries fishing on this stock to submit/update their brill time-series. Annex A1 of this working document gives an overview of the data currently available in InterCatch. Data from 2014–2021 are considered complete.

### 2. Countries with catch data

The countries contributing most to the landings of brill in the greater North Sea (27.3a47de) are The Netherlands (42 ± 2%), UK England (16 ± 1%), France (13 ± 2%), Belgium (12 ± 2%), Denmark (10 ± 2%) and Germany (4 ± 1%). The remaining countries (UK Scotland, Sweden, Norway, UK Northern Ireland and Ireland) are responsible for ≤ 1% of the landings. An overview of data available in InterCatch per country and year is provided in (Table 2.A1).

**Table 2.A1. Overview of available data in InterCatch per country and year.**

| Country | Landings data | Discard data | Length distributions Landings | Length distributions Discards |
|---|---|---|---|---|
| The Netherlands | 2014–2021 | 2014–2021 | 2014, 2016–2021 | 2014–2021 |
| UK-England | 2014–2021 | 2014–2021 | 2014–2021 | 2014–2016, 2018 |
| France | 2014–2021 | 2014–2021 | 2014–2017, 2019–2021 | No |
| Belgium | 2014–2021 | 2014–2021 | 2017–2021 | 2017–2020 |
| Denmark | 2014–2021 | 2014–2021 | 2015–2017, 2019–2020 | 2014–2017, 2019–2021 |
| Germany | 2014–2021 | 2014–2021 | 2014–2021 | 2014–2017, 2021 |
| UK Scotland | 2014–2021 | 2014–2017, 2019–2021 | 2014–2021 | 2014–2017 |
| Sweden | 2014–2021 | 2014–2021 | 2015–2021 | 2018–2021 |
| Norway | 2014–2021 | No | No | No |
| UK-Northern Ireland | 2017–2018, 2020–2021 | No | No | No |
| Ireland | 2014, 2016 | No | No | No |

InterCatch was used primarily for raising discards (and for estimating both landings and discards numbers/weights at length).

**3. Raising discard data**

If discards were not imported for a particular year-quarter-country-métier combination, they were assumed to be unknown (non-zero) and therefore raised. Discards on a year-quarter-country-métier basis were automatically matched by InterCatch to the corresponding landings. From 2014–2017, manual matching had to be done for some strata of The Netherlands and Scotland because discards estimates were provided on year level, while landings were provided per quarter (or the other way around). The matched discards-landings provided a landing-discard ratio estimate, which was then used for further raising (creating discard amounts) of the unmatched discards. The weighting factor for raising the discards was 'Landings CATON' (landings catch).

No discard estimates were calculated for the industrial bycatch strata (MIS_MIS_0_0_0_IBC).

Per year, it was investigated whether the proportion of landings for which discards weights were available **was equal or larger than 50%** compared to the total landings of that group (overview per year in Annex A1). For the period 2014–2017 this was not the case. Therefore, discards were raised using all available strata regardless of gear, season, country or area (REST group).

For 2018–2021, the 50% threshold was reached. Then, discard raising was performed on a gear level regardless of season, area or country. This approach was favoured over a more detailed one (e.g. using only strata from Area 27.7d to complete all other strata in that area). The main reasons being the fact that brill is considered as a data-limited stock, as a result of opportunistic sampling of this bycatch species, and no data call was issued to request potentially additional data.

The following groups were distinguished based on gear:

- TBB
- OTB including OTB, OTT, SSC, SDN
- GTR including GTR and GNS

The remaining gears were combined in a REST group (including MIS, FPO, DRB, LHM, LLS).

Discard rates from the available strata were sometimes higher than 100%. However, these were perceived representative for their gear group and were therefore included when estimating the discards of other strata within a gear group.

For discard raising of the REST group, all available strata were considered, except for discard rates higher than 100% from strata that had already been used in a specific gear group. For example, in 2020, discard raising was done for the OTB and TBB group separately. For the OTB group, the high discard rate (>100%) was retained. For the TBB group, no high discard rates were present (all <50%). For raising discards for the REST group (i.e. the remaining strata, not OTB or TBB), two strata from OTB with a discard rate >100% were removed. The high discard rate (>100%) of one of the GNS strata was however retained when raising the REST strata, because other GNS strata were present in the REST group and the rate was considered representative.

**4. Length allocations**

To allocate length compositions, landings and discards were handled separately; samples from landings were used only for landings and discards for discards. BMS landings strata were allocated to discard strata. No length allocations were done for logbook registered discards (these were also all 0). When length distributions (both landings and discards) had to be borrowed from other strata, allocations were performed on a gear level. The same gear groups (TBB, OTB, GTR and REST) as used for discard raising were applied. When the **threshold of 50%** was reached for the proportion of landings or discards covered by length (Annex A1), allocation of length occurred with all available information within that gear group if the gear group also reached this

50% and if ≥ 100 length measurements were available in the sampled strata (Annex A1 to this working document). When the threshold was not reached, unsampled data were pooled in the REST group and lengths were allocated using all available sampled data. The weighting factor was *'Mean Weight weighted by numbers-at-age'*.

***Landings***

The TBB group reached the threshold (50% of landings covered by length and ≥ 100 length measurements) for all years (2014–2021) except for 2015. Age allocations for all métiers within that group (e.g. TBB_DEF_>=120_0_0) were performed using the available sampled TBB data. Landings length allocations happened within the GTR group for the years 2019 and 2021. All other landings length allocations were done using all available strata (REST group).

***Discards***

The TBB group reached the threshold (50% of discards covered by length and ≥ 100 length measurements) only in 2019. All other discard length allocations were done using all available strata (REST group).

***BMS landings and Logbook registered discards***

From 2019 onwards, a limited amount of BMS landings were uploaded to InterCatch. Length allocation of BMS landings was done together with discards.

Under logbook registered discards, only zeros were available in InterCatch. These logbook registered discards were not considered for the length allocations.

## 5. Differences between old and new procedures in terms of discard tonnage

The discard data currently available for the assessment differ from the discard data used during the last assessment meeting (WGNSSK 2022) due to the change in InterCatch raising procedures.

The main difference is that prior to this benchmark, discard raising was always performed using all three gear groups (TBB, GTR, OTB) regardless of this 50% threshold and no strata were excluded with discard rates higher than 100% when raising the REST group. Table 2.A2 gives an overview of the differences in discard tonnage as a result in this change.

**Table 2.A2. Differences in discard tonnage as a result in this change between WG and benchmark.**

| | WGNSSK 2022 | | | WKBMSYSPiCT2 2023 | | | Difference (%) | | |
|---|---|---|---|---|---|---|---|---|---|
| Year | Landings | Discards | BMS | Landings | Discards | BMS | Landings | Discards | BMS |
| 2014 | 1919524 | 2308742 | | 1919524 | 2172749 | | 0.00 | −5.89 | |
| 2015 | 2470227 | 2301311 | | 2470227 | 2067236 | | 0.00 | −10.17 | |
| 2016 | 2444094 | 2673693 | | 2444094 | 2157695 | | 0.00 | −19.30 | |
| 2017 | 2207199 | 2081353 | | 2207199 | 2104447 | | 0.00 | 1.11 | |
| 2018 | 1956286 | 3488856 | | 1956286 | 3428163 | | 0.00 | −1.74 | |
| 2019 | 2147166 | 4172176 | 0004 | 2147167 | 3915166 | 0004 | 0.00 | −6.16 | 0.00 |
| 2020 | 1872411 | 2288186 | 0009 | 1872411 | 1822676 | 0009 | 0.00 | −20.34 | 0.00 |
| 2021 | 1546651 | 1514818 | 0124 | 1546651 | 6171364 | 0124 | 0.00 | −59.26 | 0.00 |

Differences are not larger than 20% with the exception of 2021. Discards are estimated 60% lower than during the previous working group. The reason is that with the WGNSSK 2022 raising procedure the GNS_DEF strata from Sweden from quarter 2 and 3 with discard rates >100% were less compensated with other strata than when they were part of the REST group (i.e. WKMBSYSPiCT2 procedure).

The InterCatch procedures as described in this working document, will be used for discard raising and length allocations in future.

#### 2.8.1.1 Annex A1: IC overview for 2011–2021 (bll.27.3a47de)

- **2011** – No landings data available, only discard data from The Netherlands present.
- **2012** – Landings from Belgium, Germany, Norway, UK England and UK Scotland, but no landings from The Netherlands as main country fishing on the stock. Discards available from Belgium, The Netherlands, UK England and UK Scotland.
- **2013** – Landings from Belgium, Denmark, France, Germany, The Netherlands, Norway, Sweden, UK England and UK Scotland present. Discards from Belgium, Denmark, The Netherlands, Sweden, UK England and UK Scotland available. However, very few strata However, few landings strata available from The Netherlands. Overall, only three strata with length distributions were provided, originating in The Netherlands.

**2014**

| **Countries** | **BEL (14%); DEN (8%); FRA (13%); GER (4%); IRE (<1%); NL (42%); NOR (1%); SWE (1%); ENG (16%); SCO (1%)** |
|---|---|
| Important gears | TBB_DEF_70-99_0_0_all<br>GTR_DEF_all_0_0_all<br>MIS_MIS_0_0_0_HC<br>OTB_DEF_70-99_0_0 |
| LAN with length | 53% |
| LAN with length per gear | GTR = 12%; OTB = 25%; REST = 6%; TBB = 69% |
| LAN length measurements | GTR = 85; OTB = 897; REST = 28; TBB = 2123 |
| DIS with length | 86% |
| DIS with length per gear | GTR = 4%; OTB = 8%; REST = 44%; TBB = 1% |
| DIS length measurements | GTR = 22; OTB = 18; REST = 280; TBB = 144 |
| LAN with DIS | 38% |
| LAN with DIS per gear | GTR = 69%; OTB = 62%; REST = 51%; TBB = 27% |

**2015**

| **Countries** | **BEL (13%); DEN (9%); FRA (12%); GER (5%); IRE (0%); NL (45%); NOR (<1%); SWE (1%); ENG (15%); SCO (1%)** |
|---|---|
| Important gears | TBB_DEF_70-99_0_0_all<br>GTR_DEF_90-99_0_0_all |

| Countries | BEL (13%); DEN (9%); FRA (12%); GER (5%); IRE (0%); NL (45%); NOR (<1%); SWE (1%); ENG (15%); SCO (1%) |
|---|---|
| | OTB_DEF_70-99_0_0<br>GNS_DEF_all_0_0_all |
| LAN with length | 19% |
| LAN with length per gear | GTR = 15%; OTB = 39%; REST = 26%; TBB = 13% |
| LAN length measurements | GTR = 104; OTB = 1769; REST = 327; TBB = 2322 |
| DIS with length | 77% |
| DIS with length per gear | GTR = 4%; OTB = 11%; REST = 40%; TBB = 4% |
| DIS length measurements | GTR = 42; OTB = 69; REST = 146; TBB = 86 |
| LAN with DIS | 42% |
| LAN with DIS per gear | GTR = 79%; OTB = 62%; REST = 43%; TBB = 31% |

**2016**

| Countries | BEL (13%); DEN (10%); FRA (12%); GER (4%); IRE (<1%); NL (41%); NOR (<1%); SWE (1%); ENG (17%); SCO (1%) |
|---|---|
| Important gears | TBB_DEF_70-99_0_0_all<br>GTR_DEF_all_0_0_all<br>MIS_MIS_0_0_0_HC<br>OTB_DEF_>=120_0_0_all |
| LAN with length | 56% |
| LAN with length per gear | GTR = 16%; OTB = 29%; REST = 53%; TBB = 71% |
| LAN length measurements | GTR = 192; OTB = 1641; REST = 101; TBB = 2555 |
| DIS with length | 73% |
| DIS with length per gear | GTR = 3%; OTB = 7%; REST = 57%; TBB = 1% |
| DIS length measurements | GTR = 17; OTB = 25; REST = 63; TBB = 74 |
| LAN with DIS | 45% |
| LAN with DIS per gear | GTR = 81%; OTB = 66%; REST = 61%; TBB = 33% |

**2017**

| **Countries** | **BEL (12%); DEN (11%); FRA (13%); GER (3%); IRE (0%); NL (42%); NOR (<1%); SWE (1%); ENG (15%); NO-IRE (<1%); SCO (1%)** |
|---|---|
| Important gears | TBB_DEF_70-99_0_0_all<br>GTR_DEF_all_0_0_all<br>OTB_CRU_90-119_0_0_all<br>OTB_DEF_>=120_0_0_all |
| LAN with length | 66% |
| LAN with length per gear | GTR = 5%; OTB = 40%; REST = 4%; TBB = 88% |
| LAN length measurements | GTR = 25; OTB = 1466; REST = 33; TBB = 5029 |
| DIS with length | 82% |
| DIS with length per gear | GTR = 4%; OTB = 27%; REST = 6%; TBB = 17% |
| DIS length measurements | GTR = 2; OTB = 129; REST = 1; TBB = 268 |
| LAN with DIS | 40% |
| LAN with DIS per gear | GTR = 74%; OTB = 72%; REST = 14%; TBB = 24% |

**2018**

| **Countries** | **BEL (12%); DEN (10%); FRA (16%); GER (4%); IRE (0%); NL (40%); NOR (1%); SWE (1%); ENG (16%); NO-IRE (<1%); SCO (2%)** |
|---|---|
| Important gears | TBB_DEF_70-99_0_0_all<br>GTR_DEF_>=220_0_0_all<br>TBB_DEF_>=120_0_0_all<br>OTB_DEF_70-99_0_0<br>OTB_DEF_>=120_0_0_all |
| LAN with length | 54% |
| LAN with length per gear | GTR = 1%; OTB = 13%; REST = 0%; TBB = 82% |
| LAN length measurements | GTR = 64; OTB = 618; TBB = 2951 |
| DIS with length | 32% |
| DIS with length per gear | GTR = 1%; OTB = 2%; REST = 0%; TBB = 68% |
| DIS length measurements | GTR = 17; OTB = 58; TBB = 170 |
| LAN with DIS | 64% |

| Countries | BEL (12%); DEN (10%); FRA (16%); GER (4%); IRE (0%); NL (40%); NOR (1%); SWE (1%); ENG (16%); NO-IRE (<1%); SCO (2%) |
|---|---|
| LAN with DIS per gear | GTR = 55%; OTB = 60%; REST = 0%; TBB = 71% |

**2019**

| Countries | BEL (10%); DEN (9%); FRA (14%); GER (6%); IRE (0%); NL (43%); NOR (<1%); SWE (1%); ENG (16%); SCO (1%) |
|---|---|
| Important gears | TBB_DEF_70-99_0_0_all<br>OTB_DEF_>=120_0_0_all<br>GTR_DEF_>=220_0_0_all<br>TBB_DEF_>=120_0_0_all<br>OTB_CRU_70-99_0_0_all |
| LAN with length | 66% |
| LAN with length per gear | GTR = 61%; OTB = 29%; REST = 1%; TBB = 86% |
| DIS with length | 60% |
| DIS with length per gear | GTR = 0%; OTB = 10%; REST = 0%; TBB = 56% |
| LAN with DIS | 69% |
| LAN with DIS per gear | GTR = 55%; OTB = 46%; REST = 3%; TBB = 85% |

**2020**

| Countries | BEL (9%); DEN (11%); FRA (11%); GER (5%); IRE (0%); NL (44%); NOR (<1%); SWE (1%); ENG (17%); NO-IRE (<1%); SCO (1%) |
|---|---|
| Important gears | TBB_DEF_70-99_0_0_all<br>TBB_DEF_>=120_0_0_all<br>OTB_DEF_100-119_0_0_all<br>OTB_CRU_90-119_0_0_all<br>OTB_CRU_70-99_0_0_all |
| LAN with length | 59% |
| LAN with length per gear | GTR = 19%; OTB = 27%; REST = 5%; TBB = 82% |
| DIS with length | 90% |
| DIS with length per gear | GTR = <1%; OTB = 20%; REST = 0%; TBB = 49% |
| LAN with DIS | 59% |
| LAN with DIS per gear | GTR = 2%; OTB = 56%; REST = <1%; TBB = 70% |

**2021**

| **Countries** | **BEL (10%); DEN (14%); FRA (15%); GER (4%); IRE (0%); NL (37%); NOR (<1%); SWE (1%); ENG (18%); NO-IRE (<1%); SCO (1%)** |
|---|---|
| Important gears | TBB_DEF_70-99_0_0_all<br>TBB_DEF_>=120_0_0_all<br>GTR_DEF_>=220_0_0_all<br>OTB_CRU_90-119_0_0_all<br>OTB_DEF_>=120_0_0_all |
| LAN with length | 58% |
| LAN with length per gear | GTR = 53%; OTB = 28%; REST = 1%; TBB = 75% |
| DIS with length | 69% |
| DIS with length per gear | GTR = 0%; OTB = 13%; REST = 0%; TBB = 45% |
| LAN with DIS | 50% |
| LAN with DIS per gear | GTR = 0%; OTB = 62%; REST = 0%; TBB = 58% |

## 2.8.2 WD Annex 2: Development and revision of survey indices for brill in the North Sea, Skagerrak, Kattegat and English Channel (ICES divisions 27.4a-c, 27.3a and 27.7d-e)

*Authors: Damian Villagra, Lies Vansteenbrugge, and Klaas Sys (ILVO, Belgium)*

### 1. Introduction and objective

This document describes how standardized survey indices were derived for Brill (*Scophthalmus rhombus)* in Subarea 4 and divisions 3.a and 7.d–e (North Sea, Skagerrak and Kattegat, English Channel; bll.27.3a47de) from all available DATRAS surveys in the stock area as prepared during WKFISHDIS2 (Seawise, 2022). The main objective was to obtain a unique exploitable biomass index for the entire stock area and move away from a spatially-limited index based on national fleets or single surveys.

For this purpose: (1) the dataset was explored to identify spatial-temporal and gear-specific trends and gaps, that could hinder the model's robustness and likely lead to inaccurate predictions; (2) survey and commercial length frequency distribution were compared to identify match/mismatch and to determine an appropriate cut-off length to accurately represent the stock's exploitable biomass; (3) different models were fitted and validated to finally (4) provide yearly, biannual or quarterly stock biomass estimates.

### 2. Data exploration

#### *Compiled dataset*

The compiled dataset was filtered to the stock's area (ICES Subarea 4 and divisions 3.a and 7.d–e; Figure 2.B1) and included six surveys (BITS, BTS, DYFS, FR-CGFS, NS-IBTS and SNS) executed by eight countries (Belgium, Denmark, France, Germany, Great-Brittain, the Netherlands, Norway and Sweden). The survey dataset spanned the period 1971–2021 and 3 quarters (1, 3, and 4). Three different gears were used by 42 different vessels: BT used in BTS, DYFS and SNS (beam trawls); GOV_CL used in FR-CGFS and NS-IBTS (Demersal trawl (bottom trawl) with clean gear and high headline net: herring bottom trawls, GOV with groundgear A) and TV used in BITS (TV-3 trawls). Night hauls were removed to avoid considering different catch rates related to different activity regimes during night-time. Weights are calculated for all length samples using a length-weight key combining all available information. Length-weight information is available from the late 1990s as shown in the table below. Most information and the longest time-series is available for the Beam Trawl Surveys (BTS), followed by the Baltic International Trawl Survey (BITS), the Sole Net Survey (SNS) and Demersal Young Fish Survey (DYFS). Length-weight relationships are consistent across years, surveys and quarters, with the exception of the year 2005 and the French CGFS having significantly deviating slope and intercept (note: sample size was lower for CGFS compared to other surveys).

| Survey | Years with length-weight information |
|---|---|
| BITS | 1994; 2009:2021 |
| BTS | 1996:2021 |
| DYFS | 2003:2021 |
| FR-CGFS | 2014:2017; 2019; 2021 |
| NS-IBTS | 2004; 2007:2021 |
| SNS | 2004:2021 |


**Figure 2.B1. Haul locations (shoot positions) by year of all included surveys from 1971 to 2021 in the stock area (ICES Subarea 4 and divisions 3.a and 7.d–e).**

### *Haul data*

The data shows a clear increase in haul number and spatial coverage throughout time from 1971 to 2021 (Figure 2.B1). Prior to 1985, there are less hauls and hauls do not homogeneously cover the stock area (Figure 2.B1; Figure 2.B2). From 1988 onwards, the eastern English Channel is sampled (7.d) and from 1990 onwards it is sampled with two different gears (Figure 2.B3). The western English Channel is only sampled from 2006 onwards. Since 1985, the central and southern North Sea (4.b–c) is surveyed by both BT and GOV_CL, while the northern North Sea (4.a), Skagerrak and Kattegat (3.a.20–21) are most often sampled by GOV_CL (Figure 2.B3). From 1996 onwards, the TV gear was used in surveys covering Division 3.a (Figure 2.B2; Figure 2.B3). Most hauls were executed in 3.a.20 (Kattegat) using this gear.

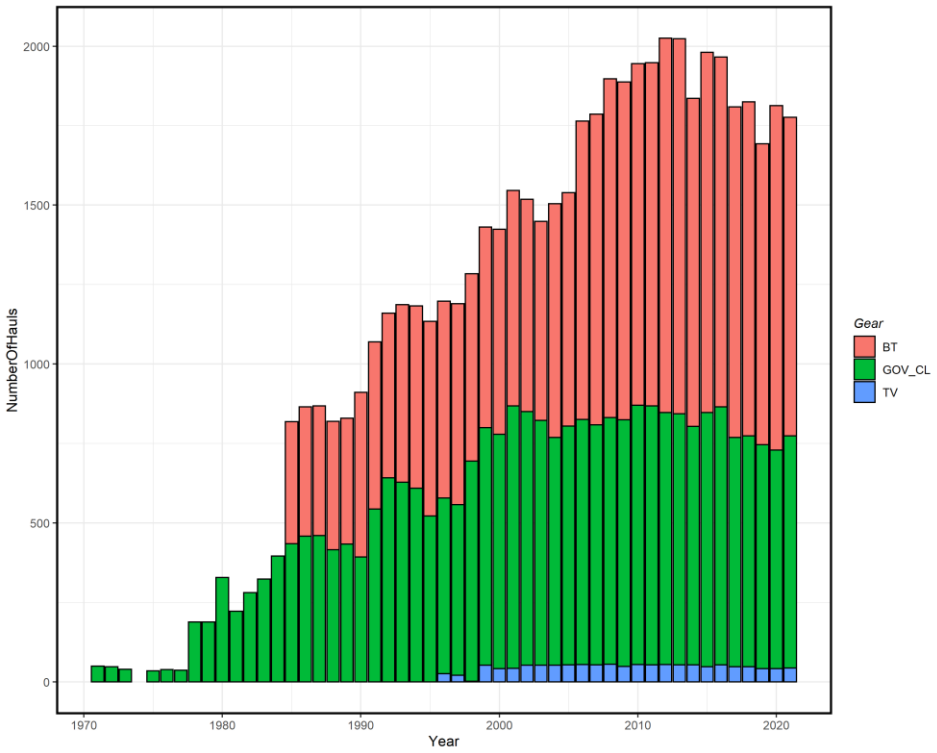


**Figure 2.B2. Haul count by gear from 1971 to 2021.**

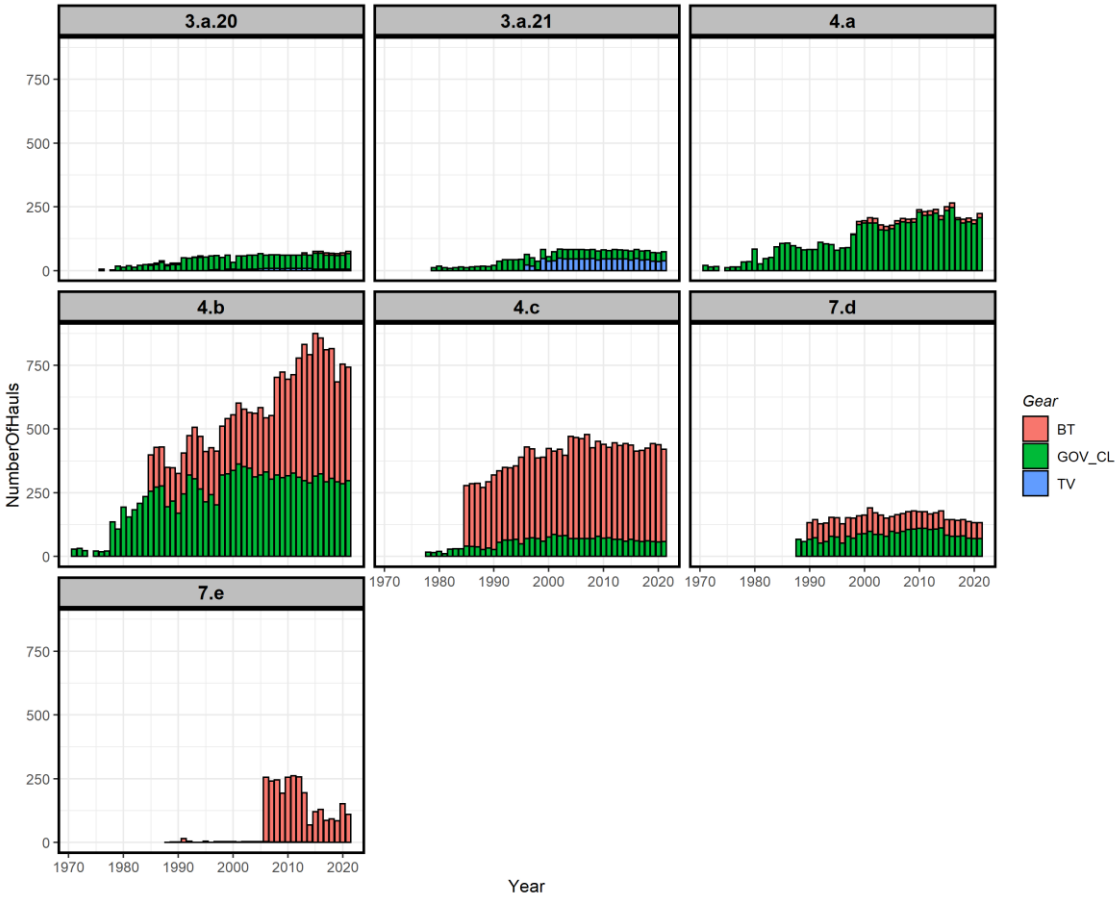


**Figure 2.B3. Haul count by gear from 1971 to 2021 for each ICES Division.**

In addition to the differences in gear per area and adding new gears through time, there is also variation per quarter (Figure 2.B4). Quarter 1 and 3 are mostly sampled throughout the time-series.

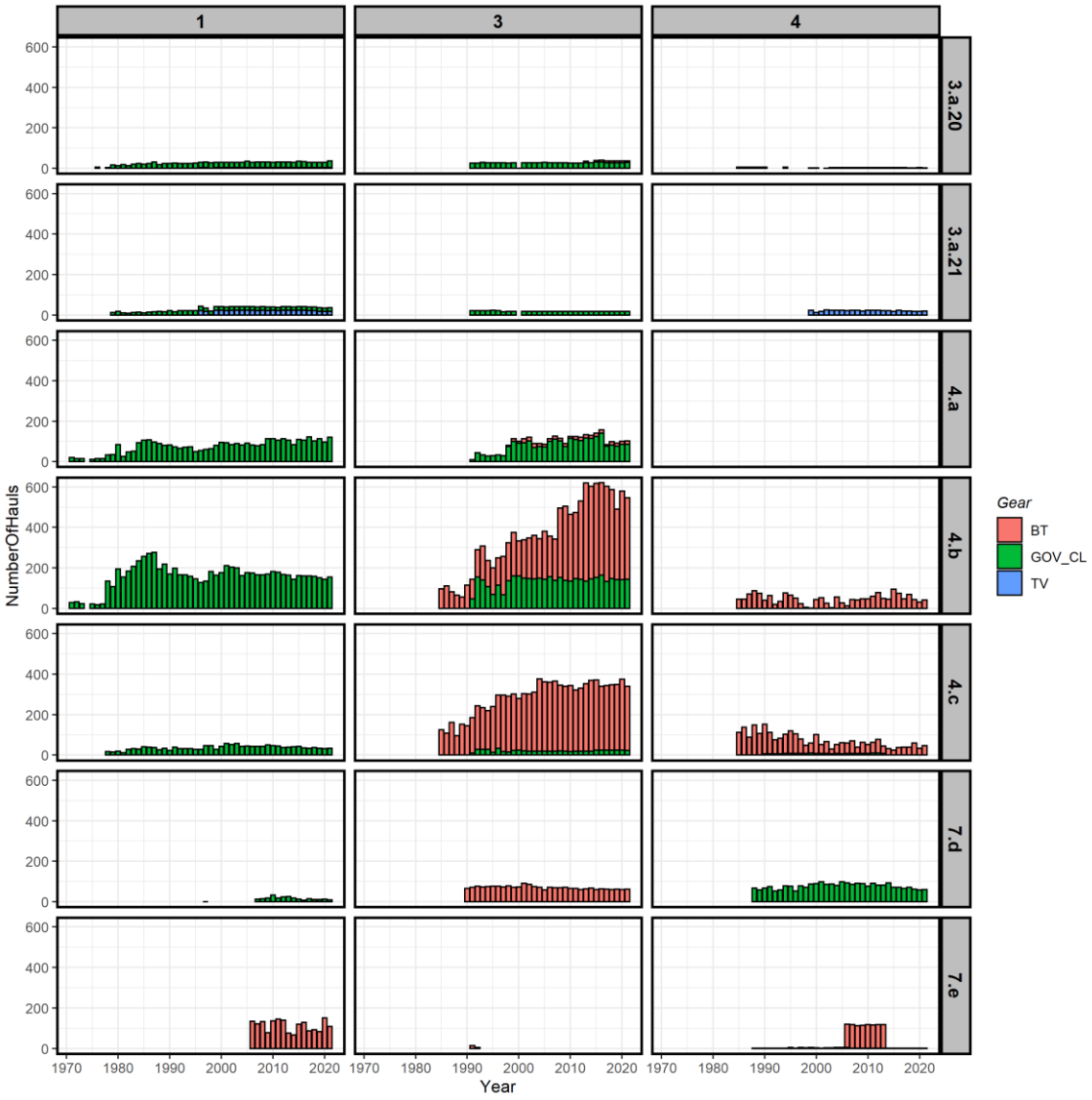


**Figure 2.B4. Haul count by gear from 1971 to 2021 for each ICES Division and quarter.**

### *Length data*

To determine an appropriate cut-off length for exploitable biomass, commercial length data (InterCatch) were compared to length data from these surveys for the years 2014–2021 (which is the time-series available for commercial data; Figure 2.B6). In general, the length frequency distributions are similar for commercial and survey data. In some years, surveys catch more small fish than commercial trips, which is related to the mesh size. On the other hand, commercial data contain more large fish compared to the survey data.

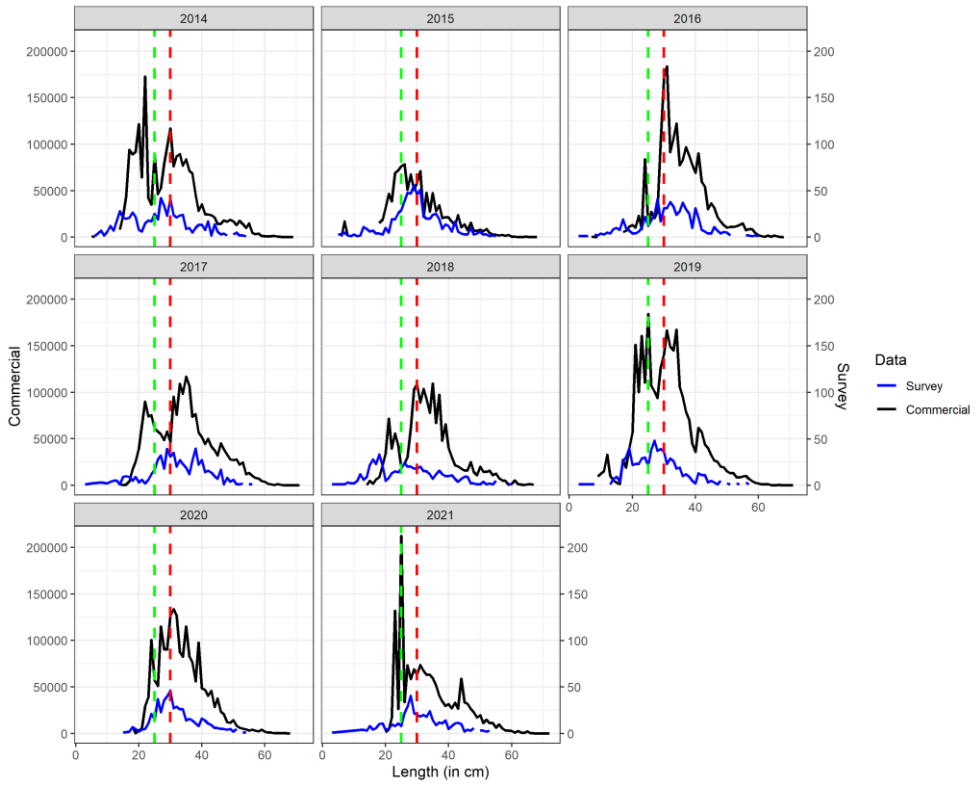


**Figure 2.B5. Length frequency distribution for commercial (black; left *y*-axis) and survey (blue; right *y*-axis) data. The green and red dashed lines represent theoretical cut-off length at 25 and 30 cm respectively.**

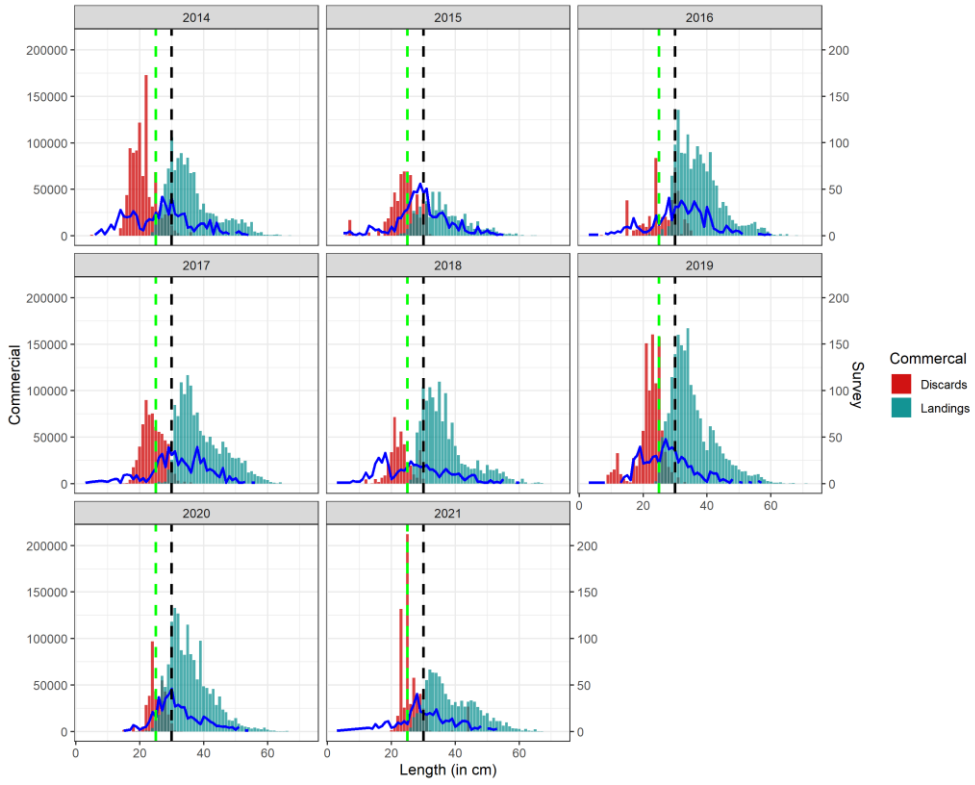


**Figure 2.B6. Length frequency distribution for survey (blue line; right *y*-axis) and commercial data (split in landings (green) and discards (red); left *y*-axis). The green and black dashed lines represent theoretical cut-off length at 25 and 30 cm respectively.**

There is no Minimum Conservation Reference Size (MCRS) imposed by e.g. the EU for brill in the stock area. However, some fleets are bounded by MCRS measures from PO's (Producer Organization) or national authorities. Depending on these measures, commercial landing size varies over the years. Setting the limit for exploitable biomass at 25 cm seems to include most of the brill landed across years.

### *Final dataset*

The final dataset only retained brill equal to or larger than 25 cm to analyse the survey distribution of exploitable biomass across the stock area. From 1971 to 1990 brill is rarely and inconsistently caught in survey hauls (Figure 2.B7). From 1990 onwards, the presence of brill in the hauls is higher and relatively constant through time. These differences are likely caused by the introduction of new gears and increased spatial coverage of the surveys through time.

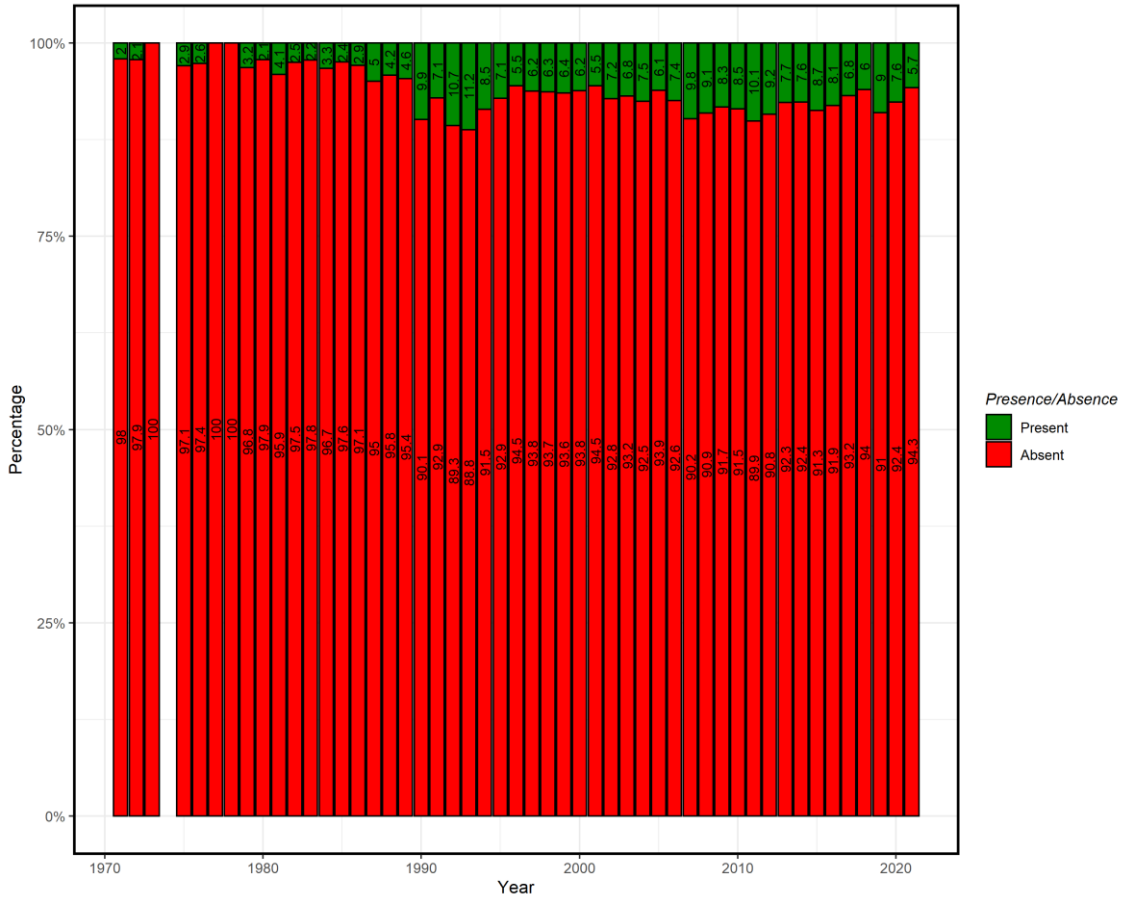


**Figure 2.B7. Percentage of presence/absence of exploitable brill (≥25cm) in survey hauls from 1971 to 2021.**

Catchability seems to differ largely between gears. BT and GOV_CL caught brill with similar frequencies, with an average presence of 8.04 ± 3.05% and 4.62 ± 1.97% in the hauls respectively, while for the TV gear, brill was caught in 39.26 ± 12.84% of the hauls (Figure 2.B8). Although this could be caused by the distribution of gears in areas, as TV gear is only used in Division 3.a, even when TV gear was not used in survey hauls (before 1996), the proportion of brill caught is relatively high in Division 3.a.21 compared to other divisions/areas (Figure 2.B9).

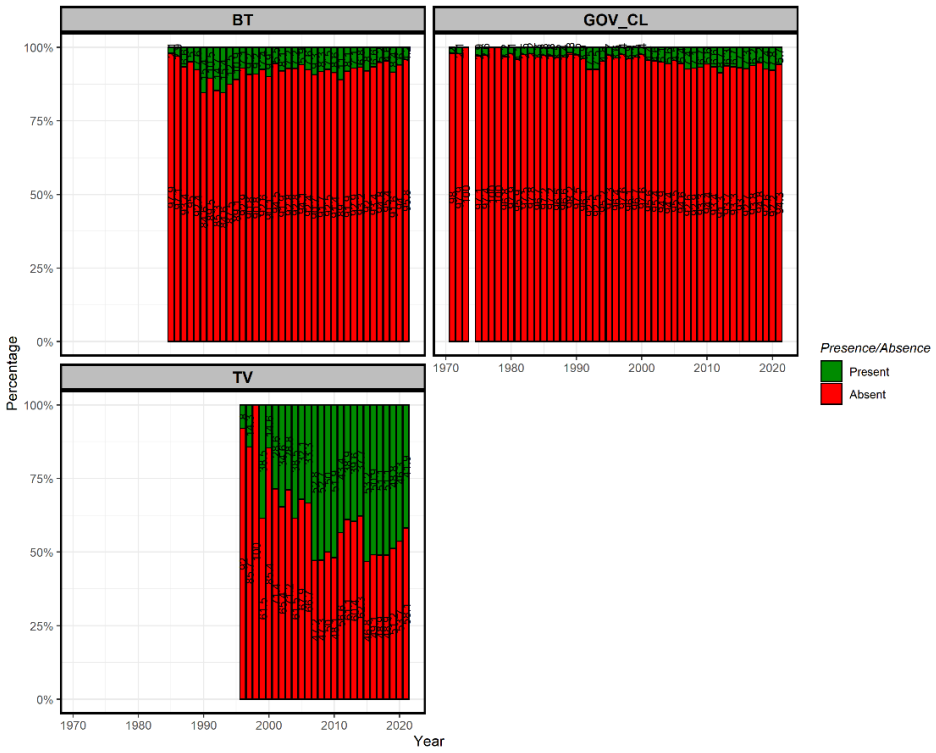


**Figure 2.B8. Percentage of presence/absence of exploitable brill (≥25cm) in survey hauls from 1971 to 2021 by gear.**

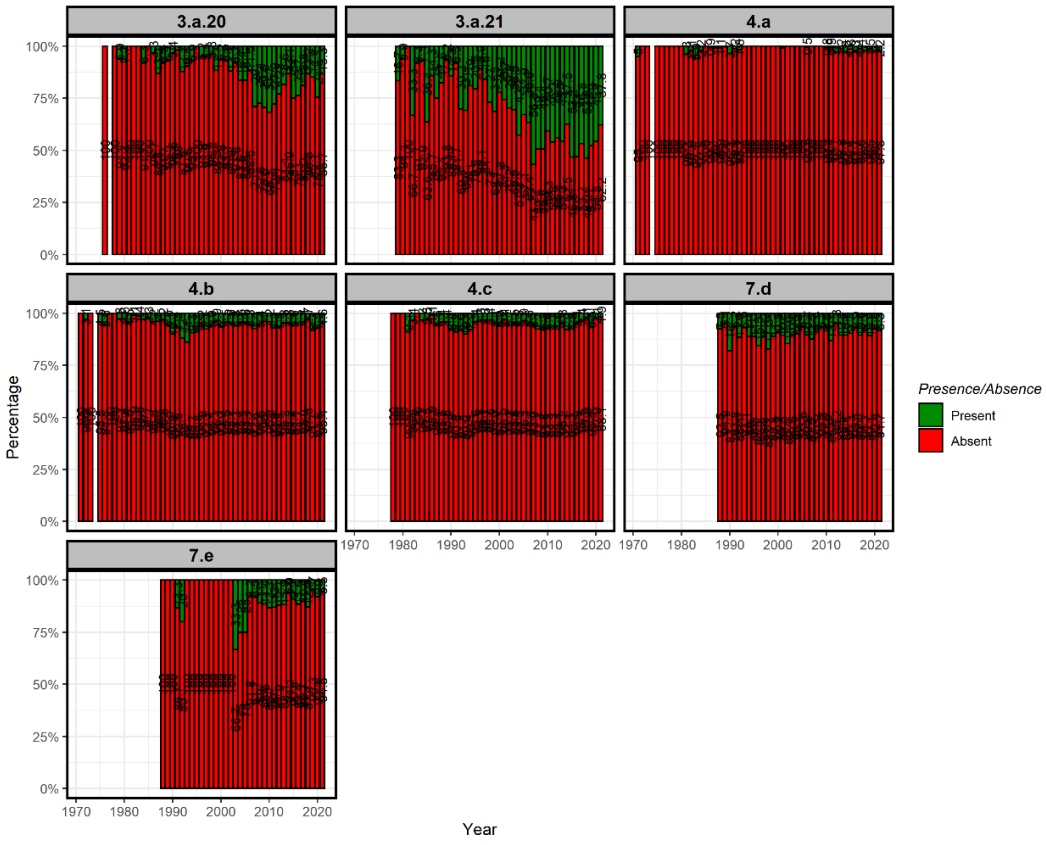


**Figure 2.B9. Percentage of presence/absence of exploitable brill (≥25cm) in survey hauls from 1971 to 2021 by area.**

The presence of brill in survey hauls over the three quarters was quite similar (Figure 2.B10).

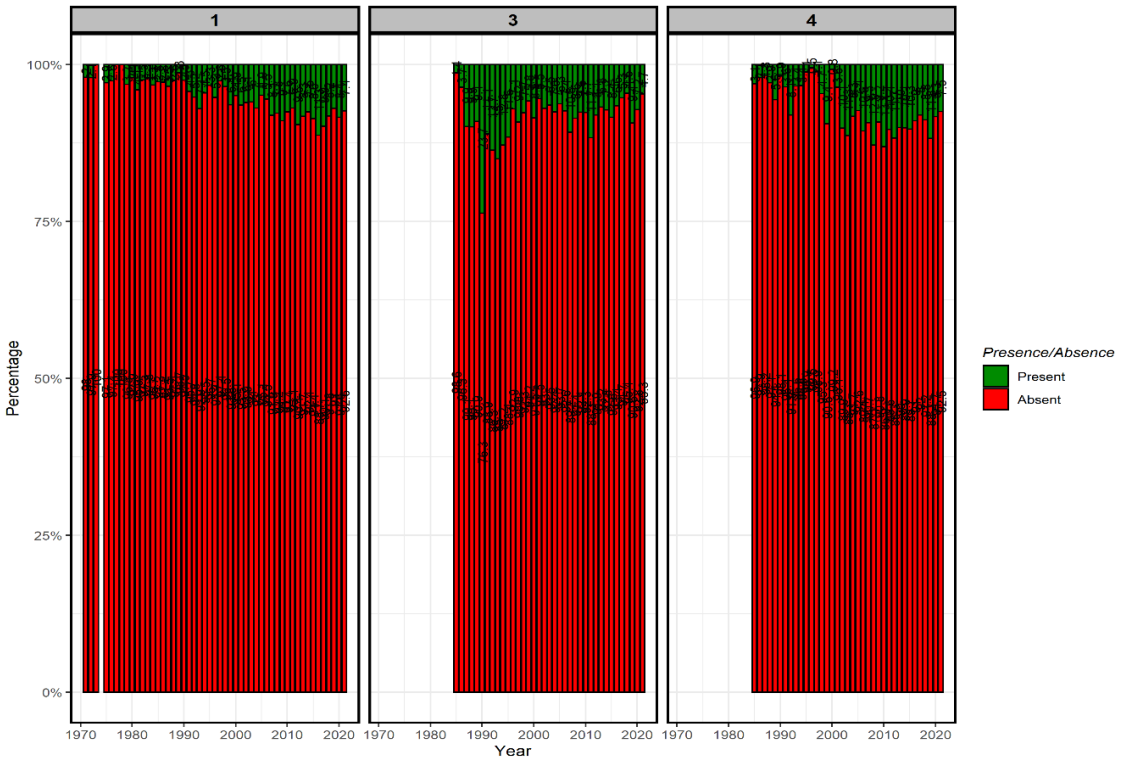


**Figure 2.B10. Percentage of presence/absence of exploitable brill (≥25cm) in survey hauls from 1971 to 2021 by quarter.**

The particularly high percentage of brill presence reported for the TV gear was further explored to verify whether this is caused by a higher biomass in Division 3.a or due to differences in gear catchability. Figure 2.B11 shows comparable higher presence/absence in quarter 1 for both GOV_CL and TV gears. The mean CPUE (of the positive observations) in Division 3.a.20–21 are also similar between gears (GOV_CL and TV), with the exceptions of some years, where the mean CPUE appears to be almost double for the TV gear compared to the GOV_CL gear (Figure 2.B12). Especially in 3.a.21, a gradual increase in CPUE can be observed toward the most recent years. Figure 2.B12 also shows that the BT gear is more efficient at catching brill compared to the GOV_CL gear.

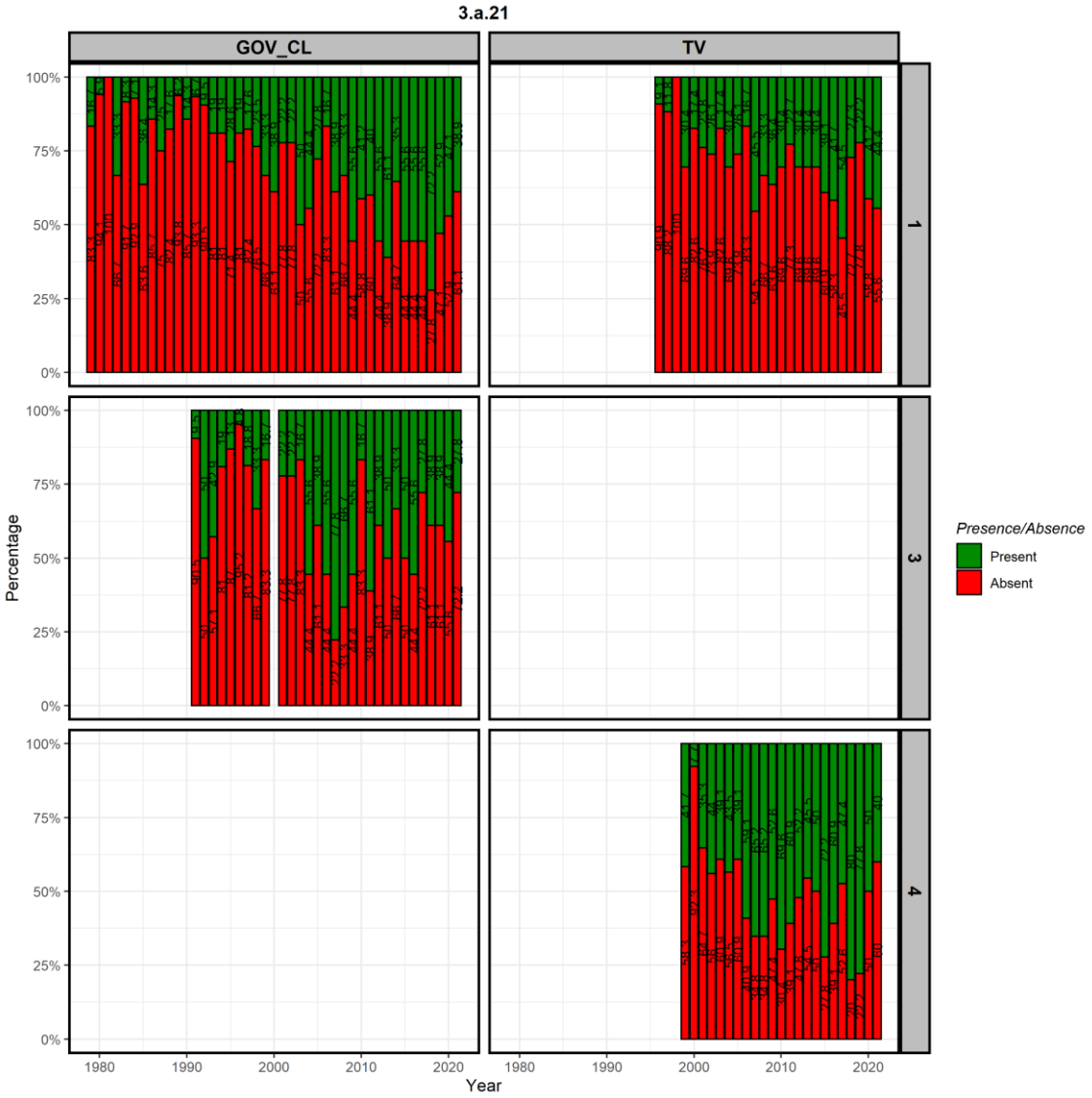


**Figure 2.B11. Percentage of presence/absence of exploitable brill (≥25cm) in survey hauls from 1971 to 2021 by gear and quarter for Division 3.a.21 (Kattegat).**

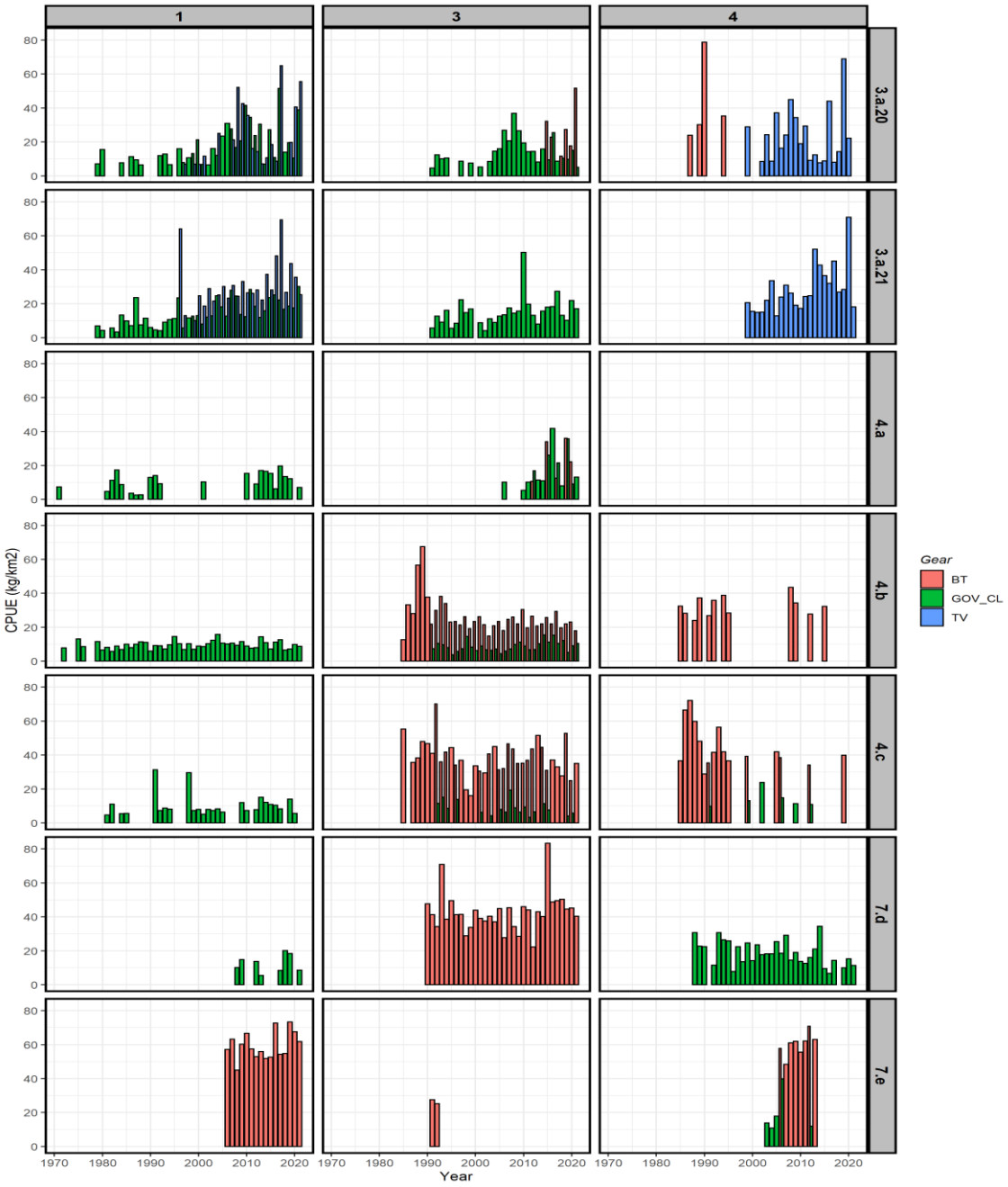


**Figure 2.B12. Positive observations for exploitable brill biomass (≥25cm) in mean CPUE (kg/km2) for survey hauls from 1971 to 2021 by gear, quarter and area.**

The survey time-series shows very little to no coverage for the stock area until the end of the 70s. Relevant brill catches in survey hauls only start to occur from the late 80s to early 90s (Figure 2.B13) when survey effort increases significantly (Figure 2.B2). Brill catches have a patchy distribution which varies from year-to-year (Figure 2.B13, Figure 2.B14, Figure 2.B15 and Figure 2.B16). Biomass (shown as CPUE in kg/km²) is concentrated in the southern North Sea, but rectangles with high catches per unit of effort (30 kg/km²) occur in divisions 3.a21 and 7.d and 7.e.

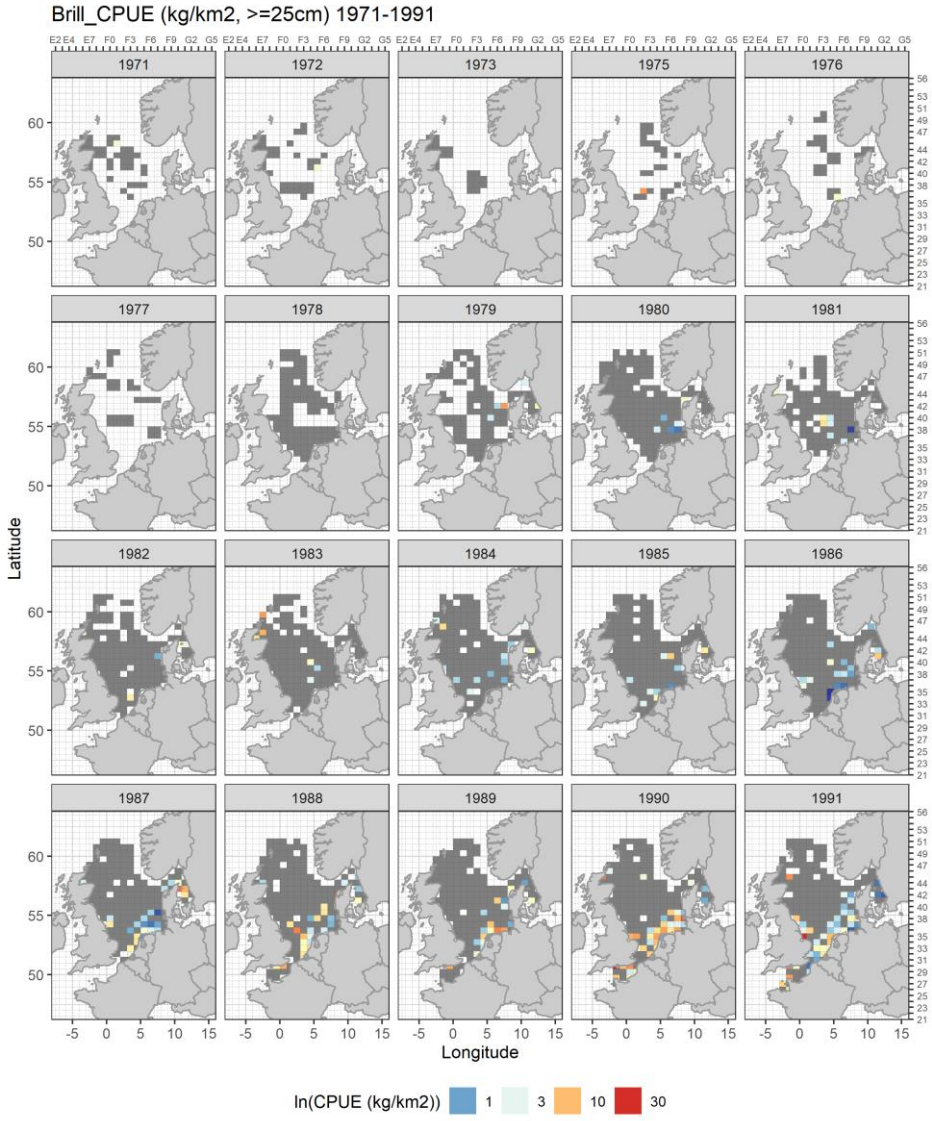


**Figure 2.B13. Total exploitable brill (≥25cm) survey CPUE (kg/km²) per year in the stock area from 1971 to 1991.**

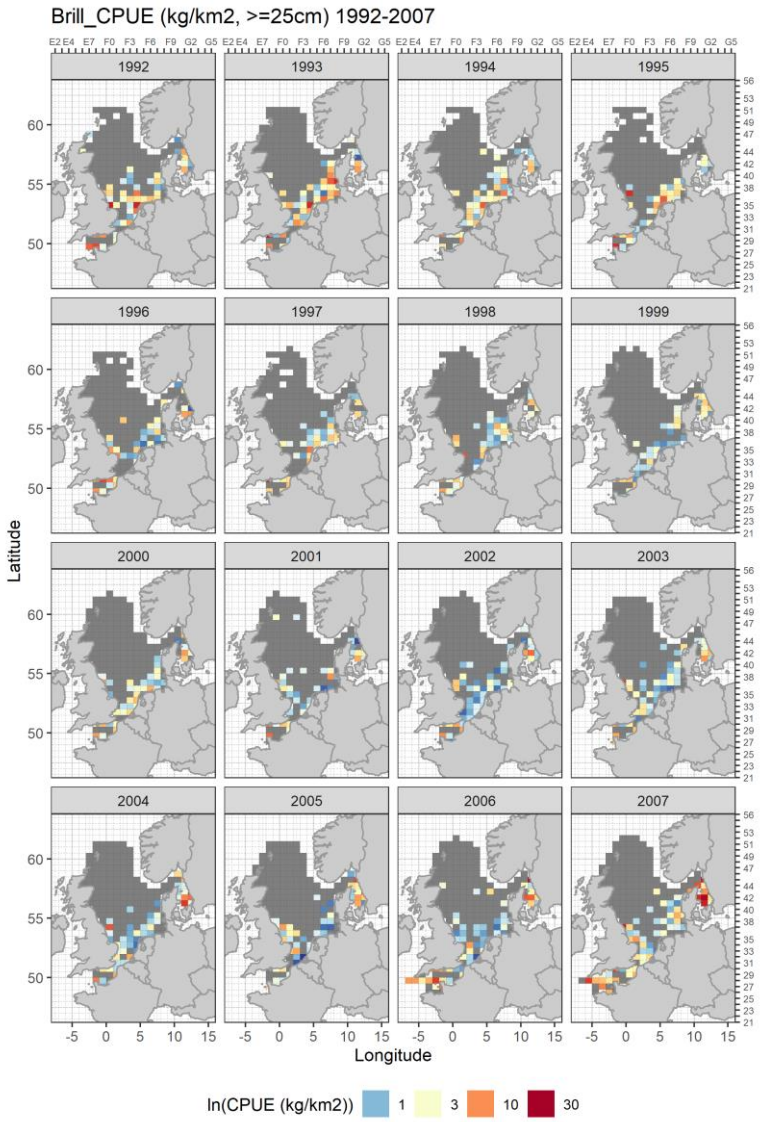


**Figure 2.B14. Total exploitable brill (≥25cm) survey CPUE (kg/km²) per year in the stock area from 1992 to 2007.**

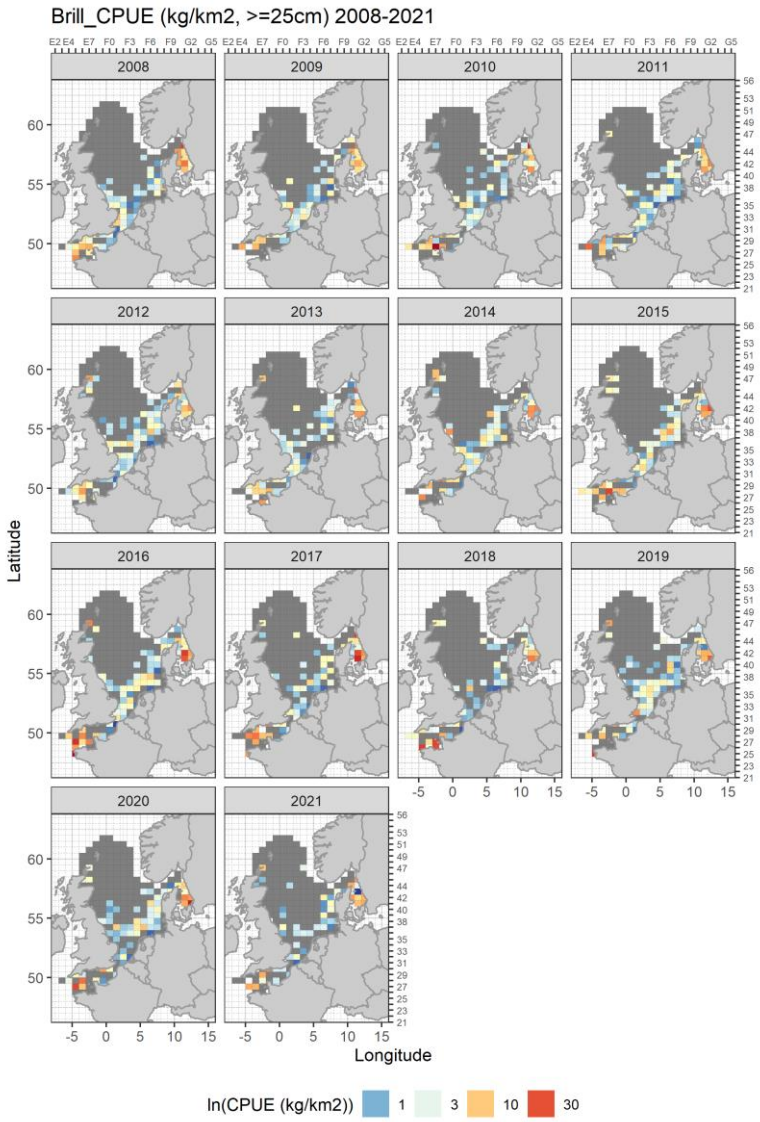


**Figure 2.B15. Total exploitable brill (≥25cm) survey CPUE (kg/km²) per year in the stock area from 2008 to 2021.**

Total catches per unit of effort for the whole time-series (1971–2021) show that surveys cover the entire stock area in quarter 1 and all but the western English Channel (7.e) in quarter 3. Surveys in quarter 4 cover mainly the English Channel, Skagerrak and Kattegat (Figure 2.B16).

The coverage of the stock area by quarter varies over the years (Annex B1). From 1971 to 1984, only quarter 1 surveys were done, covering the North Sea, Skagerrak and Kattegat from 1982 onwards. From 1988, the eastern English Channel (7.d) is sampled in quarter 4. From 2006 onwards, the western English Channel is surveyed in the first and fourth quarter. The coverage of the survey in the fourth quarter is limited and sampling stops in that quarter in 2014. Although surveys in quarter 3 started from 1985, coverage of the stock area was restricted to the southeastern North Sea. It was only in 1992 that the whole stock area was covered with the exception of the western English Channel.

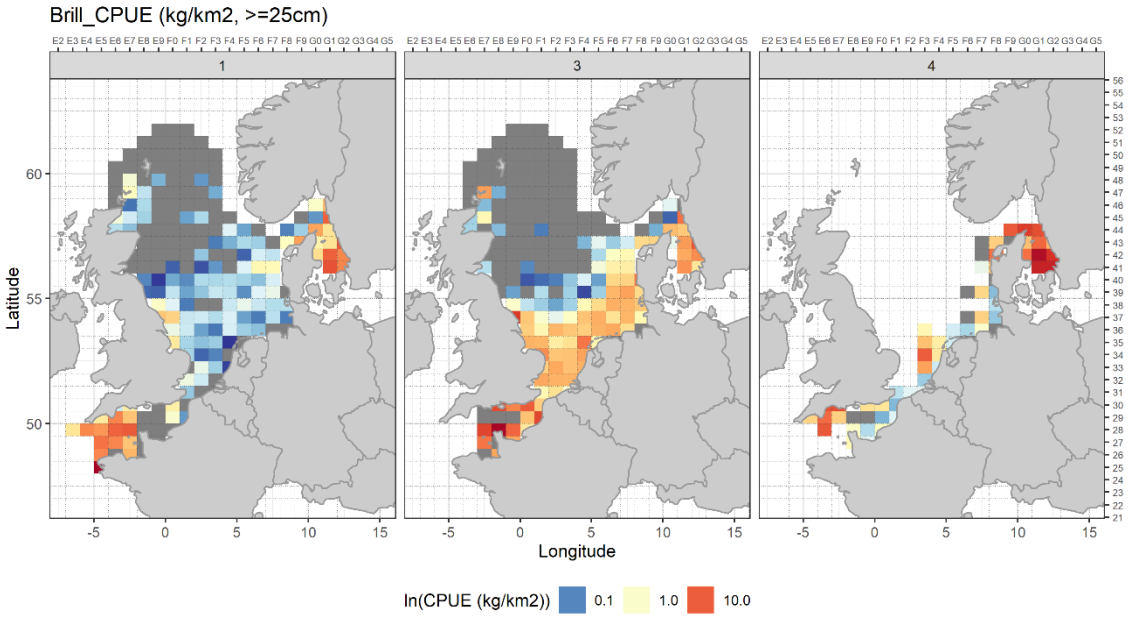


**Figure 2.B16. Total exploitable brill (≥25cm) survey CPUE (kg/km²) per quarter in the stock area from 1971 to 2021.**

### *Data exploration conclusions*

- Brill equal to or larger than 25 cm was retained in the dataset to allow estimating exploitable biomass.
- Considerable variation is present in the dataset regarding coverage in area, gear, quarter and year and their interactions.
- From 1985 onwards, approximately 800 hauls are sampled by 2 gears.
- Presence/absence proportions appeared stable from 1990 onwards.
- From 1988, most of the stock area was covered by the dataset, with the exception of 7.e.
- Maximum stock area coverage by quarter was attained in 1992, with the exception of 7.e.
- The TV gear was present in the dataset from 1996 onwards, but covered only quarter 1. From 1999 onwards, it covers both quarter 1 and 4.

→ *Based on these observations, the dataset was filtered to retain data from 1999 onwards to develop a survey biomass index.*

→ *However, in order to provide information of the stock's evolution before 1999, data from the 1st semester of years between **1983 to 1998** were used to develop an "historical" biomass index.*

- In the further analyses, different variables should be considered. year, quarter, gear, ship and area.
- The lack of data in the western English Channel (7.e) between 1999 and 2005 should also be considered.

## 3. Modelling survey indices

Based on the data exploration conclusions, an exploitable biomass index was made covering the entire stock area and the period 1999–2021 in which gear and spatio-temporal variation was minimized (see §3.1). Another exploitable biomass index was made using data from 1983–1998 covering only Area 4 and Division 3.a (see §3.2).

***Model framework for index 1999–2021***

Two model configurations were defined using general additive models (GAM) to account for the spatial-temporal (year, quarter and space) variation in data availability, different gears used and their catchability. In both approaches the data predictions were made on a biannual (semester) basis. As listed before, the data were also trimmed to exclude data before 1999 and brill smaller than 25 cm.

***One model per semester (split data)***

Data

For this approach, the data were split into two semesters, with the first one including data coming from the first quarter (Semester 1) and the second one including data from the third and fourth quarter (Semester 2) to build two individual models (1.a and 1.b).

Model framework

This model configuration included a fixed spatial effect (2 dimensional smoother), a temporal trend (1 dimensional smoother), spatio-temporal effect (3 dimensional smoother), depth effect (1 dimensional smoother), gear fixed effect, ship random effect and a linear offset based on the log of the swept-area. Finally, the observational error was assumed to follow a Tweedie distribution (Figure 2.B17 and Figure 2.B18).

```
model1.a <- gam(bio.adult ~ s(lon, lat, bs=c('ds'), k=256, m=c(1,0.5)) +     # fixed spatial effect (2 dimensional smoother)
                as.character(Year) +                                          # temporal trend (1 dimensional smoother)
                ti(ctime, lon, lat, d=c(1,2), bs=c('ds','ds'), k=c(10,40), m=list(c(1,0), c(1,0.5))) +  # spatiotemporal effect (3 dimensional smoother)
                s(Depth, bs='ds', k=5, m=c(1,0)) +   # depth effect (1 dimensional smoother)
                 Gear +                               # fixed gear effect REMOVED FOR THIS QUARTER, ONLY ONE GEAR GOV_CL
                s(Ship, bs = "re") +                 # random ship effect
                offset(log(SweptArea)),              # linear offset
                family = tw(),                       # observation error assumed to follow a Tweedie distribution
                data = brill_data99[brill_data99$Quarter == 1,])
```

**Figure 2.B17. Model 1.a (Semester 1 = Quarter 1).**

```
model1.b <- gam(bio.adult ~ s(lon, lat, bs=c('ds'), k=256, m=c(1,0.5)) +     # fixed spatial effect (2 dimensional smoother)
                as.character(Year) +                                          # temporal trend (1 dimensional smoother)
                ti(ctime, lon, lat, d=c(1,2), bs=c('ds','ds'), k=c(10,40), m=list(c(1,0), c(1,0.5))) +  # spatiotemporal effect (3 dimensional smoother)
                s(Depth, bs='ds', k=5, m=c(1,0)) +   # depth effect (1 dimensional smoother)
                Gear +                               # fixed gear effect
                s(Ship, bs = "re") +                 # random ship effect
                offset(log(SweptArea)),              # linear offset
               family = tw(),                        # observation error assumed to follow a Tweedie distribution
               data = brill_data99[brill_data99$Quarter %in% c(3,4),])
```

**Figure 2.B18. Model 1.b (Semester 2 = Quarter 3+4).**

Model outputs and validation

For both the first and second semester, the predicted biomass and standard errors (se) values at the southwestern margin of the stock distribution in the Western English Channel (7.e) showed substantially larger values. This was observed for a few ICES statistical rectangles during the years for which data are not available in that region (1999–2005). It was therefore concluded that this likely represents artificial biomass and these ICES rectangles (below latitude 48.75° N) were removed from the prediction grid.

Both models show an almost identical trend, with relatively larger uncertainty (CV) between 1999–2004, however the index for semester one reported a consistently larger uncertainty.

*Model 1.a (Semester 1)*

Model 1.a explained 57.6% of the deviance and reported an AIC of 16855.88. The QQ plot shows that the residuals follow the Tweedie distribution closely (Figure 2.B19). The uncertainty around the estimates (CV) remained almost constantly very high throughout the time-series (147–172%, Figure 2.B20). The predicted survey index values for the first semester range from 2 240 931 to 8 071 851 (Figure 2.B21).

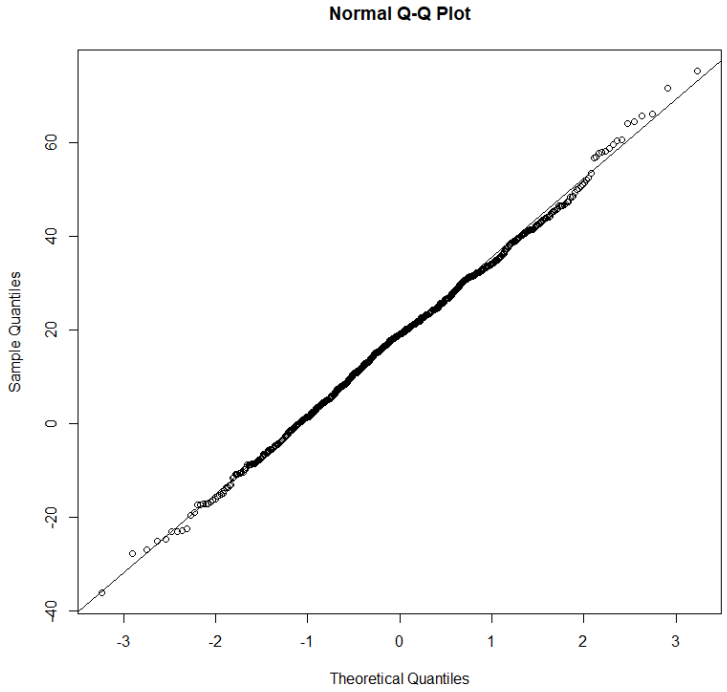


```
Family: Tweedie(p=1.178)
Link function: log

Formula:
bio.adult ~ s(lon, lat, bs = c("ds"), k = 256, m = c(1, 0.5)) +
    as.character(Year) + ti(ctime, lon, lat, d = c(1, 2), bs =
    "ds"), k = c(10, 40), m = list(c(1, 0), c(1, 0.5))) + s(Dep
    bs = "ds", k = 5, m = c(1, 0)) + Gear + s(Ship, bs = "re")
    offset(log(SweptArea))

Parametric coefficients:
                      Estimate Std. Error t value Pr(>|t|)
(Intercept)             5.5980     2.1630   2.588  0.00967 **
as.character(Year)2000  0.2009     0.4060   0.495  0.62066
as.character(Year)2001  0.4693     0.4782   0.981  0.32649
as.character(Year)2002  0.5887     0.5100   1.154  0.24839
as.character(Year)2003  0.4215     0.5088   0.828  0.40746
as.character(Year)2004  0.5772     0.4912   1.175  0.23998
as.character(Year)2005  0.2241     0.4890   0.458  0.64679
as.character(Year)2006  0.2419     0.4772   0.507  0.61218
as.character(Year)2007  0.7259     0.4691   1.547  0.12179
as.character(Year)2008  0.5682     0.4759   1.194  0.23255
as.character(Year)2009  0.6116     0.4700   1.301  0.19319
as.character(Year)2010  0.5523     0.4590   1.203  0.22893
as.character(Year)2011  0.4862     0.4675   1.040  0.29829
as.character(Year)2012  1.1438     0.4567   2.505  0.01227 *
as.character(Year)2013  1.2005     0.4554   2.636  0.00840 **
as.character(Year)2014  0.9668     0.4628   2.089  0.03674 *
as.character(Year)2015  1.0565     0.4510   2.342  0.01919 *
as.character(Year)2016  1.1405     0.4555   2.504  0.01229 *
as.character(Year)2017  1.2139     0.4614   2.631  0.00853 **
as.character(Year)2018  0.7510     0.4671   1.608  0.10792
as.character(Year)2019  0.7476     0.4712   1.587  0.11264
as.character(Year)2020  0.7512     0.4619   1.626  0.10392
as.character(Year)2021  0.7392     0.4796   1.541  0.12331
GearGOV_CL             -0.9631     2.5443  -0.379  0.70505
GearTV                 -1.0403     2.5581  -0.407  0.68426
---
Signif. codes:  0 ‘***’ 0.001 ‘**’ 0.01 ‘*’ 0.05 ‘.’ 0.1 ‘ ’ 1

Approximate significance of smooth terms:
                   edf Ref.df      F  p-value
s(lon,lat)     125.642    255 22.242  < 2e-16 ***
ti(ctime,lon,lat)  39.160    351  0.252 4.92e-05 ***
s(Depth)         3.308      4 21.723  < 2e-16 ***
s(Ship)          5.933     12  1.310  0.00288 **
---
Signif. codes:  0 ‘***’ 0.001 ‘**’ 0.01 ‘*’ 0.05 ‘.’ 0.1 ‘ ’ 1

R-sq.(adj) =  0.309   Deviance explained = 57.6%
-REML = 8518.6  Scale est. = 363.92    n = 10801
```

**Figure 2.B19. QQplot and summary for Model 1.a.**


**Figure 2.B20. Coefficient of variation (CV) by year for predictions obtained using Model 1.a**

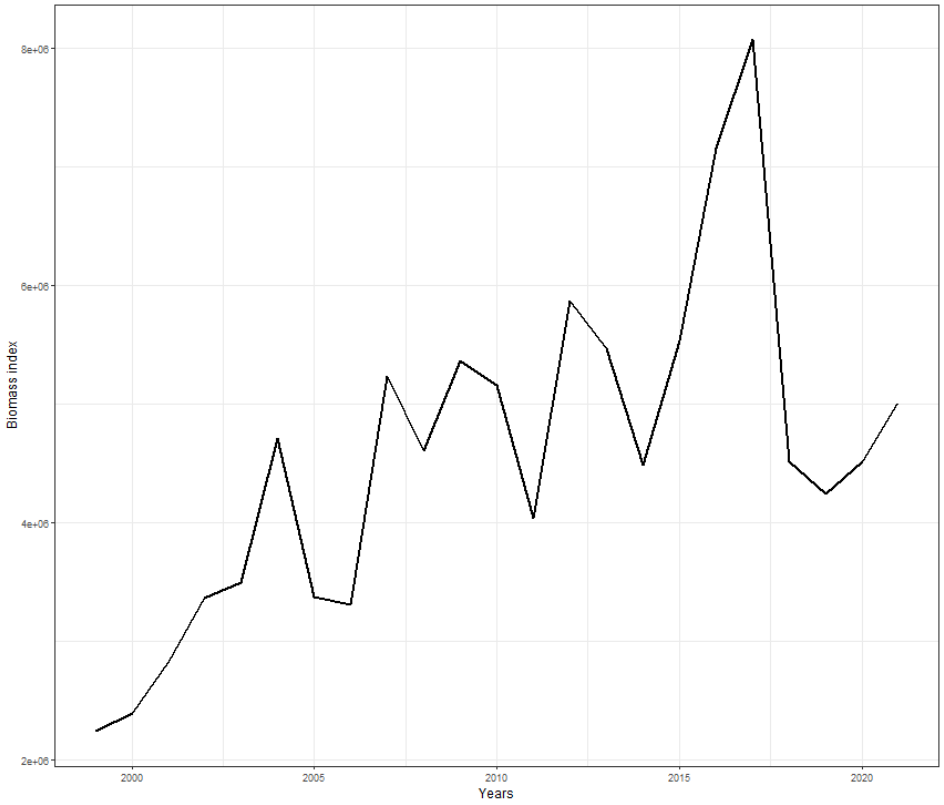


**Figure 2.B21. Survey index trend for the 1st semester obtained using Model 1.a**

*Model 1.b (Semester 2)*

Model 1.b explained 49.9% of the deviance and reported an AIC of 44217.91. The QQ plot shows that the residuals slightly deviate with respect to the Tweedie distribution (Figure 2.B22). The uncertainty around the estimates (CV) is smaller compared to the one obtained with model 1.a. The uncertainty is relatively larger at the beginning of the time-series (1999–2004), compared to the more recent years (2005 onwards, Figure 2.B23). The predicted survey index values for the second semester range from 1 527 890 to 3 776 003. (Figure 2.B24).

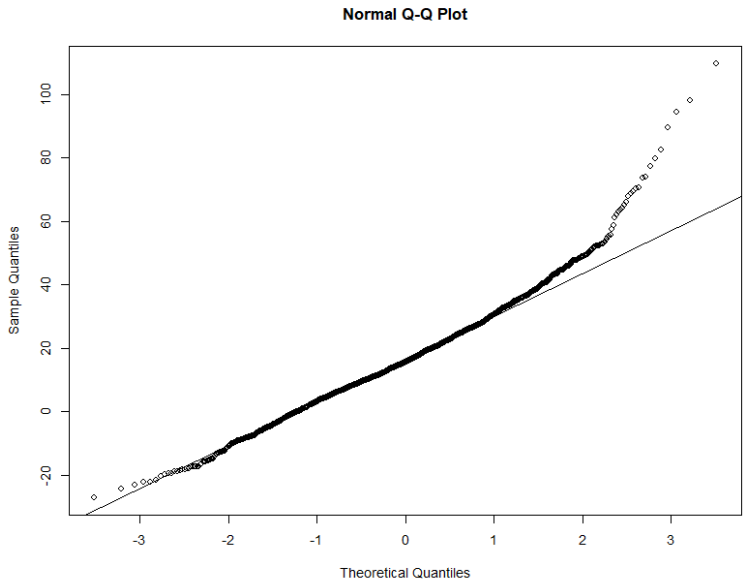


```
Parametric coefficients:
                     Estimate Std. Error t value Pr(>|t|)
(Intercept)           5.48748    0.33479  16.391  < 2e-16 ***
as.character(Year)2000  0.44498    0.18992   2.343 0.019136 *
as.character(Year)2001  0.09009    0.23119   0.390 0.696785
as.character(Year)2002  0.26749    0.24723   1.082 0.279280
as.character(Year)2003  0.26827    0.24876   1.078 0.280855
as.character(Year)2004  0.29036    0.24215   1.199 0.230515
as.character(Year)2005  0.03868    0.24541   0.158 0.874746
as.character(Year)2006  0.23431    0.24208   0.968 0.333088
as.character(Year)2007  0.70342    0.23787   2.957 0.003107 **
as.character(Year)2008  0.68576    0.24039   2.853 0.004338 **
as.character(Year)2009  0.45026    0.24182   1.862 0.062625 .
as.character(Year)2010  0.70528    0.23909   2.950 0.003183 **
as.character(Year)2011  0.96434    0.23493   4.105 4.06e-05 ***
as.character(Year)2012  0.82094    0.23799   3.449 0.000562 ***
as.character(Year)2013  0.67789    0.24047   2.819 0.004821 **
as.character(Year)2014  0.92414    0.23771   3.888 0.000101 ***
as.character(Year)2015  0.92924    0.23824   3.900 9.62e-05 ***
as.character(Year)2016  0.65189    0.24489   2.662 0.007772 **
as.character(Year)2017  0.39888    0.25317   1.576 0.115143
as.character(Year)2018  0.16004    0.25776   0.621 0.534685
as.character(Year)2019  0.67489    0.24979   2.702 0.006900 **
as.character(Year)2020  0.70278    0.25164   2.793 0.005230 **
as.character(Year)2021 -0.10169    0.27940  -0.364 0.715903
GearGOV_CL            -1.42426    0.23435  -6.077 1.24e-09 ***
GearTV                 0.30811    0.86448   0.356 0.721539
---
Signif. codes:  0 '***' 0.001 '**' 0.01 '*' 0.05 '.' 0.1 ' ' 1

Approximate significance of smooth terms:
                   edf Ref.df      F  p-value
s(lon,lat)       156.360    255 32.744  < 2e-16 ***
ti(ctime,lon,lat)  79.672    351  1.444 1.97e-05 ***
s(Depth)            3.377      4 22.627  < 2e-16 ***
s(Ship)            22.330     28  4.057  < 2e-16 ***
---
Signif. codes:  0 '***' 0.001 '**' 0.01 '*' 0.05 '.' 0.1 ' ' 1

R-sq.(adj) =  0.302   Deviance explained = 49.9%
-REML =  22341  Scale est. = 294.84    n = 29584
```

**Figure 2.B22. QQplot and summary for Model 1.b.**

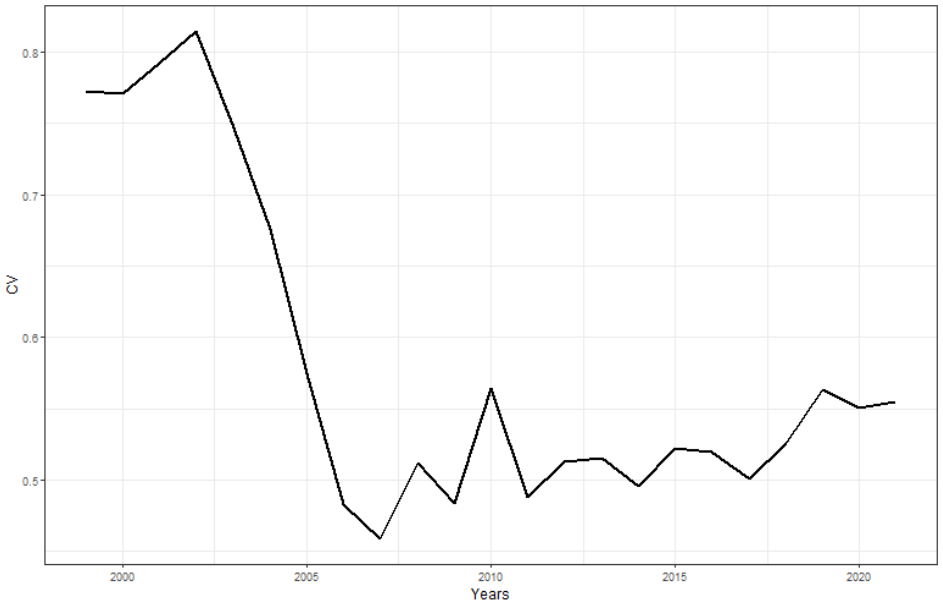


**Figure 2.B23. Coefficient of variation (CV) by year (second semester) for predictions obtained using Model 1.b**

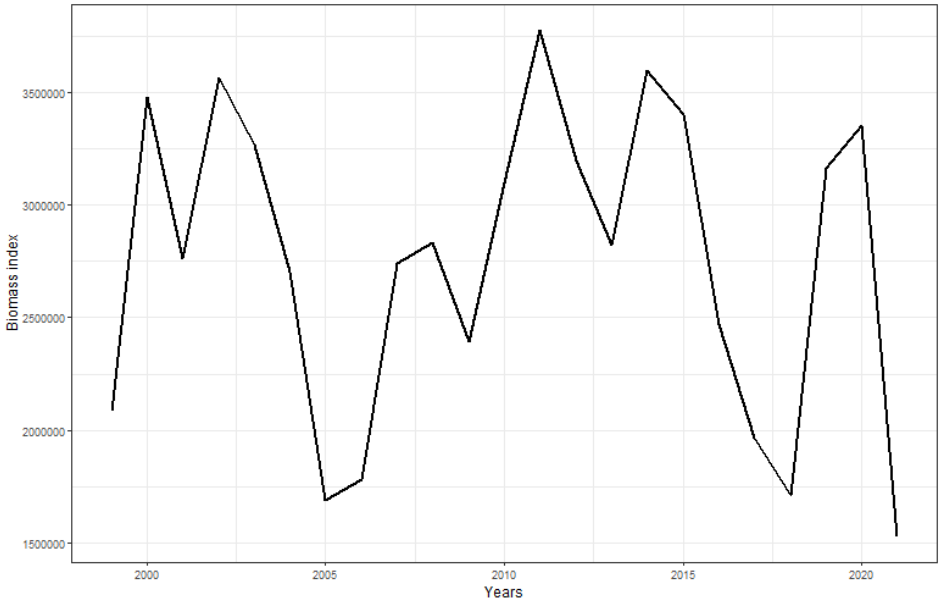


**Figure 2.B24. Survey index trend for the second semester obtained using Model 1.b**

Conclusion on one model per semester (split data)

No similar trend can be observed when comparing the survey index obtained using model 1.a and 1.b. This is likely to be caused by the high CV registered in both model runs (mainly semester 1), which likely distorted the shape of the curve throughout the time-series. This is probably even more the case at the beginning of the time-series were both indices report highest uncertainty. The limited amount and absence of data (gear overlap) in the Western English Channel between 1999–2005 likely causes this strong uncertainty around the estimated values. It is therefore impossible to determine which trend is the "correct" one. A model framework using all data (both semesters) could provide more information to the model and might help to reduce this uncertainty. The following section tries this approach and uses one model for 2 semesters.

***One model for two semesters (all quarters included)***

Data

For this approach, the whole dataset served as input to the model. Instead of building individual models per semester, the model included semester as a parameter to allow biannual predictions. Two different models were tested (2.a and 2.b, see below). After performing preliminary runs with relatively few knots, strange residual patterns were observed for both models. To address this issue, the spatial knots were doubled. No such patterns remained in the models presented below.

Model framework

This model configuration is similar to the previous one (§3.1.1.2), with the exception of the inclusion of the estimation of parameters for each semester. More specifically, the models include an interaction between year and semester (1 dimensional smoother), spatio-temporal effect (3 dimensional smoother), fixed spatial effect by semester (2 dimensional smoother), depth fixed effect by semester (1 dimensional smoother), gear fixed effect, ship random effect and a linear offset based on the log of the swept-area. Finally, the observational error was assumed to follow a Tweedie distribution. The difference between model 2.a (Figure 2.B25) and 2.b (Figure 2.B26) lies in the exclusion and inclusion respectively of a semester specific parameter estimation for the spatio-temporal effect.

```
model2.a <- gam(bio.adult ~ #s(lon, lat, bs=c('ds'), k=128, m=c(1,0.5)) +     # fixed spatial effect (2 dimensional smoother)
                as.character(Year)*as.character(semester) +                   # temporal trend (1 dimensional smoother)
                ti(ctime, lon, lat, d=c(1,2), bs=c('ds','ds'), k=c(10,40), m=list(c(1,0), c(1,0.5))) +  # spatiotemporal effect (3 dimensional smoother)
                s(lon, lat, bs=c('ds'), k=256, m=c(1,0.5), by = as.factor(semester)) +
                s(Depth, bs='ds', k=5, m=c(1,0), by = as.factor(semester)) +   # depth effect (1 dimensional smoother)
                Gear +                          # fixed gear effect
                s(Ship, bs = "re") +            # random ship effect
                offset(log(SweptArea)),         # linear offset
                family = tw(),                  # observation error assumed to follow a Tweedie distribution
                data = brill_data99)
```

**Figure 2.B25. Model 2.a**

```
model2.b <- gam(bio.adult ~ #s(lon, lat, bs=c('ds'), k=128, m=c(1,0.5)) +     # fixed spatial effect (2 dimensional smoother)
                as.character(Year)*as.character(semester) +                   # temporal trend (1 dimensional smoother)
                ti(ctime, lon, lat, d=c(1,2), bs=c('ds','ds'), k=c(10,40), m=list(c(1,0), c(1,0.5)), by = as.factor(semester)) + # spatiotemporal effect (3
dimensional smoother)
                s(lon, lat, bs=c('ds'), k=256, m=c(1,0.5), by = as.factor(semester)) +
                s(Depth, bs='ds', k=5, m=c(1,0), by = as.factor(semester)) +   # depth effect (1 dimensional smoother)
                Gear +                          # fixed gear effect
                s(Ship, bs = "re") +            # random ship effect
                offset(log(SweptArea)),         # linear offset
                family = tw(),                  # observation error assuemd to follow a Tweedie distribution
                data = brill_data99)
```

**Figure 2.B26. Model 2.b**

Model validation and outputs

As reported for models 1.a and 1.b, models 2.a and 2.b showed larger predicted biomass and standard errors (se) values at the southwestern margin of the stock distribution in the Western English Channel (7.e). This was observed for a few ICES statistical rectangles during the years for which data are not available in that region (1999–2005). It was therefore concluded that this was likely to represent artificial biomass and that these ICES squares (below latitude 48.75°) were removed from the prediction grid.

Both models show an almost identical trend, with a larger uncertainty (CV) for estimations on the second semester (Figure 2.B28 and Figure 2.B31).

*Model 2.a*

Model 2.a explained 52.3% of the deviance and reported an AIC of 61297.28. The QQ plot shows that the residuals slightly deviate with respect to the Tweedie distribution (Figure 2.B27). The uncertainty around the estimates is larger for semester 2 and especially at the beginning of the time-series (Figure 2.B28). Uncertainty for the first semester remains fairly low throughout the time-series. Despite the larger uncertainty reported for semester 2, the obtained survey indices show a consistent trend for both semesters (Figure 2.B29) with values ranging from 4 119 947 and 14 873 887. Differences in direction (increase vs. decrease) between the indices throughout the time-series are likely caused by the uncertainty around each point estimate.

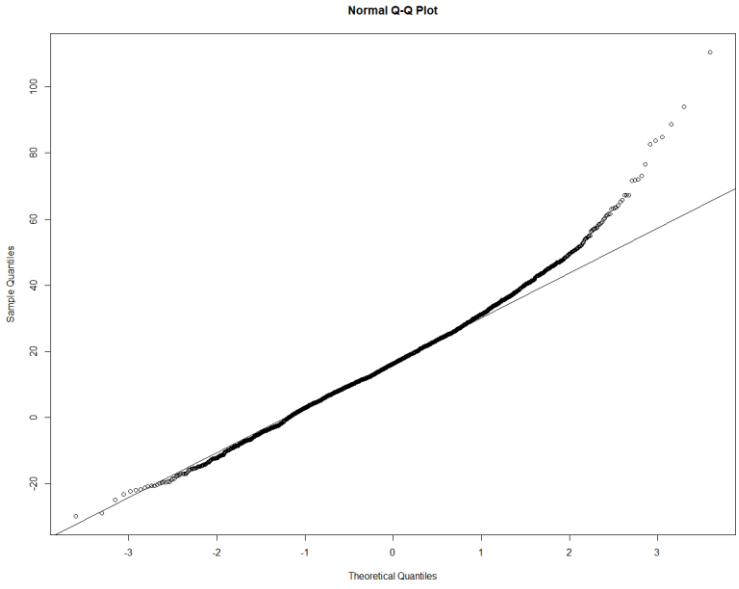


```
Parametric coefficients:
                                                Estimate Std. Error t value Pr(>|t|)
(Intercept)                                      5.87031    0.38862  15.105  < 2e-16 ***
as.character(Year)2000                           0.26357    0.33852   0.779  0.43623
as.character(Year)2001                           0.64212    0.36642   1.752  0.07971 .
as.character(Year)2002                           0.80018    0.38913   2.056  0.03976 *
as.character(Year)2003                           0.60307    0.39165   1.540  0.12362
as.character(Year)2004                           0.62565    0.37975   1.648  0.09945 .
as.character(Year)2005                           0.10728    0.38507   0.279  0.78056
as.character(Year)2006                           0.05557    0.36863   0.151  0.88017
as.character(Year)2007                           0.59197    0.36057   1.642  0.10065
as.character(Year)2008                           0.43221    0.36796   1.175  0.24016
as.character(Year)2009                           0.50539    0.36210   1.396  0.16280
as.character(Year)2010                           0.45646    0.35547   1.284  0.19911
as.character(Year)2011                           0.41473    0.36089   1.149  0.25048
as.character(Year)2012                           0.92378    0.35305   2.617  0.00889 **
as.character(Year)2013                           0.87275    0.35805   2.437  0.01479 *
as.character(Year)2014                           0.68406    0.36455   1.876  0.06060 .
as.character(Year)2015                           0.78414    0.35158   2.230  0.02573 *
as.character(Year)2016                           0.97093    0.34885   2.783  0.00538 **
as.character(Year)2017                           1.05546    0.35012   3.015  0.00257 **
as.character(Year)2018                           0.54036    0.36302   1.489  0.13662
as.character(Year)2019                           0.39646    0.36597   1.083  0.27868
as.character(Year)2020                           0.46927    0.35827   1.310  0.19026
as.character(Year)2021                           0.58464    0.36326   1.609  0.10754
as.character(semester)2                          0.05643    0.38768   0.146  0.88427
GearGOV_CL                                      -1.71204    0.11555 -14.817  < 2e-16 ***
GearTV                                          -1.06542    0.23652  -4.505 6.67e-06 ***
as.character(Year)2000:as.character(semester)2   0.21000    0.37905   0.554  0.57957
as.character(Year)2001:as.character(semester)2  -0.52944    0.39563  -1.338  0.18083
as.character(Year)2002:as.character(semester)2  -0.59969    0.40377  -1.485  0.13749
as.character(Year)2003:as.character(semester)2  -0.49818    0.40210  -1.239  0.21537
as.character(Year)2004:as.character(semester)2  -0.49375    0.38399  -1.286  0.19851
as.character(Year)2005:as.character(semester)2  -0.15182    0.39196  -0.387  0.69852
as.character(Year)2006:as.character(semester)2   0.16779    0.36749   0.457  0.64798
as.character(Year)2007:as.character(semester)2   0.08674    0.35216   0.246  0.80545
as.character(Year)2008:as.character(semester)2   0.11972    0.35963   0.333  0.73922
as.character(Year)2009:as.character(semester)2  -0.28764    0.35785  -0.804  0.42150
as.character(Year)2010:as.character(semester)2   0.04532    0.35207   0.129  0.89757
as.character(Year)2011:as.character(semester)2   0.44580    0.35865   1.243  0.21388
as.character(Year)2012:as.character(semester)2  -0.13980    0.35165  -0.398  0.69096
as.character(Year)2013:as.character(semester)2  -0.26067    0.35915  -0.726  0.46797
as.character(Year)2014:as.character(semester)2   0.12240    0.36521   0.335  0.73752
as.character(Year)2015:as.character(semester)2  -0.03039    0.35210  -0.086  0.93122
as.character(Year)2016:as.character(semester)2  -0.41741    0.34725  -1.202  0.22936
as.character(Year)2017:as.character(semester)2  -0.71126    0.35203  -2.020  0.04334 *
as.character(Year)2018:as.character(semester)2  -0.41756    0.36819  -1.134  0.25677
as.character(Year)2019:as.character(semester)2   0.23930    0.36466   0.656  0.51168
as.character(Year)2020:as.character(semester)2   0.23019    0.35822   0.643  0.52050
as.character(Year)2021:as.character(semester)2  -0.67717    0.36712  -1.845  0.06511 .
---
Signif. codes:  0 '***' 0.001 '**' 0.01 '*' 0.05 '.' 0.1 ' ' 1

Approximate significance of smooth terms:
                                edf Ref.df      F  p-value
ti(ctime,lon,lat)            98.542    351  1.360  < 2e-16 ***
s(lon,lat):as.factor(semester)1 120.992    255 10.966  < 2e-16 ***
s(lon,lat):as.factor(semester)2 154.140    255 13.309  < 2e-16 ***
s(Depth):as.factor(semester)1    3.462      4 24.291  < 2e-16 ***
s(Depth):as.factor(semester)2    3.290      4 17.689  < 2e-16 ***
s(Ship)                         13.224     30  1.402 1.24e-06 ***
---
Signif. codes:  0 '***' 0.001 '**' 0.01 '*' 0.05 '.' 0.1 ' ' 1

R-sq.(adj) =  0.281   Deviance explained = 52.3%
-REML =  30971  Scale est. = 304.84    n = 40385
```

**Figure 2.B27. QQplot and summary for Model 2.a**

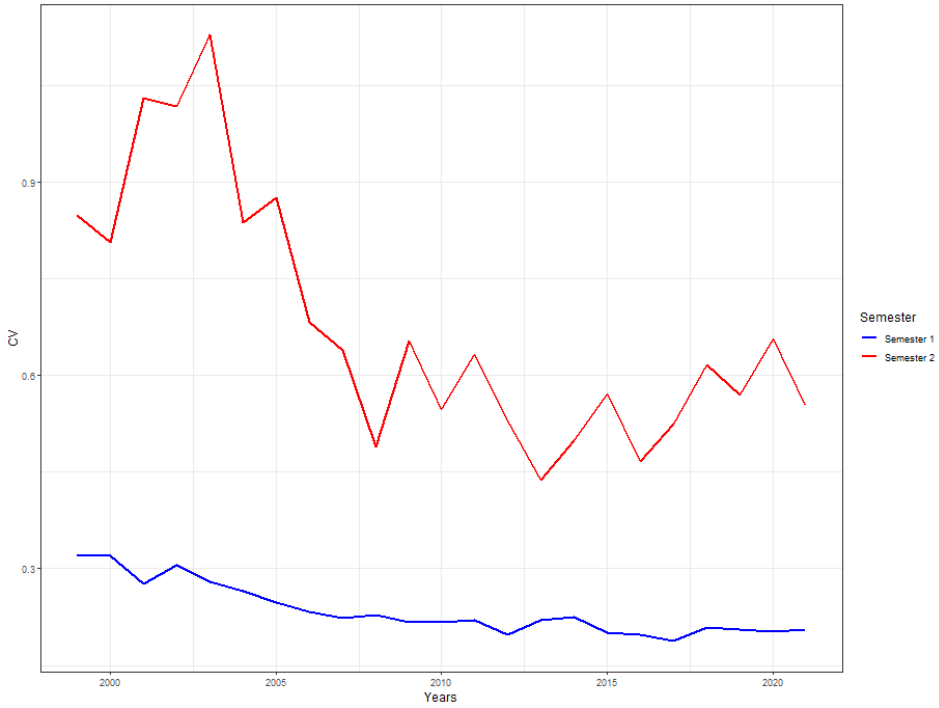


**Figure 2.B28. Coefficient of variation (CV) by year for predictions obtained using Model 2.a**

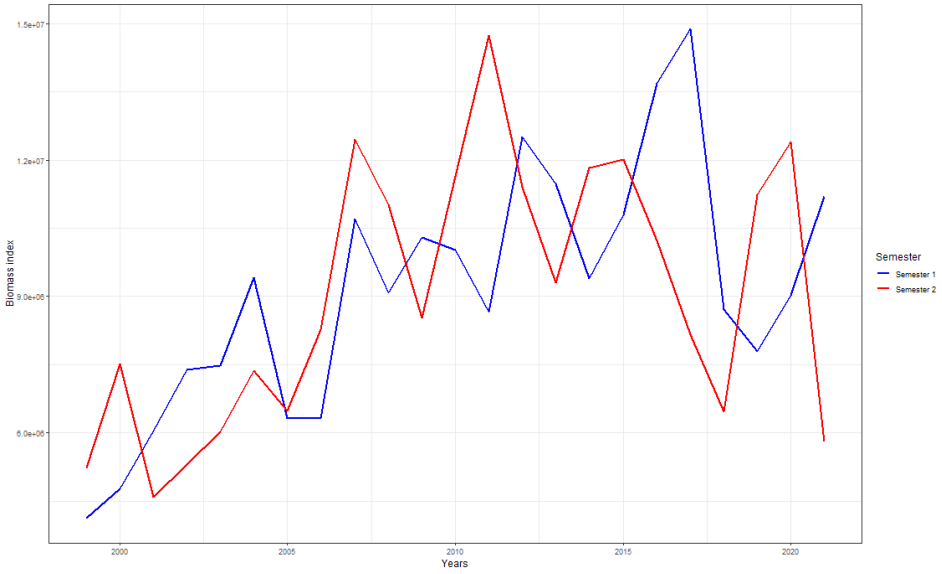


**Figure 2.B29. Survey index trend for both semesters obtained using Model 2.a**

*Model 2.b*

Model 2.b shows outputs almost identical with model 2.a, explaining 52.4% of the deviance and has an AIC of 61 335.37. In the same way, the QQ plot shows that the residuals slightly deviate with respect to the Tweedie distribution (Figure 2.B30). In both semesters, the uncertainty around the estimates (CV) is larger at the beginning of the time-series (1999–2004) and then remains relatively low (Figure 2.B31). This is likely to be explained by the relatively lower amount of data available for these years and in specific areas of the stock (i.e. 7.e). The obtained survey index shows a consistent trend for both semesters (Figure 2.B32) with values ranging from 4 583 505 to 14 727 207.

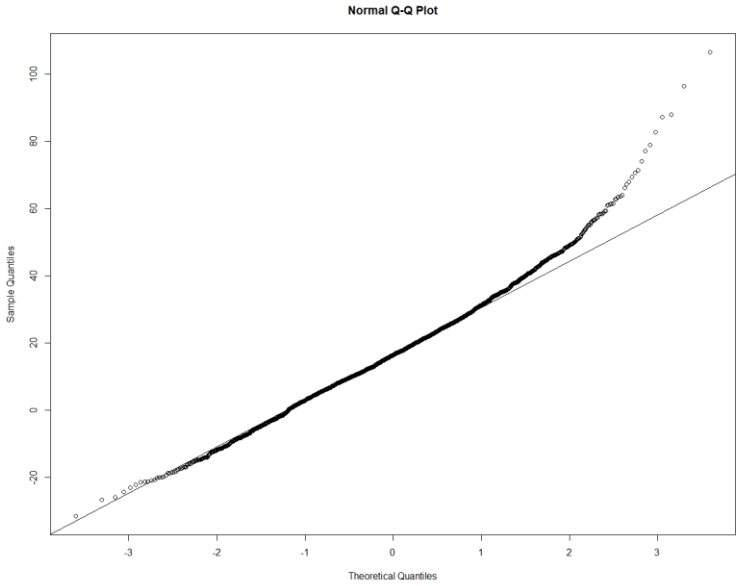


```
Parametric coefficients:
                                                  Estimate Std. Error t value Pr(>|t|)
(Intercept)                                        5.90542    0.43597  13.545  < 2e-16 ***
as.character(Year)2000                             0.11596    0.34739   0.334  0.73854
as.character(Year)2001                             0.30526    0.41470   0.736  0.46167
as.character(Year)2002                             0.45967    0.46920   0.980  0.32724
as.character(Year)2003                             0.38658    0.47491   0.814  0.41565
as.character(Year)2004                             0.51770    0.45972   1.126  0.26012
as.character(Year)2005                             0.04261    0.45520   0.094  0.92543
as.character(Year)2006                            -0.09186    0.43868  -0.209  0.83414
as.character(Year)2007                             0.51411    0.43135   1.192  0.23332
as.character(Year)2008                             0.49204    0.43542   1.130  0.25847
as.character(Year)2009                             0.66721    0.43011   1.551  0.12085
as.character(Year)2010                             0.55706    0.42195   1.320  0.18677
as.character(Year)2011                             0.34936    0.42917   0.814  0.41562
as.character(Year)2012                             0.84431    0.42666   1.979  0.04784 *
as.character(Year)2013                             0.90938    0.42234   2.153  0.03131 *
as.character(Year)2014                             0.83723    0.42800   1.956  0.05046 .
as.character(Year)2015                             1.00359    0.41622   2.411  0.01590 *
as.character(Year)2016                             1.06143    0.41590   2.552  0.01071 *
as.character(Year)2017                             1.11202    0.42407   2.622  0.00874 **
as.character(Year)2018                             0.72724    0.43008   1.691  0.09086 .
as.character(Year)2019                             0.69696    0.43096   1.617  0.10584
as.character(Year)2020                             0.73067    0.42399   1.723  0.08484 .
as.character(Year)2021                             0.66072    0.44218   1.494  0.13513
as.character(semester)2                           -0.32437    0.50522  -0.642  0.52085
GearGOV_CL                                        -1.68534    0.11633 -14.488  < 2e-16 ***
GearTV                                            -1.04439    0.23737  -4.400 1.09e-05 ***
as.character(Year)2000:as.character(semester)2     0.36727    0.40917   0.898  0.36940
as.character(Year)2001:as.character(semester)2    -0.14325    0.50071  -0.286  0.77481
as.character(Year)2002:as.character(semester)2    -0.10660    0.55752  -0.191  0.84837
as.character(Year)2003:as.character(semester)2    -0.02338    0.56095  -0.042  0.96675
as.character(Year)2004:as.character(semester)2    -0.09718    0.54144  -0.179  0.85755
as.character(Year)2005:as.character(semester)2     0.16646    0.53819   0.309  0.75709
as.character(Year)2006:as.character(semester)2     0.53803    0.52380   1.027  0.30435
as.character(Year)2007:as.character(semester)2     0.37118    0.51683   0.718  0.47265
as.character(Year)2008:as.character(semester)2     0.34530    0.52099   0.663  0.50747
as.character(Year)2009:as.character(semester)2    -0.04175    0.51183  -0.081  0.93550
as.character(Year)2010:as.character(semester)2     0.40489    0.50543   0.801  0.42309
as.character(Year)2011:as.character(semester)2     0.91033    0.51004   1.785  0.07430 .
as.character(Year)2012:as.character(semester)2     0.27519    0.50948   0.540  0.58910
as.character(Year)2013:as.character(semester)2     0.03129    0.50697   0.062  0.95079
as.character(Year)2014:as.character(semester)2     0.34737    0.51032   0.681  0.49608
as.character(Year)2015:as.character(semester)2     0.14392    0.50012   0.288  0.77353
as.character(Year)2016:as.character(semester)2    -0.14408    0.50285  -0.287  0.77448
as.character(Year)2017:as.character(semester)2    -0.45525    0.51379  -0.886  0.37559
as.character(Year)2018:as.character(semester)2    -0.30121    0.52082  -0.578  0.56303
as.character(Year)2019:as.character(semester)2     0.27887    0.51585   0.541  0.58879
as.character(Year)2020:as.character(semester)2     0.34029    0.51082   0.666  0.50531
as.character(Year)2021:as.character(semester)2    -0.35937    0.53772  -0.668  0.50393
---
Signif. codes:  0 '***' 0.001 '**' 0.01 '*' 0.05 '.' 0.1 ' ' 1

Approximate significance of smooth terms:
                                          edf Ref.df      F  p-value
ti(ctime,lon,lat):as.factor(semester)1 51.769    351  0.370  < 2e-16 ***
ti(ctime,lon,lat):as.factor(semester)2 68.965    351  0.947  < 2e-16 ***
s(lon,lat):as.factor(semester)1       120.390    255 10.475  < 2e-16 ***
s(lon,lat):as.factor(semester)2       154.241    255 12.804  < 2e-16 ***
s(Depth):as.factor(semester)1           3.457      4 24.458  < 2e-16 ***
s(Depth):as.factor(semester)2           3.288      4 17.679  < 2e-16 ***
s(Ship)                                13.229     30  1.397 1.05e-06 ***
---
Signif. codes:  0 '***' 0.001 '**' 0.01 '*' 0.05 '.' 0.1 ' ' 1

R-sq.(adj) =  0.285   Deviance explained = 52.4%
-REML =  30990  Scale est. = 304.84    n = 40385
```

**Figure 2.B30. QQplot and summary for Model 2.b**

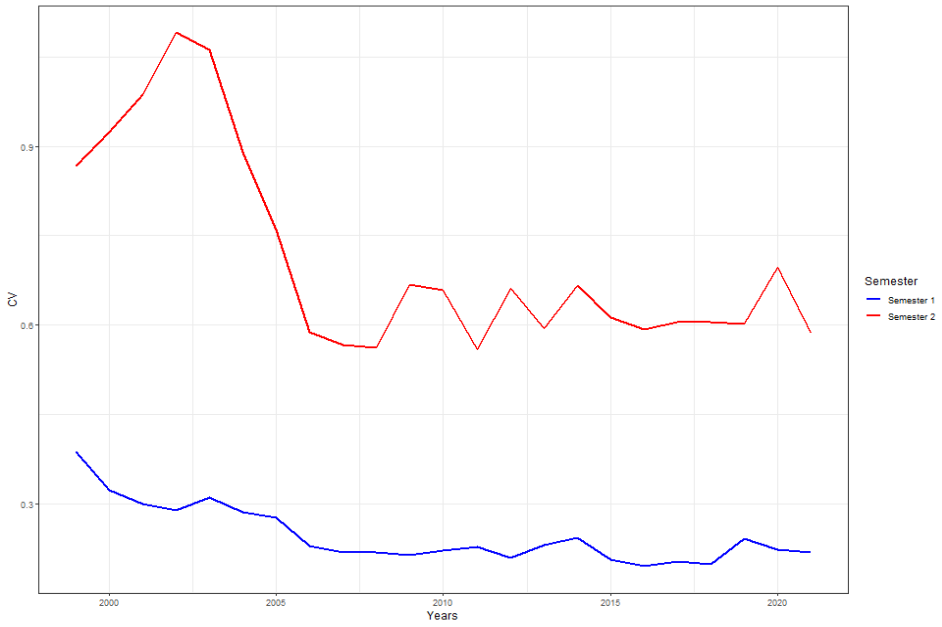


**Figure 2.B31. Coefficient of variation (CV) by year for predictions obtained using Model 2.b**

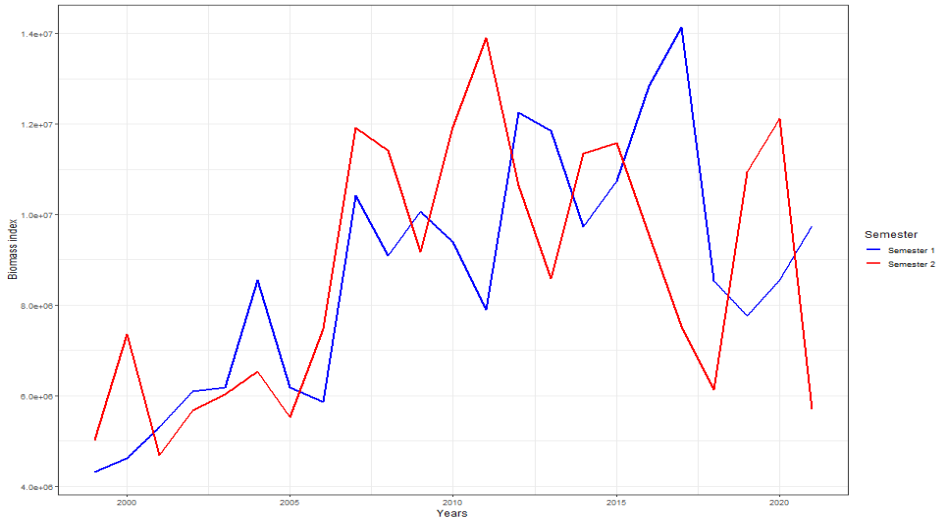


**Figure 2.B32. Survey index trend for both semesters obtained using Model 2.b**

Conclusions on one model for two semesters (all quarters included)

A model framework that included all data (model 2.a and 2.b) could be more robust for the purpose of making a survey index for the North Sea brill assessment. Model 2.a and 2.b showed almost identical patterns and relative uncertainty throughout the time-series, it was decided to choose the most parsimonious model. Model 2.a was selected, as it has a slightly lower AIC ($\Delta$AIC=38.09), explaining the same amount of deviance (52.4 vs. 52.3%), whereas being simpler (Annex B2).

***Model framework for index 1983–1998***

Data prior to the year 1999 is available but restricted to a certain quarter of the year, certain divisions/regions of the stock area and with only specific gear covering it. An exploitable biomass survey index was calculated for the years 1983–1998 using only data from Area 4 and Division 3.a.

### *Data*

The data were trimmed to include the years 1983 to 1998. Data on the English Channel is not available during this period and therefore not included in the analysis. Furthermore, the data were filtered to the first quarter (1st semester) and to the GOV_CL gear, because other quarters do not present consistent data and other gears are rarely present during this period.

### *Modelling framework*

The model framework was adjusted excluding the gear and semester effect (Figure 2.B33)

```
model1.a <- gam(bio.adult ~ s(lon, lat, bs=c('ds'), k=256, m=c(1,0.5)) +     # fixed spatial effect (2 dimensional smoother)
                as.character(Year) +                    # temporal trend (1 dimensional smoother)
                ti(ctime, lon, lat, d=c(1,2), bs=c('ds','ds'), k=c(10,40), m=list(c(1,0), c(1,0.5))) +  # spatiotemporal effect (3 dimensional smoother)
                s(Depth, bs='ds', k=5, m=c(1,0)) +    # depth effect (1 dimensional smoother)
                 # Gear +                               # fixed gear effect REMOVED FOR THIS QUARTER, ONLY ONE GEAR GOV_CL
                s(Ship, bs = "re") +                  # random ship effect
                offset(log(SweptArea)),               # linear offset
                family = tw(),                          # observation error assumed to follow a Tweedie distribution
                data = brill_data83_99)
```

**Figure 2.B33. Model 1.a used to model the "historical" data (1983–1998).**

### *Model output and validation*

The model explained only 36.3% of the deviance and reported an AIC of 4189.203. The QQ plot shows that the residuals follow the Tweedie distribution closely (Figure 2.B34). The uncertainty around the estimates (CV) is fairly low throughout the time-series, with a unique peak in 1997 (Figure 2.B35). The predicted survey index values ranged from 146 660 to 1 283 270. (Figure 2.B36). The highest biomass was estimated for 1991 and the lowest in 1997. The large uncertainty and low estimated value for 1997 is explained by especially low survey catches for that year compared to the rest of the years.

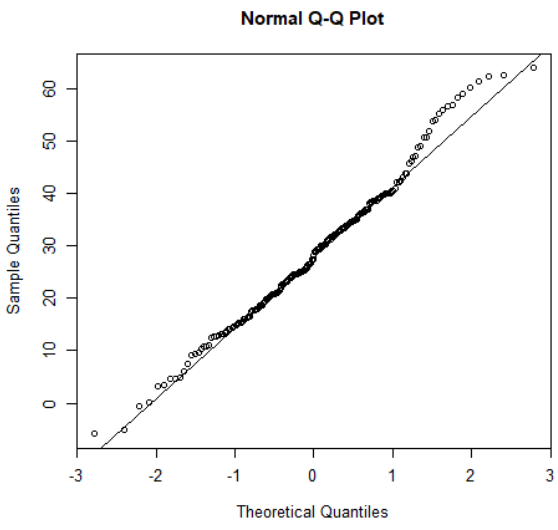


```
Family: Tweedie(p=1.164)
Link function: log

Formula:
bio.adult ~ s(lon, lat, bs = c("ds"), k = 256, m = c(1, 0.5)) +
    as.character(Year) + ti(ctime, lon, lat, d = c(1, 2), bs = c("ds",
    "ds"), k = c(10, 40), m = list(c(1, 0), c(1, 0.5))) + s(Depth,
    bs = "ds", k = 5, m = c(1, 0)) + s(Ship, bs = "re") + offset(log(SweptArea))

Parametric coefficients:
                          Estimate Std. Error t value Pr(>|t|)
(Intercept)               4.53367    0.39890  11.365   <2e-16 ***
as.character(Year)1984    0.22474    0.48883   0.460   0.6457
as.character(Year)1985   -0.04034    0.50478  -0.080   0.9363
as.character(Year)1986   -0.13549    0.50078  -0.271   0.7867
as.character(Year)1987    0.38996    0.46678   0.835   0.4035
as.character(Year)1988   -0.30074    0.54550  -0.551   0.5814
as.character(Year)1989   -0.52773    0.57242  -0.922   0.3566
as.character(Year)1990    0.02645    0.51491   0.051   0.9590
as.character(Year)1991    0.69885    0.46477   1.504   0.1327
as.character(Year)1992    0.64376    0.47826   1.346   0.1783
as.character(Year)1993    0.64188    0.47308   1.357   0.1749
as.character(Year)1994    0.27006    0.50974   0.530   0.5963
as.character(Year)1995   -0.07036    0.54197  -0.130   0.8967
as.character(Year)1996    0.53672    0.50859   1.055   0.2913
as.character(Year)1997   -1.35700    0.72077  -1.883   0.0598 .
as.character(Year)1998    0.19810    0.52338   0.379   0.7051
---
Signif. codes:  0 '***' 0.001 '**' 0.01 '*' 0.05 '.' 0.1 ' ' 1

Approximate significance of smooth terms:
                   edf Ref.df     F  p-value
s(lon,lat)      47.321    255 0.988  < 2e-16 ***
ti(ctime,lon,lat) 10.540    351 0.091 4.44e-05 ***
s(Depth)         2.608      4 1.745   0.0169 *
s(Ship)          2.635     18 0.187   0.1861
---
Signif. codes:  0 '***' 0.001 '**' 0.01 '*' 0.05 '.' 0.1 ' ' 1

R-sq.(adj) =   0.13   Deviance explained = 36.3%
-REML = 2093.9  Scale est. = 400.19    n = 5542
```

**Figure 2.B34. QQplot and summary for Model 1.a.**

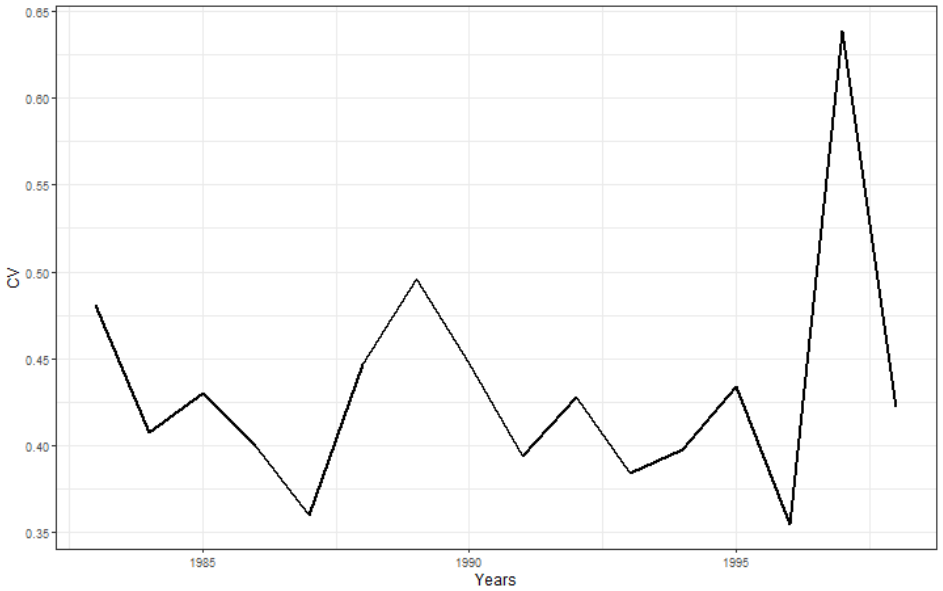


**Figure 2.B35. Coefficient of variation (CV) by year (second semester) for predictions obtained using Model 1.b**

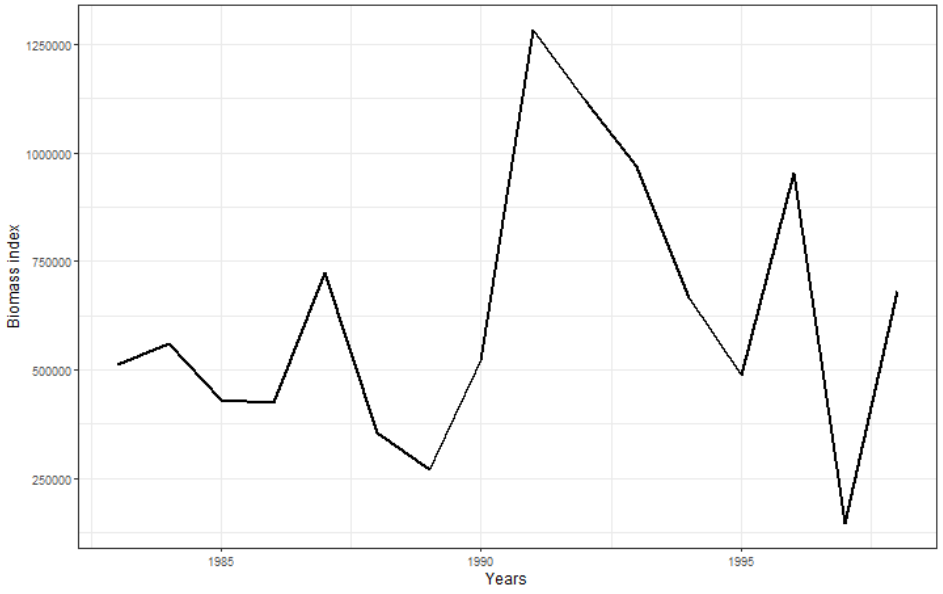


**Figure 2.B36. Survey index trend for the second semester obtained using Model 1.b**

***General conclusions and yearly estimates of survey indices***

The first approach (building individual models by semester) did not show consistent trends between both obtained indices. We are unsure which model is providing a correct picture of the stock's exploitable biomass evolution. This difference between the model outputs lies in the early years of the time-series for which the second semester model estimates higher biomass values compared to the 1st semester. This is likely linked to the high prediction uncertainty due to the limited amount or lack of data for the Western English Channel between 1999–2005. The second part of the time-series (2005–2022) does show consistency between the prediction made by both models. However, uncertainty for the semester 1 index is very large, making it unsure if this is truly the stock's trend throughout the time-series.

On the other hand, models 2.a and 2.b show relatively lower uncertainties around the predicted biomass index and a similar survey trend for both semesters. We therefore concluded that using a model framework that included all data (model 2.a and 2.b) would be more robust for the purpose of making a survey index for the North Sea brill assessment. Model 2.a and 2.b showed almost identical patterns and relative uncertainty throughout the time-series, it was decided to choose the most parsimonious model. Model 2.a was selected, as it has a slightly lower AIC ($\Delta$AIC=38.09), explaining the same amount of deviance (52.4 vs. 52.3%), whereas being simpler.

Additionally, an index covering the period 1983–1998 was calculated, which only focused on the first semester, Area 4 and Division 3.a and the GOV_CL gear. Although, this index does not cover the entire stock area and is limited to a single gear, it could help inform the SPiCT model on the stock's biomass further in the past.

The obtained final models were then used to predict the yearly biomass of the stock, confidence intervals along with coefficients of variation around the estimates. This was performed using functions developed in the surveyIndex package (Berg *et al*., 2014; Berg, 2021; https://github.com/casperwberg/surveyIndex) and adapted to provide biannual estimates. In this approach, the biomass was predicted considering differences in swept-area for each grid cell, by dividing the size of each grid cell by the mean. This was performed to consider the presence of continental masses or latitudinal differences (i.e. larger grids towards lower latitudes) in the biomass predictions. The indices, upper and lower limits of the confidence intervals, standard errors and coefficients of variation obtained from the 1983–1998 semester 1 index and the biannual (semester 1 and 2) 1999–2021 are presented in Table 2.B1 and Table 2.B3.

These three indices provide information on the spatio-temporal evolution of the Greater North Sea brill stock's biomass and serve as input (including estimated uncertainties) for inclusion in the SPiCT assessment model.

**Table 2.B1. Yearly prediction, upper and lower CI, standard error (se) and coefficient of variation (CV) for the 1st semester of the 1983–1998 index.**

| Year | Prediction | Upper CI | Lower CI | CV |
|---|---|---|---|---|
| 1983 | 513044.0 | 273907.7 | 1873888 | 0.48 |
| 1984 | 560278.7 | 318366 | 1623636 | 0.41 |
| 1985 | 430801.4 | 239740 | 1341477 | 0.43 |
| 1986 | 424467.8 | 234343.9 | 1162194 | 0.40 |
| 1987 | 725130.2 | 454927.1 | 1918511 | 0.36 |
| 1988 | 353976.0 | 180509.8 | 1079986 | 0.45 |

| Year | Prediction | Upper CI | Lower CI | CV |
|---|---|---|---|---|
| 1989 | 271308.3 | 135117.6 | 983411 | 0.50 |
| 1990 | 520670.2 | 273206.1 | 1636981 | 0.45 |
| 1991 | 1283269.6 | 773079.3 | 3742926 | 0.39 |
| 1992 | 1120779.1 | 653945.5 | 3620600 | 0.43 |
| 1993 | 969545.5 | 615430.2 | 2859934 | 0.38 |
| 1994 | 667242.5 | 381190.2 | 1871903 | 0.40 |
| 1995 | 487818.6 | 266500.2 | 1510611 | 0.43 |
| 1996 | 952653.6 | 575234 | 2379403 | 0.35 |
| 1997 | 146659.9 | 48799.16 | 627102.6 | 0.64 |
| 1998 | 680382.2 | 374229.8 | 2024959 | 0.42 |

**Table 2.B3. Yearly prediction, upper and lower CI, standard error (se) and coefficient of variation (CV) for semester 1 and 2 (S1 and S2 respectively) obtained using model 2.a for the 1999–2021 index.**

| Year | Prediction | | Upper CI | | Lower CI | | CV | |
|---|---|---|---|---|---|---|---|---|
| | S1 | S2 | S1 | S2 | S1 | S2 | S1 | S2 |
| 1999 | 4119947 | 5224304 | 2689367 | 3960164 | 10168951 | 95494861 | 0.33 | 0.80 |
| 2000 | 4768627 | 7524136 | 3370092 | 5414219 | 10910110 | 170913929 | 0.29 | 0.86 |
| 2001 | 6038475 | 4583505 | 4318476 | 3197953 | 13395583 | 128053976 | 0.28 | 0.92 |
| 2002 | 7388701 | 5310228 | 5361404 | 3828541 | 17481344 | 182603153 | 0.30 | 0.97 |
| 2003 | 7483429 | 6030672 | 5140149 | 4093495 | 17217832 | 401203678 | 0.30 | 1.15 |
| 2004 | 9405231 | 7369404 | 6361223 | 5043272 | 19532248 | 206120270 | 0.28 | 0.93 |
| 2005 | 6317122 | 6492799 | 4338484 | 4783708 | 12371171 | 118187457 | 0.26 | 0.80 |
| 2006 | 6326258 | 8272215 | 4492475 | 6309332 | 11093873 | 155390764 | 0.23 | 0.80 |
| 2007 | 10698702 | 12458714 | 7933841 | 9516859 | 18482079 | 175246457 | 0.21 | 0.73 |
| 2008 | 9074656 | 11018556 | 6809441 | 8695922 | 15977672 | 84876075 | 0.21 | 0.57 |
| 2009 | 10290885 | 8530177 | 7422509 | 6537668 | 17531034 | 65900017 | 0.21 | 0.58 |
| 2010 | 10011846 | 11640032 | 7278016 | 8898318 | 17283555 | 85453521 | 0.22 | 0.57 |
| 2011 | 8666372 | 14727207 | 6268417 | 11438925 | 15681484 | 122968907 | 0.23 | 0.59 |
| 2012 | 12515605 | 11392920 | 9567200 | 9180850 | 22297959 | 81967037 | 0.21 | 0.55 |
| 2013 | 11473038 | 9303350 | 8614933 | 7440010 | 21554783 | 58885085 | 0.23 | 0.52 |
| 2014 | 9395805 | 11820332 | 7046210 | 9642464 | 16777096 | 84640385 | 0.22 | 0.54 |

| Year | Prediction | | Upper CI | | Lower CI | | CV | |
|---|---|---|---|---|---|---|---|---|
| | S1 | S2 | S1 | S2 | S1 | S2 | S1 | S2 |
| 2015 | 10787386 | 12003911 | 8630946 | 9392735 | 18460708 | 70466539 | 0.19 | 0.50 |
| 2016 | 13692123 | 10224802 | 10532276 | 8287103 | 23062431 | 73012621 | 0.20 | 0.54 |
| 2017 | 14873887 | 8155839 | 11756909 | 6436140 | 25163824 | 67077273 | 0.19 | 0.59 |
| 2018 | 8721902 | 6475363 | 6625420 | 4931404 | 15673223 | 50757587 | 0.22 | 0.58 |
| 2019 | 7788911 | 11236719 | 5797999 | 9014248 | 13440908 | 222926607 | 0.21 | 0.80 |
| 2020 | 9026989 | 12403567 | 6927157 | 9506935 | 16447879 | 168960155 | 0.22 | 0.72 |
| 2021 | 11203587 | 5811350 | 8480233 | 4544561 | 19925851 | 46377775 | 0.21 | 0.58 |

## References

Berg, C.W., Nielsen, A., Kristensen, K., 2014. Evaluation of alternative age-based methods for estimating relative abundance from survey data in relation to assessment models. Fisheries Research 151, 91–99; DOI: 10.1016/j.fishres.2013.10.005.

SeaWise consortium, 2022. Deliverable 5.2: Report on historic and future spatial distribution of fished stocks. https://github.com/tokami/fishdish

### 2.8.2.1 Annex B1: Total observed exploitable brill (≥25 cm) catches during surveys in the bll.27.3a47de stock area by year and quarter from 1971 to 2021. Grey rectangles represent sampled hauls with no brill caught.

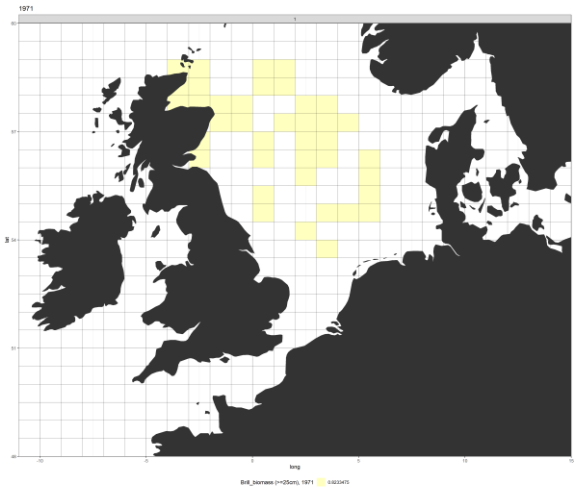


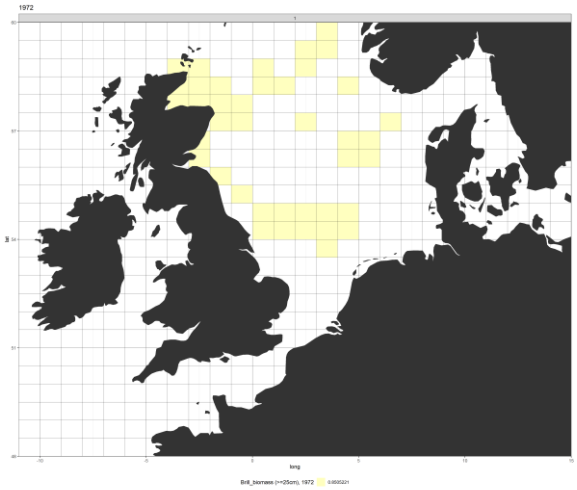


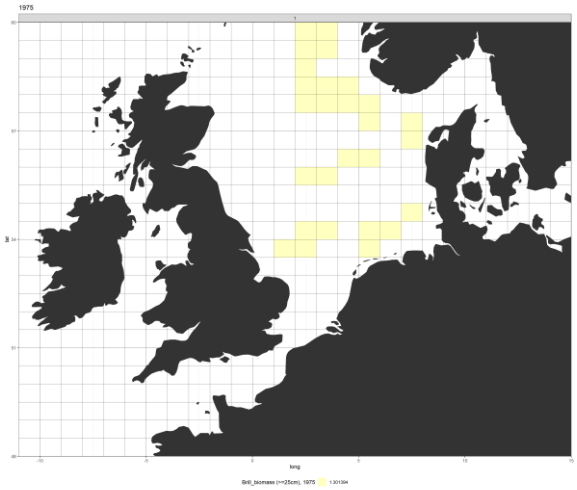
1975
lat
long
Brill_biomass (>=15cm), 1975 1.30 1.304

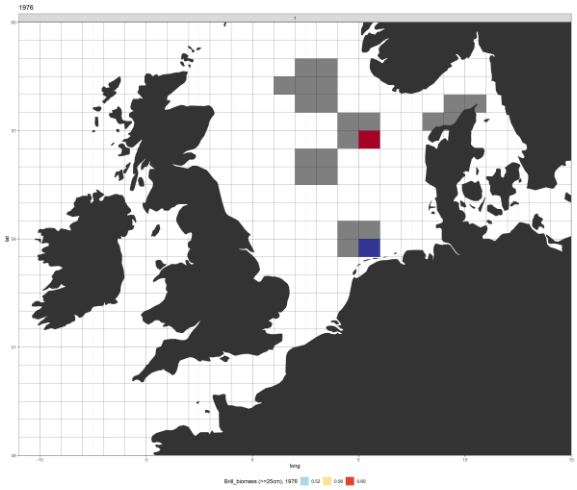
1976
lat
long
Brill_biomass (>=25cm), 1976 0.52 0.56 0.60

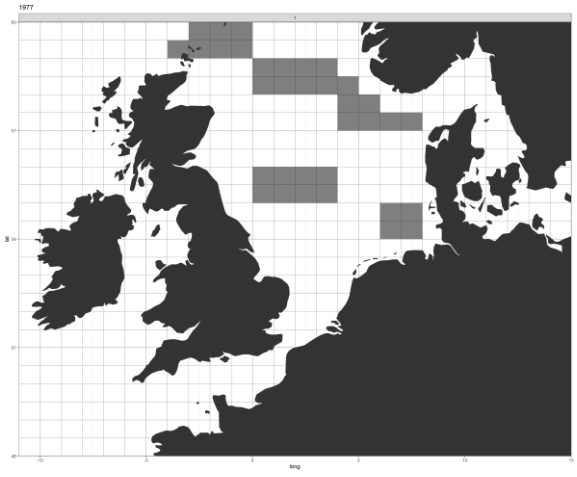
1977
lat
long

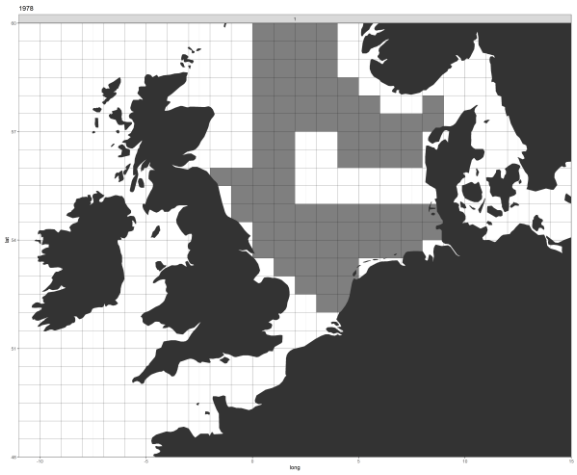
1978
lat
long

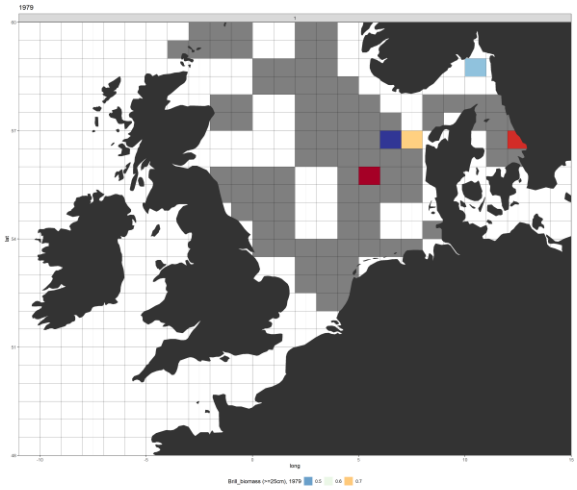
1979
lat
long
Brill_biomass (>=25cm), 1979 0.5 0.6 0.7

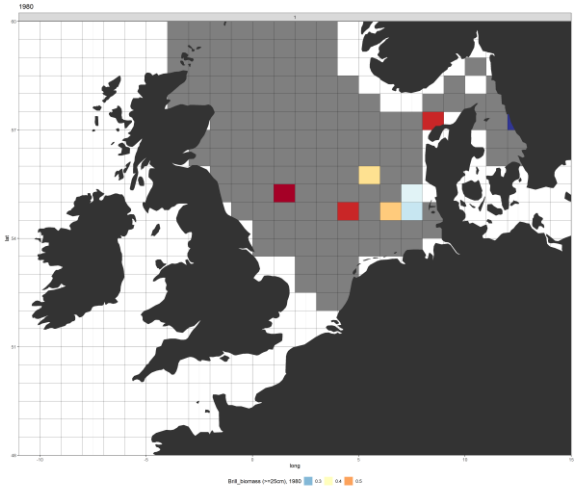
1980
lat
long
Brill_biomass (>=25cm), 1980 0.3 0.4 0.5

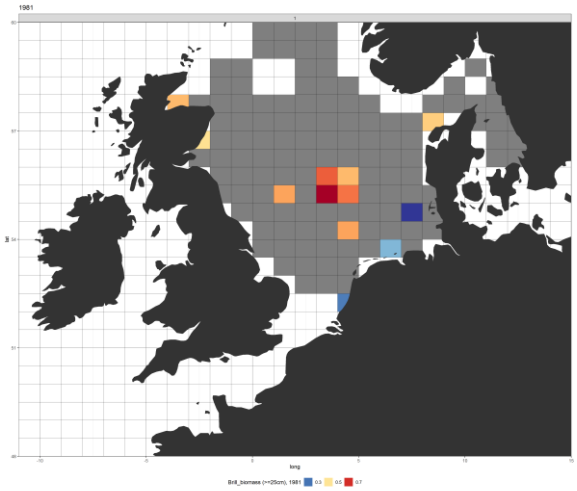
1981
long
Brill_biomass (>=25cm), 1981 0.3 0.5 0.7

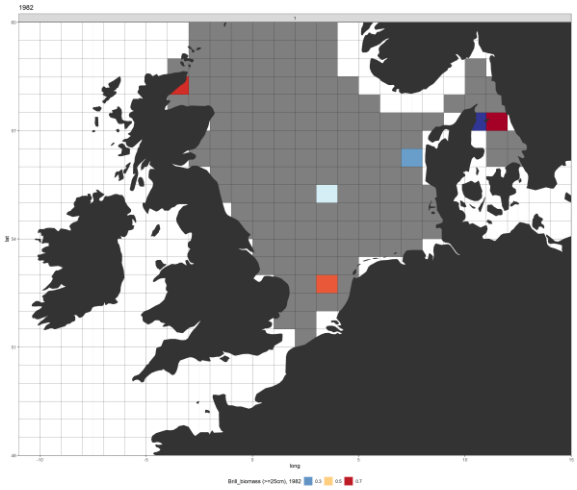
1982
long
Brill_biomass (>=25cm), 1982 0.3 0.5 0.7

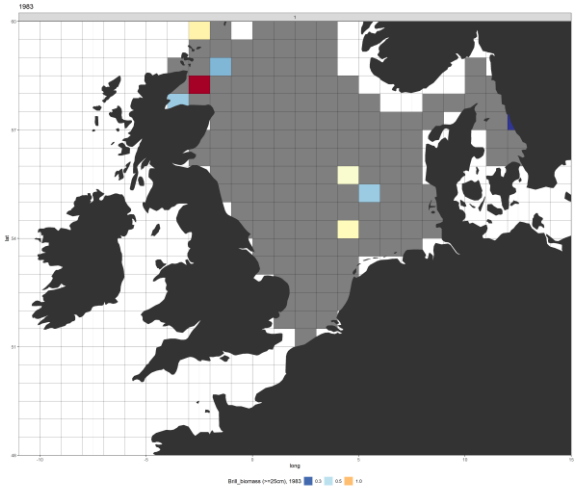
1983
long
Brill_biomass (>=25cm), 1983 0.3 0.5 1.0

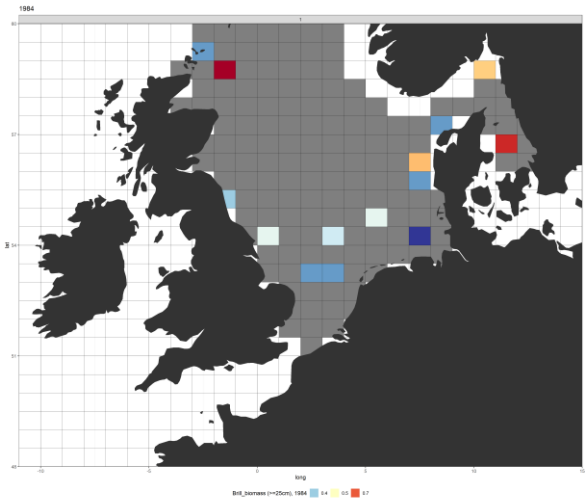
1984
long
Brill_biomass (>=25cm), 1984 0.4 0.5 0.7

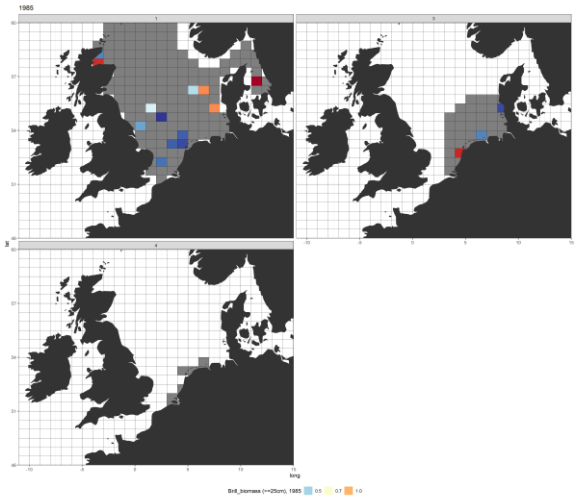
1985
long
Brill_biomass (>=25cm), 1985 0.5 0.7 1.0

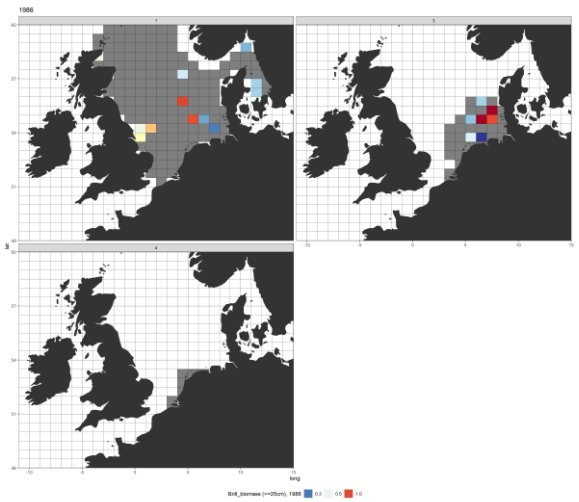
1986
long
Brill_biomass (>=25cm), 1986 0.3 0.5 1.0

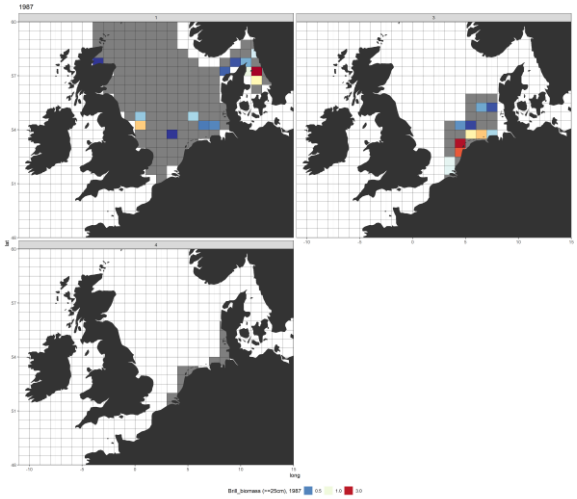
1987
long
Bm$_$biomass (<=25cm), 1987 0.5 1.0 3.0

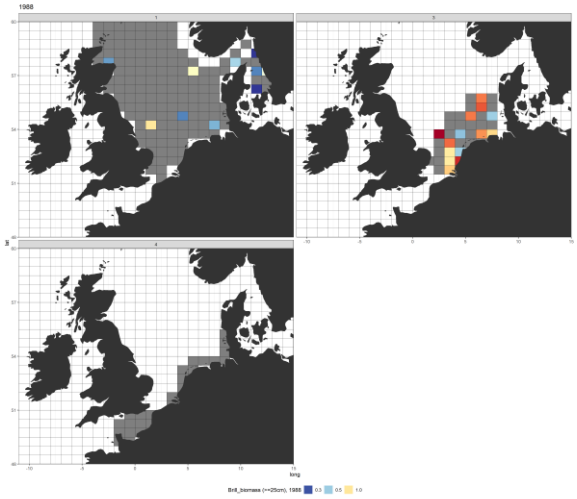
1988
long
Bm$_$biomass (<=25cm), 1988 0.3 0.5 1.0

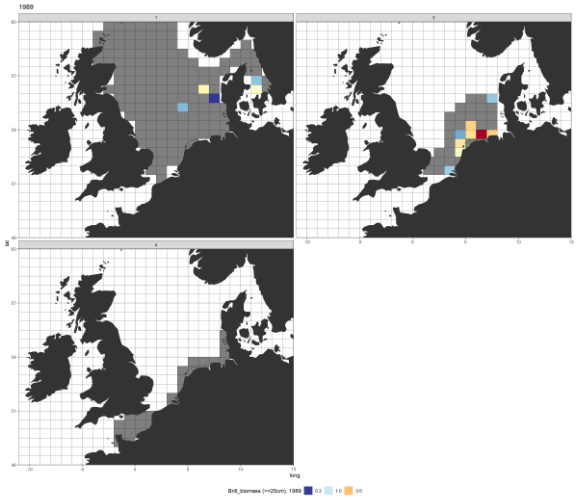
1989
long
Bm$_$biomass (<=25cm), 1989 0.3 1.0 3.0

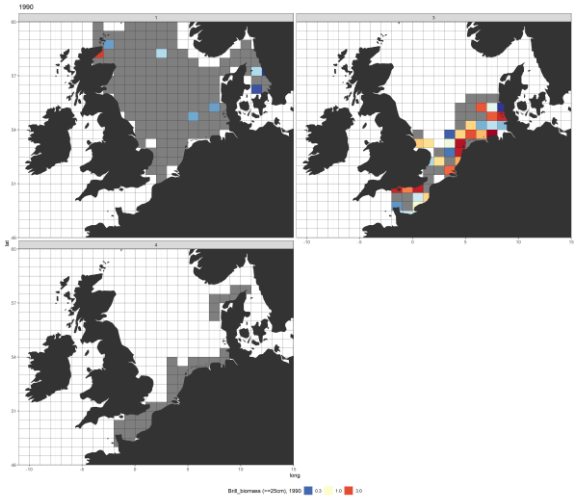
1990

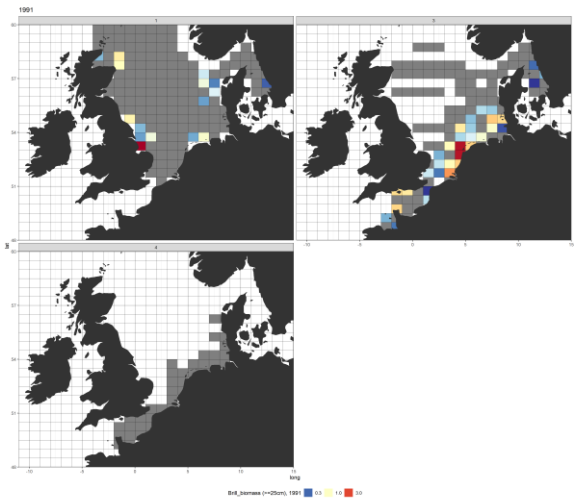
1991

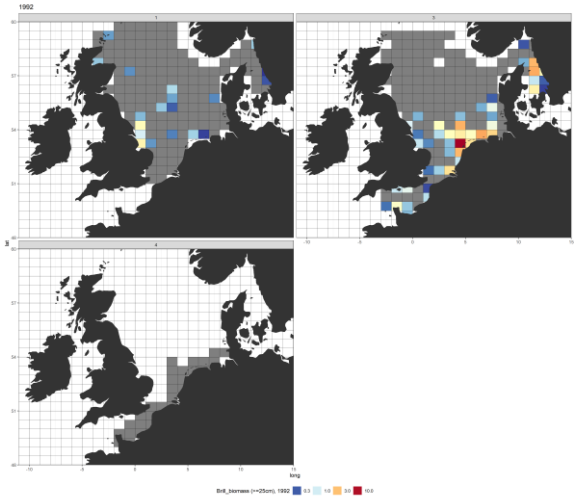
1992

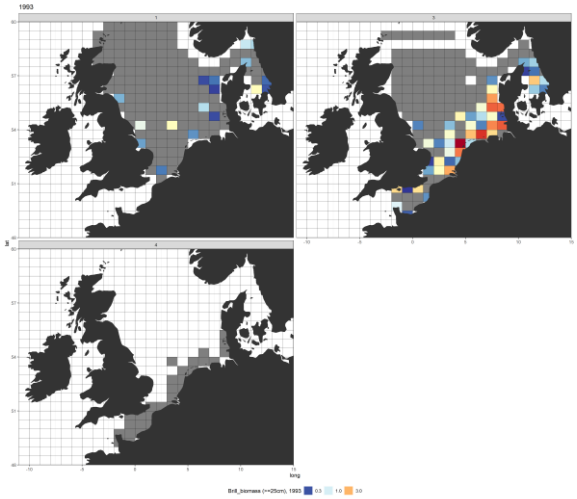
1993
long
Brill_biomass (>=25cm), 1993 0.3 1.0 3.0

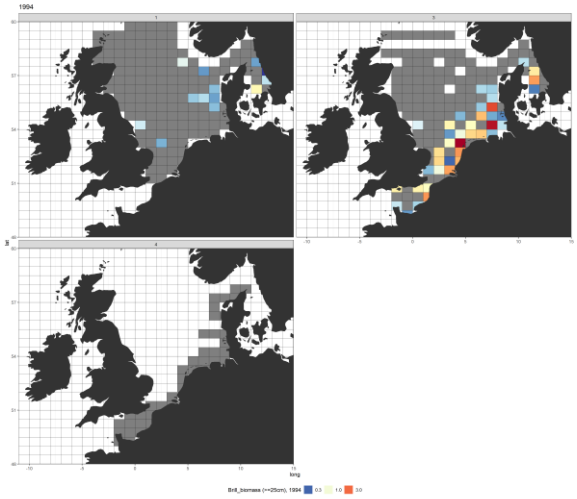
1994
long
Brill_biomass (>=25cm), 1994 0.3 1.0 3.0

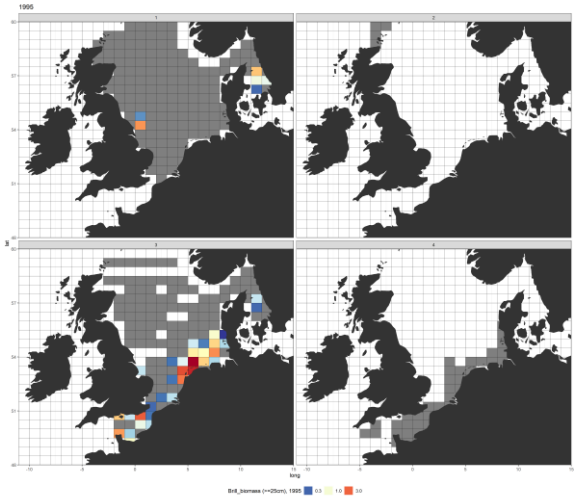
1995
long
Brill_biomass (>=25cm), 1995 0.3 1.0 3.0

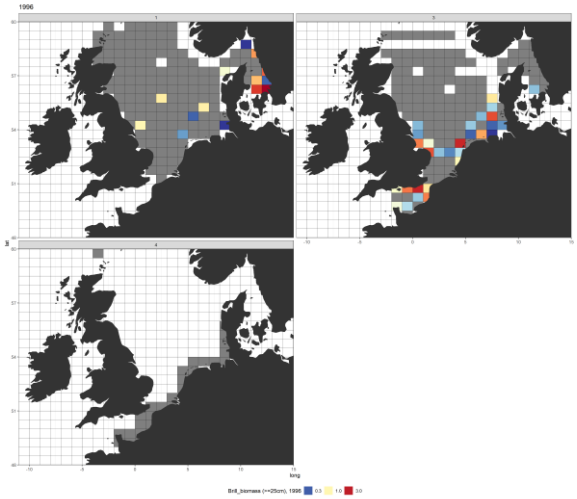
1996

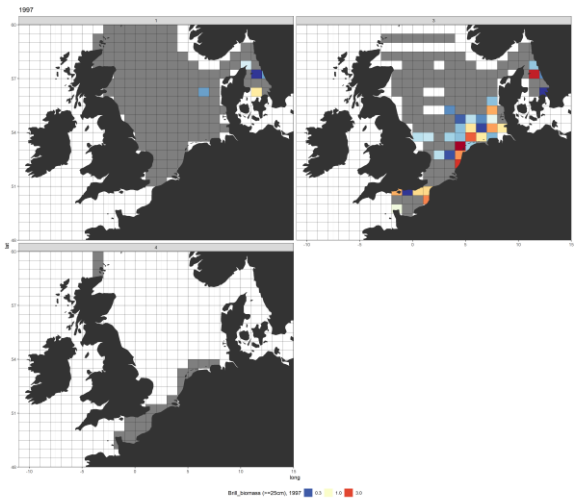
1997

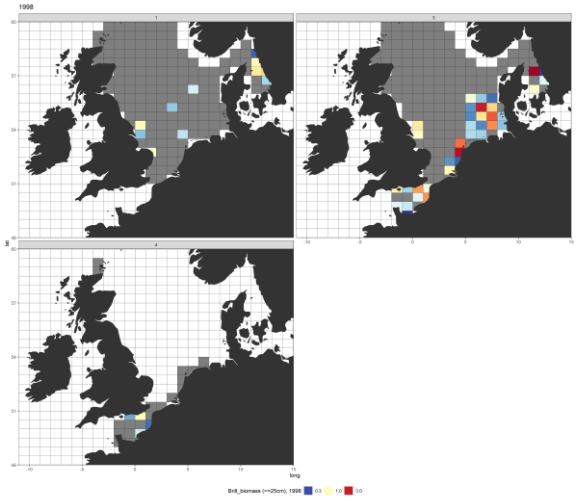
1998

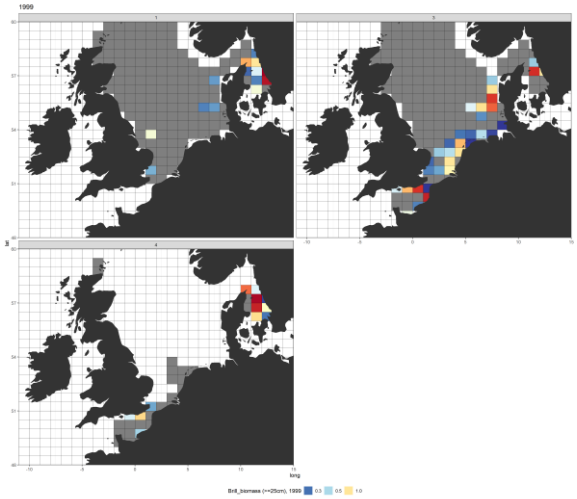
1999

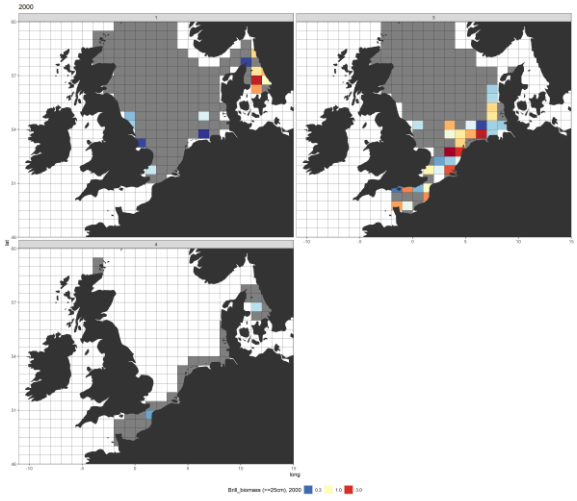
2000

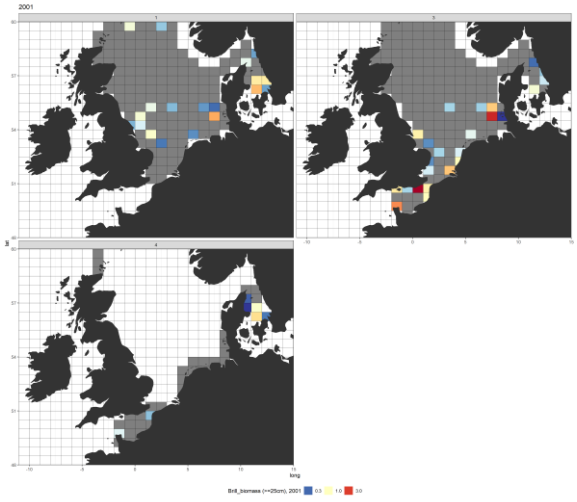
2001

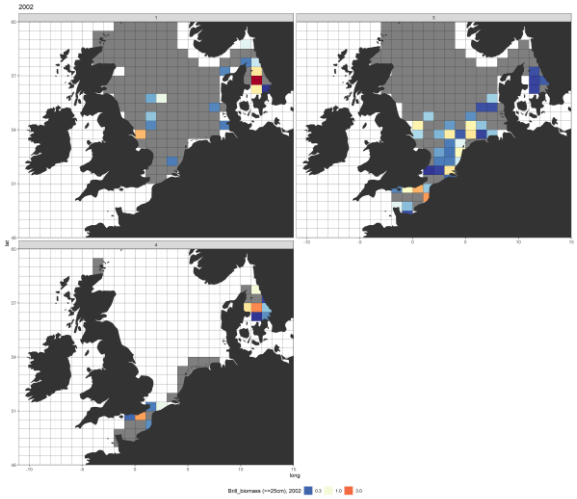
2002

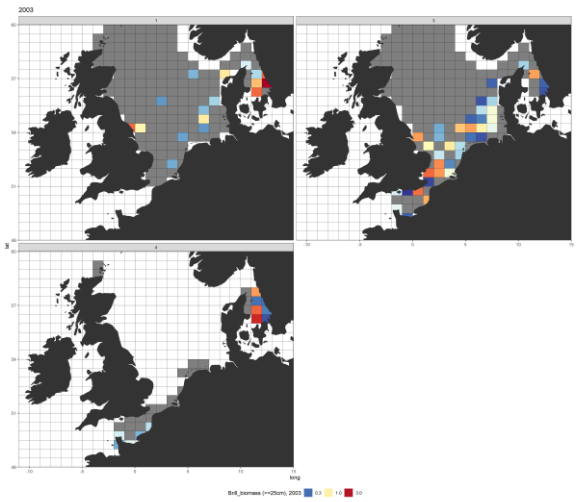
2003

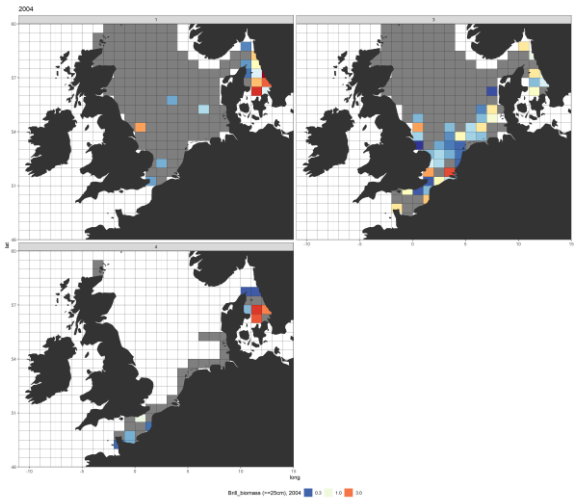
2004

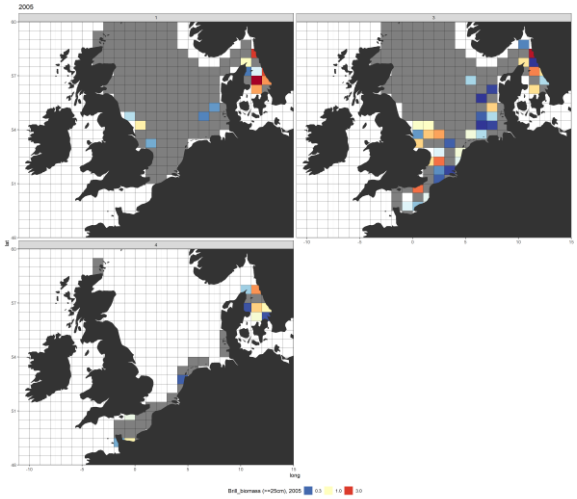
2005

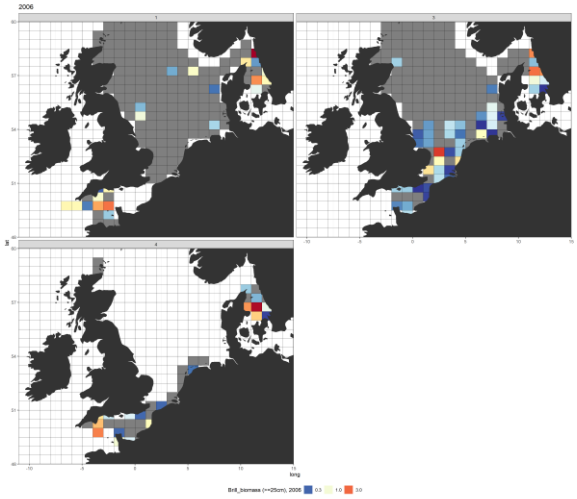
2006

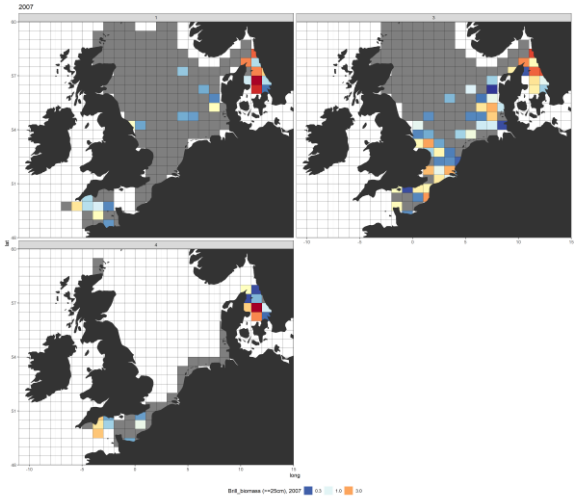
2007

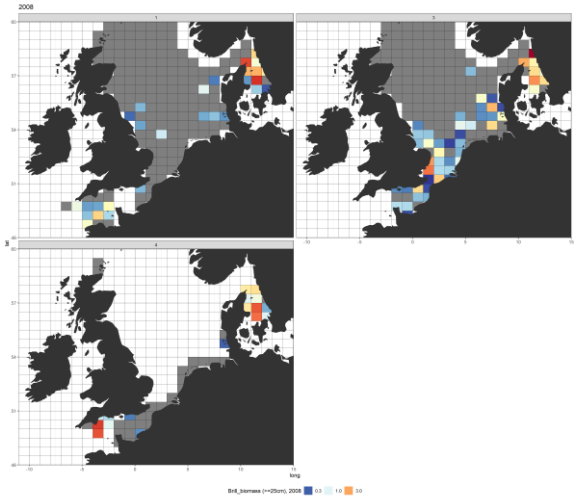
2008

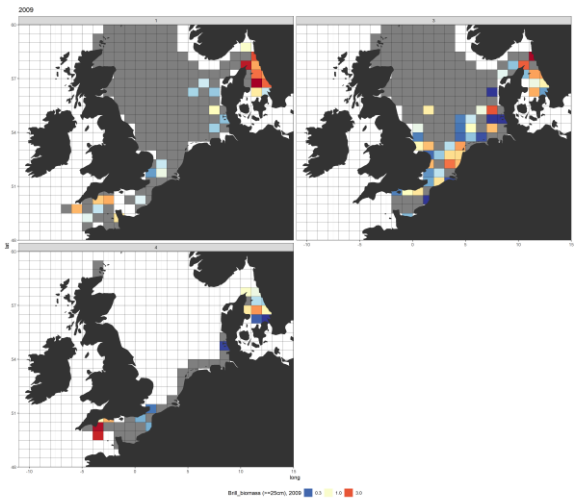
2009

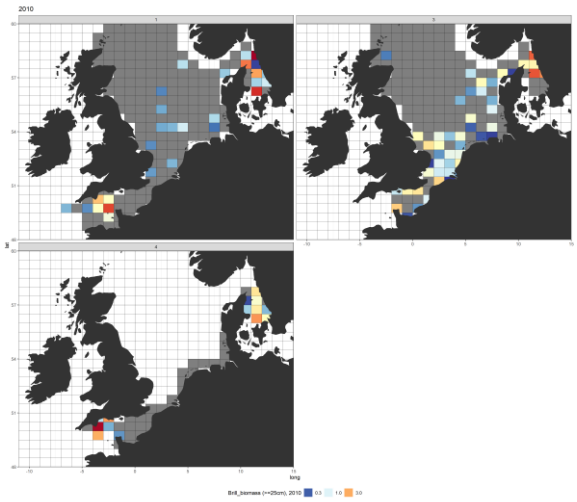
2010

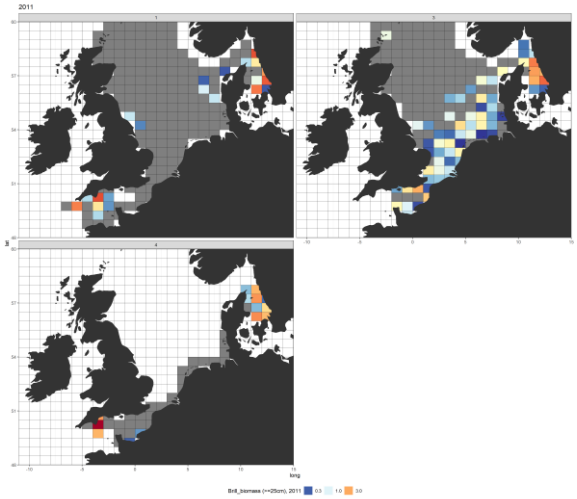
2011

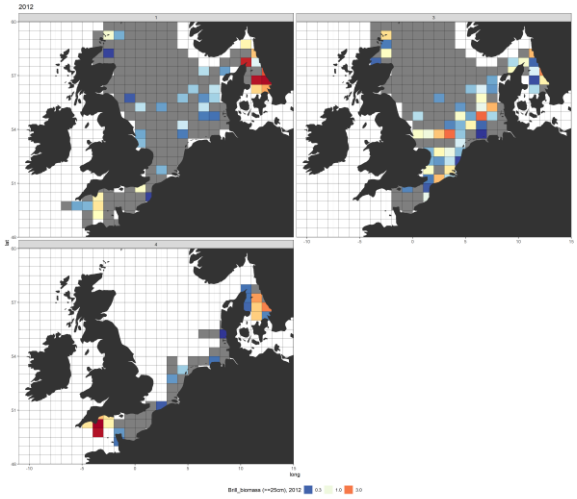
2012

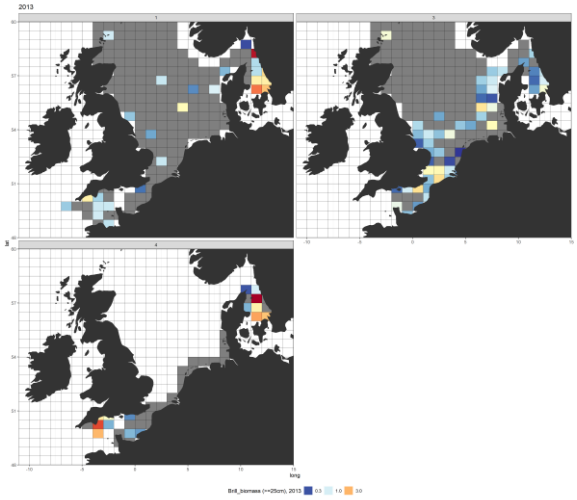
2013

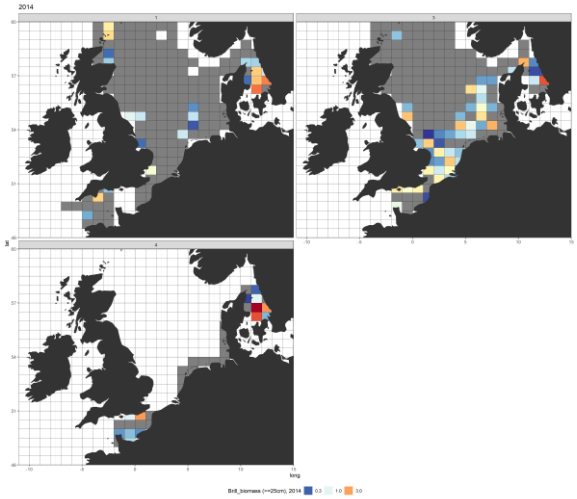
2014

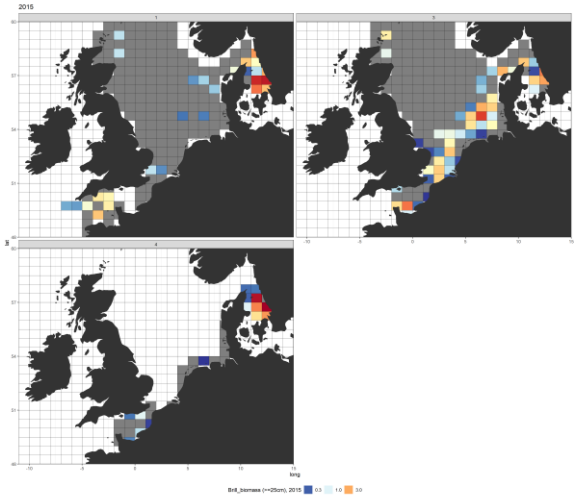
2015

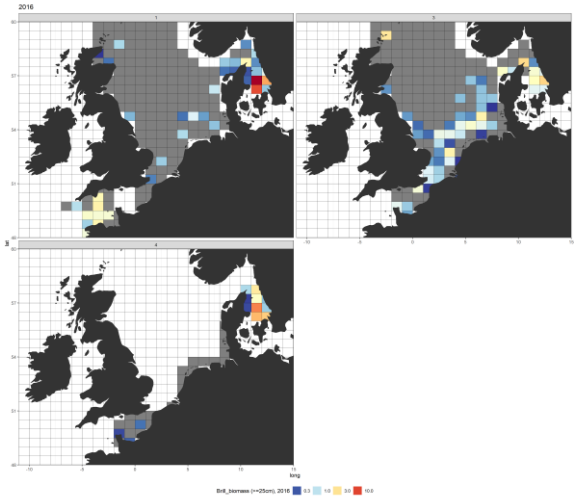
2016

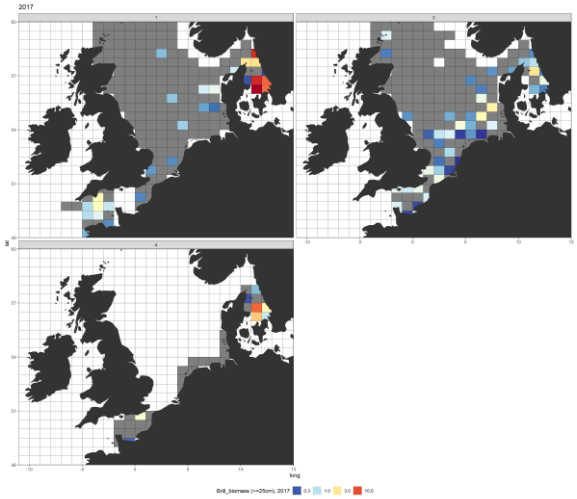
2017

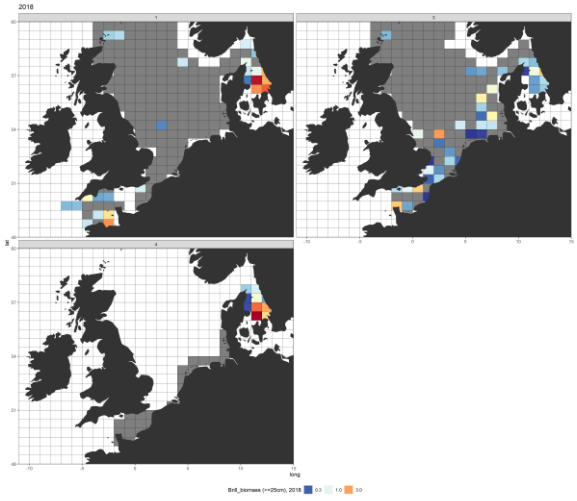
2018

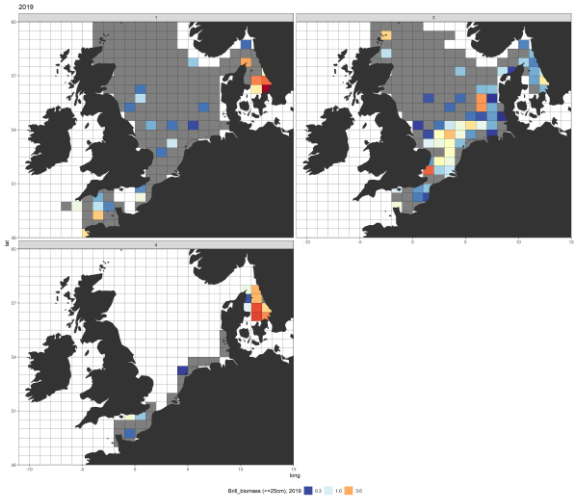
2019

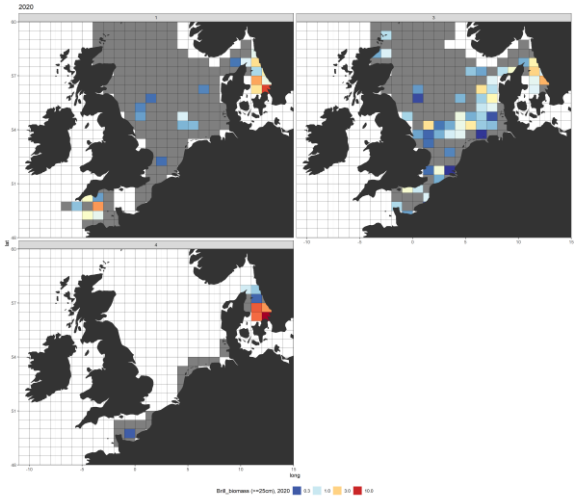
2020

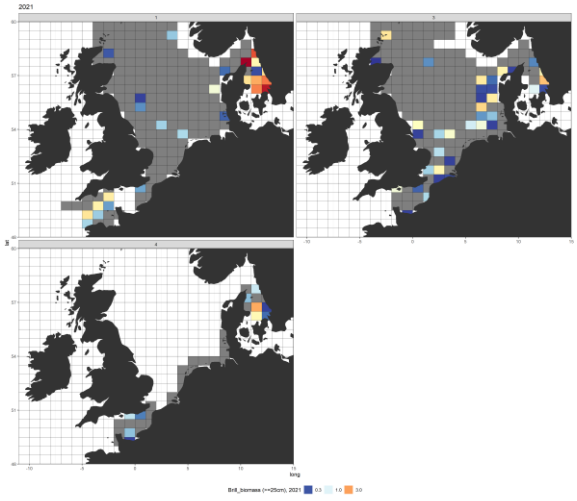
2021

### 2.8.2.2 Annex B2: Predicted exploitable brill (≥ 25cm) biomass obtained using the model 2.a in the bll.27.3a47de stock area by quarter from 1999 to 2021.

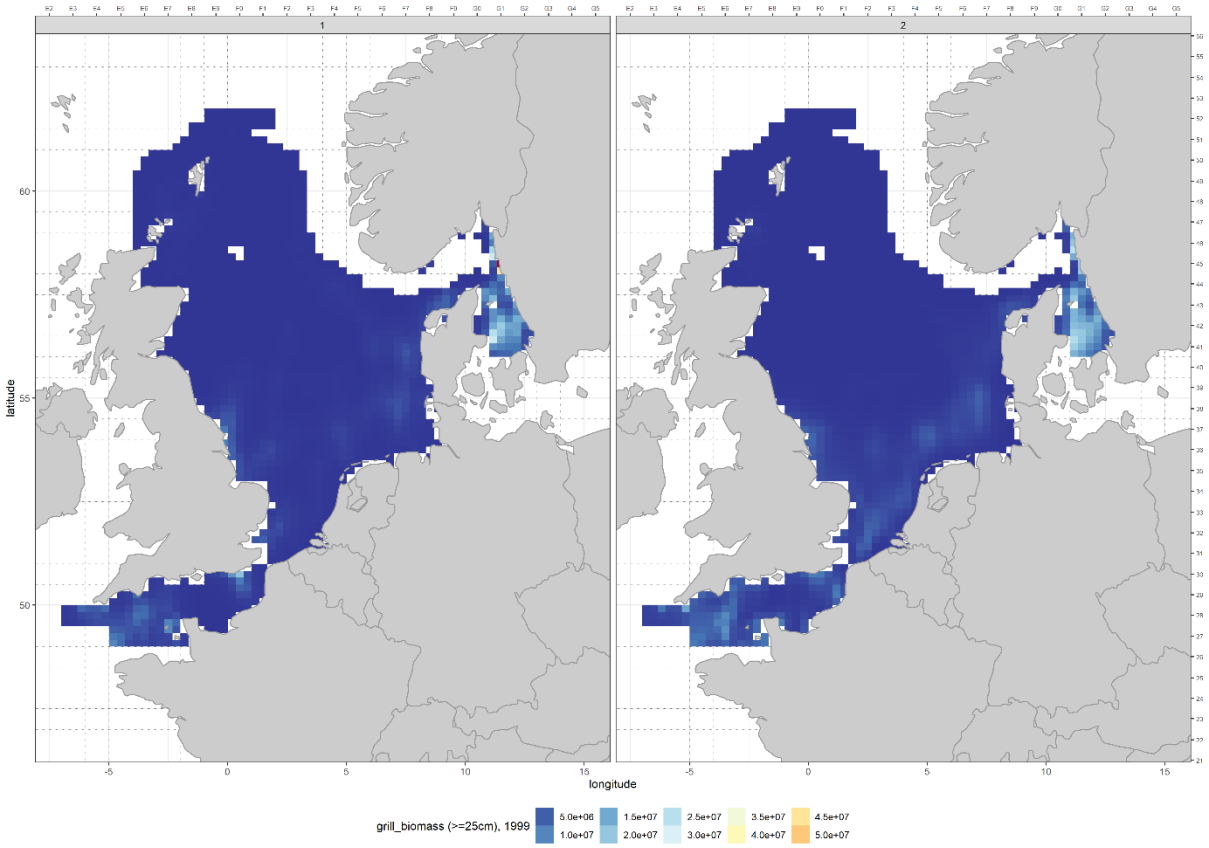


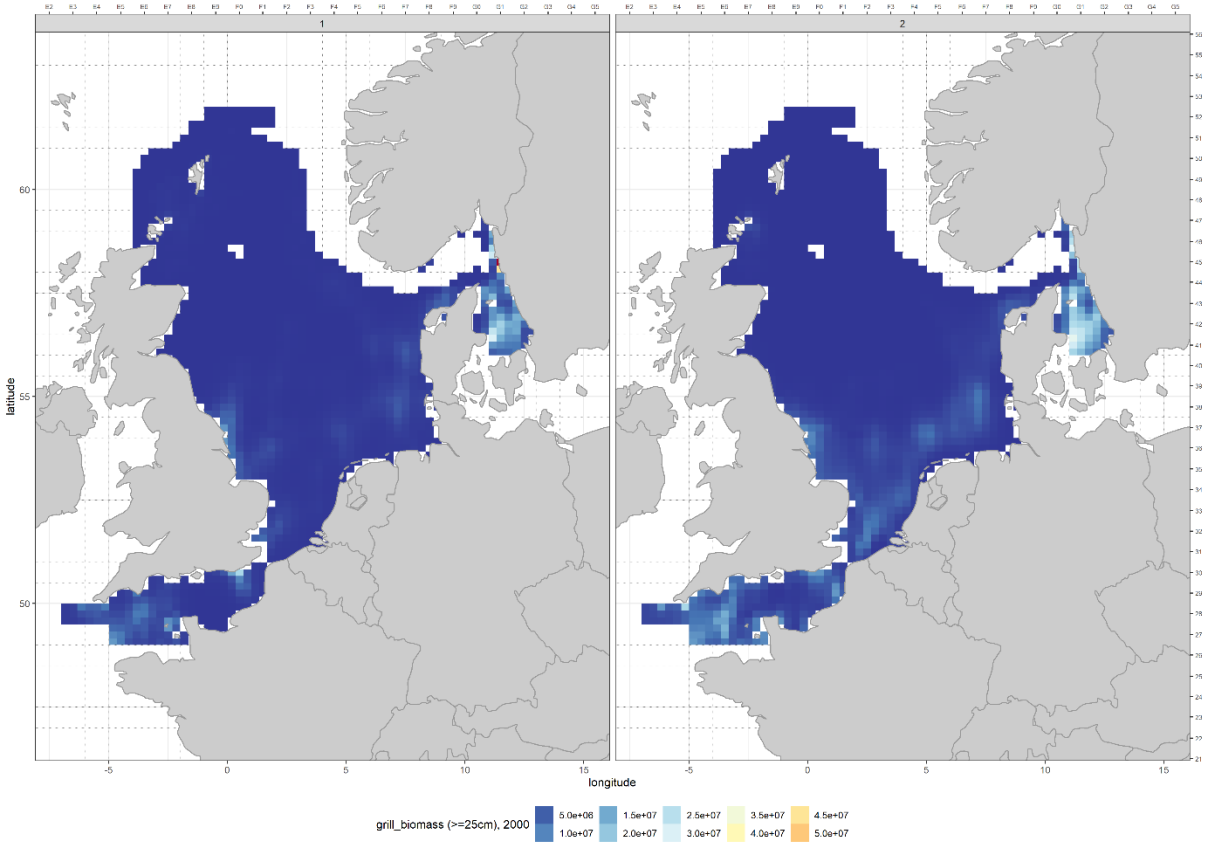

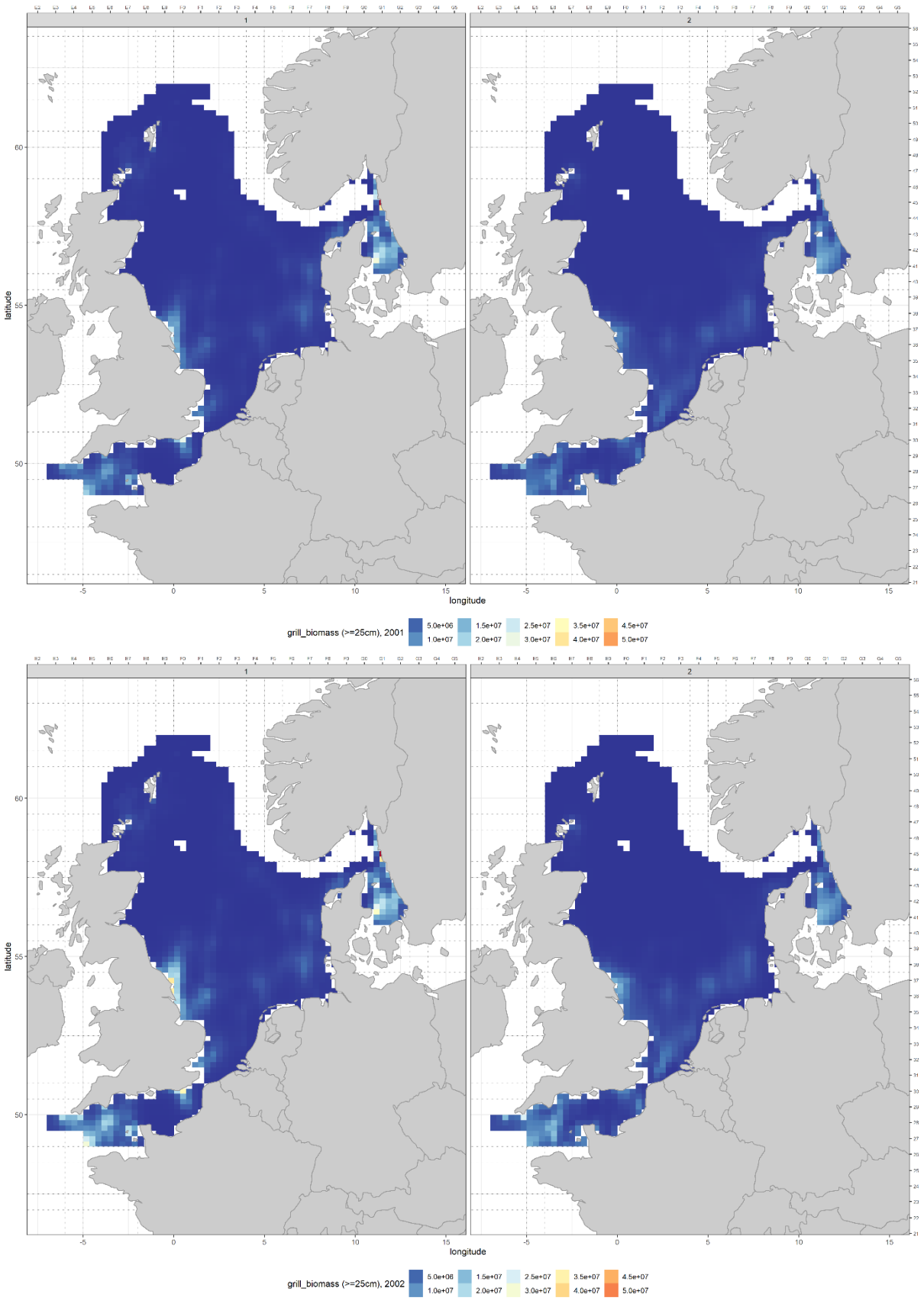
1
2
60
55
50
latitude
-5
0
5
10
15
longitude
grill_biomass (>=25cm), 2001
5.0e+06
1.0e+07
1.5e+07
2.0e+07
2.5e+07
3.0e+07
3.5e+07
4.0e+07
4.5e+07
5.0e+07
grill_biomass (>=25cm), 2002

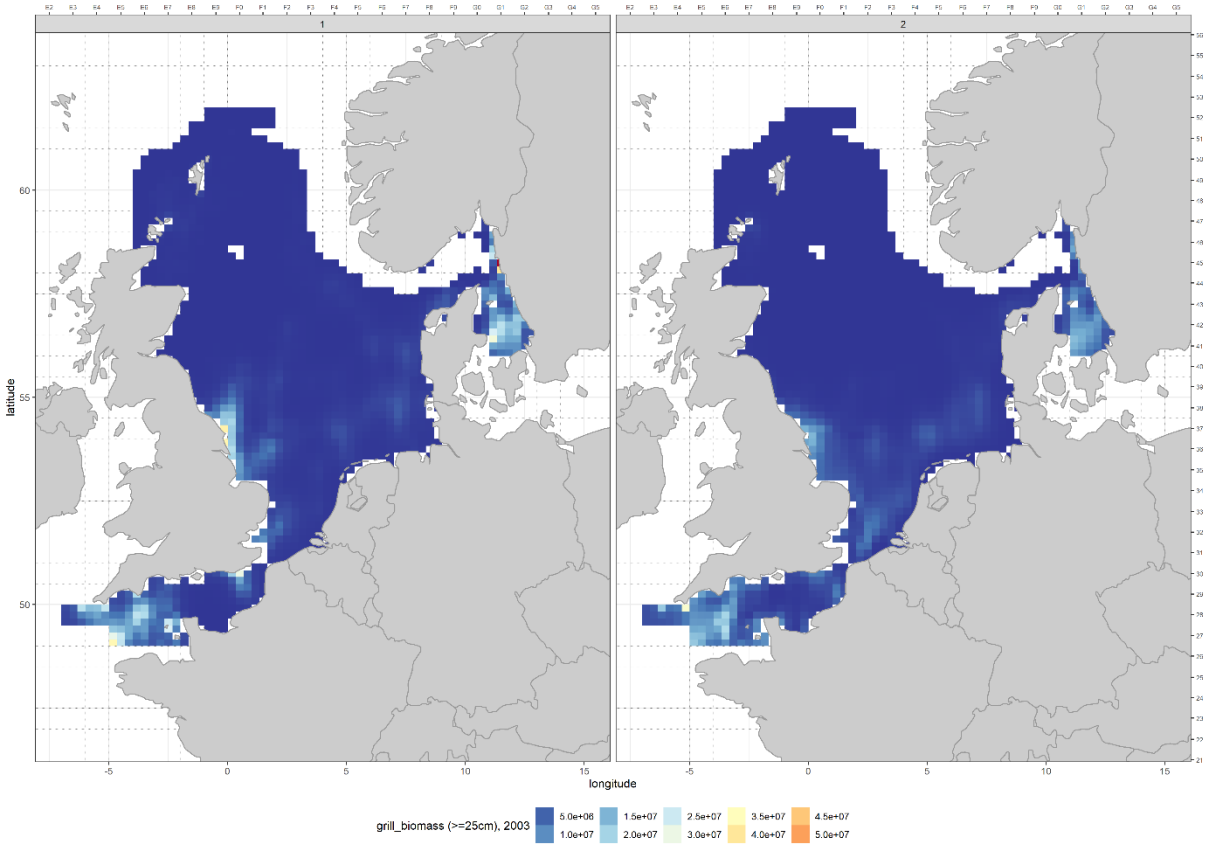
1
2
60
55
50
latitude
-5
0
5
10
15
longitude
grill_biomass (>=25cm), 2003
5.0e+06
1.0e+07
1.5e+07
2.0e+07
2.5e+07
3.0e+07
3.5e+07
4.0e+07
4.5e+07
5.0e+07

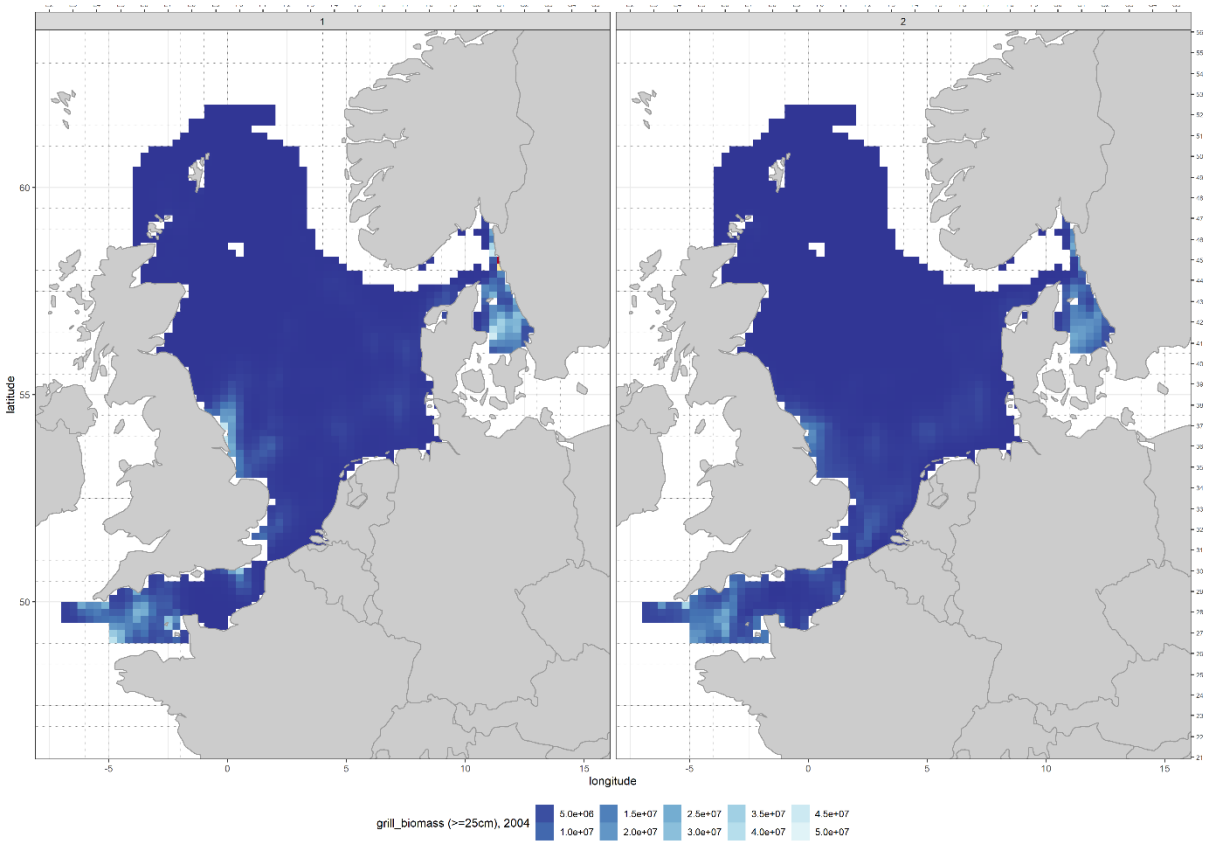
1
2
60
55
50
latitude
-5
0
5
10
15
longitude
grill_biomass (>=25cm), 2004
5.0e+06
1.0e+07
1.5e+07
2.0e+07
2.5e+07
3.0e+07
3.5e+07
4.0e+07
4.5e+07
5.0e+07

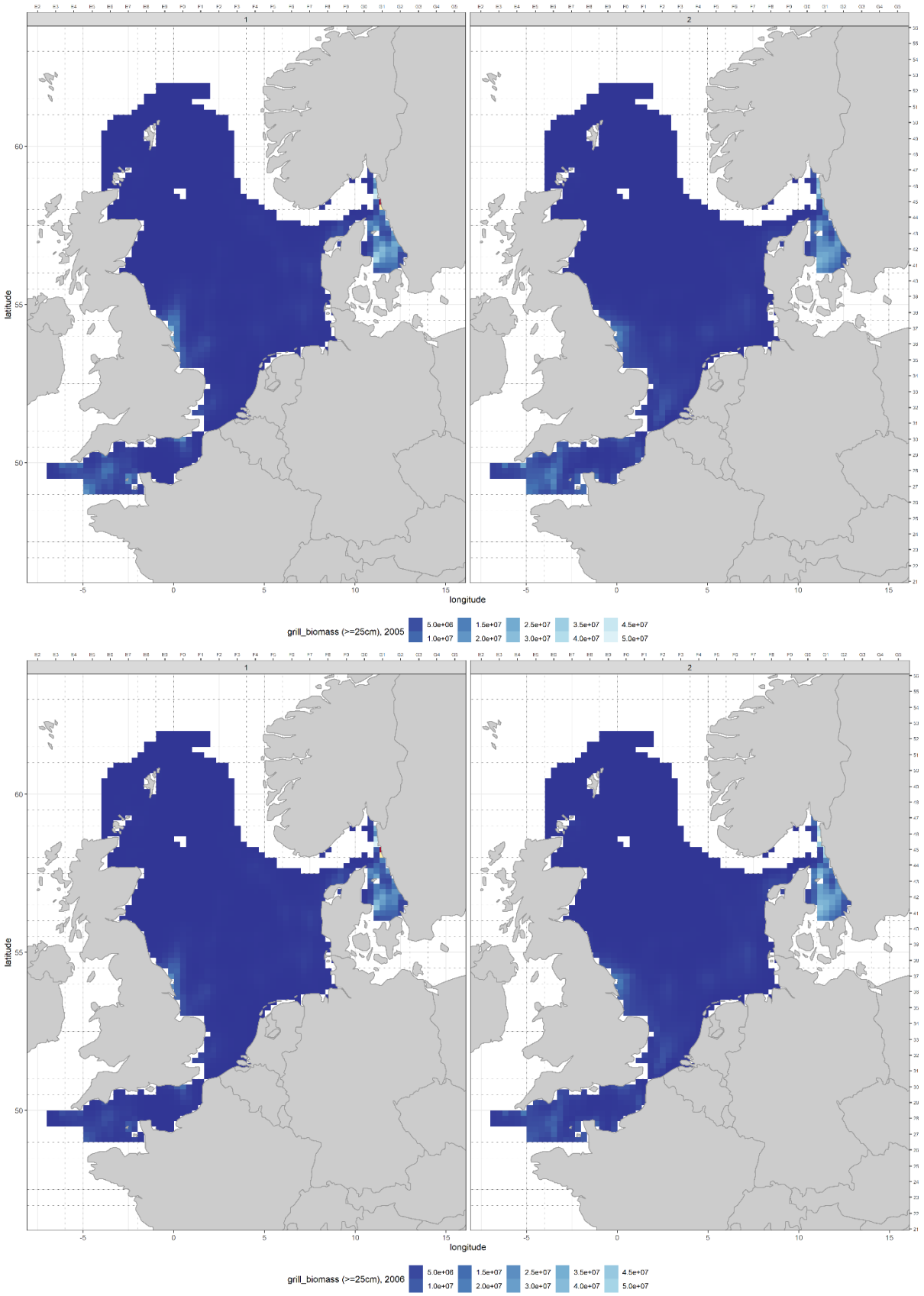
1
2
60
55
50
latitude
-5
0
5
10
15
longitude
grill_biomass (>=25cm), 2005
5.0e+06
1.0e+07
1.5e+07
2.0e+07
2.5e+07
3.0e+07
3.5e+07
4.0e+07
4.5e+07
5.0e+07
grill_biomass (>=25cm), 2006

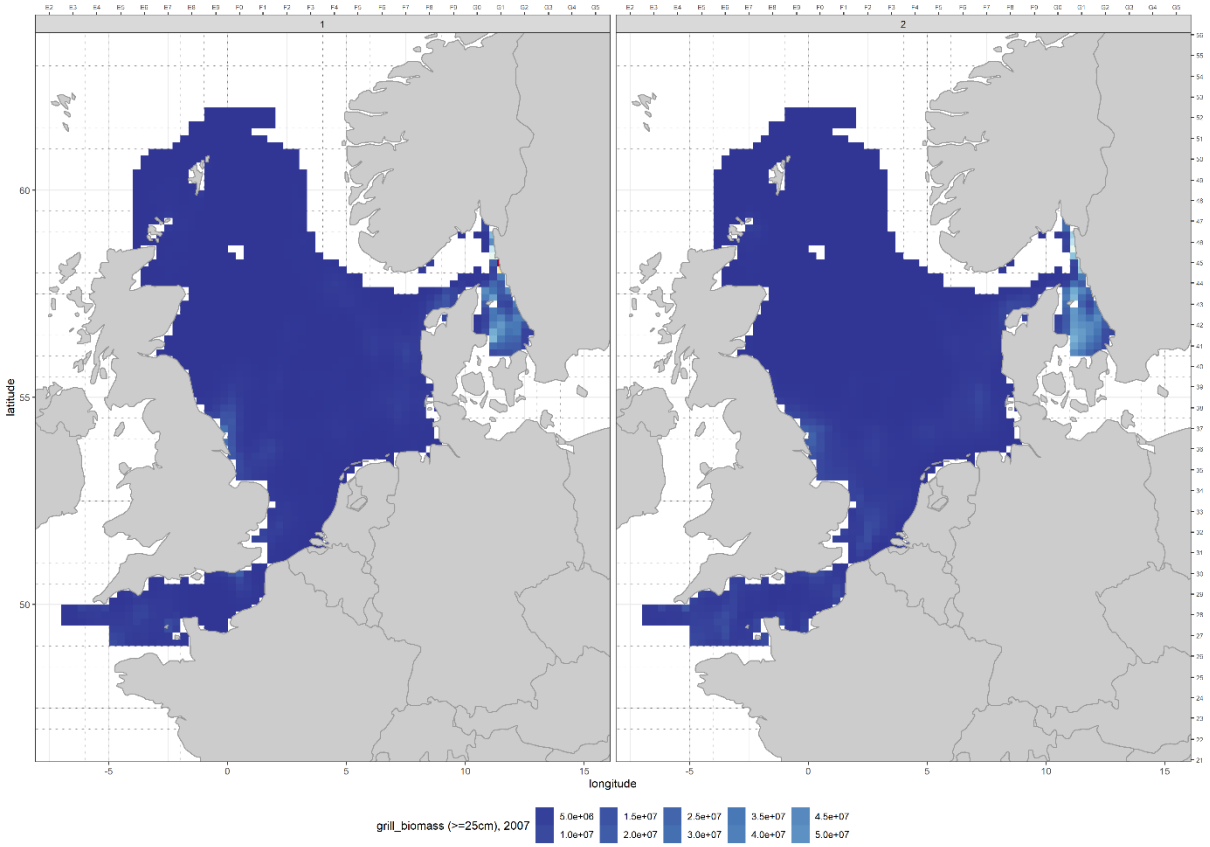
1
2
60
55
50
latitude
-5
0
5
10
15
longitude
grill_biomass (>=25cm), 2007
5.0e+06
1.0e+07
1.5e+07
2.0e+07
2.5e+07
3.0e+07
3.5e+07
4.0e+07
4.5e+07
5.0e+07

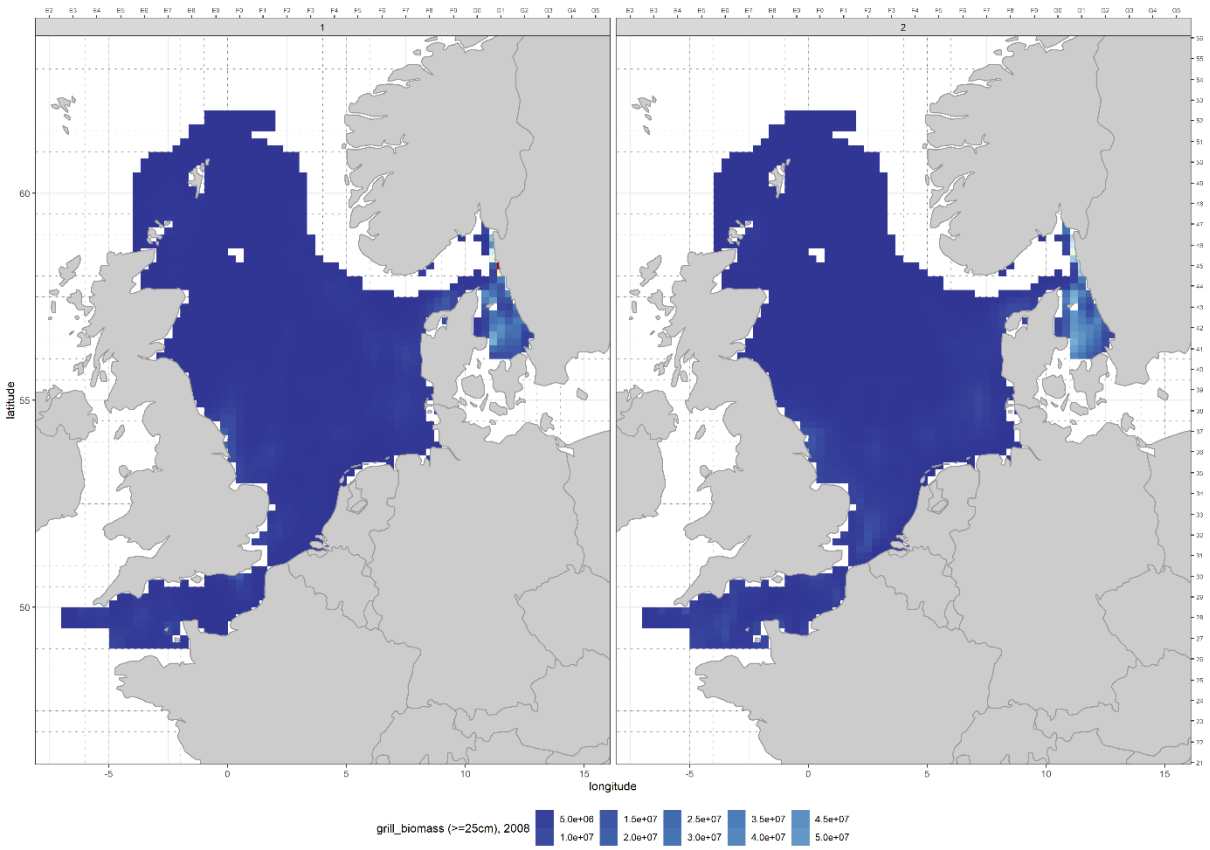
1
2
60
55
50
latitude
-5
0
5
10
15
longitude
grill_biomass (>=25cm), 2008
5.0e+06
1.0e+07
1.5e+07
2.0e+07
2.5e+07
3.0e+07
3.5e+07
4.0e+07
4.5e+07
5.0e+07

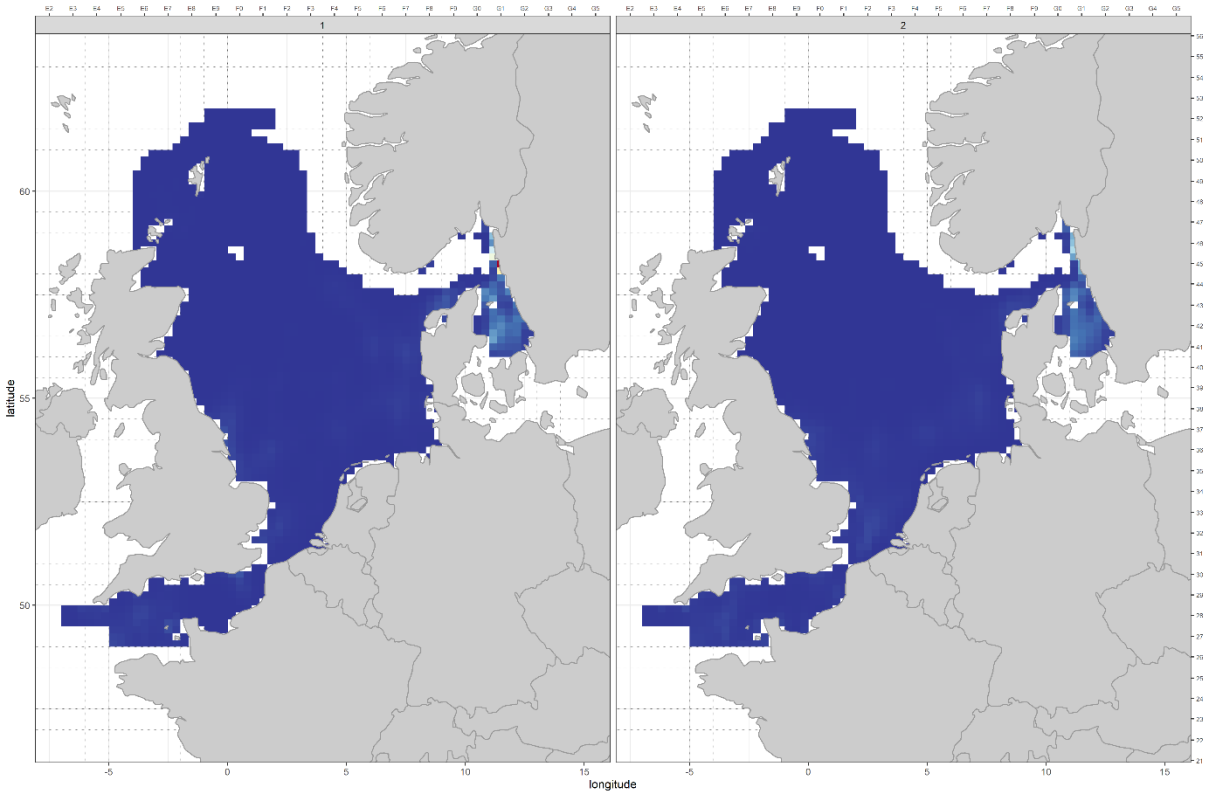
1
2
60
55
50
latitude
-5
0
5
10
15
longitude
grill_biomass (>=25cm), 2009
5.0e+06
1.0e+07
1.5e+07
2.0e+07
2.5e+07
3.0e+07
3.5e+07
4.0e+07
4.5e+07
5.0e+07

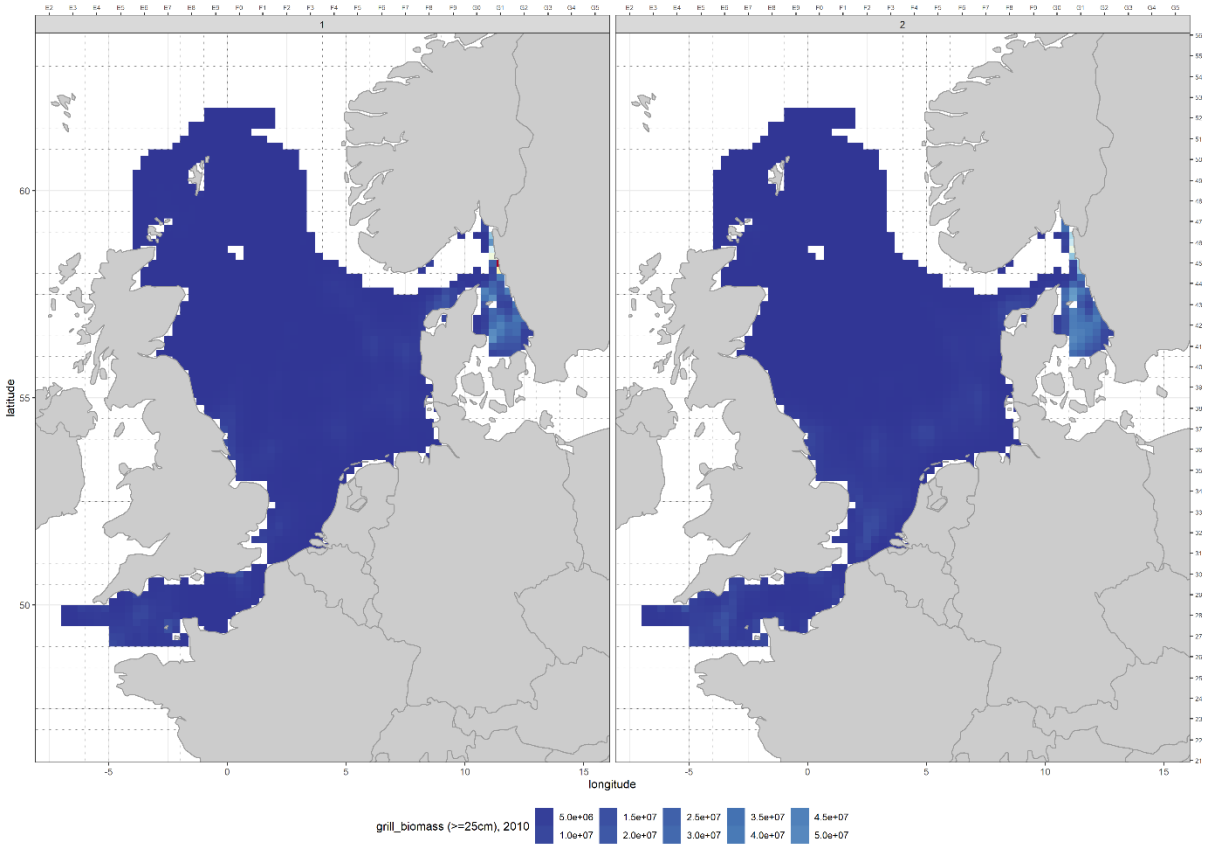
1
2
60
55
50
latitude
-5
0
5
10
15
longitude
grill_biomass (>=25cm), 2010
5.0e+06
1.0e+07
1.5e+07
2.0e+07
2.5e+07
3.0e+07
3.5e+07
4.0e+07
4.5e+07
5.0e+07

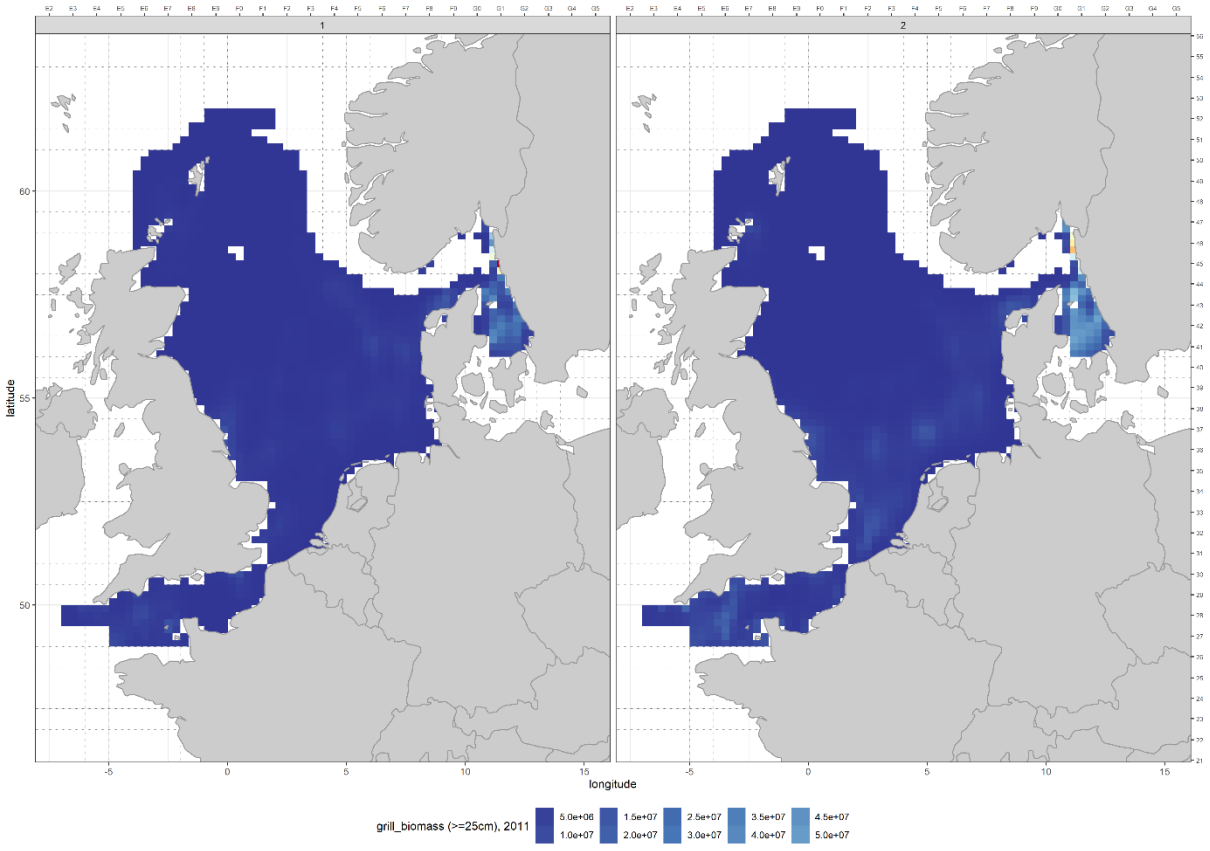
1
2
60
55
50
latitude
-5
0
5
10
15
longitude
grill_biomass (>=25cm), 2011
5.0e+06
1.0e+07
1.5e+07
2.0e+07
2.5e+07
3.0e+07
3.5e+07
4.0e+07
4.5e+07
5.0e+07

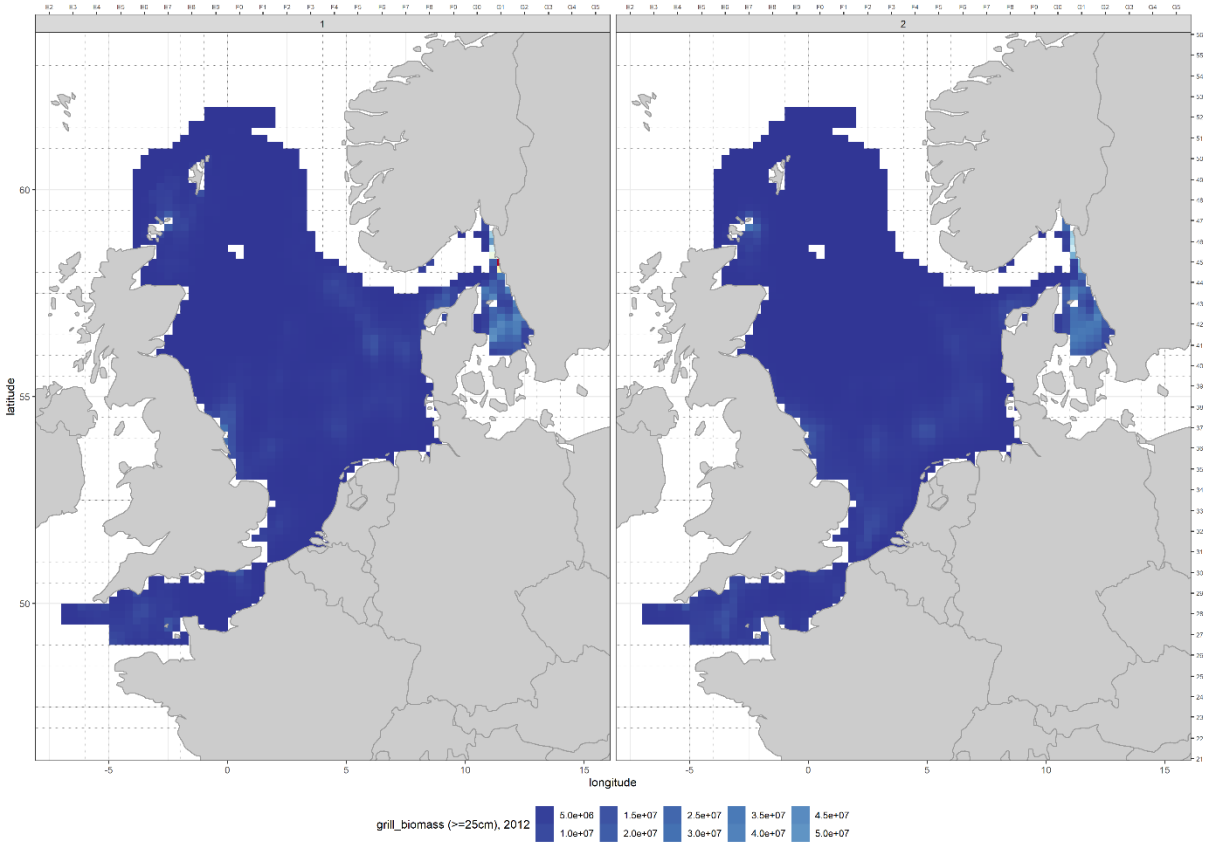
1
2
60
55
50
latitude
-5
0
5
10
15
longitude
grill_biomass (>=25cm), 2012
5.0e+06
1.0e+07
1.5e+07
2.0e+07
2.5e+07
3.0e+07
3.5e+07
4.0e+07
4.5e+07
5.0e+07

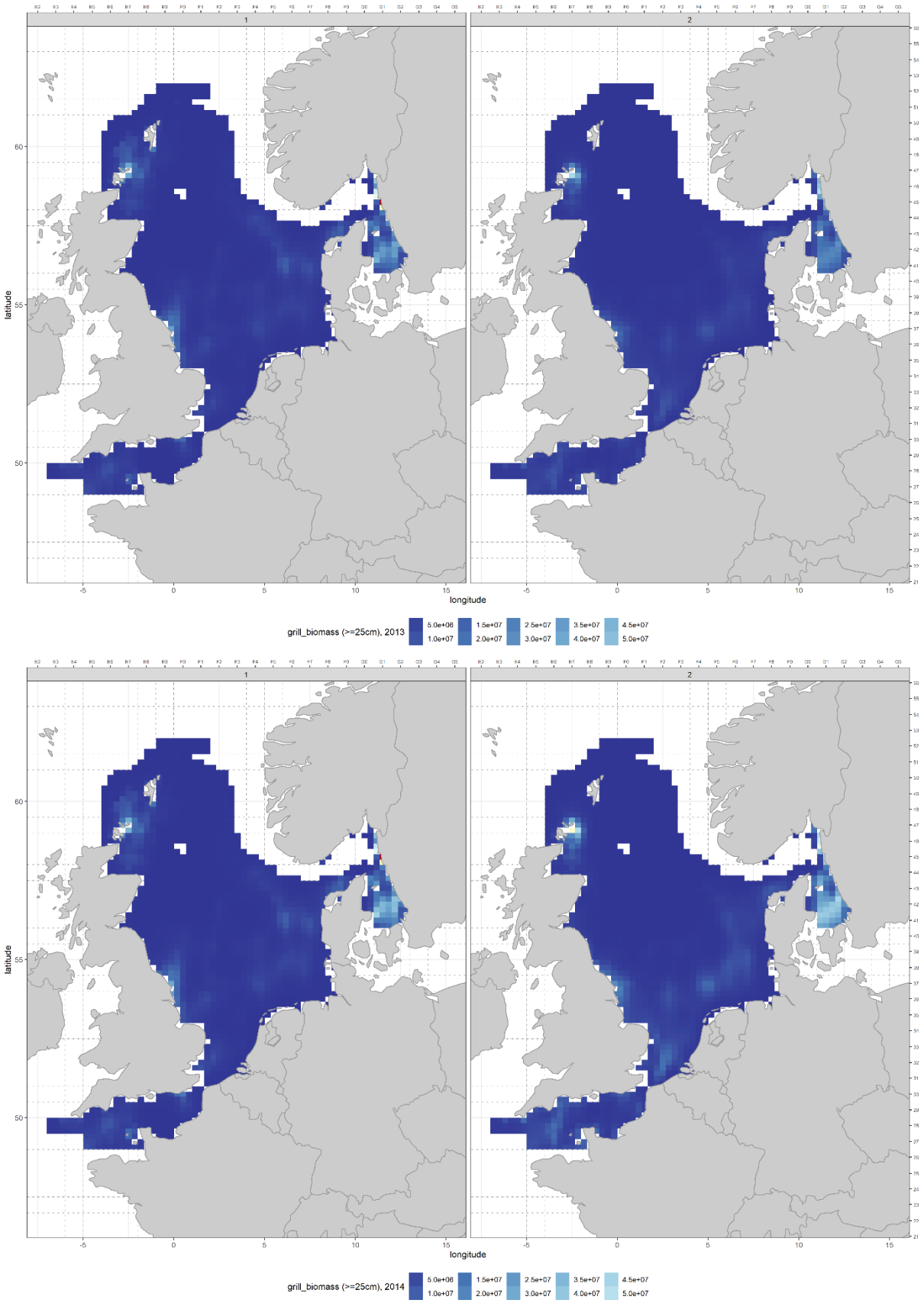
1
2
latitude
longitude
60
55
50
-5
0
5
10
15
grill_biomass (>=25cm), 2013
5.0e+06
1.0e+07
1.5e+07
2.0e+07
2.5e+07
3.0e+07
3.5e+07
4.0e+07
4.5e+07
5.0e+07
grill_biomass (>=25cm), 2014

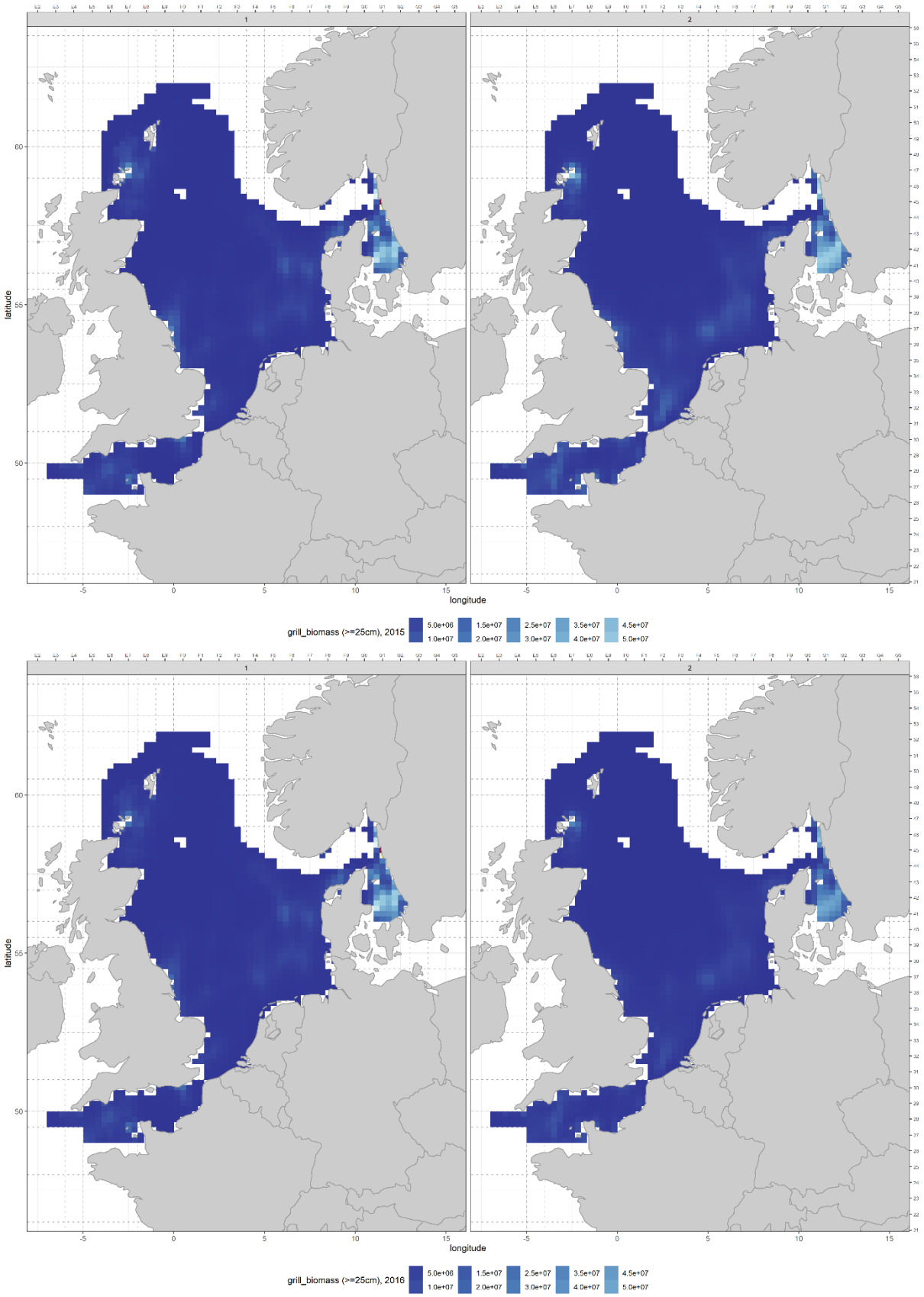
1
2
60
55
50
latitude
-5
0
5
10
15
longitude
grill_biomass (>=25cm), 2015
5.0e+06
1.0e+07
1.5e+07
2.0e+07
2.5e+07
3.0e+07
3.5e+07
4.0e+07
4.5e+07
5.0e+07
grill_biomass (>=25cm), 2016

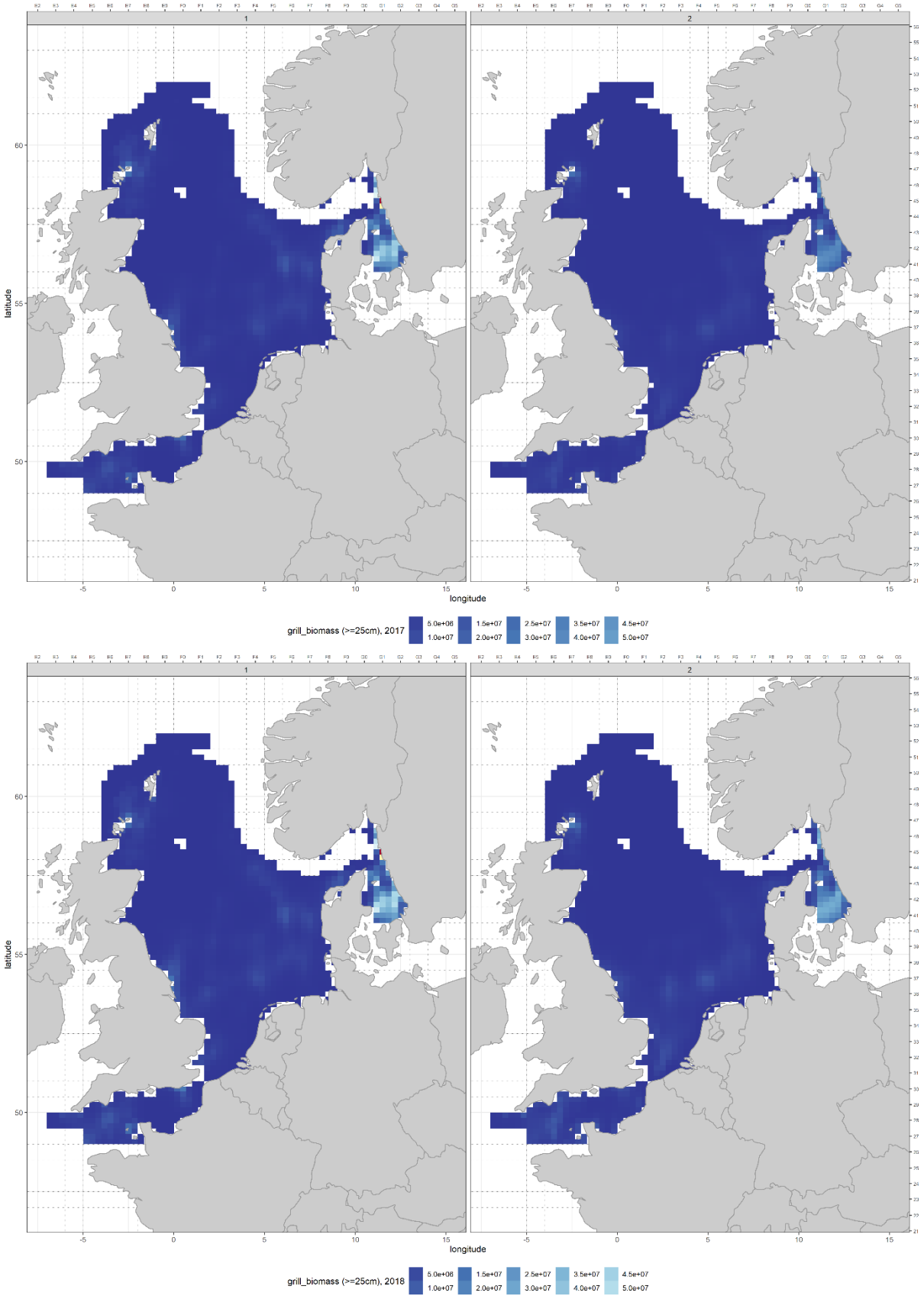
1
2
60
55
50
latitude
-5
0
5
10
15
longitude
grill_biomass (>=25cm), 2017
5.0e+06
1.0e+07
1.5e+07
2.0e+07
2.5e+07
3.0e+07
3.5e+07
4.0e+07
4.5e+07
5.0e+07
grill_biomass (>=25cm), 2018

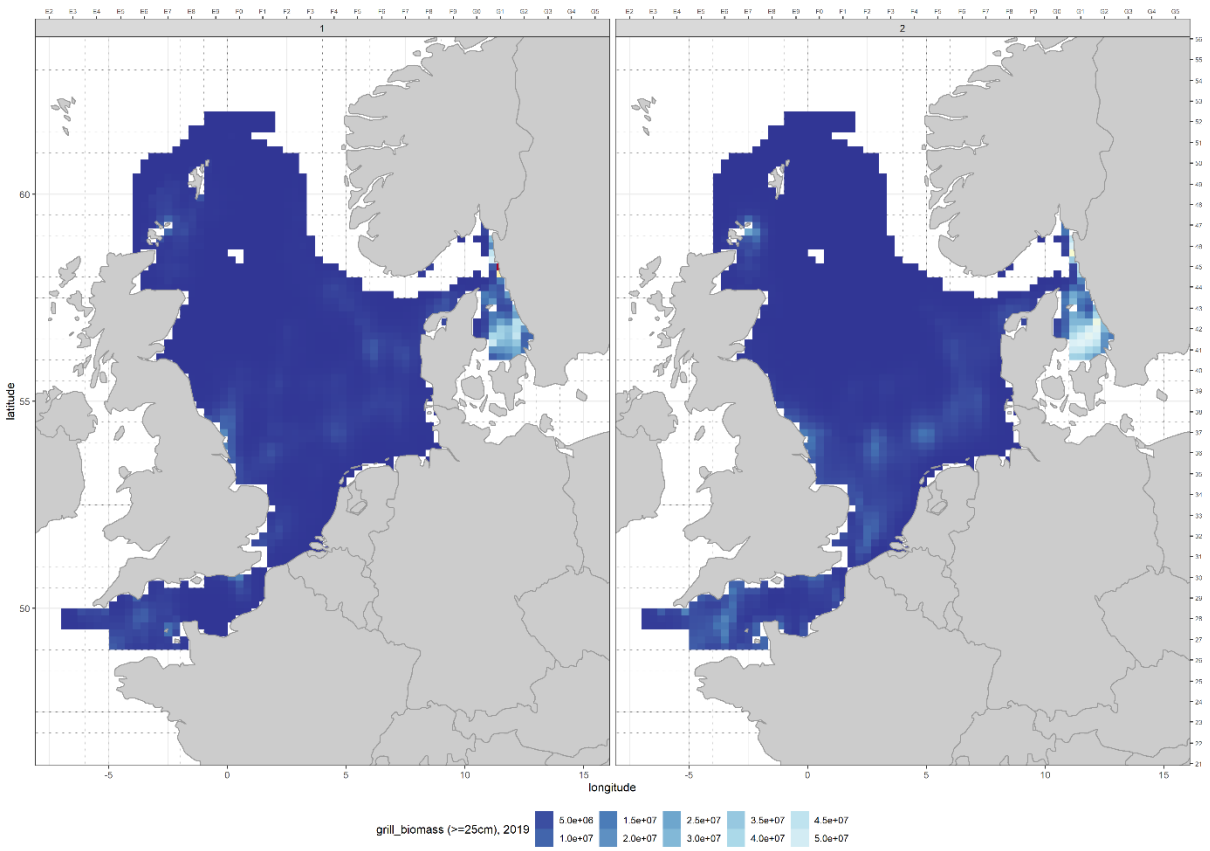
1
2
60
55
50
latitude
-5
0
5
10
15
longitude
grill_biomass (>=25cm), 2019
5.0e+06
1.0e+07
1.5e+07
2.0e+07
2.5e+07
3.0e+07
3.5e+07
4.0e+07
4.5e+07
5.0e+07

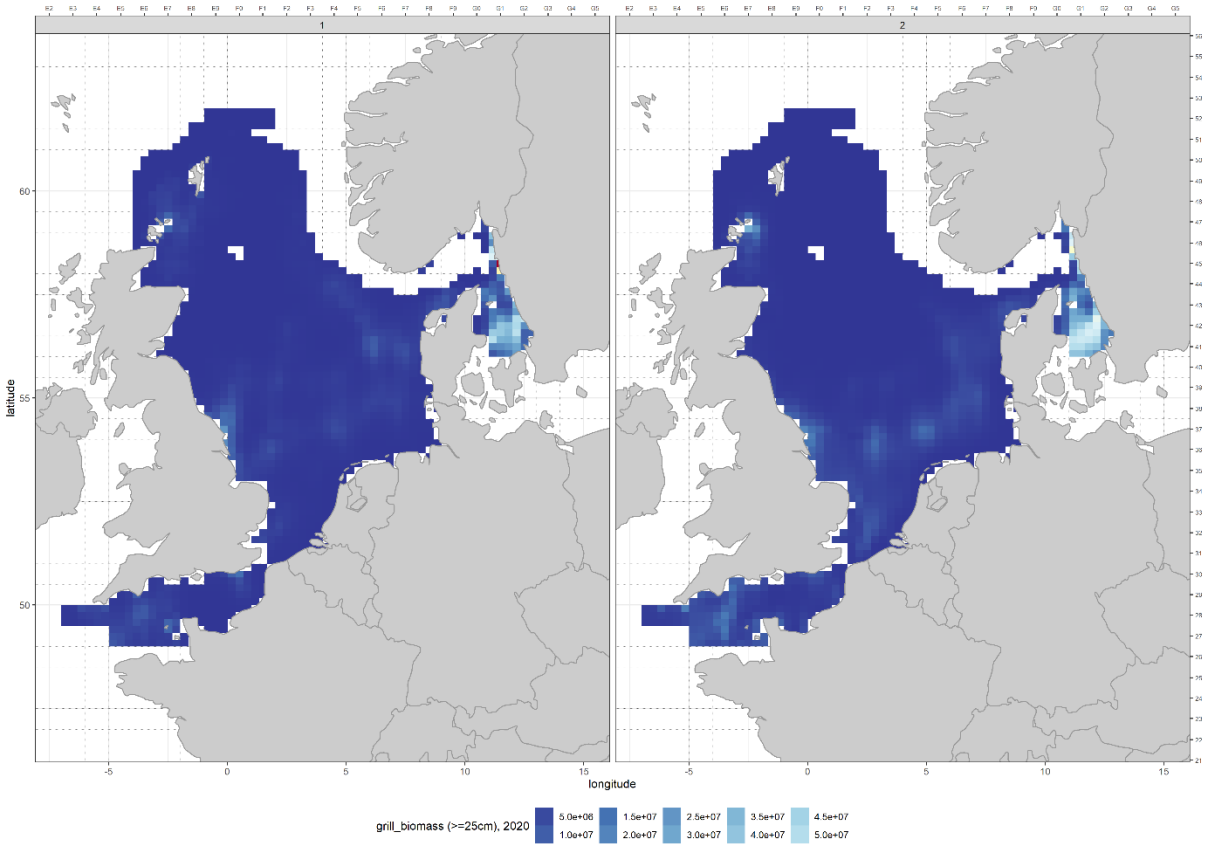
1
2
60
55
50
latitude
-5
0
5
10
15
longitude
grill_biomass (>=25cm), 2020
5.0e+06
1.0e+07
1.5e+07
2.0e+07
2.5e+07
3.0e+07
3.5e+07
4.0e+07
4.5e+07
5.0e+07

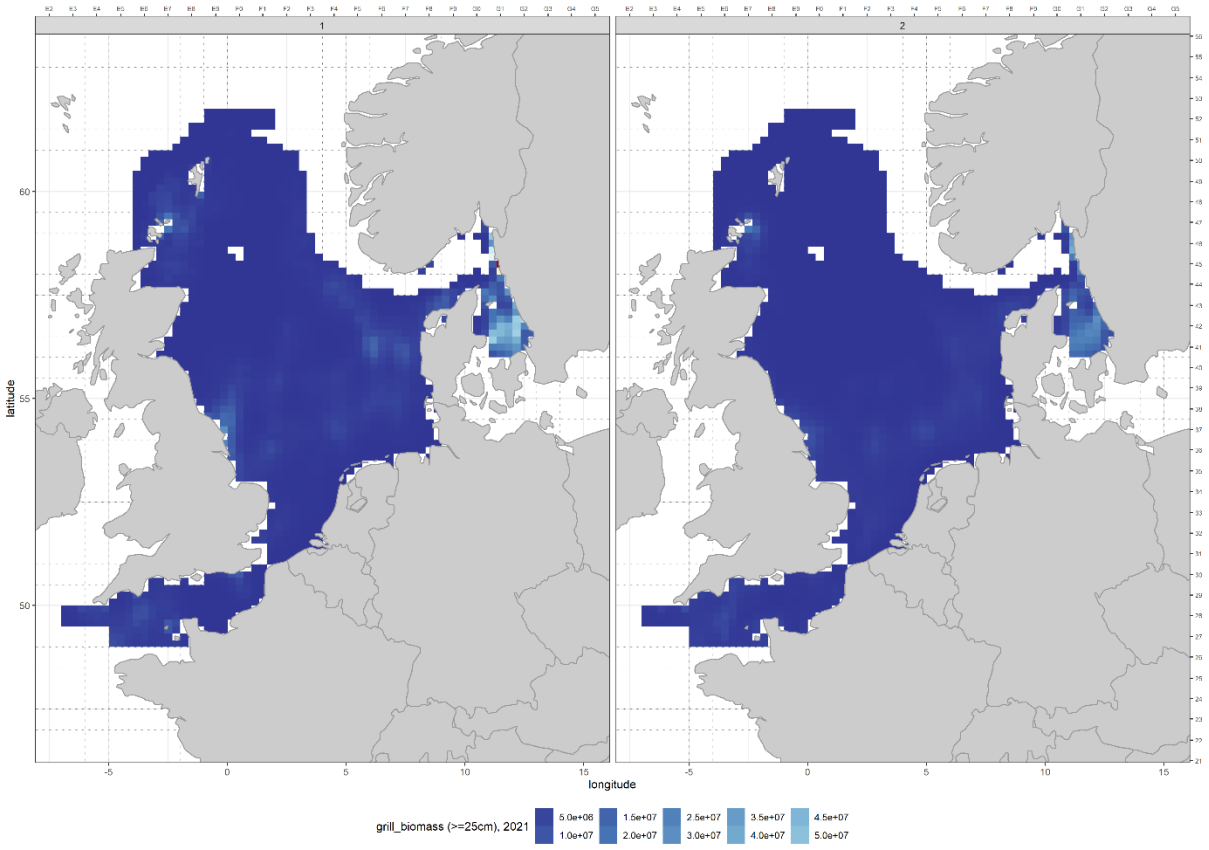
1
2
60
55
50
latitude
-5
0
5
10
15
longitude
grill_biomass (>=25cm), 2021
5.0e+06
1.0e+07
1.5e+07
2.0e+07
2.5e+07
3.0e+07
3.5e+07
4.0e+07
4.5e+07
5.0e+07

## 2.8.3 WD Annex 3: Life-history parameters for brill (*Scophthalmus rhombus*) in areas 27.3a47de (Greater North Sea)

*Author: Lies Vansteenbrugge and Damian Villagra (ILVO, Belgium)*

**1. Introduction**

Life-history information is important for evaluating the plausibility of the estimated production function by SPiCT. This information can help to set informative priors on for example r (the intrinsic rate of population increase).

To calculate the different life-history parameters, the commercial data from InterCatch was used from 2014–2021 (i.e. the available time-series), complemented with survey data (same data as is used for the survey index; see WD 2), Belgian commercial data on maturity, information from literature and from the FishLife package (Thorson *et al*., 2017; Thorson, 2020).

**2. Background information on life cycle characteristics of brill**

Compiled from van der Hammen *et al*. (2013) and Vandamme *et al*. (2020): Brill occurs in relatively low abundance throughout its distributional range. The species inhabits shallow soft bottom habitats where they feed on crustaceans and fish. Brill matures over a protracted period (March–July) and has an intermittent release of eggs, which is characteristic for an 'income spawner'. Pelagic eggs are spawned offshore and larvae are transported by wind-driven currents to the surf zone of sandy beach nurseries. Early demersal juveniles are restricted to the shallow sandy grounds on exposed shores. Large specimens can be observed to a depth of about 100 m.

**3. Length at first capture (Lc)**

Length at first capture (Lc) is defined as the first length class where abundance is larger than or equal to half of the maximum abundance. Using the available commercial catch data (InterCatch), the Lc is shown per year in Table 2.C1 and varies over the years. The total Lc was estimated as 210 mm and the average Lc was 226 mm.

The survey dataset contains data from 1999–2021 (same dataset as used for the survey index). The Lc in the survey data are influenced by years of strong recruitment or by years with few large specimen caught (Table 2.C1). The total Lc was estimated at 240 mm and the average Lc was 204 mm.

**Table 2.C1. Length at first capture (Lc) by year for commercial catches (2014–2021) and survey data (1999–2021).**

| Year | Survey Lc (mm) | Year | Survey Lc (mm) | Year | Survey Lc (mm) | Catch Lc (mm) |
|---|---|---|---|---|---|---|
| 1999 | 250 | 2007 | 180 | 2014 | 140 | 170 |
| 2000 | 260 | 2008 | 150 | 2015 | 250 | 250 |
| 2001 | 160 | 2009 | 140 | 2016 | 240 | 290 |
| 2002 | 260 | 2010 | 150 | 2017 | 260 | 210 |
| 2003 | 250 | 2011 | 220 | 2018 | 150 | 210 |
| 2004 | 240 | 2012 | 290 | 2019 | 170 | 210 |
| 2005 | 150 | 2013 | 110 | 2020 | 260 | 240 |
| 2006 | 150 | | | 2021 | 260 | 230 |

### 4. Maximum observed length in the stock ($L_{max}$)

The maximum observed length in the stock ($L_{max}$) was calculated as the 99th percentile of the length frequency distribution being 542 mm (Figure 2.C1). For this calculation, only landings data were retained.

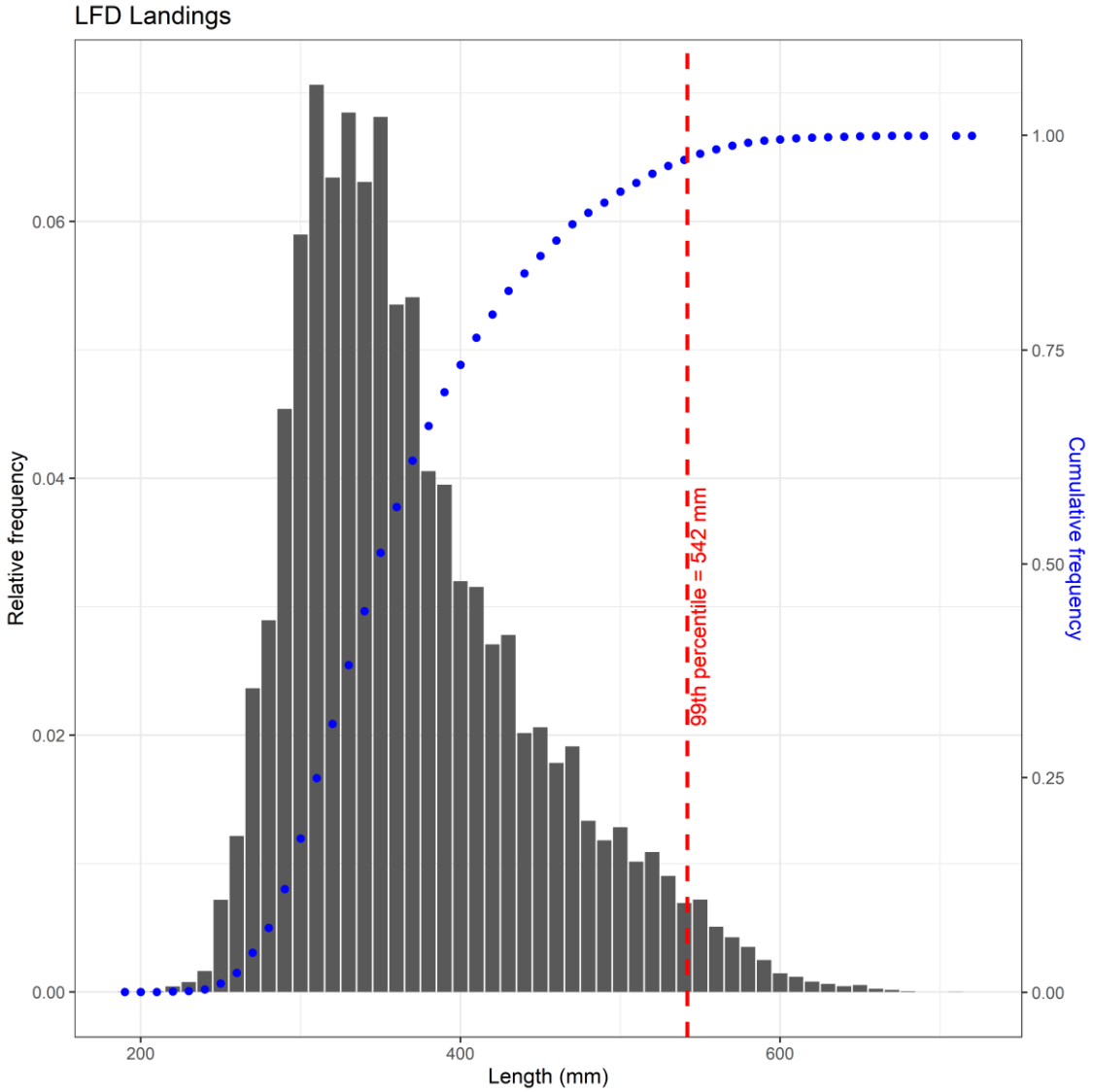


**Figure 2.C1. Landings length frequency distribution, relative (left *y*-axis) and cumulative (right *y*-axis) with indication of the 99th percentile corresponding to $L_{max}$.**

When using the survey dataset (all data, 1999–2021), $L_{max}$ is estimated at 503 mm (Figure 2.C2).

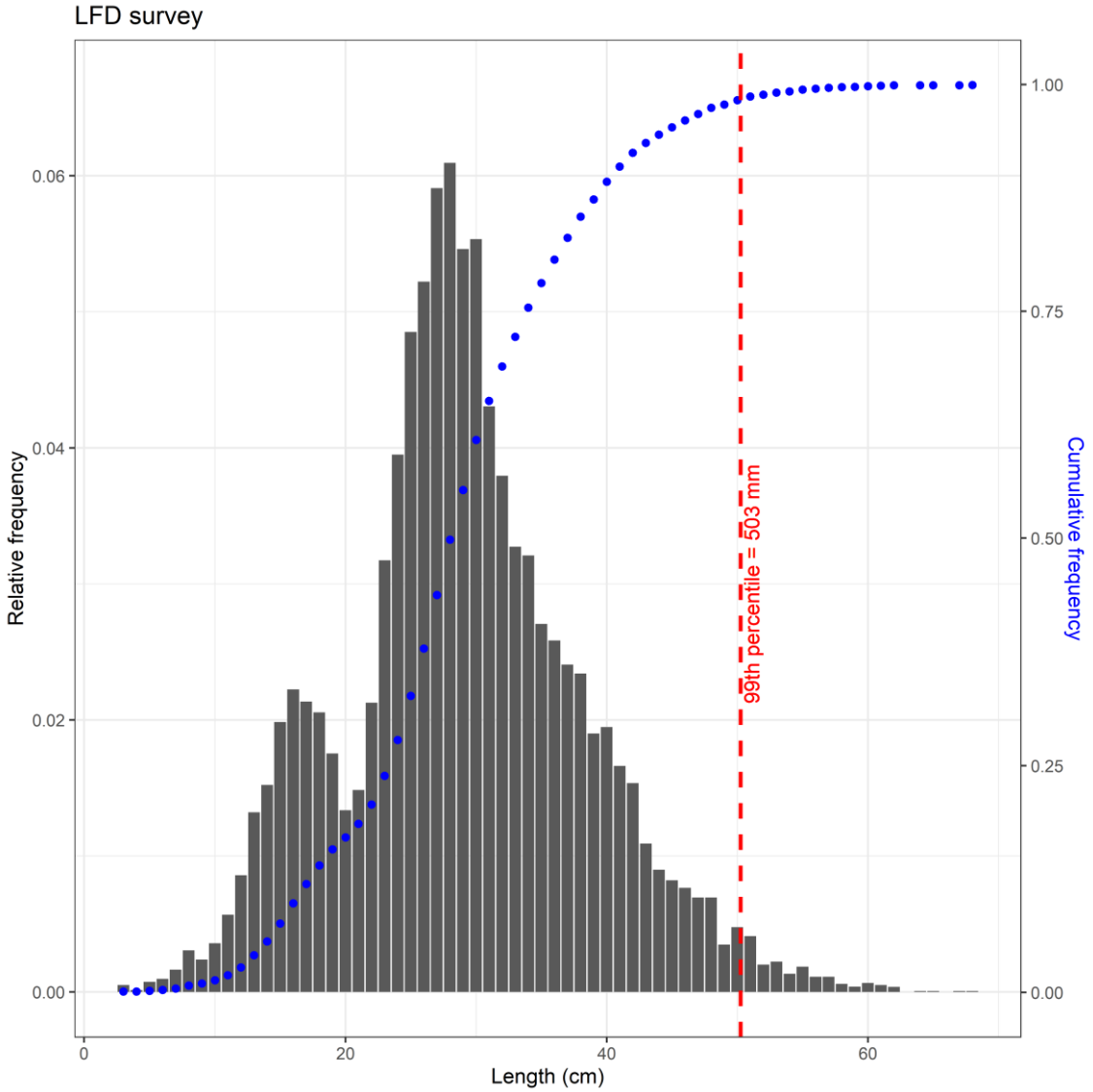


**Figure 2.C2. Length frequency distribution of survey data, relative (left *y*-axis) and cumulative (right *y*-axis) with indication of the 99th percentile corresponding to $L_{max}$.**

### 5. Asymptotic length ($L_{inf}$)

The asymptotic length was estimated using the statistical relationship provided by Garcia-Carrerras *et al*. (2016):

$$\log_{10} L_\infty = 0.068260\ (\pm 0.010451) + 0.969112\ (\pm\ 0.006318)\ \log_{10} L_{\max}$$

Using commercial landings data and $L_{max}$ as calculated in §4 using catch data, this resulted in $L_{inf}$ = 522 mm. Using survey data and $L_{max}$ as calculated in §4 using survey data, this resulted in $L_{inf}$ = 521 mm.

Using the von Bertalanffy Growth Model ($Length \sim Linf\ *\ (1\ -\ exp(-K * (Age - t0)))$) applied to the survey data, the asymptotic length was estimated at 348 mm for males and 468 mm for females. These values are likely to be underestimated because the survey methodology is not considered appropriate to target large brill.

Van der Hammen *et al*. (2013) investigated $L_{inf}$ using Dutch survey and market samples. They found sexual dimorphism for brill in the North Sea, with females reaching a larger maximum body size than males (Table 2.C2).

**Table 2.C2. Asymptotic length by sex from van der Hammen *et al*. (2013).**

| Sex | $L_{inf}$ (mm) |
|---|---|
| Males | 433 |
| Females | 580 |

FishBase[3] gives an $L_{inf}$ estimate of 566 mm for females in the southern North Sea. The estimates for males (388 mm) are considered questionable.

The FishLife package from James Thorson and his shiny R visualization estimate $L_{inf}$ at 413 mm (Figure 2.C5.; Table 2.C4).

### 6. Brody coefficient (K)

Using the von Bertalanffy Growth Model ($Length \sim Linf\ *\ (1\ -\ exp(-K * (Age - t0)))$) applied to the survey data, the Brody coefficient (K) was estimated at 0.71 years[2] for males and 0.466 years[2] for females.

Van der Hammen *et al*. (2013) provide estimates for the growth rate K by sex for the southern North Sea using the model of Somers (1988). For males K = 0.48 and for females K = 0.38. The highest somatic growth takes place in the second half of the year.

FishBase[2] estimates K = 0.320 for females in the southern North Sea. The estimates for males (0.590) are considered questionable.

The FishLife package from James Thorson and his shiny R visualization tool show that individual growth (K) varies around 0.5 (Figure 2.C5). From the FishLife package the predictive mean for K = 0.436 (Table 2.C4).

[3] https://www.fishbase.se/popdyn/PopGrowthList.php?ID=529

### 7. Theoretical age at zero length ($t_0$)

Using the von Bertalanffy Growth Model applied to the survey data, the theoretical age at zero length was estimated at −0.772 years for males and −0.862 years for females.

FishBase[4] estimates length zero to be reached at the theoretical age of −1.19 years for females in the southern North Sea.

### 8. Natural mortality (M)

Natural mortality is estimated by the FishLife package at 0.715 (Figure 2.C5; Table 2.C4). This value is substantially higher than for turbot (*Scophthalmus maximus*) a closely related species, where M = 0.354.

### 9. Length-at-maturity ($L_m$)

From the FishLife package, length at maturity is 19.613 cm (Figure 2.C5; Table 2.C4).

Van der Hammen *et al*. (2013) found that brill shows sex differences in size at 50% maturity: for males 18.4 cm and females 31.3 cm. However, immature males were undersampled in this study, which might have resulted in an underestimation.

The Belgian 2020 commercial data on maturity were analysed. Maturity data were available from 2017–2021, but the proportion of specimen per area, quarter, sex, catch category and maturity stage was more evenly distributed in 2020 compared to the other years. For 2020, 304 specimen were available, from which 14 brill were immature, 290 mature (Table 2.C3; length range from 23–62 cm). Using commercial data for estimating maturity is not optimal, because the proportion of immature fish could be underestimated. However, no survey data were available (due to the lack of a data call for this benchmark).

**Table 2.C3. Overview of Belgian 2020 commercial on maturity of brill.**

| | 2020 | Q1 | Q2 | Q3 | Q4 | 4 | 7.d | 7.e | Dis-cards | Land-ings | M | F |
|---|---|---|---|---|---|---|---|---|---|---|---|---|
| Immature | 14 | 4 | 1 | 4 | 5 | 4 | 10 | 0 | 4 | 10 | 6 | 8 |
| Mature | 290 | 94 | 6 | 80 | 110 | 121 | 169 | 0 | 55 | 235 | 140 | 150 |

Clear sexual differences are present with males maturing at a lower length than females (males 50% mature at 32.5 cm and females at 44 cm; Figure 2.C3).

[4] https://www.fishbase.se/popdyn/PopGrowthList.php?ID=529

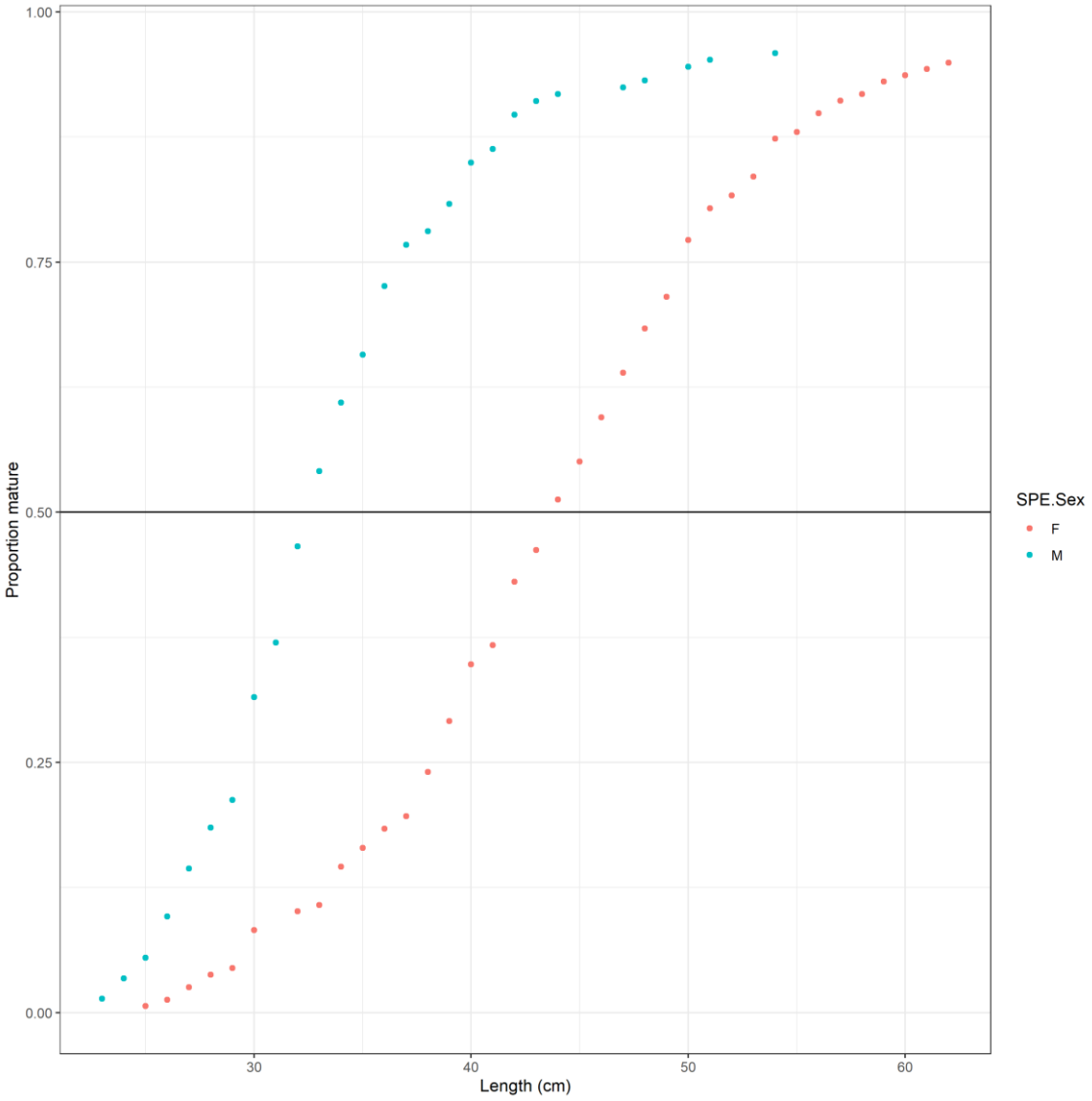


**Figure 2.C3. Maturity ogive at length using the Belgian commercial 2020 data on brill. Horizontal line presenting proportion where 50% is mature.**

## 10. Age-at-maturity ($t_m$)

From the FishLife package, age at maturity is 1.512 (Figure 2.C5; Table 2.C4).

Van der Hammen *et al*. (2013) found that brill shows sex differences in age at 50% maturity: for males age 1.1 and females age 1.6. However, immature males were undersampled in this study, which might have resulted in an underestimation.

The same Belgian dataset was used as described in §9 to explore age at maturity (Table 2.C3). Similarly to the length at maturity, sexual differences are present with males maturing approximately 1 year earlier than females (males 50% mature at age ±1.5 and females at ±2.5; Figure 2.C4).

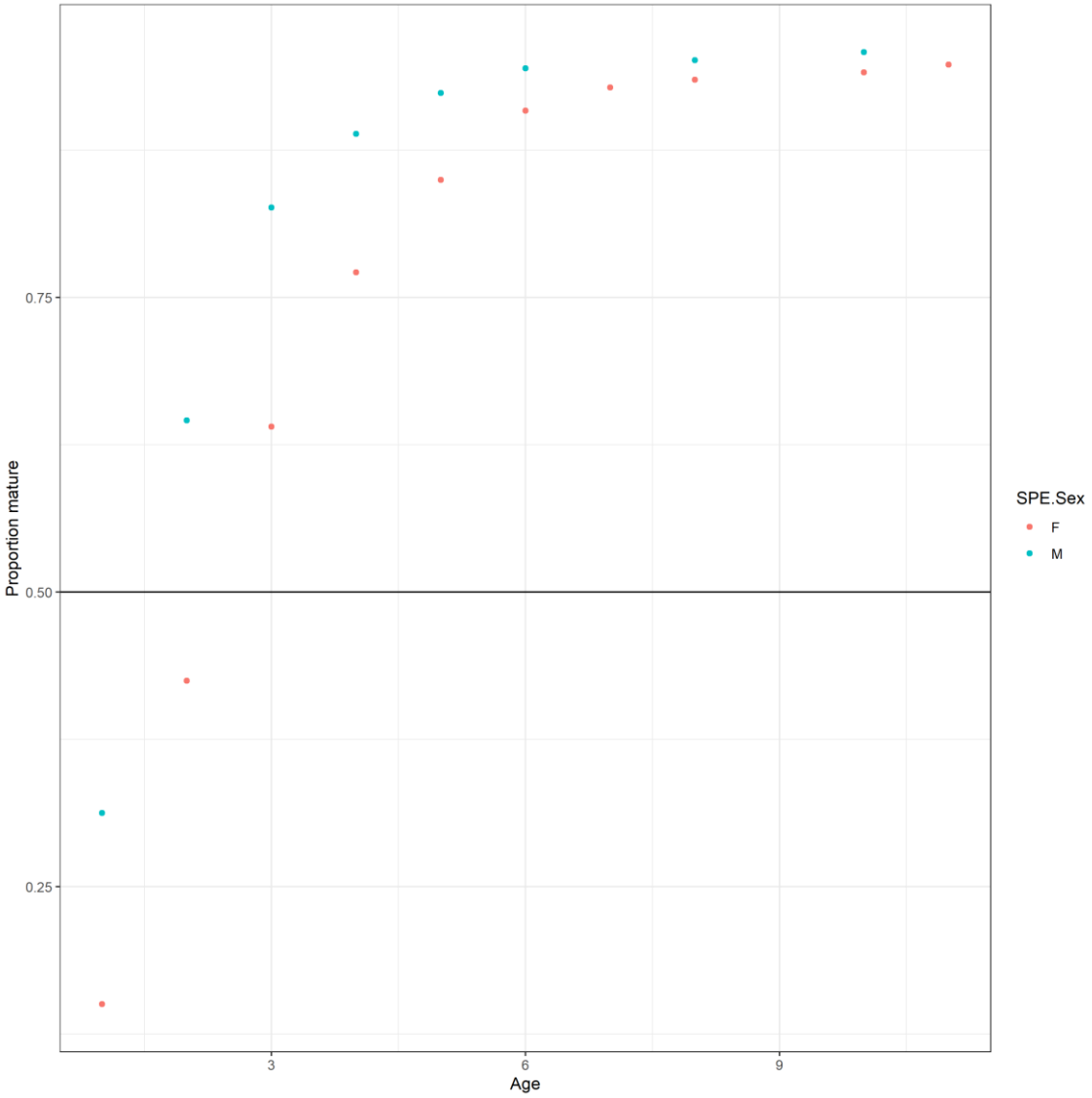


**Figure 2.C4. Maturity ogive at age using the Belgian commercial 2020 data on brill. Horizontal line presenting proportion where 50% is mature.**

### 11. Maximum age ($t_{max}$)

From the FishLife package, maximum age is 7.452 (Figure 2.C5; Table 2.C4).

Van der Hammen *et al*. (2013) estimated longevity from market sampling. The oldest brill recorded for males was age 16 (n = 2951) and for females age 22 (n = 5039).

In the available Belgian age information on brill (2017–2021), the maximum age is 14 years old for males and 12 years old for females (Table 2.C3).

**Table 2.C4. Overview of life-history traits as estimated by the FishLife package (Thorson *et al.*, 2017; Thorson, 2020).**

| Life-history parameter | | Value | Value (bias corrected) |
|---|---|---|---|
| $L_{inf}$ | Asymptotic length | 41.316 cm | 41.316 cm |
| K | Growth coefficient | 0.436 | 0.436 |
| $W_{inf}$ | Asymptotic mass | 901.638 g | 901.638 g |
| $t_{max}$ | Maximum age | 7.452 | 7.452 |
| $t_m$ | Age at maturity | 1.512 | 1.512 |
| M | Natural mortality rate | 0.715 | 0.715 |
| $L_m$ | Length at maturity | 19.613 cm | 19.613 cm |
| ln(var) | | 0.302 | 0.302 |
| rho | Autocorrelation of recruitment variability | 1.581 | 1.581 |
| ln(MASPS) | Maximum annual spawners per spawner in excess of replacement | 37.233 | 37.233 |
| ln(margsd) | Marginal standard deviation of recruitment variability | 0.559 | 0.559 |
| h | Steepness | 2.380 | 2.380 |
| logitbound h | | 15.379 | 15.379 |
| ln($F_{MSY}$ over M) | Fishing mortality ratio at MSY | 6.443 | 6.443 |
| ln($F_{MSY}$) | Fishing mortality at MSY | 4.668 | 4.668 |
| ln(r) | Intrinsic growth rate | 0.977 | 0.977 |
| r | | 2.849 | 2.849 |
| ln(G) | Generation time | 4.011 | 4.011 |
| G | | 94.854 | 94.854 |
| Temperature | Average temperature for spatial distribution | 18.628 °C | 18.628 °C |

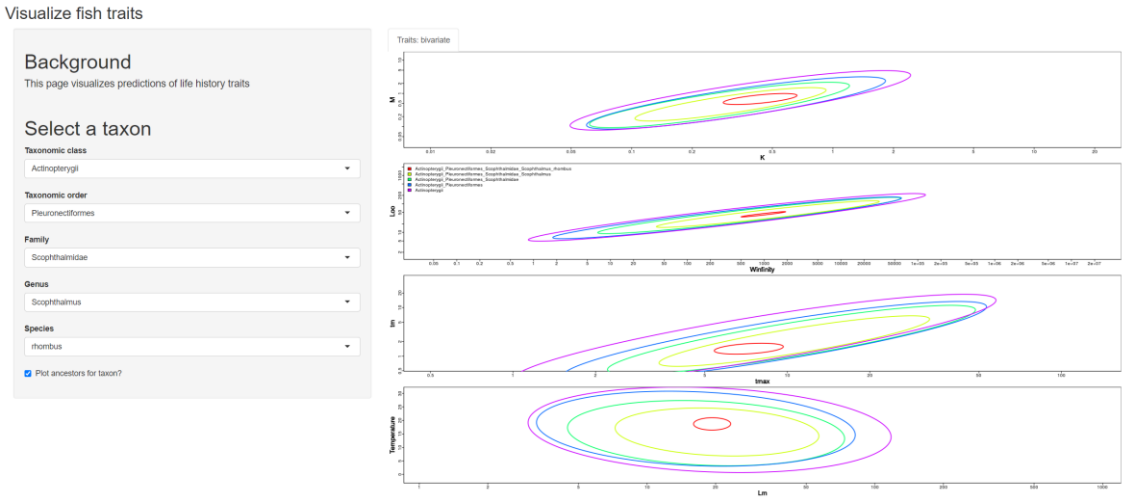


**Figure 2.C5. Visualization of *Scophthalmus rhombus* traits from Thorson *et al.* (2017); Thorson (2020); https://james-thorson.shinyapps.io/FishLife/**

## 12. Length-weight relationship (a and b parameter)

The length-weight relationship was investigated for the commercial data for the period 2014–2021 (in g and mm; Figure 2.C6). Only the sampled data were used (not the estimated length-weight).

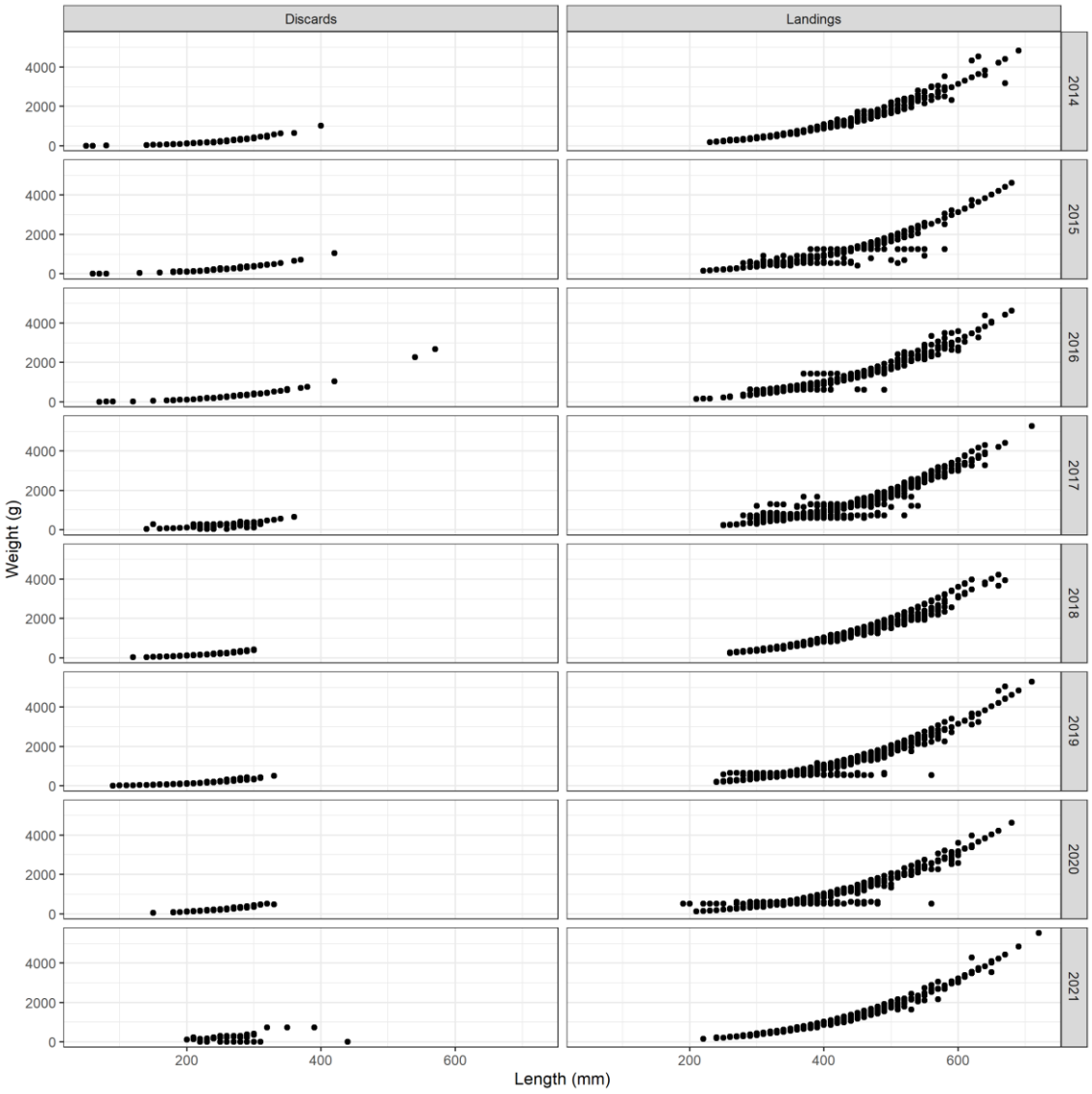


**Figure 2.C6. Length-weight relationship of the commercial brill data for the period 2014–2021 by catch category.**

Due to the limited amount length-weight information on discards, a and b parameters were calculated for landings and discards together (Table 2.C5).

**Table 2.C5. Length-weight parameters of the commercial brill data for the period 2014–2021 (discard and landings together; using g and mm).**

| Year | a | b |
|---|---|---|
| 2014 | 1.3599394e-05 | 3.0095819 |
| 2015 | 2.4315216e-05 | 2.9079952 |
| 2016 | 1.3062661e-05 | 3.0166608 |
| 2017 | 2.1601148e-05 | 2.9323129 |
| 2018 | 1.2364315e-05 | 3.0234852 |
| 2019 | 1.5096242e-05 | 2.9888694 |
| 2020 | 2.2169157e-05 | 2.9235556 |
| 2021 | 2.0599476e-06 | 3.3131908 |

It is unclear why the 2021 a and b parameters deviated from the other years (Figure 2.C7). The overall a and b parameters are 1.44e-05 and 2.99 respectively. When not considering 2021, a is higher (2.09e-05) and b is lower (2.94).

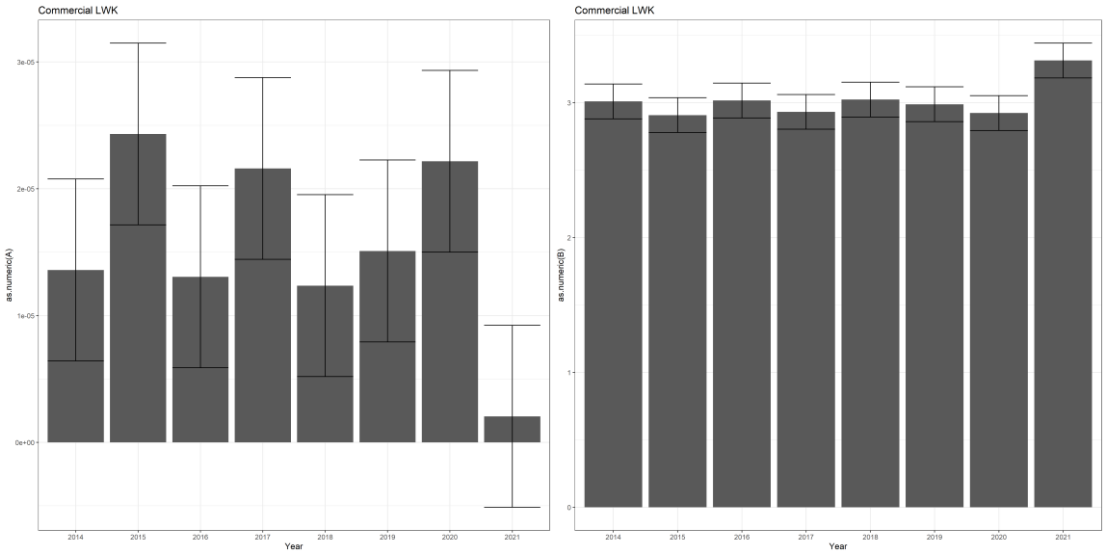


**Figure 2.C7. Variation in a (left) and b (right) parameters (± SD) over the period 2014–2021 for the commercial brill data.**

Survey data were analysed for the period 1999–2021 (same database as used for the survey index calculation; Figure 2.C8). A and b parameters were calculated per year (using g and mm; Table 2.C6).

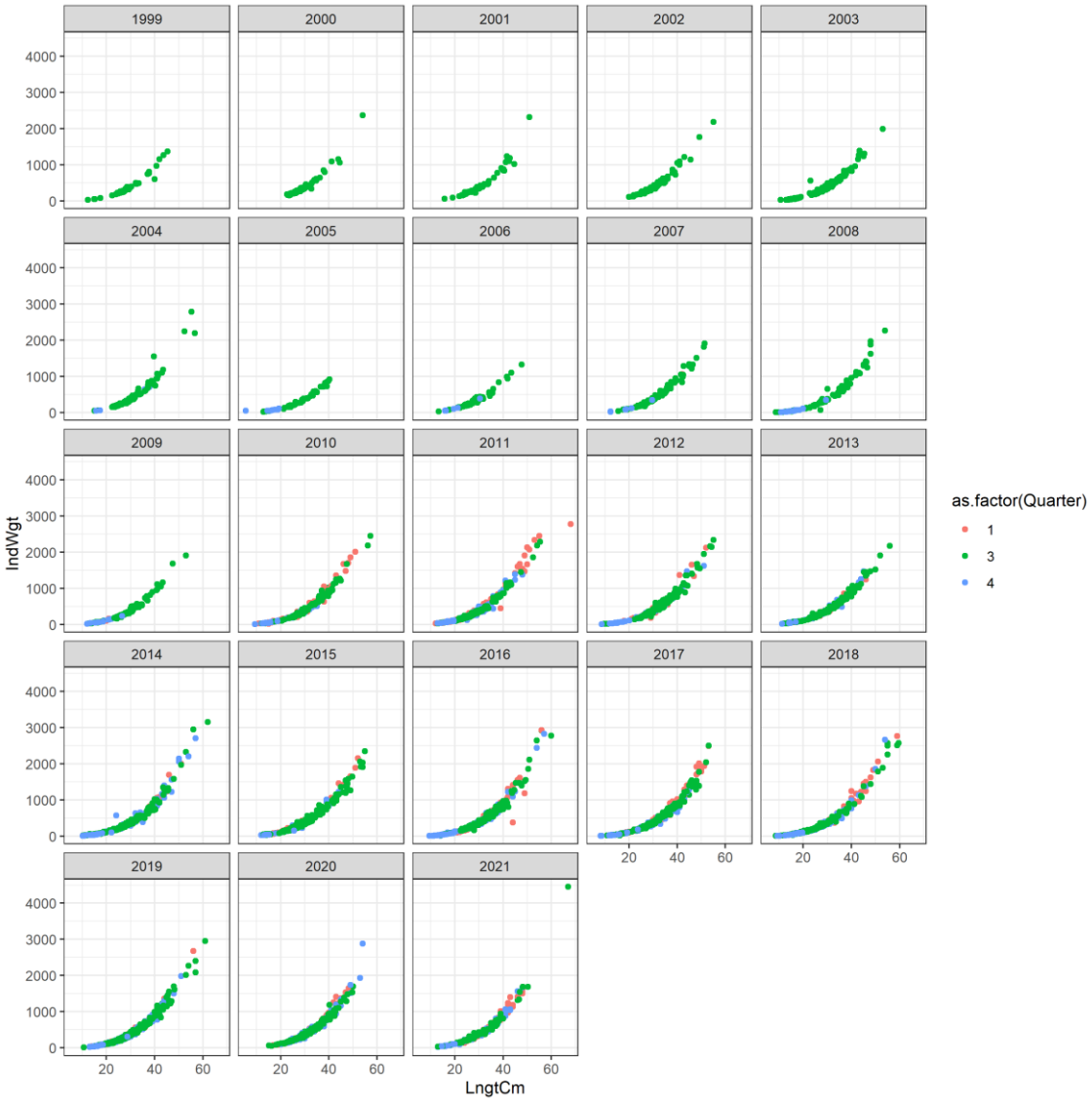


**Figure 2.C8. Length-weight relationship of the survey brill data for the period 1999–2021 by quarter.**

**Table 2.C6. Length-weight parameters of the survey brill data for the period 1999–2021 (using g and mm).**

| Year | a | b | Year | a | b |
|---|---|---|---|---|---|
| 1999 | 1.607733e-05 | 2.9752366 | **2011** | 1.303642e-05 | 3.0067983 |
| 2000 | 7.971029e-06 | 3.0909682 | **2012** | 1.043346e-05 | 3.0470139 |
| 2001 | 9.469550e-06 | 3.0639825 | **2013** | 1.592896e-05 | 2.9773692 |
| 2002 | 8.296285e-06 | 3.0855942 | **2014** | 1.479591e-05 | 2.9880918 |
| 2003 | 1.602459e-05 | 2.9776908 | **2015** | 2.307893e-05 | 2.9116815 |
| 2004 | 7.448050e-06 | 3.1074275 | **2016** | 8.483235e-06 | 3.0821534 |
| 2005 | 1.808901e-04 | 2.5328966 | **2017** | 1.034930e-05 | 3.0511323 |
| 2006 | 1.814909e-05 | 2.9478023 | **2018** | 1.259617e-05 | 3.0162306 |
| 2007 | 8.569894e-06 | 3.0806464 | **2019** | 1.407779e-05 | 2.9956410 |
| 2008 | 8.545383e-06 | 3.0813508 | **2020** | 1.293478e-05 | 3.0081594 |
| 2009 | 7.967889e-06 | 3.0984884 | **2021** | 1.211864e-05 | 3.0237026 |
| 2010 | 1.129148e-05 | 3.0397261 | | | |

A and b parameters are similar across the time-series with the exception of the year 2005. It is unclear why this year's a and b parameters deviate from the other years (Figure 2.C9). The overall a and b parameters for the survey data are 1.31e-05 and 3.01 respectively. When not considering 2005, a is lower (1.25e-05) and b is slightly higher (3.02).

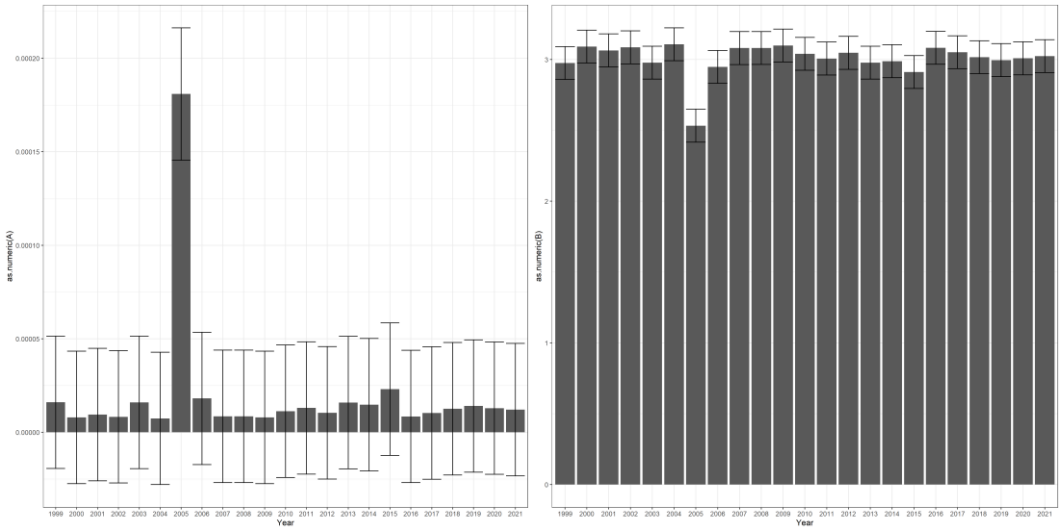


**Figure 2.C9. Length-weight relationship of the survey brill data for the period 1999–2021 by quarter.**

## 13. Estimates for priors using the life-history traits

Priors were estimated by running the SPMpriors package by Henning Winker (https://github.com/Henning-Winker/SPMpriors). Values for $L_{inf}$ and $L_m$ served as input to the flmvn_traits function. Using the information as compiled above, $L_{inf}$ was set at 51 cm (cv = 0.2) and $L_m$ at 30 cm (cv = 0.3)(Figure 2.C11 and Figure 2.C12).

When considering that the length at first capture (Lc = 22 cm) is smaller than the length at maturity ($L_m$ 50% mature = 30 cm), the following b/k and $F_{MSY}$ estimates are found (Figure 2.C10).

```
> fl2asem(stk,mc=1000,Lc=22, plot.progress = T)
              r     shape      fmsy     bmsyk
mu    0.3969507 0.7080000 0.5655002 0.3065904
logsd 0.3277572 0.3149223 0.5059285 0.1748731
```

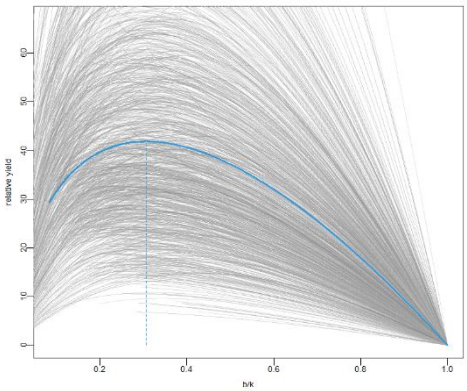


**Figure 2.C10. Finding optimal relative yield for several b/k estimates as calculated by the SPM priors package (by Henning Winker).**

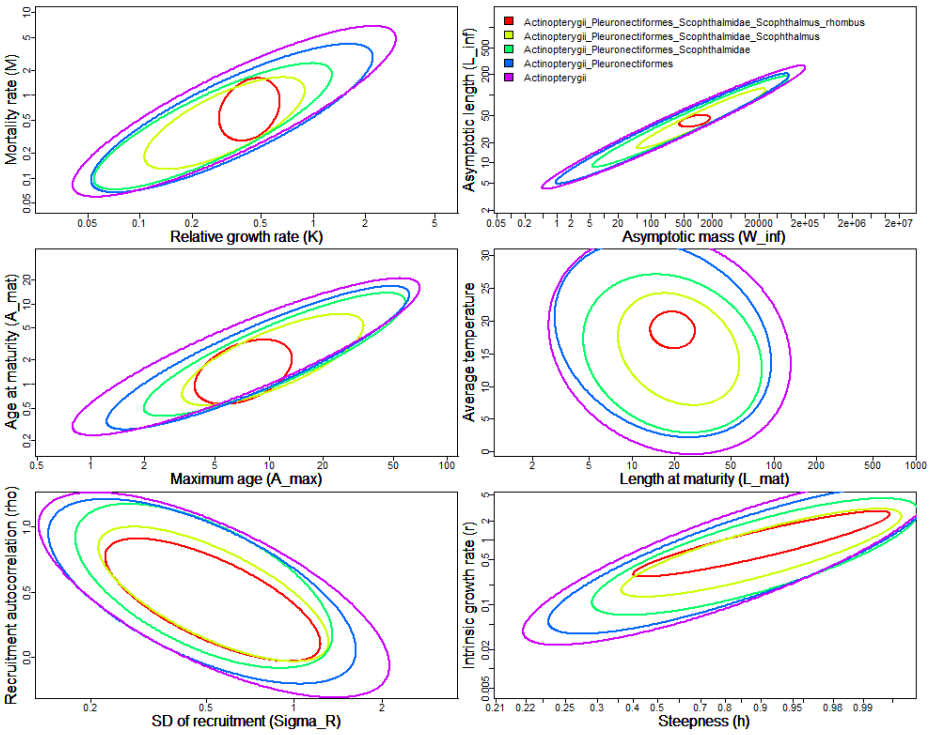


**Figure 2.C11. Estimates for life-history parameters and priors as calculated by the SPM priors package (by Henning Winker).**

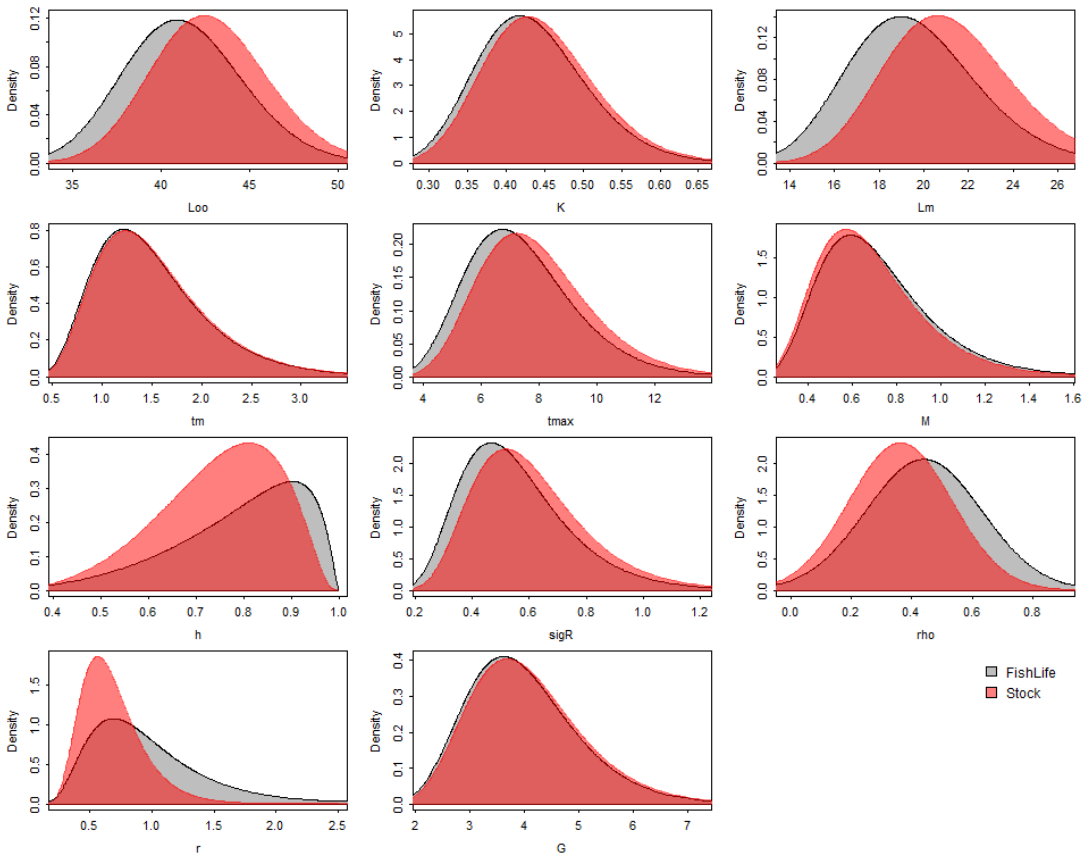


**Figure 2C.12. Estimates for life-history parameters and priors as calculated by the SPM priors package (by Henning Winker).**

## 14. References

Garcia-Carrerras, B., Jennings, S., Le Quesne, W.J.F., 2016. Predicting reference points and associated uncertainty from life histories for risk and status assessment. ICES Journal of Marine Science 73 (2), 483–493. doi:10.1093/icesjms/fsv195

Somers, I.F., 1988. On a seasonally oscillating growth function. Fishbyte 6, 8–11.

Thorson, J.T., Munch, S.B., Cope, J.M., Gao, J., 2017. Predicting life-history parameters for all fishes worldwide. Ecological Applications 27 (8), 2262–2276.

Thorson J.T., 2020. Predicting recruitment density dependence and intrinsic growth rate for all fishes worldwide using a data-integrated life-history model. Fish and Fisheries 21 (2), 237–251.

Van der Hammen, T., Poos, J.J., van Overzee, H.M.J., Heessen, H.J.L., Magnusson, A., Rijnsdorp, A.D., 2013. Population ecology of turbot and brill: What can we learn from two rare flatfish species? Journal of Sea Research 84, 96–108.

## 2.8.4 WD Annex 4: Catch statistics for brill (*Scophthalmus rhombus*) in areas 27.3a47de (Greater North Sea)

*Author: Lies Vansteenbrugge and Damian Villagra (ILVO, Belgium)*

**1. Introduction**

Historical landings were compiled from the ICES Catch Statistics website (https://www.ices.dk/data/dataset-collections/Pages/Fish-catch-and-stock-assessment.aspx). Historical nominal catches from 1950-2010 and official nominal catches from 2006-2021 were merged and analysed. In the period 1984-1989, Dutch landings were missing in Subarea 4. These data were filled by Dutch data available from the brill advice sheet. For the overlapping period 2006-2010, we chose to use the most recent time series. Differences for those years between time series were negligible (max. 3 tonnes differences).

**2. Time series 1950-2021**

Landings were below 1000 tonnes in the period 1950-1970, but steadily increased in the 1970s to around 2000 tonnes over the period 1980-2021 (Figure 1).

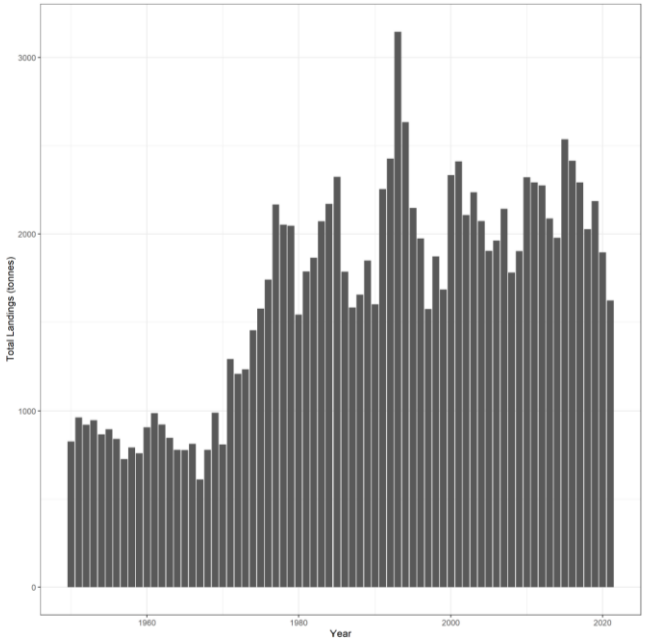


*Figure 1 Official landings for brill in 3a47de over the period 1950-2021.*

A total of 9 countries fished on this stock over the course of the time series: Belgium, Denmark, France, Germany, Ireland, The Netherlands, Norway, Sweden and the UK (including the Channel Islands Guernsey and Jersey). Especially the increase in landings of the Dutch fleet has led to the increase in landings of the stock (Figure 2).

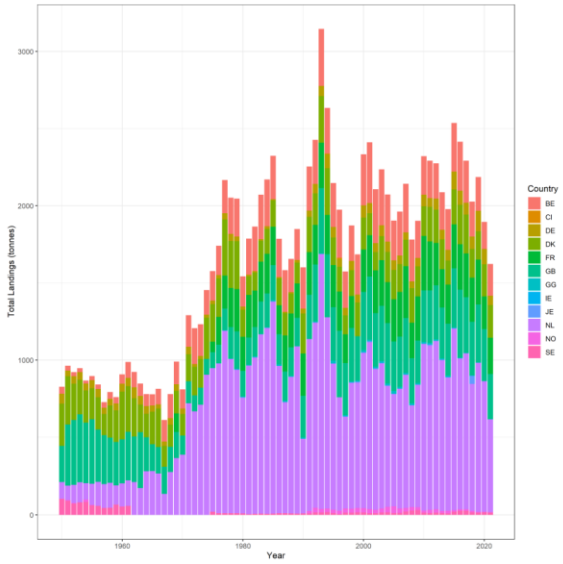


*Figure 2 Official landings by country for brill in 3a47de over the period 1950-2021.*

Throughout the time series, most of the landings originated from Subarea 4 (Figure 3). Landings in Division 3a have slightly decreased and landings in Divisions 7d,e have increased over the course of the time series (note 7d and 7e were combined in the earlier part of the time series).

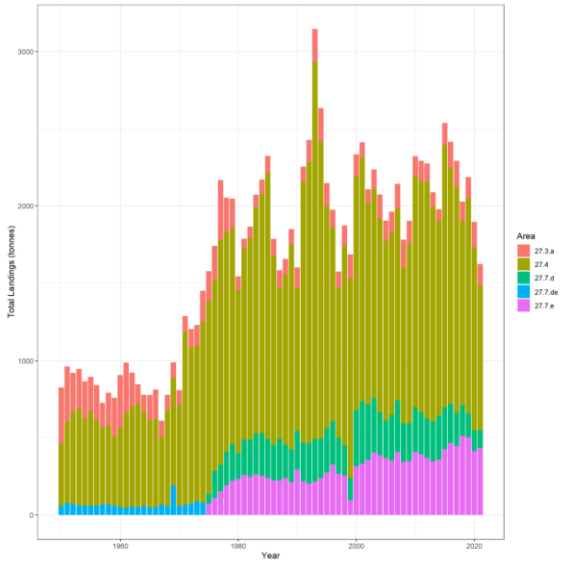


*Figure 3 Official landings by area for brill in 3a47de over the period 1950-2021.*

**3. Official landings suitable for input to SPiCT**

We compared the landing tonnage as available in InterCatch (period 2014-2021; see WD1) with the official landings statistics (Figure 4). Both series differed most in 2017 (85 tonnes), but followed the same trend.

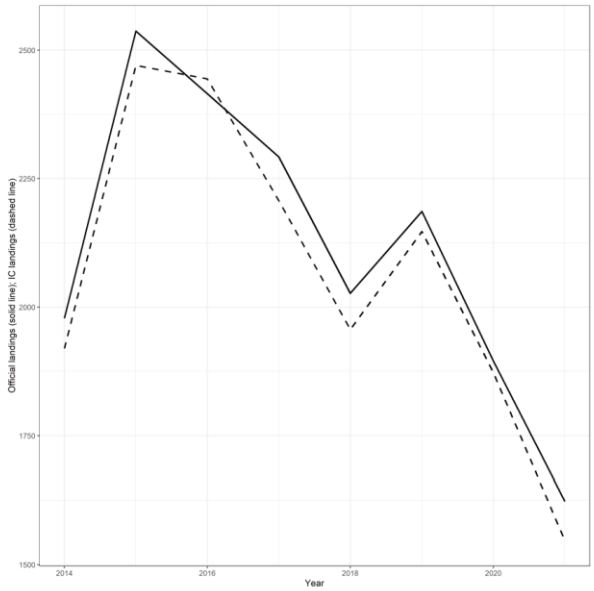


*Figure 4 Comparison between official landings statistics and landing tonnage available in InterCatch.*

**4. Overview of official landings time series from 1950-2021**

| Year | Landings (tonnes) | Year | Landings (tonnes) |
|---|---|---|---|
| **1950** | 827 | **1986** | 1786 |
| **1951** | 963 | **1987** | 1583 |
| **1952** | 922 | **1988** | 1656 |
| **1953** | 947 | **1989** | 1849 |
| **1954** | 867 | **1990** | 1601 |
| **1955** | 896 | **1991** | 2255 |
| **1956** | 842 | **1992** | 2427 |
| **1957** | 727 | **1993** | 3147 |
| **1958** | 793 | **1994** | 2634 |
| **1959** | 760 | **1995** | 2147 |
| **1960** | 907 | **1996** | 1974 |
| **1961** | 987 | **1997** | 1574 |
| **1962** | 923 | **1998** | 1872 |
| **1963** | 847 | **1999** | 1685 |
| **1964** | 780 | **2000** | 2334 |

| | | | |
|---|---|---|---|
| **1965** | 778 | **2001** | 2411 |
| **1966** | 813 | **2002** | 2107 |
| **1967** | 611 | **2003** | 2236 |
| **1968** | 779 | **2004** | 2073 |
| **1969** | 990 | **2005** | 1904 |
| **1970** | 810 | **2006** | 1962.231 |
| **1971** | 1291 | **2007** | 2142.133 |
| **1972** | 1207 | **2008** | 1780.979 |
| **1973** | 1232 | **2009** | 1902.26 |
| **1974** | 1454 | **2010** | 2320.861 |
| **1975** | 1576 | **2011** | 2292.39 |
| **1976** | 1741 | **2012** | 2275.623 |
| **1977** | 2167 | **2013** | 2088.072 |
| **1978** | 2053 | **2014** | 1978.301 |
| **1979** | 2046 | **2015** | 2537.171 |
| **1980** | 1542 | **2016** | 2415.365 |
| **1981** | 1787 | **2017** | 2292.395 |
| **1982** | 1865 | **2018** | 2026.852 |
| **1983** | 2072 | **2019** | 2186.1801 |
| **1984** | 2171 | **2020** | 1895.161252 |
| **1985** | 2324 | **2021** | 1623.1765 |

From 2014 onwards, the catch data will be replaced by the InterCatch data, which provides more detailed information on the stock's catches.
The InterCatch catches for 2014-2021 are shown in the table below.

| Year | Landings | Discards | BMS |
|---|---|---|---|
| **2014** | 1919.524 | 217.2749 | |
| **2015** | 2470.227 | 206.7236 | |
| **2016** | 2444.094 | 215.7695 | |
| **2017** | 2207.199 | 210.4447 | |
| **2018** | 1956.286 | 342.8163 | |
| **2019** | 2147.167 | 391.5166 | 0.004 |
| **2020** | 1872.411 | 182.2676 | 0.009 |
| **2021** | 1546.651 | 61.71364 | 0.124 |

## 2.8.5 WD Annex 5: Prior options and testing for North Sea brill

*Author: Henning Winker (GFCM)*

# Prior options and testing for North Sea brill

Henning Winker (GFCM)

11 January, 2023

## Contents

**1 Packages and installations** 1
1.1 Installations . . . 2

**2 Life history parameters** 2

**3 SPMpriors with FishLife** 3

**4 Leslie matrix with stock-specitic direct input** 8

**5 Setting up a generic OM for Brill** 9
5.1 Estimating priors from FLStock and SRR . . . 10
5.2 Simulating stock dynamics with evolutionary F-trajectories . . . 12

**6 Simulation testing with Spict** 16

**7 Spict estimation scenarios** 16
7.1 Quick simulation performance comparison . . . 21

```
## Warning: package 'knitr' was built under R version 4.2.2
```

## 1 Packages and installations

The following R packages are used

For generic life history parameters

- FishLife
- SPMpriors
- JABBA

As generic FLStock stock constructors

- FLCore

- FLife
- FLBRP
- FLRef

Surplus production model fitting

- spict

Note that several updates and new functions were pushed to **FLRef** on 10th of Jan of 2023, which are required to implement the below R code.

### 1.1 Installations

```
install.packages("ggplot2")
install.packages("devtools")
install.packages("TMB", type = "source")
devtools::install_github("DTUAqua/spict/spict")
devtools::install_github("james-thorson/FishLife")
devtools::install_github("henning-winker/SPMpriors")
# FLR
devtools::install_github("flr/FLCore")
devtools::install_github("flr/ggplotFL")
devtools::install_github("flr/FLBRP")
devtools::install_github("flr/FLasher")
devtools::install_github("flr/mse")
devtools::install_github("flr/FLSRTMB")
devtools::install_github("flr/FLife")
devtools::install_github("henning-winker/FLRef")
devtools::install_github("JABBAmodel/JABBA")
```

Load packages

```
# Load
library(ggplot2)
library(spict)
library(FishLife)
library(SPMpriors)
library(FLCore)
library(ggplotFL)
library(FLRef)
library(FLife)
library(JABBA)
library(ggpubr)
```

## 2 Life history parameters

Regional life history parameters of bll.27.3a47de for females were assumed assumed as follows:

```
linf = 46.8
k = 0.466
t0 = -0.862
lm = 31.3
a = 0.0000156
b = 3.01
tmax1 = 22
tmax2 =14

# check vbgf
vonbert(linf,k,t0,age=0:tmax2)
    [1] 15.48206 27.14776 34.46808 39.06163 41.94412 43.75290 44.88792 45.60016
    [9] 46.04709 46.32754 46.50353 46.61396 46.68326 46.72675 46.75403
```

An instantaneous rate of natural mortality was estimated using Then based on the maximum age estimates `tmax1 = 22` and `tmax2 = 12`

```
M1 = 4.899*tmax1^-.916
M2 = 4.899*tmax2^-.916
```

## 3 SPMpriors with FishLife

SPMpriors enables to compute two types of priors based on: (1) a Leslie Matrix approach (2) an Age-Structured Equilibrium Model

The first approach is suitable for Schaefer model formulation of the production function, whereas the second approach requires a Pella-Tomlinson production. Note that a current issue with SPMpriors is that using several traits will cancel each other out. It is therefore suggested to use only one key trait, e.g. either `tmax` or `Loo`, but not both togher.

In this example `tmax1` and `tmax2` are used, steepness (here `h`) is restricted by uniform distribution to a typically considered range of `h = c(0.6,0.9)`.

First the Leslie prior option for a Schaefer model is explored.

```
fl1 = SPMpriors::flmvn_traits(
  Genus="Scophthalmus",Species="rhombus",
  h=c(0.6,0.9),tmax=c(tmax1,0.2),Plot=TRUE)
   Closest match: Actinopterygii_Pleuronectiformes_Scophthalmidae_Scophthalmus_rhombus
```

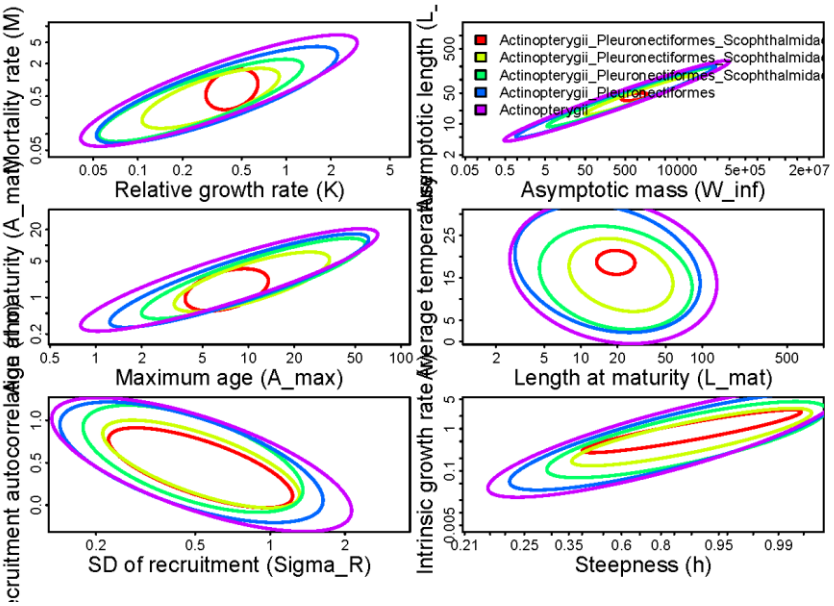
Mortality rate (M)
Relative growth rate (K)
Asymptotic length (L_
Actinopterygii_Pleuronectiformes_Scophthalmidae
Actinopterygii_Pleuronectiformes_Scophthalmidae
Actinopterygii_Pleuronectiformes_Scophthalmidae
Actinopterygii_Pleuronectiformes
Actinopterygii
Asymptotic mass (W_inf)
Maximum age (A_max)
Length at maturity (L_mat)
SD of recruitment (Sigma_R)
Steepness (h)

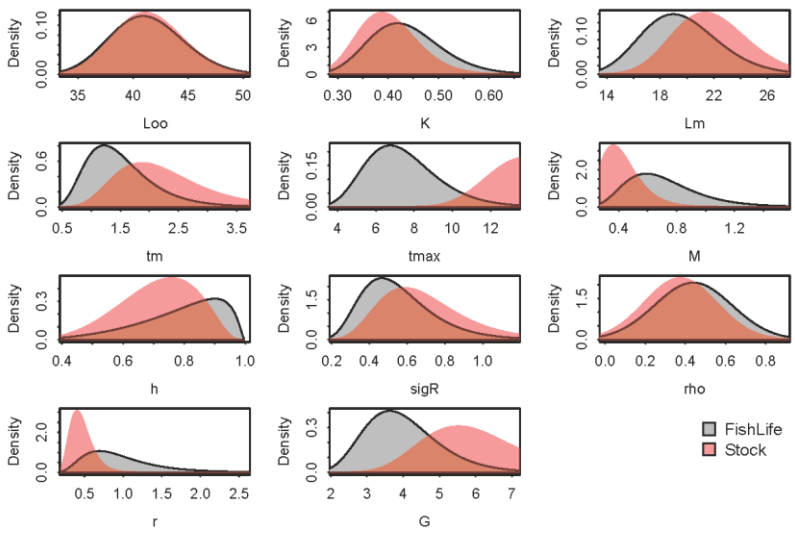


```
# too few sample, ensure more than 1000
# this is because tmax1 is outside global range
nrow(fl1$mvnstk)
   [1] 296
# increase nmc
fl1 = SPMpriors::flmvn_traits(nmc=1000000,
  Genus="Scophthalmus",Species="rhombus",
  h=c(0.6,0.9),tmax=c(tmax1,0.2),Plot=TRUE)
   Closest match: Actinopterygii_Pleuronectiformes_Scophthalmidae_Scophthalmus_rhombus
```

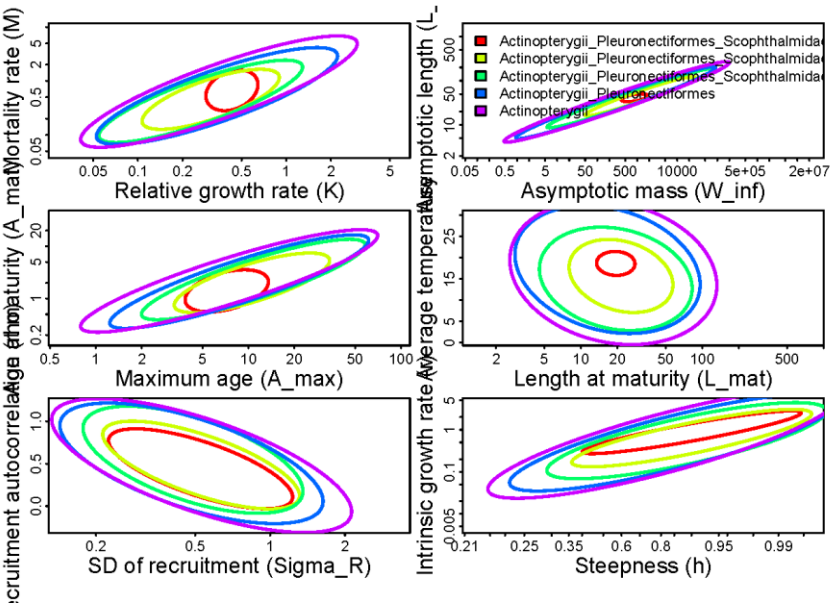
Actinopterygii_Pleuronectiformes_Scophthalmidae
Actinopterygii_Pleuronectiformes_Scophthalmidae
Actinopterygii_Pleuronectiformes_Scophthalmidae
Actinopterygii_Pleuronectiformes
Actinopterygii
Mortality rate (M)
Relative growth rate (K)
Asymptotic length (L_
Asymptotic mass (W_inf)
Maximum age (A_max)
Length at maturity (L_mat)
SD of recruitment (Sigma_R)
Steepness (h)

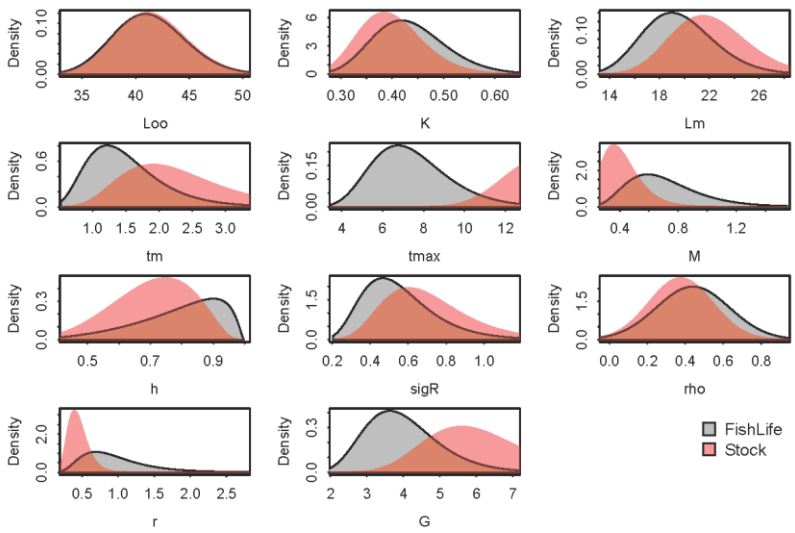


```
# Check
nrow(fl1$mvnstk)
   [1] 1296

fl2 = SPMpriors::flmvn_traits(
  Genus="Scophthalmus",Species="rhombus",
  h=c(0.6,0.9),tmax=c(tmax2,0.2),Plot=FALSE)
   Closest match: Actinopterygii_Pleuronectiformes_Scophthalmidae_Scophthalmus_rhombus

lh1=fl1$traits
lh2=fl2$traits

# Global FishLife
r.sp = lh1[lh1$trait=="r","mu.sp"]
# Tuned to tmax=22
r1 = lh1[lh1$trait=="r","mu.stk"]
# Tuned to tmax=14
r2 =lh2[lh2$trait=="r","mu.stk"]

r.sp
   [1] 0.8709
# options
r1
   [1] 0.4314
r2
   [1] 0.5304
```

```
mean(c(r1,r2))
   [1] 0.4809
```

```
# Assume Lc at 20 cm
asem1 = fl2asem(fl1,Lc=20,t0=t0,aW=1000*a,bW=b)
asem2 = fl2asem(fl2,Lc=20,t0=t0,aW=1000*a,bW=b)

asem1
                r     shape      fmsy     bmsyk
   mu    0.2341582 0.8370000 0.2827678 0.3357757
   logsd 0.2539407 0.2360257 0.4056805 0.1255510
asem2
                r     shape      fmsy     bmsyk
   mu    0.2922340 0.7910000 0.3684491 0.3256187
   logsd 0.2669539 0.2520023 0.4215298 0.1367534
```

In both cases shape of the production function is predicted to be extremely right skewed with $B_{MSY}/B0$ smaller than 0.35.

## 4 Leslie matrix with stock-specitic direct input

The recent version of the `JABBA` package provides a Leslie matrix function for use stock specific estimates to get an expected value for $r$.

The first step is build a `jbio` object and then pass this object to compute $r$ (and Generation time) with `jbleslie()`

```
# steepness from FishLife
s = lh1[lh1=="h","mu.stk"]

bio1 = jbio(amax=tmax1,nsexes=1,Loo=linf,k=k,t0=t0,aW=1000*a,bW=b,
     mat=c(lm,lm*1.2,0),M=c(M1),h=s)

bio2 = jbio(amax=tmax2,nsexes = 1,Loo=linf,k=k,t0=t0,aW=1000*a,bW=b,
     mat=c(lm,lm*1.2,0),M=c(M2),h=s)


r3 = jbleslie(bio1)$r
r4 = jbleslie(bio2)$r

r3
   [1] 0.6492533
r4
   [1] 0.7484844

median(c(r1,r2,r3,r4))
   [1] 0.5898266
```

The $r$ estimates still come out relatively high, but slightly lower than the global species mean from `FishLife`, which appears to be driven by the fairly high growth performance with a global and stock specific brody growth coefficient $k$ of around 0.45. Reducing $k$ to, e.g., 0.30, would notably reduce the stock's resilience.

## 5 Setting up a generic OM for Brill

The FLife function lhPar() is populated with some of basic life history estimates for growth,length-weight, maturity based on regional information and steepness from FishLife/SPMpriors.

```
par=lhPar(FLPar(linf=linf,k=k,t0=t0,
            a=a,b=b,a50 =2,
            s=s,m1=M1))
```

The FLife function lhEql is then used as a constructer for a basic FLBRP() object.

```
eql=lhEql(par,range = c(min = 0, max = tmax2, minfbar = 1, maxfbar = tmax2, plusgroup=tmax2))
```

Now further manipulations can be made, such as adjusting the inbuilt Gislason $M$ to a scaled Lorenzen $M$ and specifying a new maturity ogive.

```
# M
m(eql)[] = Mlorenzen(stock.wt(eql),Mref=M1,Aref=2)

mat50 = 1.9
mat95 = mat50*1.5
mat(eql) = newselex(mat(eql),FLPar(S50=mat50,mat95=mat95,Smax=1000,Dcv=0.5,Dmin=0.1))
```

It is important to then update the stock recruitment the stock recruitment relationship for a given steepness $s$ value if key biological parameters are modified.

```
# check srr parameters
params(eql)
   An object of class "FLPar"
   params
        a      b
   5987.9   92.1
   units:  NA
# update SRR given s after modifying m
eql = updsr(eql,s=s)
params(eql)
   An object of class "FLPar"
   params
       a     b
   530.8  92.1
   units:  NA
```

After making all the desired modifications the time horizon can be adjusted with fbar range. Here a time horizon from 1981-2020 is chosen.

```
# change time horizon with a fixed intial f0
f0 = 0.01
fbar(eql) = FLQuant(f0,dimnames=list(year=1971:2020))
```

Now FLBRP can be directly converted into an FLStock and the stock recruitment relationship can be extracted.

```
stk = as(eql,"FLStock")
units(stk) = standardUnits(stk) # assign units
sr = as(as(eql,"predictModel"),"FLSR")
```

Once the stock is constructed further manipulations are straight forward, such as specifying fishing selectivity using the 5-parameter selectivity function `newselex`

A new selectivity can be set by adjusting the `harvest` slot. If some dome-shaping is desired, $Smax$ has to be smaller then the plus group, $Dcv$ governs the slope of the half-normal and $Dmin$ governs the hight at the right end tail.

```
# catch before maturity
S50 = 0.8 # selectivity < age-2
S95 = 1.3
# some Doming
Smax = 100
Dcv = 0.5
Dmin = 0.2

harvest(stk) =  f0*newselex(
  harvest(stk),FLPar(S50=S50,S95=S95,
    Smax=Smax,Dcv=Dcv,Dmin=Dmin))
```

The so generated age-structured relationships for weight-at-age, maturity-at-age, natural mortality and selective are shown in Fig. 1.

```
ggplot(FLQuants(stk,"m","catch.sel","mat","catch.wt"))+
  geom_line(aes(age,data))+
  facet_wrap(~qname,scale="free")+theme_bw()
```

### 5.1 Estimating priors from FLStock and SRR

First, it is straight forward to compute the intrinsic rate of population increase from a Leslie for a specified steepness value. However, this $r$ estimate ignores selectivity and should only be used in the context of a Schaefer model with $F_{MSY} = r/2$.

```
r.leslie = mean(productivity(stk,s=s)$r)
r.leslie
   [1] 0.4910535
# Fmsy
r.leslie/2
   [1] 0.2455267
```

An alternative is to estimate $r$ and the shape parameter $n$ as function $MSY$, $VB_{MSY}$ and $VB_0$ from an age-structured equilibrium model (ASEM), where $BB$ denotes that the vulnarable (or exploitable) biomass as function of selectivity. The basic relationships for $r$ and $n$ can then be approximated as follows:

$$F_{MSY} = \frac{MSY}{VB_{MSY}}$$

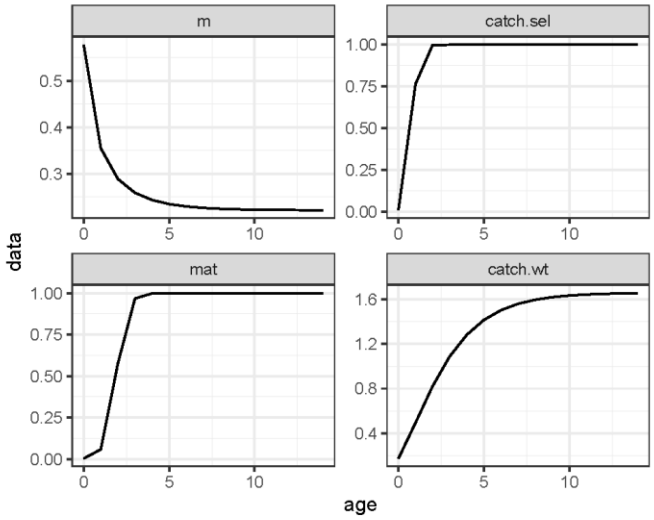


Figure 1: Specified biological and selectivtiy function for natural mortality, selectivity, maturity and somatic growth in weight-at-age

$$\frac{VB_{MSY}}{EB_0} = n^{(-\frac{1}{n-1})}$$

$$r = F_{MSY}\frac{n-1}{1-n^{-1}}$$

To compute the expected values for $r$ and $n$ (here denoted as $m$), requires the stock biology and selectivity together with the SRR as input.

```
brp = FLBRP(stk,sr)
r.pella = asem2spm(brp)

r.pella
   An object of class "FLPar"
   params
         r         m     BmsyK      Fmsy       MSY     Bmsy       B0
     0.179     0.731     0.312     0.245    87.083  355.398 1139.655
   units:  NA
```

The surplus production curves are plotted as function of the vulnerable biomass `vb` and spawning biomass `ssb` in Fig. 2, together with approximated curves of the 3-parameter Pella-Tomlinson function.

```
ggpubr::ggarrange(
plotpf(brp,rel=F),
plotpf(brp,rel=T),common.legend = T
)
```

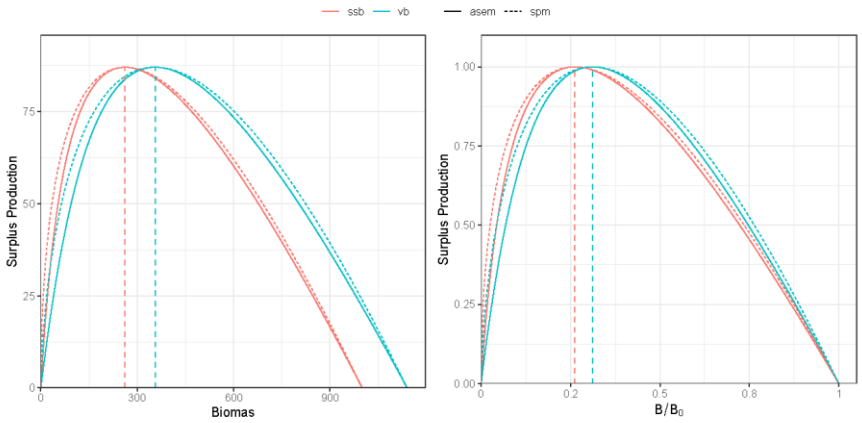


Figure 2: Specified biological and selectivtiy function for natural mortality, selectivity, maturity and somatic growth in weight-at-age

### 5.2 Simulating stock dynamics with evolutionary F-trajectories

The operating model is assumed to represent the "true" age-structured stock dynamics for evaluating the estimation accuracy of Spict. The "true" MSY based reference points can be easily added to the `FLStock` by extending it to `FLStockR`.

```
# Estimate refpts
brp = computeFbrp(stk,sr,proxy="msy",blim=0.3,type="btgt")
   Computing Fmsy with Btgt = Bmsy

    Blim = 0.3 with Btgt corresponding to Fmsy
stk = FLStockR(stk)
stk@refpts = Fbrp(brp)
# check
stk@refpts
   An object of class "FLPar"
   params
       Fmsy     Btgt     Blim     Flim      Yeq       B0       R0
      0.268  261.886   78.566    0.554   87.083 1000.000  486.028
   units:  NA
```

```
ploteq(brp)
```

`FLRef` provides generic functions to create F-trajectory for generating a wider range of plausible states for the OM, including `rffwd` and `fudc`. Here, the `fudc` function is used for illustration, which generates and up-down-constant F-pattern with the option to add random noise.

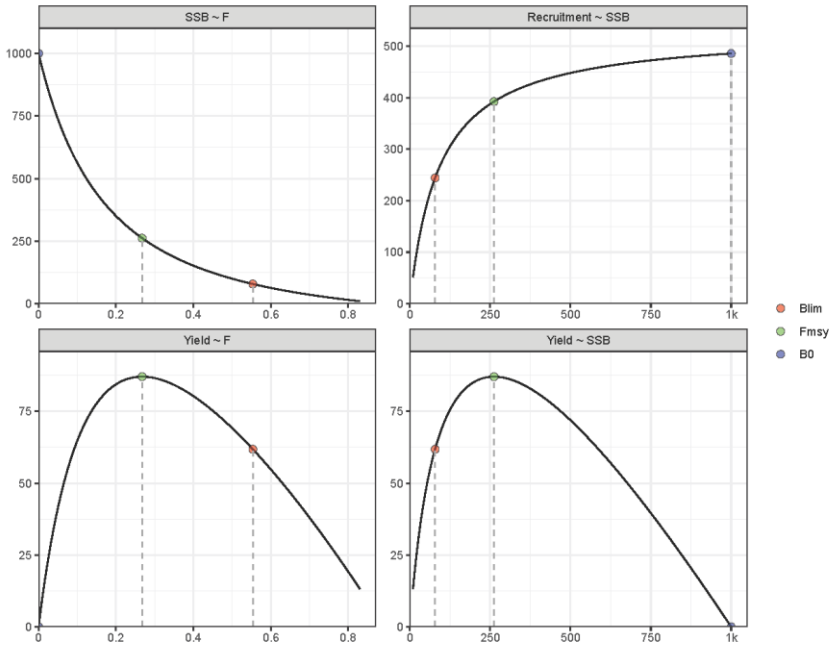


Figure 3: Equilibrium curves Recruitment, SSB, F and Landings and estimated MSY-based reference points for the Brill OM

```
its = 100
# propagate desired iterations
stki <- propagate(stk, its)
# Create F-pattern up-down-constant
fmsy = Fbrp(brp)["Fmsy"]
f = fudc(stk,fhi=2,flo=0.9,fref=fmsy,sigmaF=0)
fy = fudc(stki,fhi=2,flo=0.9,fref=fmsy,sigmaF=0.2)
plot(f,fy,iter(fy,1),iter(fy,2),
     iter(fy,3),iter(fy,5),iter(fy,6))+
  ylab("F")+theme_bw()+theme(legend.position = "none")
   Warning: Ignoring unknown parameters: linewidth
```

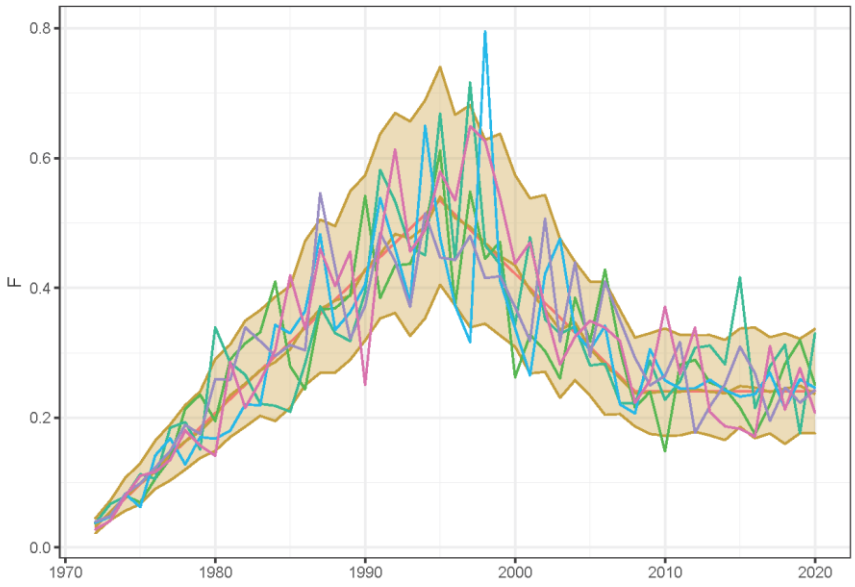


Figure 4: Simulated up-down-constant F-pattern without and with random noise for 5 random iterations

The stock dynamics can then be forecasted by adding random recruitment.

```
set.seed(123)
its = 100
# Random recruitment deviations with sigR = 0.5 and AR1 rho = 0.3
rec_devs = ar1rlnorm(0.3, 1971:2020, its, 0, 0.5)
# project Fs over om horizon
om <- ffwd(stki,sr,
             fbar=fy, # add F here
             deviances=rec_devs)
```

```
om@refpts = stk@refpts
```

```
plotAdvice(om)
```

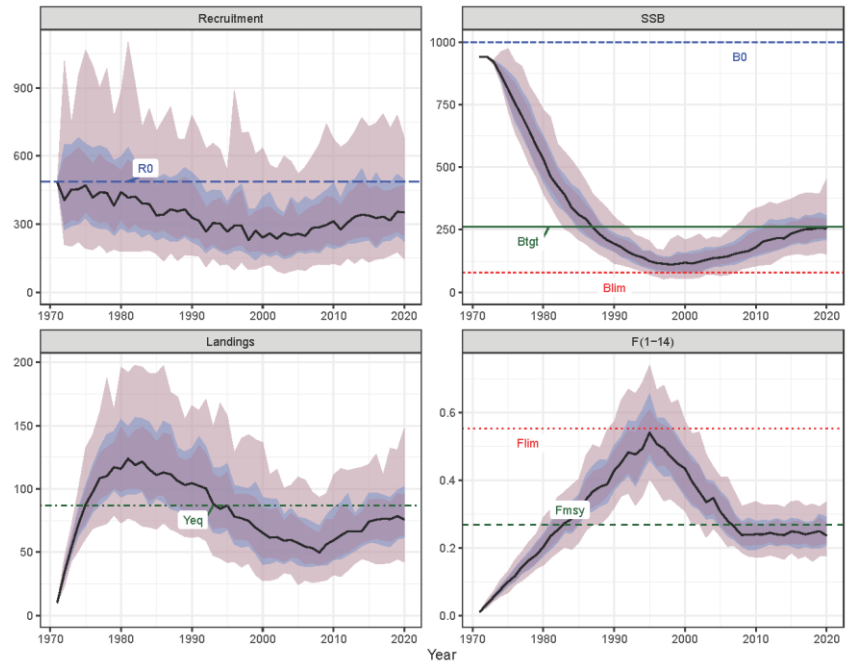


Figure 5: Simulated population dynamics compared to reference points from the off-the-shelf OM for brill based on 100 iterations

The last step is to generate the observed survey index using the `FLRef` function `bioidx.sim()`. By default, the index assumes the same fishing selectivity in the stock object (but see `?bioidx.sim`. In this case, a moderate observation error of `sigma=0.25` is assumed and the catchability coefficient $q$ that scales the exploitable biomass to the index is set as `q = 0.001`. The index is assumed to start in 1999.

```
idx = window(bioidx.sim(om,sigma=0.25,q=0.001),start=1999)
```

```
flqs= FLQuants("B/Bmsy"=ssb(om)/om@refpts["Btgt"],
               "F/Fmsy"=fbar(om)/om@refpts["Fmsy"],
               "Catch/MSY"=catch(om)/om@refpts["Yeq"]
               ,Index=idx@index%/%yearMeans(idx@index))

ggplot(iter(flqs,1:20))+
```

```
  geom_line(aes(year,data,col=ac(iter)),alpha=0.5)+
  theme_bw()+facet_wrap(~qname)+
  theme(legend.position = "none")+geom_hline(yintercept = 1,linetype=2)+
  scale_color_manual(values=c(rainbow(20)))
```

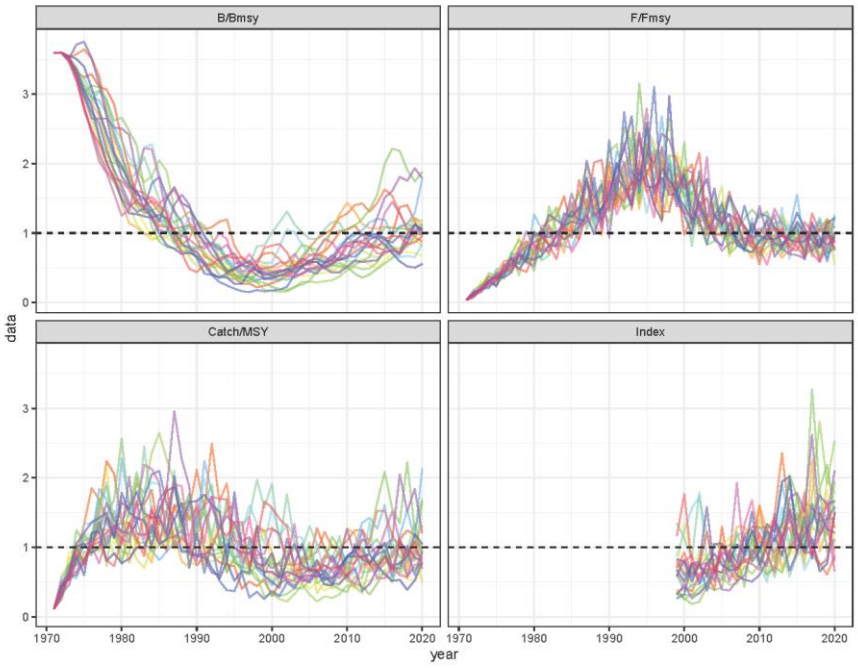


Figure 6: Individual iterations of simulated trajectories of $B/B_{MSY}$, $F/F_{MSY}$, $Catch/MSY$ and the normalized CPUE indices from the off-the-shelf OM for brill shown for the first 20 iterations

## 6 Simulation testing with Spict

## 7 Spict estimation scenarios

Initial trials indicated that the default settings are not suitable to fit Spict with historical catch data that are longer than the index. Therefore, a function `spict.simplify` was explored to stabilise the models when including the historical catch time series preceding the index of abundance.

```
#' spict.simplify
#'
#' Function to simplify spict to make it fast and robust as an MP
```

```
#'
#' @param inp spict input time series
#' @param r.pr lognormal r prior, untransformed mean,log.sd, phase
#' @param bk.pr lognormal initial depletion prior
#' @param shape.pr lognormal prior for shape
#' @param pe lognormal prior of process error on biomass
#' @param fdevs lognormal F penalty
#' @param ce lognorlam Catch penalty
#' @param dteuler time step resolution
spict.simplify = function(inp,r.pr=c(0.2,0.5,1),# r prior
                          bk.pr=c(0.8,0.3,1), # bk prior
                          shape.pr=c(2,0.01,1),
                          pe=c(1,0.3,1),
                          fdevs=c(4,0.5,1),
                          ce=c(0.1,0.1,1),
                          dteuler=1){

  inp$dteuler=dteuler
  inp$priors$logbkfrac <- c(log(bk.pr[1])-bk.pr[2]^2/2,bk.pr[2],bk.pr[3]) # this is  the bk prior
  inp$priors$logalpha <- c(0,0,0) # deactivate ratio of proc to obs error
  inp$priors$logbeta <- c(0,0,0) # deactivate catch to f devs
  inp$priors$logsdb <- c(log(pe[1])-0.5*pe[2]^2, pe[2], pe[3]) # process error
  inp$priors$logsdf <- c(log(fdevs[1])-0.5*fdevs[2]^2, fdevs[[2]], fdevs[3])
  inp$priors$logsdc <- c(log(ce)[1]-0.5*ce[2]^2, ce[2], ce[3]) #
  inp$priors$logn <- c(log(shape.pr[1]),shape.pr[2],shape.pr[3]) # Reduce shape CV
  inp$priors$logr <- c(log(r.pr[1])-0.5*r.pr[2]^2,r.pr[2],r.pr[3]) # r piror
  return(inp)

}
```

The four scenarios explored were:

(1) `Schaefer.rlo` Schaefer model with low r1 prior $r$ =`{r} round(r1,3)`
(2) `Fox.rlo` model with low 0.5$r$1 prior $r$ =`{r} round(r1/2,3)`
(3) `Schaefer.rhi` model with high r3 prior $r$ =`{r} round(r3,3)`
(4) `Fox.rhi` model with low 0.5$r$3 prior $r$ =`{r} round(r3/2,3)`

Below a simple wrapper function is presented that:

- Fits the 4 Spict scenarios
- Applies `spict2FLStockR` to convert Spict fits into simplified `FLStock` objects
- Apply `stock2ratios` to convert OM into a simplified `FLStock` object
- Combines all into a `FLStocks` object output

```
runi <- function(om,idx,it,dteuler=1/4){
# index
dfi =as.data.frame(iter(window(idx@index,start=1999),it))
# catch
# Short
dfcs = as.data.frame(iter(window(om@catch,start=1999),it))
# Long
dfcl = as.data.frame(iter(window(om@catch,start=1971),it))
```

```
# Create Spict Default input
inp = list(obsC=dfcs$data,timeC=dfcs$year,
           obsI=dfi$data,timeI=dfi$year)
inpl = list(obsC=dfcl$data,timeC=dfcl$year,
           obsI=dfi$data,timeI=dfi$year)

inp$dteuler = dteuler
# low r prior Schaefer
r1
inps.lo = spict.simplify(inpl,r.pr=c(r1,0.4,1),# r prior
                         bk.pr=c(0.95,0.3,1), # bk prior
                         shape.pr=c(2,0.01,1),
                         pe=c(0.07,0.3,1),
                         dteuler=dteuler)
# Fox
inpf.lo = spict.simplify(inpl,r.pr=c(r1/2,0.4,1),# r prior
                         bk.pr=c(0.95,0.3,1), # bk prior
                         shape.pr=c(1.01,0.01,1),
                         pe=c(0.07,0.3,1),
                         dteuler=dteuler)

# long-time seris
# hi r prior
r3
# schaefer
inps.hi = spict.simplify(inpl,r.pr=c(r3,0.4,1),# r prior
                         bk.pr=c(0.95,0.3,1), # bk prior
                         shape.pr=c(2,0.01,1),
                         pe=c(0.07,0.3,1),
                         dteuler=dteuler)
# Fox model from OM
inpf.hi = spict.simplify(inpl,r.pr=c(r3/2,0.4,1),# r prior
                         bk.pr=c(0.95,0.3,1), # bk prior
                         shape.pr=c(1.01,0.01,1),
                         pe=c(0.07,0.3,1),
                         dteuler = dteuler)

# make list of spict fits
fits = list(
  schaefer.lo=fit.spict(inps.lo),
  fox.lo=fit.spict(inpf.lo),
  schaefer.hi =fit.spict(inps.hi),
  fox.hi=fit.spict(inpf.lo)
)
# convert spict in FLStockR
res = FLStocks(lapply(fits,function(x){
 spict2FLStockR(x,rel=T)
}))
# cut forecast
res = window(res,end=2020)
# Add om for comparison
flom = stock2ratios(iter(om,it))
res = FLStocks(c(om=flom,res))
```

```
return(res)
}
```

```
res = runi(om,idx,it=1,dteuler=1/4)

plot(res,metrics=list("B/Bmsy"=ssb,"F/Fmsy"=fbar,Catch=landings))+
  geom_hline(yintercept = 1,linetype=2)+theme_bw()
```

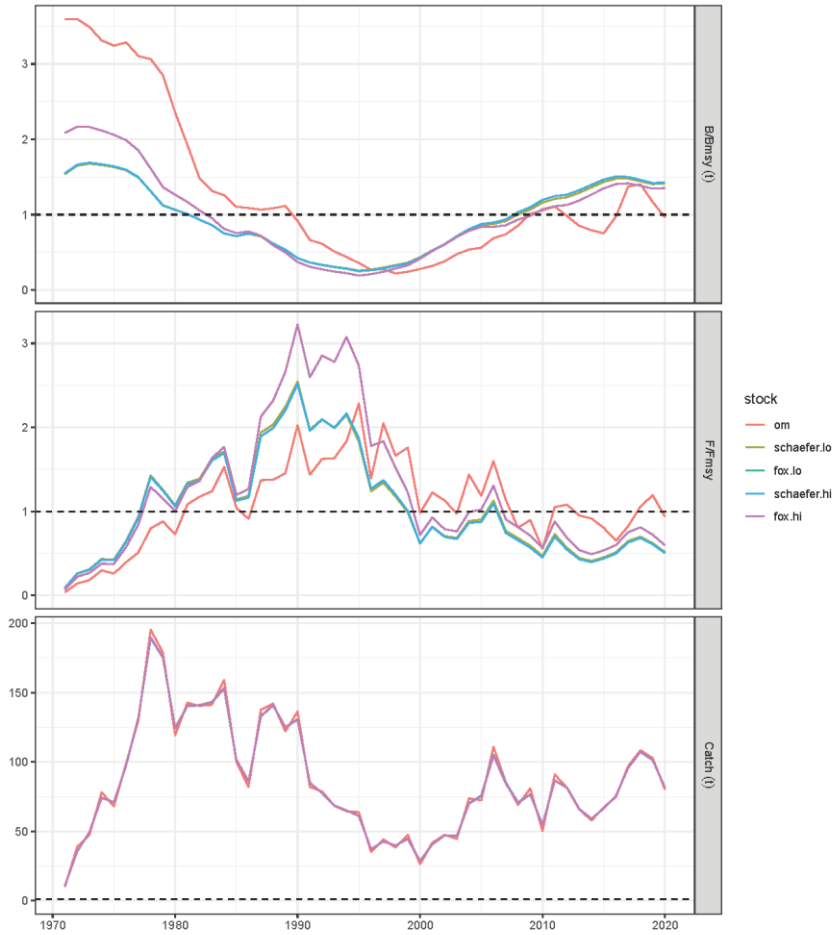


Figure 7: OM and estimated trajectories of $B/B_{MSY}$ and $F/F_{MSY}$ for the first iteration

### 7.1 Quick simulation performance comparison

```
sims = runi(om,idx,it=1,dteuler = 1)
sims =FLStocks(lapply(sims,function(x)propagate(x,its)))

for(i in 2:its){
  out=runi(om,idx,it=i,dteuler=1)
  for(j in 1:length(out)) iter(sims[[j]],i) = out[[j]]}

sims= FLStocks(Map(function(x,y){
  x@name=y
  x},x=sims,y=as.list(names(sims))))
```

```
plot(sims,metrics=list("B/Bmsy"=ssb,"F/Fmsy"=fbar))+
  geom_hline(yintercept = 1,linetype=2)+theme_bw()
```

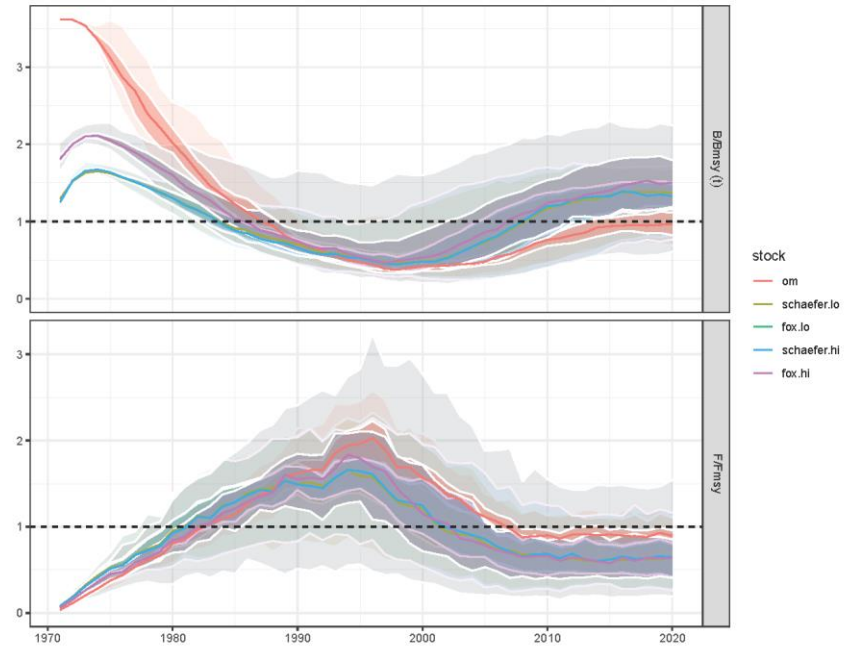


Figure 8: OM and estimated trajectories of $B/B_{MSY}$ and $F/F_{MSY}$ for 100 iterations

Several runs failed to converge the hessian, but these failed runs were not quantified removed for this initial evaluation.

By making use of **FLQuants** in is reasonably straight forward compute some estimation error with respect to the "true" value of $B_{MSY}$ and $F_{MSY}$ for the terminal year 2020.

```
simt= window(sims,start=2015)
bias.b = FLQuants(lapply(simt[2:5],function(x){
  log(ssb(x))-log(window(ssb(simt$om)))
}))
bias.f = FLQuants(lapply(simt[2:5],function(x){
  log(fbar(x))-log(window(fbar(simt$om)))
}))

out = rbind(
  data.frame(as.data.frame(bias.b),what="BBmsy"),
  data.frame(as.data.frame(bias.f),what="FFmsy")
)
```

```
ggplot(out,aes(x=qname,data,fill=qname))+
  geom_boxplot(outlier.shape = NA)+
  facet_wrap(~what)+
  geom_hline(yintercept = 0,col=2)+theme_bw()+
  xlab("Scenario")+ylab("Error")+ylim(-2,2)
```

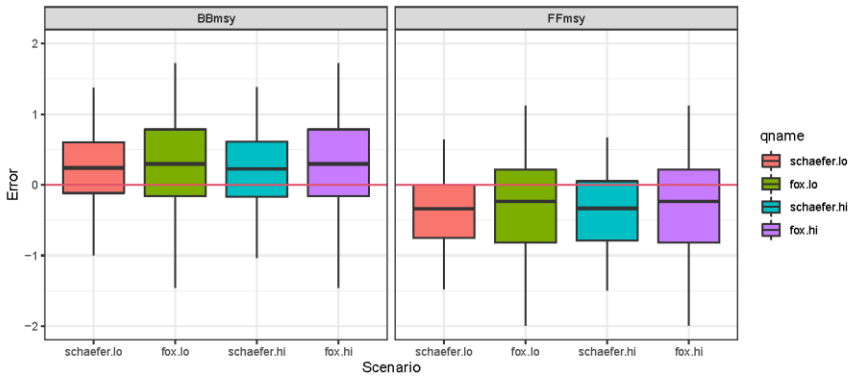


Figure 9: Boxplot showing estimation errors of $log(B/B_{MSY})$ and $log(F/F_{MSY})$ for 2020 with respect to the true quantities of the OM

All Spict scenarios showed fairly strong positive bias about the perception of stock status. The Fox models show the largest bias although the production is closer to the "true" age-structured dynamics of the OM and the Fmsy estimate is the same for prior means. One possible explanation the distortion between vulnerable biomass (vb) and ssb, where vb is linear proportional to ssb. However, this distortion appears minimal given the assumed maturity (for ssb) and selectivity (for vb) interacting with growth, natural mortality and the SRR (Figure 10). Another possible explanation is that the positive is caused by not capturing the interaction between the recruitment and age-structured lag-effects which may drive the population dynamics during the rebuilding phase, which coincides here with the observation period for the survey index.

```
asem.vb = asem2spm(brp,quant="vb")

df1 = data.frame(as.data.frame(iterMedians(vb(om))/asem.vb["Bmsy"]),qname="vb")
df2 = data.frame(as.data.frame(iterMedians(ssb(om))/stk@refpts[2]),qname="ssb")
df = rbind(df1,df2)

ggplot(df,aes(year,data,color=qname))+geom_line()+
  theme_bw()+ylab(expression(B/B[MSY]))+geom_hline(yintercept = 1,linetype=2)
```

\begin{figure}

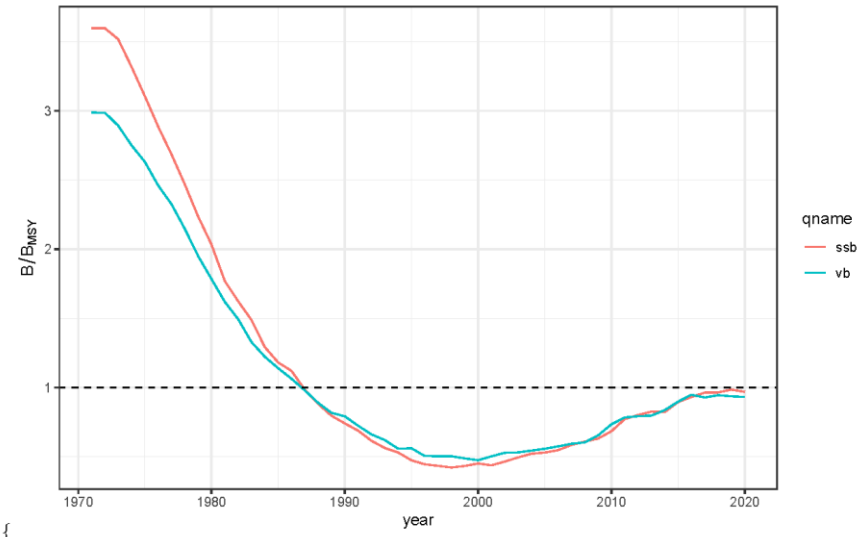


{

}

\caption{Median Trajectories of $VB/VB_{MSY}$ and $SB/SB_{MSY} for 100 OM iteratsions} \end{figure}

```
theme(legend.title = element_blank())
 List of 1
  $ legend.title: list()
   ..- attr(*, "class")= chr [1:2] "element_blank" "element"
  - attr(*, "class")= chr [1:2] "theme" "gg"
```

```
  - attr(*, "complete")= logi FALSE
  - attr(*, "validate")= logi TRUE
```

# 3 Boarfish in Celtic Seas, English Channel, and Bay of Biscay

## boc.27.6-8 – *Capros aper* in subareas 6–8

## 3.1 Introduction

Boarfish (*Capros aper*) is a small, pelagic, laterally compressed, planktivorous shoaling species (Egerton *et al*., 2017; White *et al*., 2011). They primarily inhabit continental shelves and edges, often in large dense shoals at depths of 40–600 m (Coad *et al*., 2014; Egerton *et al*., 2017). It's distribution ranges from Norway to Senegal in the Northeast Atlantic and includes the Mediterranean and Aegean seas and the islands of the Azores, Canaries, Madeira, and the Great Meteor Seamount (Holgersen, 1954; Quéro, 1986; Kaya and Ozaydin, 1996; Egerton *et al*., 2017; Coad *et al*., 2014). A genetic study conducted in 2013 of samples from the Northeast Atlantic and Mediterranean suggested that boarfish in ICES subareas 4, 6, 7 ,8 and northern part of 9.a are a single stock (Farrell *et al*., 2016). This distribution is slightly broader than the current EC TAC area (27.6, 7 and 8) and for the purposes of assessment, only data from these areas were utilized.

### 3.1.1 Fishery information

The first recorded landing of boarfish was in 1999. Landings remained low (< 1000 t pa) until 2007 whereupon a rapid expansion of the fishery took place in the mid-2000s (peaking at 144 kt in 2010) with Ireland, Denmark and Scotland the main fishers. The expansion of the fishery was associated with developments in the pumping and processing technology for boarfish catches. The fishery targets dense shoals and catches are generally free from bycatch. The fishery is carried out primarily via pelagic pair trawl using 32–54 mm mesh trawls.

Management measures were first introduced in 2011, prior to this the fishery was unregulated. In several years since the introduction of the TAC, the full quota has not been taken due to a number of factors including administrative and economic reasons. Ireland is the main participant in the fishery, with the majority of the TAC. Denmark and Scotland are the other main participants although in some years, only minimal catches were taken by these nations.

In the past two years, the fishery has noticed an increase in the abundance of boarfish, in the southern Celtic Sea, where boarfish had been sparse for many years. There has also been a shift in distribution, with fishable marks being observed along the western Irish coast even up to 57°N.

### 3.1.2 Current assessment and advice

During 2012 and 2013, an assessment was developed based on the Schaefer state space surplus production model (Meyer and Millar 1999) using catch data and fishery-independent information from an acoustic survey (BFAS/WESPAS) and indices from 6 separate national groundfish surveys. The 2013 assessment provided an estimate of stock status and was used to provide MSY based advice ($F_{MSY}$ = 0.23) for 2014. However, following the update assessment in 2014, and concerns raised by the ADG that the model was unsuitable for category 1 advice, the assessment was downgraded to category 3 and accepted for trends only based advice. Since 2018, catch advice has been issued biennially although the assessment has been updated and presented annually to WGWIDE. The history of boarfish advice is given in Table 3.1.

The assessment output has been relatively stable in recent years. It is heavily influenced by the acoustic survey which commenced in 2011 and has an informative prior on catchability (q = 1, sd = 0.25). Information prior to the start of the fishery in the mid-2000s is sparse. Highest catches occurred prior to the start of the acoustic time-series when the fishery was unregulated. The groundfish indices are characterized by high uncertainty, and variable temporal coverage. Moreover, each survey only covers a portion of the stock distribution. A summary of the output from the 2022 update assessment is shown in Figure 3.1.

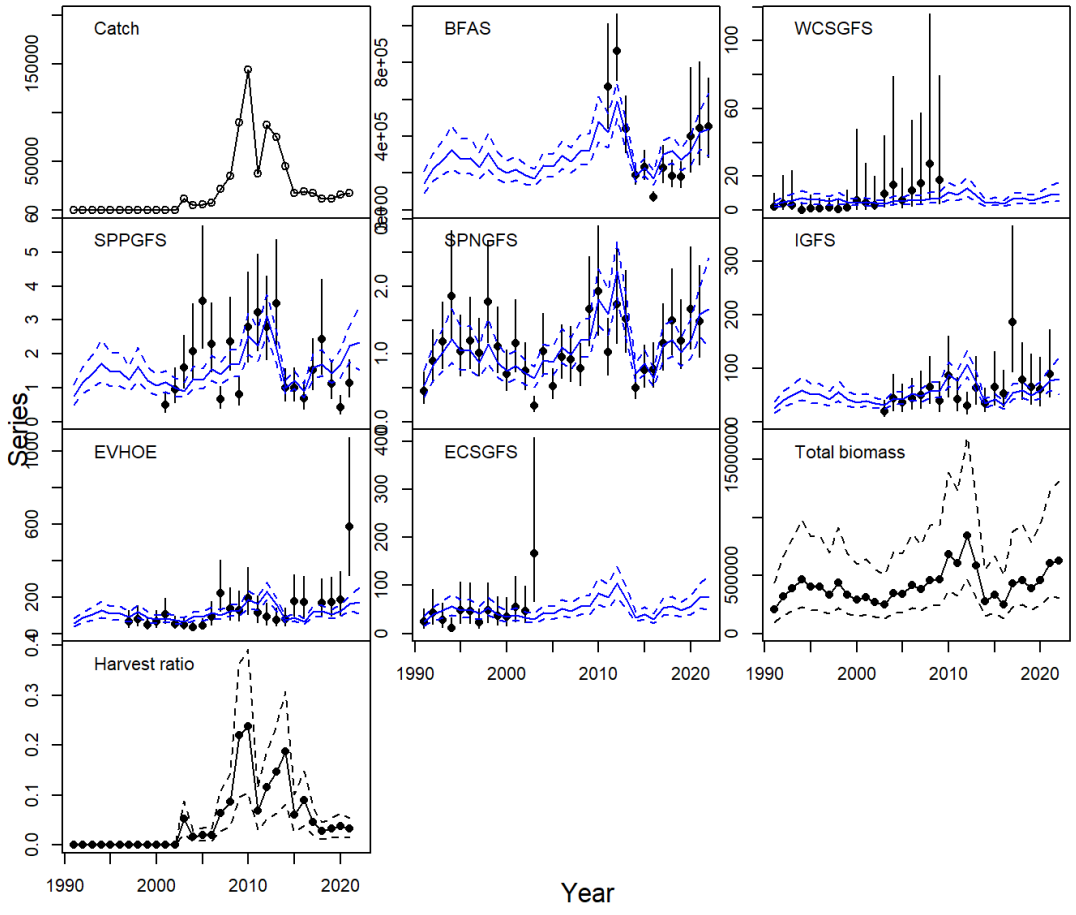


**Figure 3.1. WGWIDE 2022 Boarfish update assessment summary.**

**Table 3.1. History of advice, catch and management.**

| Year | ICES advice | Catch corresponding to advice | TAC * | ICES catch |
|---|---|---|---|---|
| 2001 | None | - | None | 120 |
| 2002 | None | - | None | 91 |
| 2003 | None | - | None | 11387 |
| 2004 | None | - | None | 5151 |
| 2005 | None | - | None | 5959 |
| 2006 | None | - | None | 7137 |
| 2007 | None | - | None | 21576 |
| 2008 | None | - | None | 34751 |
| 2009 | None | - | None | 90370 |
| 2010 | None | - | None | 144047 |

| Year | ICES advice | Catch corresponding to advice | TAC * | ICES catch |
|---|---|---|---|---|
| 2011 | None | - | 33000 | 37096 |
| 2012 | No increase in catches | 82000 | 82000 | 87355 |
| 2013 | MSY approach | 82000 | 82000 | 75409 |
| 2014 | MSY approach | 133957 | 133957 | 45231 |
| 2015 | DLS approach | 53296 | 53292 | 17766 |
| 2016 | Precautionary approach | ≤ 42637 | 42637 | 19315 |
| 2017 | Precautionary approach (-36% relative to previous advice) | ≤ 27288 | 27288 | 17388 |
| 2018 | Precautionary approach | ≤ 21830 | 20380 | 11286 |
| 2019 | Precautionary approach (same advice as for 2018) | ≤ 21830 | 21830 | 11312 |
| 2020 | Precautionary advice | ≤ 19152 | 19152 | 15649 |
| 2021 | Precautionary approach (same advice as for 2020) | ≤ 19152 | 19152 | |
| 2022 | Precautionary approach | ≤ 22791 | | |
| 2023 | Precautionary approach (same advice as for 2022) | ≤ 22791 | | |

*** EU, UK and international waters of subareas 6, 7 and 8.**

## 3.2 Input data for stock assessment

### 3.2.1 Landings and discards

A time-series of landings and discards by ICES Division is available from the Working Group for Widely Distributed Species (WGWIDE). As part of this exercise, the complete dataset has been uploaded to InterCatch. The fishery operates during the first and fourth quarters. In recent years a larger proportion of the total catch has been taken in the fourth quarter. The bulk of the catches are taken in ICES divisions 7.j, 7.b, and 8.a. Historically, the largest catches have been taken in 7.j although between 2016 and 2019, an increased proportion of the catch was taken in Northern Biscay (8.a). Discard estimates are only available for some fleets including demersal fleets from Spain, Ireland and the UK and pelagic freezers from Netherlands and Germany. The full time-series of landings and discards by country are given in Table 3.2.

During the initial years of the fishery when catches increased to over 100 kt the catch consisted of fully mature fish and a range of size classes. As the fishery has taken place further south, smaller size classes have appeared in the catch length profile, consistent with the increased proportion of young fish in southern waters. Sampling of discards indicates a similar size distribution to the landed fraction. Boarfish is discarded largely as it is an unwanted species in all but the target fisheries and is actively avoided as the spiny body tends to damage other species in mixed catches.

Comprehensive sampling of the commercial catch has been carried out since 2007. Length frequency, sex, weight and maturity information is routinely collected. While otoliths have been

taken they have not been read since the initial ageing studies were carried out in 2010–2012. Under a self-sampling scheme, Irish vessels retain a sample from each haul which is frozen and delivered to scientists when the vessel returns to port (often the catch is landed into Denmark or Faroe). Using appropriate samples for allocating to unsampled catch, the annual catch at length estimates are calculated by the InterCatch platform and are shown in Figure 3.2.

**Table 3.2. Boarfish landings by country, total discards and TAC by year (1999–2021).**

| Year | Denmark | Germany | Ireland | Netherlands | England | Poland | Scotland | Spain | Discards | Total | TAC |
|---|---|---|---|---|---|---|---|---|---|---|---|
| 1999 | | | 63 | | | | | | | 63 | |
| 2000 | | | 458 | | | | | | | 458 | |
| 2001 | | | 120 | | | | | | | 120 | |
| 2002 | | | 46 | | | | | | | 46 | |
| 2003 | | | 460 | | | | | | 10143 | 10604 | |
| 2004 | | | 675 | | | | | | 4465 | 5140 | |
| 2005 | | | 242 | | | | | | 5818 | 6061 | |
| 2006 | | | 2772 | | | | | | 4391 | 7163 | |
| 2007 | | | 17608 | | | | 772 | | 2985 | 21365 | |
| 2008 | 3098 | | 21584 | | | | 0 | | 10051 | 34734 | |
| 2009 | 15059 | | 68629 | | | | | | 6654 | 90342 | |
| 2010 | 39805 | | 89748 | | | | 9241 | | 6562 | 145357 | |
| 2011 | 7797 | | 20619 | | | | 2813 | | 5792 | 37021 | 33000 |
| 2012 | 19888 | | 55949 | | | | 4884 | | 6640 | 87361 | 82000 |
| 2013 | 13184 | | 52250 | | | | 4380 | | 1284 | 71097 | 82000 |
| 2014 | 8758 | | 34632 | | | | 38 | | 1806 | 45234 | 133957 |
| 2015 | 29 | 5 | 16325 | 375 | 104 | | 0 | | 944 | 17782 | 53296 |
| 2016 | 337 | 7 | 15974 | 212 | 21 | | | | 1245 | 17795 | 47637 |
| 2017 | 548 | | 15485 | 182 | 0 | | | | 1218 | 17433 | 27288 |
| 2018 | 94 | | 9513 | 172 | 0 | | 0 | 54 | 1364 | 11198 | 21830 |
| 2019 | 757 | | 9910 | 318 | 30 | | | 2 | 547 | 11564 | 21830 |
| 2020 | 196 | | 14666 | 416 | 62 | 109 | | 1 | 208 | 15660 | 19152 |
| 2021 | 4322 | | 11923 | 781 | 45 | 44 | 9 | 11 | 650 | 17785 | 19152 |

0 = <0.5 t

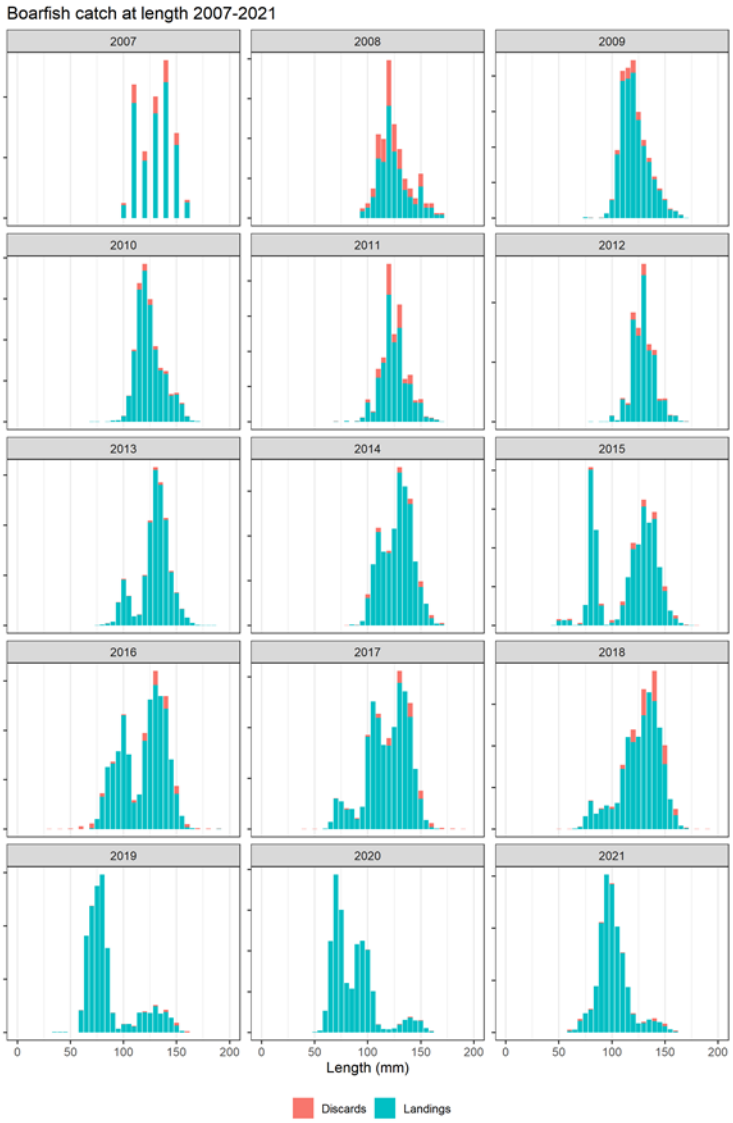


**Figure 3.2. Catch length distribution.**

## 3.2.2 Acoustic Surveys

### 3.2.2.1 BFAS/WESPAS

The Boarfish Acoustic Survey (BFAS) was first conducted in 2011, in cooperation with the fishing industry. The survey was designed as an extension of the Malin Shelf Herring Acoustic survey (MSHAS) providing a continuation of coverage to 47.5°N and was carried out on a commercial vessel deploying a towed body with a 38 kHz split-beam transducer. The survey collects acoustic data continuously along a series of parallel transects with a spacing of 15 nm with CTD stations and opportunistic trawling also. In 2012 the survey switched from 24 hour operations to daylight only (04:00–00:00) as it was noted from the 2011 survey that boarfish shoals tend to disperse during the hours of darkness such that acoustic detection becomes difficult. Following the 2013 survey, a revised target strength model (Fässler *et al.*, 2013) was applied to the historic dataset.

Since 2016, both the Malin Shelf Herring and Boarfish surveys have been carried out on the RV Celtic Explorer. Collectively, these surveys are known as the Western European Shelf Pelagic Acoustic Survey (WESPAS). The survey runs for approximately 6 weeks from mid-June to the end of July. Since 2017, the survey has been conducted from South to North, previously the

northern herring survey had been conducted first. Starting the survey at the southern boundary improves alignment with the French acoustic survey in the Bay of Biscay (PELGAS).

The StoX software package has been used to calculate an estimate of TSB/SSB since 2016, prior to this bespoke software was used. Biological sampling is carried out during the survey via targeted trawling on acoustic registrations for the purposes of mark identification and to determine species size structure. On average 25–40 trawl hauls are carried out on each survey. The catch is sampled for length frequency and biological characteristics (weight, sex, maturity, otolith extraction).

During the early years of the survey, sampling indicated that the detected stock was almost fully mature with fish under 10 cm relatively rare in the samples. In later years, smaller fish were more common, particularly in the southernmost Celtic Sea stratum. In 2020 and 2021, a significant proportion of the biomass estimate comprised of recently recruited fish as shown in Figure 3.3.

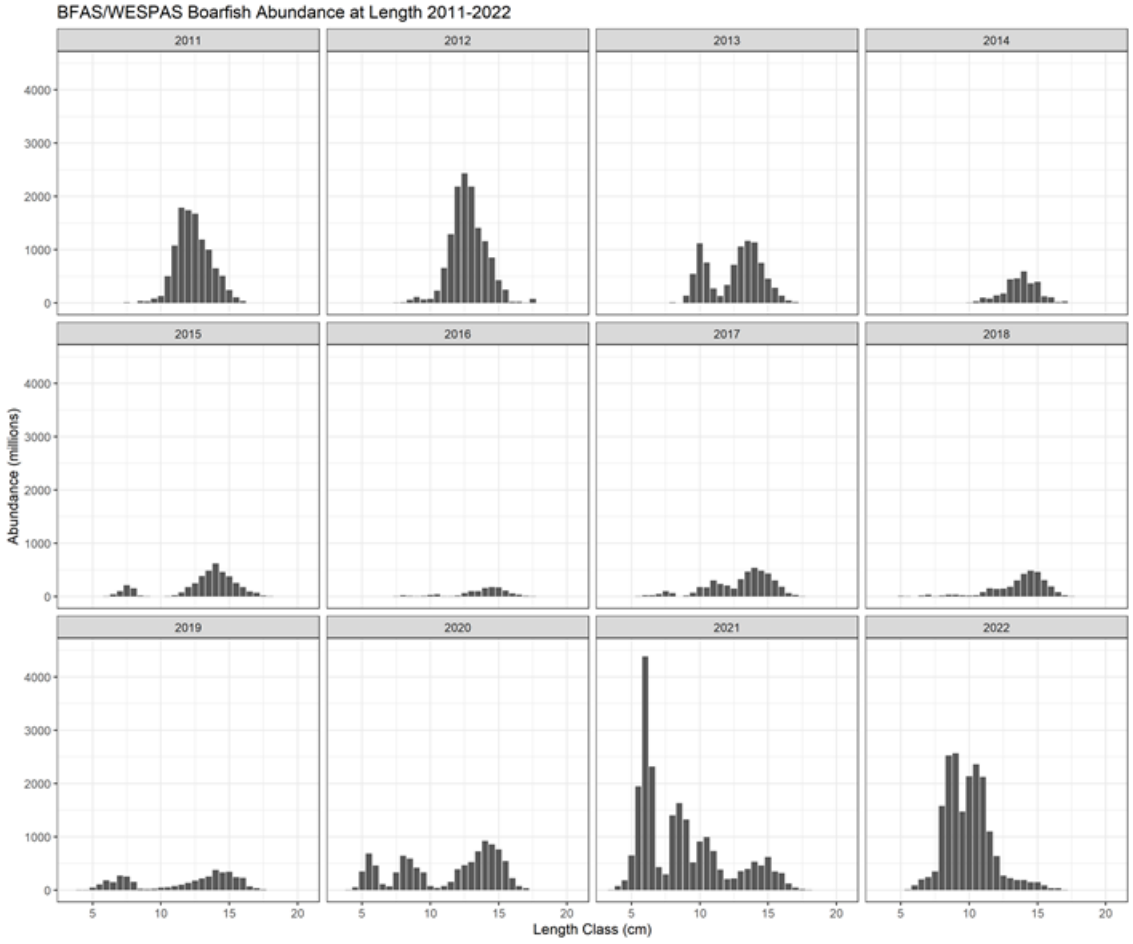


**Figure 3.3. BFAS/WESPAS boarfish abundance at length.**

### 3.2.2.2 PELGAS

The PELGAS survey is carried out each year by the French National Institute for Ocean Science, Ifremer. It is an acoustic survey designed to monitor the abundance of small pelagic fish in the Bay of Biscay with a focus on anchovy and sardine and is carried out in May. Initially, boarfish was not a target species for the survey, as it was rarely encountered and no estimate of abundance was calculated, although length sampling of any catch resulting from trawling was carried out. Since 2014, the occurrence of boarfish has increased in Northern Biscay and a TSB estimate has been calculated. Note that no survey was carried out in 2020. Sampling of boarfish catches indicates that Biscay is an important area for juvenile fish. For 2021 and 2022, when significant

quantities of boarfish were detected, the length data indicates that the biomass is comprised almost exclusively of recently recruited fish Figure 3.4.

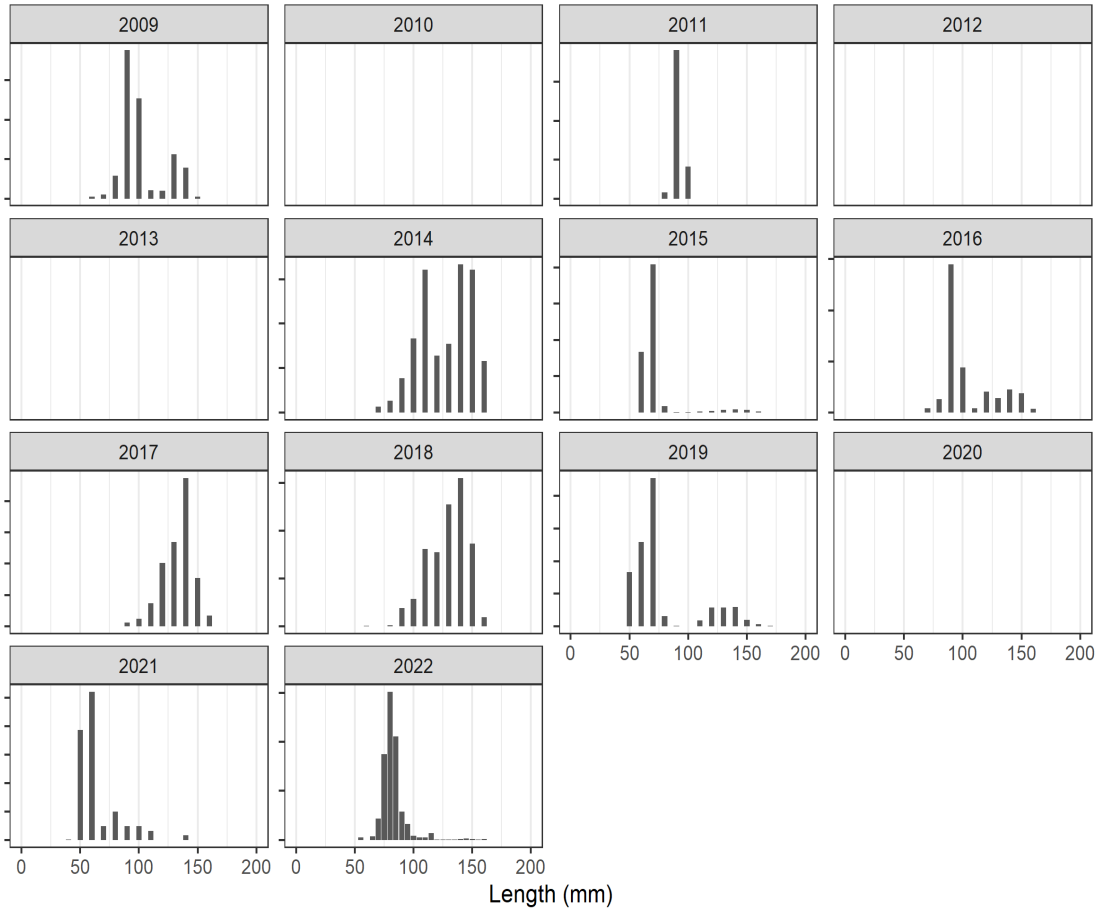


**Figure 3.4. Length sampling of boarfish from PELGAS (Bay of Biscay).**

The following changes to survey design and vessel are potential sources of bias in the time-series of TSB/SSB estimates.

- Industry vs. Research vessel (towed body vs .hull mounted transducer, noise)
- No inter-calibration
- Change in survey timing/direction (2017 onwards)
- Survey design (number strata, abundance estimation tool)
- Uncertainty regarding Southern boundary and alignment with PELGAS. 6- week gap prior to 2017, reduced to 2–3 weeks following change in survey direction to South-North.
- Some (probably minimal) uncertainty regarding the Northern boundary with boarfish reported by the Scottish component of the Malin Shelf Herring Survey in 2018 (north of 59°N)

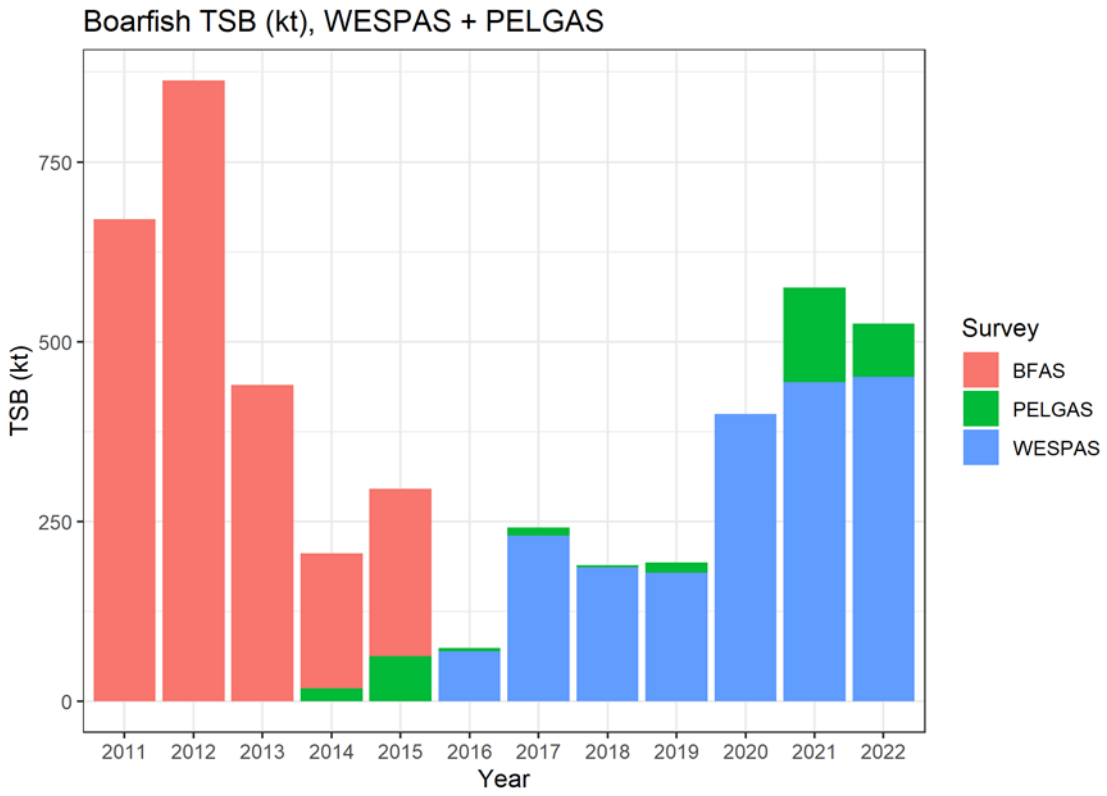


**Figure 3.5. Estimates of boarfish TSB from acoustic surveys.**

**Table 3.3 Acoustic survey estimates of boarfish TSB**

| Year | BFAS/WESPAS | CV | PELGAS | TOTAL |
|---|---|---|---|---|
| 2011 | 670 176 | 21.2 | - | 670 176 |
| 2012 | 863 446 | 10.6 | - | 863 446 |
| 2013 | 439 897 | 17.5 | - | 439 897 |
| 2014 | 187 779 | 15.1 | 17 593 | 205 372 |
| 2015 | 232 624 | 17.0 | 62 652 | 295 276 |
| 2016 | 69 690 | 19.0 | 4 475 | 74 165 |
| 2017 | 230 062 | 21.9 | 11 247 | 241 309 |
| 2018 | 186 252 | 19.9 | 3 378 | 189 630 |
| 2019 | 179 156 | 25.4 | 14 137 | 193 293 |
| 2020 | 399 872 | 34.8 | NA | 399 872 |
| 2021 | 443 777 | 31.0 | 131 186 | 574 963 |
| 2022 | 451 415 | 24.0 | 74 127 | 525 542 |

### 3.2.3 Groundfish Surveys

The current boarfish assessment utilizes indices from 6 individual IBTS surveys.

1. EVHOE (Q4 French Bay of Biscay Survey 1999–2021, ex 2017).
2. IGFS (Q4 Irish Groundfish Survey 2003–2021)
3. SPPGFS (Q4 Spanish Porcupine Bank Survey 2001–2021)
4. SPPNGFS (Q4 Spanish North Coast Survey 1990–2021)
5. WCSGFS (Q1 and Q4 West of Scotland 1985–2009)
6. ECSGFS (Q3/4, English Channel/Celtic Sea Survey 1982–2003)

The Scottish Q1 and Q4 surveys (WCSCFG) were redesigned in 2010 (and henceforth named SCOWCGFS) and are considered separate time-series. The EVHOE survey in 2017 was curtailed due to vessel breakdown with fewer than 30% of the planned hauls completed. Boarfish is frequently encountered by all western IBTS surveys. Only the Scottish surveys have an encounter rate lower than 50%, although there are indications of a decline in the proportion of zero hauls since approximately 2000, perhaps indicating a northern range expansion in the stock. Further south, in the Bay of Biscay, Celtic Sea and on the Porcupine Bank approximately 50–75% of hauls consistently contain boarfish. Since 2000, the number of hauls has been relatively constant (Figure 3.6).

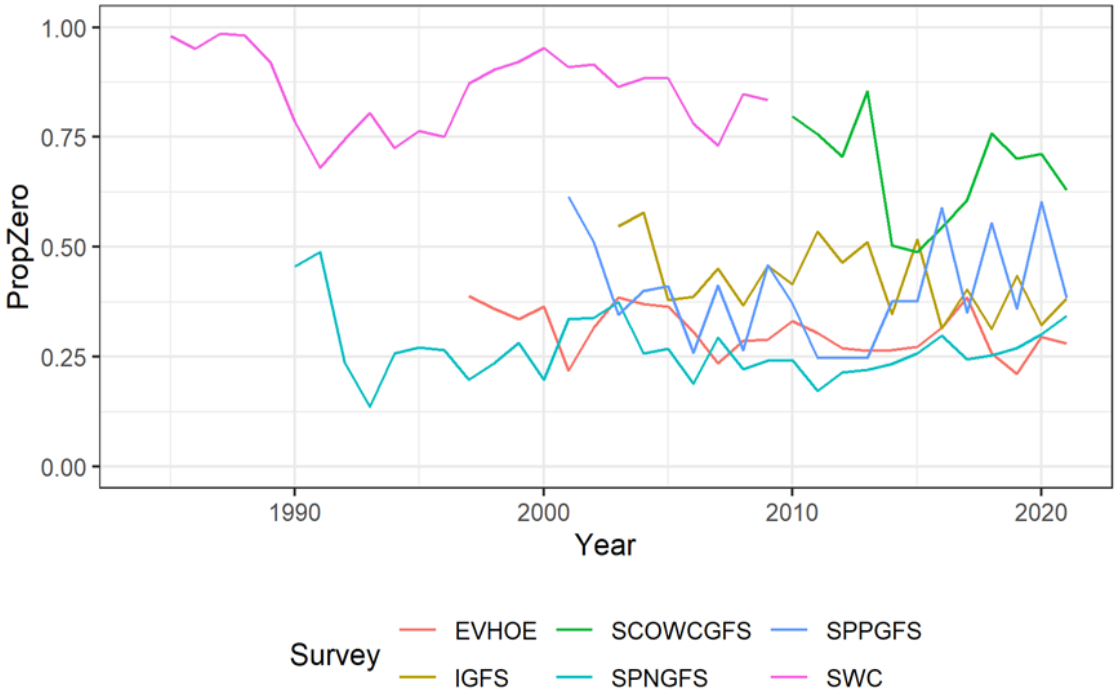


**Figure 3.6. Proportion of hauls with zero catch of boarfish by IBTS survey and year.**

Boarfish is a pelagic schooling species with an affinity to the seabed during winter when the IBTS surveys are conducted. As such, catch rates vary widely with occasional very large hauls. The indices are calculated within a Bayesian framework using the delta lognormal model whereby the probability of a positive catch and the catch rate (kg/30 min) are modelled separately before being combined to generate an index. Year and ICES statistical rectangle are explanatory variables for both the presence and catch rate models, providing both an index and estimate of uncertainty for the assessment. Note that the SCOWCGFS survey index (2011-present) is not used in the current assessment.

The highest catch rates are found in the northern part of the Bay of Biscay (covered by the EVHOE survey) and are associated with the shelf edge region. The Celtic Sea and west and north coasts of Ireland are also associated with higher catch rates. Although boarfish is frequently encountered to the west of Scotland, on the Porcupine Bank and in the southern part of the Bay of Biscay and the northern Spanish shelf, catch rates in these areas are significantly lower although this may partly be explained by the various gears used in these areas such as the heavier groundgear deployed in 6.a and the Baka trawl used on the Spanish survey. The mean catch rate for the period 2003–2021 by ICES statistical rectangle is shown in Figure 3.7.

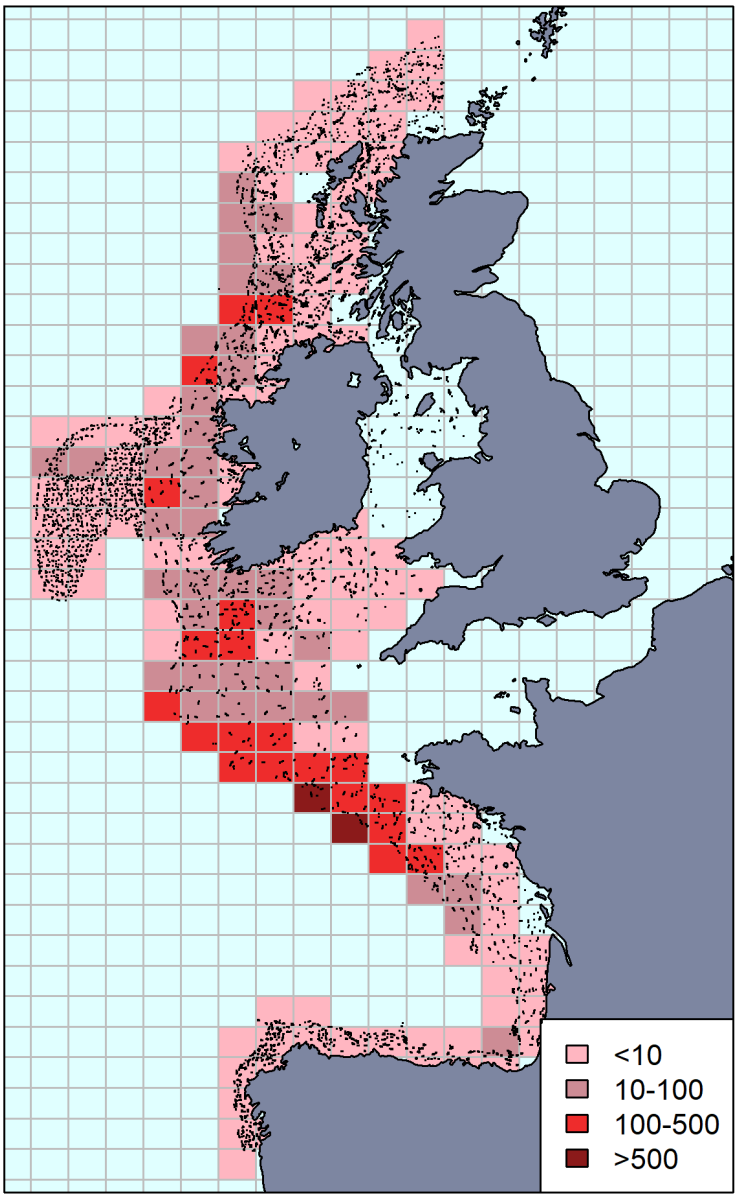


**Figure 3.7. IBTS mean catch rate of boarfish (kg/30 min) by ICES statistical rectangle 2002–2021.**

IBTS surveys routinely sample the entire catch in each haul (occasionally subsampling if the catch is particularly large) for length. Boarfish initially grow rapidly until they reach maturity at 4–5 years old. In several surveys, years modes size classes below 10 cm are evident in the length frequency distribution in particular from the Southern-most surveys (EVHOE, SPNGFS) and more recently the Irish (IGFS) survey indicating that these areas may be important for young, immature fish. Scottish surveys and the Porcupine bank survey are both associated with fully mature fish although a mode at approximately 10 cm is evident from the Scottish survey in the most recent years (Figure 3.8).

Since the IBTS indices were originally explored for use within the current Bayesian stock assessment model, there have been advances in the field of index standardization for use within stock assessment, in particular with regard to spatio-temporal modelling. This approach, typified by the VAST (Vector Autoregressive Spatio-Temporal) model, Thorson and Barnett (2017) implements a delta model capable of dealing with zeros and a continuous positive distribution but explicitly models spatial and spatio-temporal correlations in a pair of models. This approach offers the advantage of allowing for vessel (survey) effects such that separate surveys (with

potentially different sampling schemes) can be combined into a single index and can accommodate missing data.

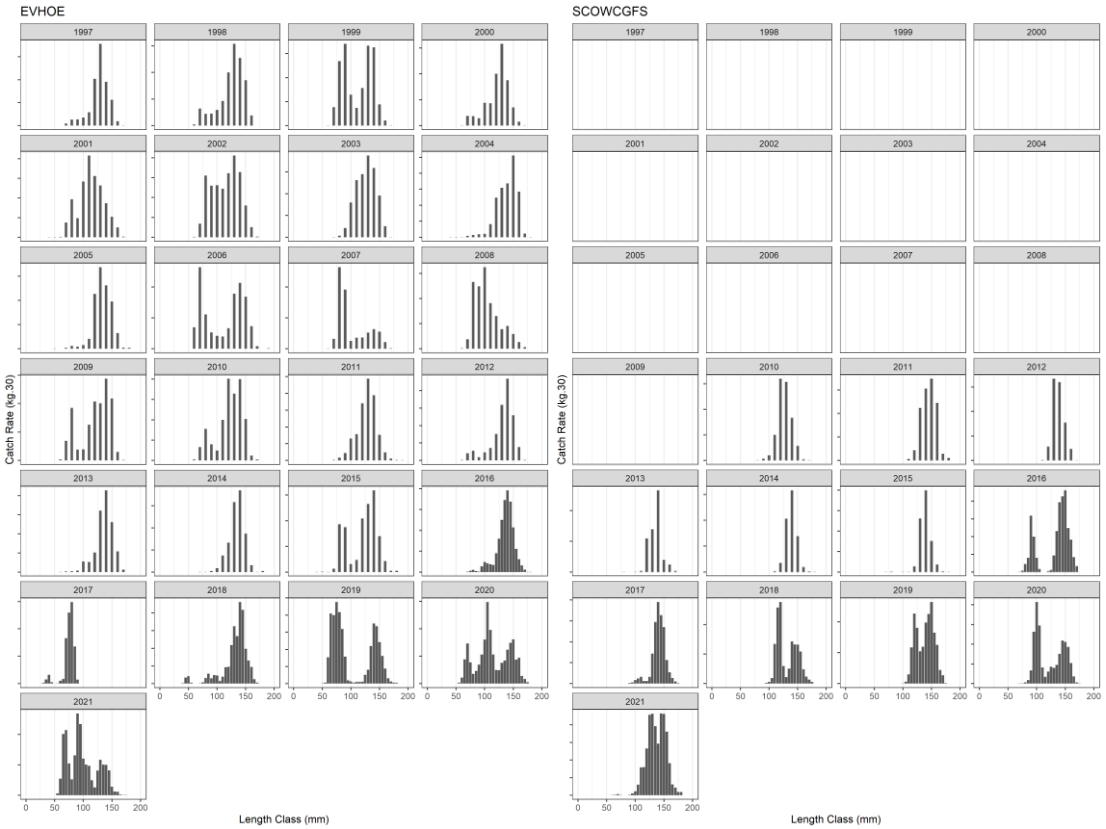


**Figure 3.8. Annual length frequency for total boarfish catch from EVHOE (left) and SCOWCGFS (right) surveys.**

For the current exercise, VAST is fitted to a combined survey dataset consisting of haul level catch rates of boarfish (kg per 30 min). The period considered is 1999 to present to coincide with the available catch time-series and corresponding to the period of consistent survey effort. The English-channel survey has been excluded as it ceased in 2003. The redesigned Scottish west coast Q1 and Q4 surveys (available since Q4 2010) have been included. For the purposes of combining these surveys the Q1 survey has been considered aligned with the Q4 survey (i.e. the survey year has been reduced by 1) such that each year of data consists of data from Q4 Irish, French, Spanish and Scottish surveys and the subsequent Scottish Q1 survey in the following year. A minor number of hauls have been excluded on the basis they were in areas that were infrequently surveyed (the Irish and Clyde Seas).

The model's spatial domain therefore consists of the majority of the Western European shelf where boarfish is understood to inhabit. The model establishes a grid consisting of 200 knots, the positions of which are dependent on the local sampling intensity. Overall, the dataset consists of 13,289 hauls. A number of fits were explored based on length-based subsets of the total catch to estimate indices based on all size classes and those corresponding to mature/immature fractions.

VAST implements two model components for encounter probability and positive catches, which are assumed to be lognormally distributed (a gamma distribution yielded a poorer model fit). The linear predictors include year-effects, survey effects and spatial and spatio-temporal variability. The R package FishStatsUtils (Thorson. 2018) implements a number of functions to examine VAST outputs and can be used to generate diagnostic plots to explore the model fit and an estimated index based on the summed density over the survey area along with estimates of uncertainty. Initially, VAST was fit to each of the surveys individually (with the exception of the

ECSGFS) with estimation of spatial correlation only. A second model including spatio-temporal correlation was also fitted.

The final VAST model was fitted to the complete dataset (all surveys and years from 1999) for catch rates based on

- All length classes
- Length classes < = 65 mm (immature, ages <2)
- Length classes >65 mm (age 2 and over)
- Length classes < = 100 (ages <3)
- Length classes >100 mm (age 3 and over)

Spatial and spatio-temporal correlations were estimated and separate runs were made with and without a survey (vessel) effect. All models appeared to converge with satisfactory diagnostics. Inclusion of a vessel effect would appear to be important, perhaps unsurprising given variations in survey protocols, gears and the separate geographic domains for each survey. A number of candidate indices for use within a SPiCT assessment are generated. The index corresponding to catch rates based on all length classes is shown in Figure 3.9.

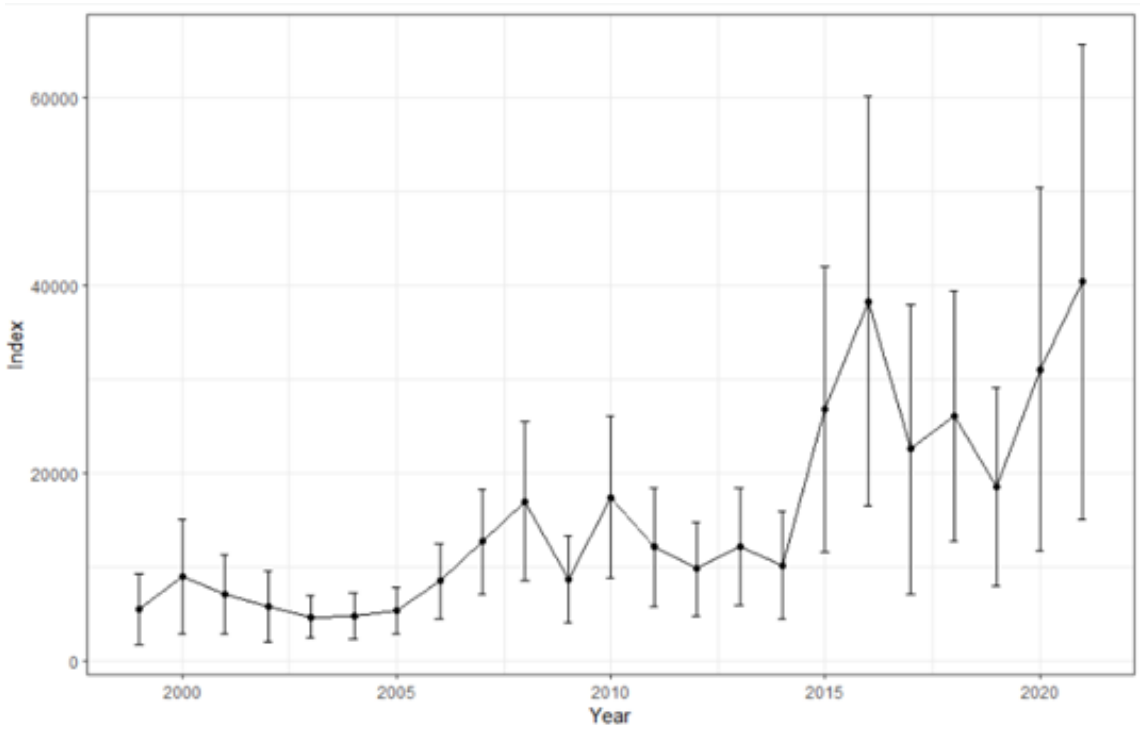


**Figure 3.9. VAST estimated IBTS boarfish index.**

A number of alternative model fits were conducted to explore the sensitivity of the proposed index to individual surveys and individual data points associated with high catch rates.

A leave one out analysis was conducted whereby the model was refit to data after excluding one of the survey time-series. The resulting index from each of these fits is shown in Figure 3.10.

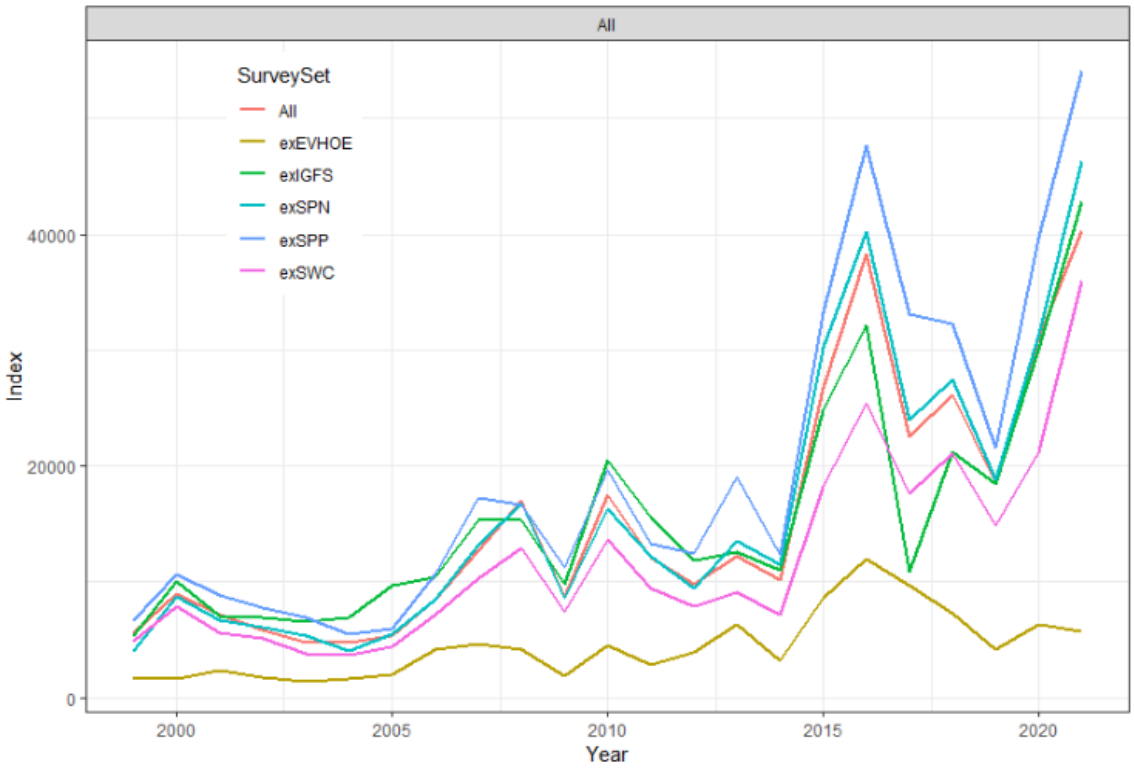


**Figure 3.10. VAST index leave one out analysis. The index is recalculated following the exclusion of one survey from the dataset.**

Figure 3.10 indicates that the EVHOE survey is the most influential in terms of the index, unsurprising given that it is associated with the highest catch rates and an average encounter rate of approximately 75%. Of the remaining surveys, the Scottish west coast and Irish groundfish are most influential, in particular in 2017 when the Irish survey undertook additional stations in the area normally covered by EVHOE which could not be completed due to vessel breakdown. The influence of the Scottish survey increases in the most recent period. Removing either of the Spanish surveys has a lower effect in the estimated index. These surveys are associated with relatively low catch rates and take place on the boundaries of the stock distribution.

An alternative VAST model was also fit excluding the survey effect. While the effect is considered to be significant when included, it's removal has a relatively minor effect on the overall index (Figure 3.11).

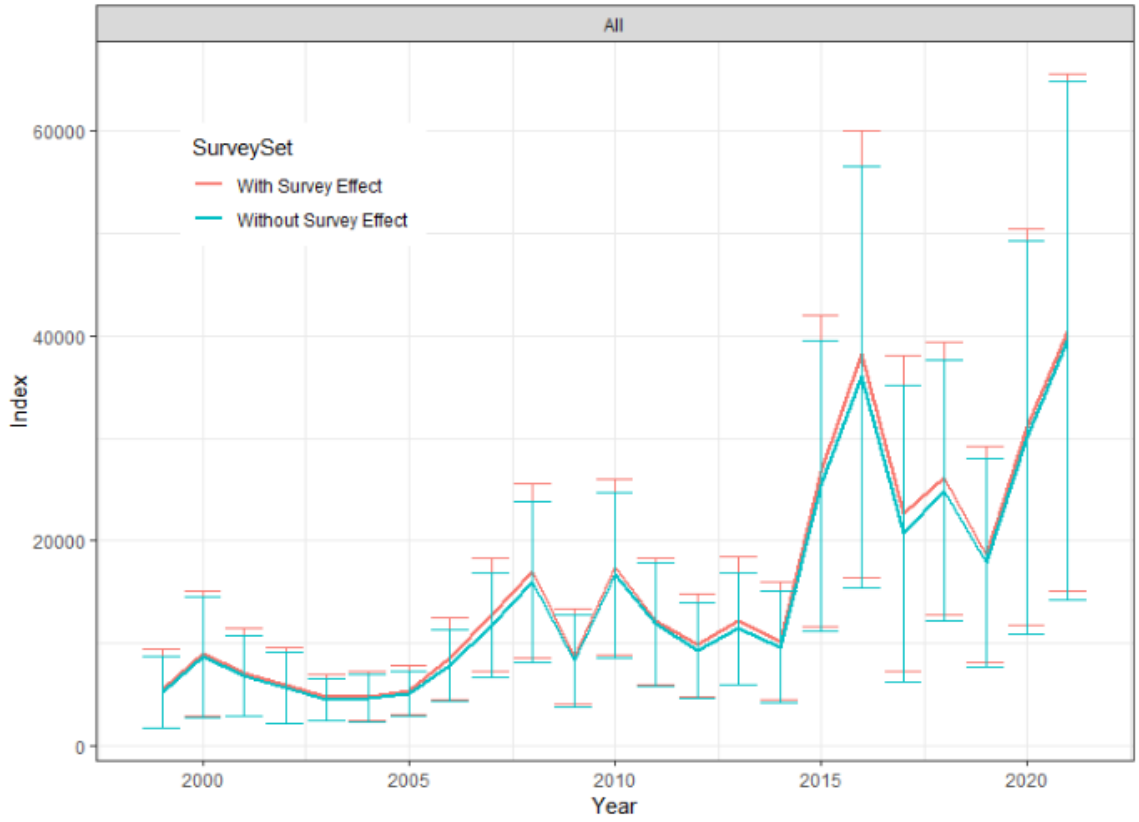


**Figure 3.11. VAST index with and without survey effect.**

Finally, the impact of large individual hauls on the index was explored. Although a delta lognormal observation model is assumed when configuring VAST, it is instructive to investigate the relative importance of individual hauls, in particular for schooling species. Figure 3.12 compares the original index with an alternative calculated when the 10 hauls with the highest catch rates are excluded in each year. Although a less variable index with narrower confidence intervals is estimated for this alternative dataset, it can be seen that the information contained in the dataset comprising lower catch rates is comparable to that when all hauls are included.

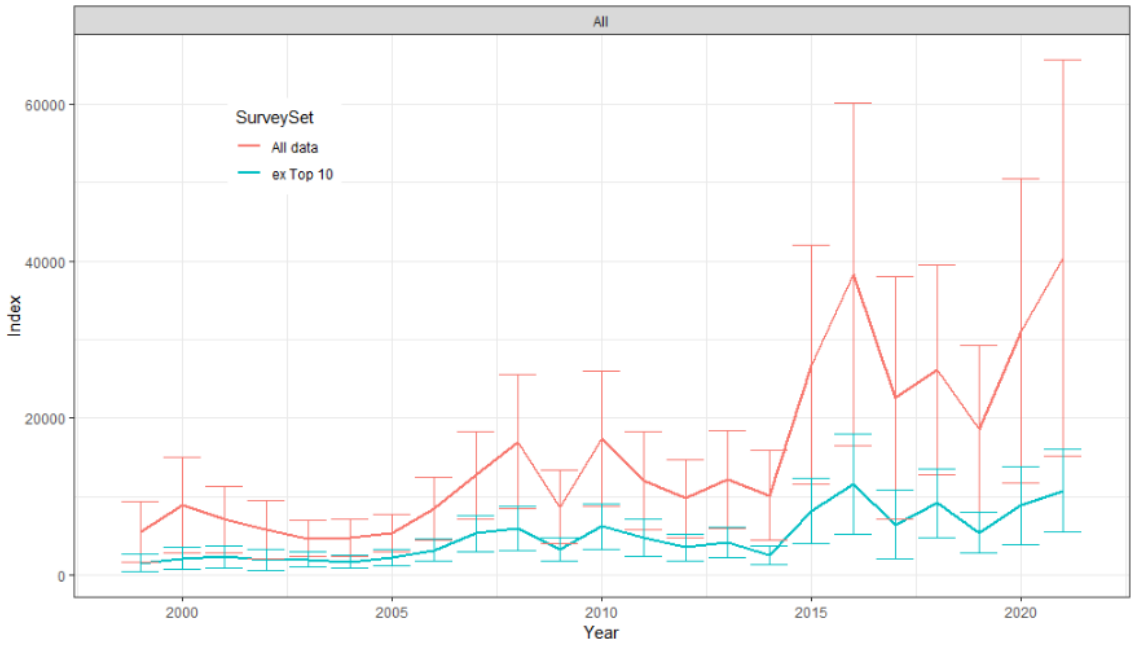


**Figure 3.12. VAST index based on all hauls (red) and excluding 10 highest catch rates in each year (blue).**

## 3.2.5 Life-history Parameters

### 3.2.5.1 Length

Comprehensive length sampling is carried out by the commercial catch sampling programme (landings (since 2007) and discards), the acoustic and groundfish surveys (Table 3.2). Initially, length measurements were taken to the nearest cm before protocols were updated to the ½ cm (2008 for catch, 2021 for the PELGAS acoustic survey)

**Table 3.2. Minimum ($L_{min}$) and maximum lengths ($L_{max}$), length at maturity ($L_{50}$) and length at first capture ($L_c$) for commercial catch, acoustic and two groundfish surveys.**

| Year | Catch ($L_{min}$,$L_c$,$L_{max}$) | WESPAS Acoustic Survey ($L_{min}$,$L_{50}$,$L_{max}$) | PELGAS Acoustic Survey ($L_{min}$,$L_{50}$,$L_{max}$) | IGFS Groundfish Survey ($L_{min}$,$L_{50}$,$L_{max}$) | EVHOE Groundfish Survey ($L_{min}$,$L_{50}$,$L_{max}$) |
|---|---|---|---|---|---|
| 1999 | | | | | 30,90,170 |
| 2000 | | | | | 20,110,170 |
| 2001 | | | | | 20,100,180 |
| 2002 | | | | | 20,90,190 |
| 2003 | | | | 20,130,180 | 30,120,170 |
| 2004 | | | | 20,130,190 | 30,130,180 |
| 2005 | | | | 20,140,190 | 20,130,180 |
| 2006 | | | | 10,140,180 | 10,70,190 |
| 2007 | 100,130,160 | | | 10,130,170 | 20,80,180 |
| 2008 | 95,120,170 | | | 30,130,190 | 20,90,190 |
| 2009 | 75,120,170 | | | 20,120,180 | 20,90,180 |
| 2010 | 60,120,180 | | | 20,130,170 | 20,110,190 |
| 2011 | 70,125,170 | 75,125,165 | | 20,130,190 | 20,120,190 |
| 2012 | 70,130,170 | 75,125,175 | | 20,130,180 | 20,120,180 |
| 2013 | 70,130,185 | 80,130,175 | | 10,140,180 | 20,130,190 |
| 2014 | 30,130,220 | 100,140,180 | 70,130,160 | 20,140,180 | 20,130,180 |
| 2015 | 45,125,190 | 60,140,185 | 60,70,160 | 20,140,180 | 20,90,190 |
| 2016 | 30,125,270 | 70,140,185 | 70,90,160 | 15,140,185 | 10,135,180 |
| 2017 | 40,120,290 | 55,135,180 | 90,140,160 | 30,140,185 | 25,70,90[1] |
| 2018 | 30,130,250 | 50,140,205 | 60,130,160 | 10,140,185 | 20,100,180 |
| 2019 | 10,80,470 | 40,130,180 | 50,70,170 | 10,140,210 | 15,70,180 |
| 2020 | 50,80,210 | 40,125,170 | No survey | 10,100,180 | 10,90,180 |
| 2021 | 40,100,190 | 35,80,180 | 40,60,140 | 15,95,195 | 20,75,185 |
| 2022 | | 55,100,175 | 50,80,160 | | |

[1] Limited coverage.

### 3.2.5.2 Length-weight

Data to support length-weight analyses are available from sampling of the commercial fishery and summer acoustic survey from 2011–2022. The fishery largely takes place in quarters 1 and 4 so separate analyses have been carried out for data from fishery samples in Jan–Apr (Q1/2), survey samples in Jun–Jul and fishery samples from (Sep–Dec). a and b parameters of the growth function W = aLb were estimated by fitting a linear model in R (lm) to log transformed length and weight data for each year.

In Figure 3.13, the blue lines correspond to fits from data collected in quarters 3 and 4 (i.e. from the fishery). The red lines use sampling data from the fishery in quarter 1 with occasional catches in quarter 2. The green lines are largely based on observations taken during the acoustic survey which takes place at spawning time in summer (June/July). While the length weight relationships from data collected during winter are similar, specimens tend to be heavier during summer.

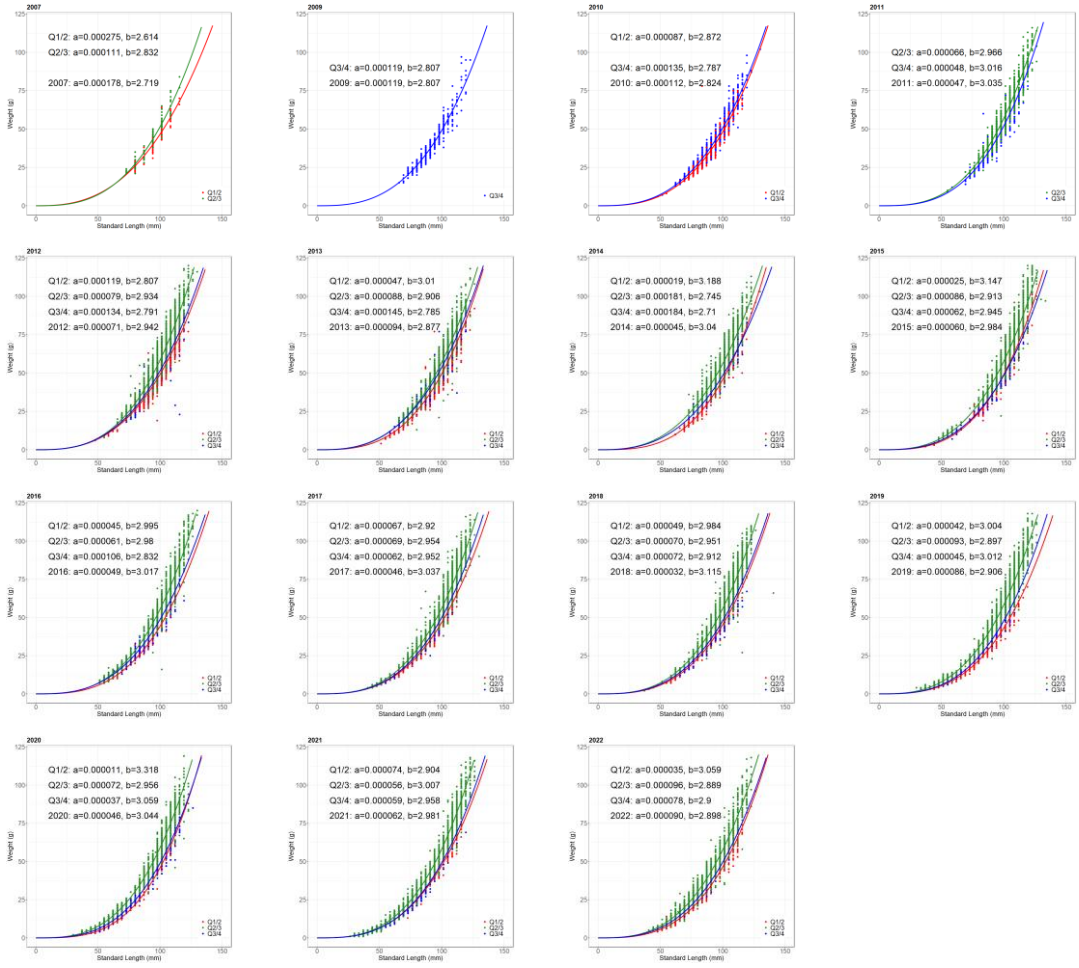


**Figure 3.13. Length-weight regressions for catch and acoustic survey samples.**

### 3.2.5.3 Length at maturity

Maturity staging (8-point scale, 3 and above considered mature) is carried out on samples from the commercial fishery and also during the WESPAS acoustic survey where extensive trawl sampling is carried out (on average, ~850 fish are sampled annually for maturity staging). R package sizeMat (Torrejon-Magallanes J, 2020) was used to fit a maturity ogive to annual survey data as shown in Figure 3.14.

The study of White *et al*. (2011) estimated an overall value (both sexes) for L50 of 85.7 mm with sex-specific values of 80.5 mm for females and 87.8 mm for males. Although few immature fish

are collected in some years, estimates from the acoustic survey data presented below range from 58–75 mm (standard length). Based on the relationship between total and standard length (SL = 1.34386 + 0.715 x TL), the equivalent TL range is 79 mm–103 mm. There may be evidence of year-class variability of maturation. Comparing data from the 2020 and 2021 surveys, both of which contain a significant number of immature specimens, all fish under 75 mm in 2020 were immature whereas all fish greater than 60 mm SL were considered mature in 2021.

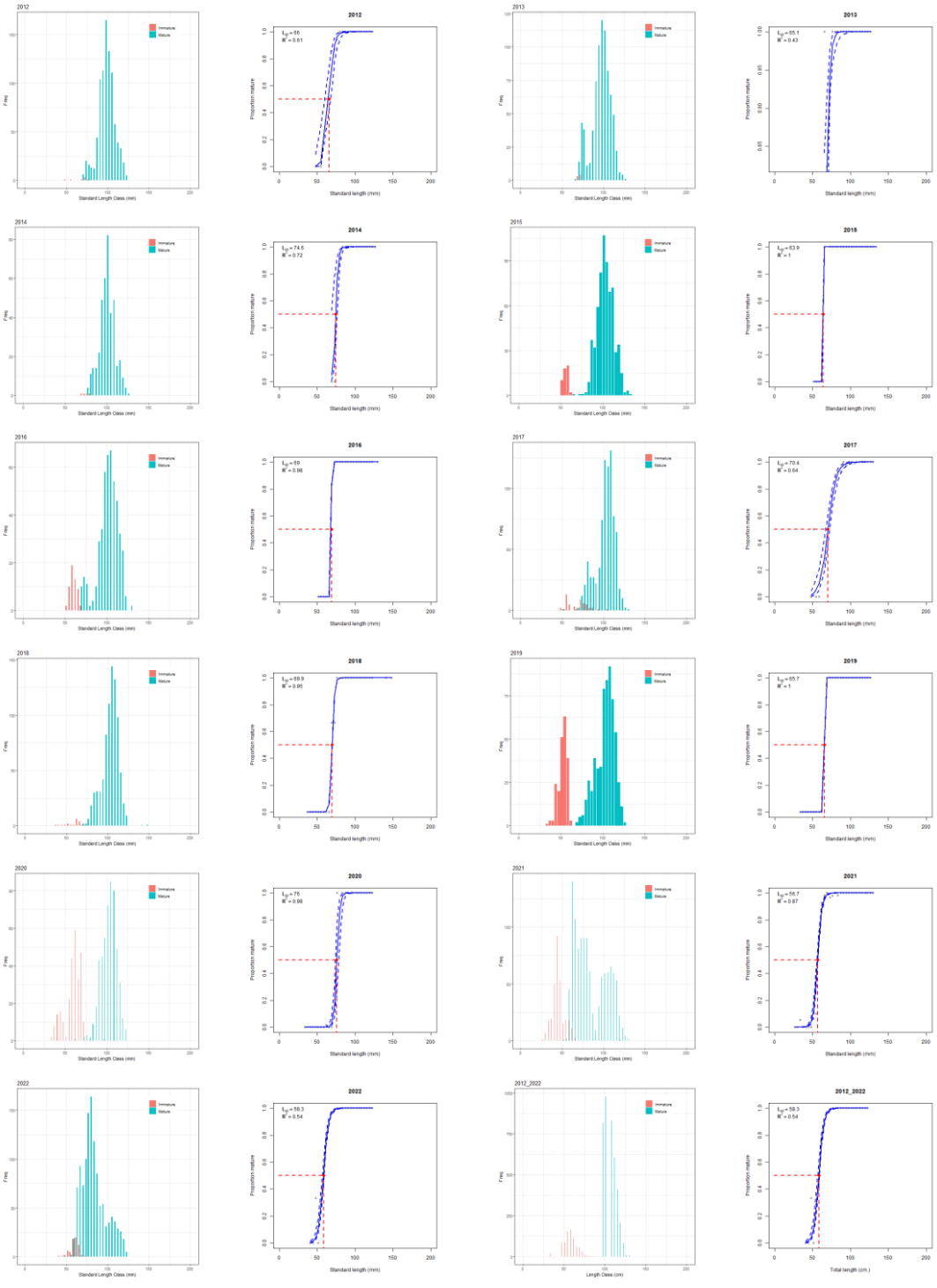

**Figure 3.14. Maturity ogives fit to acoustic survey sample data.**

### 3.2.5.4 Ageing, von Bertalanffy growth parameters

During initial investigations around the start of the targeted fishery, 868 boarfish samples were obtained from the fishery and research vessels in May, June, October and November of 2007 from 6.aS, 7.b, 7.g, 7.h, and 7.j and were used to investigate the growth of boarfish (White *et al*., 2011). At this time, age reading protocols were also developed (Hüssy *et al*., 2012a) and an ALK constructed. White *et al*. (2011) noted a maximum age of 26, relatively late maturing (A50 = 5.25 years), K = 0.186 yr-1 and an asymptotic length of 129 mm.

Hüssy *et al*. (2012b) investigated sexual dimorphism in the growth characteristics of boarfish from samples collected in 2009 and 2010. Although females are on average larger than males there is no significant difference in length at maturity nor age at maturity (L50 = 97 mm, A50 = 3.4 yrs). Growth is dimorphic with a common $t_0$ but significantly different K and $L_{inf}$ values with K = 0.145 yr-1 for females and 0.181 for males and $L_{inf}$ = 165 mm and 144 mm for females and males respectively.

Ageing of boarfish fishery and survey samples ceased in 2011 (although collection of otoliths has continued). An updated analysis to include all aged samples collected up to 2011 leads to the following updated estimates:

**Table 3.3: Updated boarfish von Bertalanffy life-history estimates.**

| **Female (age range 2–31)** | | | | | | | | |
|---|---|---|---|---|---|---|---|---|
| **$L_{inf}$** | | | **K** | | | **$t_0$** | | |
| 2.5% | 50% | 97.5% | 2.5% | 50% | 97.5% | 2.5% | 50% | 97.5% |
| 159 | 160 | 161 | 0.138 | 0.143 | 0.149 | -4.57 | -4.29 | -4.03 |

| **Male (age range 1–30)** | | | | | | | | |
|---|---|---|---|---|---|---|---|---|
| **$L_{inf}$** | | | **K** | | | **$t_0$** | | |
| 2.5% | 50% | 97.5% | 2.5% | 50% | 97.5% | 2.5% | 50% | 97.5% |
| 146 | 147 | 148 | 0.156 | 0.165 | 0.172 | -4.64 | -4.27 | -3.97 |

Growth is relatively rapid until the fish is mature with little to distinguish between ages 5–10 in terms of length. At the time of the ageing studies, the population consisted of a significant proportion of relatively old fish (PG 15+) consistent with a stock experiencing only light exploitation. The fishery at this time was concentrated in areas to the SW of Ireland (7.j), exploiting dense shoals on the shelf break. Few immature samples were obtained therefore the age length key was sparse for the youngest ages. Recently, work has restarted to establish routine ageing of both fishery and survey samples.

### 3.2.5.5 Natural mortality

Using the method described by King, (1995), that natural mortality will reduce a population to 1% of its initial size over the lifespan of the stock, and based on a maximum observed age of 31, a natural mortality estimate of 0.16 was calculated. This is a similar estimate to the total mortality estimate from 2007 (0.17) when landings were relatively low. Estimates from IBTS data from 2003–2006 ranged from 0.09 to 0.2 with a mean of 0.16 (ICES, 2012).

### 3.2.5.6 Model priors

SPiCT can be configured to supply priors for model parameters. Defaults are uninformative and may lead to unrealistic parameter estimates. Information is available for a number of model parameters that can be used to provide more informative priors than the defaults.

#### 3.2.5.6.1 Intrinsic growth rate (r)

Candidate priors for intrinsic growth rate, r, are available from the FishLife R package (Thorson, 2020), the SPMPriors R package (Winker, 2020), the current surplus production assessment model (ICES, 2022) and Trenkel and Rochet (2003).

The FishLife package estimates a value for r of 0.65. A summary of estimates for *Capros aper* is shown in Figure 3.15. However, information in FishBase on boarfish is sparse. Moreover, several of the data sources are derived from studies undertaken on boarfish likely from other populations, notably from the Aegean Sea where both growth rate and asymptotic length are different (estimates of K of ~ 0.4 for the Aegean population, double that of NE Atlantic studies). Attempts to refit the model using either a subset of the available data or including more recent data were unsuccessful.

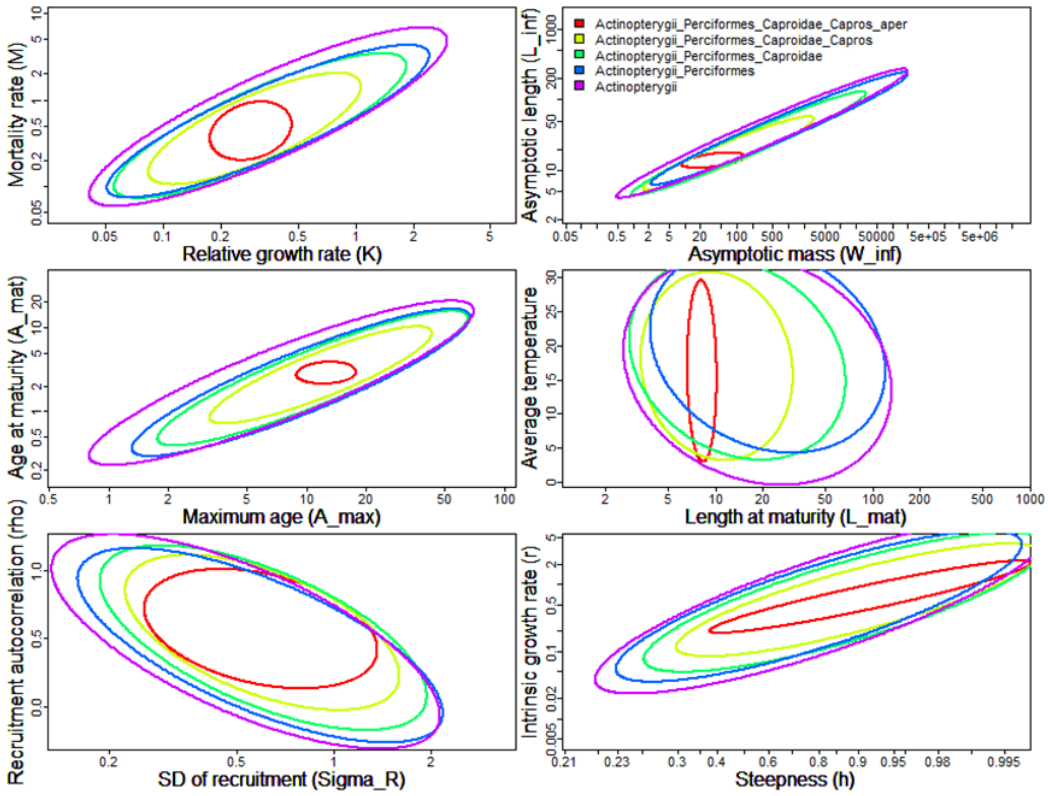


**Figure 3.15. Summary of Caper aper life-history estimates using the R package FishLife.**

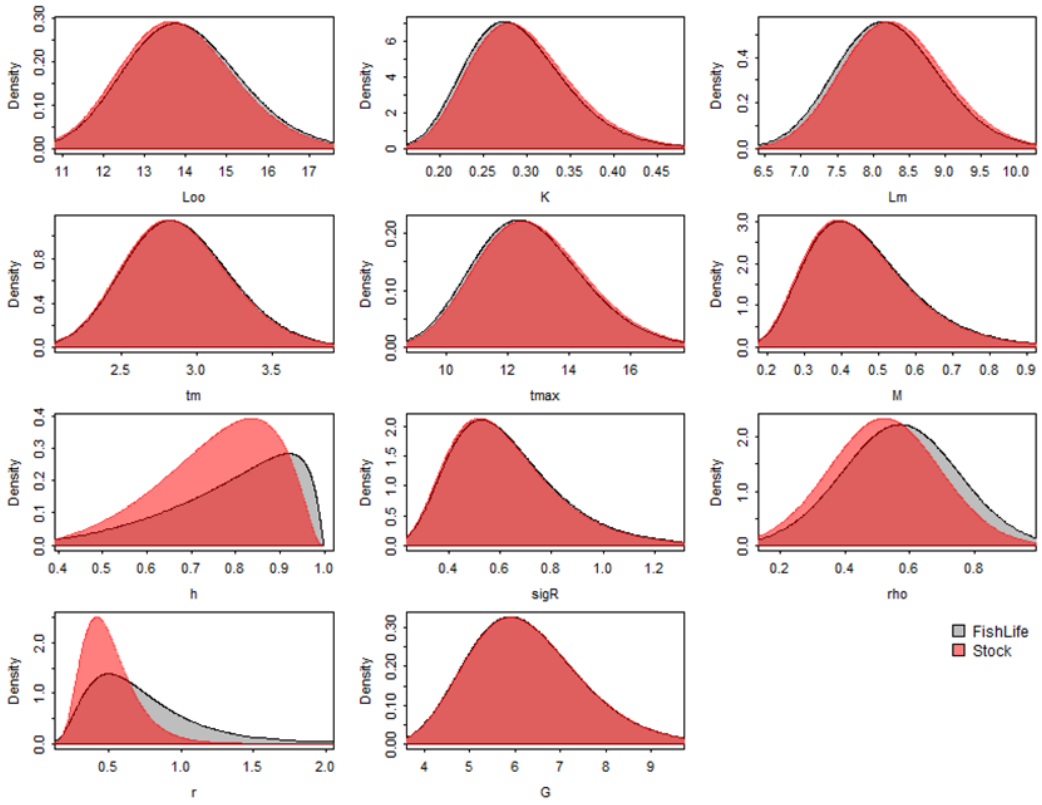


**Figure 3.16. Summary of life-history parameters from R package SPMPriors for boarfish.**

The SPMPriors R package generates surplus production priors from FishLife and yields an estimate for r of 0.47 (Figure 3.16). The r parameter from FishLife was translated into Pella-Tomlinson SPM priors through an age-structured model using the fl2asem function in SPMPriors to give an r value of 0.29. Trenkel and Rochet (2003) published a study which included an estimate of 0.31 for boarfish in the Celtic Sea. The most recent update assessment estimates an r value of 0.34, with a standard deviation of 0.17. The table below summarizes the available information on intrinsic growth rate for NE Atlantic boarfish

| Value | Source |
|---|---|
| 0.64 | FishLife (FishBase) |
| 0.47 | SPM Priors |
| 0.34 | Current Assessment (WGWIDE 2022) |
| 0.31 | Trenkel and Rochet 2003 |
| 0.29 | fl2asem |

#### 3.2.5.6.2 Shape parameter (n)

Little information is available on the likely value for the production curve shape parameter, n. The current assessment model is a Schaefer model which assumes an n = 2. Meta-analyses conducted by Thorson *et al*. (2012) estimated n for 147 species pooled and on 4 taxonomic orders. Boarfish is in the Perciformes order for which the authors estimated a shape parameter value of 1.064, with a standard deviation of 0.562.

#### 3.2.5.6.3 Initial Depletion fraction (bkfrac)

Prior to 2006, there was no targeted fishery for boarfish. Although discarding is understood to have occurred, it was not quantified. Discarding estimates from some fleets from the period

around the start of the fishery vary from 3–10 kt. These fleets did not target boarfish and it would seem likely discarding occurred at similar levels prior to the availability of these estimates. It is reasonable to assume that the stock was not heavily exploited prior to the fishery commencing such that the initial depletion is likely to be low or moderate.

The first 4 data points in the catch series (1999–2002) are, by an order of magnitude, the lowest in the time-series. They represent reported catches prior to the establishment of the fishery and precede the start of the discard time-series.

## 3.3 Stock assessment

A range of exploratory SPiCT assessments were conducted for each of 3 different datasets comprising

1. Catch and TSB index from acoustic surveys
2. Catch and VAST groundfish survey index
3. Catch, acoustic TSB and groundfish survey indices

Individual fits were used to explore the model diagnostics and response to assumptions with regard to a number of model inputs. Individual SPiCT assessments are uniquely identified by a combination of a run number denoting the input dataset (1,2 or 3) and a fit number. Initial assessments for each dataset were run using SPiCT default parameter values. Information was incrementally included in the form of parameter priors to fine tune the assessment and explore sensitivity to assumptions. Additional fits were explored during the benchmark workshop following plenary discussions.

Assessments explored the effects of:

1. Increasing the uncertainty in relation to individual data years, specifically
   a) Increased uncertainty for the first 4 years of catch data (1999–2002) when no discard estimates are available. For 2003–2005, significant discarding is reported (4–10 kt) whereas catches are low (<1 kt) as the target fishery has not yet become established and it is likely this situation also applies to 1999–2002 such that catch is underestimated.
   b) The PELGAS acoustic survey was not conducted in 2020, due to COVID-19 impacts. In 2019 and 2021 TSB estimates were 14 kt and 131 kt respectively for this survey. It is therefore reasonable to assume that in the intervening year, a total estimate based only on the WESPAS survey results is likely associated with increased uncertainty.
   c) The VAST derived index from the combined groundfish surveys indicates increased uncertainty in years with lower survey coverage. These include the early years of the survey index (1999–2002) when some of the surveys had not started and 2017, when significant survey effort was lost due to vessel breakdown. The effects of increased uncertainty in these years was also investigated.
2. Prior information on initial depletion. The target fishery for boarfish only became established several years after the start of the available data. While discarding is known to have taken place, it is reasonable to assume that the stock was not heavily exploited prior to 2005. This assumption is supported by the catch sampling in the initial years of the target fishery. Exploratory assessments therefore considered a range of scenarios for the initial biomass depletion (bkfrac). Initial depletion values of 0.2, 0.5 and 0.8 were tested to explore assumptions of heavy, moderate and light exploitation rates at the start of the assessment period (1999).
3. Prior information on production curve shape parameter (n) is limited. Priors based on a Schaeffer production curve (n=2), as used in the current stock assessment for this stock and alternatives from the Thorsen *et al* (2012) meta-analysis are explored.

4. Prior information on intrinsic growth rate (r). Various estimates for this parameter are available from literature, the current assessment and helper packages such as FishLife and SPM-Priors.
5. Prior information on survey catchability. Fishery-independent information is available from a targeted acoustic survey and an index of abundance from a VAST model fit to catch rates recorded by a number of Western IBTS surveys. The acoustic survey has been designed to provide TSB estimates for the entire boarfish stock, covering the majority of the stock distribution and achieving spatial containment on the northern, western (seaward) and eastern (land) boundaries. On the southern boundary where the primary survey has not achieved containment in the most recent period, estimates of boarfish biomass are available from a separate acoustic survey such that an estimate for the entre stock is available and an assumption of a survey catchability close to unity is appropriate.
6. While observation errors are estimated by SPiCT when fitting to all data including catch and survey, several assessments were explored when priors are provided for the appropriate parameters; sdc, sdi

SPiCT assessments were evaluated using residual analysis (calc.osa.resid, calc.process.resid) , 5 year retrospective runs (retro), initial value trials (check.ini) with 30 randomly generated initial parameter values and hindcast analysis (hindcast). Based on the SPiCT checklist the following criteria were considered when evaluating an assessment

1. Convergence
2. Finite variable parameter estimates
3. OSA residual patterns, bias, autocorrelation
4. Process error residual patterns, bias, autocorrelation
5. Mohn's rho for biomass (max absolute value of 0.2) and fishing mortality (max absolute value of -0.15)
6. Magnitude of uncertainty in biomass and fishing mortality (max 1 order of magnitude)
7. Estimated shape of the production curve
8. Assessments that failed to meet criteria in terms of convergence and finite parameter estimates are not considered further. Information on the OSA and process residuals, retrospective performance and uncertainty were the primary metrics used to evaluate the quality of individual assessment fits.

### 3.3.1 Run 1 (catch and acoustic Survey)

Estimates of TSB from the acoustic surveys are available from 2011 onwards whereas the catch data starts in 1999 such that there is a significant period prior to the start of the survey with no fishery-independent dataset. Moreover, this coincides with the period when the fishery was unregulated and expanded rapidly with the peak in catches occurring prior to the start of the acoustic survey time-series.

The SPiCT fits for this dataset are summarized in Table 3.3.1. Cells with red text indicate diagnostics that fail the SPiCT checklist or, in the case of parameter estimates, they highlight assessments that have unreasonable parameter values.

**Table 3.3.1. SPiCT fits for run 1 (catch and acoustic survey datasets)**

| Fit | Uncertainty (factor/years) | | Priors (log(x),y) | | | | | | Diagnostics | | | | | Parameters/States | | | | | | |
|---|---|---|---|---|---|---|---|---|---|---|---|---|---|---|---|---|---|---|---|---|
| | Catch | Index | bkfrac | n | r | q | sdc | sdi | OSA Res (Catch/ Index) | Proc. Res (B/F) | Retro (B/F) | Unc. (B/F) | Bmsyk | B/$B_{MSY}$ | F/$F_{MSY}$ | $B_{MSY}$ (kt) | $F_{MSY}$ | MSY (kt) | K | R |
| 1 | | | | | | | | | OK | F | ✓/× | 1/5 | 0.46 | 2.55 | 0.06 | 461 | 0.47 | 215 | 1.0Mt | 0.75 |
| 2 | | | 0.5,0.5 | | | | | | Catch | F | ✓/✓ | 1/2 | 0.32 | 0.93 | 0.59 | 113 | 0.29 | 33 | 358kt | 0.22 |
| 3 | 6 | | | | | | | | OK | F | ✓/✓ | 3/2 | 0.30 | 0.24 | 1.47 | 364 | 0.15 | 54 | 1.2Mt | 0.1 |
| 4 | 6 | | 0.5,0.5 | | | | | | OK | F | ✓/✓ | 1/1 | 0.36 | 0.75 | 0.70 | 123 | 0.28 | 35 | 346kt | 0.26 |
| 5 | 6 | 2 (2020) | 0.5,0.5 | | | | | | OK | F | ✓/✓ | 1/1 | 0.36 | 0.74 | 0.71 | 123 | 0.24 | 35 | 343kt | 0.27 |
| 6 | 6 | 2 (2020) | 0.5,0.5 | | | 0.9,0.5 | | | OK | F | ✓/× | 2/3 | 0.40 | 2.28 | 0.13 | 257 | 0.28 | 71 | 638kt | 0.33 |
| 7 | 6 | 2 (2020) | 0.2,0.5 | | | | | | OK | F | ✓/✓ | 1/1 | 0.37 | 0.70 | 0.72 | 130 | 0.28 | 36 | 356kt | 0.27 |
| 8 | 6 | 2 (2020) | 0.2,0.5 | | | 0.9,0.5 | | | OK | F | ✓/✓ | 1/2 | 0.42 | 2.20 | 0.14 | 276 | 0.27 | 75 | 656kt | 0.36 |
| 9 | 6 | 2 (2020) | 0.8,0.5 | | | 0.9,0.5 | | | OK | F | ✓/× | 2/3 | 0.40 | 2.27 | 0.13 | 255 | 0.28 | 70 | 632kt | 0.33 |
| 10 | 6 | 2 (2020) | 0.8,0.5 | | | | | | OK | F | ✓/✓ | 1/1 | 0.36 | 0.76 | 0.70 | 120 | 0.29 | 34 | 335kt | 0.27 |
| 11 | 6 | 2 (2020) | 0.8,0.5 | 2,0.5 | | 0.9,0.5 | | | OK | F | ×/× | 1/2 | 0.49 | 1.88 | 0.19 | 321 | 0.23 | 72 | 654kt | 0.43 |
| 12 | 6 | 2 (2020) | 0.8,0.5 | 1.2,0.5 | | 0.9,0.5 | | | OK | F | ✓/× | 1/2 | 0.40 | 2.31 | 0.13 | 250 | 0.28 | 70 | 630kt | 0.33 |
| 13 | 6 | 2 (2020) | 0.8,0.5 | | 0.34,0.5 | 0.9,0.5 | | | OK | F | ×/× | 2/3 | 0.41 | 2.26 | 0.13 | 257 | 0.28 | 71 | 632kt | 0.34 |
| 14 | 6 | 2 (2020) | 0.8,0.5 | 1.2,0.5 | 0.34,0.5 | 0.9,0.5 | | | OK | F | ✓/✓ | 1/1 | 0.40 | 2.32 | 0.13 | 249 | 0.29 | 72 | 627kt | 0.34 |
| 15 | 6 | 2 (2020) | 0.5,0.5 | 1.2,0.5 | 0.34,0.5 | 0.9,0.5 | | | OK | F | ✓/✓ | 1/1 | 0.40 | 2.32 | 0.13 | 252 | 0.29 | 72 | 634kt | 0.34 |
| 16 | 6 | 2 (2020) | 0.2,0.5 | 1.2,0.5 | 0.34,0.5 | 0.9,0.5 | | | OK | F | ✓/✓ | 1/1 | 0.40 | 2.29 | 0.13 | 260 | 0.29 | 74 | 651kt | 0.34 |
| 17 | 6 | 2 (2020) | 0.2,0.5 | 2,0.5 | 0.35,0.5 | 0.9,0.5 | | | OK | F | ✓/× | 1/2 | 0.47 | 1.90 | 0.19 | 323 | 0.22 | 72 | 684kt | 0.39 |
| | | | | | | | | | | | | | | | | | | | | |
| 20 | 6 | 2 (2011- | 0.2,0.5 | | | | 0.2,0.2 | | Catch | OK | ✓/✓ | 1/1 | 0.29 | 0.66 | 0.70 | 137 | 0.26 | 35 | 469kt | 0.17 |
| 21 | 6 | 2 (2011- | 0.2,0.5 | | | | 0.2,0.2 | | Catch | OK | ✓/✓ | 1/1 | 0.40 | 0.64 | 0.63 | 151 | 0.27 | 40 | 380kt | 0.31 |
| | | | | | | | | | | | | | | | | | | | | |
| 30 | 6 | 2 (2011- | 0.5,0.5 | | | | 0.2,0.2 | | Catch | OK | ✓/✓ | 1/1 | 0.30 | 0.73 | 0.64 | 124 | 0.28 | 34 | 413kt | 0.19 |
| 31 | 6 | 2 (2011- | 0.5,0.5 | | | | 0.2,0.2 | | Catch | OK | ✓/✓ | 1/1 | 0.39 | 0.66 | 0.63 | 145 | 0.27 | 39 | 371kt | 0.31 |
| 32 | 6 | 2 (2011- | 0.5,0.5 | | 0.2,0.1 | | 0.2,0.2 | | Catch | OK | ✓/✓ | 1/1 | 0.33 | 0.64 | 0.74 | 139 | 0.25 | 34 | 420kt | 0.20 |
| 33 | 6 | 2 (2011- | 0.5,0.5 | 2,0.001 | | | 0.2,0.2 | | Catch | OK | ✓/✓ | 1/1 | 0.50 | 0.71 | 0.47 | 157 | 0.31 | 49 | 314kt | 0.62 |
| 34 | 6 | 2 (2011- | 0.5,0.5 | | 0.4,0.1 | | 0.2,0.2 | | Catch | OK | ✓/✓ | 1/1 | 0.43 | 0.68 | 0.56 | 148 | 0.29 | 42 | 345kt | 0.40 |
| 35 | 6 | 2 (2011- | 0.5,0.5 | | | 1.0,0.1 | 0.2,0.2 | | Catch | OK | ×/× | 1/3 | 0.45 | 2.04 | 0.14 | 310 | 0.24 | 75 | 696kt | 0.37 |
| 36 | 6 | 2 (2011- | 0.5,0.5 | | | 0.9,0.1 | 0.2,0.2 | | Catch | OK | ×/× | 1/3 | 0.44 | 2.16 | 0.11 | 325 | 0.26 | 84 | 741kt | 0.38 |
| | | | | | | | | | | | | | | | | | | | | |
| 40 | 6 | 2 (2011- | 0.8,0.5 | | | | 0.2,0.2 | | Catch | OK | ✓/✓ | 1/1 | 0.30 | 0.76 | 0.62 | 119 | 0.29 | 34 | 391kt | 0.20 |
| 41 | 6 | 2 (2011- | 0.8,0.5 | | | | 0.2,0.2 | | Catch | OK | ✓/✓ | 1/1 | 0.39 | 0.67 | 0.63 | 142 | 0.27 | 38 | 365kt | 0.30 |
| 42 | 6 | 2 (2011- | 0.8,0.5 | | | 1.0,0.5 | 0.2,0.2 | | Catch | OK | ✓/✓ | 1/2 | 0.46 | 1.63 | 0.23 | 281 | 0.19 | 53 | 608kt | 0.31 |
| | | | | | | | | | | | | | | | | | | | | |
| 50 | 6 (1999- | | 0.8,0.5 | | | | 0.2,0.2 | | Catch & Index | OK | ✓/✓ | 1/1 | 0.36 | 0.69 | 0.64 | 136 | 0.27 | 37 | 374kt | 0.27 |
| 51 | 6 | 1.5 | 0.8,0.5 | | | | 0.2,0.2 | | Catch | OK | ✓/✓ | 1/1 | 0.38 | 0.68 | 0.64 | 140 | 0.27 | 38 | 370kt | 0.29 |
| 52 | 6 | 1.5 | 0.8,0.5 | | | | 0.2,0.2 | | Catch | OK | ✓/✓ | 1/1 | 0.39 | 0.68 | 0.62 | 141 | 0.27 | 39 | 363kt | 0.31 |
| 53 | 6 | 1.5 | 0.8,0.5 | | | | 0.2,0.2 | | Catch | OK | ✓/✓ | 1/1 | 0.40 | 0.67 | 0.58 | 140 | 0.29 | 41 | 348kt | 0.35 |

The assessment using the default SPiCT settings (fit 1) is characterized by very high uncertainties (particularly in fishing mortality), poor retrospective performance and an unrealistic biomass trajectory prior to the onset of the fishery. Implementing a prior for initial depletion elevates the initial biomass and including additional uncertainty in catch prior to 2003 and on the acoustic survey data point for 2020 improves the overall model fit (*e.g.* fit 4). However, estimates for the

survey catchability are unrealistic (~6) and the absolute biomass in the terminal year is estimated to be around 100 kt with a peak at the onset of the fishery around 300 kt (the fishery extracted ~500 kt between 2007 and 2013). The observation error on the catches is large and the model predicted catch is well below actual catches in several years (under-fitting by a cumulative 100 kt during the peak of the fishery). The large fluctuation in catch when the (unregulated) fishery initially grew followed by a cut on the introduction of management (TAC) measures is challenging for the model to replicate. Accompanying the large estimate of observation error in catch is a strong autocorrelation in the fishing mortality process error residuals. The value of the prior assumed for bkfrac is relatively unimportant with respect to the stock status and production function, when compared to the run with a default assumption (Figure 3.3.1)

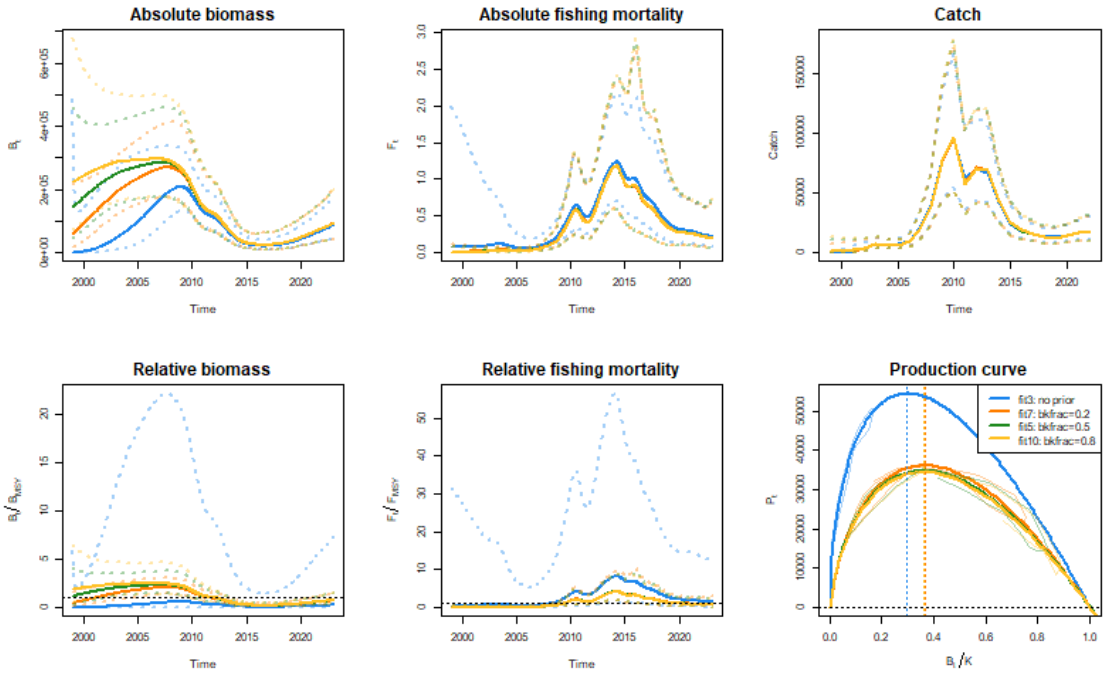


**Figure 3.3.1 Comparison of SPiCT assessments with varying assumptions on bkfrac (no other non-default priors).**

Specifying strong priors on survey catchability (stock containment is assumed) and catch observation error (catches are well documented) leads to an alternative model fit and a different stock status with respect to MSY (Figure 3.3.2).

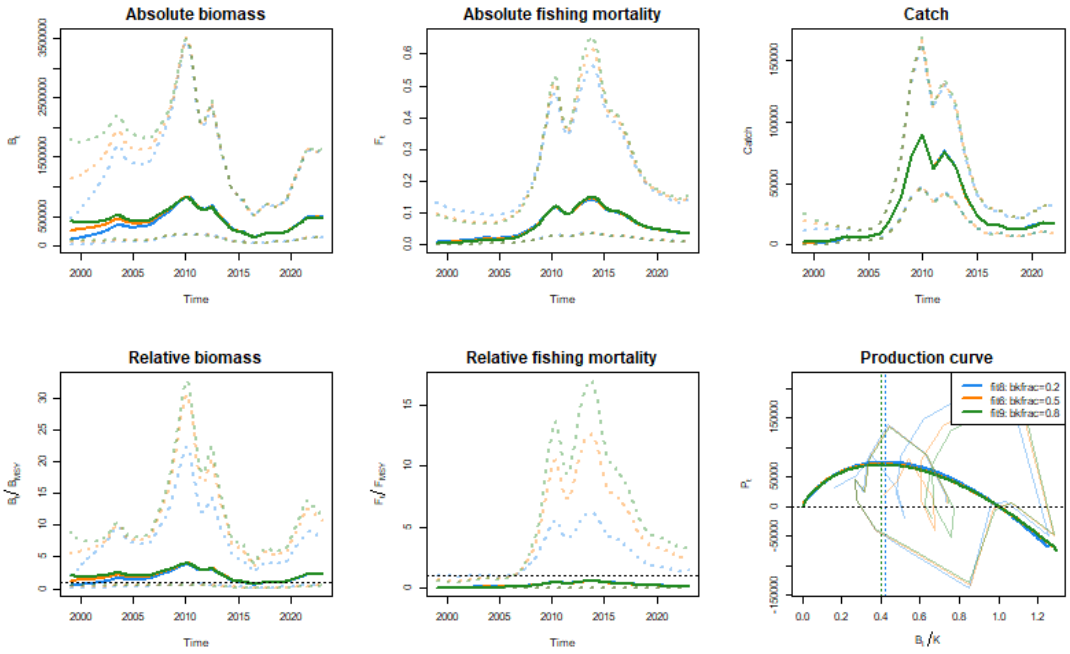


**Figure 3.3.2 Comparison of SPiCT assessments with varying assumptions on bkfrac and prior on survey catchability (log(q) = 0.9, sd = 0.5).**

To reduce the high uncertainty, additional fits were made with various combinations of priors on the production curve shape parameter and the intrinsic growth rate. Fits with these parameters estimated without prior information indicate a tendency for n values closer to a Fox model (n = 1) rather than Schaeffer (n = 2). Estimates for r vary between 0.22 and 0.36, in line with the available information from other sources. Figure 3.3.3 compares 3 fits (bkfrac = 0.2,0.5,0.8) with a prior on log(q) (log (0.9),0.5), log(n) (log(1.2), sd = 0.5) and log(r) (log(0.34), sd = 0.5).

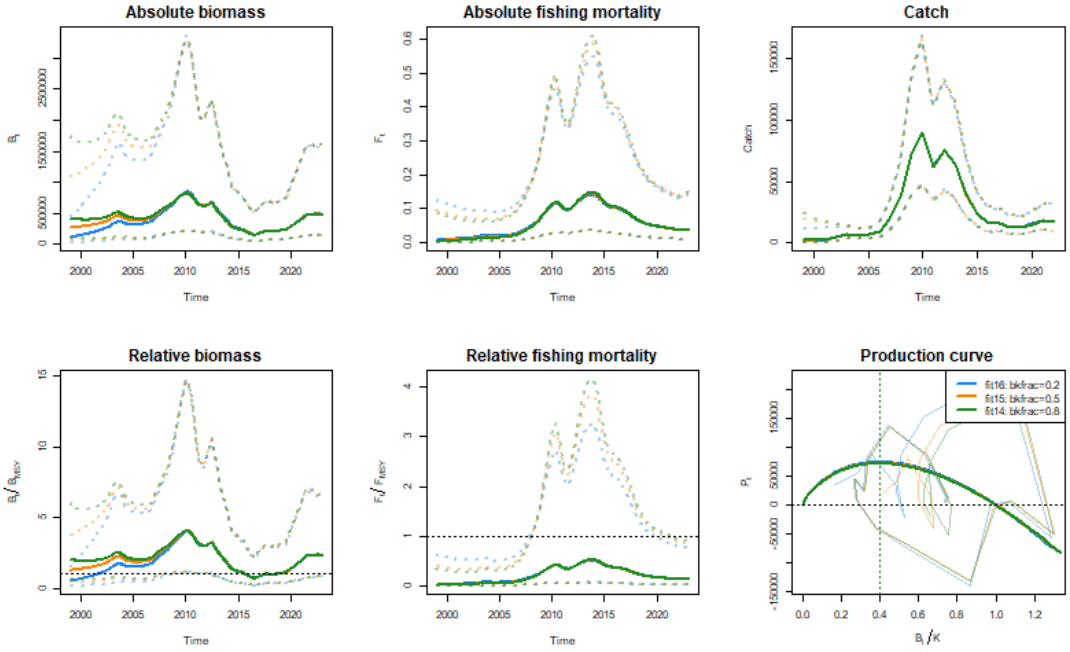


**Figure 3.3.3 Comparison of SPiCT assessments with varying assumptions on bkfrac and prior on survey catchability (log(q) = 0.9, sd = 0.5).**

Providing a prior estimate for log(n) and log(r) reduces the assessment uncertainty to acceptable levels (*i.e.* <1 order of magnitude for both fishing mortality and biomass). However, the process error residuals for fishing mortality display strong autocorrelation and are related to the poor fit to the catch data with catches significantly underestimated in several years when catch was high (2009,2010,2012) and overestimated in 2011. Associated with this are high estimates of parameter sdc (~0.8).

Additional runs were carried out, specifying a prior for sdc and forcing the assessment to more closely fit the catch time-series (fit 42 - Figure 3.3.4).

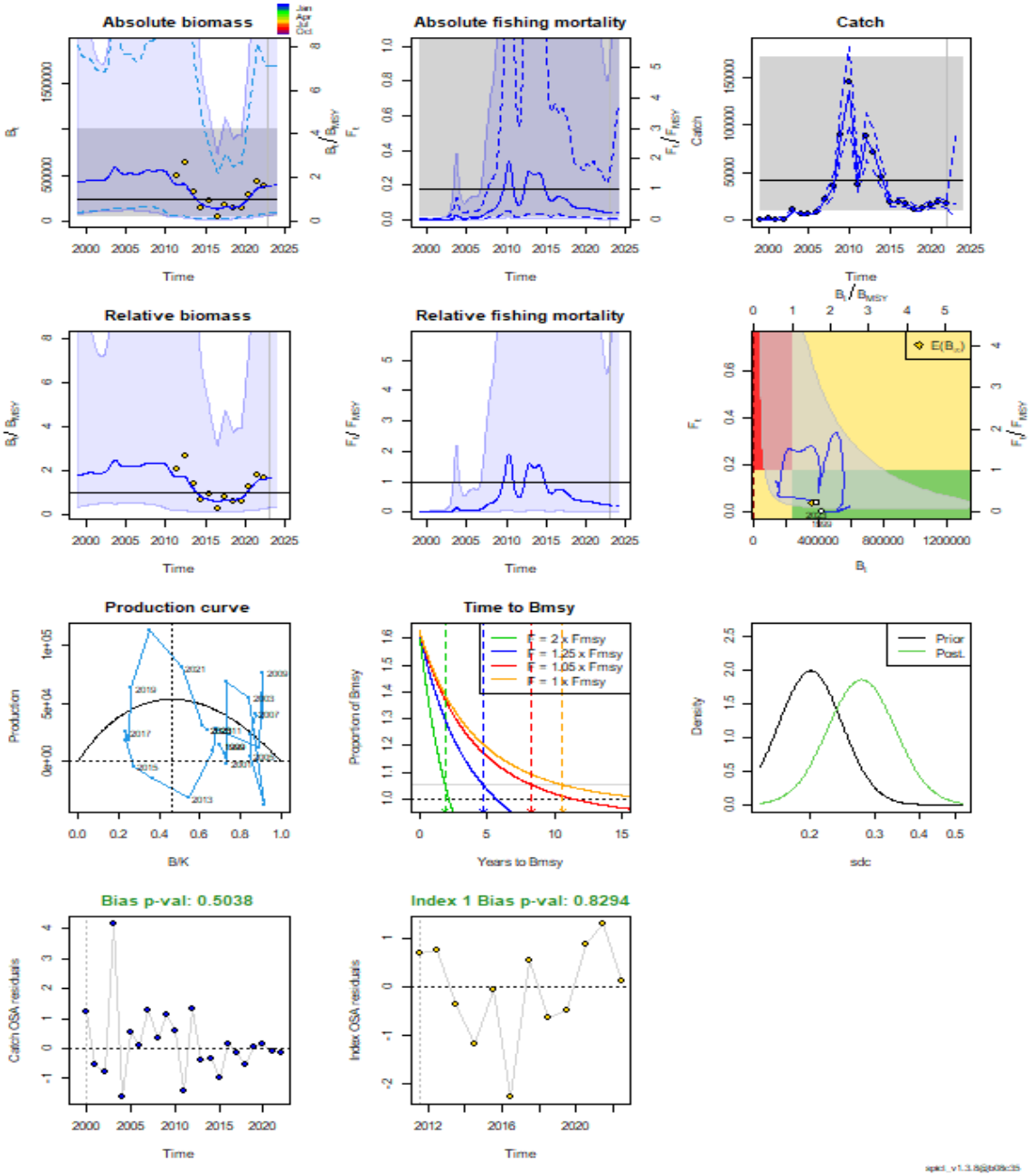


| Parameter | Est | Lo | Hi | Log |
|---|---|---|---|---|
| alpha | 1.180 | 0.142 | 9.829 | 0.165 |
| beta | 0.263 | 0.113 | 0.614 | -1.336 |
| R | 0.314 | 0.018 | 5.457 | -1.158 |
| m | 53829 | 9480 | 305649 | 10.894 |

| Parameter | Est | Lo | Hi | Log |
|---|---|---|---|---|
| K | 608440 | 195031 | 1898158 | 13.319 |
| q | 1.352 | 0.328 | 5.580 | 0.302 |
| n | 1.640 | 0.072 | 37.093 | 0.494 |
| sdb | 0.316 | 0.065 | 1.531 | -1.152 |
| sdf | 1.051 | 0.610 | 1.809 | 0.049 |
| sdi | 0.373 | 0.171 | 0.810 | -0.987 |
| sdc | 0.276 | 0.182 | 0.420 | -1.287 |
| alpha | 1.180 | 0.142 | 9.829 | 0.165 |
| beta | 0.263 | 0.113 | 0.614 | -1.336 |
| R | 0.314 | 0.018 | 5.457 | -1.158 |

**Figure 3.3.4 Run 1, Fit 42 summary and parameter estimates.**

In attempting to more closely replicate the catch time-series, the process error residual diagnostics are improved but at the expense of a poorer fit for the OSA residuals. In addition, the assessment is associated with high uncertainty and retrospective issues with peels 3,4 and 5 failing to achieve convergence.

### 3.3.2 Run 2 (Catch and Groundfish Survey Index)

A number of exploratory fits were made to the dataset consisting of catch and the stock abundance index calculated using the VAST model, informed by 6 individual groundfish surveys. In this case, the fishery-independent data are available for the complete duration of the catch data. A similar approach was adopted as for run 1. The default run was compared to alternatives incorporating increased uncertainty in the dataseries (catch data before 2003, index data before 2003 and in 2017) and priors on n and r. The run 2 fits are summarized in Table 3.3.2.

**Table 3.3.2 – SPiCT fits for run 2 (catch and acoustic survey datasets)**

| Fit | Uncertainty (factor/years) | | Priors (log(x),y) | | | | | | Diagnostics | | | | | Parameters/States | | | | | | | | | |
|---|---|---|---|---|---|---|---|---|---|---|---|---|---|---|---|---|---|---|---|---|---|---|---|
| | Catch | Index | bkfrac | n | r | q | sdc | sdi | OSA Res (Catch/ Index) | Proc. Res (B/F) | Retro (B/F) | Unc. (B/F) | bmsyk | B/BMSY | F/FMSY | BMSY (kt) | FMSY | MSY (kt) | K (Mt) | r | q | n |
| 1 | | | | | | | | | Catch Normality, | F Auto | ×/× | 7/4 | 0.56 | 0.52 | 0.04 | 15,458 | 0.06 | 919 | 27.0 | 0.16 | | 2.74 |
| 2 | | | 0.5,0.5 | | | | | | Catch | F | ×/× | 2/5 | 0.68 | 1.72 | 0.09 | 1,997 | 0.11 | 211 | 2.0 | 0.57 | | 5.4 |
| 3 | 6 | | | | | | | | Index | F | ×/× | 6/3 | 0.56 | 0.62 | 0.05 | 9,757 | 0.06 | 602 | 17.5 | 0.17 | | 2.70 |
| 4 | 6 | | 0.5,0.5 | | | | | | No convergence | | | | | | | | | | | | | | |
| 5 | 6 | | 0.2,0.5 | | | | | | OK | F | ✓/× | 1/4 | 0.69 | 1.37 | 0.04 | 3,667 | 0.08 | 299 | 5.3 | 0.47 | | 5.76 |
| 6 | 6 | | 0.8,0.5 | | | | | | OK | F | ✓/✓ | 2/7 | 0.38 | 4.63 | 0.01 | 3,104 | 0.13 | 387 | 8.2 | 0.13 | | 1.06 |
| 7 | 6 | 2 (1999-02,2017) | 0.8,0.5 | | | | | | OK | F | ✓/✓ | 2/7 | 0.37 | 5.22 | 0.01 | 1,946 | 0.17 | 329 | 5.3 | 0.17 | | 1.00 |
| 8 | 6 | 2 (1999- | 0.5,0.5 | | | | | | OK | F | ×/× | 2/5 | 0.67 | 1.83 | 0.15 | 868 | 0.15 | 130 | 13.0 | 0.74 | | 4.97 |
| 9 | 6 | 2 (1999- | 0.8,0.5 | 2,0.5 | | | | | OK | F | ✓/✓ | 1/6 | 0.50 | 3.46 | 0.03 | 1,951 | 0.12 | 238 | 3.9 | 0.24 | | 1.99 |
| 10 | 6 | 2 (1999- | 0.8,0.5 | 2,0.5 | | | | | OK | F | ✓/× | 1/6 | 0.49 | 3.62 | 0.03 | 1,991 | 0.13 | 248 | 4.1 | 0.23 | | 1.86 |
| 11 | 6 | 2 (1999- | 0.8,0.5 | 2,0.5 | 0.34,0.5 | | | | OK | F | ✓/× | 1/4 | 0.50 | 3.27 | 0.04 | 1,231 | 0.16 | 191 | 2.5 | 0.31 | | 1.99 |
| 12 | 6 | 3 (1999- | 0.8,0.5 | 2,0.5 | 0.34,0.5 | | | | OK | F | ✓/× | 1/5 | 0.48 | 3.78 | 0.03 | 1,170 | 0.19 | 216 | 2.4 | 0.34 | | 1.82 |
| 13 | 2 | 2 (1999- | 0.8,0.5 | | | | | | Catch | F | ✓/✓ | 2/5 | 0.36 | 5.53 | 0.01 | 1,681 | 0.20 | 327 | 4.7 | 0.18 | | 0.94 |
| 14 | 6 | 3 (1999- | 0.8,0.5 | 1.2,0.5 | 0.34,0.5 | | | | OK | F | ✓/× | 1/5 | 0.40 | 4.72 | 0.01 | 1,055 | 0.26 | 279 | 2.6 | 0.31 | | 1.17 |
| 15 | 6 | 3 (1999- | 0.5,0.5 | 1.2,0.5 | 0.34,0.5 | | | | OK | F | ✓/× | 1/4 | 0.41 | 4.25 | 0.02 | 744 | 0.26 | 190 | 1.8 | 0.32 | | 1.23 |
| 16 | 6 | 2 (1999- | 0.2,0.5 | 1.2,0.5 | 0.34,0.5 | | | | OK | F | ✓/× | 1/3 | 0.42 | 3.38 | 0.06 | 450 | 0.24 | 110 | 1.1 | 0.32 | | 1.32 |

No fit with these data had acceptable diagnostics with respect to uncertainty and process error residuals. The initial fit using the default SPiCT settings has very poor diagnostics including extremely high uncertainty. A bkfrac prior is required in order to prevent the assessment from simply fitting a smooth monotonic increase through the entire index time-series which leads to unreasonable estimates of several production/MSY parameters and in effect a one way trip with stock abundance increasing throughout the assessment period. Minor improvements to the assessment diagnostics can be achieved by increasing the data uncertainty in years with poorer data and specifying priors on r and n. An example output (fit 16) is shown in Figure 3.3.5.

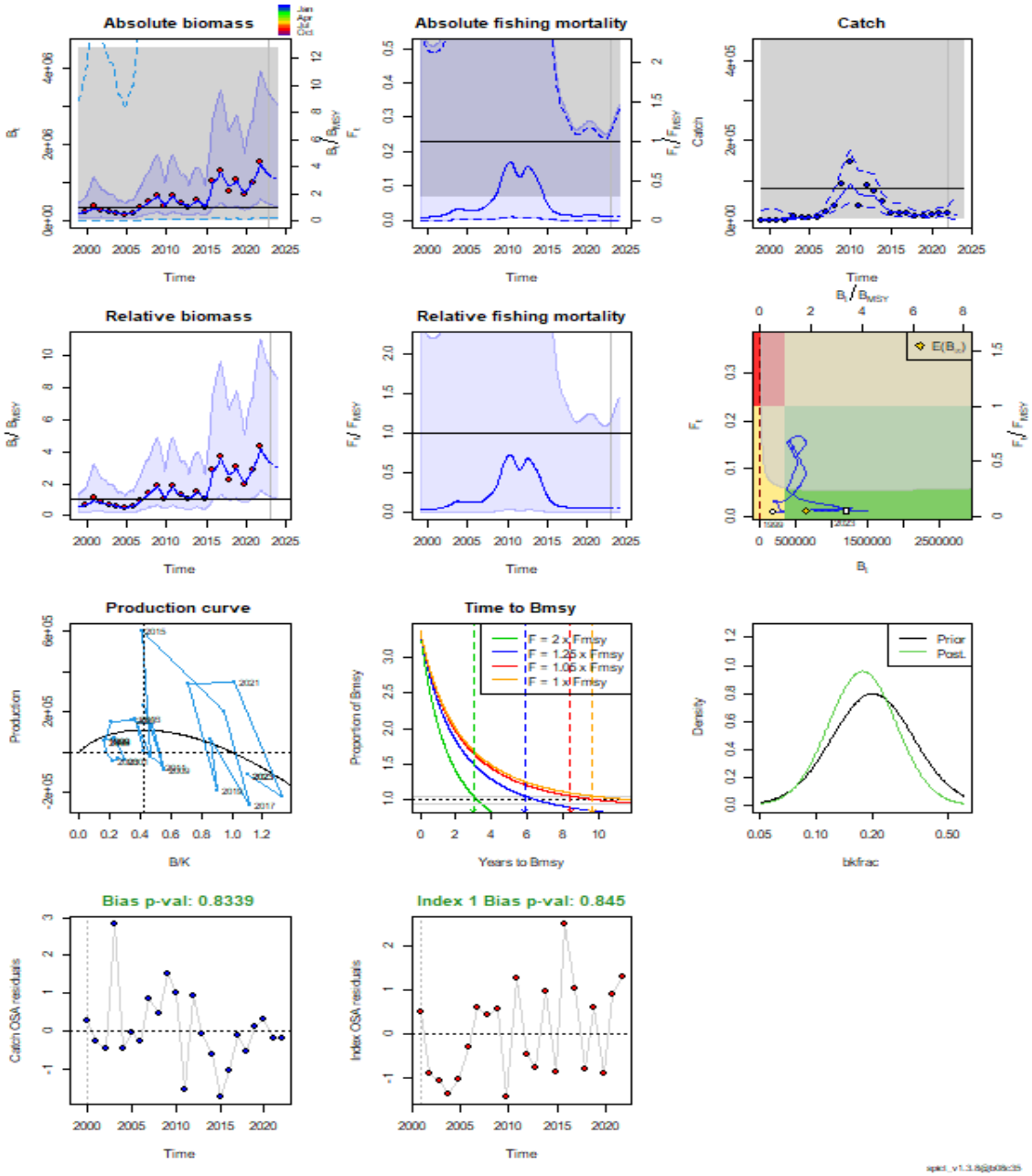


**Figure 3.3.5 Run 2, fit 16 summary.**

## 3.3.3 Run 3 - Catch, acoustic survey and groundfish survey index

### 3.3.3.1 Continuous groundfish survey index

Utilizing both fishery-independent data sources provides SPiCT with 2 separate indices (along with the catch data). The groundfish (VAST) index covers the full period for which catch data are available, albeit with reduced survey coverage prior to 2003 whereas the acoustic survey TSB index is only available from 2011 onwards. Figure 3.3.6 summarizes the available data.

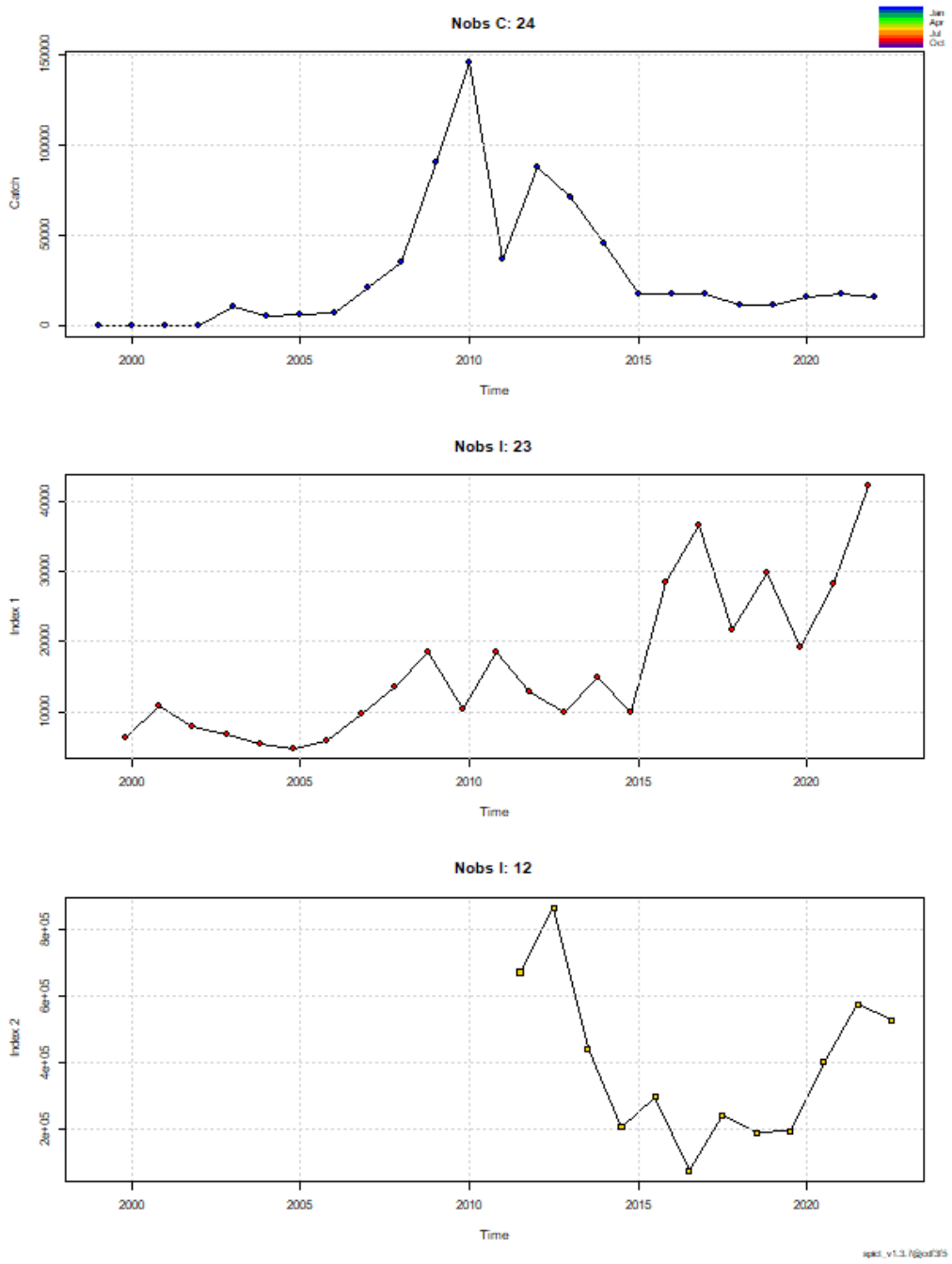


**Figure 3.3.6 Run 3 SPiCT input data (top - catch, middle - groundfish index, bottom - acoustic index).**

A number of exploratory SPiCT fits were investigated with this input data. Selected fits are summarized in Table 3.3.3.

**Table 3.3.3 – SPiCT fits (selected) for run 3 (catch, acoustic and groundfish survey datasets**

| Fit | Uncertainty (factor/years) | | | Priors (log(x),y) | | | | | | Diagnostics | | | | | Parameters/S | | | | |
|---|---|---|---|---|---|---|---|---|---|---|---|---|---|---|---|---|---|---|---|
| | Catch | Acoustic Index | Groundfish Index | bkfrac | n | r | q | sdc | sdi | OSA Res (Catch/ Index) | Proc. Res (B/F) | Retro (B/F) | Unc. (B/F) | bmsyk | B/$B_{MSY}$ | F/$F_{MSY}$ | $B_{MSY}$ (kt) | $F_{MSY}$ | MSY (kt) |
| 1 | | | | | | | | | | Catch Norm, | F Auto | ×/✓ | 5/4 | 0.53 | 0.854 | 0.048 | 7,674 | 0.059 | 450 |
| 5 | 6 | | | | | | | | | GF | F | ×/✓ | 3/3 | 0.53 | 1.036 | 0.062 | 4,400 | 0.065 | 285 |
| 9 | 6 | | 2 (1999- | 0.8,0.5 | | | | | | | F | ✓/✓ | 2/7 | 0.41 | 4.25 | 0.012 | 3,329 | 0.117 | 389 |
| 10 | 6 | | 2 (1999- | 0.5,0.5 | | | | | | | F | ✓/✓ | 1/6 | 0.59 | 2.069 | 0.054 | 2,117 | 0.099 | 209 |
| 12 | 6 | | 2 (1999- | 0.8,0.5 | 2.0,0.5 | | | | | | F | ✓/✓ | 1/6 | 0.49 | 3.312 | 0.019 | 3,424 | 0.1 | 343 |
| 13 | 6 | | 2 (1999- | 0.8,0.5 | 2.0,0.5 | 0.31,0.5 | | | | | F | ✓/✓ | 1/6 | 0.51 | 3.008 | 0.028 | 1,993 | 0.13 | 259 |
| 15 | 6 | 2 (2020) | 2 (1999- | 0.8,0.5 | | | 0.1,0.5;0.9,0.5 | | | | F | ✓/✓ | 1/2 | 0.65 | 1.823 | 0.248 | 280 | 0.231 | 65 |
| 16 | 6 | 2 (2020) | 2 (1999- | 0.8,0.5 | 2.0,0.1 | | 0.1,0.5;0.9,0.5 | | | | F | ✓/✓ | 1/1 | 0.50 | 2.642 | 0.157 | 211 | 0.244 | 51 |
| 17 | 6 | 2 (2020) | 2 (1999- | 0.8,0.5 | 2.0,0.1 | 0.31,0.1 | 0.1,0.5;0.9,0.5 | | | | F | ✓/✓ | 1/1 | 0.50 | 2.698 | 0.214 | 245 | 0.159 | 39 |
| 18 | 6 | 2 (2020) | 2 (1999- | 0.8,0.5 | 2.0,0.5 | 0.31,0.5 | 0.1,0.5;0.9,0.5 | | | | F | ✓/✓ | 1/1 | 0.49 | 2.697 | 0.177 | 225 | 0.199 | 45 |
| 19 | 6 | 2 (2020) | 2 (1999- | 0.8,0.5 | | 0.31,0.5 | 0.1,0.5;0.9,0.5 | | | | F | ×/× | 1/1 | 0.48 | 2.78 | 0.169 | 217 | 0.206 | 45 |
| 20 | 6 | 2 (2020) | 2 (1999- | 0.8,0.5 | 2.0,1.0 | 0.31,0.5 | 0.1,0.5;0.9,0.5 | | | | F | ✓/✓ | 1/1 | 0.49 | 2.745 | 0.172 | 220 | 0.203 | 45 |
| 21 | 6 | 2 (2020) | 2 (1999- | 0.5,0.5 | 2.0,1.0 | 0.31,0.5 | 0.1,0.5;0.9,0.5 | | | | F | ✓/✓ | 1/1 | 0.51 | 2.41 | 0.185 | 253 | 0.189 | 47 |
| 22 | 6 | 2 (2020) | 2 (1999- | 0.5,0.5 | 2.0,1.0 | | 0.1,0.5;0.9,0.5 | | | | F | ✓/✓ | 1/1 | 0.61 | 1.889 | 0.207 | 275 | 0.225 | 62 |
| 24 | 6 | 2 (2020) | 2 (1999- | 0.5,0.5 | 1.2,0.5 | 0.34,0.5 | 0.1,0.5;0.9,0.5 | | | | F | ✓/✓ | 1/1 | 0.44 | 2.939 | 0.138 | 201 | 0.238 | 48 |
| 25 | 6 | 2 (2020) | 2 (1999- | 0.5,0.5 | | | 0.1,0.5;0.9,0.5 | | | No convergence | | | | | | | | | |
| 26 | 6 | 2 (2020) | 2 (1999- | 0.5,0.5 | 1.2,1.0 | 0.34,0.5 | 0.1,0.5;0.9,0.5 | | | | F | ×/✓ | 1/1 | 0.49 | 2.553 | 0.167 | 234 | 0.207 | 48 |
| 27 | 6 | 2 (2020) | 2 (1999- | 0.8,0.5 | 2.0,0.5 | | 0.1,0.5;0.9,0.5 | | | | F | ✓/✓ | 1/1 | 0.53 | 2.466 | 0.17 | 223 | 0.238 | 53 |
| 28 | 6 | 2 (2020) | 2 (1999- | 0.8,0.5 | 2.0,0.5 | 0.3,0.5 | 0.1,0.5;0.9,0.5 | | | | F | ✓/✓ | 1/1 | 0.49 | 2.711 | 0.178 | 225 | 0.197 | 44 |
| 29 | 6 | 2 (2020) | 2 (1999- | 0.8,0.5 | 2.0,0.5 | 0.4,0.5 | 0.1,0.5;0.9,0.5 | | | | F | ✓/✓ | 1/1 | 0.51 | 2.59 | 0.173 | 223 | 0.217 | 44 |
| 30 | 6 | 2 (2020) | 2 (1999- | 0.8,0.5 | 2.0,0.5 | 0.5,0.5 | 0.1,0.5;0.9,0.5 | | | | F | ✓/✓ | 1/1 | 0.52 | 2.5 | 0.17 | 223 | 0.232 | 52 |

As with previous data configurations, the SPiCT fit with default parameter priors (fit 1) has poor diagnostics in a number of categories and high uncertainty. Increasing the uncertainty for data before 2003 for both the catch (fit 5) and groundfish index (fit 9) leads to minor diagnostic improvements only. Fits incorporating priors on bkfrac, log(n) and log(r) (fits 10–13) were also investigated but all displayed high uncertainty and strong autocorrelation in the fishing mortality process error. Examining the parameter estimates for these runs indicates a quite different perception to previous runs with unrealistic MSY estimates of 200–500 kt and carrying capacity of 4–15Mt. There is significant disagreement between the fishery independent indices during the initial years of the acoustic survey (2011–2015). The acoustic survey indicates a rapidly decreasing stock abundance with relatively large annual changes whereas the groundfish index is relatively low and stable. The assessment is fitting better to the longer, smoother data series from the groundfish index and largely ignoring the acoustic survey such that the estimated observation error is high. In contrast to earlier fits with only the acoustic survey providing fishery independent data, and the survey catchability is unreasonably low (often less than 0.1). As discussed earlier, the acoustic survey is considered to achieve almost complete containment of the stock and therefore would expect to have a catchability close to 1.

Fits 15–30 all use priors for the survey catchabilities (0.9 for the acoustic survey and 0.1 for the groundfish survey). As seen in the fits for run 1, specifying a prior close to 1 for the acoustic survey leads to a significantly different assessment fit. Uncertainty is reduced, particularly for biomass and more realistic estimates for MSY and K result. However, consistent issues remain with autocorrelation in the fishing mortality process error, linked to the high observation error

on catch and it is also necessary to provide priors on both log(n) and log(r) to ensure acceptable retrospective performance. Fits assuming a Schaeffer production curve (n = 2) were better than those with lower (Fox model) n values, in contrast to earlier runs were a value of n closer to 1 yielded better diagnostics. The assessment with this data configuration is relatively insensitive to a range of assumptions (0.3–0.5) on the intrinsic growth rate. Figure 3.3.7 shows the output for fit 20 (log(n) prior of log(2), sd = 0.5, log(r) = log(0.34), sd = 0.5).

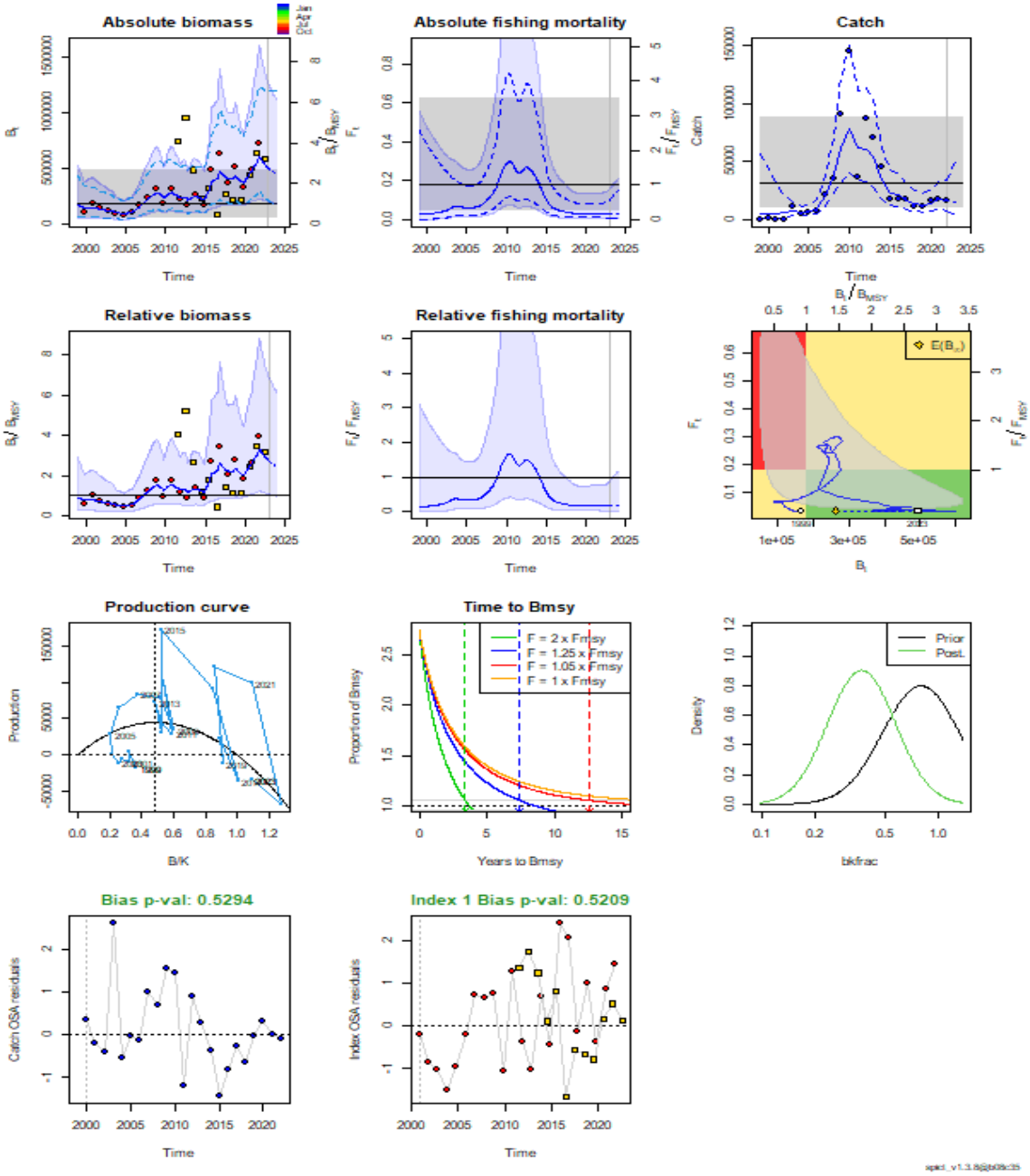


| Parameter | Est | Lo | Hi | Log |
|---|---|---|---|---|
| alpha1 | 0.769 | 0.196 | 3.010 | -0.263 |
| alpha2 | 2.497 | 1.220 | 5.112 | 0.915 |
| beta | 1.677 | 0.709 | 3.965 | 0.517 |
| r | 0.379 | 0.161 | 0.894 | -0.969 |
| m | 44747 | 20394 | 98179 | 10.709 |
| K | 452357 | 216851 | 943627 | 13.022 |
| q1 | 0.059 | 0.031 | 0.112 | -2.834 |

| Parameter | Est | Lo | Hi | Log |
|---|---|---|---|---|
| q2 | 0.912 | 0.467 | 1.784 | -0.092 |
| n | 1.866 | 0.594 | 5.863 | 0.624 |
| sdb | 0.343 | 0.180 | 0.655 | -1.069 |
| sdf | 0.511 | 0.275 | 0.951 | -0.671 |
| sdi1 | 0.264 | 0.109 | 0.641 | -1.332 |
| sdi2 | 0.857 | 0.543 | 1.353 | -0.154 |
| Sdc | 0.857 | 0.549 | 1.340 | -0.154 |

**Fig 3.3.7 Run 3, fit 20 summary and selected parameter estimates.**

Regardless of the assumptions with respect to bkfrac, survey catchability, production curve shape and intrinsic growth rate, the assessment consistently fits more closely to the groundfish index with high observation error estimates for both catch and the acoustic survey. Given that boarfish is a primary target species for the acoustic survey and is supported by a species-specific target strength model study (Fassler *et al.*, 2013) whereas the groundfish index is a by-product of a number of demersal trawl surveys, the information from the acoustic survey is considered likely to be the most representative of the stock trends. This survey also concurs with anecdotal information from fishers' experience on the fishing grounds but is in contrast to the groundfish index, particularly in the initial years of the acoustic survey. Furthermore, the groundfish index indicates a low stock abundance prior to the onset of the fishery when a larger, relatively lightly exploited population might be expected. When combined, the available groundfish surveys data covers the majority of the stock distribution and consist of a significant number of hauls with boarfish consistently present on a significant proportion such that the data are likely informative. Recognizing that these surveys have changed throughout the period of the assessment, further exploratory assessments were conducted on a split index.

### 3.3.3.2 Split Groundfish Survey Index

The VAST index is derived from a number of separate Western IBTS surveys between 1999 to present (see section 3.2.3). During this period, some surveys underwent design changes, including vessel changes (both enforced and planned). The following list describes the most important updates to the surveys upon which the index is based:

- 1997 – EVHOE survey commences. Thalassa 2 with random stratified design and GOV gear.
- 1998 – SWC-IBTS new vessel, GOV gear.
- 2001 – Spanish Porcupine survey commences. PORB gear.
- 2003 – IGFS survey commences. Celtic Explorer, GOV gear.
- 2011 – SWC redesigned (change of sampling scheme, switch to daylight only), GOV gear. Survey renamed SCOWCGFS.
- 2013 – Spanish north coast survey (8.c) new vessel. BAK gear.
- 2016 – EVHOE updates sampling design and drops some (deeper) strata.
- 2017 – EVHOE coverage severely reduced due to vessel issues.
- 2021 – Spanish north coast survey utilizes second vessel due to technical issues.

The VAST model configured to estimate a stock level abundance index utilizes a survey effect which should account for some of the variability that may be due to individual survey/vessel/gear effects. The most significant change occurred in 2011 with the update to the Scottish west coast survey, which is conducted in both quarters 1 and 4. Although treated as a separate survey within VAST, the raw data suggests a significant increase in both the proportion of hauls containing boarfish and catch rate following the survey redesign. For the purposes of the assessment, the index was therefore split at this point.

A number of SPiCT fits were conducted with the split VAST index (*i.e.* 3 separate survey indices). The input data are shown in Figure 3.3.8.

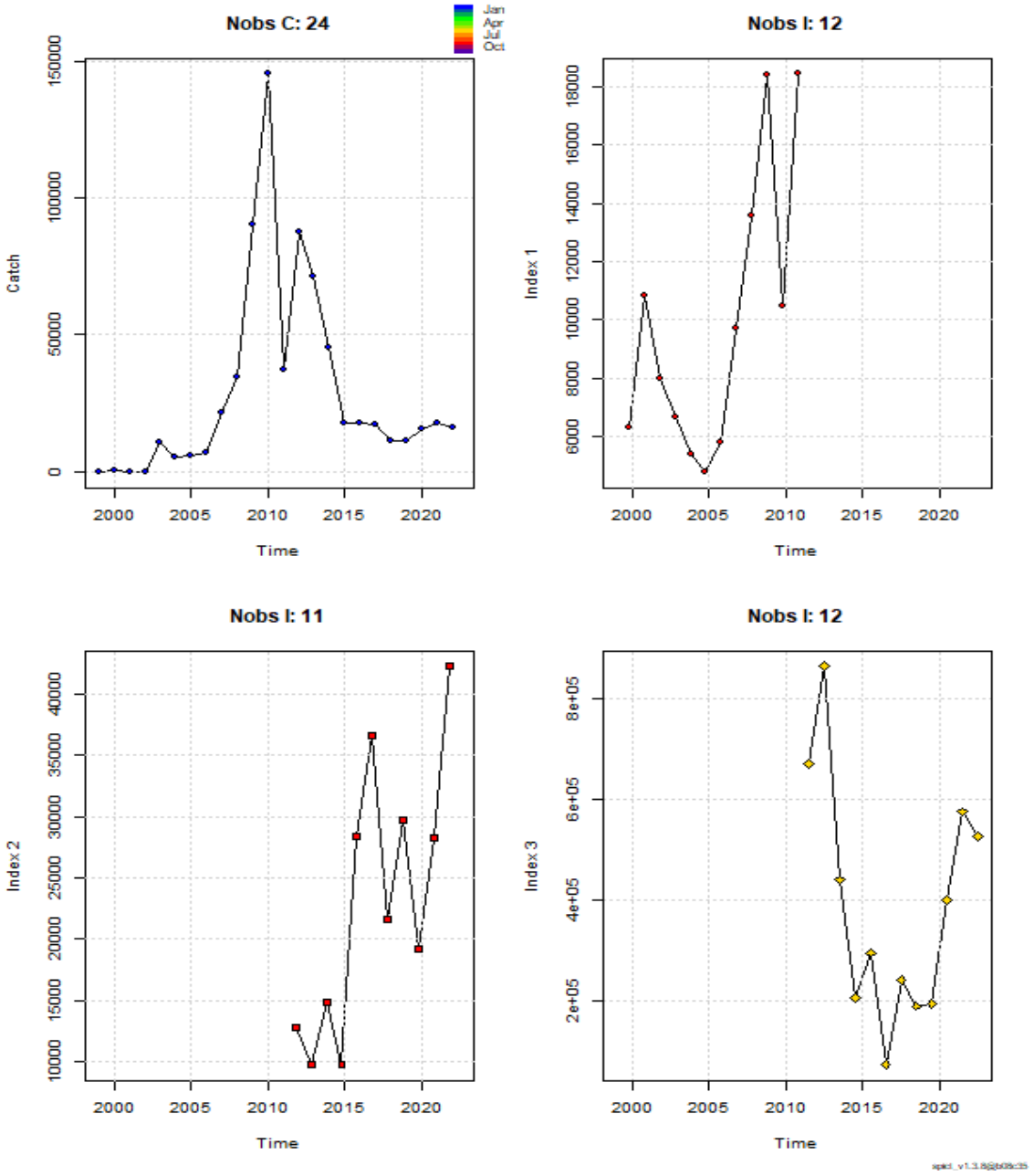


**Figure 3.3.8 Run 3 SPiCT input data with split groundfish index (top left - catch, top right – groundfish 1999–2011, bottom left – groundfish 2012 onward, bottom right - acoustic index)**

Initial fits with default priors failed to meet the SPiCT checklist criteria on a number of points including assessment uncertainty, poor catch residuals, autocorrelation in the F process error and failure to converge for a number of retrospective peels (see Table 3.3.3.2).

Inclusion of additional uncertainty in some input data in some years (as described in earlier sections), an assumed low initial depletion (bkfrac = 0.8), a catchability for the acoustic survey (log(q) = 0.9, sd-0.5), an assumption that the acoustic survey is generally more precise than the groundfish survey index (as indicated by the annual CV estimates (see Tables 3.3) and a prior on the catch observation error (logsdc = log(0.5), sd = 0.2) led to a number of improvements (e.g. fit 47) although issues remained around uncertainty in estimates of F and the fishing mortality

process error. Priors of the production function shape parameter (n) and the intrinsic growth rate (r) help to reduce assessment uncertainty whereas they are only slightly modified by the fit. Figure 3.3.9 shows the summary output and parameter estimates from fit 47 with further details of selected fits given in Table 3.3.4.

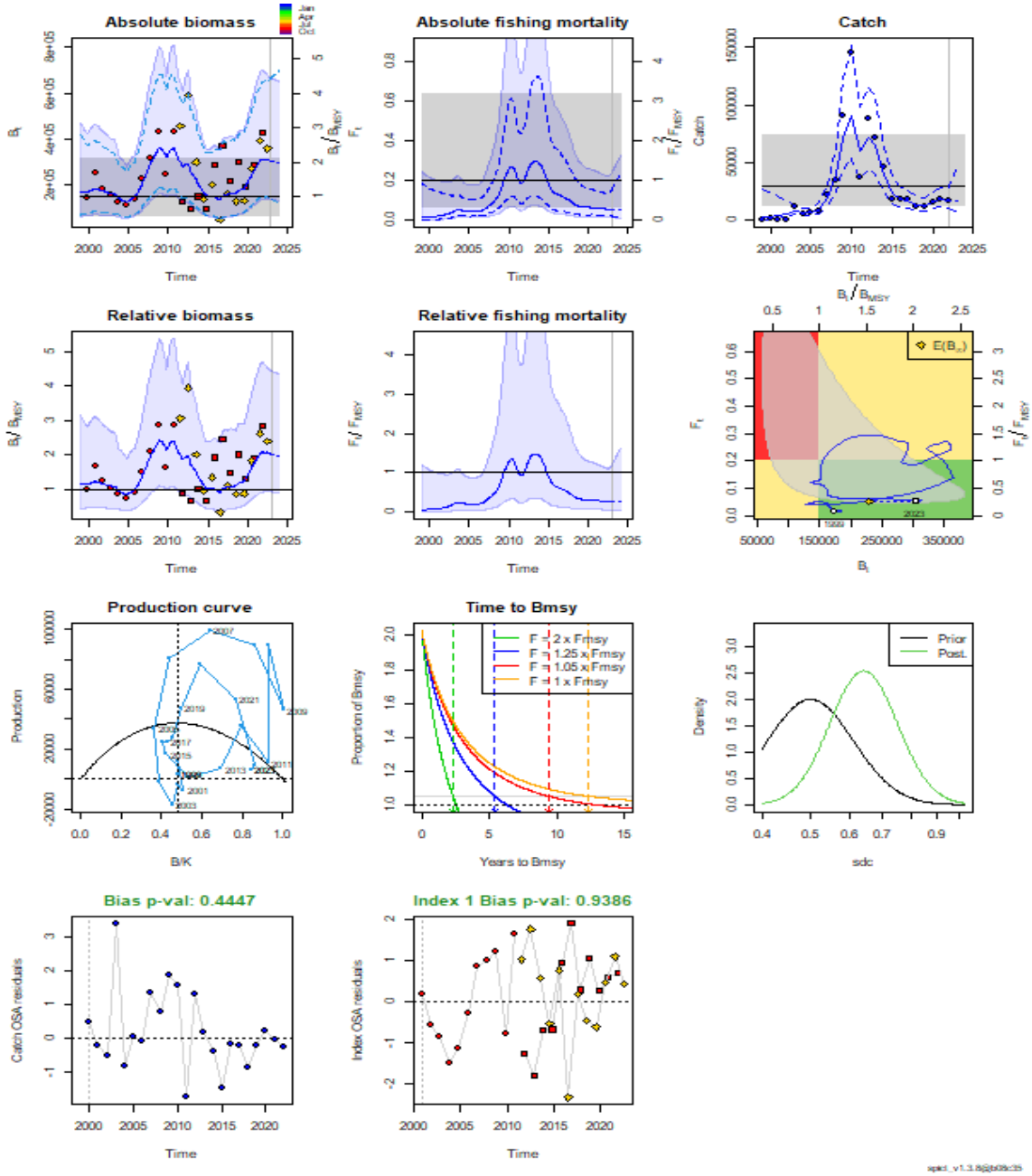


| Parameter | Est | Lo | Hi | Log |
|---|---|---|---|---|
| alpha1 | 0.992 | 0.390 | 2.521 | -0.008 |
| alpha2 | 2.104 | 1.035 | 4.274 | 0.744 |
| alpha3 | 1.504 | 0.598 | 3.783 | 0.408 |
| beta | 1.289 | 0.538 | 3.088 | 0.254 |
| r | 0.388 | 0.181 | 0.832 | -0.946 |
| m | 37319 | 18000 | 77333 | 10.527 |
| K | 358823 | 195839 | 657449 | 12.791 |
| q1 | 0.043 | 0.024 | 0.077 | -3.150 |
| q2 | 0.099 | 0.051 | 0.190 | -2.316 |

| Parameter | Est | Lo | Hi | Log |
|---|---|---|---|---|
| q3 | 1.463 | 0.763 | 2.805 | 0.380 |
| n | 1.786 | 0.734 | 4.348 | 0.580 |
| sdb | 0.298 | 0.165 | 0.537 | -1.211 |
| sdf | 0.497 | 0.247 | 0.997 | -0.699 |
| sdi1 | 0.295 | 0.157 | 0.557 | -1.220 |
| sdi2 | 0.626 | 0.372 | 1.055 | -0.468 |
| sdi3 | 0.448 | 0.255 | 0.788 | -0.803 |
| Sdc | 0.640 | 0.470 | 0.872 | -0.446 |

**Figure 3.3.9 Run 3, fit 47 summary and selected parameter estimates.**

<< landscape/figures >>

The effect of specifying a prior on the observation noise on catches was investigated, given the poor fit to the observed catches (high sdc) when this parameter is freely estimated.

With no prior on logsdc (fit 48) a relatively high value is estimated for this parameter (~0.83) with a significant underestimate of the catch in several years such that the total underestimate of catch exceeds 100 kt for the period when catches were relatively high. Lower priors on sdc lead to a closer fit to the observed catches and an acceptable diagnostic with respect to autocorrelation of the process error on fishing mortality which is poor when logsdc is estimated without a prior. However, other model diagnostics deteriorate, for example, the residuals of the fit to the catch exceed the threshold of the normality test and the assessment uncertainty is increased to 2 or 3 orders of magnitude for both fishing mortality and biomass. Varying the prior on sdc has a relatively minor effect on the shape of the production curve and the assessment of stock status with respect to MSY (Figure 3.3.10). Lower priors on sdc lead to improved fit to the catch data and better diagnostics for the fishing mortality process errors but a deterioration in the OSA residuals. The estimates of survey catchability are around 1.5 for the acoustic survey for all fits with this dataset. For the groundfish index, q estimates for each of the periods differ, with the second period q estimated at approximately twice that of the first period.

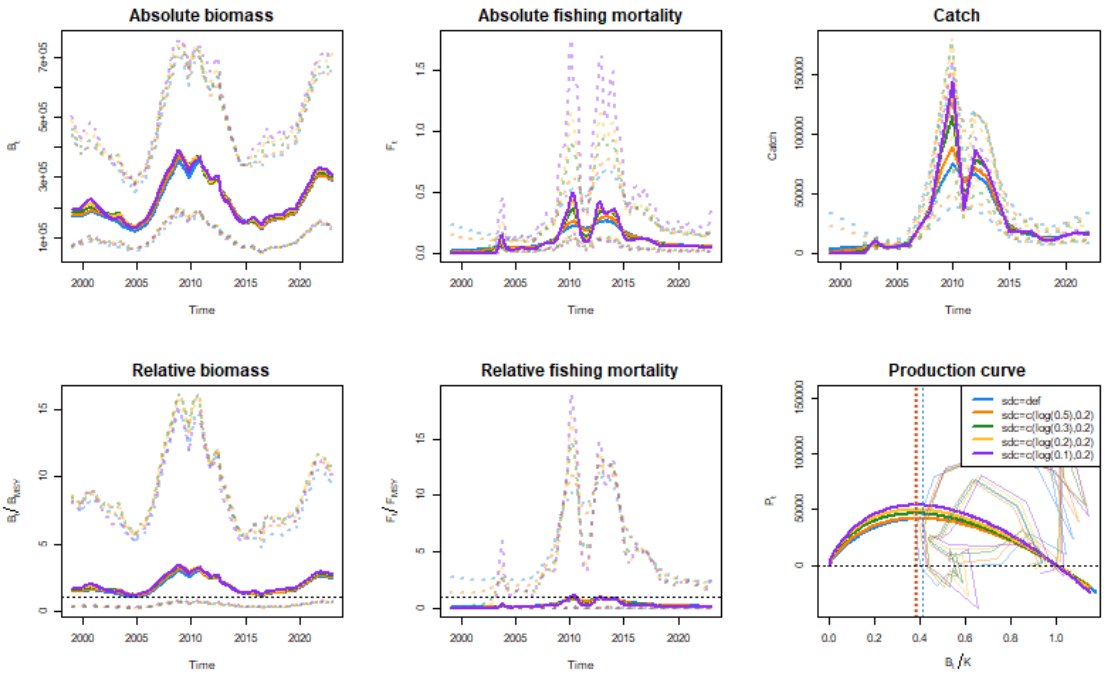


**Figure 3.3.10 Comparison of SPiCT assessments by catch observation error (sdc) prior.**

Although reasonable estimates for n and r are available from fits using default priors, specifying stronger priors can lead to reduction in assessment uncertainty. A number of fits (53–57) were made with informative priors for r (0.29, 0.34, 0.47) and n (1.2,2). A comparison of these fits is shown in Figure 3.3.11.

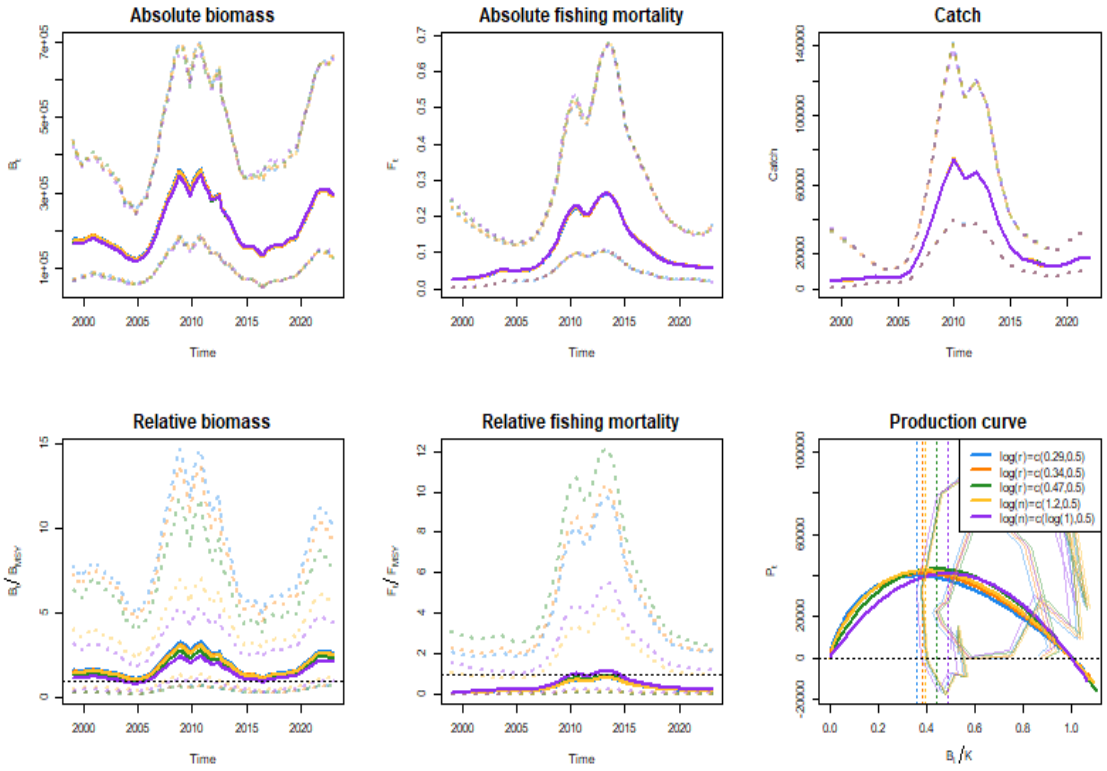


**Figure 3.3.11 Comparison of SPiCT assessments for alternative priors on r and n.**

Assessment output is relatively insensitive to the range of r and n priors tested. The principal benefit is a reduction in uncertainty, particularly for fishing mortality. A prior on the shape parameter is more effective in achieving this reduction compared to intrinsic growth rate.

Figure 3.3.12 provides a comparison between a number exploratory assessments used to investigate the effect of priors individually and in combination.

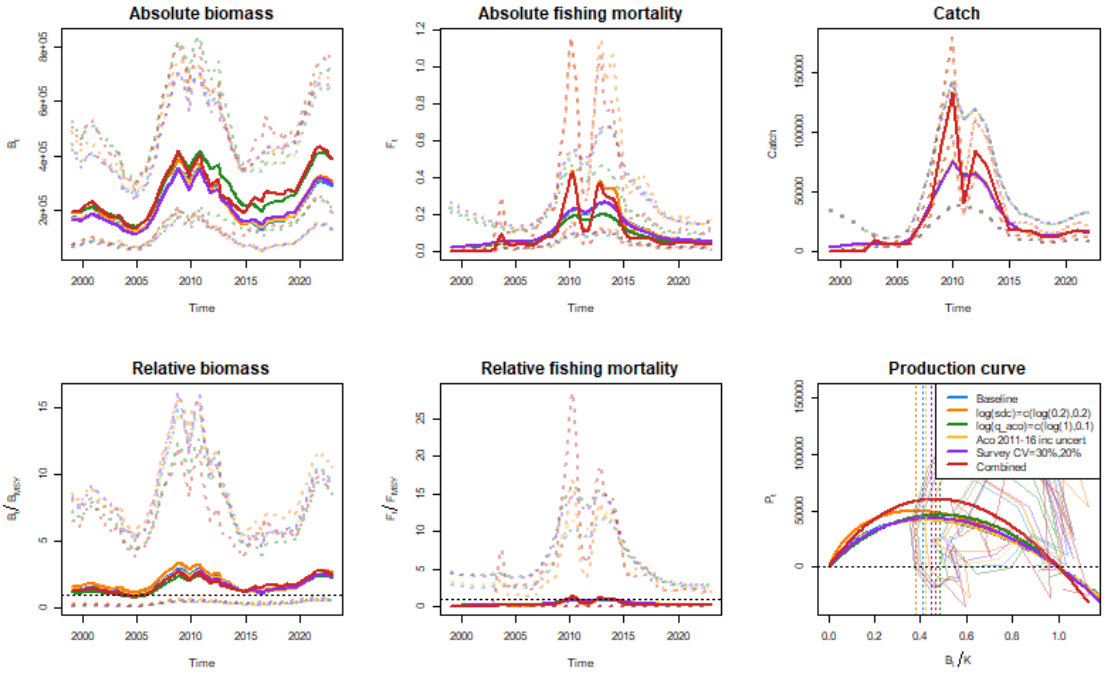


**Figure 3.3.12 Comparison of SPiCT assessments for individual priors and the combination of priors**

The overall trends in biomass and fishing mortality are similar for each run with a strong increase in stock size prior to the onset of the fishery which leads to a decrease before a recovery in stock size since 2015 to levels similar to that earlier in the time-series. Forcing the assessment to follow the catch more closely leads to a more variable (and probably realistic) estimate of fishing mortality during the years of high exploitation. A tighter prior on the acoustic survey catchability leads to a more optimistic view of the stock status in the recent period.

### 3.3.4 Final assessment

No final assessment was presented.

## 3.4 Future considerations/recommendations

- Investigate potential reasons for conflict in fishery-independent data sources.
- Length sampling information is available from the fishery and the surveys such that a length based model is worthy of investigation.
- This stock may be subject to recruitment pulses which challenge the underlying assumptions and therefore suitability of a surplus production model such as SPiCT.
- Acoustic dead zone/changing vertical distribution may lead to bias in the acoustic survey time-series.
- Boarfish is common in groundfish hauls, occasionally in large quantities. Lower catch rates during the early years of the time-series do not seem consistent with the presence of a significant (unfished) stock. Investigate the potential impact of changes in survey protocols, sampling design, deliberate avoidance of large hauls of (non-target) pelagic species.

## 3.5 Reviewer report

Boarfish is currently a category 3 stock and accepted for trend-based advice. Before 2005, there was no market for boarfish in Europe and, thus, boarfish in subareas 6–8 were not directly targeted by fisheries. With the technological development to target this species and the start of a directed fisheries in 2007, catches increased sharply and peaked with 150000 tons in 2010. After the introduction of a TAC and mesh size restrictions in 2011, catches fell to around 30000 tons before they doubled again in 2012 and after that declined quickly too low levels around 15000 tons. After the high catches from 2007–2013, the search time for fishing vessels was high and only a few fishing vessels stayed engaged in the fishery.

Two abundance indices were presented, one based on an acoustic survey targeting boarfish from 2011 onward and one based on a spatio-temporal model (VAST) of several different groundfish surveys with varying time-series length. The abundance index based on the groundfish survey goes back to 1990, but the index was considered more reliable from 1999 onward. The abundance index based on the groundfish surveys suggests a continuously increasing abundance throughout the time-series with the highest increase from 2014 to 2015, while the acoustic survey suggests a decrease in abundance from 2011 to 2014 and an increase from 2015 to 2019 to 2021.

The SPiCT assessment with both survey indices showed high uncertainty and did not pass diagnostic tests. Thus, the SPiCT assessment of boarfish in areas 6–8 was not considered suitable for providing management advice. The SPiCT assessment with only the acoustic index and a prior on the initial depletion level showed more promising results. However, one point of concern was the estimated catchability coefficient of below 1 (even if a prior distribution was used) and the estimated high historic biomass that is in direct conflict to the trend of the groundfish survey. While the lower catchability coefficient (and lower estimated biomass relative to the biomass based on the acoustic survey) could be explained by the fact that SPiCT estimates the exploitable stock biomass (ESB) while the biomass of the acoustic survey corresponds to the total-stock biomass (TSB), the problem of conflicting indices or assessment trends with the groundfish survey remains. Several potential factors affecting the reliability of the groundfish survey were discussed, such as diel vertical and seasonal spawning migrations, the change in length/age structure in the survey catches, as well as changes in the survey design. These aspects should be revisited in future, and it should be decided together with survey experts if the catches of boarfish in these surveys can be considered representative of their abundance. A length-based model could also be considered given the amount of and importance of length-structured data for this stock. The exploratory stock synthesis assessment with catches, the acoustic survey and length composition data gave promising results supporting the historical high standing biomass that decreased as a consequence of the high fishing pressure from 2007–2013. However, the problem of the conflicting surveys was also apparent in the stock synthesis model, as the model did not converge when including the groundfish survey index. Since the SPiCT assessment was rejected for this stock, ICES empirical rules such as the rfb-rule will be used to provide advice for the stock. These were not discussed during this benchmark, other than the presented abundance indices and probably further external evaluation is needed during or after the assessment working group.

### 3.5.1 Conclusions

SPiCT assessment model ***was not accepted*** as the basis for providing advice for boarfish in the North Sea.

An integrated model should be explored in future to account for the change in stock productivity over time and the good amount of size information available for this stock.

## 3.6 References


Coad, J. O., Hussy, K., Farrell, E. D., & Clarke, M. W. (2014). The recent population expansion of boarfish, *Capros aper* (Linnaeus, 1758): interactions of climate, growth and recruitment. Applied Ichthyology, 30, 463–471. https://doi.org/10.1111/jai.12412

Egerton, S., Culloty, S., Whooley, J., Stanton, C., Ross, R.P. (2017). Boarfish (*Capros aper*): review of a new capture fishery and its valorization potential, *ICES Journal of Marine Science*, 74 (8), 2059–2068. https://doi.org/10.1093/icesjms/fsx048

Farrell, E. D., Carlsson, J. E. L. & Carlsson, J. 2016. Next gen pop gen: Implementing a high-throughput approach to population genetics in boarfish (*Capros aper*). *Open Science*, 3, 160651.

Fässler, S. M. M., O'Donnell, C. & Jech, J.M. (2013). Boarfish (*Capros aper*) target strength modelled from magnetic resonance imaging (MRI) scans of its swimbladder. ICES Journal of Marine Science, 70, 1451–1459.

Holgersen H. 1954. First record of the boarfish, *Capros aper* in Norway. Aktietrykkeriet i Stavanger, 17: 1–11.

Hüssy, K., Coad, J. O., Farrell, E. D., Clausen, L. A., & Clarke, M. W. (2012a). Age verification of boarfish (*Capros aper*) in the Northeast Atlantic. *ICES Journal of Marine Science*, *69*(1), 34–40.

Hüssy K., Coad J. O., Farrell E. D., Clausen L. W., Clarke M. W. (2012b). Sexual dimorphism in size, age, maturation, and growth characteristics of boarfish (*Capros aper*) in the Northeast Atlantic. ICES Journal of Marine Science, 69: 1729–1735.

ICES. 2012. Report of the Working Group on Widely Distributed Stocks (WGWIDE), 21 – 27 August 2012, Lowestoft, United Kingdom. ICES CM 2012/ACOM:16.931 pp. http://doi.org/10.17895/ices.pub.21088804

ICES. 2022. Working Group on Widely Distributed Stocks (WGWIDE). ICES Scientific Reports. 4:73. 922 pp. http://doi.org/10.17895/ices.pub.21088804

Kaya M., Özaydin O. 1996. A preliminary investigation on biology of *Capros aper* (L., 1758) (Pisces: Caproidae). Turkish Journal of Zoology, 20: 51–55.

King, M. (1995) Fisheries biology, assessment and management

Meyer, R. & Millar, R.B. 1999. BUGS in Bayesian stock assessments. *Canadian Journal of Fisheries and Aquatic Sciences*, 56, 1078–1087.

Quero, J. C. (1986). Caproidae. In Fishes of the North-eastern Atlantic and the Mediterranean, pp. 777–779. Ed. By P. J. P. Whitehead, M-L. Bauchot, J-C. Hureau, J. Nielsen, and E. Tortonese. UNESCO, Paris.

Thorson, J. T., Branch, T. A., Cope, J. M., Jensen, O. (2012). Spawning biomass reference points for exploited marine fishes, incorporating taxonomic and body size information. Canadian Journal of Fisheries and Aquatic Sciences, 69(9), 1556- 1568.

Thorson, J. T. & Barnett, L. A. K. (2017). Comparing estimates of abundance trends and distribution shifts using single- and multispecies models of fishes and biogenic habitat. ICES J. Mar. Sci., 74: 1311–1321, 10.1093/icesjms/fsw193.

Thorson, J. T. (2018). FishStatsUtils: Utility functions for spatio-temporal analysis. https://github.com/James-Thorson/FishStatsUtils

Thorson, J. T. (2020). Predicting recruitment density dependence and intrinsic growth rate for all fishes worldwide using a data-integrated life-history model. Fish and Fisheries, 21: 237–251. John Wiley & Sons, Ltd. https://doi.org/10.1111/faf.12427.

Torrejón-Magallanes, Edgar. (2016). 'sizeMat': An R package to estimate size at sexual maturity. R package version 1.1.2, https://CRAN.R-project.org/package=sizeMat.

Trenkel, V.M. & Rochet, M.J. (2003). Performance of indicators derived from abundance estimates for detecting the impact of fishing on a fish community. Canadian Journal of Fisheries and Aquatic Sciences, 60(1), 67–85.

White, E., Minto, C., Nolan, C. P., King, E., Mullins, E., and Clarke, M. (2011). First estimates of age, growth, and maturity of boarfish (*Capros aper*): a species newly exploited in the Northeast Atlantic. -ICES Journal of Marine Science, 68: 61–66.

Winker, H. 2021. SPMPriors: SPM prior generation with FishLife[2].

[2] https://github.com/Henning-Winker/SPMpriors

## 3.7 Working documents

### 3.7.1 WD Annex 1: SPiCT Assessment of Northeast Atlantic Boarfish (boc.27.6-8)

# 1 Introduction

Boarfish (Capros aper) is a small, pelagic, laterally compressed, planktivorous shoaling species (Egerton et al. 2017, White et al. 2011). They primarily inhabit continental shelves and edges, often in large dense shoals at depths of 40-600m (Coad and Hussy 2012, Egerton et al. 2017). It's distribution ranges from Norway to Senegal in the Northeast Atlantic and includes the Mediterranean and Aegean seas and the islands of the Azores, Canaries, Madeira, and the Great Meteor Seamount (Holgersen, 1954; Quéro, 1986; Kaya and Ozaydin, 1996, Egerton et al. 2017, Coad and Hussy, 2012).

Results from a genetic study of 839 samples conducted in 2013 to elucidate the population structure of boarfish in the Northeast Atlantic and Mediterranean Sea identified a number of distinct genetic populations (fig 1.1).

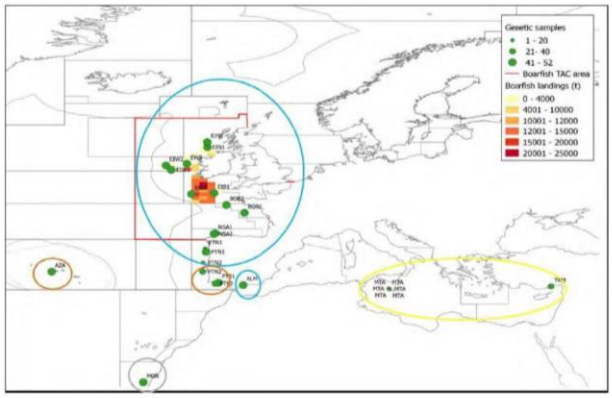


Fig 1.1 Boarfish samples included in the genetic stock identification. Population clusters identified by multiple analyses are indicated by colour coded markers and circles.

Boarfish was first targeted in 2001 although landings remained low (<1000t pa) until 2006. A rapid expansion of the fishery took place in the mid-2000s, aided by developments in pumping technology. The fishery targets dense shoals and catches are generally free from bycatch. The fishery is carried out primarily via pelagic pair trawl using 32-54mm mesh trawls.

Management measures were first introduced in 2011, prior to this the fishery was unregulated. In several years since the introduction of the TAC, the full quota has not been taken due to a number of factors including administrative and economic reasons. Ireland is the main participant in the fishery, with the majority of the TAC. Denmark and Scotland are the other main participants although in some years, only minimal catches were taken by these nations.

# 2 Assessment History

During 2012 and 2013, an assessment was developed based on the Schaefer state space surplus production model (Meyer and Millar 1999) using catch data and fishery independent information from an acoustic survey and indices from 6 separate national groundfish surveys. The 2013 assessment provided an estimate of stock status and was used to provide MSY based advice ($F_{MSY}$ = 0.23) for 2014. However, following the update assessment of 2014, and concerns raised by the ADG that the model was unsuitable for category 1 advice, the assessment was downgraded and accepted for trends only based advice. Since 2018, catch advice has been issued biennially although the assessment has been updated and presented annually to WGWIDE.

The assessment output has been relatively stable in recent years. It is heavily influenced by the acoustic survey which commenced in 2011 and has an informative prior on catchability (q=1, sd=0.25). Information prior to the start of the fishery in the mid-2000s is sparse. Highest catches occurred prior to the start of the acoustic time series when the fishery was unregulated. The groundfish indices are characterised by high uncertainty, and variable temporal coverage. Moreover, each survey only covers a portion of the stock distribution. A summary of the output from the 2022 update assessment is shown in figure 2.1.

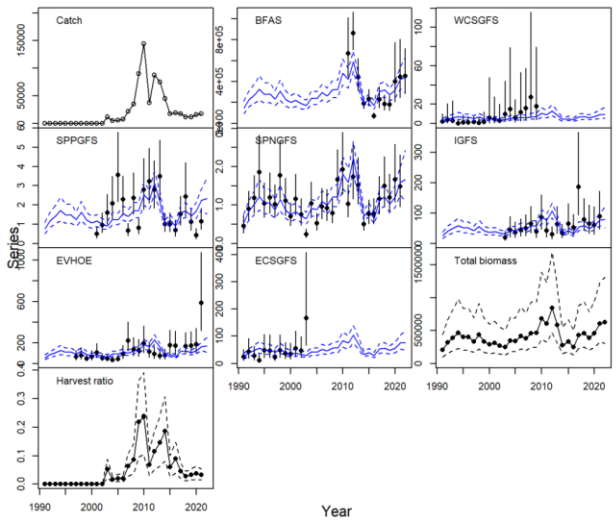


Fig. 2.1: WGWIDE 2022 Boarfish update assessment summary

# 3 Catch Data

Prior to 2006, there was no targeted boarfish fishery. A fishery was established in the mid 2000's with the development of pumping and processing technologies and catches increased rapidly (peaking at 144kt in 2010) with Ireland, Denmark and Scotland the main fishers. The fishery remained unregulated until 2010 when the European Commission introduced regulations in relation to mesh size. In 2011, a TAC was set for the first time and catches were reduced. Following the development of a Schaefer state space surplus production model, MSY based advice was given in 2014. However, the assessment model was subsequently downgraded to category 3 and advice has been given on the basis of the assessment biomass trend since this time. Since 2018, advice has been given biennially. In recent years only the Irish fleet has participated in the fishery with total annual catch lower than the TAC.

A time series of landings and discards by ICES division and is available from the relevant ICES expert group (WGWIDE). As part of this exercise, the complete dataset has been uploaded to Intercatch. Prior to 2007, no sampling of the catch was carried out. Initially sampling was funded nationally but has since been included under the DCF and comprehensive sampling has continued. Length frequency, sex, weight and maturity information is routinely collected. While otoliths have been taken they have not been read since the initial ageing studies were carried out in 2010-2012.

Discard estimates are only available for some fleets including demersal fleets from Spain, Ireland and the UK and pelagic freezers from Netherlands and Germany. The full time series of landings and discards by country are given in tables 3.1-3.3.

| Year | Ireland | Scotland | Denmark | England | Germany | Netherlands | Spain | Poland |
|---|---|---|---|---|---|---|---|---|
| 1999 | 63 | | | | | | | |
| 2000 | 458 | | | | | | | |
| 2001 | 120 | | | | | | | |
| 2002 | 46 | | | | | | | |
| 2003 | 460 | | | | | | | |
| 2004 | 675 | | | | | | | |
| 2005 | 242 | | | | | | | |
| 2006 | 2772 | | | | | | | |
| 2007 | 17608 | 772 | | | | | | |
| 2008 | 21584 | 0 | 3098 | | | | | |
| 2009 | 68629 | | 15059 | | | | | |
| 2010 | 89748 | 9241 | 39805 | | | | | |
| 2011 | 20619 | 2813 | 7797 | | | | | |
| 2012 | 55949 | 4884 | 19888 | | | | | |
| 2013 | 52250 | 4380 | 13184 | | | | | |
| 2014 | 34632 | 38 | 8758 | | | | | |
| 2015 | 16325 | 0 | 29 | 104 | 5 | 375 | | |
| 2016 | 15974 | | 337 | 21 | 7 | 212 | | |
| 2017 | 15485 | | 548 | 0 | | 182 | | |
| 2018 | 9513 | 0 | 94 | 0 | | 172 | 54 | |
| 2019 | 9910 | | 757 | 30 | | 318 | 2 | |
| 2020 | 14666 | | 196 | 62 | | 416 | 1 | 109 |
| 2021 | 11923 | 9 | 4322 | 45 | | 781 | 11 | 44 |

Table 3.1: Boarfish landings by country and year (1999-2021)

| Year | Ireland | Netherlands | Spain | Germany | England | Scotland | Lithuania |
|---|---|---|---|---|---|---|---|
| 2003 | 132 | 1198 | 8813 | | | | |
| 2004 | 49 | 837 | 3579 | | | | |
| 2005 | 78 | 733 | 5007 | | | | |
| 2006 | 47 | 411 | 3933 | | | | |
| 2007 | 345 | 23 | 2617 | | | | |
| 2008 | 903 | 738 | 8410 | | | | |
| 2009 | 349 | 1258 | 5047 | | | | |
| 2010 | 103 | 512 | 5947 | | | | |
| 2011 | 98 | 185 | 5461 | 49 | | | |
| 2012 | 164 | 88 | 6365 | | 23 | | |
| 2013 | 80 | 11 | 1119 | 22 | 52 | | |
| 2014 | 41 | 477 | 1119 | 117 | 50 | 1 | |
| 2015 | 116 | | 801 | | 25 | 3 | |
| 2016 | 22 | | 869 | | 348 | 4 | 1 |
| 2017 | 191 | | 640 | | 386 | 1 | |
| 2018 | 95 | | 525 | | 744 | 0 | |
| 2019 | 298 | | 240 | | 7 | 1 | |
| 2020 | 74 | | 133 | | 0 | 1 | |
| 2021 | 9 | | 594 | | 46 | | |

Table 3.2: Boarfish discards by country and year (1999-2021)

| Year | Landings | Discards | Total |
|---|---|---|---|
| **1999** | 63 | | 63 |
| **2000** | 458 | | 458 |
| **2001** | 120 | | 120 |
| **2002** | 46 | | 46 |
| **2003** | 460 | 10143 | 10604 |
| **2004** | 675 | 4465 | 5140 |
| **2005** | 242 | 5818 | 6061 |
| **2006** | 2772 | 4391 | 7163 |
| **2007** | 18380 | 2985 | 21365 |
| **2008** | 24683 | 10051 | 34734 |
| **2009** | 83688 | 6654 | 90342 |
| **2010** | 138795 | 6562 | 145357 |
| **2011** | 31228 | 5792 | 37021 |
| **2012** | 80720 | 6640 | 87361 |
| **2013** | 69813 | 1284 | 71097 |
| **2014** | 43428 | 1806 | 45234 |
| **2015** | 16837 | 944 | 17782 |
| **2016** | 16550 | 1245 | 17795 |
| **2017** | 16215 | 1218 | 17433 |
| **2018** | 9834 | 1364 | 11198 |
| **2019** | 11017 | 547 | 11564 |
| **2020** | 15451 | 208 | 15660 |
| **2021** | 17135 | 650 | 17785 |

Table 3.3: Boarfish landings, discards by year (1999-2021)

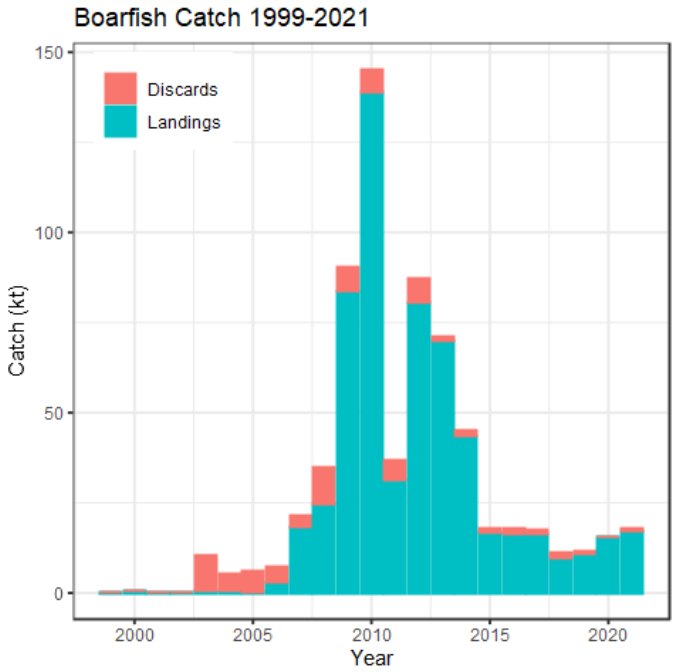


Fig. 3.1 Boarfish catch 1999-2021.

Catch Distribution

The fishery operates during the first and fourth quarters (see fig 3.3). In recent years a larger proportion of the total catch has been taken in the fourth quarter. The bulk of the catches are taken in ICES divisions 7.j, 7.b, and 8.a. Historically, the largest catches have been taken in 7.j although between 2016 and 2019, an increased proportion of the catch was taken in Northern Biscay (8.a). The distribution of catch by ICES statistical rectangle for Irish landings (of which the bulk of the total catch is comprised) are shown in figure 3.2.

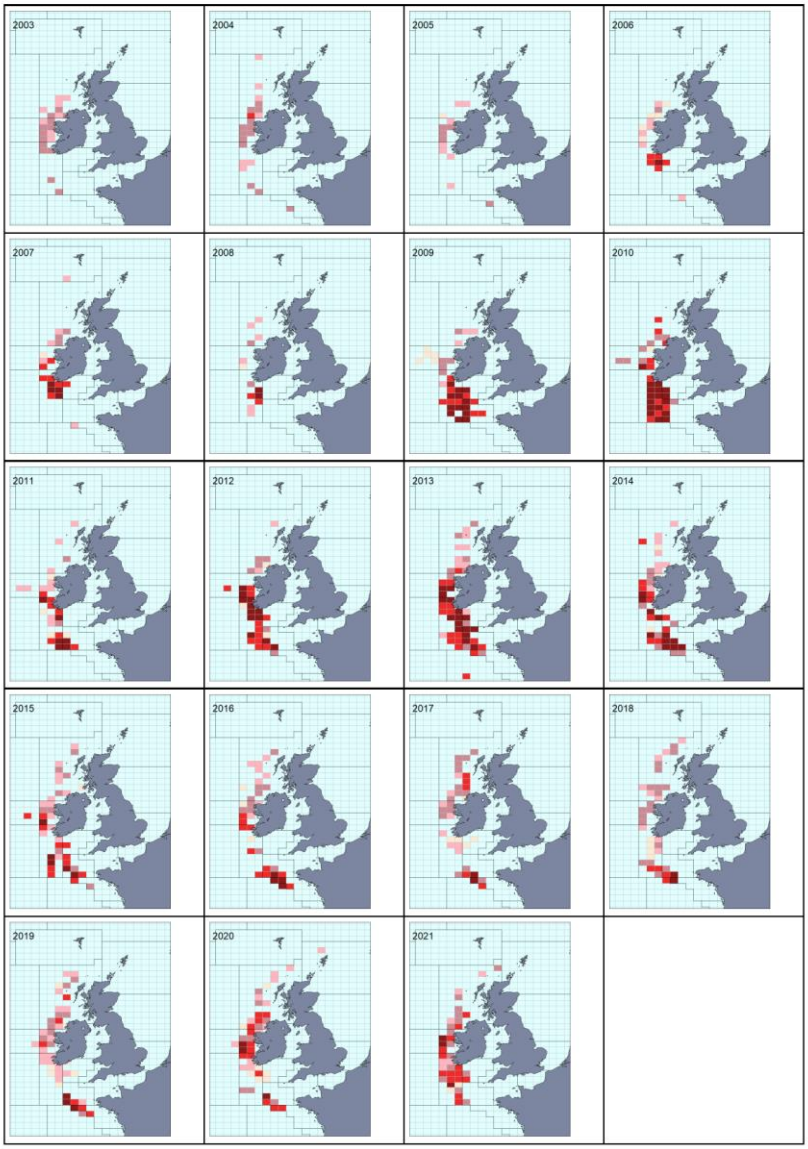


Fig 3.2: Irish catch by ICES statistical rectangle 2003-2021

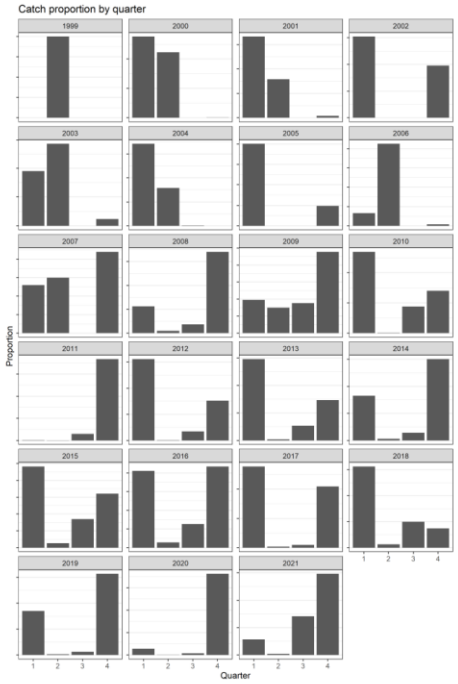


Fig 3.3 – Catch proportion by quarter

Comprehensive sampling of the commercial catch is carried out. Under a self-sampling scheme, Irish vessels retain a sample from each haul which is frozen and delivered to scientists when the vessel returns to port (often the catch is landed into Denmark or Faroe). Using appropriate samples for allocating to unsampled catch, the annual catch at length estimates are calculated by the InterCatch platform and are shown in figure 3.4.

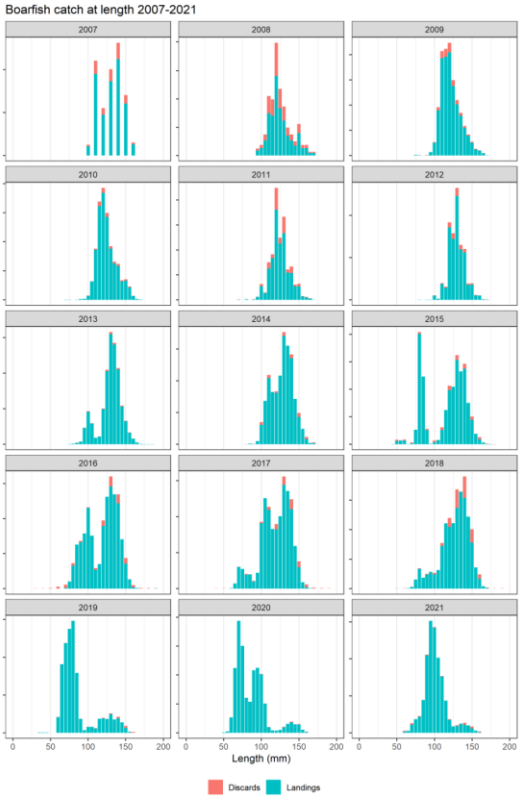


Fig 3.4 – Catch length distribution

During the initial years of the fishery when catches increased to over 100kt the catch consisted of fully mature fish and a range of size classes. Since 2015, the fishery has taken place further south and smaller size classes have appeared in the catch length profile, consistent with the increased proportion of young fish in southern waters. Sampling of discards indicates a similar size distribution to the landed fraction. Boarfish is discarded largely as it is an unwanted species in all but the target fisheries and is actively avoided as the spiny body tends to damage other species in mixed catches. See section 5 for a comparison of length profiles from catch and survey data.

# 4 Survey Data

## 4.1 Acoustic Surveys

The Boarfish Acoustic Survey (BFAS) was first conducted in 2011, in cooperation with the fishing industry. The survey was designed as an extension of the Malin Shelf Herring Acoustic survey providing a continuation of coverage to 47.5°N and was carried out on a commercial vessel deploying a towed body with a 38kHz split beam transducer. The survey collects acoustic data continuously along a series of parallel transects with a spacing of 15nm with CTD stations and opportunistic trawling also. In 2012 the survey switched from 24 hour operations to daylight only (04:00-00:00) as it was noted from the 2011 survey that boarfish shoals tend to disperse during the hours of darkness such that acoustic detection becomes difficult. Following the 2013 survey, a revised target strength model (Fässler et al 2013) was applied to the historic dataset.

Since 2016, both the Malin Shelf Herring and Boarfish surveys have been carried out on the RV Celtic Explorer. Collectively, these surveys are known as the Western European Shelf Pelagic Acoustic Survey (WESPAS). The survey runs for approximately 6 weeks from mid-June to the end of July. Since 2017, the survey has been conducted from South to North, previously the northern herring survey had been conducted first. Starting the survey at the southern boundary improves alignment with the French acoustic survey in the Bay of Biscay (PELGAS).

The StoX software package has been used to calculate an estimate of TSB/SSB since 2016, prior to this bespoke software was used. Biological sampling is carried out during the survey via targeted trawling on acoustic registrations for the purposes of mark identification and to determine species size structure. On average 25-40 trawl hauls are carried out on each survey. The catch is sampled for length frequency and biological characteristics (weight, sex, maturity, otolith extraction).

Figure 4.1 contains a composite of the acoustic registrations (NASC) for the complete survey time series. Identical scales have been used for each annual plot to aid comparison.

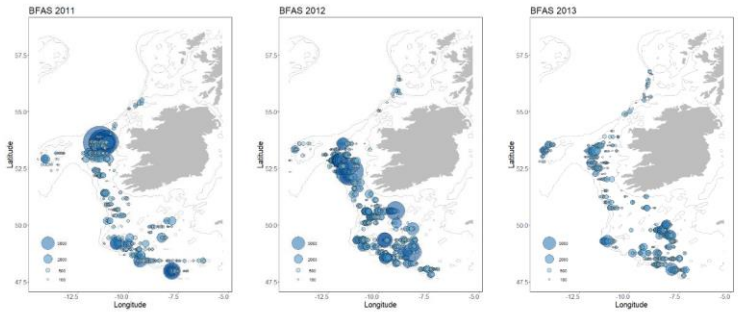

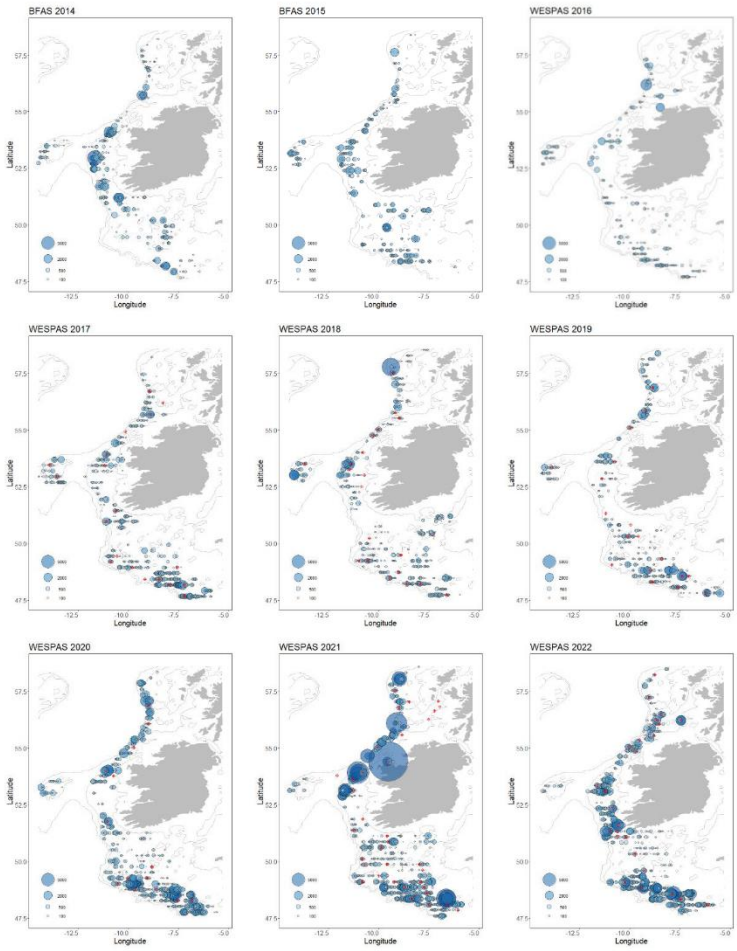


Fig 4.1: Boarfish acoustic survey NASC 2011-2022

The time series of TSB and SSB is shown in figure 4.2 and the annual abundance at length in shown in figure 4.3.

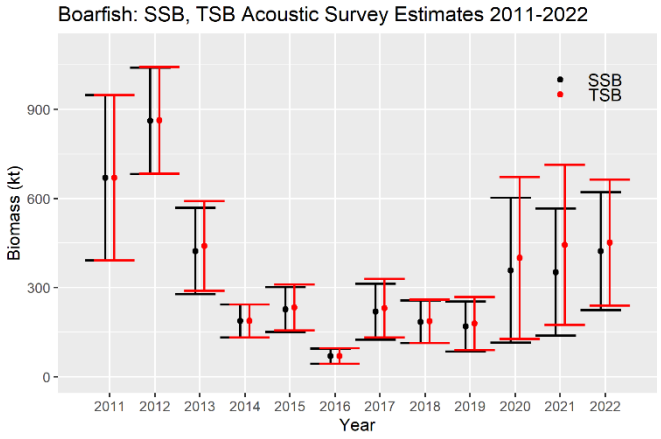


Fig. 4.2: BFAS/WESPAS acoustic survey estimates of TSB/SSB for boarfish.

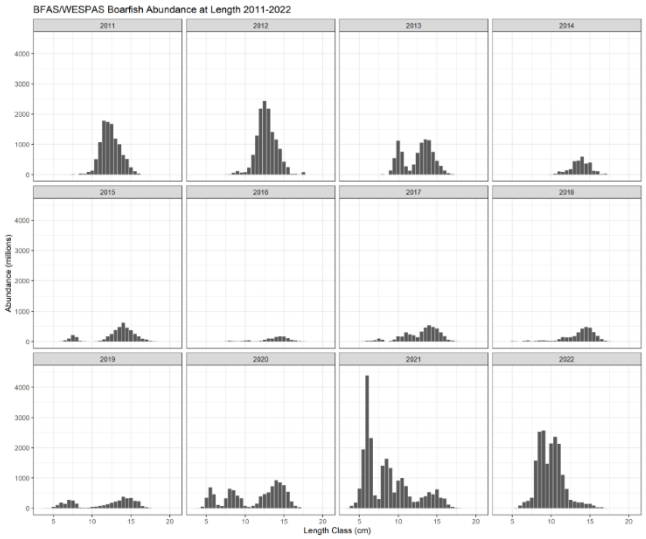


Fig 4.3: BFAS/WESPAS boarfish abundance at length.

During the early years of the survey, sampling indicated that the detected stock was almost fully mature with fish under 10cm relatively rare in the samples. In later years, smaller fish were more common, particularly in the southernmost Celtic Sea stratum. In 2020 and 2021 a significant proportion of the biomass estimate comprised recently recruited fish.

PELGAS

The PELGAS survey is carried out each year by the French National Institute for Ocean Science, Ifremer. It is an acoustic survey designed to monitor the abundance of small pelagic fish in the Bay of Biscay with a focus on anchovy and sardine and is carried out in May. Initially, boarfish was not a target species for the survey as it was rarely encountered and no estimate of abundance was calculated although length sampling of any catch resulting from trawling was carried out. Since 2014, the occurrence of boarfish has increased in Northern Biscay and a TSB estimate has been calculated. Figure 4.4 shows the location of boarfish detections and the estimated survey TSB from 2014 to 2022. Note that no survey was carried out in 2020. For 2021 and 2022 the southernmost transects of the WESPAS survey are also shown.

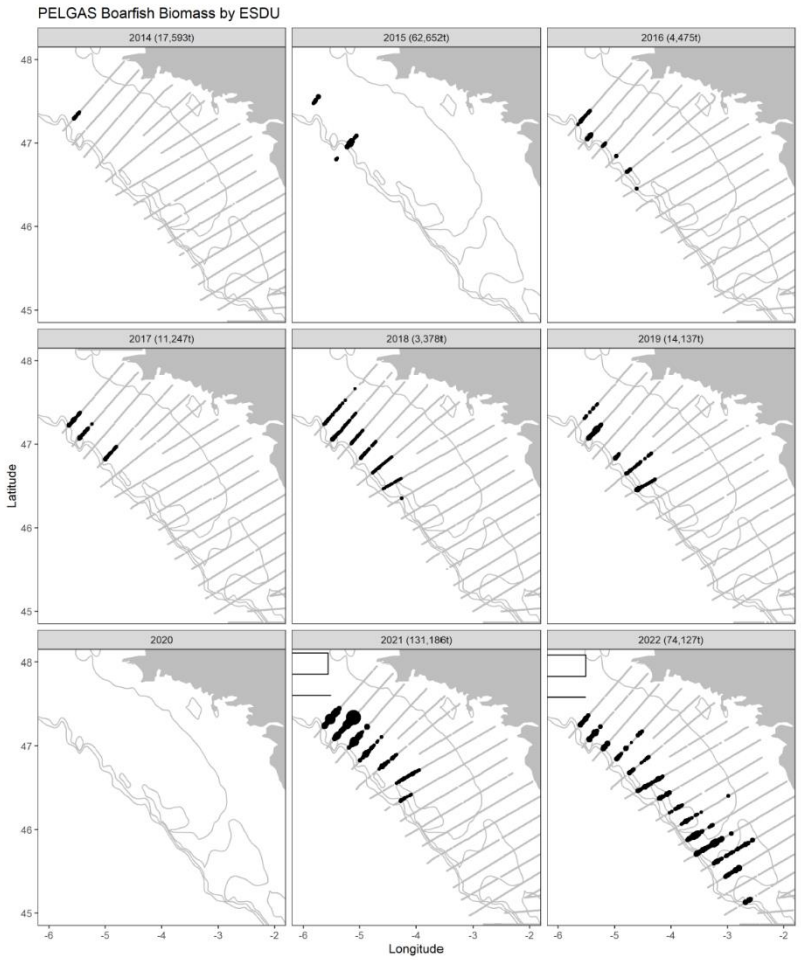


Fig 4.4. Boarfish acoustic detections by the French PELGAS survey.

Sampling of boarfish catches indicates that Biscay is an important area for juvenile fish. For 2021 and 2022 when significant quantities of boarfish were detected, the length data indicates that the biomass is comprised almost exclusively of recently recruited fish.

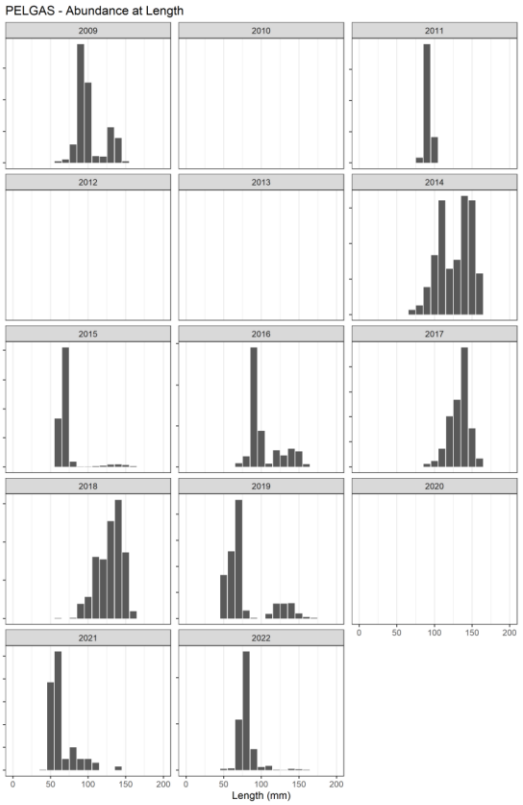


Fig 4.5 Length sampling of boarfish from PELGAS (Bay of Biscay)

A summary of the available acoustic estimates is given in the table below.

| Year | Vessels/Equipment | Design | Number echotraces | Abundance Estimation Tool | PELGAS (South of 47) |
|---|---|---|---|---|---|
| 2011 | MFV Feluoca – EK60 + towed body transducer<br>RV Celtic Explorer – EK60 + drop keel mounted transducer | ICES SR based strata, North-South direction, 7.5 and 15nmi transect spacing, 24 hour operations | 977 | Bespoke R code | Single echotrace (no estimate) |
| 2012 | MFV Father McKee – EK60 + towed body transducer<br>RV Celtic Explorer – EK60 + drop keel mounted transducer | ICES SR based strata, North-South. 04:00-00:00. | 1130 | Bespoke R code | No boarfish detected |
| 2013 | MFV Feluoca – EK60 + towed body transducer<br>RV Celtic Explorer – EK60 + drop keel mounted transducer | ICES SR based strata, North-South. 04:00-00:00. | 1074 (reduced density) | Bespoke R code | No boarfish detected |
| 2014 | MFV Feluoca – EK60 + towed body transducer<br>RV Celtic Explorer – EK60 + drop keel mounted transducer | ICES SR based strata, North-South. 04:00-00:00. | 611 (much reduced in south) | Bespoke R code | Low abundances (18kt) |
| 2015 | MFV Feluoca – EK60 + towed body transducer<br>RV Celtic Explorer – EK60 + drop keel mounted transducer | ICES SR based strata, North-South. 04:00-00:00. | 681 | Bespoke R code | Significant (63kt) |
| 2016 | RV Celtic Explorer – EK60 + drop keel mounted transducer | 7 stock based strata. North-South, 04:00-00:00. | 394 | StoX | Some detections (4kt) |
| 2017 | RV Celtic Explorer – EK60 + drop keel mounted transducer | 5 stock based strata. South-North, 04:00-00:00. | 1116 | StoX | Some detections (11kt) |
| 2018 | RV Celtic Explorer – EK60 + drop keel mounted transducer | 5 stock based strata. South-North, 04:00-00:00. | 817 | StoX | Some detections (3kt) |
| 2019 | RV Celtic Explorer – EK60 + drop keel mounted transducer | 5 stock based strata. South-North, 04:00-00:00. | 667 | StoX | Some detections (3kt) |
| 2020 | RV Celtic Explorer – EK60 + drop keel mounted transducer | 5 stock based strata. South-North, 04:00-00:00. | 928 | StoX | No survey |
| 2021 | RV Celtic Explorer – EK60 + drop keel mounted transducer | 5 stock based strata. South-North, 04:00-00:00. | 976 | StoX | Largest in time series (131kt) |
| 2022 | RV Celtic Explorer – EK60 + drop keel mounted transducer | 5 stock based strata. South-North, 04:00-00:00. | 1060 | StoX | Increased southern extent (74kt) |

The following changes to survey design and vessel are potential sources of bias in the time series of TSB/SSB estimates.

- Industry vs Research vessel (towed body vs hull mounted transducer, noise)
- No inter-calibration
- Change in survey timing/direction (2017 onwards)
- Survey design (number strata, abundance estimation tool)
- Uncertainty regarding Southern boundary & alignment with PELGAS. 6 week gap prior to 2017, reduced to 2-3 weeks following change in survey direction to South-North.
- Some (probably minimal) uncertainty regarding the Northern boundary with boarfish reported by the Scottish component of the Malin Shelf Herring Survey in 2018 (north of 59°N)

Figure 4.6 shows the combined estimates of TSB from the available surveys.

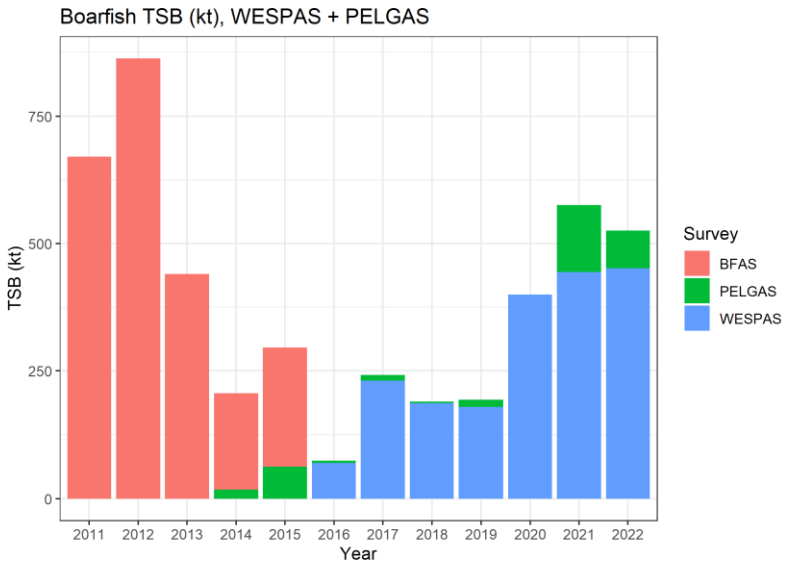


Fig 4.6 Estimates of boarfish TSB from acoustic surveys.

## 4.2 Groundfish Surveys

The current boarfish assessment utilises indices from 6 individual IBTS surveys.

1. EVHOE (Q4 French Bay of Biscay Survey 1999-2021, ex 2017).
2. IGFS (Q4 Irish Groundfish Survey 2003-2021)
3. SPPGFS (Q4 Spanish Porcupine Bank Survey 2001-2021)
4. SPPNGFS (Q4 Spanish North Coast Survey 1990-2021)
5. WCSGFS (Q1 & Q4 West of Scotland 1985-2009)

6. ECSGFS (Q3/4, English Channel/Celtic Sea Survey 1982-2003)

The Scottish Q1 and Q4 surveys (WCSCFG) were redesigned in 2010 (and henceforth named SCOWCGFS) and are considered a separate time series.

The indices are calculated within a Bayesian framework using the delta lognormal model whereby the probability of a positive catch and the catch rate (kg/30 min) are modelled separately before being combined to generate an index. Year and ICES statistical rectangle are explanatory variables for both the presence and catch rate models - providing both an index and estimate of uncertainty for the assessment. The most recent indices were calculated for the 2021 assessment and are shown in figure 4.7. Note that the SCOWCGFS survey index (2011-present) is not used in the current assessment.

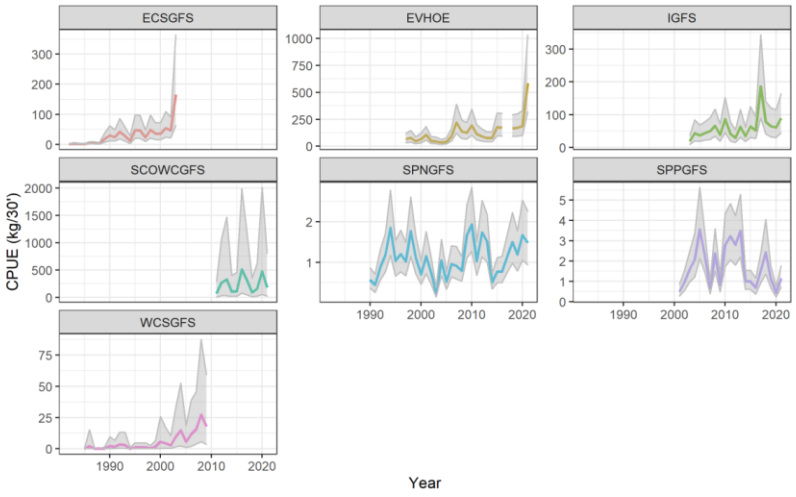


Fig 4.7 – Delta Lognormal indices used by the current boarfish stock assessment (excluding SCOWCGFS).

The number of hauls carried out by each survey is shown in figure 4.8.

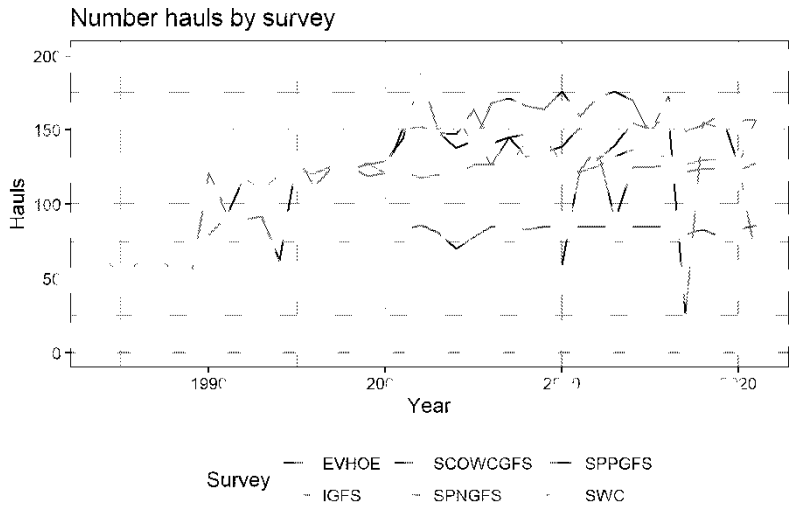


Fig 4.8: Number of hauls by IBTS survey by year

Since 2000, the number of hauls is relatively constant. The EVHOE survey in 2017 was curtailed due to vessel breakdown with fewer than 30% of the planned hauls completed. The Scottish surveys (SWC and SCOWCGFS) consist of both a Q1 and Q4 survey.

Boarfish is frequently encountered by all Western IBTS surveys. Only the Scottish surveys have an encounter rate of lower than 50% although there are indications of a decline in the proportion of zero hauls since approximately 2000 - perhaps indicating a northern range expansion in the stock. Further south, in the Bay of Biscay, Celtic Sea and on the Porcupine Bank approximately 50-75% of hauls consistently contain boarfish (fig. 4.9)

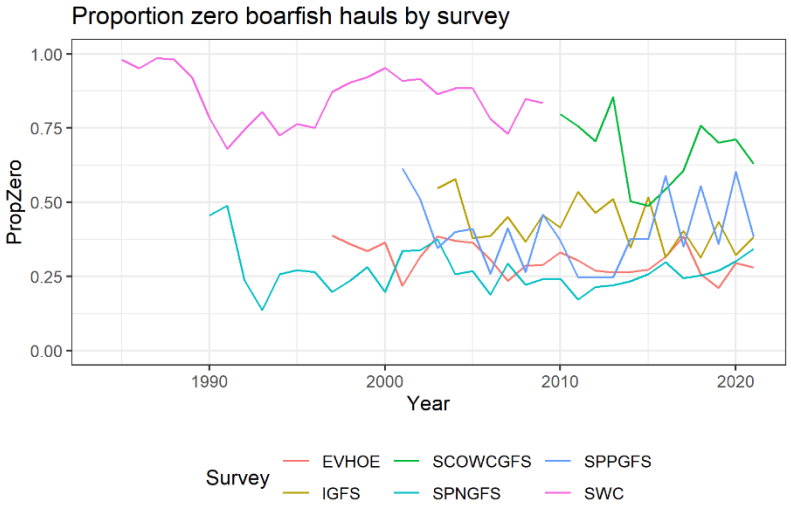


Fig 4.9 – Proportion of hauls with zero catch of boarfish by IBTS survey and year.

The distribution of hauls and presence absence by ICES statistical rectangle are shown in 4.10.

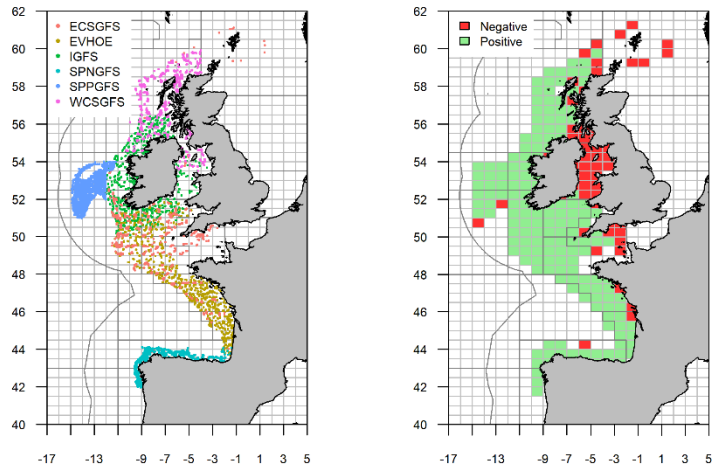


Fig 4.10: Haul positions and presence/absence of boarfish by ICES statistical rectangle (full time series).

Boarfish is a pelagic schooling species with an affinity to the seabed during the winter months when the IBTS surveys are conducted. As such, catch rates vary widely with occasional very

large hauls. The mean catch rate for the period 2003-2021 by ICES statistical rectangle is shown in figure 4.11.

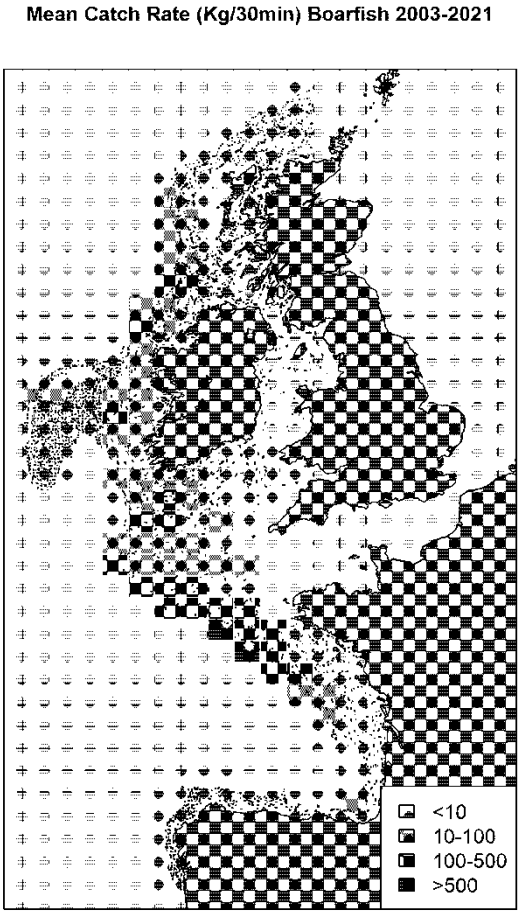


Fig 4.11 IBTS mean catch rate of boarfish (kg/30min) by ICES statistical rectangle 2002-2021

The highest catch rates are found in the northern part of the Bay of Biscay (covered by the EVHOE survey) and are associated with the shelf edge region. The Celtic Sea and west and northern coasts of Ireland are also associated with higher catch rates. Although boarfish is frequently encountered to the west of Scotland, on the Porcupine Bank and in the southern part of the Bay of Biscay and the northern Spanish shelf, catch rates in these areas are significantly lower although this may partly be explained by the various gears used in these areas such as the heavier ground gear deployed in 6a and the Baka trawl used on the Spanish survey.

IBTS surveys routinely sample the entire catch in each haul (occasionally subsampling if the catch is particularly large) for length. Figure 4.12 shows the annual length frequency for each

survey. For the earlier years in most surveys boarfish length was taken to the nearest cm before ½ cm increments were used for this relatively small species.

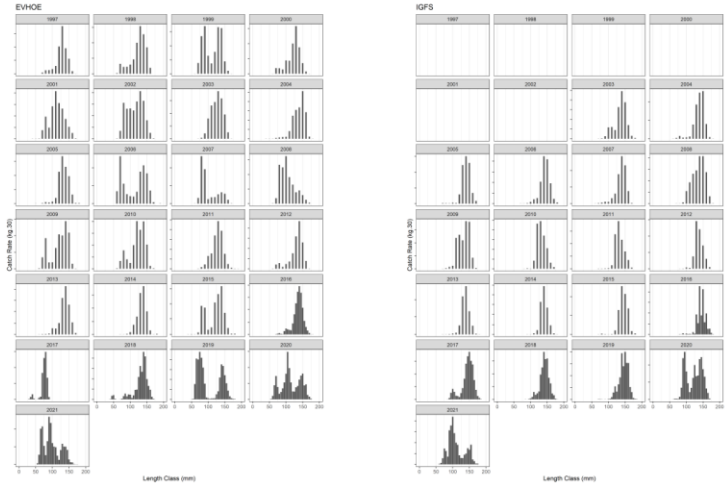


Fig 4.12 – Annual length frequency for total boarfish catch from EVHOE (left) and IGFS (right) surveys.

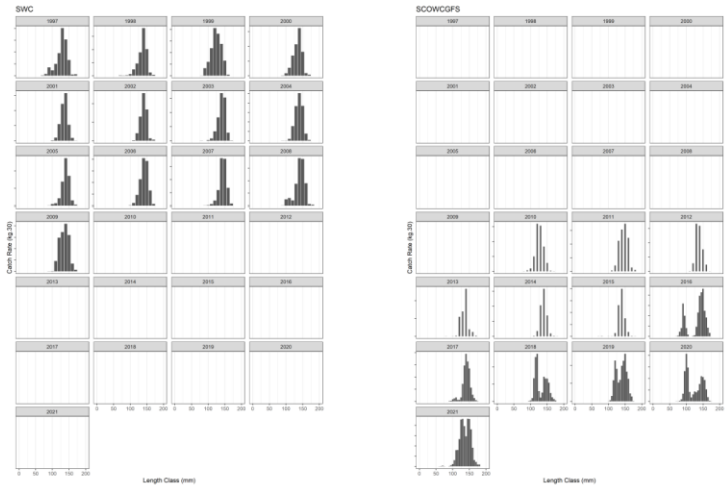


Fig 4.12 (cont.) – Annual length frequency for total boarfish catch from SWC (left) and SCOWCGFS (right) surveys.

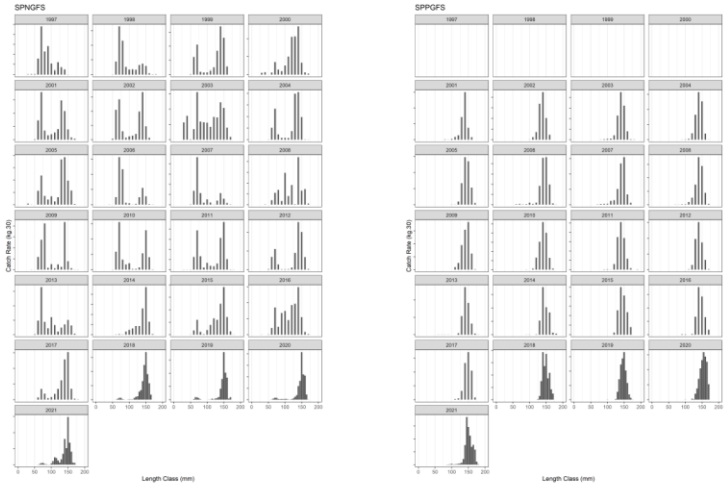


Fig 4.12 (cont.) – Annual length frequency for total boarfish catch from Spanish Shelf (left) and Spanish Porcupine (right) surveys.

Boarfish initially grow rapidly until they reach maturity at 4-5 years old. In several surveys and years modes size classes below 10cm are evident in the length frequency distribution in particular from the Southern-most surveys (EVHOE, SPNGFS) and more recently the Irish (IGFS) survey indicating that these areas may be important for young, immature fish. Scottish surveys and the Porcupine bank survey are both associated with fully mature fish although a mode at approximately 10cm is evident from the Scottish survey in the most recent years.

Since the IBTS indices were originally explored for use within the current Bayesian stock assessment model, there have been advances in the field of index standardisation for use within stock assessment, in particular with regard to spatio-temporal modelling. This approach, typified by the VAST (Vector Autoregressive Spatio-Temporal) model of Thorsen (ref) implements a delta model capable of dealing with zeros and a continuous positive distribution but explicitly models spatial and spatiotemporal correlations in a pair of models. This approach offers the advantage of allowing for vessel (survey) effects such that separate surveys (with potentially different sampling schemes) can be combined into a single index and can accommodate missing data.

For the current exercise, VAST is fitted to a combined survey dataset consisting of haul level catch rates of boarfish (kg per 30min). The period considered is 1999 to present to coincide with the available catch time series and corresponding to the period of consistent survey effort. The English-channel survey has been excluded as it ceased in 2003. The redesigned Scottish west coast Q1 and Q4 surveys (available since Q4 2010) have been included. For the purposes of combining these surveys the Q1 survey has been considered aligned with the Q4 survey (i.e. the survey year has been reduced by 1) such that each year of data consists of data from Q4 Irish, French, Spanish and Scottish surveys and the subsequent Scottish Q1 survey in the following year. A minor number of hauls have been excluded on the basis they were in areas that were infrequently surveyed (the Irish and Clyde Seas).

The model spatial domain therefore consists of the majority of the Western European shelf where boarfish is understood to inhabit. The model establishes a grid consisting of 200 knots, the positions of which are dependent on the local sampling intensity. Overall, the dataset consists of

13,289 hauls. A number of fits were explored based on length-based subsets of the total catch to estimate indices based on all size classes and those corresponding to mature/immature fractions.

VAST implements two model components for encounter probability and positive catches, which are assumed to be log-normally distributed (a gamma distribution yielded a poorer model fit). The linear predictors include year-effects, survey effects and spatial and spatio-temporal variability.

The R package FishStatsUtils implements a number of functions to examine VAST outputs and can be used to generate diagnostic plots to explore the model fit and an estimated index based on the summed density over the survey area along with estimates of uncertainty.
Initially, VAST was fit to each of the surveys individually (with the exception of the ECSGFS) with estimation of spatial correlation only. A second model including spatiotemporal correlation was also fit. The results of these fits are shown in figure 4.13. The black line and grey shading correspond to the fit using the existing Bayesian frame work which does not explicitly model spatial correlations but rather uses ICES statistical rectangle as an explanatory variable in both the encounter probability model and the positive catch rate model. The red lines are the result of the VAST fit incorporating spatial correlation only and are generally in good agreement with the Bayesian results. The blue lines correspond to the VAST model with the additional inclusion of spatio-temporal variability. Models incorporating spatio-temporal correlations exhibit reduced residual variance and lower AIC. In general, the index is in agreement with the Bayesian and spatial VAST fits, reflecting the relative importance of variability in average spatial pattern as opposed to interannual changes. Some differences can be seen in the most recent period for the IGFS and EVHOE surveys, both of which have recorded significant increases in catch rates in recent years.

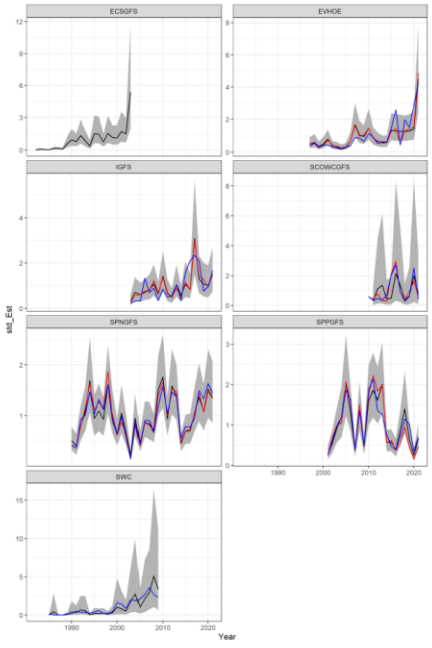

Fig 4.13 – Bayesian and VAST fits for individual IBTS surveys.

VAST was then fit to the complete dataset (all surveys and years from 1999) for catch rates based on

- All length classes
- Length classes <=65mm (immature, ages <2)
- Length classes >65mm (age 2 and over)
- Length classes <=100 (ages <3)
- Length classes >100mm (age 3 and over)

Spatial and spatio-temporal correlations were estimated and separate runs were made with and without a survey (vessel) effect. All models appeared to converge with satisfactory diagnostics. Inclusion of a vessel effect would appear to be important, perhaps unsurprising given variations in survey protocols, gears and the separate geographic domains for each survey. A number of candidate indices for use within a SPiCT assessment are generated. The index corresponding to catch rates based on all length classes is shown in figure 4.14.

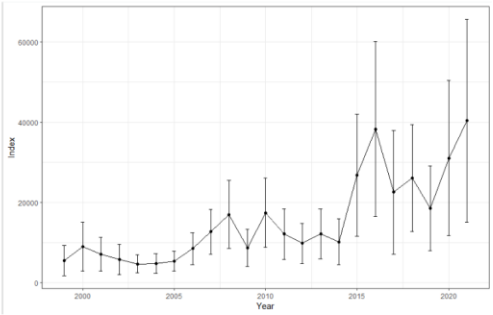


Fig 4.14 VAST estimated IBTS boarfish index.

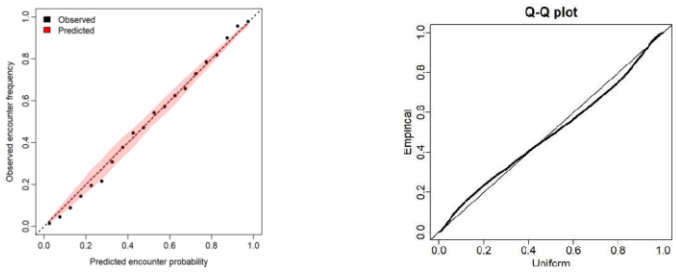


Fig 4.15: residual diagnostics predicted encounter probability vs observed encounter probability (left) and QQ plot for positive catches (right)

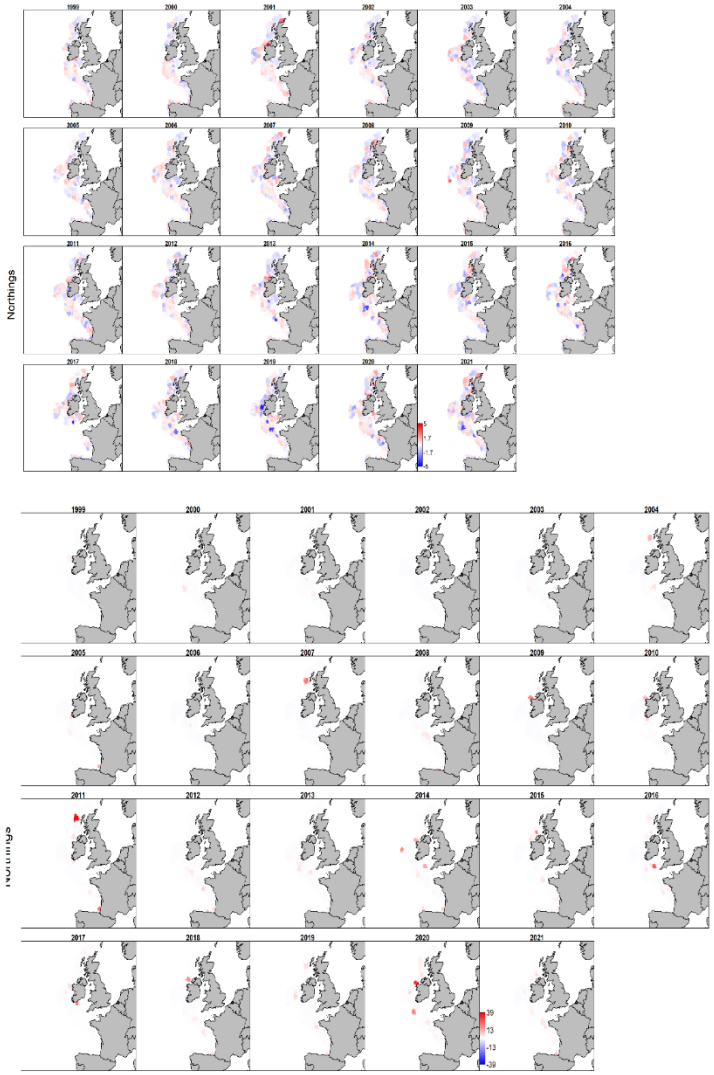


Fig 4.16 Pearson residuals for (top) encounter model and (bottom) catch rate

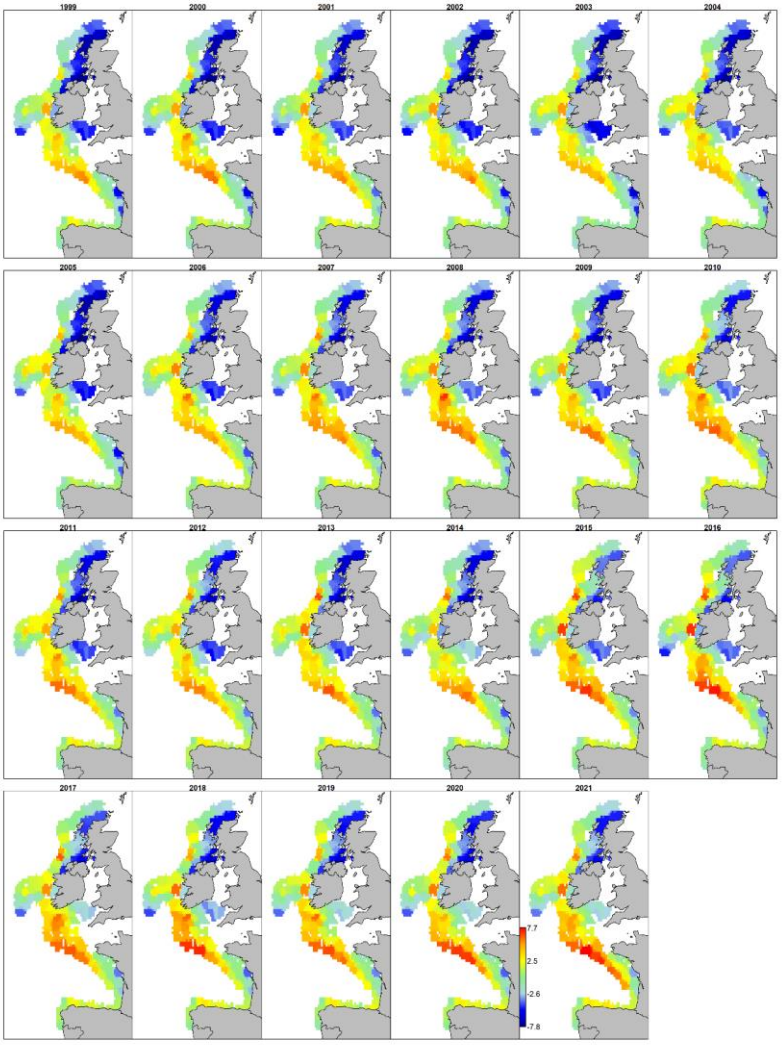


Fig 4.17: Boarfish - predicted (log) density

A retrospective analysis was carried out, refitting the VAST model following successively removing the most recent year of data, up to 5 years.

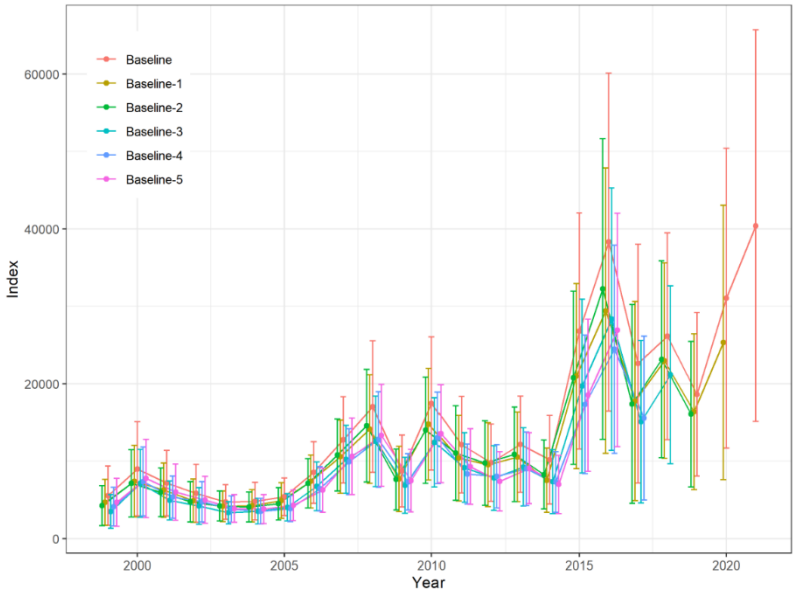


Fig 4.18: VAST Index retrospective analysis. Data on the year axis is jittered to aid comparison.

# 5 Length Composition Comparisons

Comprehensive length sampling is available for the commercial catch, acoustic and groundfish surveys. Comparisons between each of the groundfish surveys, the catch (from 2007) and acoustic survey (WESPAS component, 2011 onwards) are shown in figure 5.1

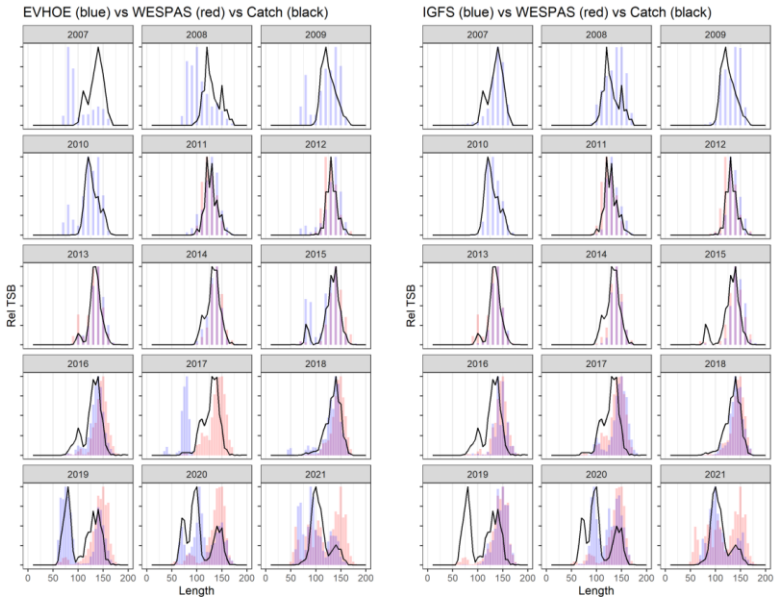


Fig 5.1 – length frequency comparison comparing catch (black line), acoustic survey (red bars) and groundfish surveys (blue bars) - EVHOE (left), IGFS (right).

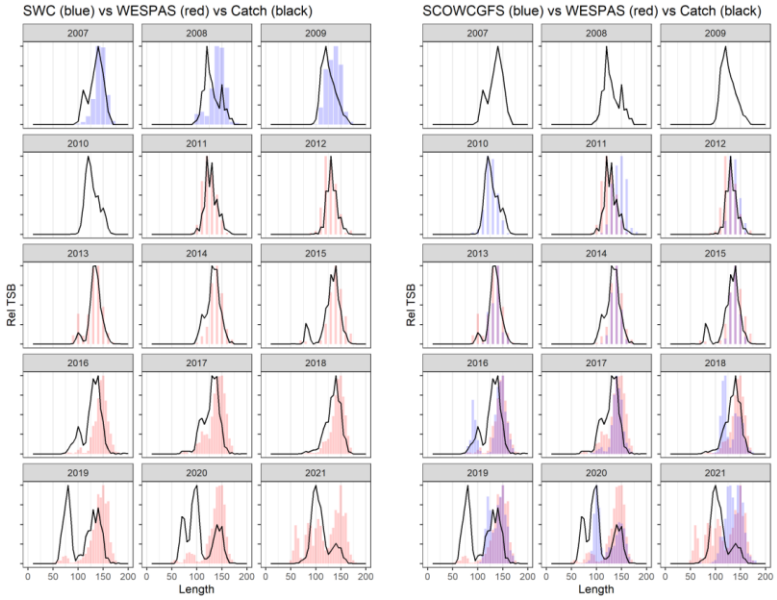


Fig 5.2 (cont.) – length frequency comparison comparing catch (black line), acoustic survey (red bars) and groundfish surveys (blue bars) - SWC (left), SCOWCGFS (right).

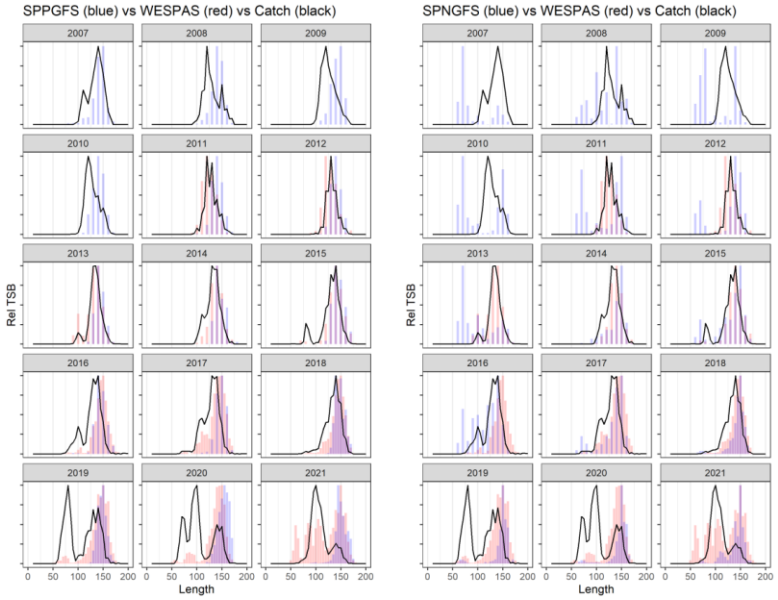


Fig 5.3 (cont.) – length frequency comparison comparing catch (black line), acoustic survey (red bars) and groundfish surveys (blue bars) - SPPGFS (left), SPNGFS (right).

Comparing the acoustic survey with the catch (2011-2022) indicates strong agreement in the early years of the survey (2011-2015). During this period both the fishery and the majority of the biomass detected by the acoustic survey was in division 7.j. Significant catches were taken in both quarters 1 and 4. Between 2016 and 2018 slightly larger fish were found in the survey. This period coincided with an increase in survey biomass in the Northern survey strata (west of Scotland) and increased catches in Northern Biscay. In the most recent years, the catch has comprised an increasing proportion of immature fish which are occasionally (e.g. 2021) but not routinely detected by the WESPAS acoustic survey. The PELGAS survey however, which covers waters to the south of the WESPAS survey area regularly detects immature boarfish in particular in 2021 and 2022.

The EVHOE IBTS survey catches regularly consist of a large proportion of juveniles in agreement with catch, particularly in more recent years when the catch has been taken further south. The IGFS length profile is regularly in agreement with the fishery as both take place in similar locations. The Scottish west coast survey exhibits poorer agreement but is indicative of expansion of range in recent years. It indicates a lower proportion of juveniles than more southern surveys.

No juveniles have been detected during the survey conducted on the Porcupine bank whereas the other Spanish survey from 8.c regularly detects juveniles. As a collective, the groundfish surveys cover the majority of the boarfish distribution and offer comprehensive coverage of both juvenile and adult phases. As an indication of their ability to track stock development, figure 5.4 depicts the development of the length profile from the catch sampling, the acoustic survey and 2 groundfish surveys. All four data sources are on broad agreement regarding the length structure of the stock in recent years.

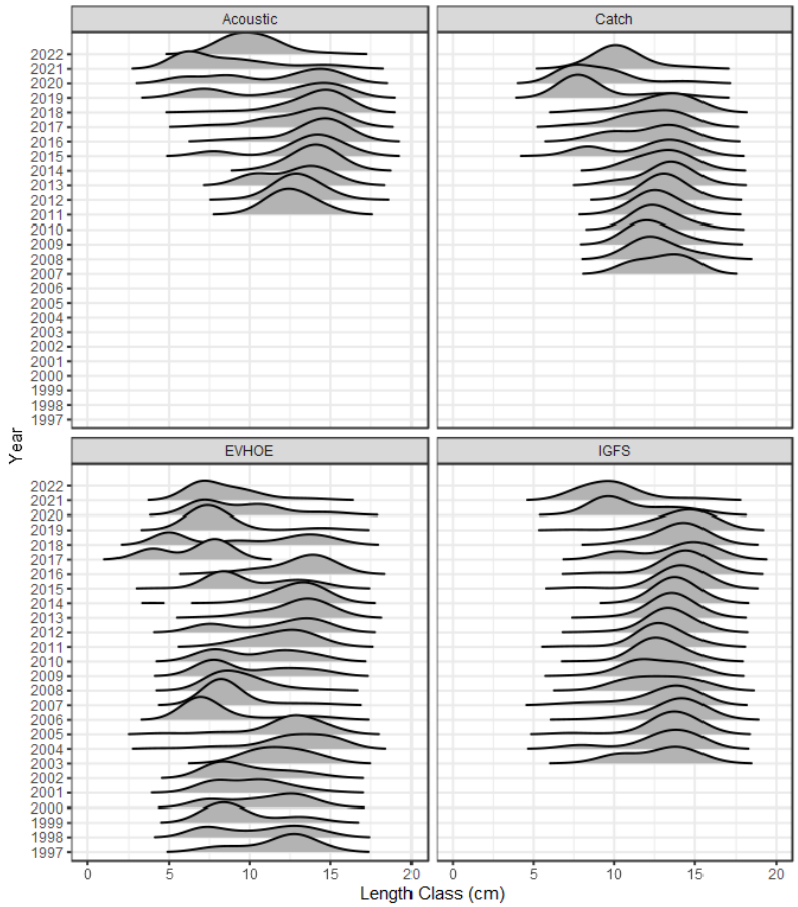


Fig 5.4 Length frequency ridgeplots for catch, WESPAS and EVHOE and IGFS groundfish surveys.

# 6 Population Parameters

## 6.1 Length

Comprehensive length sampling is carried out by the commercial catch sampling programme (landings (since 2007) and discards), the acoustic and groundfish surveys. Initially, length measurements were taken to the nearest cm before protocols were update to the half-cm (2008 for catch, 2021 for the PELGAS acoustic survey).

The length sampling of commercial catch and from the acoustic survey is shown in figure 6.1. The red dashed line corresponds to the length at first capture ($L_c$), the smallest length class with an abundance greater than half the maximum. The blue line represents $L_{max}$, the 99$^{th}$ percentile of the recorded lengths. The values are tabulated below in table 6.1.

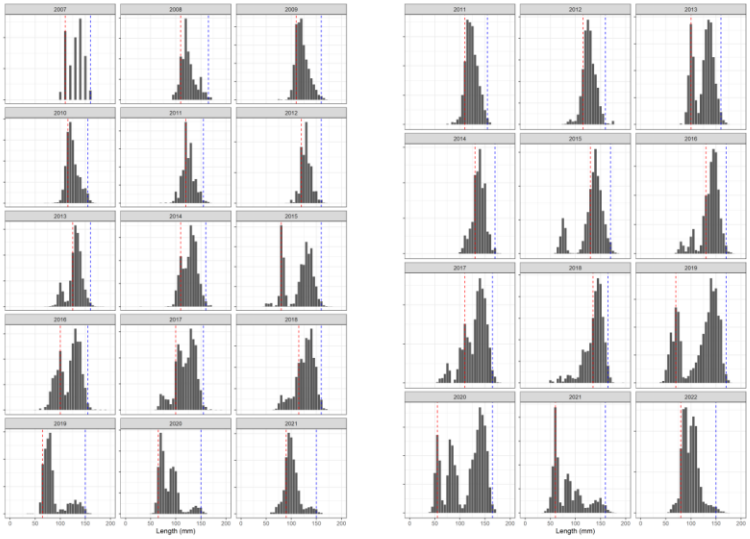


Fig 6.1 Annual length frequency for commercial catch (left) and acoustic survey (right). The red dashed line indicates $L_c$ and the blue $L_{max}$ (99$^{th}$ percentile).

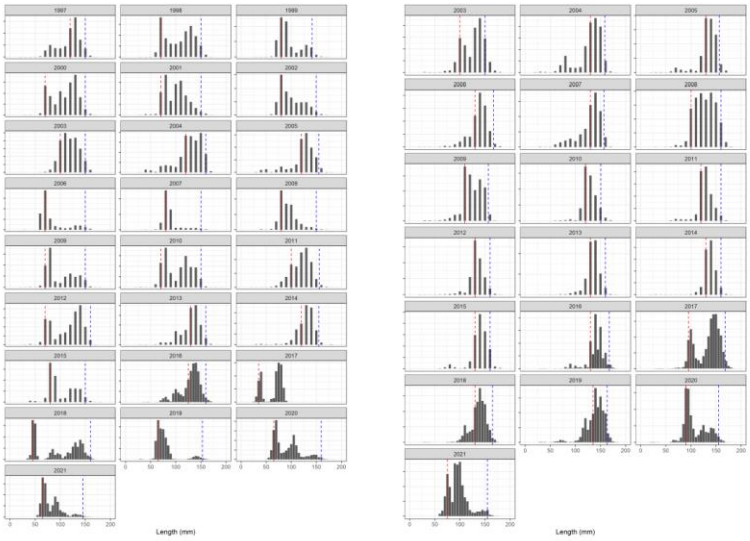


Fig 6.1 (cont) Annual length frequency for EVHOE groundfish survey (left) and IGFS groundfish survey (right). The red dashed line indicates $L_c$ and the blue $L_{max}$ ($99^{th}$ percentile).

| Year | $L_c$ | | | | $L_{max}$ | | | |
|---|---|---|---|---|---|---|---|---|
| | Catch | Acoustic Survey | EVHOE | IGFS | Catch | Acoustic Survey | EVHOE | IGFS |
| 2007 | 110 | | 80 | 130 | 160 | | 150 | 155 |
| 2008 | 110 | | 80 | 100 | 165 | | 150 | 160 |
| 2009 | 110 | | 70 | 110 | 160 | | 150 | 155 |
| 2010 | 115 | | 70 | 120 | 155 | | 150 | 150 |
| 2011 | 120 | 110 | 100 | 120 | 155 | 155 | 155 | 160 |
| 2012 | 120 | 115 | 70 | 130 | 160 | 160 | 160 | 160 |
| 2013 | 125 | 100 | 130 | 130 | 160 | 160 | 160 | 160 |
| 2014 | 110 | 130 | 120 | 130 | 160 | 170 | 155 | 160 |
| 2015 | 80 | 130 | 80 | 130 | 160 | 170 | 150 | 160 |
| 2016 | 100 | 130 | 125 | 130 | 155 | 170 | 160 | 165 |
| 2017 | 100 | 110 | | 95 | 155 | 165 | | 170 |
| 2018 | 115 | 135 | 45 | 130 | 160 | 165 | 160 | 165 |
| 2019 | 65 | 70 | 65 | 135 | 150 | 170 | 155 | 165 |
| 2020 | 65 | 55 | 65 | 90 | 150 | 165 | 160 | 155 |
| 2021 | 90 | 60 | 65 | 75 | 150 | 160 | 145 | 155 |
| 2022 | | 80 | | | | 150 | | |

Table 6.1 Lc, Lmax statistics for commercial catch, acoustic survey and EVHOE, IGFS groundfish surveys

## 6.2 Length-Weight

Data to support length-weight analysis are available from sampling of the commercial fishery and the summer acoustic survey from 2011-2022. The fishery largely takes place in quarters 1 and 4 so separate analysis have been carried out for data from fishery samples in Jan-Apr (Q1/2), survey samples in Jun-Jul and fishery samples from (Sep-Dec). a and b parameters of the growth function $W = aL^b$ were estimated by fitting a linear model in R (lm) to log transformed length and weight data for each year.

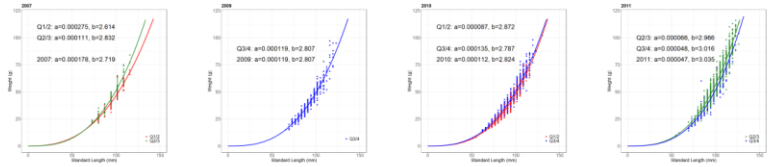

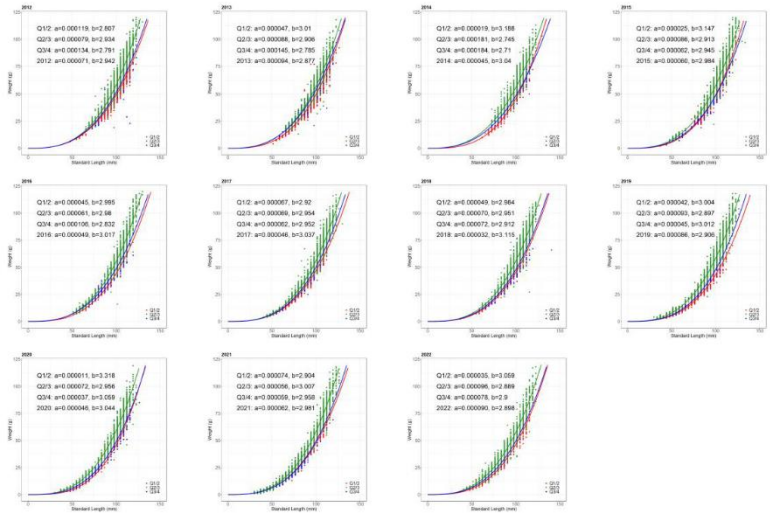


Fig 6.3. length-weight regressions for catch and acoustic survey samples.

| Year | a | B |
|---|---|---|
| 2007 (White et al) | 0.000054 | 2.91 |
| 2007 | 0.000178 | 2.72 |
| 2009 | 0.000109 | 2.81 |
| 2010 | 0.000112 | 2.82 |
| 2011 | 0.000047 | 3.04 |
| 2012 | 0.000071 | 2.94 |
| 2013 | 0.000094 | 2.88 |
| 2014 | 0.000045 | 3.00 |

| Year | a | b |
|---|---|---|
| 2015 | 0.000060 | 2.98 |
| 2016 | 0.000049 | 3.02 |
| 2017 | 0.000046 | 3.04 |
| 2018 | 0.000032 | 3.12 |
| 2019 | 0.000086 | 2.91 |
| 2020 | 0.000046 | 3.04 |
| 2021 | 0.000062 | 2.98 |
| 2022 | 0.000090 | 2.90 |

Table 6.3 Length-weight a,b parameters from sampling of the commercial fishery and summer acoustic survey 2007-2022.

In figure 6.3 the blue lines correspond to fits from data collected in quarters 3 and 4 (i.e. from the fishery). The red fits use sampling data from the fishery in quarter 1 with occasional catches in quarter 2. The green data points are largely based on observations taken during the acoustic survey which takes place at spawning time in summer (June/July). While the length weight relationships from data collected during the winter months are similar, specimens tend to be heavier during the summer.

## 6.3 Length at Maturity

Maturity staging (8 point scale, 3 and above considered mature) is carried out on samples from the commercial fishery and also during the WESPAS acoustic survey. The commercial fishery largely takes place outside of spawning time. However, the acoustic survey is conducted in June and July when spawning aggregations occur (Blanchard and Vandermeirsch, 2005) and extensive trawl sampling is carried out (on average, ~850 fish are sampled annually for maturity staging).

R package *sizeMat* (Torrejon-Magallanes J (2020)) was used to fit a maturity ogive to annual survey data:

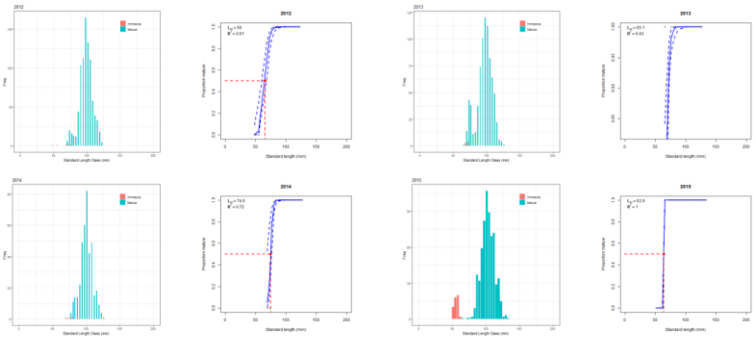

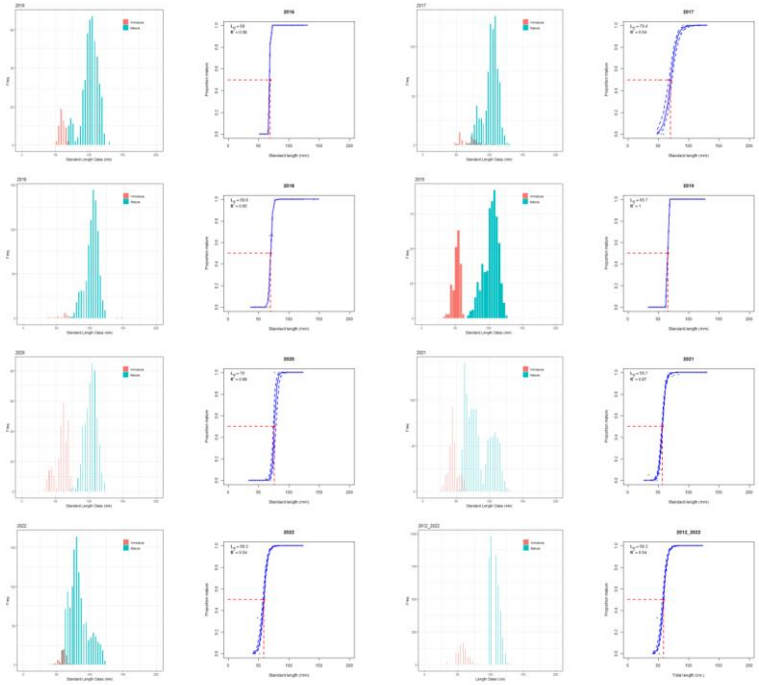

Fig 6.4 Maturity ogives fit to acoustic survey sample data.

The study of White et al (2011) estimated an overall value (both sexes) for $L_{50}$ of **85.7mm** with sex-specific values of 80.5mm for females and 87.8mm for males. Although few immature fish are collected in some years, estimates from the acoustic survey data presented above range from **58-75mm** (standard length). Based on the relationship between total and standard length (SL = 1.34386 + 0.715 x TL), the equivalent TL range is 79mm-103mm. There may be evidence of year class variability in maturation. Comparing data from the 2020 and 2021 surveys, both of which contain a significant number of immature specimens, all fish under 7.5cm in 2020 were immature whereas all fish greater than 60mm SL were considered mature in 2021.

## 6.4 Ageing, Von Bertalanffy Growth Parameters

During initial investigations around the start of the targeted fishery, 868 boarfish samples were obtained from the fishery and research vessels in May, June, October and November of 2007 from 6aS, 7b, 7g, 7h and 7j and were used to investigate the growth of boarfish (White *et al* 2011). At this time, age reading protocols were also developed (Hussy *et al* 2012a) and an ALK constructed. White *et al* (2011) noted a **maximum age of 26**, relatively late maturing ($A_{50}$ = 5.25 years), K = **0.186 $yr^{-1}$** and an asymptotic length of **129mm**.

Hussy *et al* (2012b) investigated sexual dimorphism in the growth characteristics of boarfish from samples collected in 2009 and 2010. Although females are on average larger than males there is no significant difference in length at maturity nor age at maturity ($L_{50}$=**9.7cm**, $A_{50}$=3.4yrs). Growth is dimorphic with a common $t_0$ but significantly different K and $L_{inf}$ values with K=0.145 $yr^{-1}$ for females and 0.181 for males and $L_{inf}$ = **165mm and 144mm** for females and males respectively.

Ageing of boarfish fishery and survey samples ceased in 2011 (although collection of otoliths has continued). An updated analysis to include all aged samples collected up to 2011 leads to the following updated estimates

| Female (age range 2-31) | | | | | | | | |
|---|---|---|---|---|---|---|---|---|
| $L_{inf}$ | | | K | | | $t_0$ | | |
| 159 | **160** | 161 | 0.138 | **0.143** | 0.149 | -4.57 | -4.29 | -4.03 |

| Male (age range 1-30) | | | | | | | | |
|---|---|---|---|---|---|---|---|---|
| $L_{inf}$ | | | K | | | $t_0$ | | |
| 146 | **147** | 148 | 0.156 | **0.165** | 0.172 | -4.64 | -4.27 | -3.97 |

The ALK constructed from ageing of commercial fishery samples from 2011 is shown below.

| | 1 | 2 | 3 | 4 | 5 | 6 | 7 | 8 | 9 | 10 | 11 | 12 | 13 | 14 | 15+ |
|---|---|---|---|---|---|---|---|---|---|---|---|---|---|---|---|
| 7 | 1 | 1 | | | | | | | | | | | | | |
| 7.5 | 1 | 1 | | | | | | | | | | | | | |
| 8 | | 1 | | | | | | | | | | | | | |
| 8.5 | | 1 | 1 | | | | | | | | | | | | |
| 9 | | 1 | 1 | | | | | | | | | | | | |
| 9.5 | | | 1 | | | | | | | | | | | | |
| 10 | | | 1 | | | | | | | | | | | | |
| 10.5 | | | 2 | 10 | 3 | | | | | | | | | | |
| 11 | | | 1 | 29 | 14 | 2 | 2 | | | | | | | | |
| 11.5 | | | | 9 | 21 | 21 | 18 | 2 | 2 | 1 | | | | | |
| 12 | | | | 4 | 17 | 22 | 38 | 12 | 8 | | | | | | 1 |
| 12.5 | | | | | 5 | 9 | 42 | 37 | 14 | 6 | 2 | | 1 | 1 | 1 |
| 13 | | | | | 2 | 4 | 31 | 28 | 24 | 12 | 6 | 2 | 3 | 1 | 5 |
| 13.5 | | | | | 1 | 3 | 25 | 22 | 21 | 14 | 6 | 5 | 4 | 2 | 11 |
| 14 | | | | | | | 6 | 8 | 18 | 22 | 8 | 3 | 7 | 1 | 20 |
| 14.5 | | | | | | 1 | 1 | 2 | 3 | 8 | 1 | 6 | 6 | 6 | 30 |
| 15 | | | | | | | 1 | 1 | | 2 | 2 | 2 | 5 | 2 | 19 |
| 15.5 | | | | | | | | | | 2 | | | | 2 | 19 |
| 16 | | | | | | | | | | | | | | | 8 |
| 16.5 | | | | | | | | | | | | | | | 1 |
| 17 | | | | | | | | | | | | | | | 1 |
| 17.5 | | | | | | | | | | | | | | | 1 |
| 18 | | | | | | | | | | | | | | | 1 |
| 18.5 | | | | | | | | | | | | | | | 1 |

Table 6.4 Boarfish age-length key from 2011 samples.

Growth is relatively rapid until the fish is mature with little to distinguish between ages 5-10 in terms of length. At the time of the study the population consisted of a significant proportion of relatively old fish (PG 15+) consistent with a stock experiencing only light exploitation. The fishery at this time was concentrated in areas to the SW of Ireland (7.j), exploiting dense shoals on the shelf break. Few immature samples were obtained and the key is spare for the youngest ages. Recently, work has restarted to establish routine ageing both fishery and survey samples.

## 6.5 Natural Mortality

Based on an assumption that the natural mortality will reduce a population to 1% of its initial size over the lifespan of the stock, and based on a maximum observed age of 31, this model yields a natural mortality estimate of **0.16** (King, 1995). This is a similar estimate to the total mortality estimate from 2007 (0.17) when landings were relatively low. Estimates from IBTS data from 2003-2006 ranged from 0.09 to 0.2 with a mean of 0.16 (ICES, 2012).

## 6.6 Conditioning of model priors

SPiCT can be configured to supply priors for model parameters. Defaults are uninformative and may lead to unrealistic parameter estimates. Information is available for a number of model parameters that can be used to provide more informative priors than the defaults which may lead to unrealistic parameter estimates

Intrinsic Growth Rate (r)

Candidate priors for intrinsic growth rate r are available from the FishLife R package (Thorson 2020), the SPMPriors R package (github.com/henning-winker/SPMpriors), the current surplus production assessment model (ICES, 2022) and Trenkel and Rochet (2003).

The FishLife package estimates a value for r of 0.65. A summary of estimates for *Capros aper* is shown in figure 6.5. However, information in FishBase on boarfish is sparse. Moreover, several of the data sources derive from studies undertaken on boarfish likely from other populations, notably from the Aegean Sea where both growth rates and asymptotic length are different (estimates of K of ~ 0.4 for the Aegean population, double that of NE Atlantic studies). Attempts to refit the model using either a subset of the available data or including more recent data were unsuccessful.

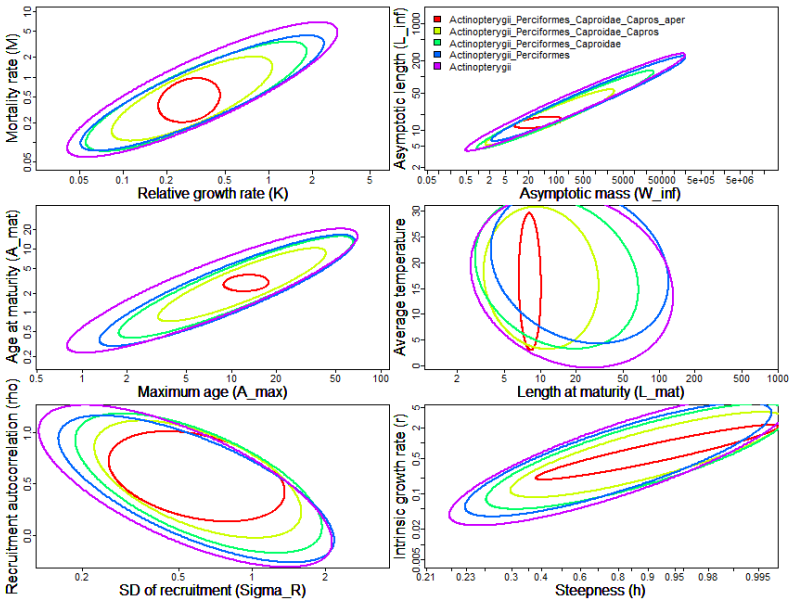


Fig. 6.5 FishLife Plot_taxa(Search_species(Genus="Capros", Species="aper")$match_taxonomy,mfrow=c(3,2) )

The SPMPriors R package extends the FishLife dataset to generate priors for stock assessments using multivariate-normal Monte Carlo simulations which can be tuned using existing estimates of stock lie history parameter such as $L_{inf}$ and $L_{mat}$. Estimates from SPMPriors for *Capros aper* with an $L_\infty = 16.0$ cm and $L_m = 9.7$ cm (Hüssy et al. 2012) are shown in figure 6.6 and yields an estimate for r of 0.47.

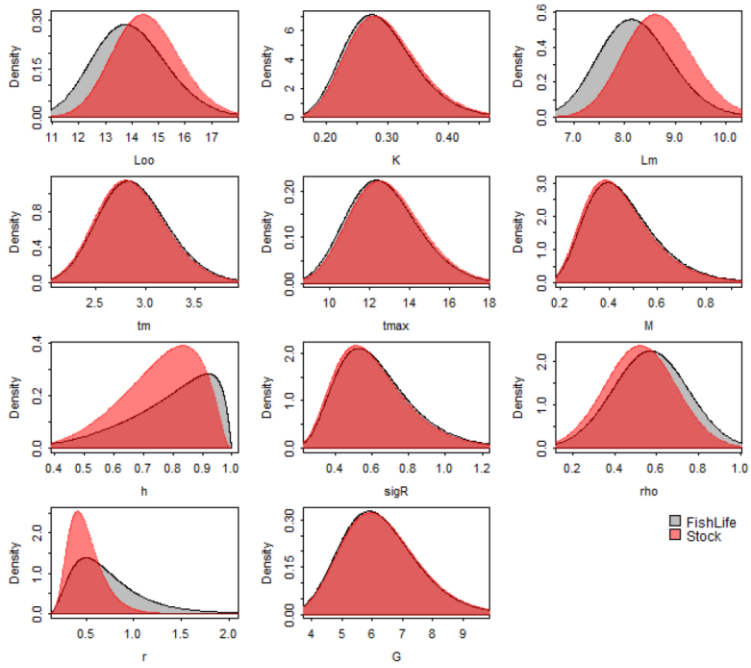


Fig 6.6 Life history parameter estimates from SPMPriors with no tuning info.

| trait | mu.sp | cv.sp | mu.stk | cv.stk | lc.stk | uc.stk | upper quant |
|---|---|---|---|---|---|---|---|
| Loo | 13.8966 | 0.1009 | 14.5304 | 0.0862 | 12.7714 | 16.5316 | 0.9 |
| K | 0.2854 | 0.2021 | 0.2907 | 0.2008 | 0.2249 | 0.3758 | 0.9 |
| Lm | 8.2003 | 0.0880 | 8.6650 | 0.0787 | 7.7427 | 9.6972 | 0.9 |
| tm | 2.8691 | 0.1232 | 2.8457 | 0.1229 | 2.4317 | 3.3303 | 0.9 |
| tmax | 12.6135 | 0.1434 | 12.7739 | 0.1429 | 10.6343 | 15.3440 | 0.9 |
| M | 0.4379 | 0.3260 | 0.4273 | 0.3255 | 0.2844 | 0.6421 | 0.9 |
| h | 0.9197 | 0.1544 | 0.8344 | 0.1750 | 0.6069 | 0.9473 | 0.9 |
| sigR | 0.5910 | 0.3499 | 0.5758 | 0.3521 | 0.3723 | 0.8906 | 0.9 |
| rho | 1.7692 | 0.3136 | 1.6866 | 0.3253 | 1.3405 | 2.1220 | 0.9 |
| r | 0.6465 | 0.5409 | 0.4698 | 0.3338 | 0.2456 | 0.8988 | 0.9 |
| G | 6.1426 | 0.2051 | 6.1939 | 0.2063 | 4.7761 | 8.0326 | 0.9 |

Translation of MVN stocks into Pella-Tomlinson SPM priors through an age-structured model using fl2asem function

| | r | shape | Fmsy | bmsyk |
|---|---|---|---|---|
| mu | 0.2969 | 0.575 | 0.513 | 0.2719 |
| logsd | 0.299 | 0.3531 | 0.5544 | 0.2078 |

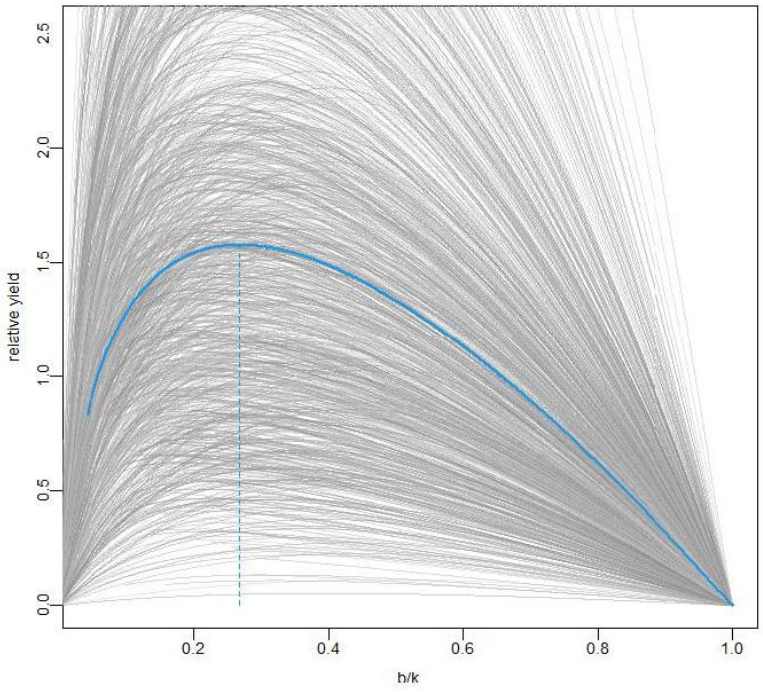


Trenkel and Rochet (2003) published a study on the performance of indicators derived from abundance estimates from groundfish surveys, with an estimate of intrinsic growth rate r for boarfish in the Celtic Sea of 0.31. The most recent update assessment for boarfish, carried out in 2022 using a state space Schaefer surplus production model estimates an r value of 0.34, with a standard deviation of 0.17. The key parameter values from the assessment are given below (ICES, 2022):

**Table 3.6.3.1. Boarfish in ICES Subareas 27.6, 7, 8. Key parameter estimates from the exploratory Schaeffer state space surplus production model. Posterior parameter distributions are provided in Figure 3.6.3.5**

| Parameter | Mean | SD | 2.5 | 25 | 50 | 75 | 97.5 |
|---|---|---|---|---|---|---|---|
| r | 0.34 | 0.17 | 0.06 | 0.22 | 0.33 | 0.45 | 0.70 |
| K | 685102 | 511831 | 310500 | 443300 | 550600 | 730600 | 2116000 |
| $F_{MSY}$ | 0.17 | 0.08 | 0.03 | 0.11 | 0.17 | 0.23 | 0.35 |
| $B_{MSY}$ | 171276 | 127958 | 77625 | 110825 | 137650 | 182650 | 529000 |
| MSB | 626304 | 295825 | 308800 | 450800 | 565050 | 729900 | 1314975 |

The table below summarises the available information on intrinsic growth rate for NE Atlantic Boarfish

| Value | Source |
|---|---|
| 0.64 | FishLife (Fishbase) |
| 0.47 | SPM Priors (Linf=160, Lm=9.7) |
| 0.29 | fl2asem |
| 0.34 | Current Schaeffer SP Assessment (WGWIDE 2022) |
| 0.31 | Trenkel & Rochet 2003 |

# 7 Exploratory Assessments

Run numbers are associated with a particular dataset, fit numbers with a model configuration such that the combination of run and fit uniquely identifies an assessment.

## 7.1 Datasets (runs)

| Run | Acronym | Data | Year Range |
|---|---|---|---|
| 1 | ca | Total catch | 1999-2021 |
| | | Acoustic Survey TSB | 2011-2022 |
| 2 | cg | Total catch | 1999-2021 |
| | | IBTS VAST index | 1999-2021 |
| 3 | cag | Total catch | 1999-2021 |
| | | Acoustic Survey TSB | 2011-2022 |
| | | IBTS VAST index | 1999-2021 |

## 7.2 SPiCT Configurations (fits)

A number of exploratory SPiCT assessments were carried out for each of the 3 different datasets (runs) described above. Individual assessments (fits) explored the effects of

1. Increasing the uncertainty in relation to individual data years, specifically
    a. Increased uncertainty for the first 4 years of catch data (1999-2002) when no discarding information is available. For 2003-2005, significant discarding is reported (4-10kt) whereas catches are low (<1000t) as the target fishery has not yet become established and it is likely this situation also applies to 1999-2002.
    b. The PELGAS survey was not conducted in 2020, due to COVID-19 impacts. In 2019 and 2021 TSB estimates were 14kt and 131kt respectively for this survey. It is therefore reasonable to assume that in the intervening year, a total estimate based only on the WESPAS survey results is likely associated with increased uncertainty.
    c. The VAST derived index from the combined groundfish surveys indicates increased uncertainty in years with lower survey coverage. These include the early years of the survey index (1999-2002) when some of the surveys had not started and 2017, when significant survey effort was lost due to vessel breakdown. The effects of increased uncertainty in these years is also investigated.
2. Prior information on initial depletion. The target fishery only became established several years after the start of the available data. While discarding is known to have taken place, it is reasonable to assume that the stock was not heavily exploited prior to 2005 (supported by the population structure observed in the initial years of significant exploitation). Exploratory assessments therefore consider a number of scenarios for the initial biomass depletion (bkfrac). Initial depletion values of 0.2, 0.5 and 0.8 were tested to explore assumptions of heavy, moderate and light exploitation rates at the start of the assessment period (1999).

3. Prior information on production curve shape parameter (n).
4. Prior information on intrinsic growth rate (r).
5. Prior information on survey catchability (q).

Residual analysis (calc.osa.resid) , 5 year retrospective runs (retro) and 30 trials (check.ini) with randomly generated initial parameter values were run for each assessment. Based on the SPiCT checklist the following criteria were considered when evaluating assessment output

1. Convergence
2. Finite variable parameter estimates
3. OSA residual patterns, bias, autocorrelation
4. Mohn's rho for biomass (max 0.2) and fishing mortality (0.15)
5. Magnitude of uncertainty in biomass and fishing mortality (max 1 order of magnitude)
6. Estimated shape of the production curve

Table 7.1 describes details the assessments in terms of input data, uncertainties in data, model priors, output diagnostics and estimates for selected states and parameters. Rows shaded in red correspond to runs that failed to meet the criteria outlined above for an acceptable assessment.

| Run/Fit | Uncertainty (factor/years) | | | Priors | | | | Diagnostics | | | | Parameters/States | | | | | | |
|---|---|---|---|---|---|---|---|---|---|---|---|---|---|---|---|---|---|---|
| | Catch | Aco | GF | bkfrac | log(n) | log(r) | log(q) | OSA | Retro (B/F) | Unc. (B/F) | bmsyk | B/$B_{MSY}$ | F/$F_{MSY}$ | $B_{MSY}$ | $F_{MSY}$ | MSY | K | r |
| 1_1 | | | | | | | | ✓ | ✓/✖ | 1/5 | 0.46 | 2.55 | 0.06 | 461 | 0.47 | 215 | | |
| 1_2 | | | | 0.5,0.5 | | | | ✖ | ✓/✓ | 1/2 | 0.32 | 0.93 | 0.59 | 113 | 0.29 | 33 | | |
| 1_3 | 6 (1999-2002) | | | | | | | ✓ | ✓/✓ | 3/2 | 0.30 | 0.24 | 1.47 | 366 | 0.15 | 54 | | |
| 1_4 | 6 (1999-2002) | | | 0.5,0.5 | | | | ✓ | ✓/✓ | 1/1 | 0.36 | 0.75 | 0.70 | 123 | 0.28 | 35 | | |
| 1_5 | 6 (1999-2002) | 2 (2020) | | 0.5,0.5 | | | | ✓ | ✓/✓ | 1/1 | 0.36 | 0.74 | 0.71 | 123 | 0.24 | 35 | | |
| 1_6 | 6 (1999-2002) | 2 (2020) | | 0.5,0.5 | | | 0.9,0.5 | ✓ | ✓/✓ | 2/3 | 0.40 | 2.28 | 0.13 | 257 | 0.28 | 71 | | |
| 1_7 | 6 (1999-2002) | 2 (2020) | | 0.2,0.5 | | | | ✓ | ✓/✖ | 1/1 | 0.37 | 0.70 | 0.72 | 130 | 0.28 | 36 | | |
| 1_8 | 6 (1999-2002) | 2 (2020) | | 0.2,0.5 | | | 0.9,0.5 | ✓ | ✓/✓ | 1/2 | 0.42 | 2.20 | 0.14 | 276 | 0.27 | 75 | | |
| | | | | | | | | | | | | | | | | | | |
| 2_1 | | | | | | | | ✖ | ✖/✖ | 7/4 | 0.56 | 0.52 | 0.04 | 15,458 | 0.06 | 919 | 27.0 | 0.16 |
| 2_2 | | | | 0.5,0.5 | | | | ✖ | ✖/✖ | 2/5 | 0.68 | 1.72 | 0.09 | 1,997 | 0.11 | 211 | 2Mt | 0.57 |
| 2_3 | 6 (1999-2002) | | | | | | | ✖ | ✖/✖ | 6/3 | 0.56 | 0.62 | 0.05 | 9,757 | 0.06 | 602 | 17.5 | 0.17 |
| 2_4 | 6 (1999-2002) | | | 0.5,0.5 | | | | No Convergence | | | | | | | | | | |
| 2_5 | 6 (1999-2002) | | | 0.2,0.5 | | | | ✓ | ✓/✖ | 1/4 | 0.69 | 1.37 | 0.04 | 3,667 | 0.08 | 299 | 5.3Mt | 0.47 |
| 2_6 | 6 (1999-2002) | | | 0.8,0.5 | | | | ✓ | ✓/✓ | 2/7 | 0.38 | 4.63 | 0.01 | 3,104 | 0.13 | 387 | 8.2Mt | 0.13 |
| 2_7 | 6 (1999-2002) | | 2 (1999-2002,2017) | 0.8,0.5 | | | | ✓ | ✓/✓ | 2/7 | 0.37 | 5.22 | 0.01 | 1,946 | 0.17 | 329 | | |
| 2_8 | 6 (1999-2002) | | 2 (1999-2002,2017) | 0.5,0.5 | | | | ✓ | ✖/✖ | 2/5 | 0.67 | 1.83 | 0.15 | 868 | 0.15 | 130 | 13.9 | 0.74 |
| 2_9 | 6 (1999-2002) | | 2 (1999-2002,2017) | 0.8,0.5 | 2,0.1 | | | ✓ | ✓/✓ | 1/6 | 0.5 | 3.46 | 0.03 | 1,951 | 0.12 | 238 | 3.9Mt | 0.24 |
| 2_10 | 6 (1999-2002) | | 2 (1999-2002,2017) | 0.8,0.5 | 2,0.5 | | | ✓ | ✓/✖ | 1/6 | 0.49 | 3.62 | 0.03 | 1,991 | 0.13 | 248 | 4.1Mt | 0.23 |
| 2_11 | 6 (1999-2002) | | 2 (1999-2002,2017) | 0.8,0.5 | 2,0.5 | 0.31,0 | | ✓ | ✓/✖ | 1/4 | 0.50 | 3.27 | 0.04 | 1,231 | 0.16 | 191 | 2.5Mt | 0.31 |
| 2_12 | 6 (1999-2002) | | 2 (1999-2002,2017) | 0.8,0.5 | 2,0.5 | 0.31,0 | | ✓ | ✓/✖ | 1/5 | 0.48 | 3.78 | 0.03 | 1,170 | 0.18 | 216 | 2.4Mt | 0.34 |
| 2_13 | 6 (1999-2002) | | 2 (1999-2002,2017) | | | | | ✓ | ✓/✓ | 2/5 | 0.36 | 5.53 | 0.01 | 1,681 | 0.20 | 327 | 4.7Mt | 0.18 |

Table 7.1 – Exploratory SPiCT assessments for runs 1 (catch and acoustic survey data) and 2 (catch and groundfish index data)

| Run/Fit | Uncertainty (factor/years) | | | Priors | | | | Diagnostics | | | | Parameters/States | | | | | | |
|---|---|---|---|---|---|---|---|---|---|---|---|---|---|---|---|---|---|---|
| | Catch | Aco | GF | bkfrac | log(n) | log(r) | log(q) | OSA | Retro (B/F) | Unc. (B/F) | bmsyk | B/$B_{MSY}$ | F/$F_{MSY}$ | $B_{MSY}$ (kt) | $F_{MSY}$ | MSY | K | r |
| 3_1 | | | | | | | | ✖ | ✖/✖ | 5/4 | 0.53 | 0.85 | 0.05 | 7,674 | 0.06 | 450 | 14.4 Mt | 0.14 |
| 3_2 | | | | 0.5,0.5 | | | | ✖ | ✓/✖ | 1/4 | 0.64 | 1.75 | 0.04 | 4,478 | 0.08 | 349 | 7.0 Mt | 0.33 |
| 3_3 | | | | 0.8,0.5 | | | | ✖ | ✖/✖ | 2/6 | 0.63 | 3.76 | 0.01 | 4,125 | 0.10 | 416 | 9.7 Mt | 0.14 |
| 3_4 | | | | 0.2,0.5 | | | | ✖ | ✓/✖ | 1/4 | 0.64 | 1.45 | 0.04 | 4,239 | 0.08 | 321 | 6.6 Mt | 0.32 |
| 3_5 | 6 (1999-2002) | | | | | | | ✖ | ✖/✖ | 1/1 | 0.53 | 1.04 | 0.06 | | 0.07 | 285 | 6.6 Mt | |
| 3_6 | 6 (1999-2002) | | | 0.5,0.5 | | | | ✓ | ✓/✖ | 3/3 | 0.62 | 1.85 | 0.04 | | 0.08 | 285 | 5.6 Mt | |
| 3_7 | 6 (1999-2002) | | | 0.8,0.5 | | | | ✓ | ✖/✖ | 1/6 | 0.45 | 3.39 | 0.01 | | 0.09 | 454 | 10.6 Mt | |
| 3_8 | 6 (1999-2002) | | | 0.2,0.5 | | | | ✓ | ✓/✖ | 2/7 | 0.63 | 1.51 | 0.06 | | .08 | 222 | 4.4 Mt | |
| 3_9 | 6 (1999-2002) | | 2 (1999-2002,2017) | 0.8,0.5 | | | | ✓ | ✖/✖ | 1/5 | 0.41 | 4.25 | 0.01 | | 0.12 | 389 | 8.0 Mt | |
| 3_10 | 6 (1999-2002) | | 2 (1999-2002,2017) | 0.5,0.5 | | | | ✓ | ✓/✖ | 2/7 | 0.59 | 2.07 | 0.05 | | 0.10 | 209 | 3.5 Mt | |
| 3_11 | 6 (1999-2002) | | 2 (1999-2002,2017) | 0.8,0.5 | 2,0.1 | | | ✓ | ✓/✖ | 1/6 | 0.50 | 3.23 | 0.02 | | 0.10 | 338 | 6.8 Mt | |
| 3_12 | 6 (1999-2002) | | 2 (1999-2002,2017) | 0.8,0.5 | 2,0.5 | | | ✓ | ✓/✖ | 1/6 | 0.49 | 3.31 | 0.02 | | 0.10 | 343 | 7.0 Mt | |
| 3_13 | 6 (1999-2002) | | 2 (1999-2002,2017) | 0.8,0.5 | 2,0.5 | 0.31,0.5 | | ✓ | ✓/✖ | 1/6 | 0.51 | 3.01 | 0.03 | | 0.13 | 259 | 3.9 Mt | |
| 3_14 | 6 (1999-2002) | | 3 (1999-2002,2017) | 0.8,0.5 | 2,0.5 | 0.31,0.5 | | ✓ | ✓/✖ | 1/6 | 0.51 | 2.95 | 0.03 | | 0.14 | 240 | 3.4 Mt | |
| 3_15 | 6 (1999-2002) | | 2 (1999-2002,2017) | 0.8,0.5 | 2,0.5 | 0.31,0.5 | | ✖ | ✖/✖ | 1/6 | 0.40 | 4.61 | 0.01 | | 0.13 | 359 | 7.1 Mt | |
| 3_16 | 6 (1999-2002) | 2 (2020) | 2 (1999-2002,2017) | 0.8,0.5 | | | 0.1,0.5,0.9,0.5 | ✓ | ✓/✖ | 1/2 | 0.65 | 1.82 | 0.25 | | 0.23 | 65 | 429 kt | |
| 3_17 | 6 (1999-2002) | 2 (2020) | 2 (1999-2002,2017) | 0.8,0.5 | 2,0.1 | | 0.1,0.5,0.9,0.5 | ✓ | ✓/✓ | 1/1 | 0.50 | 2.64 | 0.16 | | 0.24 | 51 | 420 kt | |
| 3_18 | 6 (1999-2002) | 2 (2020) | 2 (1999-2002,2017) | 0.8,0.5 | 2,0.1 | 0.31,0.1 | 0.1,0.5,0.9,0.5 | ✓ | ✓/✓ | 1/1 | 0.50 | 2.70 | .021 | | 0.16 | 39 | 492 kt | |
| 3_19 | 6 (1999-2002) | 2 (2020) | 2 (1999-2002,2017) | 0.8,0.5 | 2,0.5 | 0.31,0.5 | 0.1,0.5,0.9,0.5 | ✓ | ✓/✓ | 1/1 | 0.49 | 2.70 | 0.18 | | 0.20 | 45 | 455 kt | |
| 3_20 | 6 (1999-2002) | 2 (2020) | 2 (1999-2002,2017) | 0.8,0.5 | | 0.31,0.5 | 0.1,0.5,0.9,0.5 | ✓ | ✓/✓ | 1/1 | 0.48 | 2.78 | 0.17 | | 0.21 | 45 | 450 kt | |
| 3_21 | 6 (1999-2002) | 2 (2020) | 2 (1999-2002,2017) | 0.8,0.5 | 2,1 | 0.31,0.5 | 0.1,0.5,0.9,0.5 | ✓ | ✓/✓ | 1/1 | 0.49 | 2.75 | 0.17 | | 0.20 | 45 | 492 kt | 0.38 |
| 3_22 | 6 (1999-2002) | 2 (2020) | 2 (1999-2002,2017) | 0.5,0.5 | 2,1 | 0.31,0.5 | 0.1,0.5,0.9,0.5 | ✓ | ✓/✓ | 1/1 | 0.51 | 2.41 | 0.19 | 253 | 0.19 | 48 | 499 kt | 0.39 |
| 3_23 | 6 (1999-2002) | 2 (2020) | 2 (1999-2002,2017) | 0.5,0.5 | 2,1 | | 0.1,0.5,0.9,0.5 | ✓ | ✓/✓ | 1/1 | 0.61 | 1.89 | 0.21 | 275 | 0.23 | 62 | 447 kt | 0.80 |
| 3_24 | 6 (1999-2002) | 2 (2020) | 2 (1999-2002,2017) | 0.5,0.5 | 2,1 | 0.31,0.5 | 0.1,0.5,0.9,0.5 | ✓ | ✓/✓ | 1/1 | 0.48 | 2.80 | 0.17 | 210 | 0.22 | 46 | 439 kt | 0.39 |

Table 7.1 (cont) Run 3 (catch, acoustic survey and groundfish index) configurations

## 7.3 Results

**Run 1 (catch and acoustic survey dataset)**

The acoustic survey data series does not start until 2011 such that there are several years when only catch data is available, including the period associated with the initial rapid development of the fishery and the highest level of annual catch. In general terms, the survey indicates a rapidly declining stock size between 2011 and 2015, followed by a period of stability and then growth in the most recent period with the current stock about 50% of the previous peak. The input data is shown below

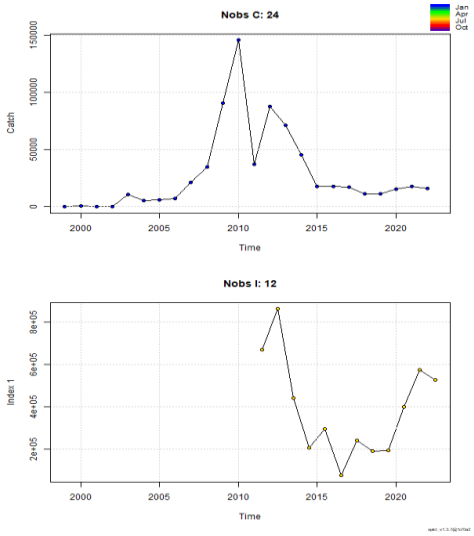


Fig 7.1 – Run 1 input data.

While all fits for this dataset converged and estimated finite parameters values, outputs were very variable and the majority of runs suffered from significant uncertainty in either biomass or fishing mortality. A numerically acceptable solution (fit 5) is obtained when the initial depletion prior is set to 0.5. This reduces the uncertainty in the early years and predicts a stock development in line with the acoustic survey index with an acceptable residual pattern.

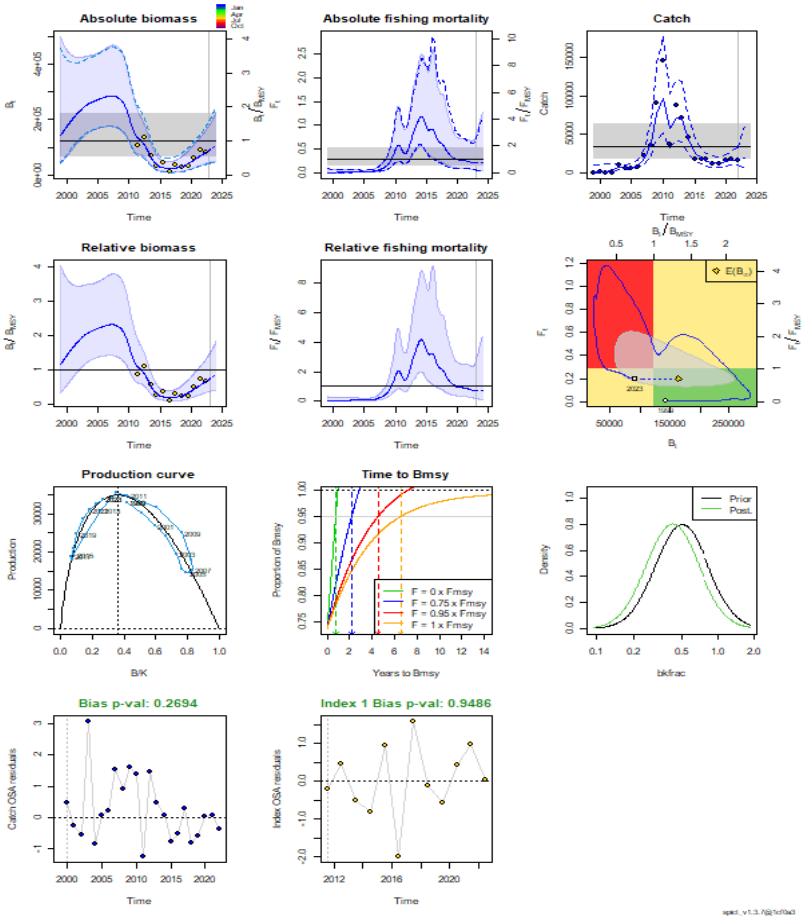


Fig 7.2: Run 1_5 summary output.

Upon examination of the parameter values, this fit is associated with an unreasonable estimate of catchability for the acoustic survey (6.4) such that the assessment considers that the survey estimate is several multiples of the real stock size. Given the extensive spatial coverage of the survey, covering the majority of the stock area, such an estimate of catchability does not seem reasonable.

By supplying a prior estimate of catchability, an alternative solution can be obtained (run 1_8), shown below

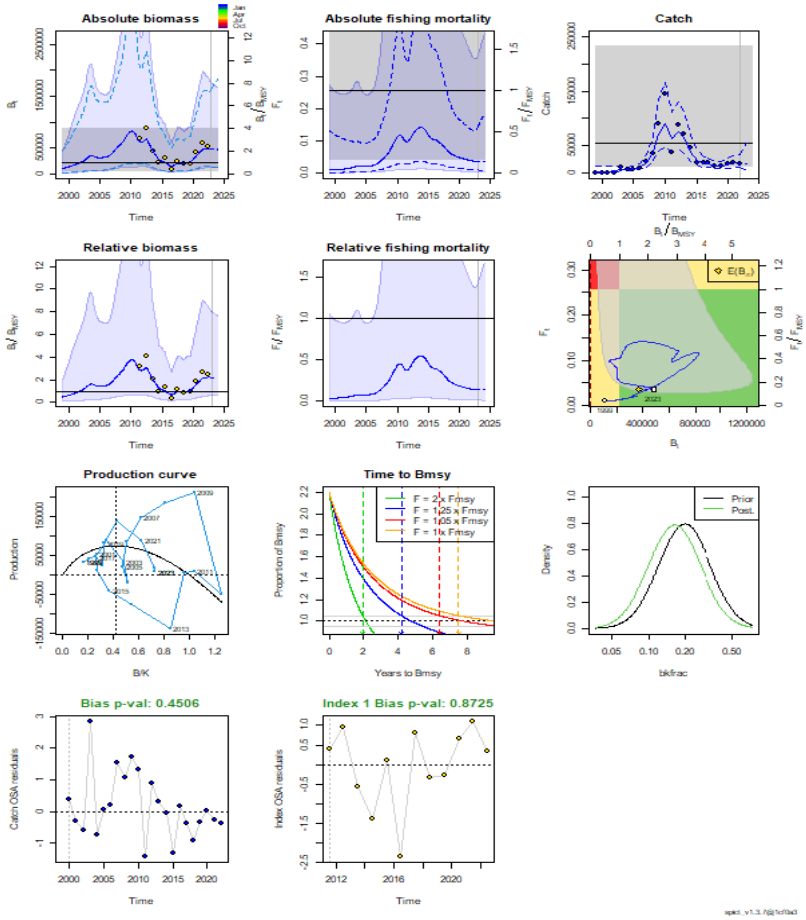


Fig 7.3: Run 1_8 summary output.

Although this run is deemed unacceptable due to uncertainty in fishing mortality, all other criteria for an acceptable assessment are met. It is clearly a very different solution to that without the prior on q in terms of the historic stock trajectory and the terminal stock status with respect to MSY points.

**Run 2 (catch and groundfish survey index dataset)**

In contrast to the acoustic survey data series, the start of the groundfish index coincides with that for catch. However, in contrast to the acoustic data, it does not indicate a period of high stock size around 2011 but rather a stock that has been increasing is size substantially since about 2015. Prior to this the index was relatively stable with short periods of more moderate growth (e.g. 2005-2009) and decline (2001-2005). The run 2 dataset is shown below

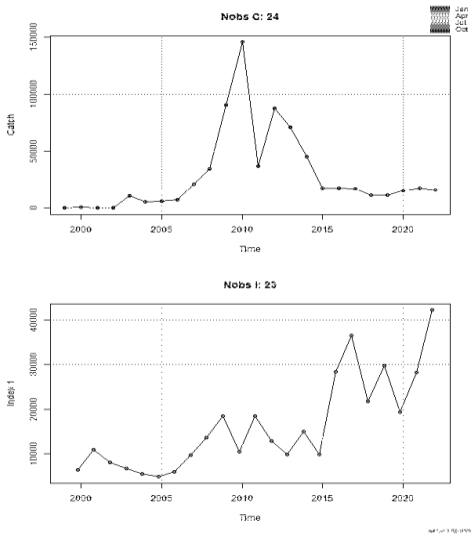


Fig 7.4: Run 2 input data.

All exploratory runs with this dataset were characterised by high levels of uncertainty. Without a prior on initial depletion, the assessment tends to fit a consistently growing stock that is currently well below $B_{MSY}$ with unreasonable estimates of MSY. When a bkfrac prior is supplied, the stock development more closely follows the shorter term signals in the index (rather than simply increasing over time). As with run 1, issues with the catch residuals can be dealt with by assuming increased uncertainty in the initial years. A similar assumption with regard to the index (to deal with years with lower survey coverage) is less impactful on the assessment output.

All assessments based on this dataset suffer from retrospective issues, likely because of the relatively significant changes in this index in the most recent years. The configuration that most closely meets the requirements for an acceptable assessment requires priors on bkfrac (0.8 i.e. lightly exploited), shape parameter n (2 i.e. Schaeffer) and the intrinsic growth rate r (0.31). The output from this assessment is given below:

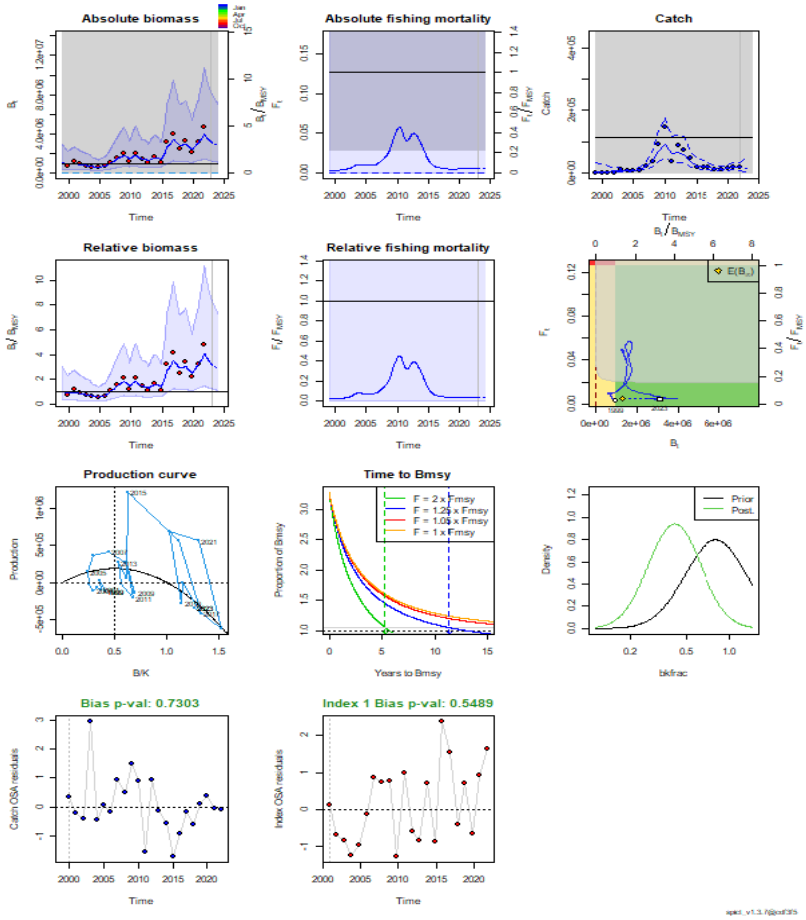


Fig 7.5 Run 2_11 summary output

**Run 3 (catch, acoustic survey and groundfish index dataset)**

Run 3 uses all available data i.e. catch, acoustic survey and the groundfish index.

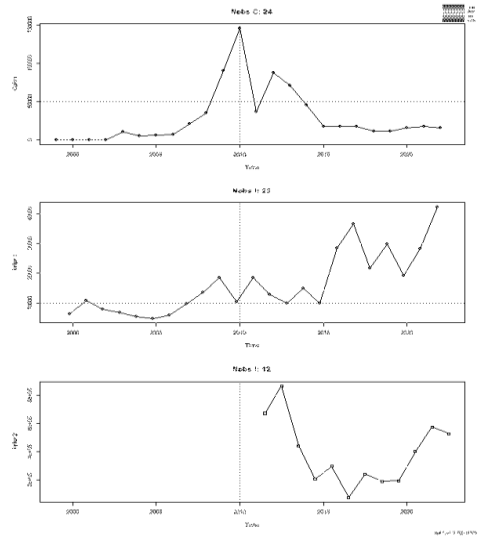


Fig 7.6 Run 3 input data

Immediately obvious from fig 7.6 is the disagreement between the indices during the period 2011-2014 when the acoustic survey points to a declining stock whereas the groundfish index is stable during this period. Both indices agree that the stock size has been increasing in the recent period although the onset of the increase appears earlier according to the groundfish data.

A number of the conclusions from runs 1 and 2 apply with this dataset also. By increasing uncertainty in some years when data is lacking, a number of the residual diagnostics can be improved. A prior on initial depletion is also required, best results are obtained assuming either moderate or low initial depletion. As with run 1, the most impactful prior is that associated with the catchability on the acoustic survey, without which it is not possible to configure an assessment that meets all the criteria for stability and uncertainty. In contrast to run 1 when an unreasonably high q was estimated in the absence of a prior, for run 3, very low values result, indicating that the survey estimates total biomass to be less than 10% of the actual and associated MSY values of 200-400kt result.

Imposing a prior on q (0.9) (along with bkfrac and n) leads to an assessment that passes each of the checklist criteria. Supplying prior information for r also helps, without it, unreasonable values for this parameter can result.

The output from run 3_22 is shown below:

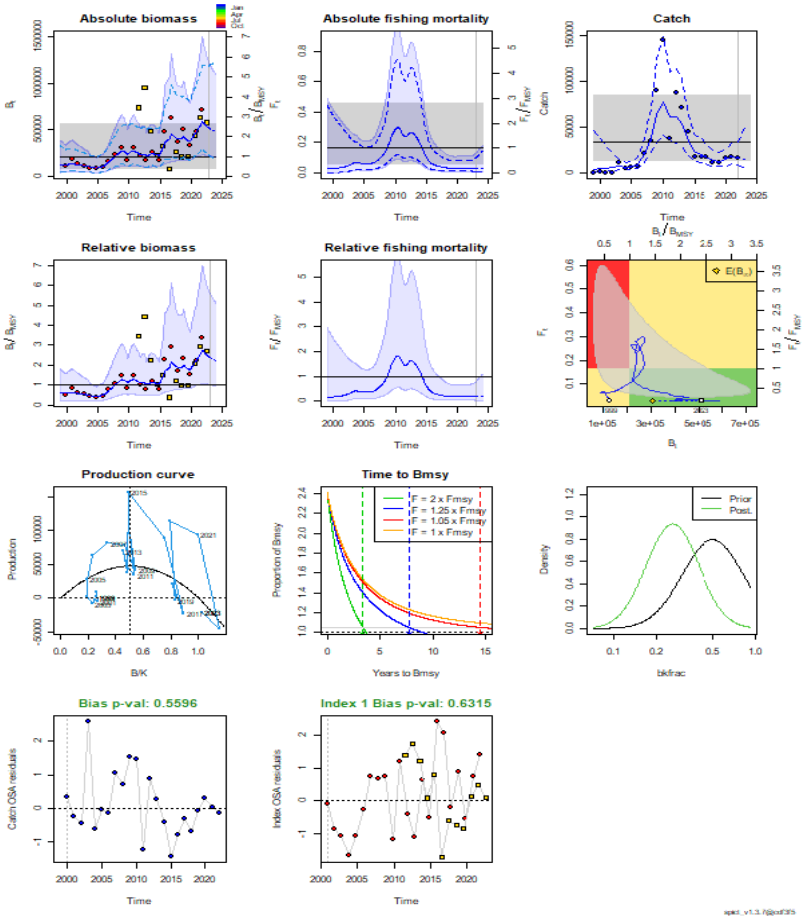


Fig 7.7 Run 3_22 summary output.

A further exploratory run which only considers the acoustic survey data from 2016 onwards was also considered. The survey design was changed at this time and, save for a switch in survey direction in 2017, has remained constant since this time. The results of this run are shown in Fig 7.8.

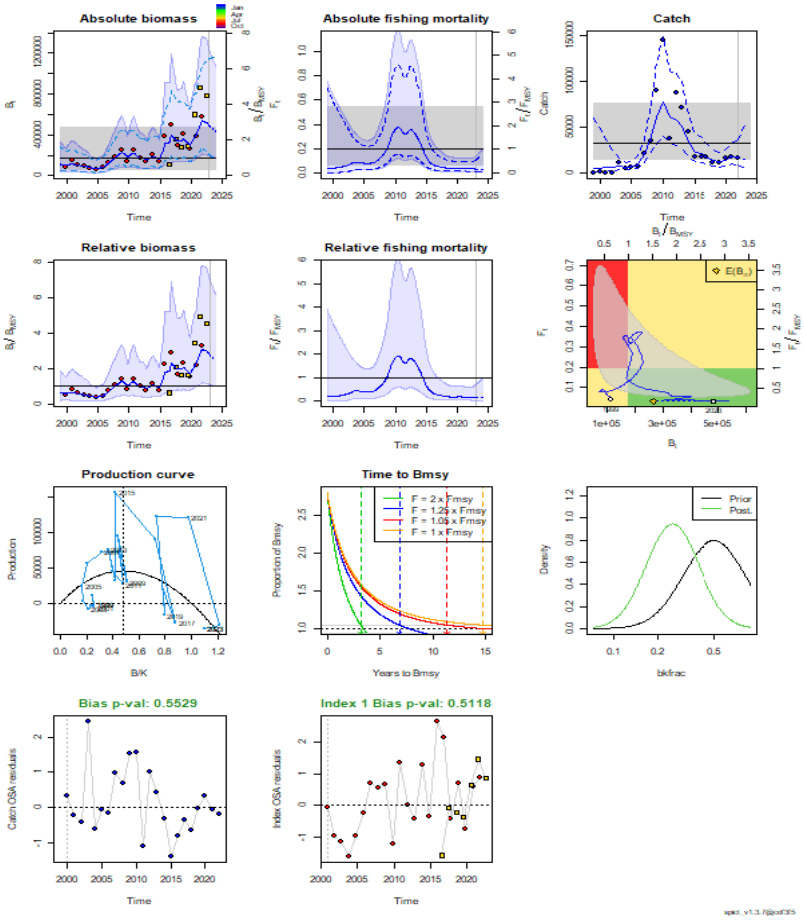


Fig 7.8 Run 3_24 summary

# 8 References

Fässler, S.M.M., O'Donnell, C. & Jech, J.M. (2013). Boarfish (capros aper) target strength modelled from magnetic resonance imaging (MRI) scans of its swimbladder. ICES Journal of Marine Science, **70**, 1451–1459.

ICES. 2012. Report of the Working Group on Widely Distributed Stocks (WGWIDE), 21 - 27 August 2012, Lowestoft, United Kingdom. ICES CM 2012/ACOM:16. 931pp.

ICES. 2022. Working Group on Widely Distributed Stocks (WGWIDE). ICES Scientific Reports. 4:73. 922 pp. http://doi.org/10.17895/ices.pub.21088804

King, M. (1995) Fisheries biology, assessment and management

Meyer, R. & Millar, R.B. 1999. BUGS in Bayesian stock assessments. *Canadian Journal of Fisheries and Aquatic Sciences*, **56**, 1078–1087.

Thorson, J. T. 2020. Predicting recruitment density dependence and intrinsic growth rate for all fishes worldwide using a data-integrated life-history model. Fish and Fisheries, 21: 237–251. John Wiley & Sons, Ltd. https://doi.org/10.1111/faf.12427.

Torrejon-Magallanes J (2020). _sizeMat: Estimate Size at Sexual Maturity_. R package version 1.1.2, <https://CRAN.R-project.org/package=sizeMat>.

Trenkel, V.M. & Rochet, M.J. (2003). Performance of indicators derived from abundance estimates for detecting the impact of fishing on a fish community. Canadian Journal of Fisheries and Aquatic Sciences, 60(1), 67–85.

White, E., Minto, C., Nolan, C. P., King, E., Mullins, E., and Clarke, M. (2011). First estimates of age, growth, and maturity of boarfish (Capros aper): a species newly exploited in the Northeast Atlantic. – ICES Journal of Marine Science, 68: 61–66.

# 4 Striped red mullet in the North Sea, eastern English Channel, Skagerrak, and Kattegat

## mur.27.3a47d – *Mullus surmuletus* in Subarea 4 and divisions 7.d and 3.a

## 4.1 Introduction

Striped red mullet (*Mullus surmuletus*) is a demersal species and is frequent in Northern European waters. Striped red mullet range from Western Africa to southern Scandinavia including the Mediterranean Sea (Heessen, 2015). Young fish are distributed in coastal areas, while adults have an offshore distribution. Benzinou *et al*. (2013) conducted stock identification studies based on otolith and fish shape in European waters. The study showed that striped red mullet can be geographically divided into two units: Western Unit (subareas 6 and 8, and divisions 7.a–c, 7.e–k, and 9.a) and Northern Unit (Subarea 4 (North Sea) and divisions 7.d (Eastern English Channel) and 3.a (Skagerrak, Kattegat)). The English Channel is considered as a mixing zone (7de).

A review of striped red mullet stock definition in the greater North Sea was realized in 2020 (Ellis, 2020). This review does not support the current stock definition used by ICES. IBTS survey from Q1 might indicate that striped red mullet in Division 3.a should be considered as a separate stock from the North Sea one. In addition, survey data and commercial data have highlighted migration pattern between the Western English Channel and the southern North Sea, with striped red mullet concentrating and mixing in the southern North Sea during summer. Thus, assessment of stripped red mullet in Subarea 4 and divisions 7.d–e may need to be assessed as a single stock or a complex one with two subpopulation mixing during summer. However, in absence of new robust scientific study, the stock identity remains unchanged.

In the English Channel, the first sexual maturity was identified on fish of 16.2 cm for the male and 16.7 cm for the female (Mahé *et al*., 2005), 16.2 cm is used for combined sex. Juveniles are found in waters of low salinity, while adults are found at high salinity. Striped red mullet prefers sandy sediments (Carpentier *et al*., 2009).

Adult red mullet feed on small crustaceans, annelid worms and molluscs, using their chin barbels to detect prey and search the mud.

### 4.1.1 Fishery information

Historically, France has taken most of the landings with a targeted fishery for striped red mullet (> 90% of landings at the beginning of the 2000s). This French fishery targeting striped red mullet is conducted by bottom trawlers using a mesh size of 70–99 mm in the eastern English Channel and in the southern North Sea.

The eastern English Channel and southern North Sea areas are also fished by trawlers of various types targeting a variety of species. Striped red mullet might be a bycatch in these fisheries.

From 2000, a Dutch targeted fishery, using fly shooters, and a UK fisheries has also developed. Landings are shared by these three fleets in the latter years. The Netherlands landed about or more than half of the total landings since the 2010s (Figure 4.2.1.1).

There is no EU TAC or MCRS applicable for this stock even if management rules exist at a national level.

### 4.1.2 Current assessment and advice

Striped red mullet in Subarea 4 and divisions 7.d and 3.a is currently assessed biennially as a Category 5 stock. Before 2021, the stock was assessed as a Category 3 stock using biomass trend from a4a using the 1 over 4 rules. However, due to both a decrease of age sampling coverage from 40% in 2014 to 8% in 2021 (Figure 4.1.2.1) and to several issue with CGFS survey index at age calculation (issue in the method and lack of sampling in UK EEZ in 2020), a4a assessment was rejected by WGNSSK and the stock was downgraded into category 5. The last ICES advice was based on average 2004–2020 ICES landings to which was applied an 80% precautionary buffer leading to a catch opportunity of no more than 1950 tonnes.

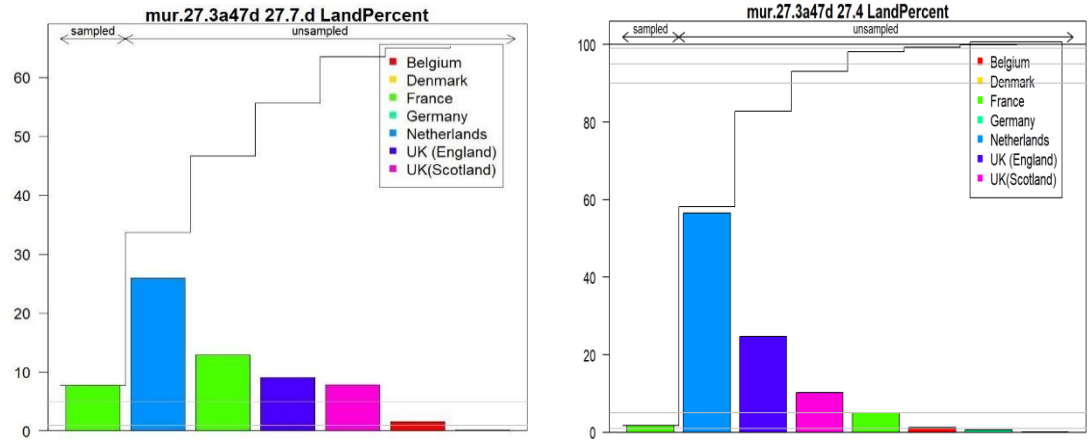


Figure 4.1.2.1. Striped red mullet in Subarea 4 and Division 7.d ICES age sampled and unsampled landings percentage by country in 2021 (percentage over the total area).

## 4.2 Input data for stock assessment

### 4.2.1 Landings and discards

Official landings data are shown by country in Table 4.2.1.1 and by area in Table 4.2.1.2. There is no indication of discard of striped red mullet. All catches are assumed to be landed. ICES estimates over the period 2004–2021 are compared with total official landings in Table 4.2.1.1. In 2021, 70% of the catches were made using demersal seines and 24% using demersal trawls.

Figure 4.2.1.1 shows that IC data and official landings are consistent over years and countries except in 2008. Official landings have increased from 1975 to 2004 to reach a maximum of 4561 tonnes, then decreased up until 2009 with a minimum of 364 tonnes. Since then landings are following recruitment event with two peaks in 2015 and 2019.

Age samples for French landings mostly in Division 7.d are available from InterCatch from 2004–2021. When possible landings age distribution were raised by quarter and if not by semester, however there is not enough information to raise data by métier. Figure 4.2.1.2 shows that most of the landings are coming from age 1 individuals.

**Table 4.2.1.1. Striped red mullet in Subarea 4 and divisions 7.d and 3.a: Official landings by country and ICES estimates of total landings (tonnes).**

| Year | Belgium | Denmark | France | Germany | NL | UK | Total | ICES estimates |
|---|---|---|---|---|---|---|---|---|
| 1975 | 0 | 0 | 140 | 0 | 0 | 0 | 140 | |
| 1976 | 0 | 0 | 156 | 0 | 3 | 1 | 160 | |
| 1977 | 0 | 0 | 279 | 0 | 12 | 1 | 292 | |
| 1978 | 0 | 0 | 207 | 0 | 25 | 3 | 235 | |
| 1979 | 0 | 0 | 212 | 0 | 32 | 11 | 255 | |
| 1980 | 0 | 0 | 86 | 0 | 25 | 4 | 115 | |
| 1981 | 0 | 0 | 44 | 0 | 19 | 1 | 64 | |
| 1982 | 0 | 2 | 32 | 0 | 18 | 2 | 54 | |
| 1983 | 0 | 0 | 232 | 0 | 15 | 1 | 248 | |
| 1984 | 0 | 0 | 204 | 0 | 0 | 3 | 207 | |
| 1985 | 0 | 1 | 135 | 0 | 0 | 4 | 140 | |
| 1986 | 0 | 1 | 84 | 0 | 0 | 3 | 88 | |
| 1987 | 0 | 2 | 40 | 0 | 0 | 3 | 45 | |
| 1988 | 0 | 1 | 35 | 0 | 0 | 4 | 40 | |
| 1989 | 0 | 0 | 37 | 0 | 0 | 5 | 42 | |
| 1990 | 0 | 0 | 524 | 0 | 0 | 13 | 537 | |
| 1991 | 0 | 0 | 208 | 0 | 0 | 11 | 219 | |
| 1992 | 0 | 0 | 431 | 0 | 0 | 14 | 445 | |
| 1993 | 0 | 0 | 516 | 0 | 0 | 18 | 534 | |
| 1994 | 0 | 0 | 308 | 0 | 0 | 14 | 322 | |
| 1995 | 0 | 0 | 2016 | 0 | 0 | 63 | 2079 | |
| 1996 | 0 | 1 | 1785 | 0 | 1 | 36 | 1823 | |
| 1997 | 0 | 1 | 731 | 0 | 0 | 48 | 780 | |
| 1998 | 0 | 1 | 2598 | 0 | 0 | 97 | 2696 | |
| 19991) | 0 | 2 | | 0 | 0 | 70 | 72 | |
| 2000 | 0 | 2 | 2590 | 13 | 235 | 93 | 2933 | |
| 2001 | 0 | 5 | 1417 | 10 | 533 | 142 | 2107 | |
| 2002 | 0 | 12 | 1346 | 9 | 326 | 82 | 1775 | |
| 2003 | 17 | 0 | 2750 | 15 | 396 | 115 | 3293 | |
| 2004 | 22 | 0 | 3618 | 26 | 804 | 91 | 4561 | 4674 |
| 2005 | 19 | 0 | 1595 | 26 | 600 | 81 | 2321 | 2350 |
| 2006 | 12 | 0 | 1030 | 17 | 293 | 69 | 1421 | 1476 |
| 2007 | 14 | 0 | 3475 | 4 | 906 | 161 | 4560 | 4604 |
| 2008 | 16 | 0 | 3249 | 18 | 873 | 313 | 4469 | 2064 |
| 2009 | 13 | 0 | 736 | 11 | 562 | 260 | 1582 | 1513 |
| 2010 | 62 | 0 | 879 | 5 | 567 | 310 | 1823 | 1919 |
| 2011 | 83 | 0 | 649 | 0 | 540 | 238 | 1510 | 1511 |
| 2012 | 38 | 0 | 155 | 0 | 367 | 138 | 698 | 726 |
| 2013 | 33 | 0 | 112 | 0 | 180 | 39 | 364 | 408 |
| 2014 | 71 | 0 | 726 | 0 | 700 | 242 | 1739 | 1718 |
| 2015 | 211 | 0 | 1615 | 0 | 2038 | 663 | 4527 | 4487 |
| 2016 | 151 | 0 | 556 | 0 | 1421 | 486 | 2614 | 2579 |
| 2017 | 93 | 0 | 784 | 0 | 978 | 349 | 2204 | 2195 |
| 2018 | 77 | 0 | 593 | 0 | 826 | 156 | 1652 | 1640 |

| Year | Belgium | Denmark | France | Germany | NL | UK | Total | ICES estimates |
|---|---|---|---|---|---|---|---|---|
| 2019 | 232 | 0 | 1408 | 0 | 1867 | 589 | 4096 | 4048 |
| 2020 | 222 | 0.202 | 723 | 0 | 1752 | 787 | 3484 | 3503 |
| 2021 | 437 | 0.606 | 593 | 0 | 1188 | 757 | 2976 | 2611 |

**No data reported by France in 1999.**

**Table 4.2.1.2. Striped red mullet in Subarea 4 and divisions 7.d and 3.a: Official landings by area (tonnes). Note: Most of the Subarea 4 catches are made in Division 4.c.**

| Year | 4 | 3.a | 7.d | Total [2)] |
|---|---|---|---|---|
| 1975 | 0 | 0 | 140 | 140 |
| 1976 | 4 | 0 | 156 | 160 |
| 1977 | 19 | 0 | 273 | 292 |
| 1978 | 30 | 0 | 205 | 235 |
| 1979 | 49 | 0 | 206 | 255 |
| 1980 | 29 | 0 | 86 | 115 |
| 1981 | 20 | 0 | 44 | 64 |
| 1982 | 19 | 0 | 33 | 52 |
| 1983 | 41 | 0 | 207 | 248 |
| 1984 | 22 | 0 | 185 | 207 |
| 1985 | 9 | 0 | 130 | 139 |
| 1986 | 5 | 0 | 82 | 87 |
| 1987 | 6 | 0 | 38 | 44 |
| 1988 | 7 | 0 | 33 | 40 |
| 1989 | 5 | 0 | 37 | 42 |
| 1990 | 33 | 0 | 504 | 537 |
| 1991 | 26 | 0 | 193 | 219 |
| 1992 | 30 | 0 | 415 | 445 |
| 1993 | 63 | 0 | 471 | 534 |
| 1994 | 58 | 0 | 264 | 322 |
| 1995 | 527 | 0 | 1552 | 2079 |
| 1996 | 264 | 0 | 1559 | 1823 |
| 1997 | 139 | 0 | 641 | 780 |
| 1998 | 389 | 0 | 2307 | 2696 |
| 1999[1)] | 35 | 0 | 37 | 72 |
| 2000 | 895 | 0 | 2038 | 2933 |
| 2001 | 810 | 0 | 1297 | 2107 |
| 2002 | 626 | 0 | 1149 | 1775 |
| 2003 | 824 | 0 | 2469 | 3293 |
| 2004 | 936 | 0 | 3625 | 4561 |
| 2005 | 728 | 0 | 1593 | 2321 |
| 2006 | 321 | 0 | 1083 | 1404 |
| 2007 | 773 | 0 | 3782 | 4555 |
| 2008 | 915 | 0 | 3536 | 4451 |

| Year | 4 | 3.a | 7.d | Total [2)] |
|---|---|---|---|---|
| 2009 | 455 | 0 | 1115 | 1570 |
| 2010 | 350 | 0 | 1468 | 1818 |
| 2011 | 305 | 0 | 1206 | 1511 |
| 2012 | 193 | 0 | 505 | 698 |
| 2013 | 98 | 0 | 266 | 364 |
| 2014 | 263 | 0 | 1476 | 1739 |
| 2015 | 800 | 0 | 3727 | 4527 |
| 2016 | 825 | 0.03 | 1789 | 2614 |
| 2017 | 652 | 0 | 1552 | 2204 |
| 2018 | 385 | 0.002 | 1267 | 1652 |
| 2019 | 1308 | 0.006 | 2788 | 4096 |
| 2020 | 1379 | 0.24 | 2103 | 3482 |
| 2021 | 1231 | 0.065 | 1745 | 2976 |

**1) No data reported by France in 1999.**

**2) Differ from Table 4.2.1.1 and Table 4.2.1.2 due to rounding.**

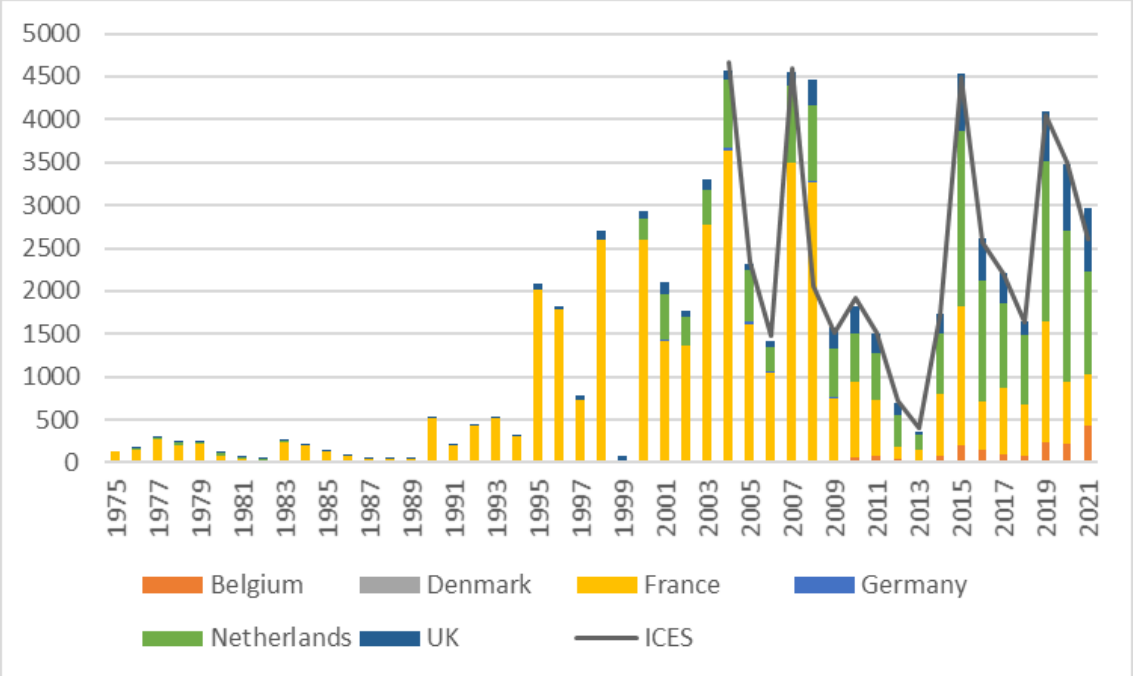


**Figure 4.2.1.1. Striped red mullet in Subarea 4 and divisions 7.d and 3.a ICES estimated landings (grey line) and official catch statistics by country.**

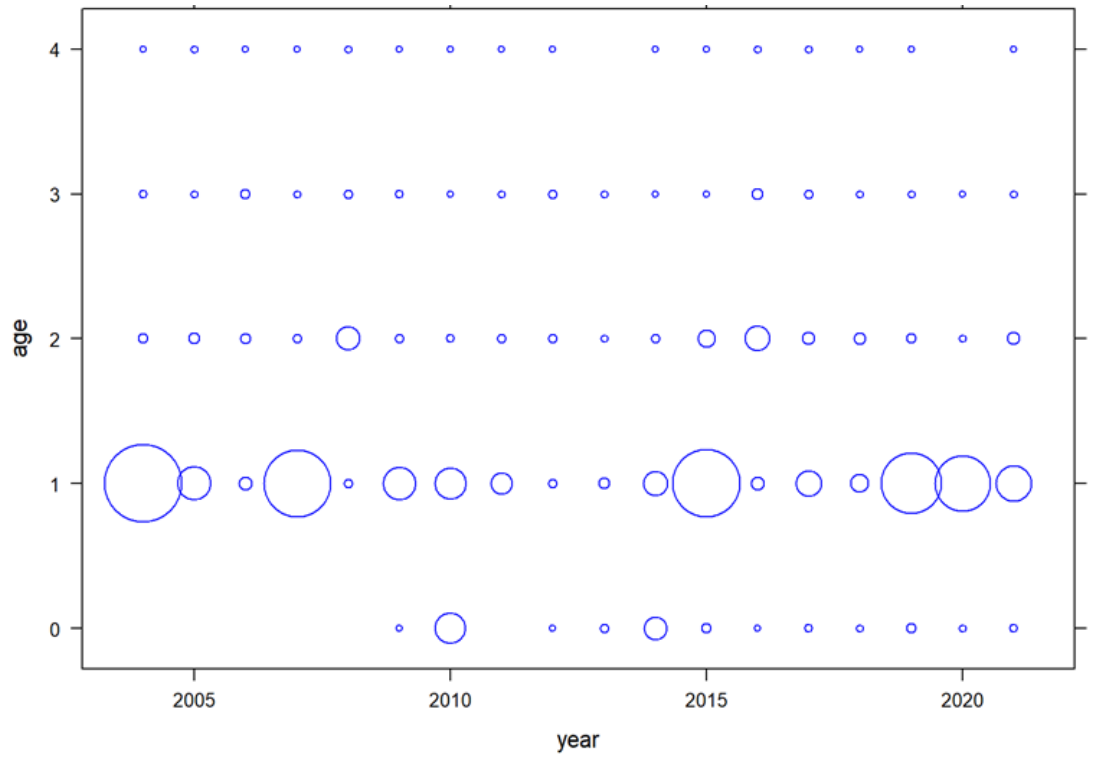


**Figure 4.2.1.2. Striped red mullet age structure (in numbers) as provided in the ICES estimated landings.**

## 4.2.2 Length frequency data

Length frequency data from commercial sampling are available from 2014–2016 and 2018–2021 (Figure 4.2.2.1). Most of the samples are coming from French commercial data with some information also provided by Netherland and the UK. In addition, sampling mainly occurred in 7.d Subdivision with only few samples in Area 4. 97.5% of the landings are composed of individuals larger than 12 cm.

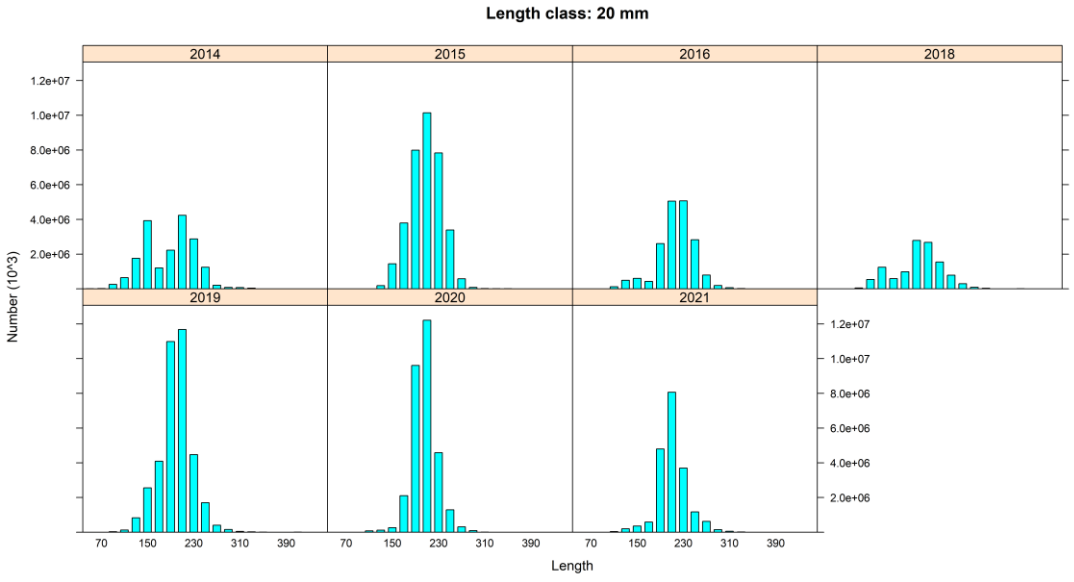


**Figure 4.2.2.1. Striped red mullet in Subarea 7.d and 4 length frequency of commercial landings by 20 mm length class from 2014–2021.**

## 4.2.3 Biomass index

### 4.2.3.1 Available data and stripped red mullet distribution

No commercial CPUE is available for stripped red mullet in Subarea 4 and divisions 3.a and 7.d. The fishery has changed from a bottom trawler to fly shooters dominated fleets in recent. Due the difficulty of assessing fly shooters fishing effort, no commercial index was developed.

However several surveys data that covered the stock area are available from DATRAS surveys, three bottom-trawl surveys NS-IBTS Q1&3 and CGFS Q4 as well as the beam trawl survey BTS Q3. NS-IBTS Q1 data are available from 1978 to 2022 with stripped red mullet started occurring from 1990. The species in Q1 is mainly distributed along the UK coast and the Southern part of the stock area (Figure 4.2.3.1). In quarter 3, two survey are available, NS-IBTS from 1991-onwards and BTS from 1985-onwards. During that quarter, stripped red mullet is mainly distributed in the Southern part of the North Sea and the Eastern English Channel (Figure 4.2.3.2 and Figure 4.2.3.3). Finally, CGFS Q4 is available from 1988-onwards in Division 7.d, in that Division stripped red mullet are mainly distributed along the coast in the Strait of Dover and the Bay of Seine in the South (Figure 4.2.3.4).

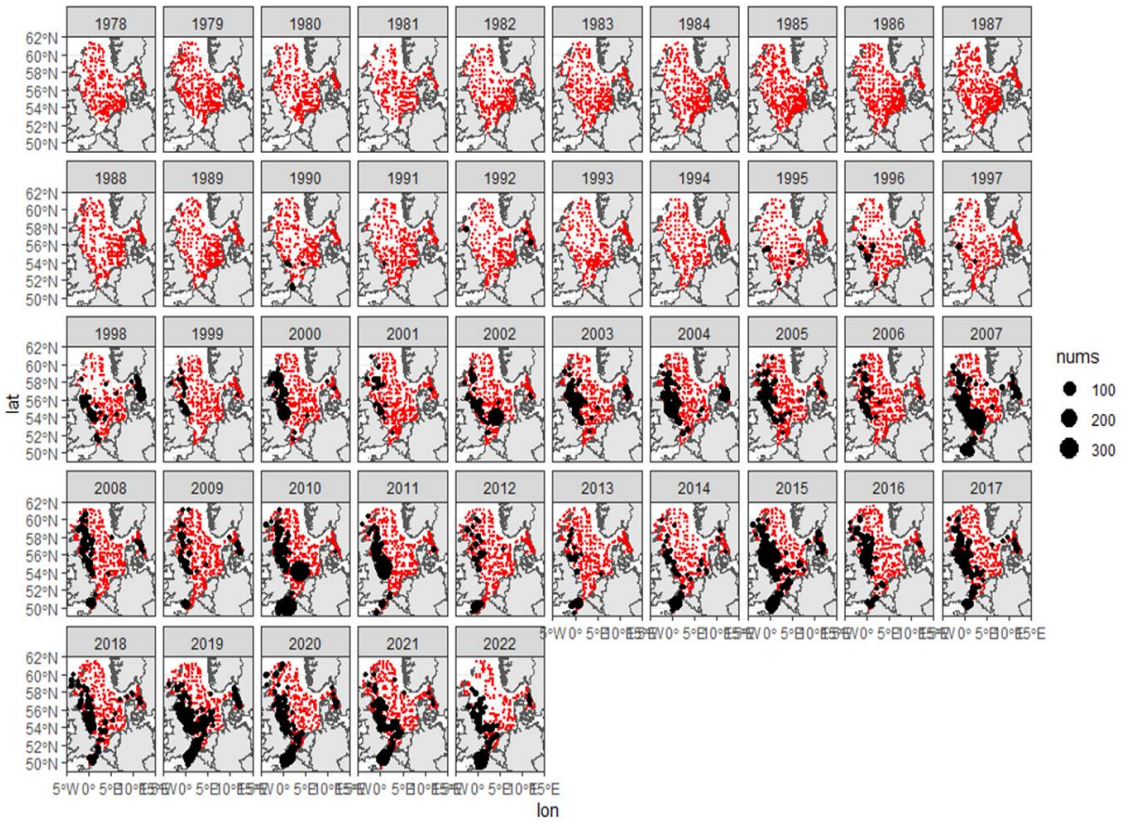


**Figure 4.2.3.1. Striped red mullet in Subarea 4 and divisions 7.d and 3.a abundance distribution in IBTS quarter 1 (in red are shown survey stations with no catch).**


**Figure 4.2.3.2. Striped red mullet in Subarea 4 and divisions 7.d and 3.a abundance distribution during IBTS quarter 3 (in red are shown survey stations with no catch).**

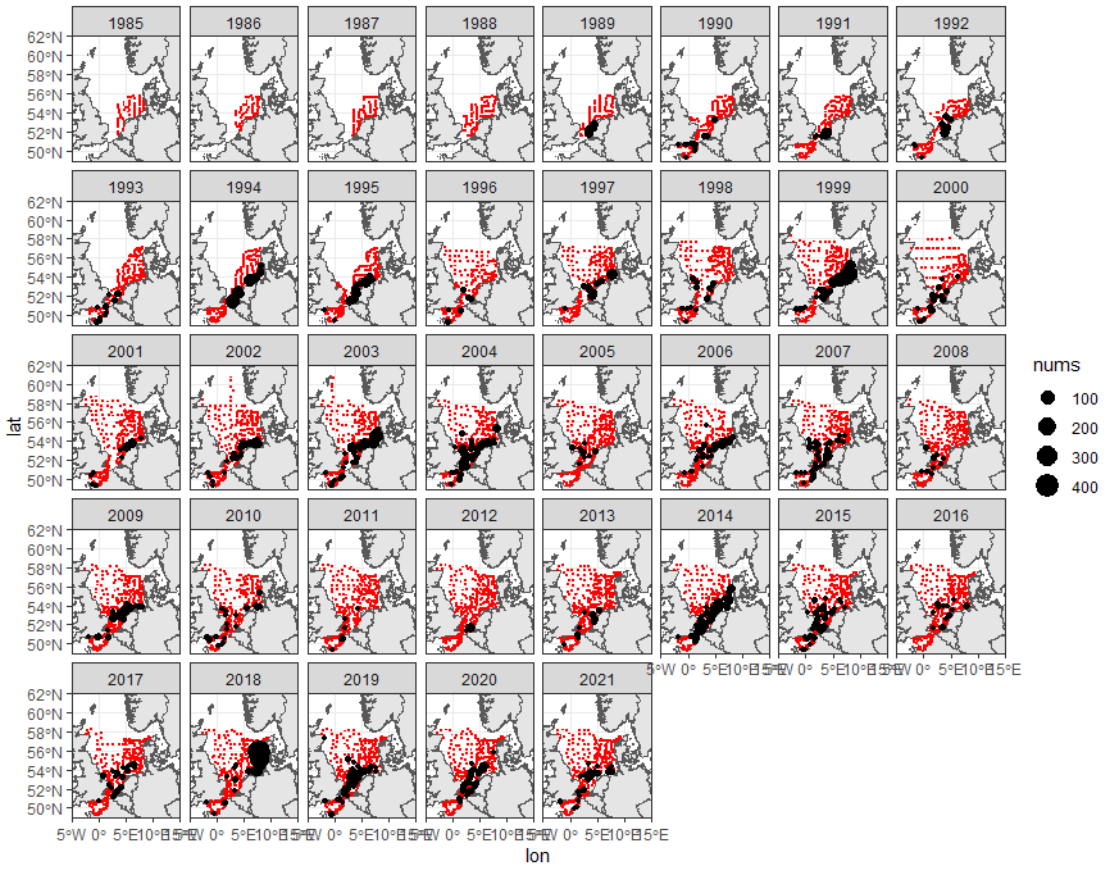


**Figure 4.2.3.3. Striped red mullet in Subarea 4 and divisions 7.d and 3.a abundance distribution during BTS quarter 3 (in red are shown survey stations with no catch).**

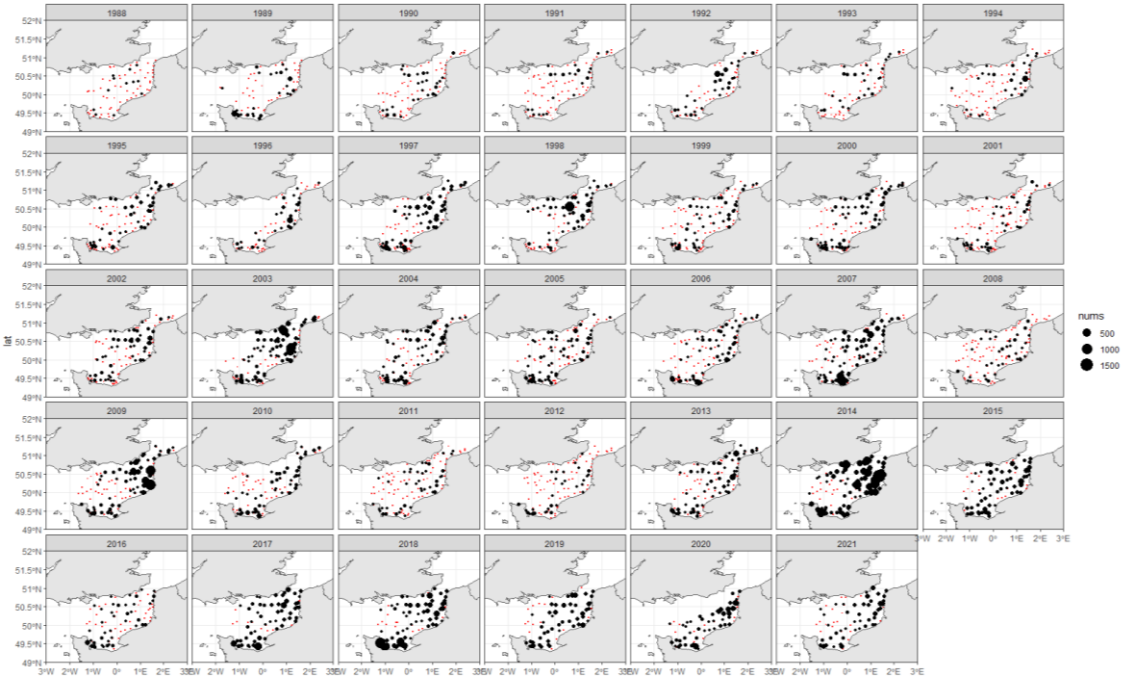


**Figure 4.2.3.4. Striped red mullet in Division 7.d abundance distribution during CGFS quarter 4 (in red are shown survey stations with no catch).**

### 4.2.3.2 Survey data selection

To estimate an exploitable biomass index for SPiCT only individuals above 12 cm were considered in the survey data, as only 2.5% of commercial landings are below 13 cm (see Section 4.2.2).

As before 1990 there is no catch of stripped red mullet in IBTS Q1, only data from 1990-onwards were used. To reduce the number of survey it was decided during the data compilation workshop to combined surveys from Q3 and 4. Only years with the three surveys, from 1991-onwards were kept in the analysis. Only few individuals are catch in the Northwest part of the North Sea during Q3 survey and all the data from that area were removed to ease the survey data standardization (Figure 4.2.3.5). Finally, in 2014 CGFS survey had to change vessel and the sampling design was updated to accommodate for the new vessel. As consequences, the Seine estuary was no longer covered by the survey, so we removed the ICES rectangle 27E8 from the dataset (Figure 4.2.3.6).

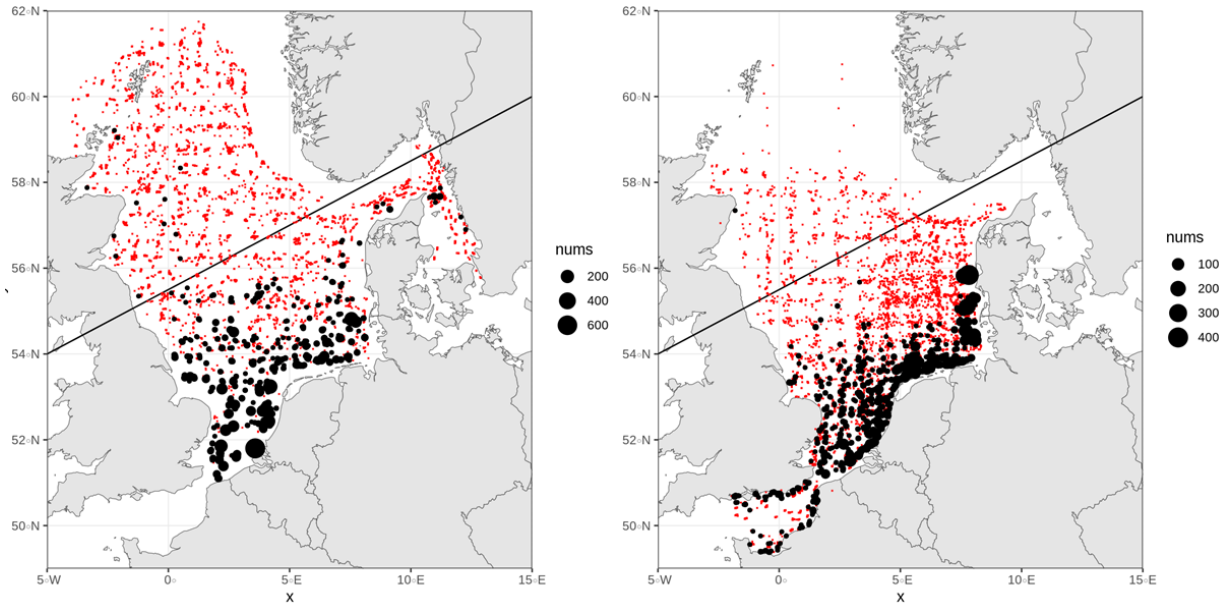


**Figure 4.2.3.5. Striped red mullet IBTS Q3 (on the left) and BTS Q3 (on the right) abundance from 1991–2021 (in red are shown survey stations with no catch). Data above the black line were removed from the dataset.**

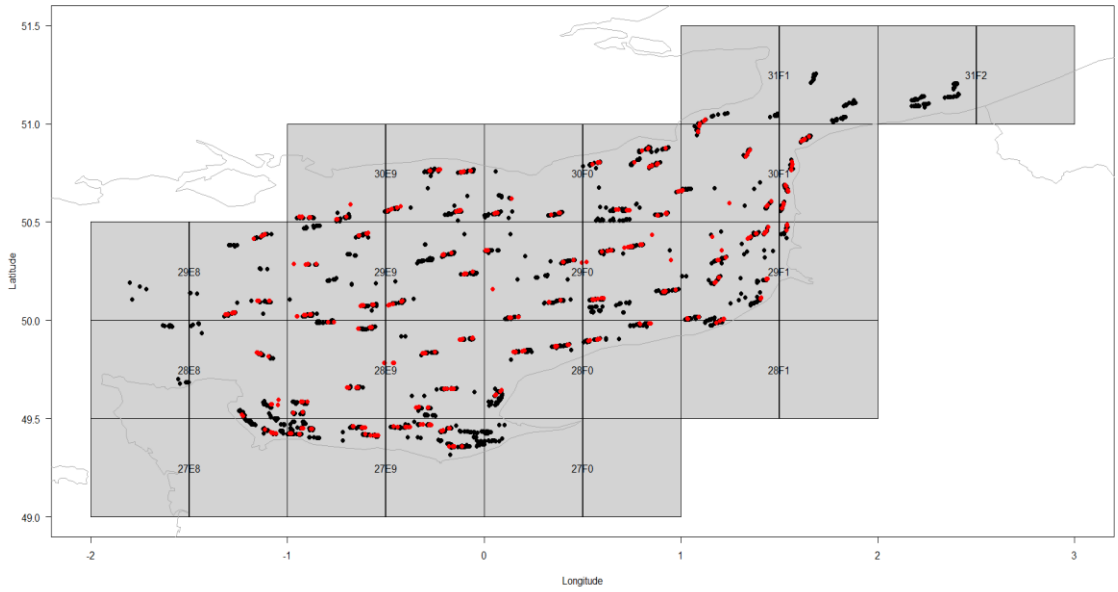


**Figure 4.2.3.6. CGFS station from 1991–2021, in black before 2014 sampled with the Gwen Drez vessel and in red from 2014-onwards sampled with using the Thalassa vessel.**

### 4.2.3.3 Biomass index standardization

To standardized biomass index collected from different vessels, gear and also quarters, two different model distributions, tweedie and delta-lognormal, were tested using general additive mixed models (GAMM). The analysis was performed separately on Q1 survey and Q3–4 survey data using surveyIndex R package (Berg *et al.*, 2014). For both seasons, several model configurations were investigated to include a fixed spatial effect (two-dimensional splines), country/vessel random effect, a time of a year and time of the day effect (two 1D splines), a depth effect (1D spline), a time varying spatial effect (three-dimensional spline) and the logarithm of the swept-

area as an offset. For the Q3–4 season, an extra gear effect was included to account for change in catchability between beam trawl and bottom trawl. The standardized biomass index was derived from the year effect included in each model configurations. The full model is described as follow:

$$g(\mu i) = Yeari + Geari + U(Country/Shipi) + f_1(loni,lati) + f_2(depthi) + f_3(Time\ of\ Yeari) + f_3(Time\ of\ dayi) + f5(loni,lati,Yeari) + offset(log(Swept\_areai))$$

where for each haul *i*,

$\mu i$ is the expected response (1/0 for the binomial model in the delta lognormal distribution or biomass for the Tweedie distribution and positive part of the delta lognormal model)

Yeari a categorical year effect

Geari a categorical gear effect (only used for Q3–4 surveys)

U is a random Country-Ship effect

$f_1$ is a 2-D thin plate regression spline ("ts") on the latitude/longitude coordinates

$f_2$ is a 1-D thin plate spline ("ts") for the bottom depth effect

$f_3$ and $f_3$ are cubic regression spline ("cc") for the Time of Year and Time of day

$f5$ is a tensor product interaction between a two-dimensional thin plate regression spline on the latitude/longitude coordinates and a cubic regression spline ("cs") on the year

$g$ is the link function (logit or log transformed response depending on the distribution)

$log(Swept\_areai)$ is an offset to standardize the response by the swept-area.

Based on AIC, the full model was selected for both season (Q1 and Q3–4 combined).

#### 4.2.3.3.1 IBTS Q1 model diagnostics and prediction

For both model distribution, residuals are not temporally autocorrelated and an over dispersion of the residuals is observed on the residuals QQplot for the model using the Tweedie distribution (Figure 4.2.3.7). 72.5% of the deviance is explained by the Tweedie GAMM model while for the delta-lognormal GAMM, 46.6% are explained by the occurrence model and 34.2% only for the lognormal model. Biomass index prediction CV are higher in the Tweedie model in general, especially at the beginning of the time-series were some year don't have any catches of Stripped red mullet above 12 cm. An increasing trend is observed but not with a lot of contrast for both model distribution (Figure 4.2.3.8). Finally, the retrospective analysis is shown in Figure 4.2.3.9. Both model distribution have a low value of MohnRho with 0.057 for the delta-lognormal model and 0.003 for the Tweedie model.

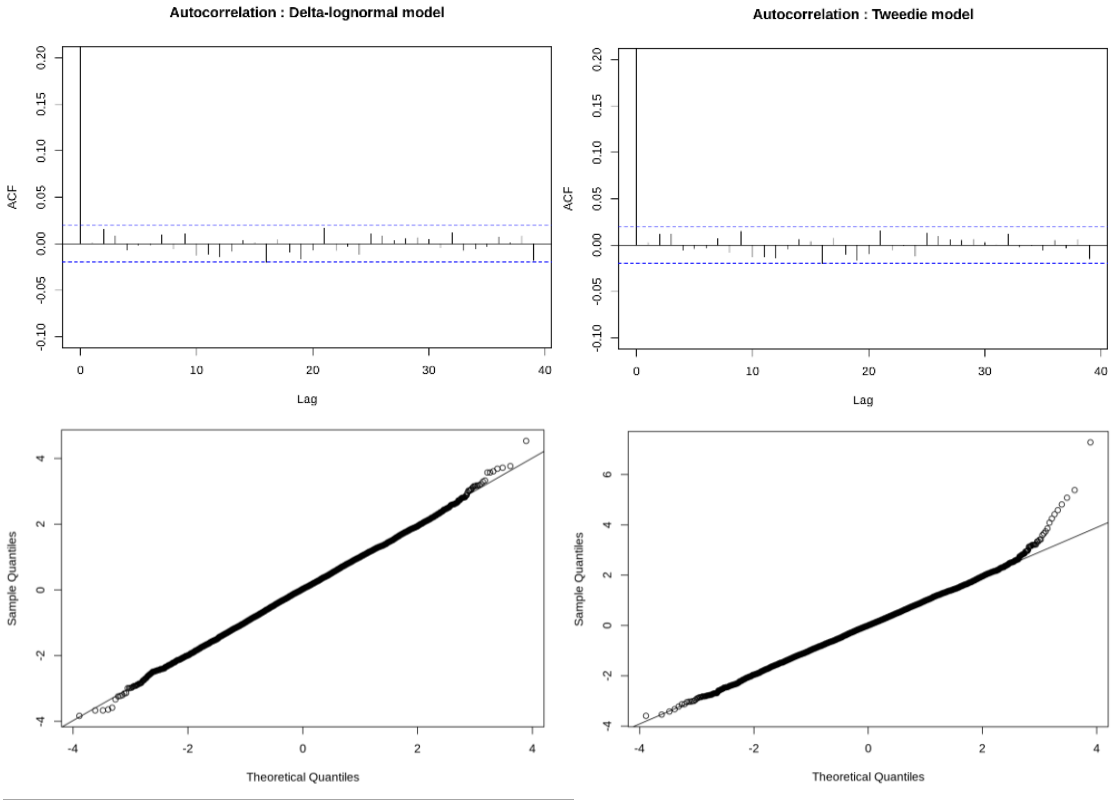


**Figure 4.2.3.7. IBTS Q1 GAMM residuals temporal autocorrelation on the top and QQ plot on the bottom for the Delta-lognormal model on the left and the Tweedie model on the right.**

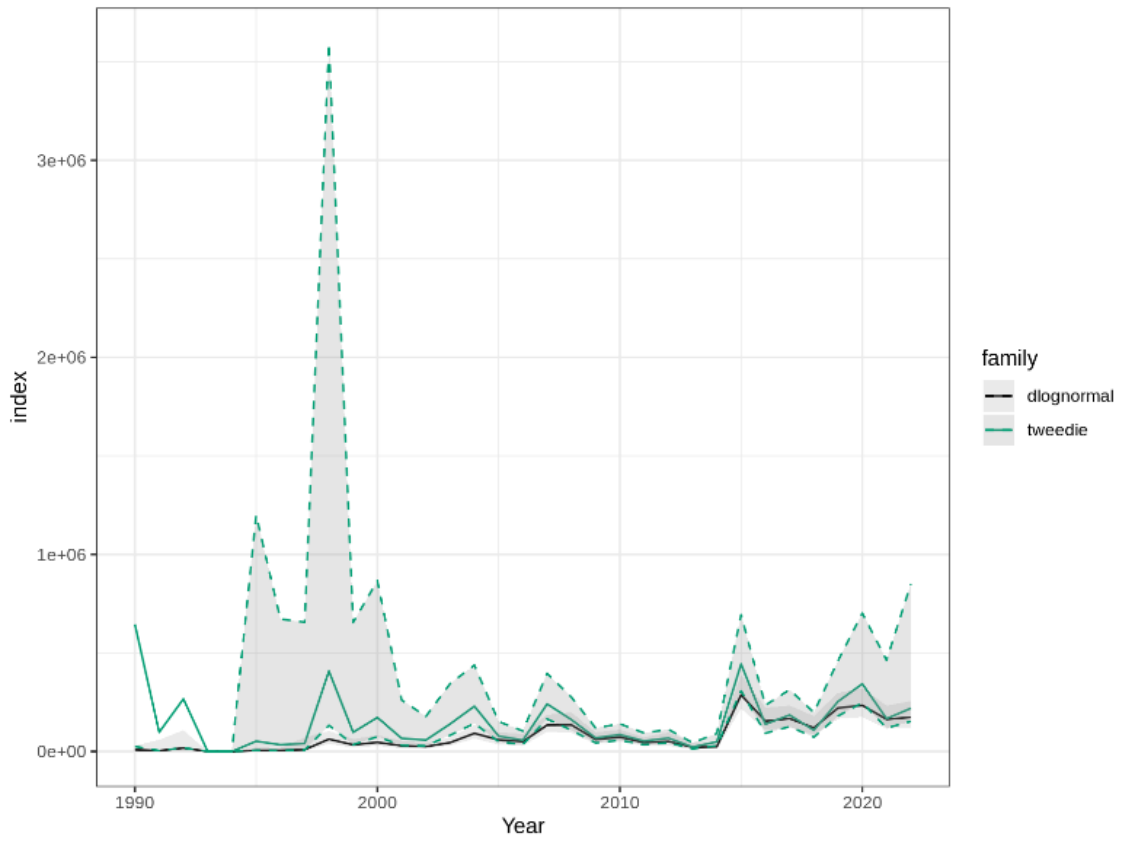


**Figure 4.2.3.8. IBTS Q1 GAMM Exploitable biomass index prediction for the delta-lognormal model in black and the Tweedie model in green.**

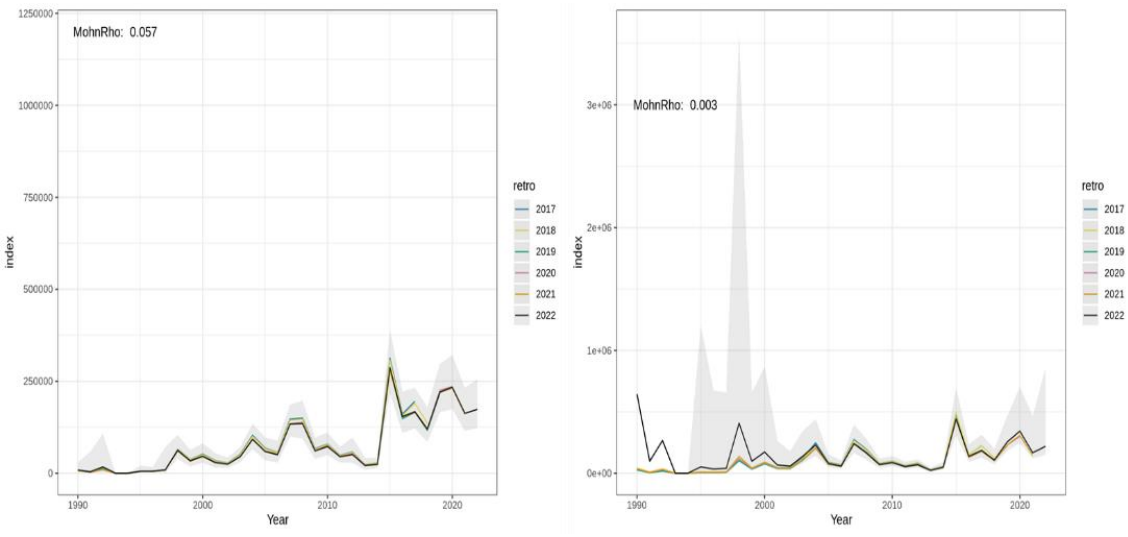


**Figure 4.2.3.9. IBTS Q1 GAMM retrospective analysis for the delta-lognormal model on the left and the Tweedie model on the right.**

#### 4.2.3.3.2 Q3–4 surveys model diagnostics and prediction

For both model distribution, residuals are not temporally autocorrelated and an over dispersion of the residuals is observed on the residuals QQplot for the model using the Tweedie distribution (Figure 4.2.3.10). 68% of the deviance is explained by the Tweedie GAMM model while for the delta-lognormal GAMM, 42% are explained by the occurrence model and 34% only for the lognormal model. Biomass index prediction CV are higher in the delta-lognormal model. Biomass trend are comparable between both model, with an increasing trend at the beginning of the time-series up until 2007, then the biomass collapse to reach a minimum in 2013. In recent years, the biomass index fluctuate following the different recruitment events (2014 and 2018 cohorts; Figure 4.2.3.11).

Finally, the retrospective analysis is shown in Figure 4.2.3.12. Both model distribution have a low value of MohnRho with 0.063 for the delta-lognormal model and –0.017 for the Tweedie model.

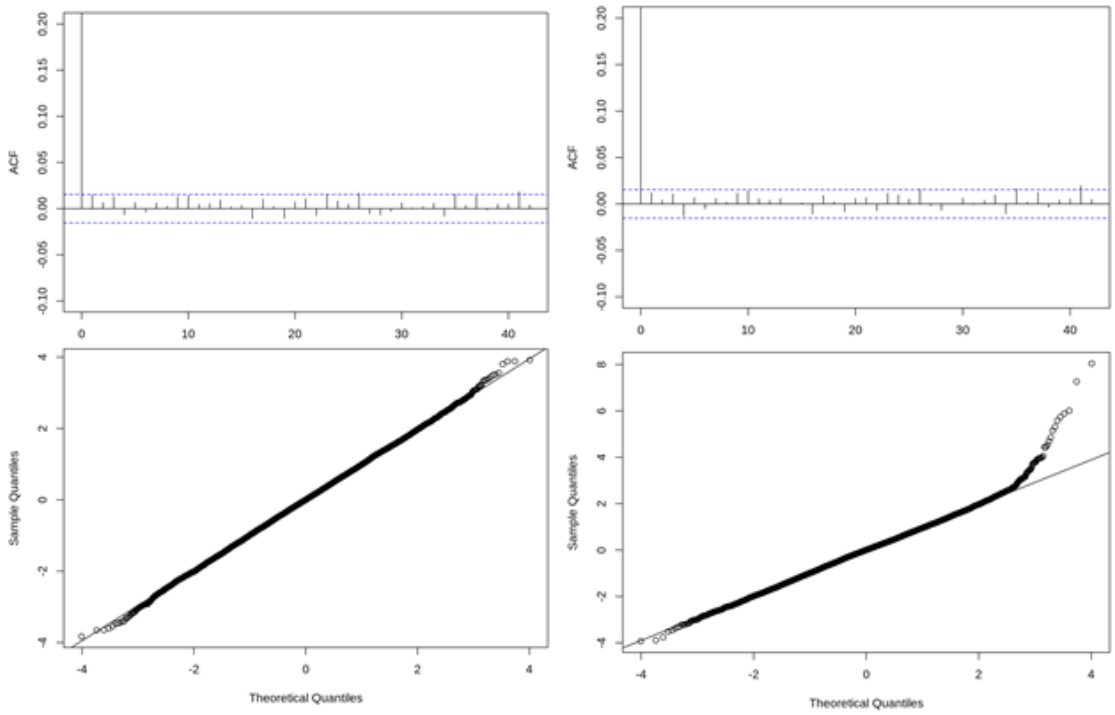


**Figure 4.2.3.10. Q3–4 surveys GAMM residuals temporal autocorrelation on the top and QQ plot on the bottom for the Delta-lognormal model on the left and the Tweedie model on the right.**

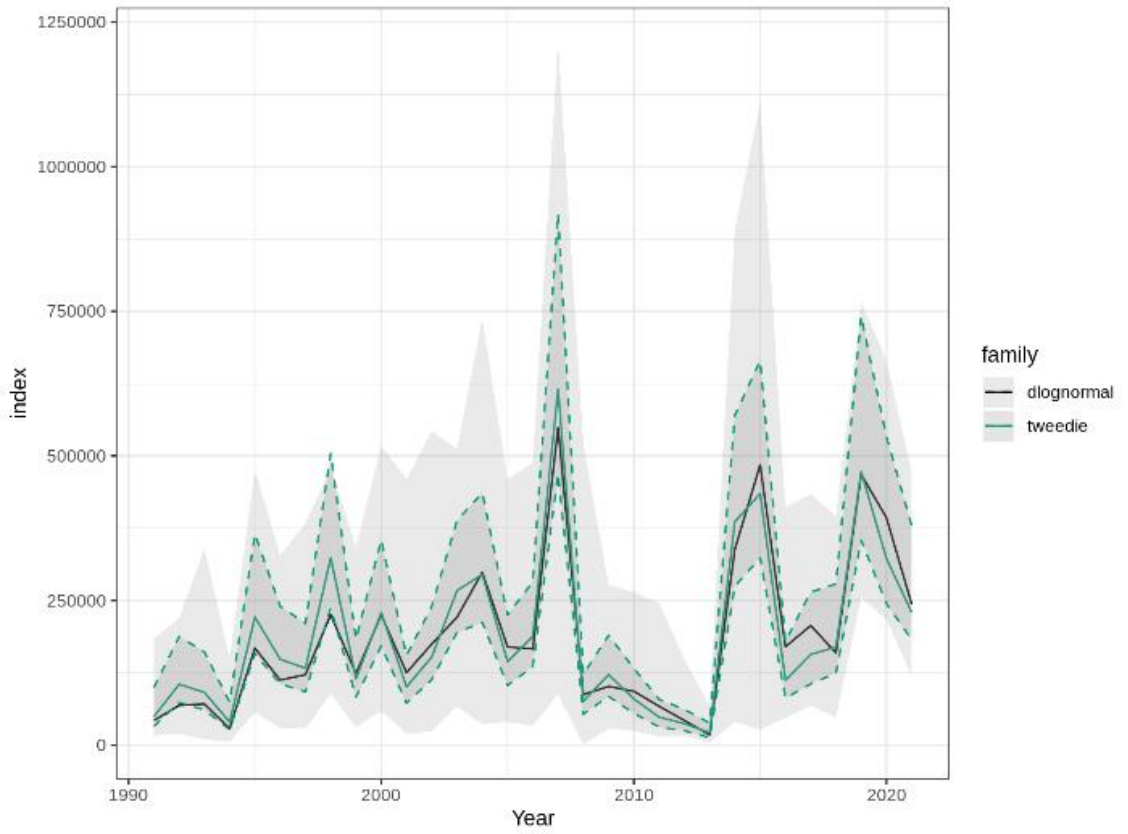


**Figure 4.2.3.11. Q3–4 surveys GAMM exploitable biomass index prediction for the delta-lognormal model in black and the Tweedie model in green.**

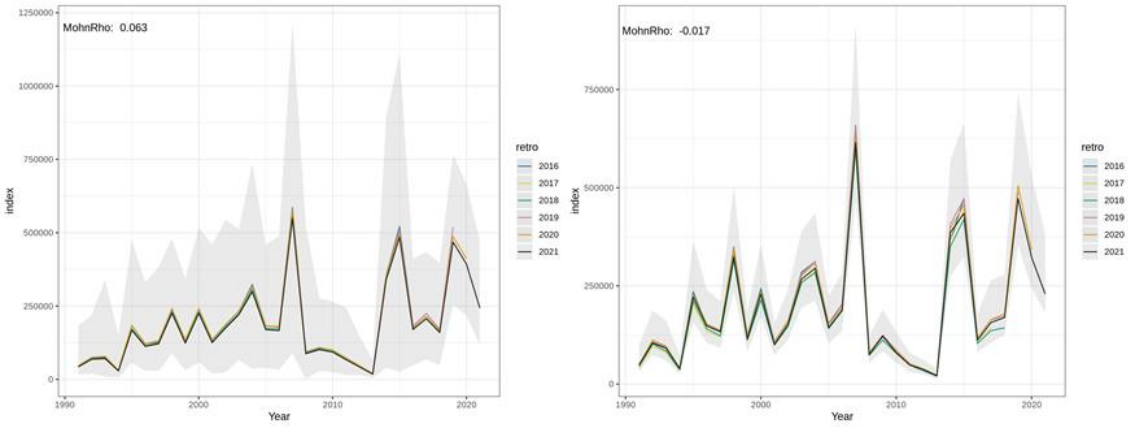


**Figure 4.2.3.12. Q3–4 surveys GAMM retrospective analysis for the delta-lognormal model on the left and the Tweedie model on the right.**

#### 4.2.3.4 Exploitable biomass index selection

Survey from the first semester and the second semester display different stripped red mullet distribution across the stock area as well as different trend in exploitable biomass. The index from the second semester gathered information from three different surveys covering the entire stock area and covering two quarters. In addition, the combined Q3–4 exploitable biomass display similar trend to the commercial landings. For those reasons, we decided to keep the combined Q3–4 index to represent exploitable biomass trend. Based on model diagnostics, the deviance explained, the CV of the predicted exploitable biomass index and the retrospective analysis, the Tweedie GAMM was selected over the delta-lognormal GAMM for the combined Q3–4 survey index. To assess the influence of each survey, we run a leave-one-out analysis showed in Figure 4.2.3.13. The trends remain similar between each run of the analysis, however removing CGFS increase the biomass index CV as most of the information is coming from that survey.

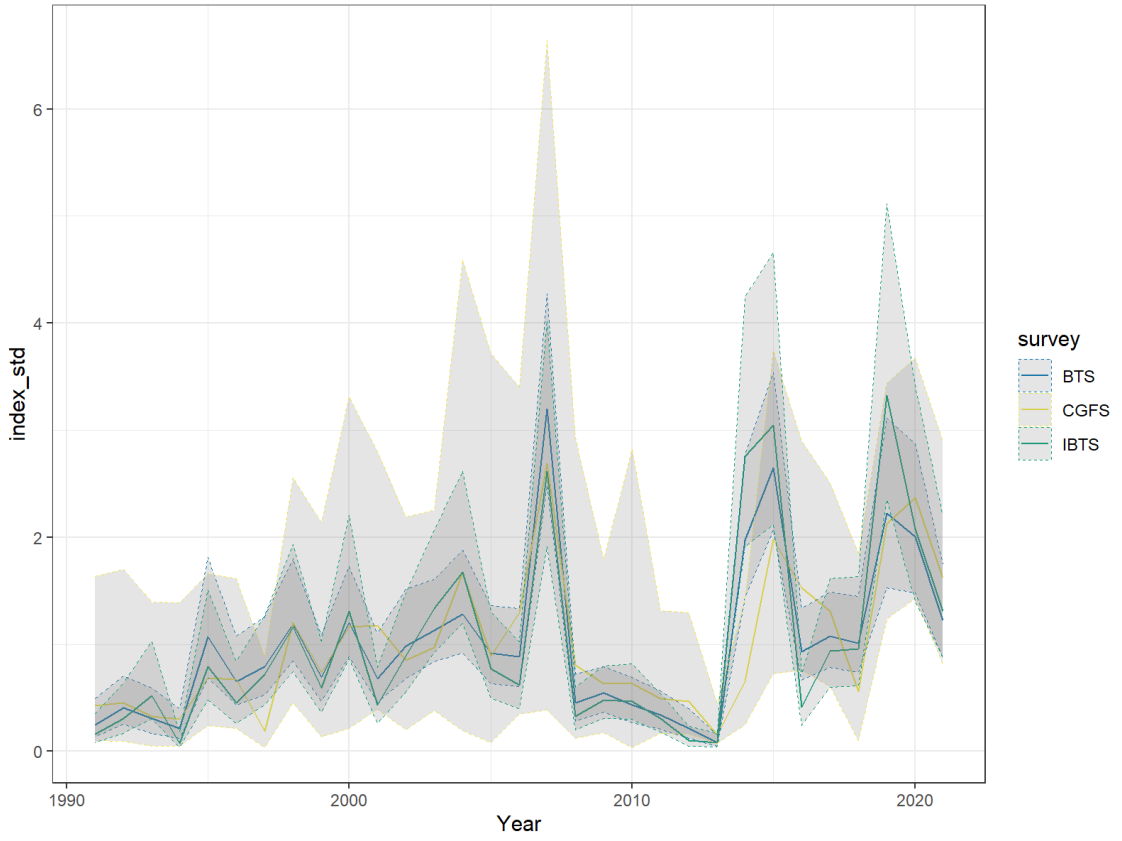


**Figure 4.2.3.13. Q3–4 surveys Tweedie GAMM survey leave one out analysis: comparison of mean standardized biomass index.**

### 4.2.4 Life-history traits

Life-history parameters were estimated using FishLife (Thorson, 2019; Figure 4.2.4.1 and Table 4.2.4.1). Growth parameter were also updated based on French age length data collected for this stock from 2006 to 2021 commercial sampling and surveys (Table 4.2.4.2; WD on updated growth parameters). $L_m$ is estimated for this stock at 16.2 cm (Mahé *et al.*, 2005).

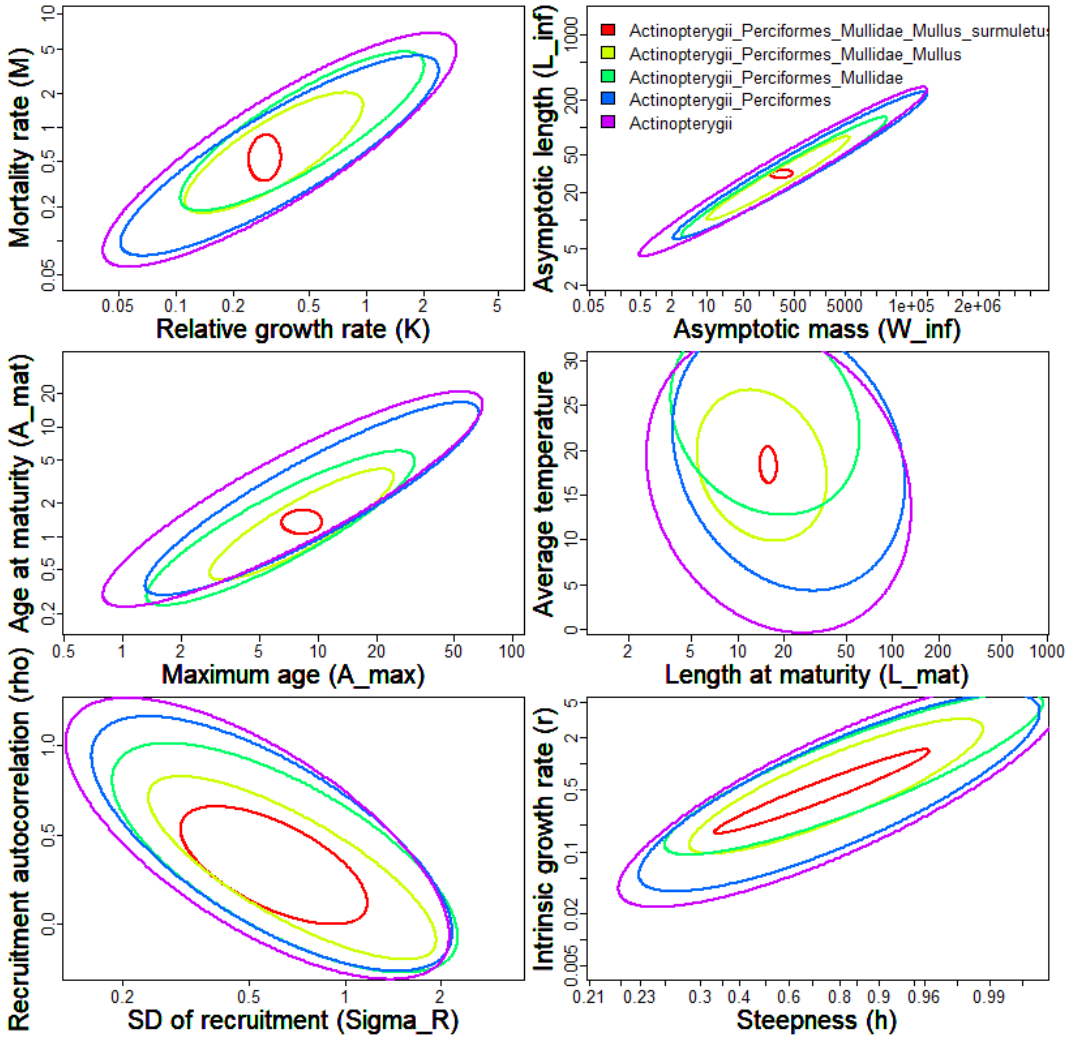


**Figure 4.2.4.1. Life-history parameters of stripped red mullet using the package FishLife.**

**Table 4.2.4.1. Estimations of the life-history parameters for stripped red mullet from FishLife.**

| Parameter | Estimates |
|---|---|
| $L_{inf}$ | 31.2 cm |
| K | 0.29 |
| $W_{inf}$ | 287 g |
| $t_{max}$ | 8.3 |
| $t_m$ | 1.4 |
| M | 0.54 |
| $L_m$ | 15.8 cm |
| r | 0.52 |

**Table 4.2.4.2. Estimations of the growth parameters for stripped red mullet in Subarea 4 and divisions 7.d and 3.a from 2006–2021 French commercial sampling and surveys.**

| Parameter | Estimates |
|---|---|
| $L_{inf}$ | 34.1 cm |
| K | 0.36 |
| $t_0$ | –1.36 |
| $t_1$ | 19.5 cm |

## 4.2.5 Summary of data available

**Table 4.2.4.1. Input data for SPiCT assessment: total landings (tonnes), Q3–4 exploitable biomass index and Q3–4 exploitable biomass index CV.**

| Year | Landing [2)] | Q3–4 survey index | Q3–4 survey index CV |
|---|---|---|---|
| 1991 | 26 | 49078.82206 | 1.367098531 |
| 1992 | 30 | 105111.1891 | 1.082567972 |
| 1993 | 63 | 91064.42033 | 1.102000326 |
| 1994 | 58 | 39807.71974 | 1.197333355 |
| 1995 | 527 | 221327.0396 | 0.934919058 |
| 1996 | 264 | 148356.1855 | 0.904791551 |
| 1997 | 139 | 132823.1734 | 0.890326694 |
| 1998 | 389 | 324082.3748 | 0.824472864 |
| 1999[1)] | 35 | 115080.1612 | 0.86713269 |
| 2000 | 895 | 229118.7828 | 0.800000085 |
| 2001 | 810 | 100656.3621 | 0.818626191 |
| 2002 | 626 | 152256.2544 | 0.830478325 |
| 2003 | 824 | 267048.005 | 0.724524555 |
| 2004 | 4674 | 295015.041 | 0.759330997 |
| 2005 | 2350 | 144345.2427 | 0.843411626 |
| 2006 | 1476 | 187865.6106 | 0.781219521 |
| 2007 | 4604 | 614625.4088 | 0.732172366 |
| 2008 | 2064 | 75536.64185 | 0.90770243 |
| 2009 | 1513 | 121928.9807 | 0.866745323 |
| 2010 | 1919 | 79927.07415 | 0.970769928 |
| 2011 | 1511 | 48348.99388 | 0.992189259 |
| 2012 | 726 | 37091.60932 | 0.99642702 |
| 2013 | 408 | 21427.65758 | 1.167061761 |
| 2014 | 1718 | 386234.8565 | 0.765018631 |
| 2015 | 4487 | 434870.3899 | 0.783186161 |
| 2016 | 2579 | 112112.0213 | 0.873253716 |
| 2017 | 2195 | 156783.1618 | 1.012725386 |
| 2018 | 1640 | 169570.4931 | 0.909520034 |
| 2019 | 4048 | 472502.9548 | 0.819497797 |
| 2020 | 3503 | 322514.3014 | 0.895237856 |
| 2021 | 2611 | 229381.2092 | 0.857364237 |

**1) No data reported by France in 1999.**

**2) Before 2004, Official landings and from 2004-onwards use ICES estimated landings**

## 4.3 Stock assessment

The stock assessment was performed using SPiCT version 1.3.7 (Pedersen and Berg, 2017). Two dataset were tested, one using all the biomass index time-series and a mix of Official landings and ICES estimated landing from 1991–2021 (models 1) and on using only ICES estimated landing and the biomass index from 2004–2021 (models 2) with various prior. In the set of model 1 tested stdevfacC was set to 1.29 before 2004 and 0.86 after to account for the higher uncertainty in Official landing data.

### 4.3.1 Priors distributions

To estimate a prior for the intrinsic rate of increase the SPMpriors package was used (Winker, 2020). The analysis is based on the information from FishLife, some life parameters were updated using data from the stock using a prior on $L_{inf}$ of c(34,0.1), K of c(0.36,0.1), $t_{max}$ of c(7,0.2) and $L_m$ of c(16.2,0.1). The output from the analysis were as followed:

| | r | shape | fmsy | bmsyk |
|---|---|---|---|---|
| mu | 0.3810302 | 0.6330000 | 0.6051821 | 0.2876750 |
| logsd | 0.1661333 | 0.3303099 | 0.4557491 | 0.1895965 |

### 4.3.2 Exploratory assessments

Different scenarios were tested for both datasets using different priors on n, bkfrac and r (Table 4.3.2.1). The different scenario were assessed based on the acceptance criteria defined by Mildenberger *et al*. (2021). The best model outputs for both datasets are shown in Figure 4.3.2.1 and 4.3.2.2. All the scenario converged for the dataset 1991–2021 but only one did for the shorter dataset. However none of the scenario were considered acceptable as the model have issue with assessing the state of the stock ($B_{MSY}$ and $F_{MSY}$). Depending on the length of the dataset considered the model changed is estimation of the stock status with always high uncertainty around $B_{MSY}$ and $F_{MSY}$ estimates. For both dataset, SPiCT has difficulties to estimates fishing mortality for this stock, even if with a shorter dataset the uncertainty around F decrease.

Table 4.3.2.1. Set of scenario tested with the two dataset from 1991–2021 and 2004–2021. Acceptance diagnostics are presented, Convergence: convergence of the SPiCT run; Finite s.d.: indicates whether all variances of the parameters are finite; Residuals: indicates whether model assumptions regarding one-step-ahead residuals have been met; Retro: indicates the presence of consistent patterns in the retrospective analysis; Prod. curve: indicates whether the shape of the production curve is realistic; Uncertainty: indicates whether the confidence intervals around $B/B_{MSY}$ and $F/F_{MSY}$ are not excessively large. In bold are the scenario presented in Figure 4.3.2.1 and 4.3.2.2.

| scenario | dataset | n | bkfrac | r (mean, sd) | Convergence | Finite sd | residuals | retro | Prod. curve | uncertainty |
|---|---|---|---|---|---|---|---|---|---|---|
| 1a | 1991–2021 | default | default | default | 1 | 0 | 0 | 1 | 0 | 0 |
| 1b | 1991–2021 | 2 | default | default | 1 | 0 | 0 | 0 | 0 | 0 |
| 1c | 1991–2021 | default | 0.4 | default | 1 | 1 | 0 | 1 | 0 | 0 |
| 1d | 1991–2021 | default | 0.5 | default | 1 | 1 | 1 | 1 | 0 | 0 |
| 1e | 1991–2021 | default | 0.7 | default | 1 | 1 | 1 | 1 | 0 | 0 |
| **1f** | **1991–2021** | **default** | **0.5** | **(0.381, 0.116)** | **1** | **1** | **1** | **1** | **0** | **0** |
| 2a | 2004–2021 | default | default | default | 0 | 0 | 0 | 0 | 0 | 0 |
| 2b | 2004–2021 | 2 | default | default | 0 | 0 | 0 | 0 | 0 | 0 |
| 2c | 2004–2021 | default | 0.4 | default | 0 | 0 | 0 | 0 | 0 | 0 |
| 2d | 2004–2021 | default | 0.5 | default | 0 | 0 | 0 | 0 | 0 | 0 |
| **2e** | **2004–2021** | **default** | **0.7** | **default** | **1** | **1** | **1** | **0** | **1** | **0** |
| 2f | 2004–2021 | default | 0.7 | (0.381, 0.116) | 0 | 0 | 0 | 0 | 0 | 0 |

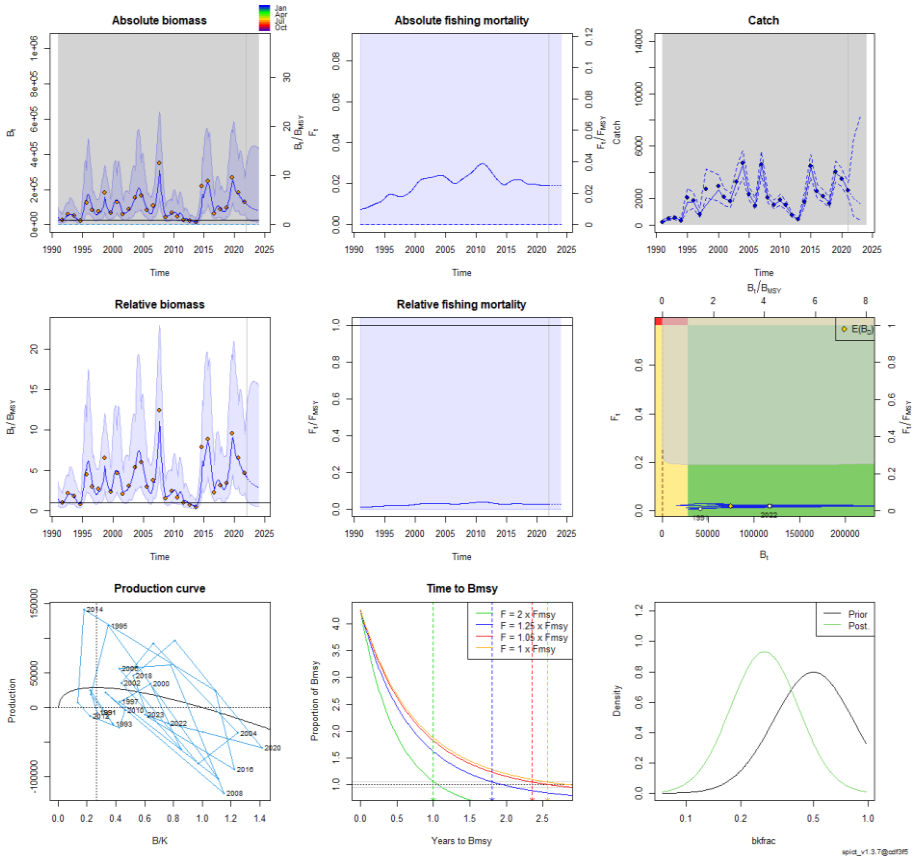


**Figure 4.3.2.1. Output from SPiCT assessment model 1f using data from 1991–2021.**

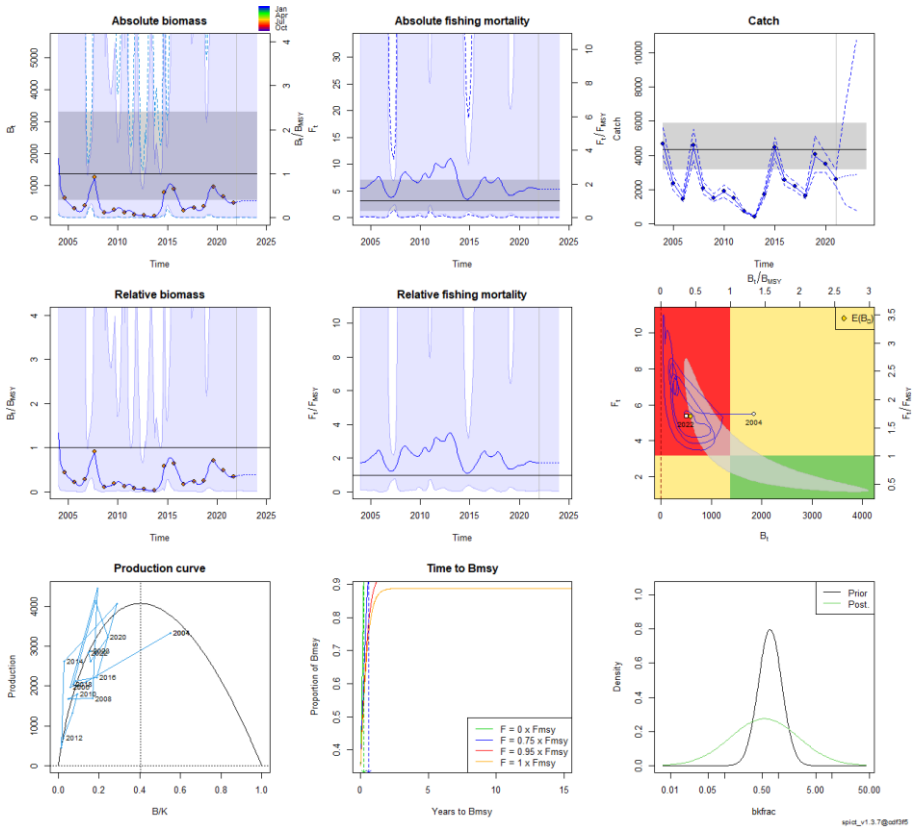


**Figure 4.3.2.2. Life-history parameters of stripped red mullet using the package FishLife.**

## 4.4 Future considerations/recommendations

No SPiCT configurations were accepted for this stock and the workshop concluded that SPiCT was not suitable for this stock. Indeed, catch are mainly driven by the recruitment and SPiCT is not able to evaluate the status of the stock and link fishing pressure to the stock dynamics.

Hypothesis have been made that the productivity of the stock change through time with an increase of the productivity especially at the beginning of the time-series. This increase of productivity is related with the expansion Northward of the species distribution. To test that hypothesis, an assessment trial using SS3 was made using all the data available from 1975–2021 (survey indices, length frequency, landings at age and total landings) and allowing change in productivity. In Figure 4.4.1 we can see that $B_0$ is estimated to have increased over time up until the mid-2000's. Further investigation of model allowing for change in stock productivity over time was recommended by the workshop to assess stripped red mullet in Subarea 4 and divisions 7.d and 3.a.

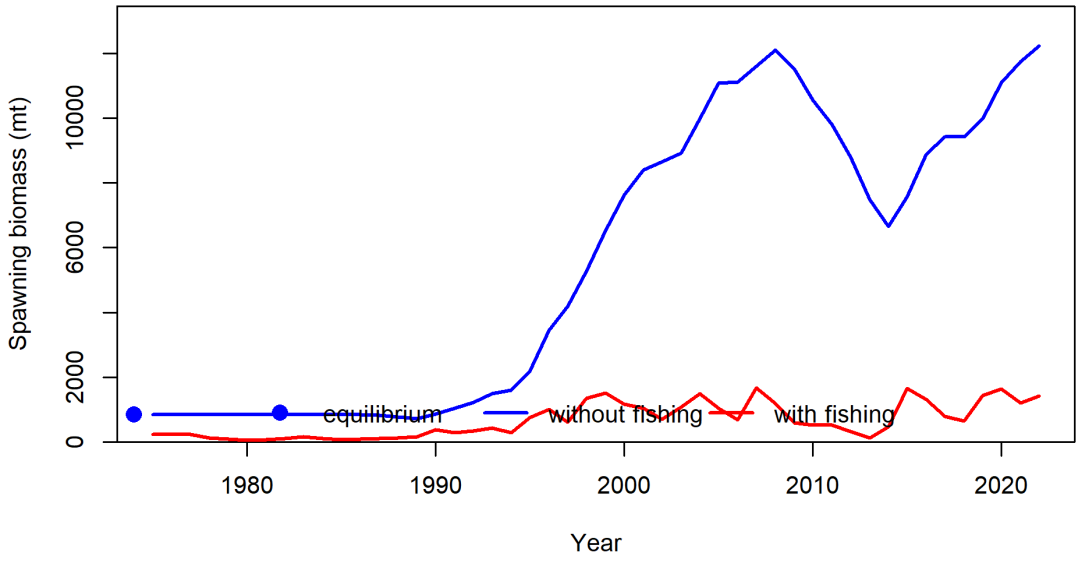


**Figure 4.4.1. Dynamics spawning-stock biomass (red) and $B_0$ (blue) as estimated by SS3 assessment trial.**

Category 3 assessment following the chr rule was proposed for this stock, using the biomass index derived from Q3–4 surveys data, the life parameters available for the stock ($L_{inf}$, K and $L_{mat}$) and the length distribution of landing data from 2014–2016 and 2018–2021.

## 4.5 Reviewer report

This stock was downgraded to category 5 in 2021. There is no TAC or MCRS for this stock.

Official landings go back to 1958, but very little was landed before 1990. IBTS also indicates that there was much lesser abundance of striped red mullet back in time, which could indicate increased productivity of the stock over time, as low initial stock size combined with very little historical exploitation is unlikely unless productivity has changed. There are also indications of Northward expansion of the stock supporting the argument of increased productivity of the stock over time. The catches are mainly driven by 1-year olds, and the survey indices are highly variable from year-to-year. Stocks with such dynamics are not well described by surplus production models, and all SPiCT runs had very high associated uncertainty and could therefore not be accepted. A length structured alternative assessment using Stock Synthesis was briefly presented and could be considered in future benchmarks. Since the SPiCT assessment was

rejected for this stock, ICES empirical rules such as the chr-rule will be used to provide advice for the stock. These were shortly presented to the group but were not thoroughly discussed during this benchmark. The presented abundance index and available length distributions can be used as input to ICES empirical rules and specifically the "*chr*-rule". Further external evaluation should be performed during or after the assessment working group on the input data and the application of the rule.

## 4.6 Conclusions

No SPiCT configurations were accepted for this stock and the workshop concluded that SPiCT was not suitable for this stock. An integrated model should be explored in future to account for the change in stock productivity over time and the moderate amount of size information available for this stock.

## 4.7 References

Cornou, A.-S., Quinio-Scavinner, M., Sagan, J., Cloâtre, T., Dubroca, L., and Billet, N. 2021. Captures et rejets des métiers de pêche français. Résultats des observations à bord des navires de pêche professionnelle en 2019. ObsMer. doi: https://doi.org/10.13155/79198. https://archimer.ifremer.fr/doc/00680/79198/.

Hoarau, G., Piquet, A. M.-T., van der Veer, H. W., Rijnsdorp, A. D., Stam, W. T., and Olsen, J. L. 2004. Population structure of plaice (*Pleuronectes platessa* L.) in northern Europe: a comparison of resolving power between microsatellites and mitochondrial DNA data. Journal of Sea Research, 51: 183–190.

Machiels, M. a. M., Kraak, S. B. M., Borges, L., and Bogaards, H. 2007. Stock assessment of North Sea plaice using surplus production models. C032/07. IMARES. https://research.wur.nl/en/publications/stock-assessment-of-north-sea-plaice-using-surplus-production-mod (Accessed 4 January 2023).

Mildenberger, T. K., Kokkalis, A., and Berg, C. W. 2021, February 20. Guidelines for the stochastic production model in continuous time (SPiCT).

## 4.8 Working document for striped red mullet: updated growth patterns

Updated growth parameters of striped red mullet (*Mullus surmuletus*) in the eastern English Channel (7D) and North Sea (IV)

Kélig Mahé (1), Romain Elleboode (1), Raphael Girardin (1)

(1) Ifremer, Laboratoire Ressources Halieutiques, 150 quai Gambetta, BP 699, 62321 Boulogne-sur-Mer, France

## 1. Growth Data

A total of 5334 striped red mullet were used from commercial sampling and surveys (IBTS, CGFS and Camanoc) from 2006 to 2021 (Table 1). This species, caught by the local trawler fleet, is known to originate solely from the eastern English Channel and the southern North Sea. All fresh specimens were examined in the laboratory for total length (TL, cm), total wet weight (W, g), sex, and macroscopic maturation stage according to N'Da and Deniel (1993). In order to estimate the age of each individual, sagittal otoliths were removed from the cranial cavity. As recommended by international expert groups (Vitale et al., 2019), two techniques were used in order to gain the most precise evaluation of the fish age: observation under transmitted light, as well as observation under reflected light before and after burning the whole otolith. Once prepared, otoliths were immersed in 5% alcohol water and layed out under a binocular microscope connected by a camera to a computer. Each sample was then analysed. Finally, in order to limit interpretation error three different experts examined each otolith.

A) By sampling year

| Age Group | 2006 | 2007 | 2008 | 2009 | 2010 | 2011 | 2012 | 2013 | 2014 | 2015 | 2016 | 2017 | 2018 | 2019 | 2020 | 2021 | Total |
|---|---|---|---|---|---|---|---|---|---|---|---|---|---|---|---|---|---|
| 0 | 28 | 11 | 3 | 89 | 45 | 1 | 44 | 20 | 66 | | 25 | 49 | 77 | 27 | 22 | 74 | 581 |
| 1 | 92 | 339 | 26 | 333 | 314 | 217 | 194 | 17 | 146 | 160 | 117 | 115 | 74 | 97 | 178 | 103 | 2522 |
| 2 | 122 | 42 | 97 | 92 | 141 | 49 | 228 | 8 | 13 | 13 | 100 | 80 | 100 | 60 | 92 | 78 | 1315 |
| 3 | 182 | 36 | 20 | 81 | 69 | 16 | 75 | 3 | 1 | | 31 | 41 | 9 | 16 | 2 | 15 | 597 |
| 4 | 47 | 7 | 18 | 11 | 95 | 9 | 21 | | 1 | | | 6 | 4 | 7 | | 1 | 227 |
| 5 | 8 | 2 | 13 | 9 | 17 | 3 | 18 | | 1 | 1 | | | | | | | 72 |
| 6 | 2 | | 1 | 1 | 7 | 1 | 3 | | | | | 1 | | | | | 16 |
| 7 | | | | 1 | 3 | | | | | | | | | | | | 4 |
| **Total** | **481** | **437** | **178** | **617** | **691** | **296** | **583** | **48** | **228** | **174** | **273** | **292** | **264** | **207** | **294** | **271** | **5334** |

B) By sampling quarter

| Age Group | Quarter 1 | Quarter 2 | Quarter 3 | Quarter 4 | Total |
|---|---|---|---|---|---|
| 0 | 104 | 10 | 47 | 420 | 581 |
| 1 | 443 | 221 | 974 | 884 | 2522 |
| 2 | 212 | 522 | 327 | 254 | 1315 |
| 3 | 61 | 353 | 131 | 52 | 597 |
| 4 | 6 | 184 | 19 | 18 | 227 |
| 5 | 1 | 61 | 7 | 3 | 72 |
| 6 | 1 | 15 | | | 16 |
| 7 | | 4 | | | 4 |
| **Total** | **828** | **1370** | **1505** | **1631** | **5334** |

Table 1 : Summary of sampling by year and quarter of sampling for each age group of striped red mullet (*Mullus surmuletus*) in the eastern English Channel (7D) and North Sea (IV).

## 2. Growth models

Four growth models were tested from the ageing data of *Mullus surmuletus* in the Eastern English Channel and the south of the North Sea from 2006 to 2021 :

- the von Bertalanffy model (1938) without constraint :

$$TL_t = TL_\infty . (1 - e^{-K.(t-t_0)})$$

- the von Bertalanffy model forced t0=0:

$$TL_t = TL_\infty - (TL_\infty . e^{-K.t})$$

- the von Bertalanffy model forced $TL_1$:

$$TL_t = TL_\infty - (TL_\infty - TL_1). e^{-K.(t-1)}$$

- the logistic model (Verhulst, 1838):

$$TL_t = \frac{TL_\infty}{1 + \left(\left(\frac{TL\infty}{TL_1}\right) - 1\right) * e^{-K.t}}$$

Where $TL_1$, $TL_t$, and $TL_\infty$ are respectively the length at age 1, at age $t$ and the asymptotic length, $K$ the rate at which the asymptote is reached, also called the growth coefficient. The best growth model was identified as the one minimizing the small-sample, bias-corrected form of the Akaike Information Criterion (AICc ; Akaike, 1974 ; Sakamo et al., 1986). The AICc balances the trade-off between the quality of fit and the number of parameters used (Pauly, 1979) while accounting for small-sample bias and is defined as:

$$AICc = 2k - 2\ln(TL) + \frac{2k(k+1)}{n-k-1}$$

Where $n$ is the sample size, k is the total number of parameters of the model and $TL$ is its likelihood.

## 3. Growth model from 2006 to 2021 for both sexes

A total of 5334 striped red mullet were used from commercial sampling and surveys (IBTS, CGFS and Camanoc) from 2006 to 2021.

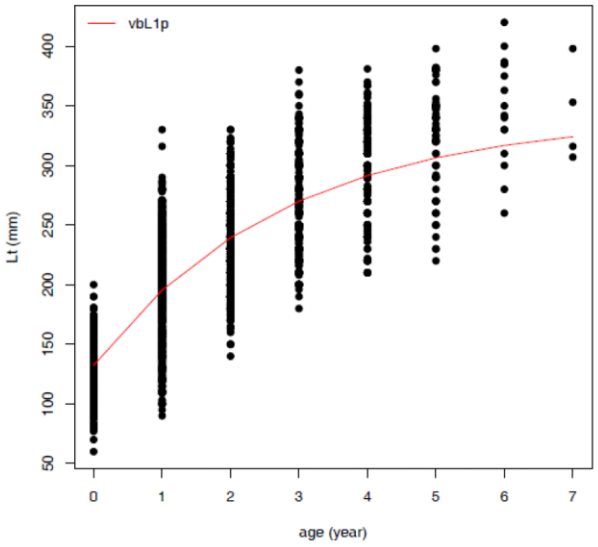


| Fish number | TL (mm) max | TL (mm) min | Age min | Age max | Growth model | TL ∞ | K | To | TL1 | AIC | Selected model |
|---|---|---|---|---|---|---|---|---|---|---|---|
| 5328 | 420 | 127.865 | 0 | 7 | vbp | 272,48 | 1,25 | | | 57996,94 | |
| 5328 | 420 | 127.865 | 0 | 7 | vbt0p | 340,66 | 0,36 | -1,36 | | 53049,15 | |
| 5328 | 420 | 127.865 | 0 | 7 | vbL1p | 340,84 | 0,36 | NA | 195,41 | 53049,15 | selected |
| 5328 | 420 | 127.865 | 0 | 7 | log.p | 307,98 | 0,74 | NA | 137,64 | 53160,62 | |

## 4. Growth models by sex from 2006 to 2021

The growth data showed that the growth of female was higher than the growth of males with at the same age group, the mean of total length for females was higher than the mean of total length for males from 2006 to 2021.

To optimize the growth model by sex, all immatures fish were used in both growth models by sex.

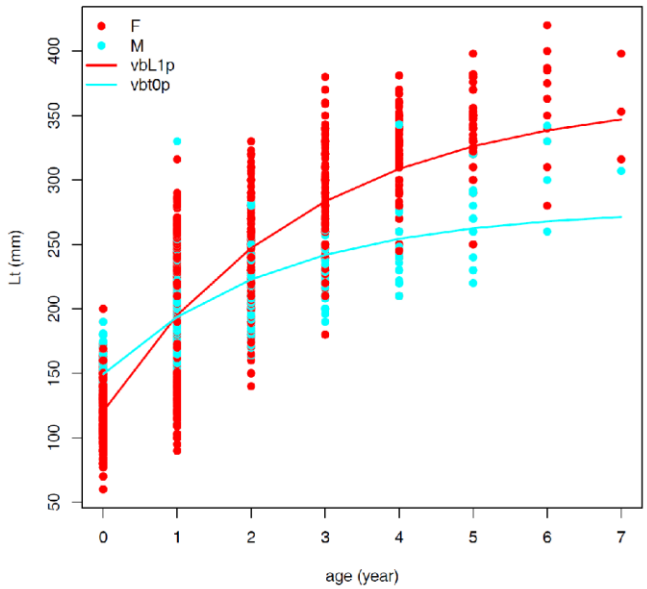


The growth model for females was the von Bertalanffy model forced mean $TL_1$ while for the males individuals, the best model was the von Bertalanffy model (1938) without constraint. Consequently, according to the growth data, the choice of growth model is important.

| Sex | Fish number | TL (mm) max | TL (mm) min | Age min | Age max | Growth model | TL ∞ | K | To | TL1 | AIC | Selected model |
|---|---|---|---|---|---|---|---|---|---|---|---|---|
| F | 3572 | 420 | 119 | 0 | 7 | vbp | 296,47 | 1,04 | | | 39918,46 | |
| F | 3572 | 420 | 119 | 0 | 7 | vbt0p | 366,37 | 0,36 | -1,10 | | 35865,70 | |
| F | 3572 | 420 | 119 | 0 | 7 | vbL1p | 366,43 | 0,36 | | 195,18 | 35865,70 | selected |
| F | 3572 | 420 | 119 | 0 | 7 | log,p | 320,17 | 0,87 | | 124,15 | 35942,35 | |
| M | 2107 | 380 | 144 | 0 | 7 | vbp | 236,43 | 1,72 | | | 22065,67 | |
| M | 2107 | 380 | 144 | 0 | 7 | vbt0p | 277,97 | 0,42 | -1,82 | | 20098,87 | selected |
| M | 2107 | 380 | 144 | 0 | 7 | vbL1p | -1472,41 | -0,01 | | 191,19 | 20329,10 | |
| M | 2107 | 380 | 144 | 0 | 7 | log,p | 265,04 | 0,69 | | 152,57 | 20116,07 | |

## 5. Growth models by year

The same analysis for each year was carried out.

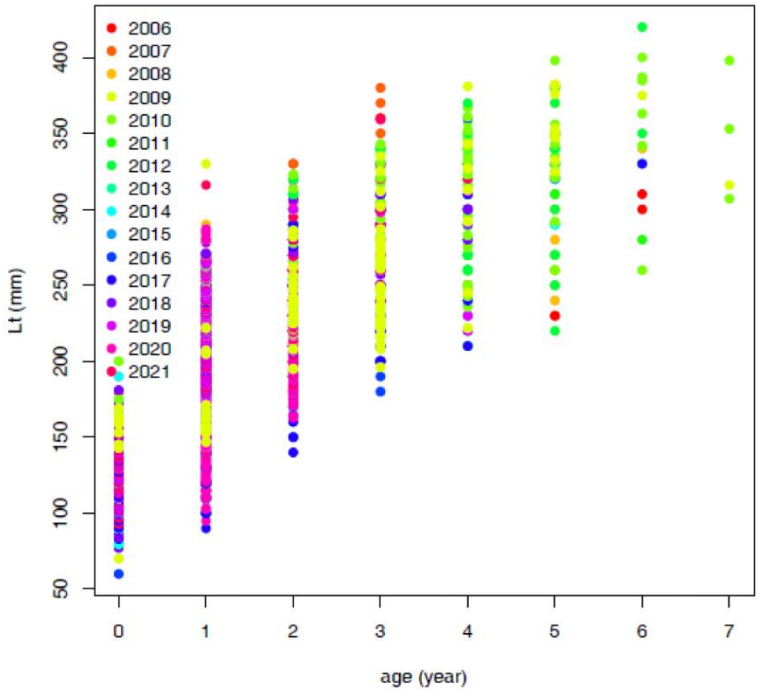

| Sampling year | Fish number | TL (mm) max | TL (mm) min | Age min | Age max | Growth model | TL ∞ | K | To | TL1 |
|---|---|---|---|---|---|---|---|---|---|---|
| 2021 | 271 | 359 | 135 | 0 | 4 | vbL1p | 299,17 | 0,56 | | 206,12 |
| 2020 | 294 | 319 | 140 | 0 | 3 | vbL1p | 271,66 | 0,35 | | 181,28 |
| 2019 | 207 | 312 | 124 | 0 | 4 | vbt0p | 230,15 | 2,04 | -0,38 | |
| 2018 | 264 | 310 | 136 | 0 | 4 | vbL1p | 241,58 | 1,73 | | 222,79 |
| 2017 | 292 | 360 | 120 | 0 | 6 | log.p | 297,13 | 0,92 | | 118,70 |
| 2016 | 273 | 300 | 120 | 0 | 3 | vbL1p | 240,08 | 1,05 | | 197,86 |
| 2015 | 174 | 320 | 187 | 1 | 5 | vbt0p | 590,80 | 0,10 | -2,81 | |
| 2015 | 174 | 320 | 187 | 1 | 5 | log.p | 393,69 | 0,39 | | 149,35 |
| 2014 | 228 | 320 | 123 | 0 | 5 | vbL1p | 357,27 | 0,32 | | 186,71 |
| 2012 | No adjusted model | | | | | | | | | |
| 2013 | 48 | 280 | 124 | 0 | 3 | vbL1p | 264,82 | 0,82 | | 202,70 |
| 2011 | 296 | 330 | 100 | 0 | 6 | vbL1p | 309,32 | 0,61 | | 188,86 |
| 2010 | 691 | 400 | 140 | 0 | 7 | vbL1p | 531,43 | 0,12 | | 192,13 |
| 2009 | 613 | 382 | 128 | 0 | 7 | vbL1p | 325,95 | 0,43 | | 199,66 |
| 2008 | No adjusted model | | | | | | | | | |
| 2007 | 434 | 380 | 179 | 0 | 5 | log.p | 388,51 | 0,67 | | 131,55 |
| 2006 | 481 | 360 | 134 | 0 | 6 | vbL1p | 315,24 | 0,41 | | 203,98 |

## 6. REFERENCES

Akaike, H. A new look at the statistical model identification. *IEEE Trans. Autom. Control.* 19, 716-723 (1974). http://dx.doi.org/10.1109/TAC.1974.1100705

Pauly, D. Gill size and temperature as governing factors in fish growth: a generalization of von Bertalanffy's growth formula. PhD Thesis, Univ. Kiel and Institut für Meereskunde (1979)

Sakamo, Y., Ishiguro, M. & Kitagawa, G. Akaike *Information Criterion Statistics.* Springer, Netherlands (1986)

Verhulst, P. F. Notice sur la loi que la population poursuit dans son accroissement. *Corresp. Math. Phys*. 10, 113-121 (1838). http://dx.doi.org/10.1371/journal.pbio.1001827
Von Bertalanffy, L. A quantitative theory of organic growth (Inquiries on growth laws II). *Hum. Biol*. 10, 181-213 (1938)

## 7. Annex 1 : all growth models by each sampling year

| Sampling year | Fish number | TL (mm) max | TL (mm) min | Age min | Age max | Growth model | TL ∞ | K | To | TL1 | AIC | Selected model |
|---|---|---|---|---|---|---|---|---|---|---|---|---|
| 2021 | 271 | 359,00 | 134,68 | 0 | 4 | vbp | 258,36 | 1,62 | | | 3115,70 | |
| 2021 | 271 | 359,00 | 134,68 | 0 | 4 | vbt0p | 299,24 | 0,56 | -1,07 | | 2532,41 | |
| 2021 | 271 | 359,00 | 134,68 | 0 | 4 | vbL1p | 299,17 | 0,56 | | 206,12 | 2532,41 | selected |
| 2021 | 271 | 359,00 | 134,68 | 0 | 4 | log.p | 274,78 | 1,11 | | 136,15 | 2537,60 | |
| 2020 | 294 | 319,00 | 139,86 | 0 | 3 | vbp | 210,45 | 2,02 | | | 3224,77 | |
| 2020 | 294 | 319,00 | 139,86 | 0 | 3 | vbt0p | 271,47 | 0,35 | -2,12 | | 3054,21 | |
| 2020 | 294 | 319,00 | 139,86 | 0 | 3 | vbL1p | 271,66 | 0,35 | | 181,28 | 3054,21 | selected |
| 2020 | 294 | 319,00 | 139,86 | 0 | 3 | log.p | 244,43 | 0,69 | | 144,04 | 3054,66 | |
| 2019 | 207 | 312,00 | 124,26 | 0 | 4 | vbp | 229,09 | 2,91 | | | 2218,76 | |
| 2019 | 207 | 312,00 | 124,26 | 0 | 4 | vbt0p | 230,15 | 2,04 | -0,38 | | 1903,54 | selected |
| 2019 | 207 | 312,00 | 124,26 | 0 | 4 | vbL1p | -106,84 | -14,17 | | 183,93 | 19843,56 | |
| 2019 | 207 | 312,00 | 124,26 | 0 | 4 | log.p | 229,35 | 2,65 | | 124,35 | 1903,86 | |
| 2018 | 264 | 310,00 | 135,53 | 0 | 4 | vbp | 238,13 | 2,88 | | | 3051,98 | |
| 2018 | 264 | 310,00 | 135,53 | 0 | 4 | vbt0p | 241,61 | 1,73 | -0,48 | | 2462,80 | |
| 2018 | 264 | 310,00 | 135,53 | 0 | 4 | vbL1p | 241,58 | 1,73 | | 222,79 | 2462,80 | selected |
| 2018 | 264 | 310,00 | 135,53 | 0 | 4 | log.p | 239,06 | 2,43 | | 135,70 | 2464,38 | |
| 2017 | 292 | 360,00 | 119,74 | 0 | 6 | vbp | 278,85 | 1,07 | | | 3235,93 | |
| 2017 | 292 | 360,00 | 119,74 | 0 | 6 | vbt0p | 348,15 | 0,36 | -1,13 | | 2936,06 | |
| 2017 | 292 | 360,00 | 119,74 | 0 | 6 | vbL1p | 348,15 | 0,36 | | 188,05 | 2936,06 | |
| 2017 | 292 | 360,00 | 119,74 | 0 | 6 | log.p | 297,13 | 0,92 | | 118,70 | 2934,12 | selected |
| 2016 | 273 | 300,00 | 119,60 | 0 | 3 | vbp | 231,95 | 1,91 | | | 2867,00 | |
| 2016 | 273 | 300,00 | 119,60 | 0 | 3 | vbt0p | 240,08 | 1,05 | -0,66 | | 2597,93 | |
| 2016 | 273 | 300,00 | 119,60 | 0 | 3 | vbL1p | 240,08 | 1,05 | | 197,86 | 2597,93 | selected |
| 2016 | 273 | 300,00 | 119,60 | 0 | 3 | log.p | 234,57 | 1,63 | | 119,89 | 2598,11 | |
| 2015 | 174 | 320,00 | 187,00 | 1 | 5 | vbp | 251,61 | 1,35 | | | 1810,44 | |
| 2015 | 174 | 320,00 | 187,00 | 1 | 5 | vbt0p | 590,80 | 0,10 | -2,81 | | 1809,25 | selected |
| 2015 | 174 | 320,00 | 187,00 | 1 | 5 | vbL1p | 590,79 | 0,10 | | 187,00 | 1809,25 | |
| 2015 | 174 | 320,00 | 187,00 | 1 | 5 | log.p | 393,69 | 0,39 | | 149,35 | 1809,25 | selected |
| 2014 | 228 | 320,00 | 122,88 | 0 | 5 | vbp | 267,11 | 1,20 | | | 2636,50 | |
| 2014 | 228 | 320,00 | 122,88 | 0 | 5 | vbt0p | 357,27 | 0,32 | -1,33 | | 2337,53 | |
| 2014 | 228 | 320,00 | 122,88 | 0 | 5 | vbL1p | 357,27 | 0,32 | | 186,71 | 2337,53 | selected |
| 2014 | 228 | 320,00 | 122,88 | 0 | 5 | log.p | 303,61 | 0,83 | | 123,92 | 2338,17 | |
| 2013 | 48 | 280,00 | 123,50 | 0 | 3 | vbp | 246,66 | 1,74 | | | 566,80 | |
| 2013 | 48 | 280,00 | 123,50 | 0 | 3 | vbt0p | 264,79 | 0,82 | -0,77 | | 448,87 | |
| 2013 | 48 | 280,00 | 123,50 | 0 | 3 | vbL1p | 264,82 | 0,82 | | 202,70 | 448,87 | selected |
| 2013 | 48 | 280,00 | 123,50 | 0 | 3 | log.p | 252,50 | 1,44 | | 123,99 | 449,61 | |
| 2012 | 583 | 420,00 | 80,00 | 0 | 6 | No adjusted model | | | | | | |
| 2011 | 296 | 330,00 | 100,00 | 0 | 6 | vbp | 284,33 | 1,08 | | | 2930,65 | |
| 2011 | 296 | 330,00 | 100,00 | 0 | 6 | vbt0p | 309,33 | 0,61 | -0,54 | | 2921,06 | |
| 2011 | 296 | 330,00 | 100,00 | 0 | 6 | vbL1p | 309,32 | 0,61 | | 188,86 | 2921,06 | selected |
| 2011 | 296 | 330,00 | 100,00 | 0 | 6 | log.p | 296,11 | 1,02 | | 114,70 | 2921,50 | |
| 2010 | 691 | 400,00 | 139,62 | 0 | 7 | vbp | 287,75 | 1,05 | | | 7444,65 | |
| 2010 | 691 | 400,00 | 139,62 | 0 | 7 | vbt0p | 531,44 | 0,12 | -2,75 | | 6866,26 | |
| 2010 | 691 | 400,00 | 139,62 | 0 | 7 | vbL1p | 531,43 | 0,12 | | 192,13 | 6866,26 | selected |
| 2010 | 691 | 400,00 | 139,62 | 0 | 7 | log.p | 398,53 | 0,38 | | 154,67 | 6871,14 | |
| 2009 | 613 | 382,00 | 127,57 | 0 | 7 | vbp | 273,66 | 1,32 | | | 6688,00 | |
| 2009 | 613 | 382,00 | 127,57 | 0 | 7 | vbt0p | 325,82 | 0,43 | -1,19 | | 5862,52 | |
| 2009 | 613 | 382,00 | 127,57 | 0 | 7 | vbL1p | 325,95 | 0,43 | | 199,66 | 5862,52 | selected |
| 2009 | 613 | 382,00 | 127,57 | 0 | 7 | log.p | 292,11 | 0,94 | | 133,21 | 5887,99 | |
| 2008 | 178 | 150,00 | 370,00 | 0 | 6 | No adjusted model | | | | | | |
| 2007 | 434 | 380,00 | 179,09 | 0 | 5 | vbp | 335,22 | 0,84 | | | 4580,85 | |
| 2007 | 434 | 380,00 | 179,09 | 0 | 5 | vbt0p | 864,12 | 0,09 | -1,90 | | 4422,14 | |
| 2007 | 434 | 380,00 | 179,09 | 0 | 5 | vbL1p | 862,94 | 0,09 | | 194,75 | 4422,14 | |
| 2007 | 434 | 380,00 | 179,09 | 0 | 5 | log.p | 388,51 | 0,67 | | 131,55 | 4412,87 | selected |
| 2006 | 481 | 360,00 | 133,93 | 0 | 6 | vbp | 266,71 | 1,49 | | | 5056,35 | |
| 2006 | 481 | 360,00 | 133,93 | 0 | 6 | vbt0p | 314,96 | 0,41 | -1,56 | | 4671,20 | |
| 2006 | 481 | 360,00 | 133,93 | 0 | 6 | vbL1p | 315,24 | 0,41 | | 203,98 | 4671,20 | selected |
| 2006 | 481 | 360,00 | 133,93 | 0 | 6 | log.p | 306,31 | 0,61 | | 157,19 | 4683,51 | |

# 5 Bay of Biscay and Atlantic Iberian waters plaice

## ple.27.89a – *Pleuronectes platessa* in Subarea 8 and Division 9.a

## 5.1 Introduction

European plaice (*Pleuronectes platessa* L.) is distributed from the Barents Sea to the Strait of Gibraltar. The stock unit covering the Bay of Biscay and Atlantic Iberian waters hence covers one or several populations located close to the southern limit of the distribution area for this species.

A study on population genetics of plaice in the Northeast Atlantic concluded in a statistically significance genetic differentiation between individuals collected in the Bay of Biscay and those sampled in the Irish Sea and North Sea, based on mitochondrial DNA (Hoarau *et al.*, 2004). However, no significant differentiation was found using nuclear microsatellites, suggesting a relatively recent differentiation.

### 5.1.1 Fishery information

Plaice can be considered a secondary commercial species in the Bay of Biscay. There has been an average twenty-fold difference between plaice landings and landings of the main commercial flatfish species in the area, the common sole (*Solea solea*, L.) since 2000.

### 5.1.2 Current assessment and advice

European plaice in Subarea 8 and Division 9.a is currently assessed biennially as a category 5 stock. No reference survey to derive a biomass index exists for this stock.

Official landings have never reached the TAC set for this stock.

## 5.2 Input data for stock assessment

### 5.2.1 Landings and discards

Available data consist mainly of landings. Estimates of discarded quantities are only available for some combinations of fleets and years in the Bay of Biscay. However, when estimated, discard rates are usually quite low (<10%)(e.g. Cornou *et al.*, 2021). Therefore, only landings were considered for stock assessment.

The dataseries of landings used by the Working Group for the Bay of Biscay and the Iberian Waters Ecoregion (WGBIE) extends from 1994 to 2021. This time-series was extended back to 1950 using the Historical Nominal Catches 1950–2010 database compiled by ICES and EUROSTAT. The incorporation of these additional data necessitated the estimation of Portuguese landings prior to 1994 (first year with available Portuguese records) and the aggregation of landings by groups of two years when high variations in reported quantities between two consecutive years made suspect a pooling of landing records. Besides, reported landings for 1968 and 1999 were replaced by NA in the series used as input for SPiCT, due to missing data from France (main contributor) for those years. As a consequence, a higher relative observation error was set for the 1950–1993 landing data in the SPiCT simulations.

**Table 5.1. Nominal landings (t) of ple.27.89a. 1950–1993: Eurostat/ICES catch data; 1994–2021: data as used by WGBIE.**

| Year | Belgium | Denmark | France | Netherlands | Portugal | Spain | UK |
|---|---|---|---|---|---|---|---|
| 1950 | | | 797 | | 33* | | |
| 1951 | | | 378 | | 33* | | |
| 1952 | | | 586 | | 33* | | |
| 1953 | | | 727 | | 33* | | |
| 1954 | | | 539 | | 33* | | |
| 1955 | | | 657 | | 33* | | |
| 1956 | | | 894 | | 33* | | |
| 1957 | | | 915 | | 33* | | |
| 1958 | | | 758 | | 33* | | |
| 1959 | | | 465 | | 33* | | |
| 1960 | | | 684 | | 33* | | |
| 1961 | | | 535 | | 33* | | |
| 1962 | | | 539 | | 51* | | |
| 1963 | | | 606 | | 33* | | |
| 1964 | | | 546 | | 33* | | |
| 1965 | | | 661 | | 33* | | |
| 1966 | | | 466 | | 33* | | |
| 1967 | | | 562 | | 33* | | |
| 1968 | | | | | 33* | | |
| 1969 | | | 607 | | 33* | | |
| 1970 | | | 404 | | 33* | | |
| 1971 | | | 585 | | 33* | | |
| 1972 | | | 276 | | 33* | | |
| 1973^ | | | 910 | | 33* | | |
| 1974^ | | | 200 | | 33* | | |
| 1975 | | | 235 | 1 | 33* | | |
| 1976 | 4 | | 184 | 1 | 33* | | |
| 1977 | | | 246 | | 33* | | |
| 1978 | 6 | | 215 | | 33* | | |
| 1979 | | 7 | 220 | | 33* | | |
| 1980 | 9 | | 235 | | 33* | | |
| 1981^ | 1 | | 94 | | 33* | | |
| 1982^ | 1 | | 336 | 9 | 33* | | |
| 1983 | | | 268 | 19 | 33* | | |
| 1984 | | | 238 | 25.75* | 33* | | |
| 1985 | | | 472 | 58 | 33* | | |
| 1986 | 4 | | 369 | 17 | 33* | | 1 |
| 1987 | 13 | | 294 | | 33* | | |
| 1988 | 18 | | 435 | | 33* | | 1 |
| 1989 | 30 | | 356* | | 33* | 4 | |
| 1990 | 29 | | 443* | | 33* | | |
| 1991 | 15 | | 444* | | 33* | | |
| 1992 | 4 | | 308 | | 33* | 17 | |
| 1993 | 8 | | 355 | | 33* | 2 | |

| Year | Belgium | Denmark | France | Netherlands | Portugal | Spain | UK |
|---|---|---|---|---|---|---|---|
| 1994 | | | 365 | | 33 | 1 | |
| 1995 | | | 319 | | | 12 | |
| 1996 | | | 248 | | | 14 | |
| 1997 | | | 255 | | | 3 | |
| 1998 | | | 219 | | | 6 | |
| 1999 | 1 | | | | | 3 | |
| 2000 | 15 | | 193 | | | 22 | |
| 2001 | | | 201 | | | 22 | |
| 2002 | 1 | | 167 | | | 11 | |
| 2003 | 1 | | 217 | | 1 | 4 | |
| 2004 | | | 229 | | 163 | 7 | |
| 2005 | 4 | | 186 | | 1 | 33 | |
| 2006 | 2 | | 248 | | 1 | 5 | |
| 2007 | 5 | | 214 | | 41 | 4 | |
| 2008 | 2 | | 98 | | 89 | 4 | |
| 2009 | 2 | | 133 | | 101 | 8 | |
| 2010 | 2 | | 200 | | 112 | 12 | |
| 2011 | 2 | | 208 | | 65 | 9 | |
| 2012 | 3 | | 183 | | 63 | 4 | |
| 2013 | 0 | | 147 | | 45 | 5 | |
| 2014 | 1 | | 164 | | 51 | 6 | |
| 2015 | 2 | | 142 | | 45 | 5 | |
| 2016 | 1 | | 121 | | 49 | 4 | |
| 2017 | 1 | | 98 | | 33 | 2 | |
| 2018 | 0 | | 90 | | 39 | 3 | |
| 2019 | 0 | | 94 | | 36 | 3 | |
| 2020 | 0 | | 76 | | 46 | 4 | |
| 2021 | 0 | | 65 | | 27 | 4 | |

*** Reconstructed data.**

**^Pooled years in the SPiCT input**

The annual landings almost monotonously decrease over the considered period, from around 800 tonnes in the 1950s to slightly less than 100 tonnes in 2021.

Limited information is available on the size composition of the catch of plaice in the Bay of Biscay. For French bottom trawlers, the main fleet landing this stock, only information regarding landed fish is available. In addition, the length distribution obtained in recent years (i.e. after 2015) may not be reflective of the real size composition of the catch, as the number of observed samples has decreased with landings of the species (Figure 5.1).

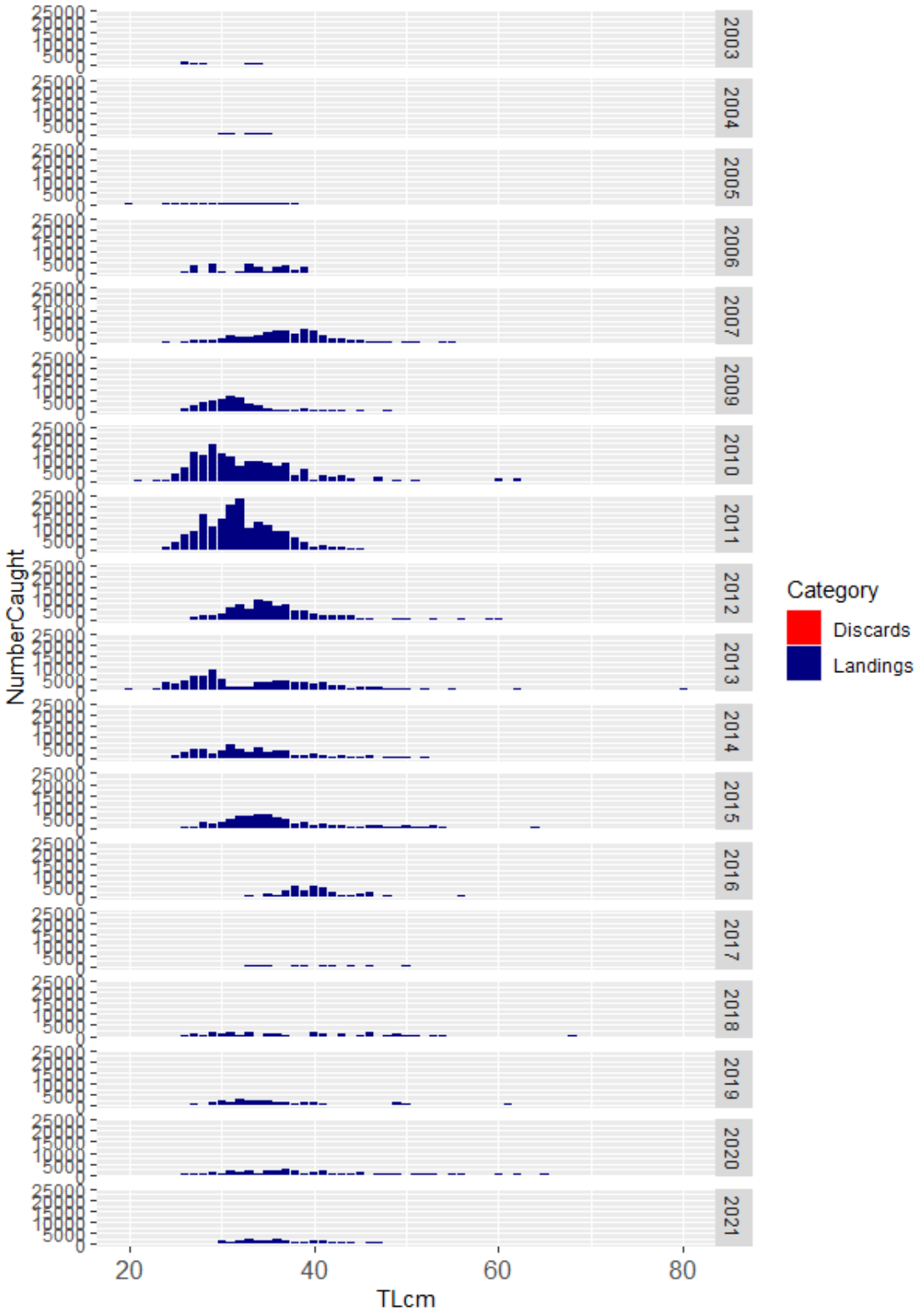


**Figure 5.1. Raised length distribution of plaice caught by French bottom trawlers (OTB, OTT) in the Bay of Biscay.**

### 5.2.2 Biomass index

As expressed in the corresponding stock annex, none of the current fishery-independent surveys provides a reliable biomass index for this stock. Concerning the Bay of Biscay, where most of the catch take place, this is mainly due to the small numbers of individuals observed during the

EVHOE (G9527, using GOV in Q4) and BTS-VIII (B1706, using beam trawl in Q4). Therefore, fishery-dependent data had to be used to provide an index of exploitable biomass for this stock. The derivation of the index was here based on landing data from the French otter trawlers, as France is the main contributor of landings for this stock and otter trawlers dominate landings for this country (around 55% for the period 2000–2021, vs. around 40% for set-nets).

The following criteria were applied to extract data for the relevant fishing vessels:

- Landings from ICES Subarea 8 and Division 9.a
- Gear codes OT, OTB and OTT
- Landings of plaice during at least 15 years
- Minimal annual number of trips with recorded plaice landings: 30
- Minimal overall landings of plaice throughout the time-series: 5 tonnes

Data are specific landings by fishing sequence as well as descriptors of the fishing sequence (ICES rectangle, métier, vessel time, date…). Due to a change in the aggregation of data (some sequences are pooled in the earlier years), only fishing sequences having taken place after 2008 were considered. The aggregation of several fishing sequences indeed decreased the frequency of zeros at the beginning of the series and was likely to create a spurious signal in the time-series of standardized LPUE. Vessel time was used to define fishing effort. Suspiciously high landings of plaice (>50 kg/hour at sea) were excluded from the dataset of fishing sequences.

A generalized additive mixed model (GAMM) was applied to describe landings per unit effort (LPUE) as a function of year, ICES rectangle, month, and a targeting factor, with vessel identifier as a random effect. Year, ICES rectangle and month were introduced as factors in the model. A Tweedie distribution of the error, with a log-link was used to account for the large proportion of zeros (49.8%) in the input data. As the distribution of residuals of the selected model displayed an excess of high values, leading to a deviation from their expected distribution, a transformation of the dependent variable was applied. LPUE where raised to the power of 0.4 to obtain an acceptable distribution of the deviance residuals.

The influence of targeting on plaice LPUE, expressed through the specific composition of landings was introduced into the model in two different ways. Following a principal component analysis on the double square root transformed LPUE, either the coordinates of fishing sequences on the main principal components or the cluster (following a classification based on the main principal components) to which a sequence belongs were used. The best model was then selected by performing an ANOVA to compare the fits of the different models. These models were:

- a model with year effect only
- a model with year, ICES rectangle and month effects
- a model with year, ICES rectangle and month effects, with targeting expressed though coordinates on the main principal components
- a model with year, ICES rectangle and month effects, with targeting expressed as a cluster

The ANOVA led to the selection of the third type of model, with targeting characterized by the coordinates on the first three principal components. The final model can be written as:

$$\log\left(\overline{LPUE_t^{0.4}}\right) \sim Year_i + Rectangle_i + Month_i + s_1(PC1) + s_2(PC2) + s_3(PC3) + Random(Vessel)$$

where $\overline{LPUE_t^{0.4}}$ is the expected value of the transformed plaice LPUE for fishing sequence $i$, and PC are the coordinates of fishing sequence $i$ on the first three principal components.

The time-series of standardized LPUE was obtained by fixing the effects of all variables except *Year*.

A back-transformation to the natural scale was done as

$$\overline{LPUE} = SE\left(\overline{LPUE^{0.4}}\right)^{1/0.4} + \overline{LPUE^{0.4}}^{1/0.4}$$

For the *stdevfacI* parameter reflecting the relative uncertainty associated to each estimated value in the time-series of the biomass index, the corresponding standard error associated with $\overline{LPUE^{0.4}}$ was used. There are however doubts on whether the choice of the standard error associated with the non back-transformed expected LPUE is appropriate.

The targeting factor, when expressed through the coordinates on the first three principal component, did not strongly modify the variation of the estimated biomass index over time compared to models only including the year effect ('Base') or the year, month and spatial effects ('Spatial'; Figure 5.2).

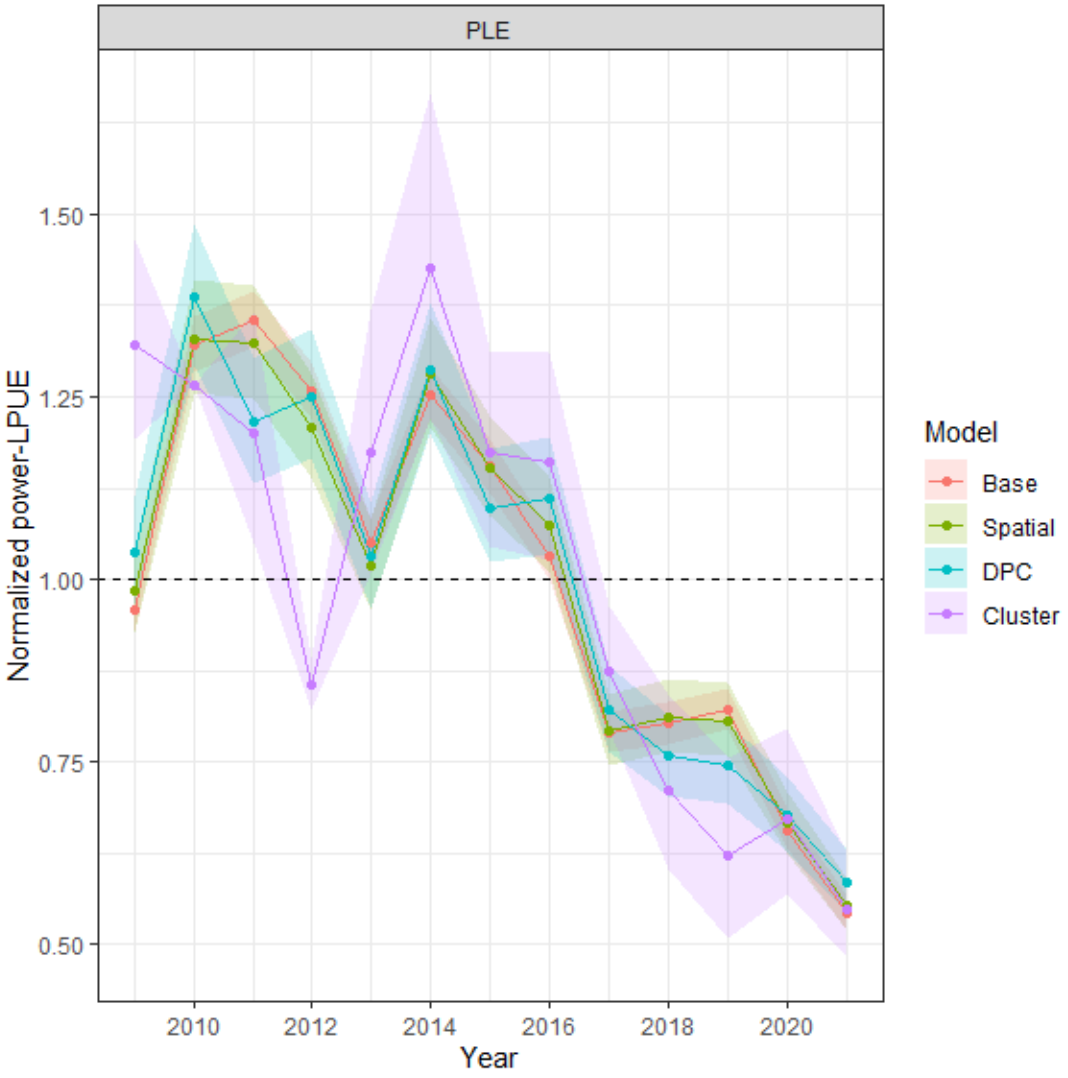


**Figure 5.2. Standardized $LPUE^{0.4}$ time-series obtained from the four GAMM tested for ple.27.89a.**

**Table 5.2. LPUE series for ple.27.89a, back-transformed to natural scale, and associated standard deviation on the original scale.**

| Year | $\overline{LPUE}$ | s.e. (original scale) |
|---|---|---|
| 2009 | 1.133 | 0.208 |
| 2010 | 2.303 | 0.420 |
| 2011 | 1.625 | 0.295 |
| 2012 | 1.739 | 0.318 |
| 2013 | 1.090 | 0.199 |
| 2014 | 1.901 | 0.346 |
| 2015 | 1.252 | 0.228 |
| 2016 | 1.252 | 0.229 |
| 2017 | 0.628 | 0.115 |
| 2018 | 0.473 | 0.087 |
| 2019 | 0.451 | 0.083 |
| 2020 | 0.381 | 0.071 |
| 2021 | 0.281 | 0.052 |

### 5.2.3 Prior distributions

*Shape parameter n of the surplus production model*

In scenarios where this *n* was constrained, this parameter was fixed to a value of 2, corresponding to a Schaefer model.

*Ratios of observation to process errors alpha and beta*

Due to limited contrast in the time-series of landings and the relatively short series of biomass index combined with a one-way trajectory of the latter, it was decided to disable the default priors on *alpha* and *beta*. Despite the fact that these default priors are relatively uninformative, this option was retained to ensure that the process errors would not be spuriously inflated due to a high uncertainty associated with the series of landings or biomass index.

Instead, the relative standard errors associated with the annual estimates of the biomass index (standardized so that their mean was equal to 1) were used to specify the relative observation error associated with the series of exploitable biomass, through the parameter *stdevfacI*.

*Intrinsic rate of increase r*

Machiels *et al*. (2007) estimated the intrinsic rate of increase of the population of plaice in the North Sea to be 0.35 or 0.30, depending on the approach applied to derive this parameter (multiple regression using available landings and LPUE data or fitting a state-space biomass surplus production model). These values are slightly higher than the estimate produced by the FishLife

package for plaice: 0.25 when applying the Fit_model function, and a mean value of 0.28 when using the Plot_taxa function. Using the flmvn_traits function from the SPM prior library and adding information about Linf (mean = 50cm, CV = 2) and length at maturity (mean = 25 cm, CV = 1) from neighbouring populations yielded a mean estimate of 0.24 and a CV of 0.15.

Based on these various estimates, two priors were tested. They were defined by median values of 0.24 and 0.35, following the minimum and maximum estimates previously mentioned. A relatively high uncertainty was associated with these values, with a standard deviation of 0.4, to have a limited constraint on the fitting of the model.

*Initial depletion fraction bkfrac*

As recommended, two prior distributions were tested for the initial depletion, reflecting in this case the biomass in 1994 relative to the carrying capacity *K*. They differed by their median value: 0.2 and 0.5, while the associated uncertainty was set rather high (s.d. = 0.5) due to the absence of information on historical level of biomass for this stock. Unlike the priors set on the intrinsic rate of increase, the informative priors defined for *bkfrac* do not reflect a level of knowledge of the stock of plaice but are applied to assess the sensitivity of the model output to this parameter.

### 5.2.4 Exploratory assessments

Different scenarios were tested to assess the sensitivity of the outcomes to different specifications of the priors. The different outcomes were then assessed in light of the acceptance criteria defined by Mildenberger *et al.* (2021). In ascending order of information provided by the priors, the trialled scenario were:

- with SPiCT default priors, with priors on alpha and beta disabled (#1)
- same as scenario #1, with surplus production model forced to a Schaefer formulation (#2)
- same as scenario #1, with additional informative prior on *r* (median at 0.24 or 0.35; #3, #4)
- with informative priors on *r* (median at 0.24 or 0.35), Schaefer formulation (#5, #6)
- with informative priors on *bkfrac* (median at 0.2 or 0.5), Schaefer formulation (#7, #8)
- with informative priors on *bkfrac* and *r*, with same median values as listed above, Schaefer formulation (#9, #10, #11, #12)

**Table 5.3. Acceptance diagnostics for the tested scenarios. 1 indicates that the acceptance criterion has been met, 0 otherwise. Convergence: convergence of the SPiCT run; Finite s.d.: indicates whether all variances of the parameters are finite; Residuals indicates whether model assumptions regarding one-step-ahead residuals have been met; Retro: indicates the presence of consistent patterns in the retrospective analysis; Prod. curve: indicates whether the shape of the production curve is realistic; Uncertainty: indicates whether the confidence intervals around $B/B_{MSY}$ and $F/F_{MSY}$ are not excessively large; Sensi. inits: indicates whether parameter estimates are sensitive to initialization values.**

| #Scenario | Scenario name | Convergence | Finite s.d. | Residuals | Retro. | Prod. curve | Uncertainty | Sensi. inits |
|---|---|---|---|---|---|---|---|---|
| 1 | Default | 0 | 0 | 0 | 0 | 1 | 0 | 0 |
| 2 | Schaefer | 0 | 0 | 0 | 0 | 1 | 0 | 0 |
| 3 | r035 | 1 | 1 | 0 | 0 | 1 | 0 | 0 |
| 4 | r024 | 1 | 1 | 1 | 0 | 1 | 0 | 0 |
| 5 | Schaefer_r024 | 1 | 1 | 0 | 0 | 1 | 0 | 0 |
| 6 | Schaefer_r035 | 0 | 0 | 0 | 0 | 1 | 0 | 0 |
| 7 | Schaefer_bk02 | 1 | 1 | 0 | 1 | 1 | 0 | 0 |

| #Scenario | Scenario name | Convergence | Finite s.d. | Residuals | Retro. | Prod. curve | Uncertainty | Sensi. inits |
|---|---|---|---|---|---|---|---|---|
| 8 | Schaefer_bk05 | 0 | 0 | 0 | 0 | 1 | 0 | 0 |
| 9 | Schaefer_r024_bk02 | 1 | 1 | 0 | 1 | 1 | 0 | 1 |
| 10 | Schaefer_r035_bk02 | 0 | 0 | 0 | 0 | 1 | 1 | 0 |
| 11 | Schaefer_r024_bk05 | 1 | 1 | 0 | 0 | 1 | 0 | 0 |
| 12 | Schaefer_r035_bk05 | 0 | 0 | 0 | 0 | 1 | 1 | 0 |

Model convergence was reached for only half of the tested scenarios. None of the considered scenarios were accepted, as at least two acceptance criteria were not met.

## 5.3 Future considerations/recommendations

The stock annex indicates " The stock unit definition of plaice (*Pleuronectes platessa*) in this area is not clear. WGNEW concluded that in the absence of specific information on stock structure". This implies that the biomass index derived from landings by fishing sequence of French trawlers operating in the Bay of Biscay may not reflect the variations of exploitable biomass along the Portuguese coast (Division 9.a). A spatial discontinuity in the distribution of plaice landings in the stock area suggests the existence of distinct subpopulations that way have distinct dynamics. This matter needs further investigation before considering the application of a unique surplus production model for the whole area.

## 5.4 Reviewer report

No fishery-independent survey time-series is available for this stock.

Although survey data exists (e.g. EVHOE and BTS-VIII), the number of individuals of plaice caught in these surveys are low, so it was not considered in the benchmark. However, future benchmarks could explore model-based indices, such that the data from the above mentioned surveys could be combined and thereby perhaps overcome the problem of few individuals observed in each individual survey.

Instead, a model based commercial LPUE index was derived. This index could only go back to 2008, because earlier data were aggregated into several fishing sequences. Concerns were raised about how well such an LPUE index reflects changes in stock biomass when the fishery does not target plaice, although the index seemed fairly robust to different target factor definitions in the model.

Another concern raised was the formula used to back-transform the LPUE index to natural scale as well as the associated uncertainty. It was not clear why the standard error was included in the formula for the back-transformation, as it should not be.

The main reason for rejecting the SPiCT assessment for this stock was however the failure to meet all the standard acceptance criteria in any of the 12 tested model runs.

The uncertainty from SPiCT was very high, and the results were quite dependent on the choice of prior on the initial depletion level.

However, there are some indications that the stock is in a depleted state. The LPUE index indicates a decreasing trend, and the ICES historical catch database reports that past landings have

been more than five times current levels, and landings have always been below the TAC in recent years.

It is, however, also worth noting that this stock is at the southern limit of the distribution area for the species, so the decrease in abundance could be driven by climate rather than fisheries or a combination of the two.

### 5.4.1 Conclusions

It was not possible for the group to recommend or approve a SPiCT assessment for this stock. The reasons for this were doubts on whether a LPUE index such as derived here would appropriately reflect changes in biomass for a stock essentially caught as a bycatch in directed fisheries on common sole or cephalopods (squids and cuttlefish), doubts linked to the back-transformation of the LPUE index to the natural scale, as well as the severe constraints that needed to be applied to reach convergence and avoid the stock fluctuating on two different states depending on the initial values. The 'one-way trip' trajectories of landings and biomass index considerably complicated the estimation of parameters and contributed to a high level of uncertainty associated with parameter estimates. Alternatively, the use of integrated models could be explored in future to account for the amount of size and age information available for this stock and spatial differences over the area of distribution of the stock.

## 5.5 References

Cornou, A.-S., Quinio-Scavinner, M., Sagan, J., Cloâtre, T., Dubroca, L., and Billet, N. 2021. Captures et rejets des métiers de pêche français. Résultats des observations à bord des navires de pêche professionnelle en 2019. ObsMer. doi: https://doi.org/10.13155/79198. https://archimer.ifremer.fr/doc/00680/79198/

Hoarau, G., Piquet, A. M.-T., van der Veer, H. W., Rijnsdorp, A. D., Stam, W. T., and Olsen, J. L. 2004. Population structure of plaice (Pleuronectes platessa L.) in northern Europe: a comparison of resolving power between microsatellites and mitochondrial DNA data. Journal of Sea Research, 51: 183–190.

Machiels, M. a. M., Kraak, S. B. M., Borges, L., and Bogaards, H. 2007. Stock assessment of North Sea plaice using surplus production models. C032/07. IMARES. https://research.wur.nl/en/publications/stock-assessment-of-north-sea-plaice-using-surplus-production-mod (Accessed 4 January 2023).

Mildenberger, T. K., Kokkalis, A., and Berg, C. W. 2021, February 20. Guidelines for the stochastic production model in continuous time (SPiCT).

# 6 Celtic Seas and the English Channel pollack

## pol.27.67 – *Pollachius pollachius* in subareas 6-7

## 6.1 Introduction

*Habitat and Stock Identification*

Pollack are a gadoid primarily found on rocky bottoms or around reef or wreck features, which is particularly true for young pollack that occur mostly inshore. The stock structure of pollack populations in this ecoregion is unclear. ICES does not necessarily advocate that subareas 6 and 7 constitutes a management unit for Pollack, and further work is required.

### 6.1.1 Fishery information

*Commercial Fishery*

Pollack is an important commercial species in divisions 6 and 7, with landing of up 9000 tonnes in the 1980s. Due to its habitat, targeted fisheries of pollack are often localized and small scale due to the high level of local knowledge required and the more specialized gear utilized. As well as the targeted fishery, a large proportion of landings are due to pollack being a valued bycatch species of a range of other fisheries using various gear across the stock area.

*Recreational*

There are considerable catches of pollack by recreational fishers, either from small boats or shore based fishers. The exact level of catch is poorly understood and difficult to estimate, but it may be a similar level to commercial landings.

### 6.1.2 Current assessment and advice

The current assessment for pol.27.67 uses a Depletion-Corrected Average Catch method. The method aims to estimate a catch that is likely to be sustainable long term. The only input to the assessment is commercial landings data, and because it is the total catch that is used, the output to the model is always similar to previous estimates. The model is unable to provide reference points, and there is no way to identify whether changes in catch are due to changes in fishing effort or stock biomass. Recent landings have been below the catch levels that have been estimated to be sustainable.

## 6.2 Input data for stock assessment

### 6.2.1 Landings and discards

#### 6.2.1.1 Official landings data

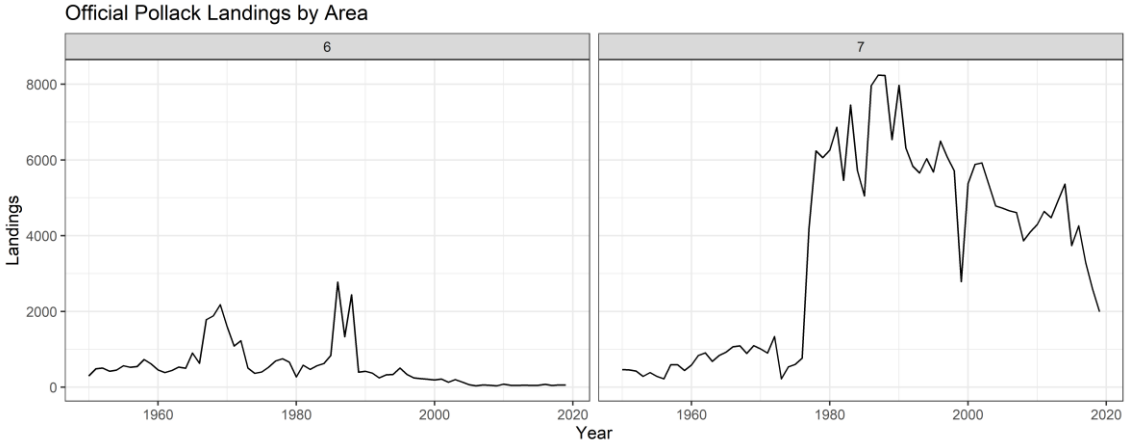


**Figure 6.1 Official landings of pollack by area.**

Pollack landings increased dramatically in the late 1970s (Figure 6.1) due to a large increase in reported French landings (Figure 6.2). The landings peaked in the late 1980s and have been in general decline since then. It was decided to use the official landings from 1986 onwards, because prior to that the values are difficult to trust, primarily because Ireland reported zero pollack landings for the previous 10 years, despite having landings in the 1960s and 1970s. It is likely that Irish landings were mis-codified with saithe during that period. Spain also reported a huge spike in landings in area 6 in the mid-1980s and these landings were removed for the assessment. There is a missing year in the French data in 1999, and this value was replaced with the mean landings of the 2 years either side. The official landings values (Table 6.1) are used for the assessment from 1986 to 2003, when InterCatch landings become available.

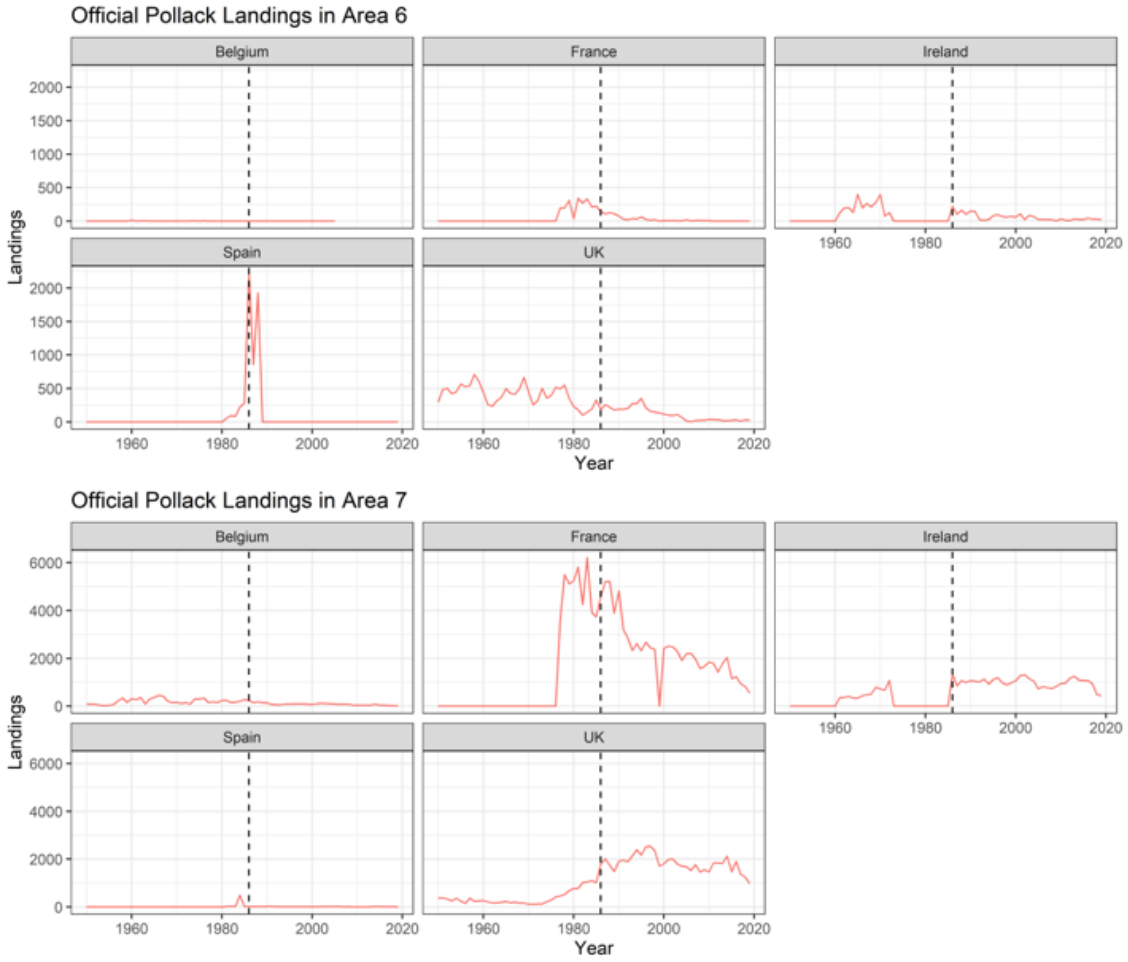


**Figure 6.2 Official pollack landings broken down by country and division.**

**Table 6.1 Official landings of pollack in areas 6 and 7 as adjusted for use in assessment (tonnes).**

| Year | Belgium | France | Germany | Ireland | Netherlands | Norway | Spain | UK | Total |
|---|---|---|---|---|---|---|---|---|---|
| 1986 | 241 | 4719 | 0 | 1558 | 0 | 0 | 17 | 1982 | 8517 |
| 1987 | 149 | 5321 | 0 | 951 | 0 | 0 | 19 | 2269 | 8709 |
| 1988 | 191 | 5339 | 0 | 1229 | 0 | 0 | 22 | 1961 | 8742 |
| 1989 | 145 | 4004 | 1 | 1097 | 0 | 0 | 18 | 1666 | 6931 |
| 1990 | 133 | 4907 | 0 | 1216 | 0 | 1 | 26 | 2106 | 8389 |
| 1991 | 76 | 3242 | 0 | 1190 | 0 | 0 | 26 | 2151 | 6685 |
| 1992 | 62 | 2870 | 0 | 1037 | 0 | 0 | 19 | 2092 | 6080 |
| 1993 | 55 | 2364 | 0 | 1149 | 0 | 0 | 7 | 2408 | 5983 |
| 1994 | 94 | 2655 | 0 | 947 | 0 | 0 | 8 | 2667 | 6371 |
| 1995 | 88 | 2379 | 3 | 1190 | 0 | 0 | 4 | 2522 | 6188 |
| 1996 | 94 | 2713 | 0 | 1287 | 6 | 1 | 5 | 2729 | 6835 |

| | | | | | | | | | |
|---|---|---|---|---|---|---|---|---|---|
| 1997 | 99 | 2457 | 1 | 1053 | 4 | 2 | 7 | 2702 | 6325 |
| 1998 | 92 | 2396 | 0 | 946 | 1 | 0 | 11 | 2494 | 5940 |
| 1999 | 86 | 2439 | 0 | 1049 | 0 | 6 | 19 | 1839 | 5438 |
| 2000 | 71 | 2433 | 2 | 1131 | 0 | 0 | 5 | 1926 | 5568 |
| 2001 | 100 | 2523 | 0 | 1382 | 0 | 0 | 9 | 2088 | 6102 |
| 2002 | 117 | 2490 | 0 | 1334 | 0 | 0 | 17 | 2095 | 6053 |
| 2003 | 113 | 2287 | 0 | 1239 | 0 | 1 | 12 | 1899 | 5551 |
| 2004 | 104 | 1916 | 0 | 1117 | 1 | 1 | 13 | 1770 | 4922 |
| 2005 | 98 | 2221 | 0 | 756 | 1 | 0 | 16 | 1700 | 4792 |
| 2006 | 78 | 2213 | 0 | 834 | 1 | 0 | 32 | 1535 | 4694 |
| 2007 | 90 | 1979 | 0 | 804 | 3 | 6 | 1 | 1787 | 4671 |
| 2008 | 76 | 1586 | 0 | 758 | 1 | 1 | 14 | 1483 | 3919 |
| 2009 | 41 | 1677 | 0 | 833 | 4 | 0 | 3 | 1580 | 4137 |
| 2010 | 35 | 1852 | 0 | 976 | 2 | 0 | 3 | 1505 | 4373 |
| 2011 | 37 | 1786 | 0 | 979 | 2 | 0 | 4 | 1881 | 4690 |
| 2012 | 43 | 1424 | 0 | 1174 | 1 | 0 | 5 | 1878 | 4525 |
| 2013 | 39 | 1791 | 0 | 1284 | 1 | 0 | 11 | 1848 | 4973 |
| 2014 | 84 | 2043 | 0 | 1121 | 1 | 0 | 14 | 2145 | 5408 |
| 2015 | 32 | 1154 | 0 | 1093 | 1 | 0 | 13 | 1495 | 3787 |
| 2016 | 42 | 1237 | 0 | 1117 | 0 | 0 | 12 | 1928 | 4337 |
| 2017 | 19 | 942 | 0 | 964 | 0 | 0 | 12 | 1393 | 3331 |
| 2018 | 21 | 819 | 0 | 515 | 9 | 0 | 13 | 1273 | 2649 |
| 2019 | 12 | 552 | 0 | 469 | 2 | 0 | 3 | 1008 | 2046 |

#### 6.2.1.2 InterCatch data

Landings and discard data for pollack are available from InterCatch are available since 2003 (Figure 6.3). France has the highest catches of pollack with the UK and Ireland also contributing significantly, but with very low catches by other countries. French landings have been in general decline since 2003, whereas catches by Ireland and England have been stable up until the last five years when they have also shown a significant decrease.

Discards have been low (approx. 1%) and are considered negligible are not included in the assessment.

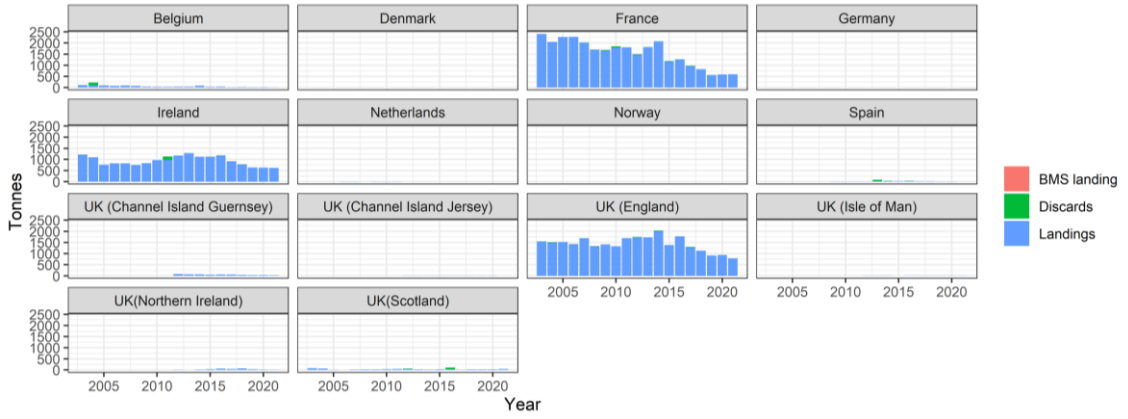


**Figure 6.3 Landings and discards of pollack from InterCatch broken down by country.**

The highest catches have historically been in 7.e, with England and France both fishing primarily there and in 7.h. Irish catches have mostly been in areas 7..g and 7.j (Figure 6.4).

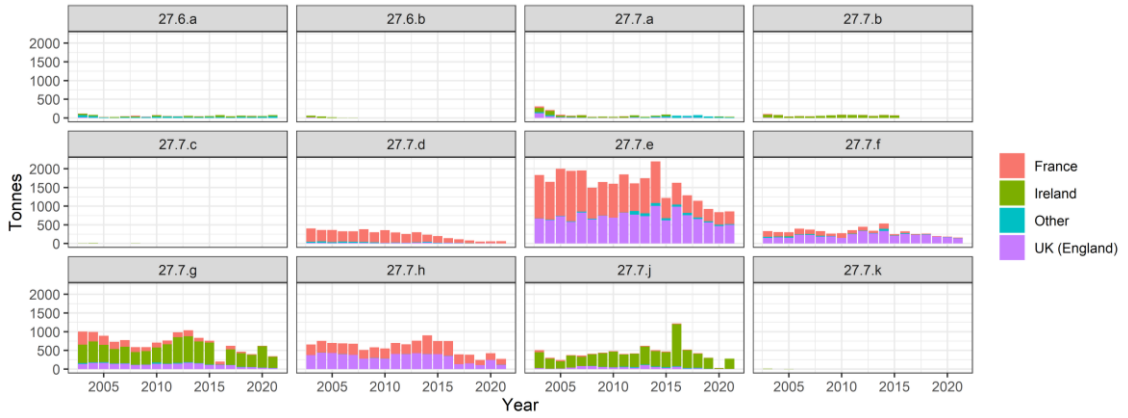


**Figure 6.4 InterCatch landings in subdivisions by country.**

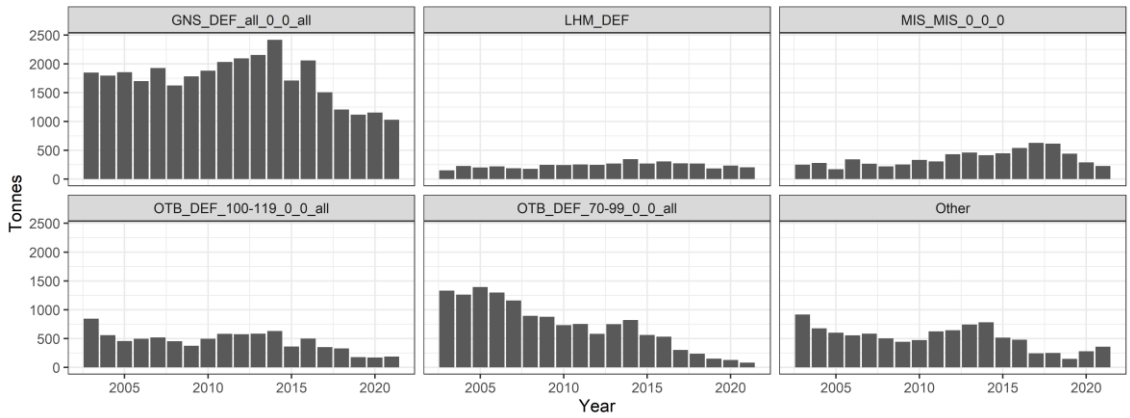


**Figure 6.5 InterCatch landings by main gear types.**

The largest contributor to landing are gillnets, followed by the otter trawl métiers. There is also a significant contribution from line métiers and other localized and specialised métiers (Figure 6.5). There are significant differences when broken down by country. England predominantly lands pollack from gillnets, whereas Ireland landings are from gillnets and miscellaneous métiers. Historically, the majority of the French landings were from the OTB métiers, although their contribution to the landings has decreased substantially in the last 10 years (Figure 6.6). A

big contributor to this reduction seems to be a change in behaviour and reduced targeting of pollack by those métiers.

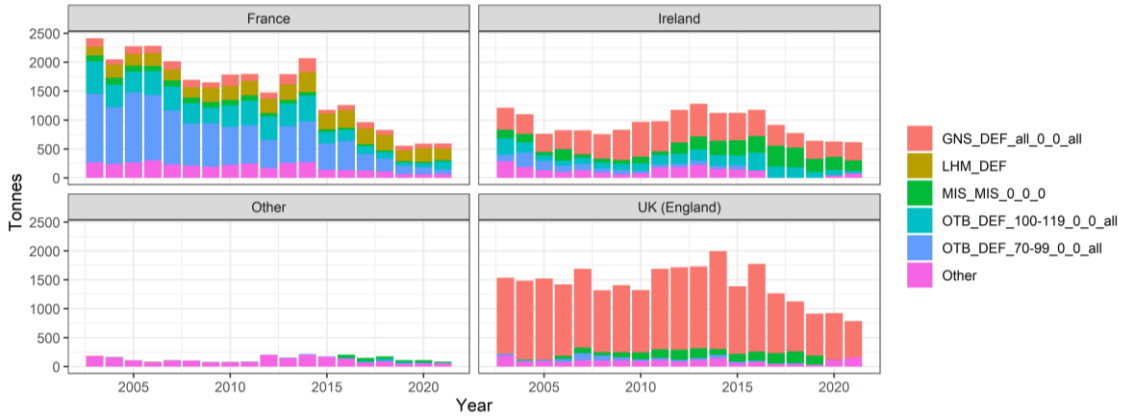


**Figure 6.6 InterCatch landings by gear type and country.**

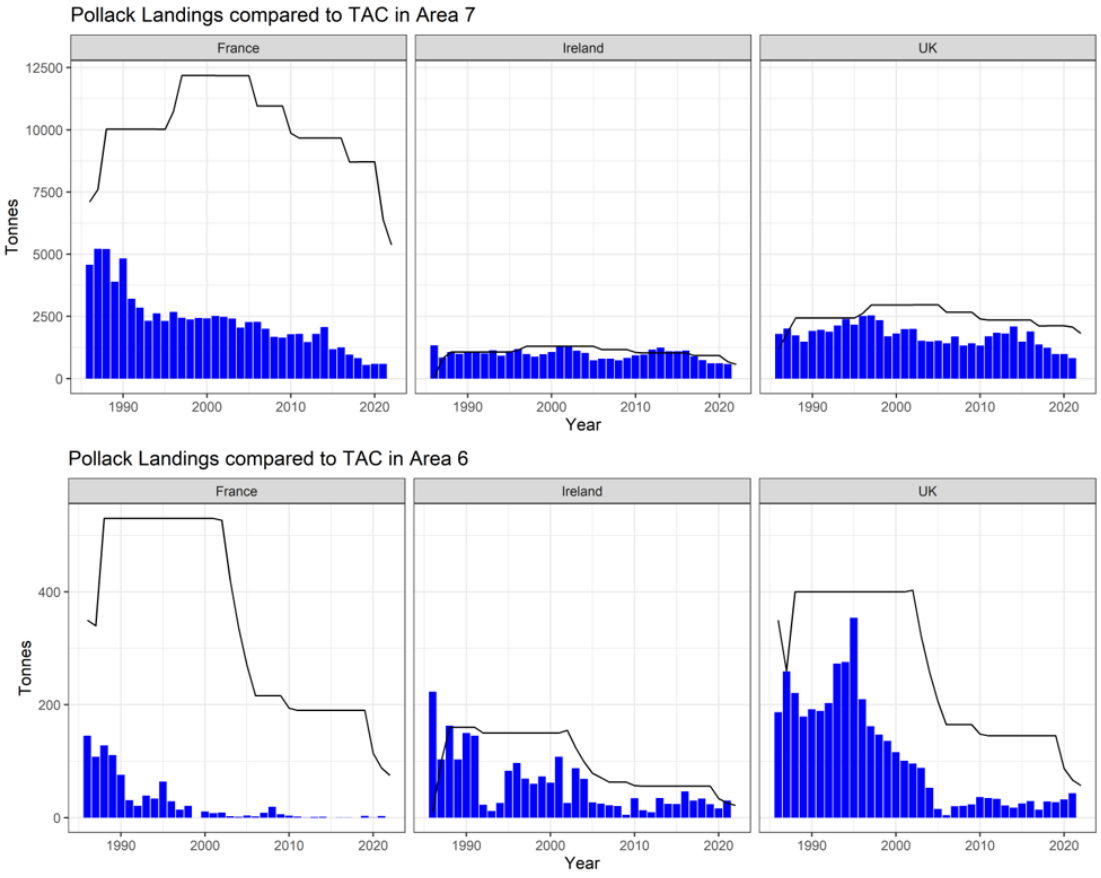


**Figure 6.7 Pollack quota uptake.**

Figure 6.7 shows the quota uptake by the main nations fishing on pollack in the area. In 2021, the combined quota for areas 6 and 7 was 6087 tonnes greater than the landings. This is primarily due to the very low French uptake of the quota. Ireland and the UK's quota has been much more fully utilized. Overall the TAC is not restrictive, because of the national breakdown, but decreasing catches might well be due to quota restraints.

Commercial landings of pollack are complex and difficult to breakdown. The métiers that target pollack are often small scale, localized and opportunistic, making it hard to appropriately

measure effort or know what is driving changes in catches. Similarly, pollack is often a small part of bycatch in larger métiers whose behaviour and catches are driven by other factors.

### 6.2.2 Recreational fisheries

Recreational fishing contributes significantly to the catches of pollack in this stock area, however it is difficult to quantify the amount of removals and the impact on the stock. The recreational sector is comprised of charter vessels, small boats and shore based anglers. This makes estimating recreational fishing levels incredibly challenging and uncertain.

The UK has estimates of recreational catches of pollack (Figure 6.8), which are reasonably stable across the six-year timeframe. The mean catches of pollack over the period are 3368 tonnes, with an estimated 1219 tonnes retained by the recreational fishers. There is very limited data on survival of released pollack, and is likely to differ based on what type of recreational fishing it ism so the effective removals from the stock may be towards the catch estimates rather than the removals estimate.

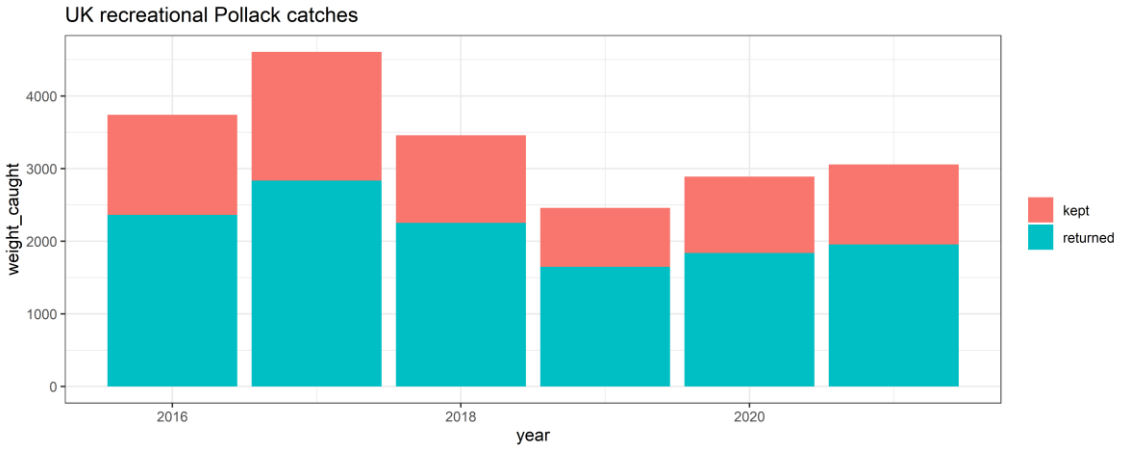


**Figure 6.8. UK estimates of recreational catches of pollack.**

Ireland has conducted preliminary work on estimated recreational catches of pollack, and although the data are not ready for inclusion in a stock assessment, it does broadly fall in line with the UK's estimates. There is very few data available for French recreational fishing of pollack.

The best available estimate of pollack recreational catches in the area comes from (Radford *et al.*, 2018) and estimates catches of approximately 3500 tonnes annually. This comes from data that is several years old, however, and assumes 100% mortality of released pollack. This value at least offers a starting point to trial through the assessment process. The UK data, although a short time-series, does show a reasonably consistent ratio between recreational and commercial catches. It is therefore reasonable to test the model assuming a consistent ratio between commercial and recreational landings, as well as an alternative hypothesis of constant recreational catches of 3500 tonnes.

### 6.2.3 Survey data

The assessment makes use of four surveys to produce an abundance index using Vector Autoregressive Spatio-Temporal (VAST). The surveys are not designed to catch pollack and often avoid either the inshore habitats, rocky substrata or hard features that make up pollack's primary habitat. These trawl surveys are conducted on clean trawlable ground which is not the core habitat for pollack so catches might not be truly representative of the pollack stock abundance and dynamics.

#### 6.2.3.1 IGFS

The Irish Groundfish Survey data goes back to 2003 and covers the main pollack fishing areas around Ireland. Pollack are not caught in large numbers, despite the large number of stations and geographic extent of the survey (Figure 6.9), and are caught at just 5% of stations fished. Catches are localized and tend to be off the northwest or southwest coast of Ireland (Figure 6.10). Catches have been low since 2015 with less than 25 fish caught each survey year. Prior to 2015 catch numbers were generally similar, but interspersed with a few years where the number of pollack caught could be 2 or 3 times higher than normal (Figure 6.11). Historically the majority of catches in the survey have also been in Subdivision 6.a, which is an area with very low pollack landings. In 2021 the number of pollack caught dropped to just four pollack in 157 stations. Due to the small number of fish sampled the survey data are quite uncertain and may experience dramatic interannual variation either due to survey changes, an unusually high catch or if some of the higher expected abundance stations are not sampled in any given year. For example, in 2018 and 2019 there were few stations inshore around the southwest tip of Ireland, which have often had the highest pollack catches, and this resulted in overall low pollack estimates for that year. Due to the localized nature of the pollack habitat the survey output is quite dependent on the stations able to be fished each year. Figure 6.11 show the breakdown of fish numbers in the survey by area. Catch numbers are highest in 6a which is in contrast to catches in the commercial fisheries which show higher catches in Area 7.

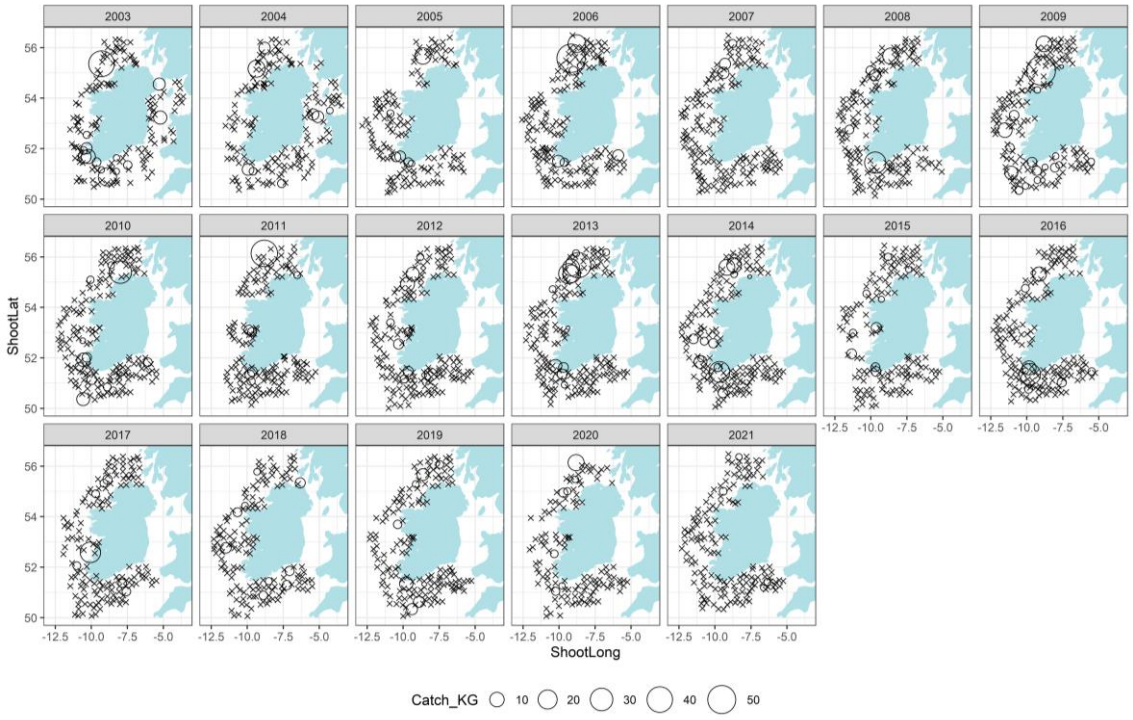

**Figure 6.9 IGFS Stations sampled and pollack caught.**

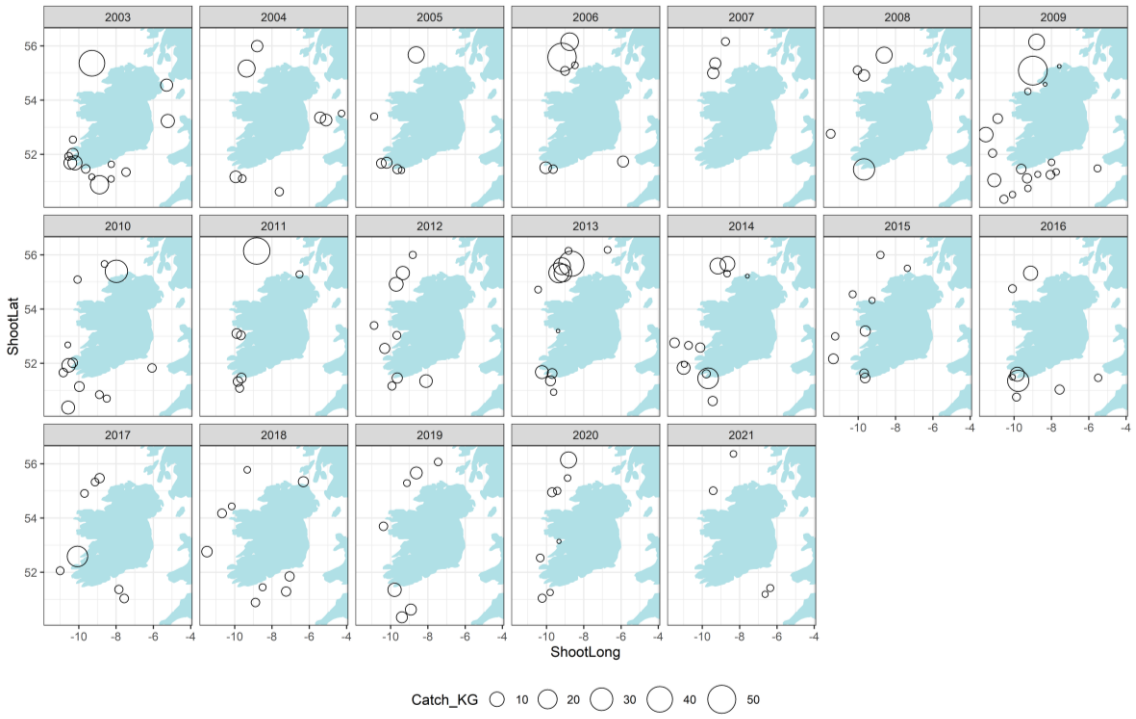


**Figure 6.10 IGFS Pollack caught (only positive stations included)**

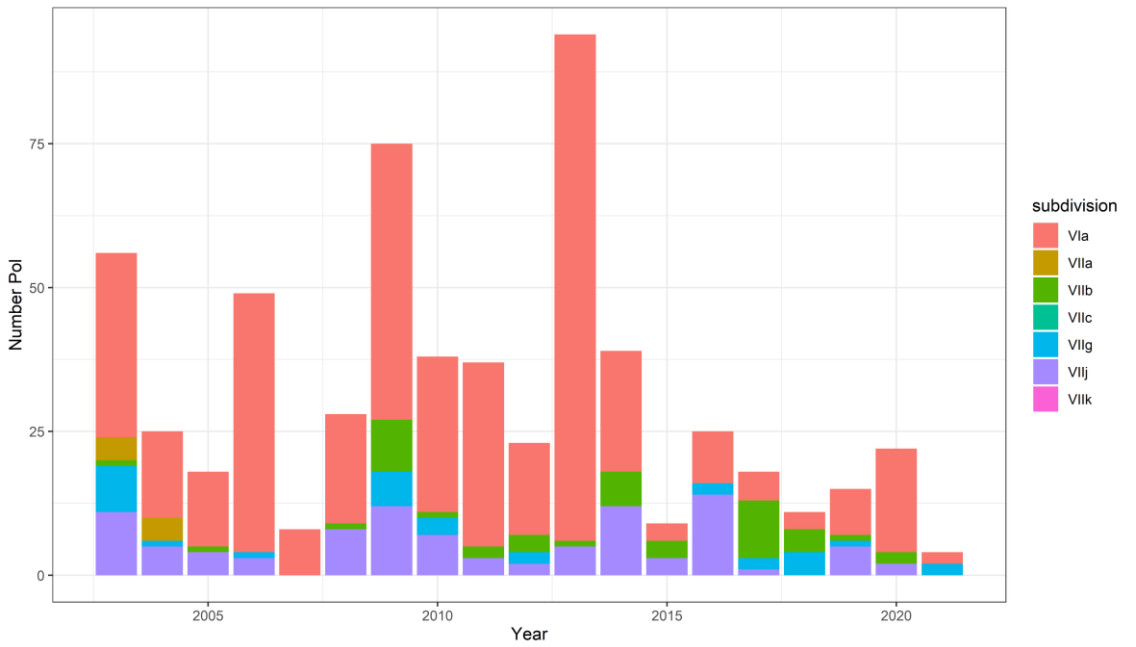


**Figure 6.11 IGFS Number of pollack caught by subdivision and year.**

### 6.2.3.2 EVHOE

The French bottom-trawl survey data goes back to 1997 and incorporates the Celtic Sea and Bay of Biscay, but for this index only the data from division 7 is included. The EVHOE survey has

historically caught pollack at less than 3% of stations, with a lot of the stations being further offshore (Figure 6.12). On average the survey catches 2 pollack per year, and has never exceeded 10 pollack in one year (Figure 6.13). In the last decade, pollack have only been caught in 4 years, which explains the downward trend in pollack catches (Figure 6.14). Although the survey has only caught 11 fish in the last decade, in the subdivisions the surveys operate, there have been nearly 20 000 tonnes of pollack landed by commercial vessels (mean 1 961 tonnes annually). The survey cannot be regarded as very representative of the fishery.

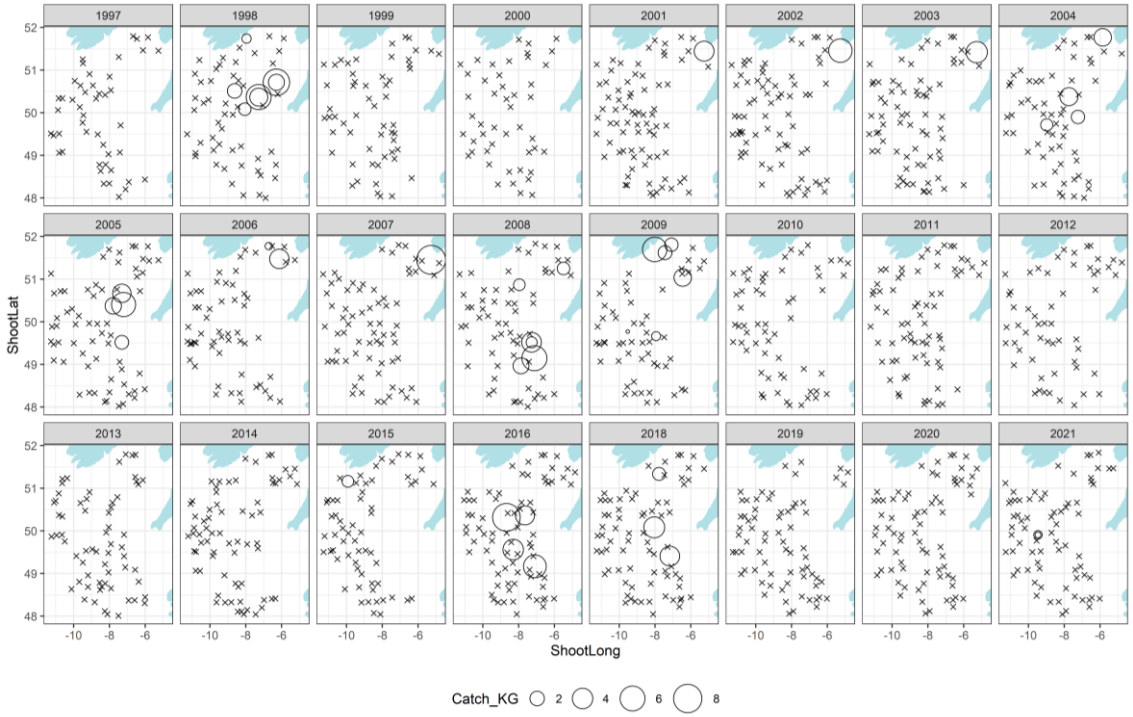


**Figure 6.12 EVHOE Stations sampled and pollack caught.**

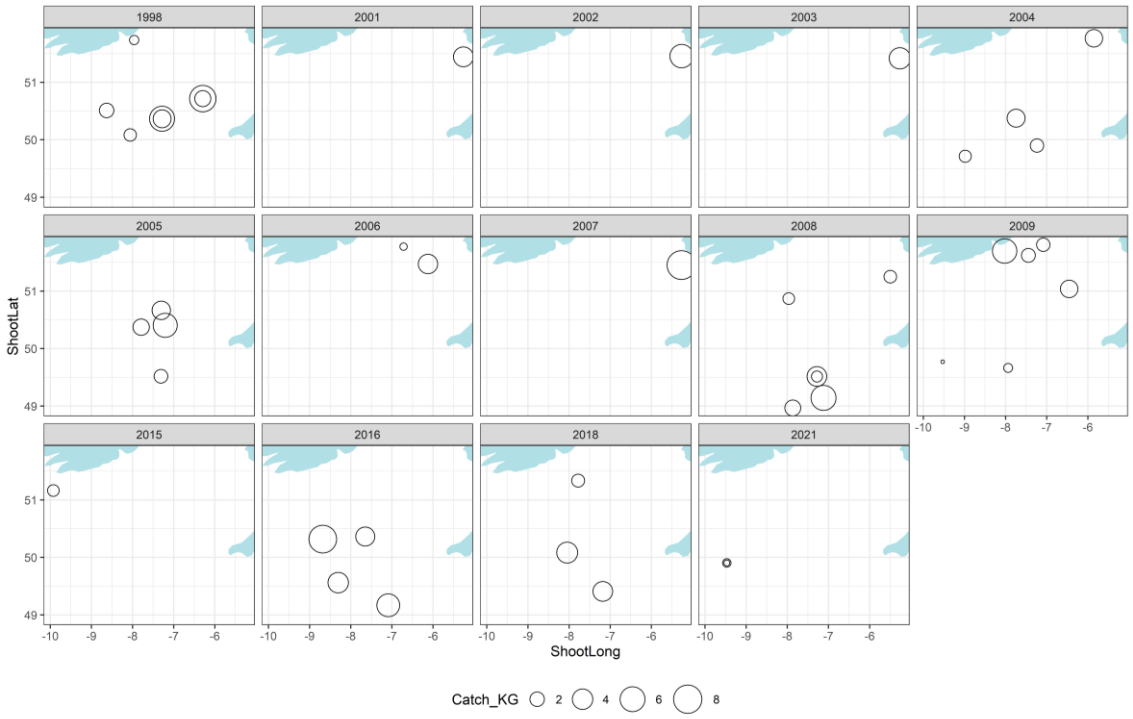


**Figure 6.13 EVHOE Pollack caught (only positive stations included).**

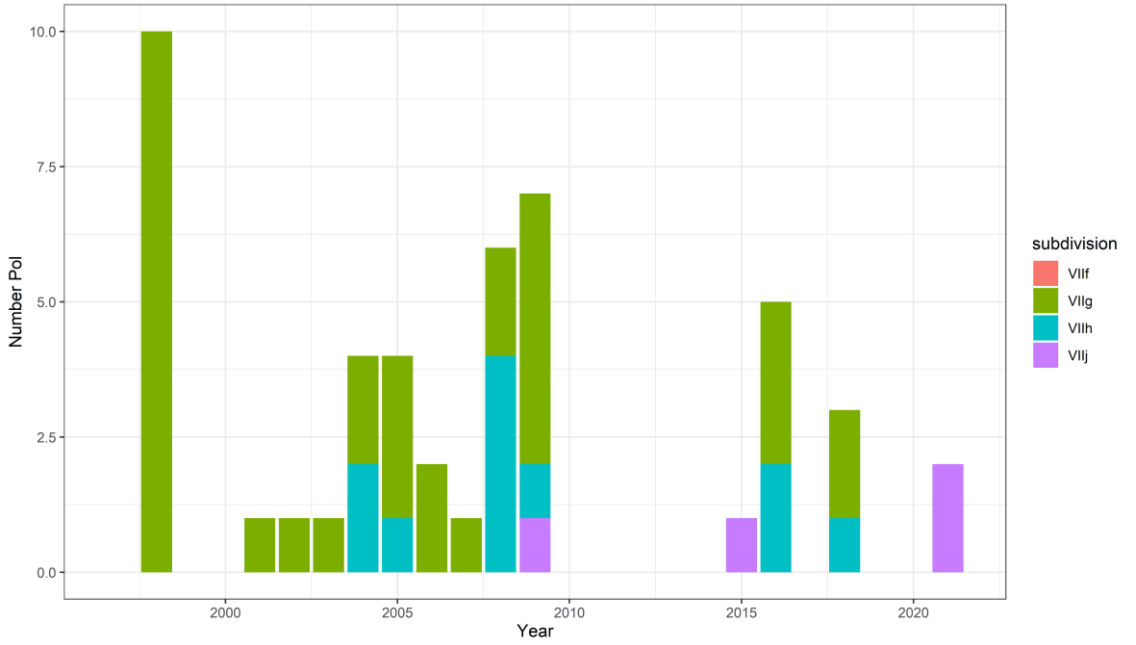


**Figure 6.14 EVHOE Number of pollack caught by subdivision and year.**

### 6.2.3.3 IAMS

The Irish Anglerfish and Megrim survey has only been running since 2016 and although designed to target those species, it does also catch pollack. The survey avoids rocky bottom locations and has few inshore stations so it does avoid the main pollack habitats. Pollack have been caught in just over 10% of stations, primarily being caught in the more coastal stations (Figure 6.15). The pattern of catches matches that found in the IGFS (Figure 6.16), although the 2020 survey was severely restricted in geography. The survey has on average caught 43 pollack annually and has been reasonable consistent in the 6 years it's been running (Figure 6.17). A significant proportion of the catches have occurred in Division 6, which has very low levels of commercial pollack landings.

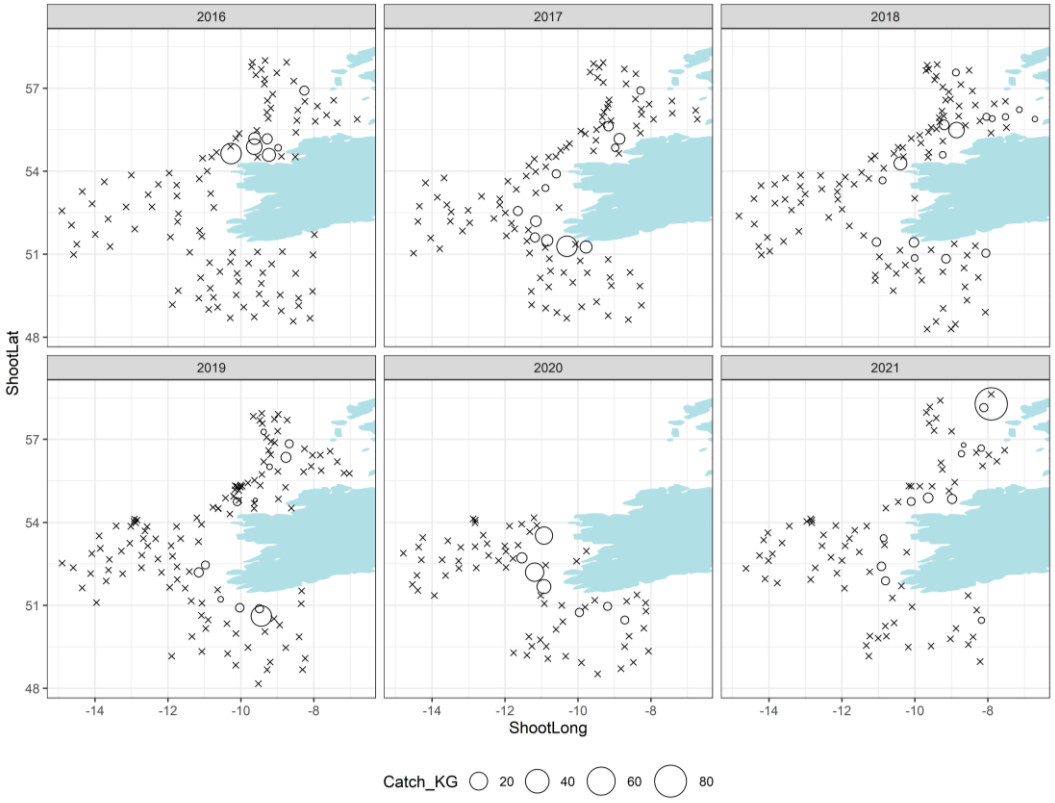


**Figure 6.15 IAMS Stations sampled and pollack caught.**

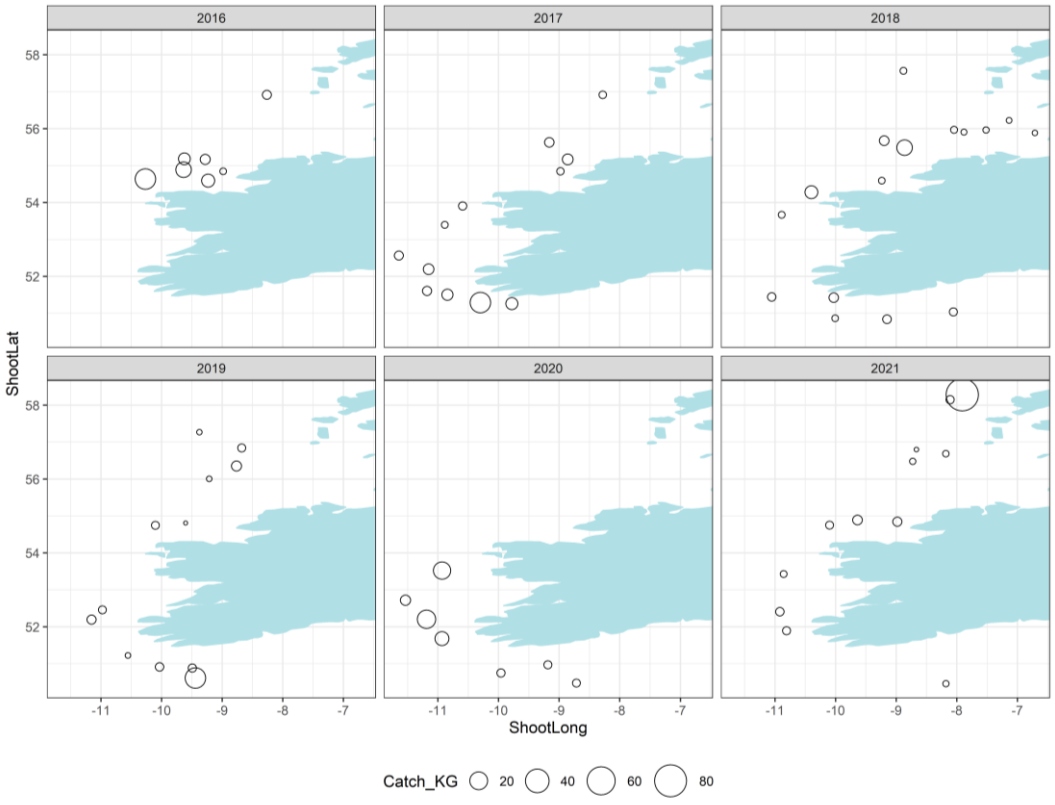


**Figure 6.16 IAMS Pollack caught (only positive stations included).**

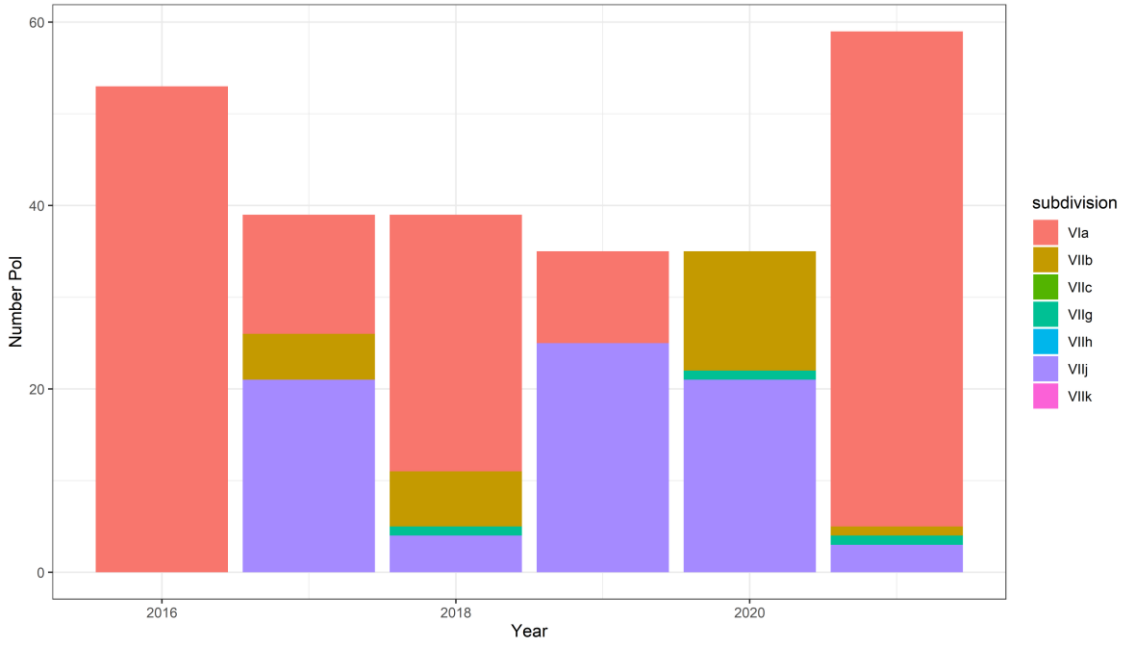


**Figure 6.17 IAMS Number of pollack caught by subdivision and year.**

### 6.2.3.4 FR-CGFS

The French Channel groundfish survey takes place in the Eastern Channel (7.d) and has data going back to 1998. Pollack have been historically caught at just 2.5% of stations with highest pollack catches being close to the French coast (Figure 6.18 and Figure 6.19). Pollack catches were much higher at the start of the time-series, with up to 167 fish caught in the 1998 but since then catches have drastically reduced. In 2011, there were unusually large catches in terms of catch weight (65 kg) in the middle of the channel, and in 2012 there were large numbers of smaller fish caught (84 fish). Since then however only 15 fish have been caught in total, and 5 of the last 6 years have had zero pollack reported by the survey (Figure 6.20).

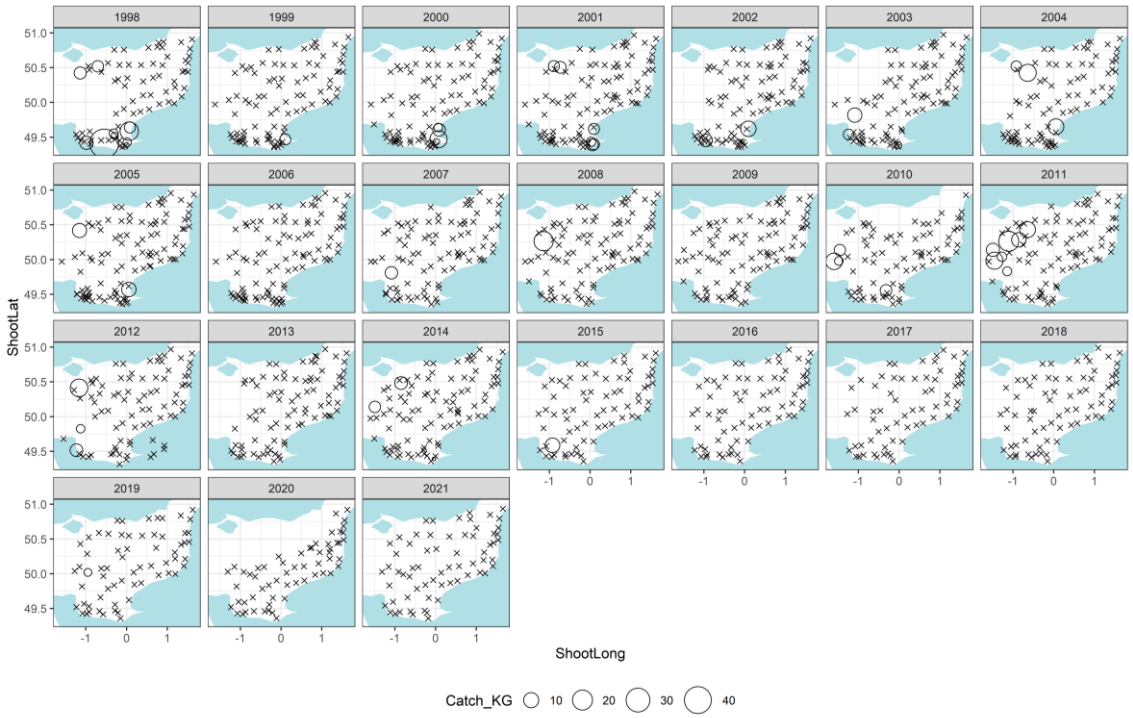


**Figure 6.18 CGFS Stations sampled and pollack caught**

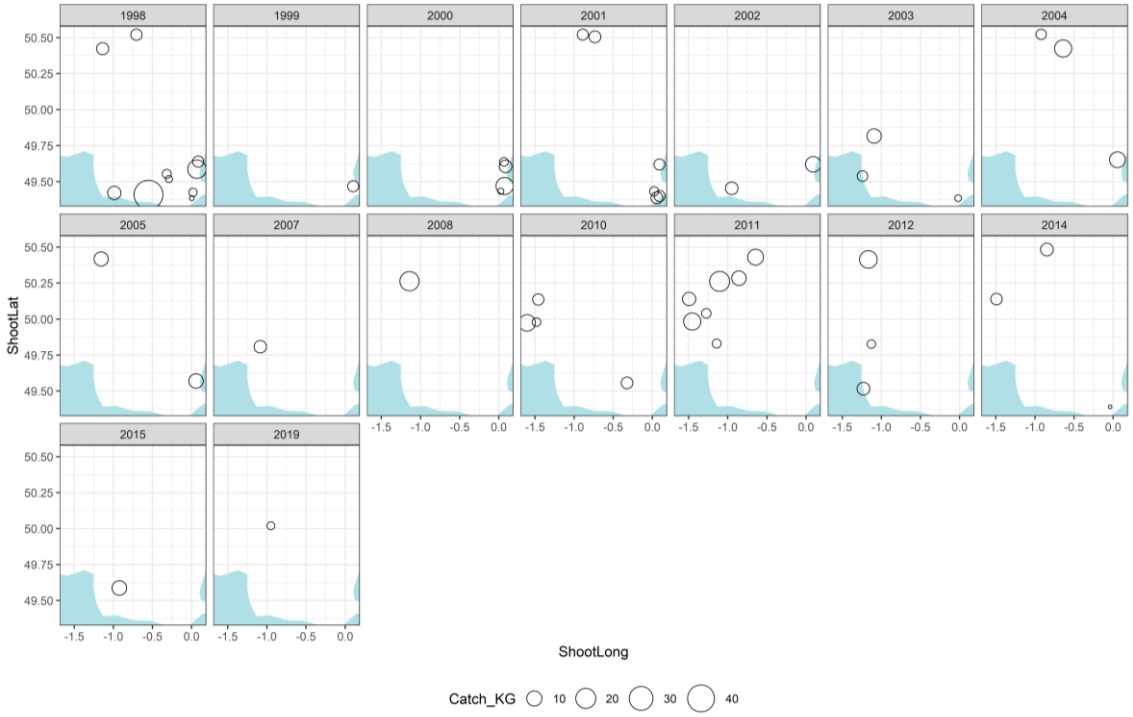


**Figure 6.19 CGFS Pollack caught (only positive stations included).**

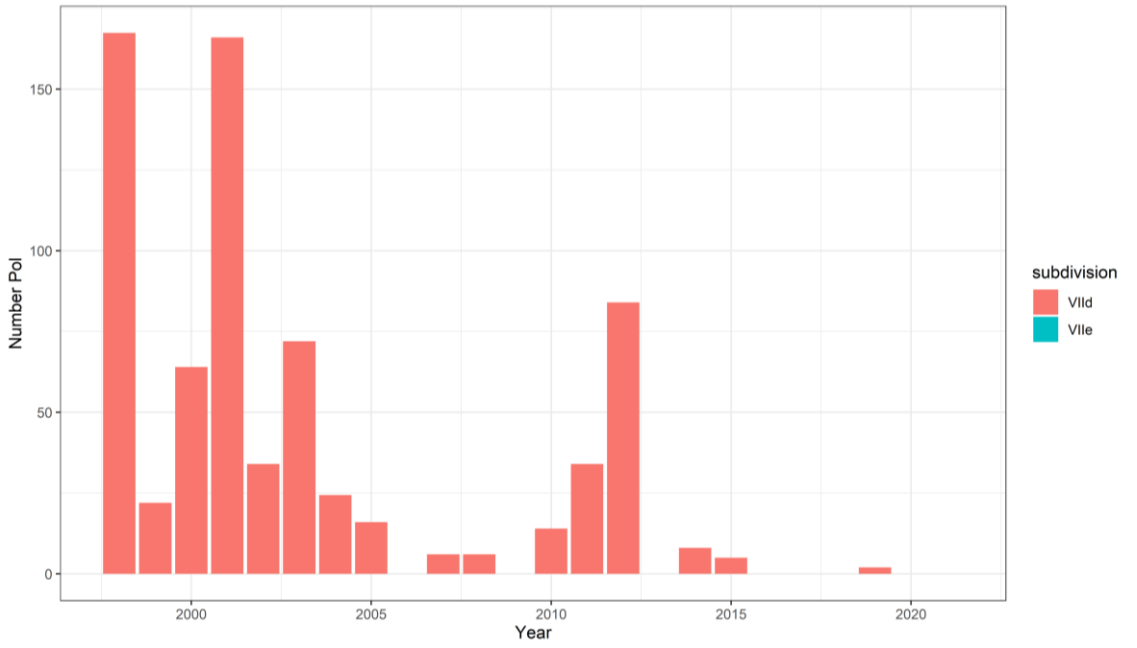


**Figure 6.20 CGFS Number of pollack caught by subdivision and year.**

## 6.2.4 VAST index

A survey index for the stock area was calculated using the VAST package. Multiple models were tested using a combination of different start dates and surveys included. The best fitting and most representative used all 4 surveys and a started in 2005. This allowed for fullest coverage of the geographic area and avoided distortion in the results coming from the IGFS sampling in the Irish Sea prior to then. Each year was independent in the model and over dispersion was turned off.

The abundance estimates from the VAST are shown in Table 6.2 and Figure 6., and they follow the trend observed in the individual survey data. There is a large uncertainty with these estimates. Figure 6. shows the density estimates of pollack as estimated by the model and show the highest pollack abundances off the northwest and southwest coast of Ireland. This is being driven by similar patterns in the IGFS and IAMS survey data. There are relatively strong pollack landings off the southwest coast of Ireland in 7j, but the model has no data in 7e where the highest pollack catches are reported. There are high estimates of pollack abundance in division 6, but there are very low commercial landings in the area. Figure 6. shows the predicted vs. observed encounter probability model diagnostics. It should be note that the spatial distribution shown in Figure 6.22 is not consistent with the know habitat preference of the species i.e. highest predicted densities are not in inshore waters.

**Table 6.2 Estimated pollack abundance from the VAST model**

| Year | Estimate metric tons | SD mt |
|---|---|---|
| 2005 | 1628 | 886 |
| 2006 | 1281 | 758 |
| 2007 | 629 | 462 |
| 2008 | 1790 | 951 |
| 2009 | 2004 | 912 |
| 2010 | 1496 | 789 |
| 2011 | 1834 | 1007 |

| Year | Estimate metric tons | SD mt |
|---|---|---|
| 2012 | 1351 | 755 |
| 2013 | 1110 | 625 |
| 2014 | 871 | 452 |
| 2015 | 1039 | 571 |
| 2016 | 1134 | 592 |
| 2017 | 821 | 447 |
| 2018 | 827 | 409 |
| 2019 | 535 | 287 |
| 2020 | 757 | 414 |
| 2021 | 418 | 230 |

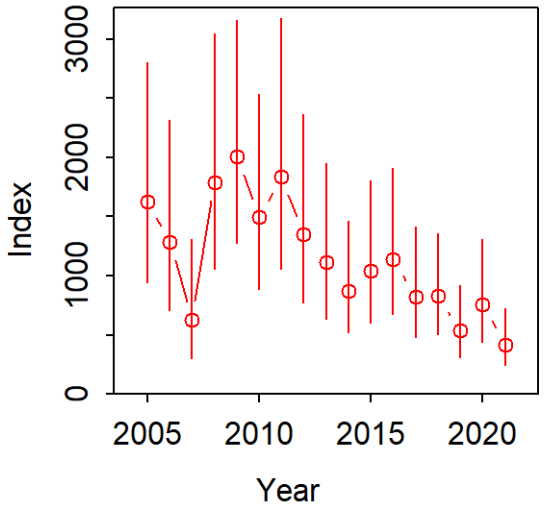


**Figure 6.21 Estimated pollack abundance from the VAST model.**

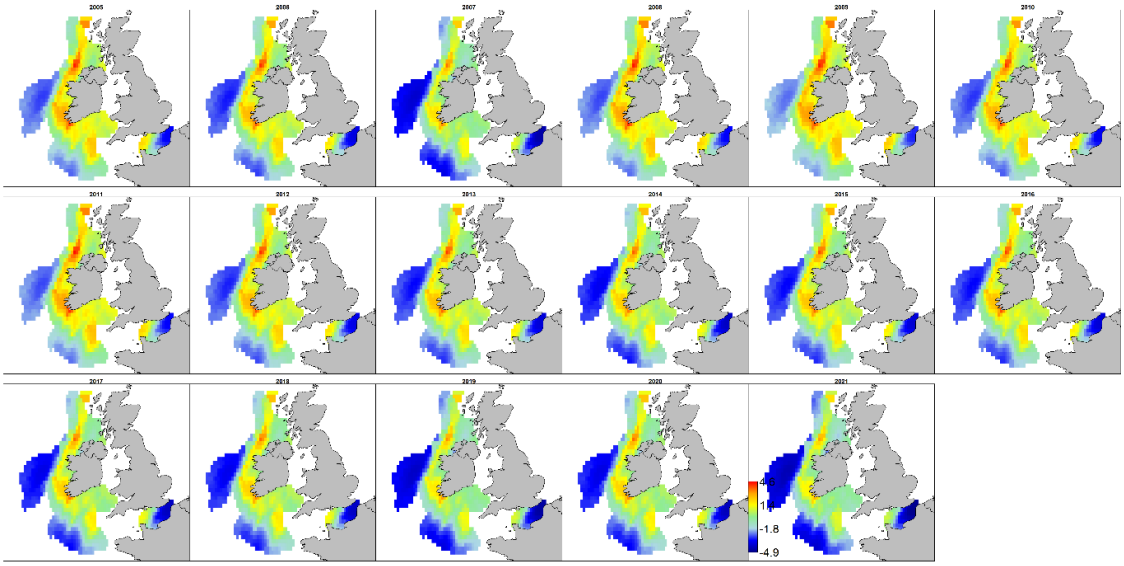

**Figure 6.22 Map of pollack density estimated from the VAST model.**

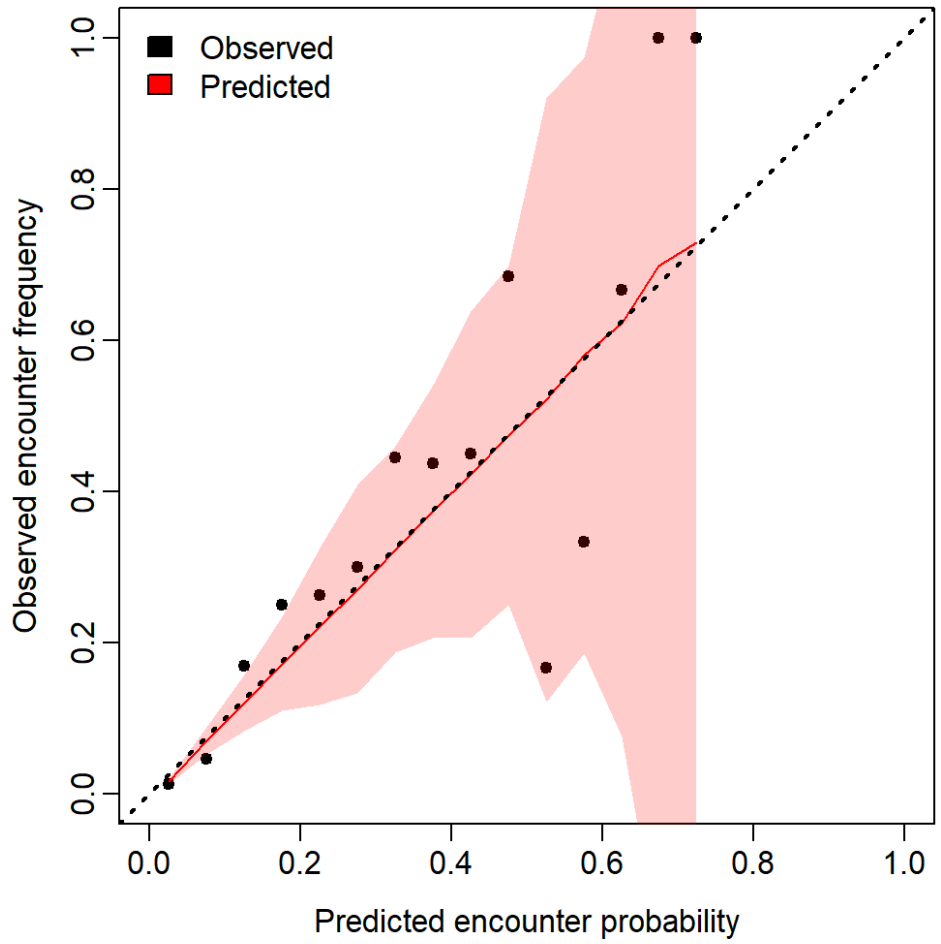


**Figure 6.23 Predicted and observed encounter probability estimated by the VAST model.**

### 6.2.5 Commercial LPUE

The possibility of producing commercial landings-per-unit-effort (LPUE) indices was explored. This is challenging for pollack because a lot of landings come from métiers that are not targeting pollack, but land small amounts as bycatch. This leads to a confusing signal from the data as the fisheries are not driven or based on pollack catches. There are a few small-scale and local fisheries that do target pollack, such as the French longline or localized gillnet métiers, but due to the scale of these it would be difficult to be sure that any index based on them would be appropriate to assessing the wider pollack stock.

## 6.3 Stock assessment

### 6.3.1 Exploratory assessments

The input data used for the exploratory assessments is shown in Figure 6.24 The catch data is comprised of official landings up until 2002 and then InterCatch landings. Recreational catches are not included at this point of the trials. Both the catch and index show a consistent downward trend.

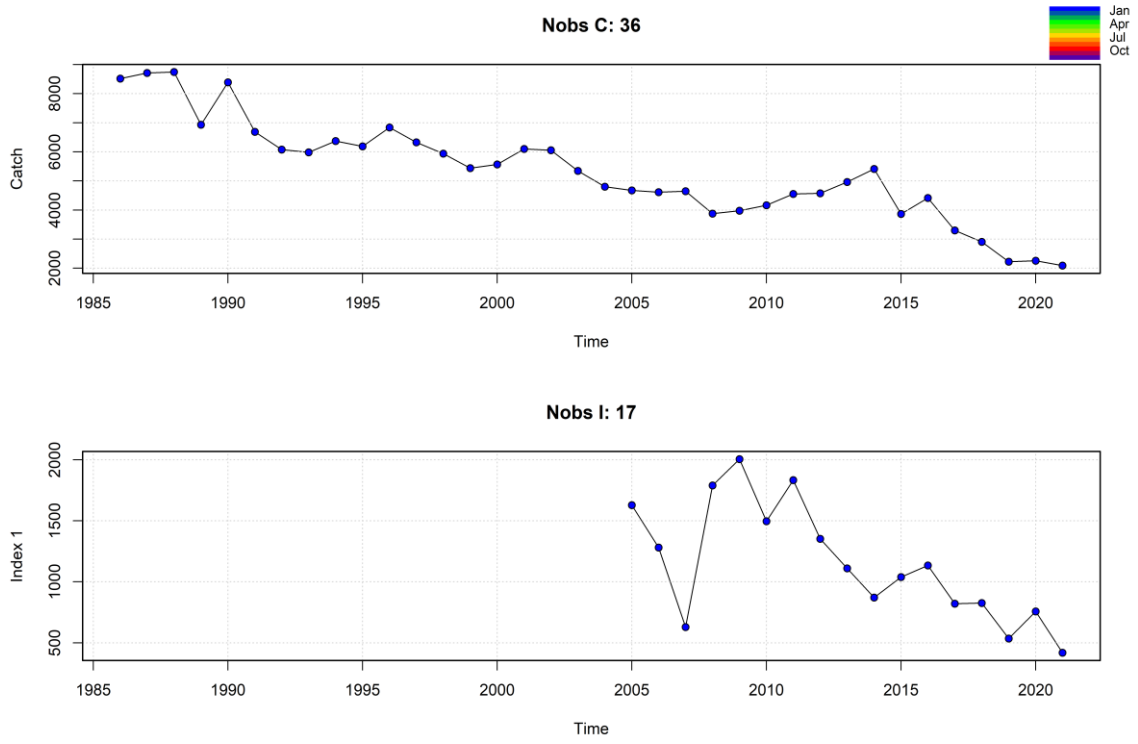


**Figure 6.24 Input data for the exploratory SPiCT assessments**

Table 6.3 shows the results of exploratory assessments using different combinations of priors on n, r and bkfrac. All of the assessments converged and showed remarkable consistency in the overall trend in the results, although there was some scaling up and down of the results. The final $B/B_{MSY}$ value ranged from 0.1 to 0.17 (mean = 0.15) and the final $F/F_{MSY}$ value ranged from 1.97 to 2.58 (mean = 2.19). In order to refine the model selection, specific issues were then investigated.

<< landscape/figures >>

## 6.3.2 Out-of-the-box SPiCT assessment

The results from the SPiCT assessment with no priors are shown in Figure 6.. The model converged, the residuals were good and produced a sensible assessment. The retrospectives were poor for the -4 and -5 peels, and there is concern on the surplus production curve. The curve is skewed to the right of centre, which would be unusual for a species like pollack.

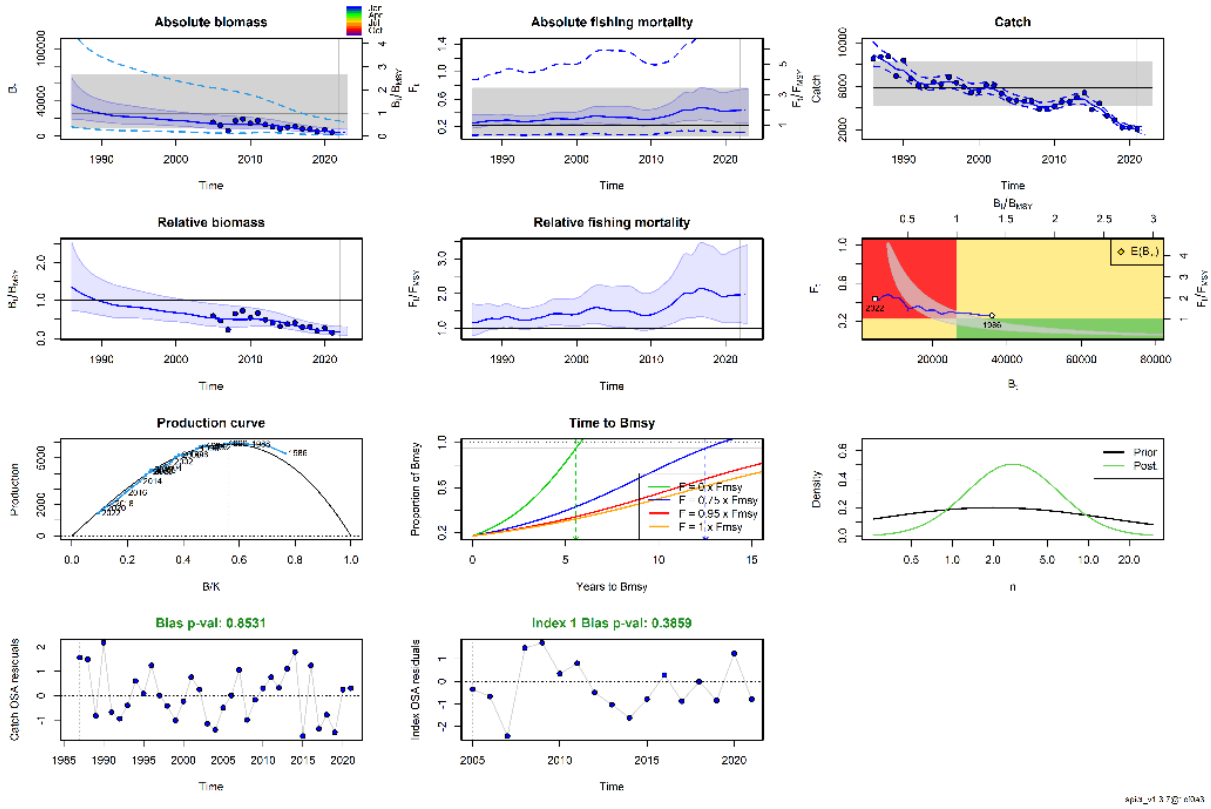


**Figure 6.25 SPiCT output "Out-of-the-box" assessment**

## 6.3.3 Fixing the surplus production curve

Several scenarios were tested of different priors on n, and the estimates of n are shown in Figure 6.. The n value had a tendency to increase over 2, indicating a skewing of the surplus production curve to the right, unless the n prior was very low or very strong. It was decided to fix the surplus production curve to be symmetrical for this stock. This had the benefit of reducing the parameters to be estimated, and fixing the curve in what would be a precautionary manner for a general demersal fish species.

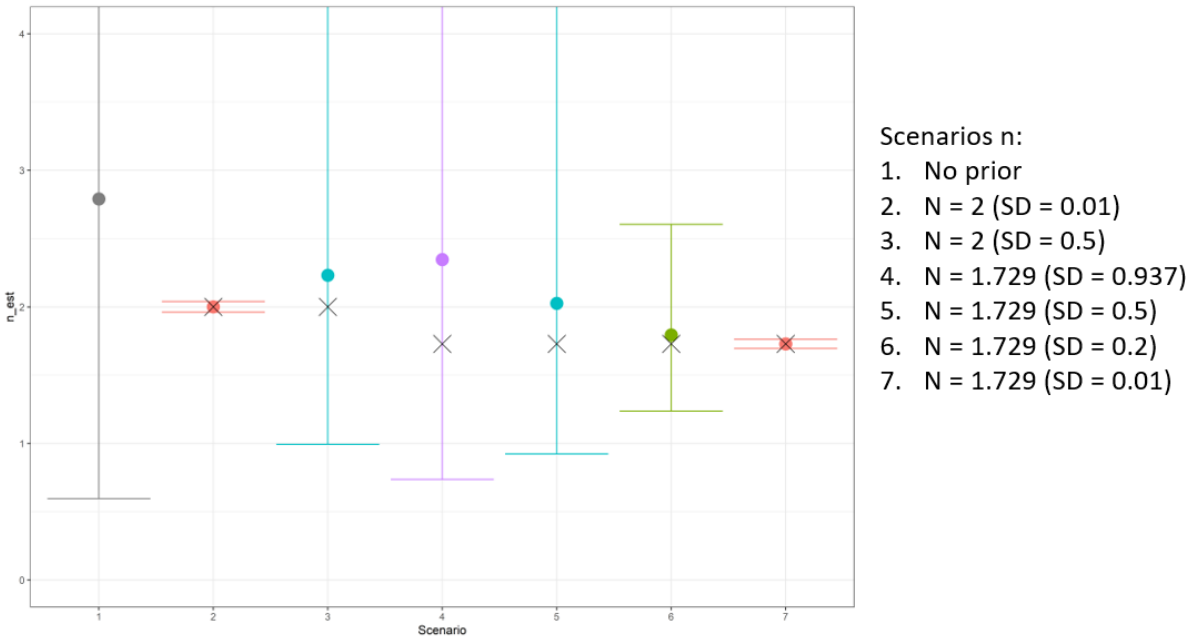


**Figure 6.26 Estimates of n (surplus production curve shape) in differing prior scenarios**

### 6.3.3.1 Fixed Surplus Production Curve

The assessment plots from the assessment with a fixed surplus production curve (n=2) are shown in Figure 6. and the outputs in Figure 6.. Judging the model on its fit the results look reasonable, although there is quite a lot of uncertainty around the r estimate (intrinsic growth rate). The model also has very little process error, with all the points fitting very closely to the surplus production curve. This would mean that observation error in the model is overestimated, but this should not overly impact on the stock status estimates. Figure 6.Figure 6. shows the retrospective analysis from this assessment and although the last 3 peels look good, as you go back further the results become increasingly poor. It was determined that an r prior might assist the model by reducing uncertainty.

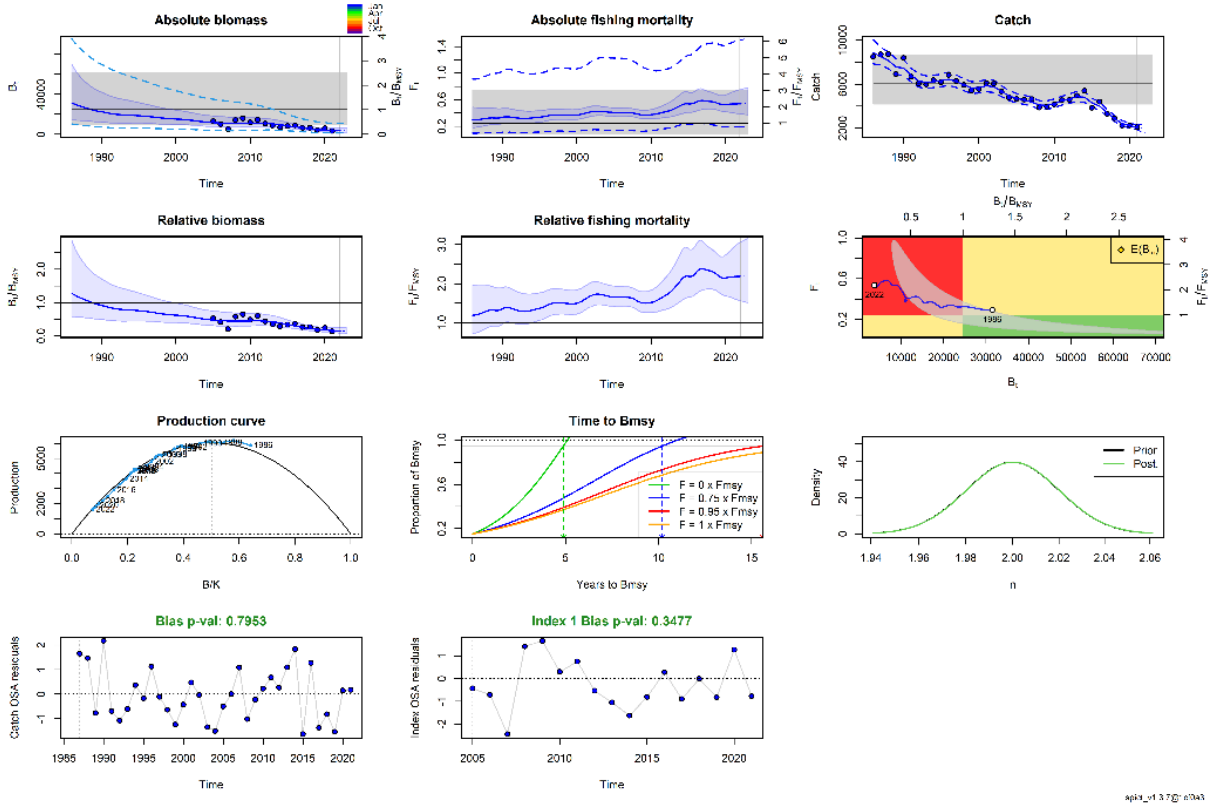


**Figure 6.27 SPiCT assessment with a fixed surplus production curve**

```
Convergence: 0  MSG: relative convergence (4)
Objective function at optimum: -11.4583182
Euler time step (years):  1/16 or 0.0625
Nobs C: 36,  Nobs I1: 17

Residual diagnostics (p-values)
    shapiro   bias    acf   LBox shapiro bias acf LBox
C    0.2767 0.7953 0.6054 0.8990       -    -   -    -
I1   0.5891 0.3477 0.3252 0.6093       -    -   -    -

Priors
     logn   ~  dnorm[log(2), 0.01^2]
 logalpha   ~  dnorm[log(1), 2^2]
  logbeta   ~  dnorm[log(1), 2^2]

Model parameter estimates w 95% CI
          estimate        cilow        ciupp    log.est
alpha    9.1598590    1.6485063   50.8963886  2.2148308
beta     0.8972217    0.3999863    2.0125863 -0.1084523
r        0.4926267    0.1631128    1.4878114 -0.7080036
rc       0.4925940    0.1631154    1.4875902 -0.7080701
rold     0.4925612    0.1630613    1.4878858 -0.7081365
m     6043.1736323 4203.0451307 8688.9258656  8.7066846
K    49070.9927509 19552.2272213 123155.3982217 10.8010234
q        0.1257955    0.0471555    0.3355810 -2.0730978
n        2.0001329    1.9613170    2.0397169  0.6932136
sdb      0.0304241    0.0054778    0.1689764 -3.4925214
sdf      0.0772151    0.0426989    0.1396330 -2.5611597
sdi      0.2786801    0.1987897    0.3906773 -1.2776906
sdc      0.0692791    0.0473343    0.1013977 -2.6696120

Deterministic reference points (Drp)
          estimate        cilow        ciupp    log.est
Bmsyd 24536.126067 9776.4391850 61578.8091119 10.107902
Fmsyd     0.246297    0.0815577     0.7437951 -1.401217
MSYd   6043.173632 4203.0451307  8688.9258656  8.706685
Stochastic reference points (Srp)
          estimate        cilow        ciupp    log.est rel.diff.Drp
Bmsys 24506.1429750 9773.434123 61447.2902708 10.106679 -0.001223493
Fmsys     0.2460701    0.081403     0.7438362 -1.402139 -0.000921994
MSYs   6030.2223345 4191.075173  8676.4326339  8.704539 -0.002147731

States w 95% CI (inp$msytype: s)
                estimate        cilow        ciupp    log.est
B_2021.94     3702.1392055 1269.9924064 10792.060352  8.2166661
F_2021.94        0.5384342    0.1933306     1.499563 -0.6190900
B_2021.94/Bmsy   0.1510698    0.0885944     0.257602 -1.8900130
F_2021.94/Fmsy   2.1881333    1.5656723     3.058065  0.7830488

Predictions w 95% CI (inp$msytype: s)
                prediction        cilow        ciupp    log.est
B_2023.00       3393.2661313 1075.4353369 10706.5991255  8.1295482
F_2023.00          0.5384344    0.1910607     1.5173799 -0.6190895
B_2023.00/Bmsy     0.1384659    0.0712902     0.2689405 -1.9771309
F_2023.00/Fmsy     2.1881343    1.5124800     3.1656167  0.7830493
Catch_2022.00   1908.3701298 1538.2229001  2367.5870071  7.5540048
E(B_inf)                 NaN          NA            NA         NaN
```

**Figure 6.28 SPiCT output of assessment with fixed surplus production curve**

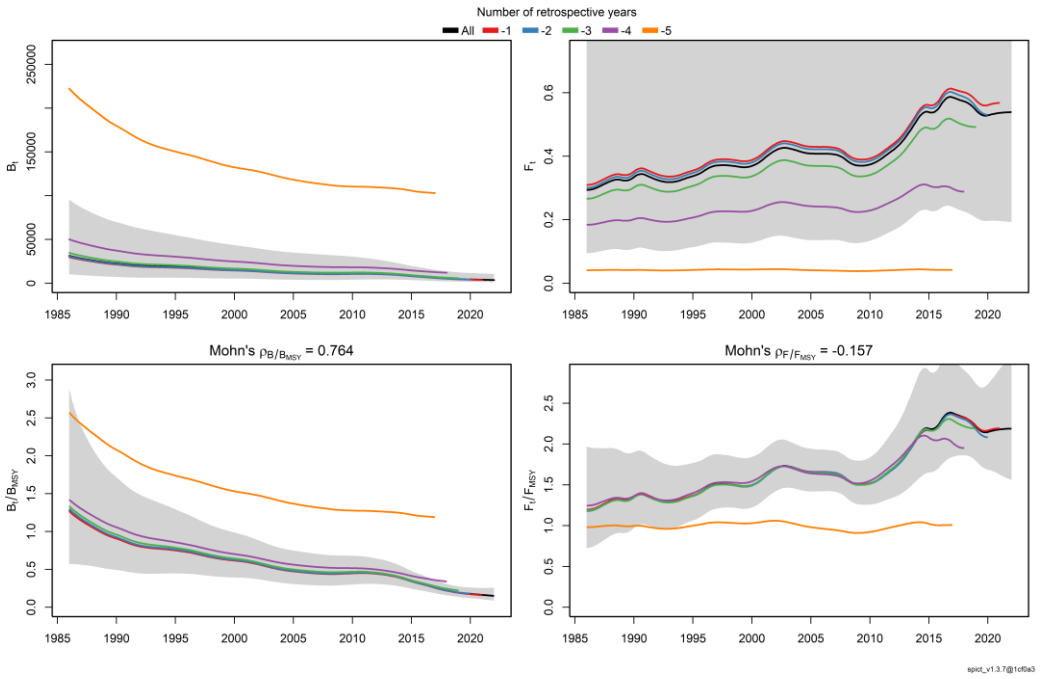


**Figure 6.29 Retrospectives of the SPiCT assessment using the fixed surplus production curve**

### 6.3.3.2 R prior

The FishLife package (Thorson, 2020) was used to determine a starting point for testing values of the r prior. For pollack this gave an r = 0.384 (SD = 1.66). This option was tested, as well as other r values, ranging from 0.3 to 0.5, and with various associated standard deviations. Figure 6. shows the estimated r value of the scenarios. Depending on the strength of the prior, the model tried pull the r value towards 0.5 where it was quite stable, however the stronger prior reduced the models uncertainty and improved the retrospective analysis.

Figure 6. shows the B/$B_{MSY}$ and F/$F_{MSY}$ time-series as estimated by the different scenarios. Regardless of the prior the results are remarkably stable. It was determined that using the FishLife prior of 0.384 and a standard deviation of 0.5 was an acceptable compromise of biologically informed prior and allowing a reasonable level of freedom.

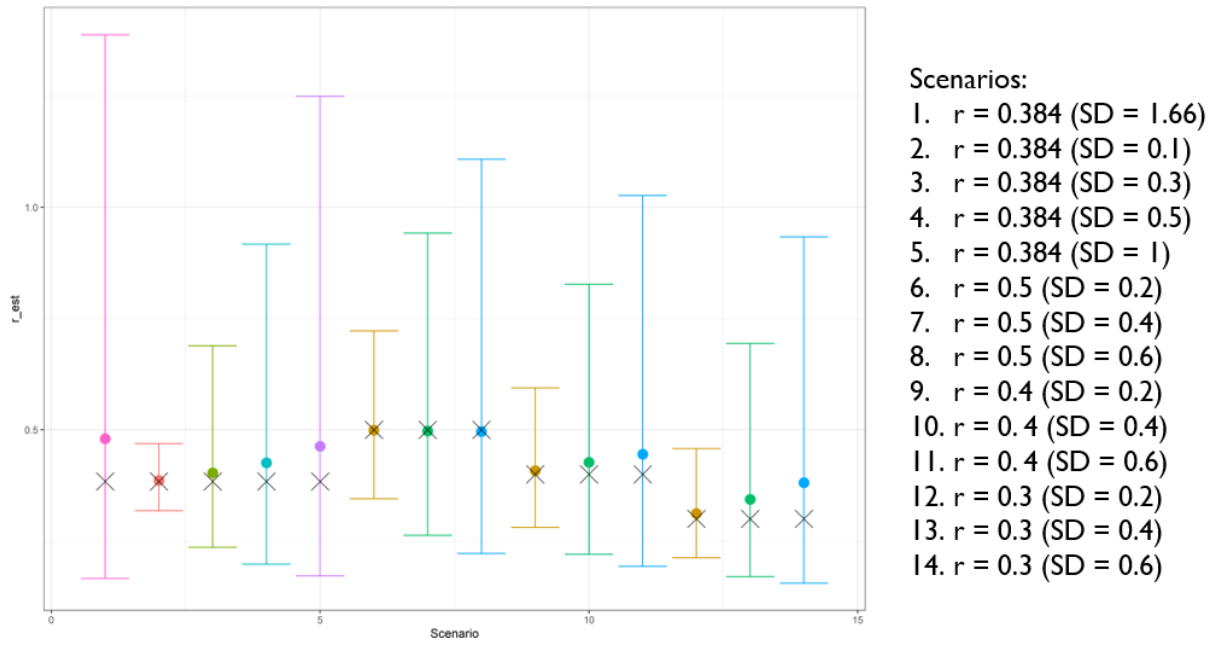


**Figure 6.30 Estimates of r (intrinsic growth rate) in differing prior scenarios**

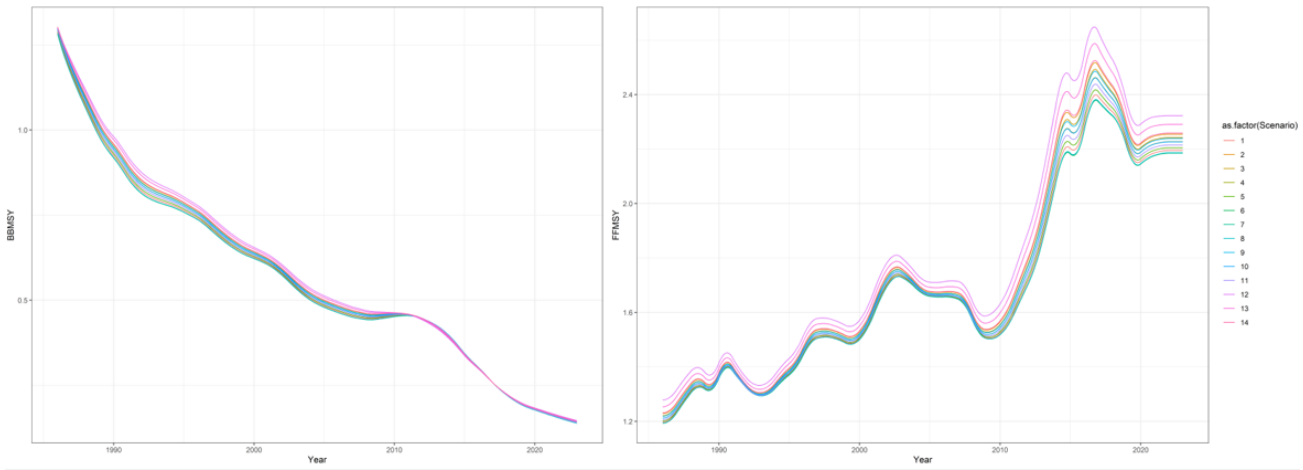


**Figure 6.31 $B/B_{MSY}$ and $F/F_{MSY}$ time-series for the r prior trial scenarios**

### 6.3.3.3 BKfrac Prior (initial depletion)

A range of values for the BKfrac prior and standard deviation were tested to determine if that would improve the model fit. The priors had a minor impact upon the scale of the stock status (Figure 6.), but no option made a notable improvement to the model. Therefore, it was decided to refrain from using any prior option and leave the model free in that regard.

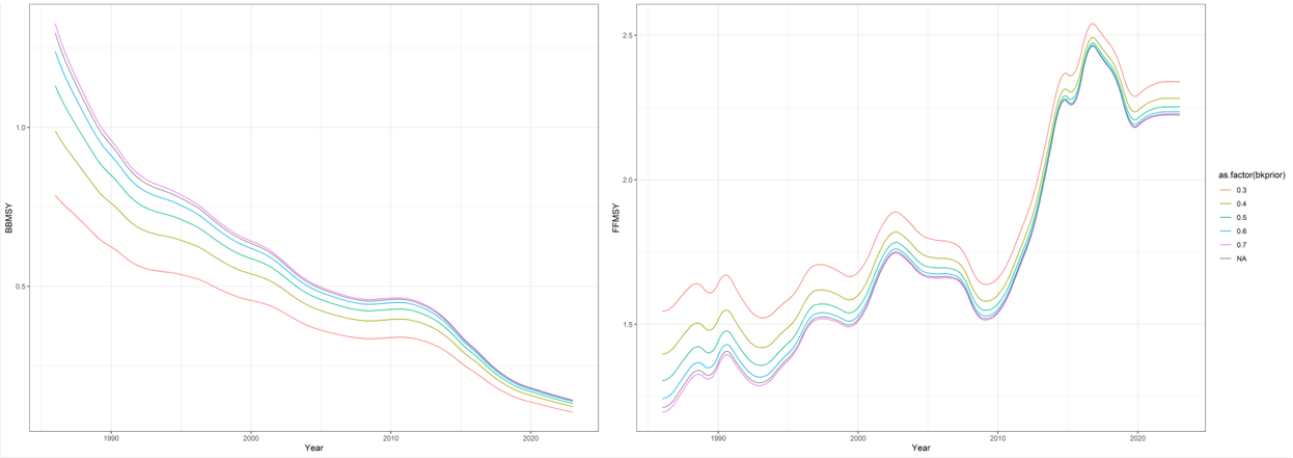


**Figure 6.32 Time-series of $B/B_{MSY}$ and $F/F_{MSY}$ from assessments using a bkfrac prior, ranging from 0.3 to 0.7**

### 6.3.3.4 Incorporating Recreational Catches

Three options were considered for including recreational catches into the assessment, as opposed to relying purely on just commercial landings. They were:

1. Recreational catches were a constant 3,500 tonnes throughout the time-series, based on (Radford et al., 2018)
2. Recreational catches were a constant proportion of commercial catches (which at the time of the recreational estimate were 1:1)
3. Recreational catches scaled to stock biomass but not at a 1:1 ratio

The issue with scenario 1 is that recreational fishing would have been catching the same amount back in the 1980s when the stock biomass could potentially have been much higher. That may or may not be a reasonable assumption, as little is known of recreational effort historically. It also means that as commercial landings drop, the recreational catch becomes increasingly dominant.

Scenario 2 has the problem that we are assuming recreational catches of approximately 8000 tonnes at the start of the time-series, which may not be reasonable. As this scenario simply increases the catch by a constant factor, from a relative reference stand point it is identical with just using the commercial landings.

Scenario 3 was tested but quickly dropped. Determining a suitable and justifiable method to scale the catch was difficult and required making ever more complex assumptions. Depending on how much you scaled the catch, the result looked very similar to one of the above scenarios.

The results of the assessments using scenarios 1 and 2, as well as that just using the commercial landings are shown in Figure 6.. There are also two different r prior options for each scenario, an r low where r=0.384 and an r high where r = 0.5. The catch plot shows the catch options differing for each scenario. The biomass trends and fishing mortality trends are similar in each scenario, but they do scale differently. As would be expected the biomass at the start was estimated to be highest in scenario 2 where the recreational catches equalled commercial catches, but by the end of the time-series the highest biomass belonged to the scenario 1 where the recreational catches were 3,500 tonnes annually. The base case had the lowest biomass because it had the lowest input catches to support. The same trend applied for the relative biomass status, only the base case and scenario 2 had the same outcome. Fishing mortality both absolute and relative was lower for the scenario with constant recreational catches. The changing shape of the production curve highlight how changing the magnitude of the catches must effect the model estimates.

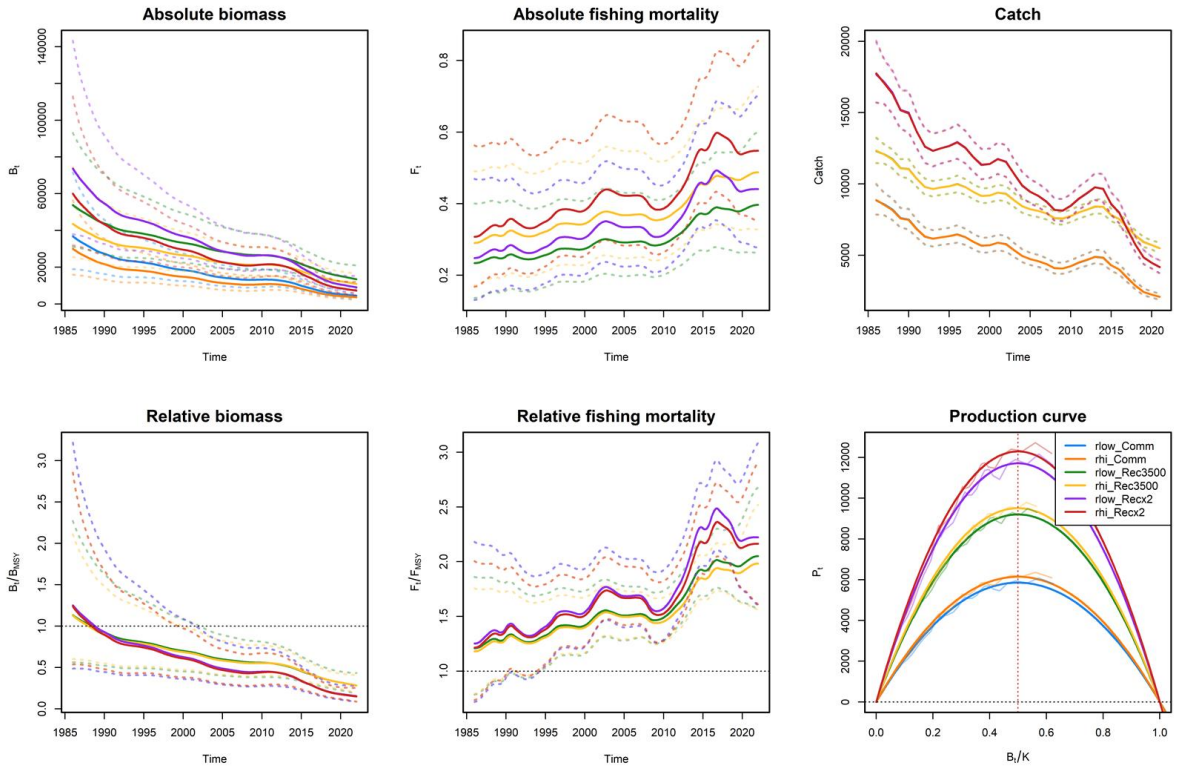


**Figure 6.33 Comparison of assessments incorporating recreational catches (rlow = r prior 0.384, rhi = r prior of 0.5; Comm = Commercial only (base scenario), Rec3500 = Recreational catch is constant 3,500 tonnes (scenario 1), Recx2 = Recreational catches equal to commercial catches(scenario 2))**

The hindcast plot from scenario 1 shows that the assessment using the constant 3,500 tonnes of recreational catches has a consistent bias towards overestimating that the stock will recover (Figure 6.1). This was not the situation for scenario 2 or when just using the commercial catch. For that reason, it was decided not to include recreational fishing as per scenario 1. Considering that the when the recreational catches were scaled 1:1 with commercial landings (scenario 2) the results were so similar, it was decided not to include recreational catches in the assessment. Including them would make the assessment less transparent, require more assumptions and complicate management advice without any benefit of having added useful input data.

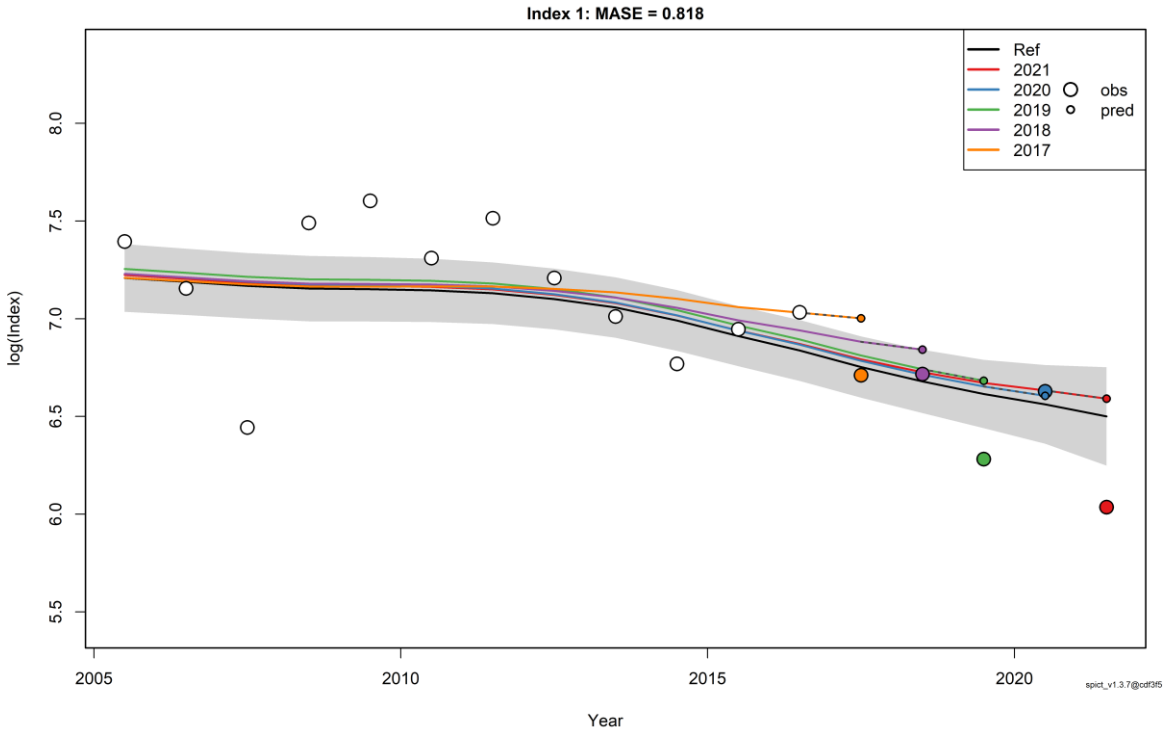


**Figure 6.14 Hindcast from the SPiCT assessment using catches with constant 3,500 tonnes of recreational catches**

### 6.3.4 Final assessment

The final assessment was determined to use the commercial landings, a fixed surplus production curve and an r prior of 0.384 (s.d. = 0.5). Although the model was robust to a variety of options, this combination was judged to have been the optimal from a performance and practical perspective. The input data are shown in Figure 6..

The parameter estimates from the assessment is shown in Figure 6. and the plots are shown in Figure 6.. The model estimates that the biomass has been decreasing the entire period, dropped below $B/B_{MSY}$ in the late 1980's and now sits around 0.13 $B/B_{MSY}$. Meanwhile the fishing mortality increased from about 1.25 $F/F_{MSY}$ until around 2015 since when it has levelled off at approximately 2.2 $F/F_{MSY}$. The production curve (Figure 6.) shows the stock being just above $B_{MSY}$ at the start of the time-series, and since then the points have consistently been moving down and to the left along the curve, as the stock biomass got consistently lower. The points all very closely fit the curve indicating low process error in the model, which is also highlighted by the high alpha estimate in Figure 6..

```
Convergence: 0  MSG: relative convergence (4)
Objective function at optimum: -13.4513877
Euler time step (years):  1/16 or 0.0625
Nobs C: 36,  Nobs I1: 17

Priors
     logn  ~  dnorm[log(2), 0.001^2] (fixed)
     logr  ~  dnorm[log(0.384), 0.5^2]
 logalpha  ~  dnorm[log(1), 2^2]
  logbeta  ~  dnorm[log(1), 2^2]

Model parameter estimates w 95% CI
            estimate         cilow          ciupp    log.est
alpha      8.3123831     1.4787097     46.7270315  2.1177463
beta       0.8841757     0.4001951      1.9534639 -0.1230994
r          0.4483900     0.2015620      0.9974776 -0.8020920
rc         0.4483899     0.2015617      0.9974786 -0.8020922
rold       0.4483898     0.2015604      0.9974844 -0.8020924
m       5999.7809482  4147.7266656   8678.8195867  8.6994782
K      53522.8918669 25999.3500174 110183.5219680 10.8878647
q          0.1201261     0.0591868      0.2438093 -2.1192132
n          2.0000005     1.9960844      2.0039242  0.6931474
sdb        0.0335982     0.0060245      0.1873751 -3.3932828
sdf        0.0774639     0.0431644      0.1390189 -2.5579426
sdi        0.2792811     0.1986628      0.3926146 -1.2755365
sdc        0.0684917     0.0468220      0.1001905 -2.6810420

Deterministic reference points (Drp)
           estimate         cilow         ciupp   log.est
Bmsyd 26761.4482928 12999.6684183 55091.7986276 10.194718
Fmsyd     0.2241949     0.1007808     0.4987393 -1.495239
MSYd   5999.7809482  4147.7266656  8678.8195867  8.699478
Stochastic reference points (Srp)
           estimate         cilow         ciupp   log.est rel.diff.Drp
Bmsys 26718.7190457 12997.3659893 54925.7401867 10.193120 -0.001599225
Fmsys     0.2239172     0.1005251     0.4987702 -1.496479 -0.001240311
MSYs   5982.7693000  4135.0048630  8656.2240392  8.696639 -0.002843440

States w 95% CI (inp$msytype: s)
                estimate         cilow         ciupp    log.est
B_2021.94     4088.1375361 1807.5405934 9246.192630  8.3158448
F_2021.94        0.4908140    0.2260131    1.065860 -0.7116900
B_2021.94/Bmsy   0.1530065    0.0872099    0.268444 -1.8772749
F_2021.94/Fmsy   2.1919440    1.5923997    3.017219  0.7847888

Predictions w 95% CI (inp$msytype: s)
                 prediction         cilow         ciupp    log.est
B_2024.00      3503.8658275 1296.5873221 9468.7612071  8.1616222
F_2024.00         0.4908145    0.2193181    1.0983993 -0.7116891
B_2024.00/Bmsy    0.1311390    0.0592194    0.2904019 -2.0314975
F_2024.00/Fmsy    2.1919462    1.4887536    3.2272822  0.7847898
Catch_2023.00  1788.3074546 1310.3211155 2440.6563509  7.4890249
E(B_inf)                NaN          NA           NA        NaN
```

**Figure 6.35 SPiCT output of the final assessment**

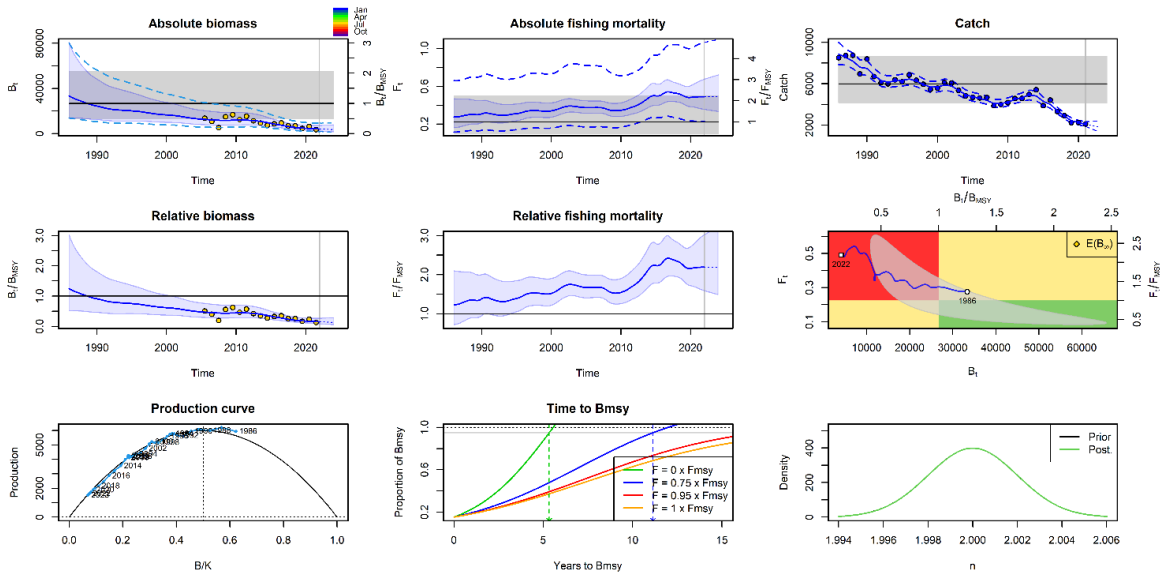


**Figure 6.36 SPiCT plots from the final assessment**

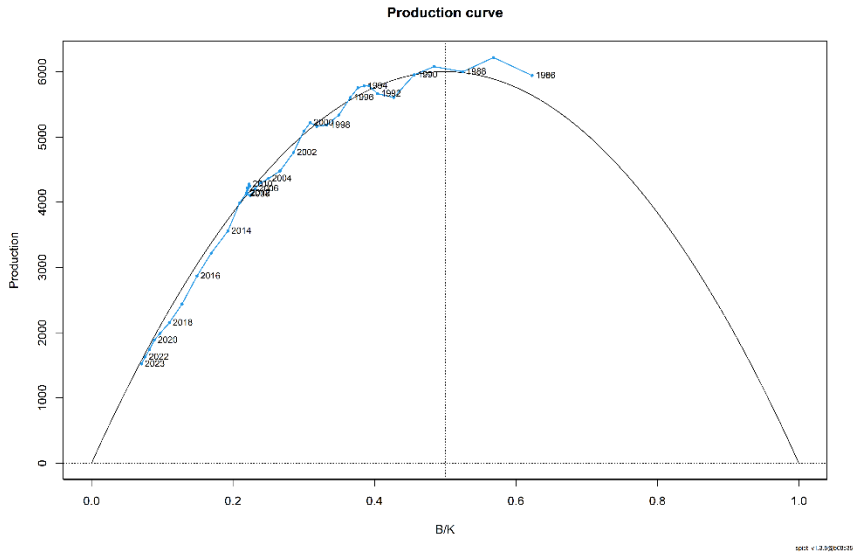


**Figure 6.37 Surplus production curve from the final assessment**

The residuals of the model were checked for violations of model assumptions. Figure 6. shows the assessment that the input data for the model is good with regards to both the autocorrelation, normality and using the one step ahead approach (OSA). The hindcast analysis of the assessment removes years of data and compares what the model predicts for the index compared to the observed result. This is shown in Figure 6., and shows that the model does a reasonable job of predicting the outcome particularly in the most recent years. The model also doesn't show any consistent bias in its predictions vs. reality.

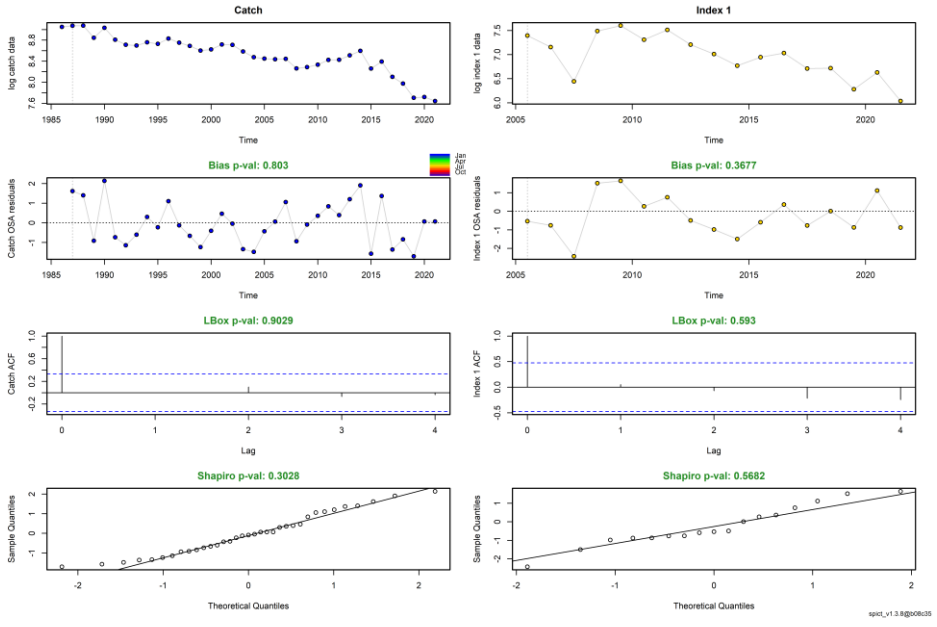


**Figure 6.38 SPiCT residual diagnostic plots for the final assessment**

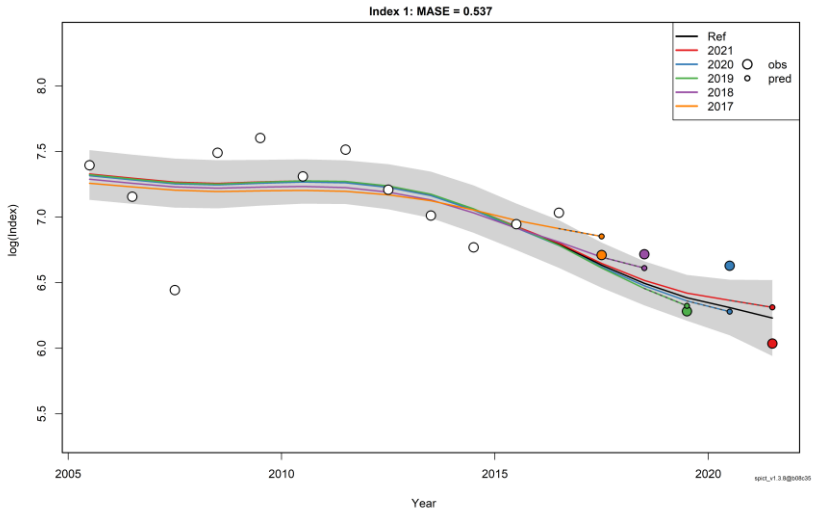


**Figure 6.39 SPiCT Hindcast analysis of the final assessment**

The model consistency was checked through analysis of retrospective patterns by peeling off the last years of data in successive model runs. The 5 year retrospective analysis (Figure 6.) shows that as more years are removed from the assessment, the outcome of the assessment produces considerable variation with the 4$^{th}$ and 5$^{th}$ peel estimating biomass to be significantly higher and fishing mortality to be significantly lower. The Mohn's Rho for $B/B_{MSY}$ is 0.259 and is -0.114 for the $F/F_{MSY}$ is also large and the biomass value would be outside the guidelines that a major retrospective pattern would be indicated by a rho value range of > 0.2 or < -0.15 outlined in WKFORBIAS (ICES, 2019).

In some cases, where the time-series is not long it might be adequate to use a 3-year retrospective analysis. This is shown in Figure 6. and the results of the analysis show far better consistency and very low Mohn's Rho values.

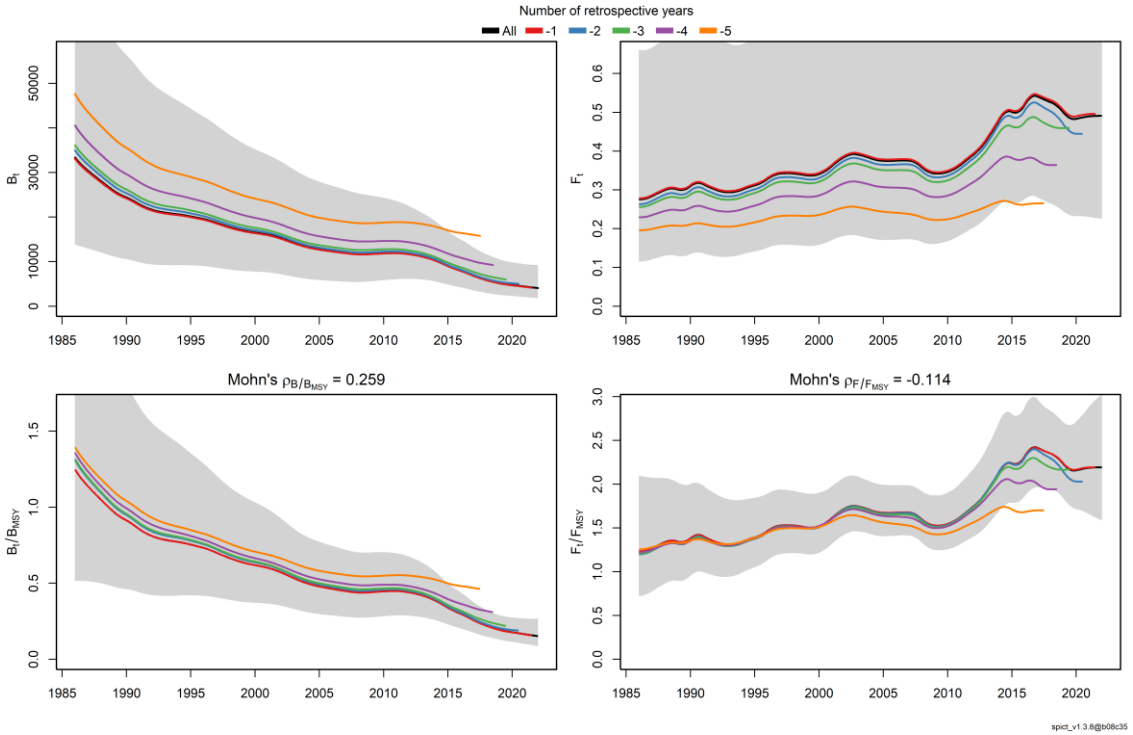


**Figure 6.40 Retrospective analysis (5 years) for the final SPiCT assessment**

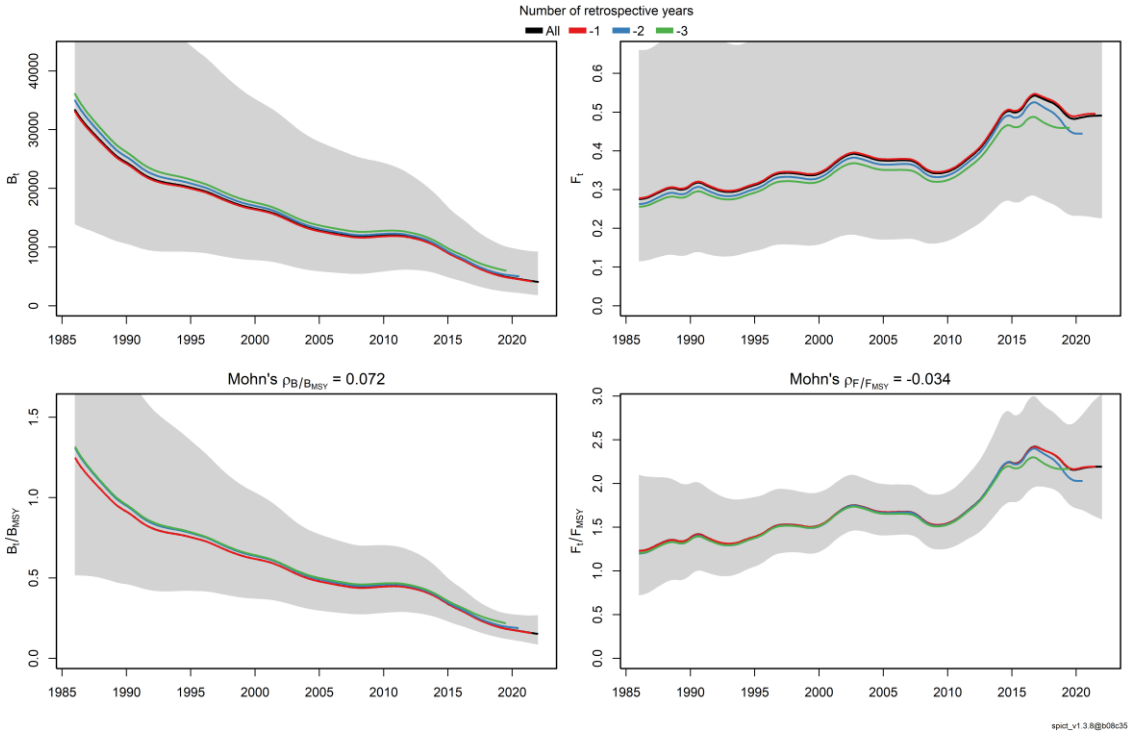


**Figure 6.41 Retrospective analysis (3 years) for the final SPiCT assessment**

In the guidelines for SPiCT (Mildenberger et al., n.d.) there is a checklist for acceptance of a SPiCT assessment. The characteristics are:

1. Model convergence: TRUE

2. Variance parameters are finite: TRUE
3. No violations of model assumptions: TRUE
4. Retrospective patterns are consistent: TRUE in 3-year analysis, FALSE for 5-year analysis
5. Production curve is realistic: TRUE, although there is very little process error
6. Assessment Uncertainty: TRUE
7. Initial values do not influence the parameter estimates; estimates should be the same as for all initial values: TRUE

## 6.4 Future considerations/recommendations

### 6.4.1 Issues with the assessment

#### 6.4.1.1 Index uncertainty and representativity

The index derived from the scientific surveys has several key issues that need to be considered.

*Low catches in the survey*

The catches in the surveys are generally very low:

- In 2021, the 3 groundfish surveys caught a total of 6 fish in 295 stations.
- The EVHOE survey has caught 31 fish throughout the entire 16 years
- The CGFS has only caught 2 fish since 2016.

A change in what station is fished or a slight change in fishing track, could quite drastically change the results. The catches have been decreasing, but with such small numbers, there is some uncertainty around this. The IAMS survey has caught by far the most pollack consistently (59 in 2021) and does not replicate the declining trend in catches and has been pretty consistent in the last 6 years.

*VAST has no 7e data*

There is currently no groundfish survey in the western channel (7.e), and no data are therefore incorporated into the model. In 2021, over 41% of landings came from 7.e.

*Representative Surveys*

There is a disconnect between the survey catches and the commercial landings. For example, the EVHOE survey has only caught 11 fish in the last decade, yet there have been nearly 20 000 tonnes landed by commercial vessels with a mean landing of 1961 tonnes in the area in that time. We know that pollack populations are mainly distributed inshore in shallower water and around wrecks and rocky reefs further off shore and that trawl surveys operate mainly in off shore areas and clean ground where pollack are only occasionally found. We also know that the locations that are being fished by the surveys and the gear used are different from the behavior of the commercial fleets. If pollack populations are declining the trajectory of the decline might well be exaggerated at the extremities of the natural range of the species.

*Density-dependent catchability*

Despite concerns about the ability of the surveys to catch pollack, the index shows a consistent decreasing trend over much of the time-series, suggesting that there may be a signal in the data. However, it is possible that the index does not correlate with pollack biomass in a linear way: when the stock is abundant it is likely to spillover into areas where they are available to be caught by trawl surveys but when the stock contracts to its main habitat of rough ground, they might become almost entirely unavailable to the survey – this would lead to an index that decreases much faster than the stock.

### 6.4.1.2 One way trip

The data used in the model is lacking in contrast to catches and abundances both in decline. This trend makes it very difficult to reliably estimate the intrinsic growth rate (r) and the carrying capacity (k). The retrospectives which fail the 5-year analysis, are also showing us that it the model is being very strongly influenced by the last few years of data, where the decline in catch and index seems to be accelerating. Going back to the -5 peel in Figure 6., when we don't use the recent data the model estimates the stock to be close to 0.5 $B/B_{MSY}$. There is a lot of uncertainty in this most recent data, due to the low survey catch numbers and decreasing commercial effort accounting for lower landings. Excluding these data years produces a very different perspective of the stock.

### 6.4.1.3 Wider context

From a model point of view, the assessment looks robust in its results, but when compared with what we know about fisheries and pollack catches in the area, however, a number of concerns present.

The model estimates that $F/F_{MSY}$ has nearly doubled from 1.2 to 2.2 since the late 1980s, and this is in strong contrast to developments in other stocks in the area. Figure 6. shows the $F/F_{MSY}$ trends for the demersal stocks from the ICES Celtic Seas ecoregion fisheries overview (ICES, 2022) with the added trend from the final pollack assessment. The vast majority of stocks have seen trending downward since the 1990's, with a few greater mortality stocks that have remained fairly constant. Pollack would be almost unique in differing from the trend seen throughout the ecoregion, with only Celtic sea cod (cod.27.7e-k) showing a moderately increasing trend, for which there are several technical measures in place to reduce cod catch and a very low quota.

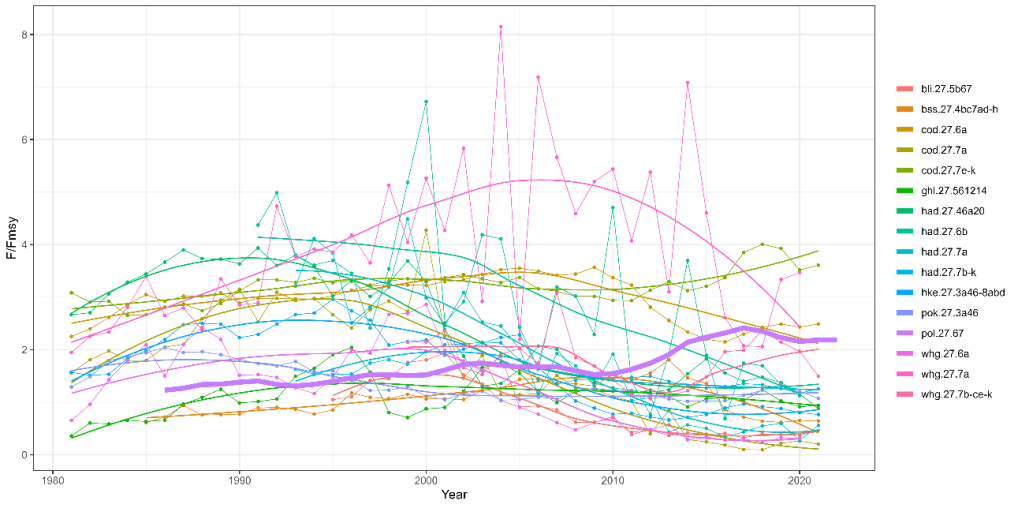


**Figure 6.42 $F/F_{MSY}$ trends of demersal stocks from the fisheries overview including Pollack as estimated by the assessment**

- As previously discussed, pollack is a species that is caught by a lot of métiers, but is targeted by very few, and those that do are relatively small scale. This is represented in Figure 6., showing data from WGMIXFISH. The métier with the largest landings are catching just a tiny proportion of pollack, for example the FRA_OTB_DEF fleet are landing just 2% of pollack and the UKE_OTB_DEF is less than 1%. The UK and Irish GNS métiers catch significantly larger proportions of pollack, but still only 28% and 21% of their landings respectively. It is only some of the French and Irish longline métiers that have strong targeting with over 50% of landings being pollack.
- We also know that the level of fishing effort in métiers catching pollack has been decreasing over time(Figure 6.). The only way F could increase over a period with decreasing effort is

through increased targeting. The decreasing effort of most métiers and only very limited small-scale targeted métiers is hard to rationalize against the apparent steady increase in fishing mortality over the last 30 years.

- There have also been some métiers that have stopped targeting pollack over the course of the time-series. For example, the French OTB fleet used to target pollack and caught over 1,200 tonnes annually in the early 2000's, however since then fisher behaviour and preference have changed and the most recent landings were less than 100 tonnes. Similarly, Irish inshore gillnetters have largely stopped targeting pollack because in recent years' catches have suffered very high levels of seal damage.
- In recent year's countries such as Ireland and the UK have not taken their full quota share (Figure 6.). This is a cause for some concerns about the status of the pollack population. Anecdotal information for the fishing industry has highlighted issues like seal depredation in gillnet fisheries as a major problem but these have not been fully quantified. Most indications suggest that the pollack stock has been in decline. However, the significant decline in effort in fleets catching pollack and decline in fishing mortality of demersal stocks in the area, suggests that the model may be overly pessimistic in its estimate of F.

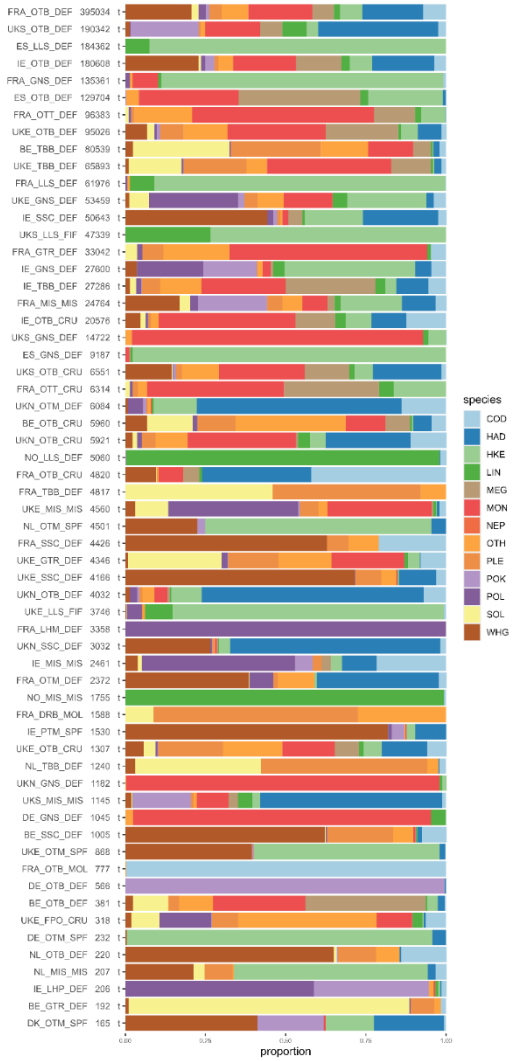


**Figure 6.43 Data from WGMIXFISH from 2019-2021 on the species composition by métier (tonnage is the total over all 3 years; the métiers are sorted from top to bottom according their landings). The main fleets that have more than a small bycatch of pollack (POL; dark purple) are UK and Irish gillnets (UKS_GNS_DEF and IE_GNS_DEF). French handlines (FRA_LHM_DEF) appear to fully target pollack but their landings are minor.**

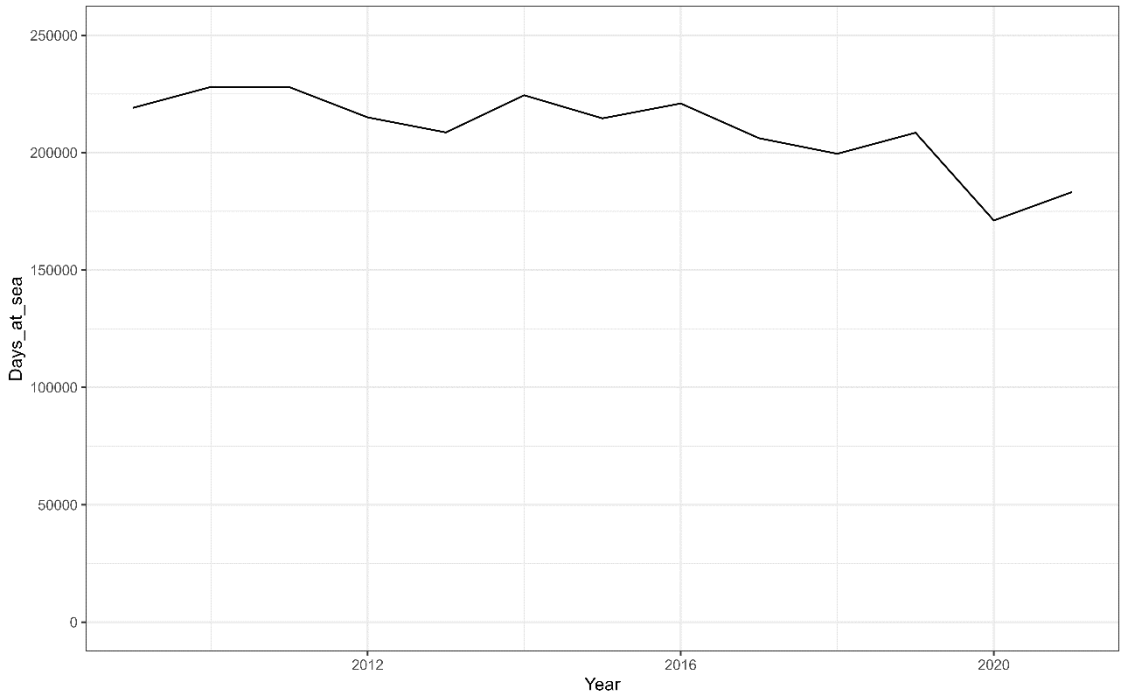


**Figure 6.44 Fishing effort of gears averaging catches of more than 10 tonnes of pollack in ICES divisions 6 and 7**

- The increased fishing mortality estimated by the model would be corroborated by a decrease in the size of fish caught over time. (Figure 6.45) is based on Irish sampling data going back to 2002. With the exception of the Pmega indicator, the evidence of a notable change in the size of fish being caught over the time isn't clear. Most of the indicators surprisingly look relatively healthy and stable.

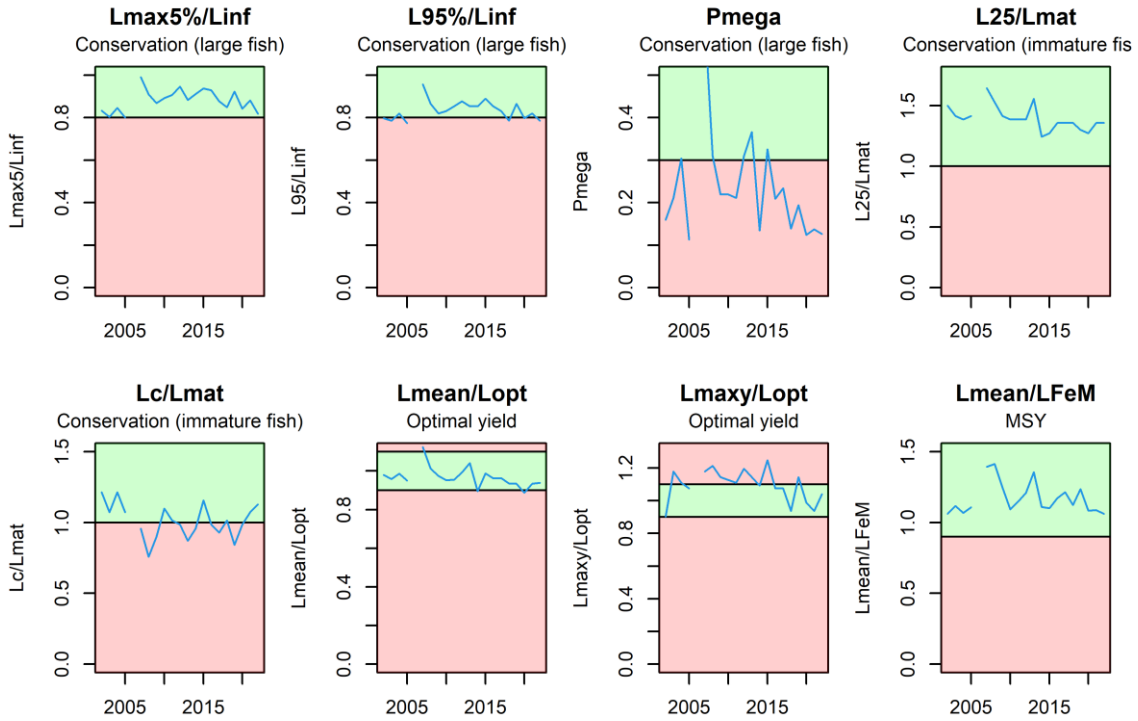


**Figure 6.45 Length Based Indicators from Irish observer data since 2002**

### 6.4.1.4 Recreational fishing

The final assessment does not include any recreational fishing catches, and instead uses just the commercial catches which we know are only about half of the story. At present there is no reasonable way to incorporate recreational fishing, but it's absence does add uncertainty to the assessment and undermines the credibility of the outcomes and any advice. Also in recent years ICES has been asked to provide management advice for recreational fisheries for pollack in this area so the current assessment does not provide a basis for advice on the recreational fisheries component of catches.

### 6.4.1.5 Stock identification

ICES does not necessarily advocate that subareas 6 and 7 constitutes a management unit for Pollack, and further work is required. Genetic work is taking place but no results are available yet.

There appears to be large differences between different areas with regards to commercial fishing, and estimates of abundance from the surveys, and the two do not always correlate. For example, there would appear to be abundance hot spots in area 6 on the IGFS, yet there are very low commercial landings from the area. Given the costal distribution of the species there may well be different populations of pollack in different areas.

## 6.5 Recommendations

There are several areas of uncertainty around the assessment that might be improved going forward. Improved survey data and new inshore surveys are hoping to allow for better sampling of pollack habitats, which would improve the representativity of the abundance index. As the availability of recreational data increases, better estimates of catches and mortality may be possible, which might allow recreational fishing to be incorporated into the model in a more robust manner. There are also genetic studies of population structure underway that might help better define stock structure.

Alternatively, the use of integrated models could be explored in future to account for the good amount of length and biological information available for this stock.

## 6.6 Reviewer report

Pollack in ICES areas 6 and 7 is currently a category 4 stock, using a catch-only method to provide catch advice (DCAC). Information about landings is available since before the 1960s, but only considered reliable since mid-1980s. InterCatch data are available since 2003. The species has probably a large amount of recreational catches, which is not quantifiable.

A new biomass index was presented, based on 4 bottom-trawl surveys and standardized using VAST. The surveys are not targeting pollack and they do not cover the area with the highest catches, which could be the main habitat of the species. In three of the four surveys, catches of pollack in the surveys are fluctuating with a large proportion of hauls without any observed individuals (up to 100% of hauls for some surveys in some years). Nevertheless, the overall trend of observed individuals is decreasing over the whole time-series. While the catches in the IAMS survey are stable, the data are only available from 2016 onward. The final survey index combining the information from all surveys shows an overall declining trend, however, with large uncertainty and a CV between 46 and 73%.

The group was presented a large amount of SPiCT runs with different settings, most importantly looking into the shape parameter and the priors on intrinsic growth rate (r) and initial depletion (bkfrac). Additionally, runs including assumptions of recreational catches were explored. Comparison plots and estimates from all runs agree that the stock is declining and likely to be overfished in the most recent years.

The final model uses a Schaefer production curve, a prior distribution for the intrinsic growth rate and vague priors about the ratios of observation to process uncertainties. The SPiCT assessment of pollack in subareas 6-7 is considered suitable for providing management advice. The assessment passed all diagnostic checks with the exception of the retrospective pattern for $B/B_{MSY}$ in the 5-year analysis; the retrospective bias was not present in a 3-year retrospective analysis. The alternative sensitivity runs showed that the results are robust over a wide range of tested alternative scenarios.

The assessment has some caveats that were presented during the benchmark meetings, but also added to the report after the meeting had ended. The abundance index is based on surveys that are not designed to catch the species and do not cover an important area of the stock distribution. Another issue is that there are open questions about the stock identity. These caveats were outside the scope of the benchmark but need to be investigated further in future.

Another explanation of the likely continuous decrease in abundance as apparent in the surveys and as suggested by the model could be declining productivity due to climate or environmental changes affecting habitat suitability rather than or in addition to the high commercial and unknown recreational fishing pressure. This should be further investigated in future.

Overall, all presented information, points to the fact that the stock is at a very low biomass level compared to likely historical levels and any trend-based rule that is not able to estimate the stock status will be less precautionary than this SPiCT assessment that has been accepted by the benchmark group despite the above-mentioned caveats.

## 6.7 Conclusions

The SPiCT assessment model was considered appropriate to be used as basis for providing advice for Pollack in ICES divisions 6 and 7.

## 6.8 References

ICES, 2022. Celtic Seas ecoregion – fisheries overview. ICES Advice: Fisheries Overviews. https://doi.org/10.17895/ICES.ADVICE.21641312

ICES. 2021. Benchmark Workshop on the development of MSY advice for category 3 stocks using Surplus Production Model in Continuous Time; SPiCT (WKMSYSPiCT). ICES Scientific Reports. 3:20. 317 pp. https://doi.org/10.17895/ices.pub.7919

ICES, 2019. Workshop on Catch Forecast from Biased Assessments (WKFORBIAS; outputs from 2019 meeting). https://doi.org/10.17895/ICES.PUB.5997

Mildenberger, T.K., Kokkalis, A., Berg, C.W., n.d. Guidelines for the stochastic production model in continuous time (SPiCT).

Radford, Z., Hyder, K., Zarauz, L., Mugerza, E., Ferter, K., Prellezo, R., Strehlow, H.V., Townhill, B., Lewin, W.-C., Weltersbach, M.S., 2018. The impact of marine recreational fishing on key fish stocks in European waters. PLoS ONE 13, e0201666. https://doi.org/10.1371/journal.pone.0201666

Thorson, J.T., 2020. Predicting recruitment density dependence and intrinsic growth rate for all fishes worldwide using a data-integrated life-history model. Fish Fish 21, 237–251. https://doi.org/10.1111/faf.12427

# 7 Pollack in Bay of Biscay and Atlantic Iberian waters

## pol.27.89a – *Pollachius pollachius* in Subarea 8 and Division 9.a

## 7.1 Introduction

*Pollachius pollachius* (Linnaeus, 1758) is restricted to the Northeast Atlantic with a main distribution from the Portuguese continental coast northwards around the British Isles, into the Skagerrak and along the Norwegian coast where it is fairly common up to the Lofoten Islands.

Pollack is a bentho-pelagic species. Outside the breeding season, it does not form large schools, but it is rarely solitary. During reproduction, individuals come together in dense formations. Juveniles live along the coast at least during their first two years; they move offshore, gaining depth (40 to 100 m) during their third year (Moreau, 1964; Quéro and Vayne, 1997). According to Moreau (1964) reproduction occurs at maximum depths of 150 m.

### 7.1.1 Fishery information

Data from the fishery indicate three main areas of exploitation, so based on a pragmatic approach three different stock units are distinguished (ICES, 2012): the southern European Atlantic shelf (ICES Subarea 8 and Division 9a), the Celtic Seas (ICES subareas 6 and 7), and the North Sea (ICES Subarea 4, including divisions 7d and 3a).

Pol.27.8.9a is mainly exploited by France and Spain, with minor contribution to landings from Portugal. In the last ten years, France was responsible for 77% of the commercial landings of the stock and Spain for 18%. In recent years, netters and longliners are catching the 51% and 38% of landings, respectively. Trawl and other gears catch the remaining 11% of landings.

Although it is known that the recreational catches may be considerable, they have not been quantified (Radford et al. 2018).

### 7.1.2 Current assessment and advice

Currently, pol.27.8.9a is considered a data-limited stocks without information on abundance or exploitation, and it is classified as ICES Category 5 stock. The last management advice was provided in 2021, and ICES advised that commercial landings should be no more than 905 tonnes in each of the years 2022 and 2023.

The first objective of this study is to compile and evaluate the available data of pol.27.8.9a in order to apply a stochastic production model in continuous time (SPiCT; Pedersen and Berg, 2007). The second objective was to test different model configurations and values of priors to achieve a robust model for the stock. In the case of any of the proposed SPiCT models was accepted, a third objective is to evaluate the suitability of the available information (length composition of landings, life-history parameters and abundance index) to perform length based assessment methods (ICES, 2022).

# 7.2 Input data for stock assessment

## 7.2.1 Landings and discards

The available data of commercial landings, as estimated by the Working Group for the Bay of Biscay and the Iberian Waters Ecoregion (WGBIE2022), extends from 1979 to 2021 (Table 7.1). There is a missing value in the series for France in 1999. In order to complete the series and used it as input for the assessment, a value for total landings was calculated as the average of the previous and next year of total landings, resulting in 1322 t. Also, because of the high uncertainty regarding to the Spanish landings in 1985, a higher uncertainty on the catch series (six times higher) was set in 1985 in the SPiCT assessment.

**Table 7.1. Commercial landings data of pollack in ICES subareas 8 and 9a by country as considered by WGBIE2022. The last column shows the values used in the SPiCT assessment.**

| | Subarea 8 | | | Division 9.a | | | Total official landings | Unallocated | Total | Total. Interpolated |
|---|---|---|---|---|---|---|---|---|---|---|
| Year | Belgium | Spain | France | UK | Spain | Portugal | | | | |
| 1979 | 0 | 1021 | 2221 | 0 | 0 | 0 | 3242 | 0 | 3242 | 3242 |
| 1980 | 1 | 1576 | 2158 | 0 | 0 | 0 | 3735 | 0 | 3735 | 3735 |
| 1981 | 1 | 902 | 2326 | 0 | 0 | 0 | 3229 | 0 | 3229 | 3229 |
| 1982 | 2 | 85 | 2185 | 2 | 32 | 0 | 2306 | 0 | 2306 | 2306 |
| 1983 | 0 | 581 | 2652 | 0 | 203 | 0 | 3436 | 0 | 3436 | 3436 |
| 1984 | 0 | 1606 | 2351 | 1 | 642 | 0 | 4600 | 0 | 4600 | 4600 |
| 1985 | 0 | 2304 | 2769 | 23 | 636 | 0 | 5732 | 0 | 5732 | 5732 |
| 1986 | 0 | 437 | 2127 | 5 | 237 | 0 | 2806 | 0 | 2806 | 2806 |
| 1987 | 0 | 584 | 2022 | 1 | 308 | 3 | 2918 | 0 | 2918 | 2918 |
| 1988 | 3 | 476 | 1761 | 6 | 329 | 7 | 2582 | 0 | 2582 | 2582 |
| 1989 | 13 | 214 | 1682 | 4 | 57 | 3 | 1973 | 0 | 1973 | 1973 |
| 1990 | 14 | 194 | 1662 | 2 | 27 | 1 | 1900 | 0 | 1900 | 1900 |
| 1991 | 1 | 221 | 1867 | 1 | 76 | 2 | 2168 | 0 | 2168 | 2168 |
| 1992 | 2 | 154 | 1735 | 0 | 65 | 2 | 1958 | 0 | 1958 | 1958 |
| 1993 | 3 | 135 | 1327 | 0 | 47 | 1 | 1513 | 0 | 1513 | 1513 |
| 1994 | 3 | 157 | 1764 | 0 | 28 | 3 | 1955 | 0 | 1955 | 1955 |
| 1995 | 6 | 153 | 1457 | 2 | 59 | 2 | 1679 | 0 | 1679 | 1679 |
| 1996 | 8 | 137 | 1164 | 0 | 43 | 2 | 1354 | 0 | 1354 | 1354 |
| 1997 | 2 | 152 | 1167 | 1 | 54 | 2 | 1378 | 0 | 1378 | 1378 |
| 1998 | 1 | 152 | 956 | 0 | 55 | 1 | 1165 | 0 | 1165 | 1165 |
| 1999 | 0 | 120 | na | 0 | 36 | 1 | 157 | 0 | 157 | 1322 |
| 2000 | 0 | 121 | 1294 | 0 | 49 | 15 | 1479 | 0 | 1479 | 1479 |
| 2001 | 0 | 346 | 1278 | 0 | 81 | 41 | 1746 | 0 | 1746 | 1746 |
| 2002 | 0 | 170 | 1722 | 0 | 35 | 45 | 1972 | 0 | 1972 | 1972 |
| 2003 | 0 | 142 | 1450 | 1 | 39 | 31 | 1663 | 0 | 1663 | 1663 |
| 2004 | 0 | 211 | 1343 | 0 | 90 | 12 | 1656 | 70 | 1726 | 1726 |
| 2005 | 0 | 306 | 1552 | 0 | 132 | 0 | 1990 | -4 | 1986 | 1986 |
| 2006 | 0 | 251 | 1596 | 171 | 102 | 0 | 2120 | 6 | 2126 | 2126 |
| 2007 | 0 | 198 | 1375 | 62 | 103 | 5 | 1743 | 104 | 1847 | 1847 |
| 2008 | 0 | 265 | 1732 | 64 | 128 | 31 | 2220 | 93 | 2313 | 2313 |
| 2009 | 0 | 218 | 1371 | 41 | 68 | 3 | 1701 | 111 | 1812 | 1812 |
| 2010 | 0 | 265 | 1170 | 44 | 91 | 2 | 1572 | 110 | 1682 | 1682 |
| 2011 | 0 | 322 | 1475 | 27 | 104 | 2 | 1930 | 102 | 2032 | 2032 |
| 2012 | 0 | 159 | 1131 | 2 | 139 | 2 | 1433 | 87 | 1520 | 1520 |
| 2013 | 0 | 251 | 1346 | 8 | 110 | 3 | 1718 | 93 | 1811 | 1811 |
| 2014 | 0 | 185 | 1612 | 19 | 93 | 1 | 1910 | 49 | 1959 | 1959 |
| 2015 | 0 | 195 | 1244 | 37 | 78 | 18 | 1573 | 37 | 1610 | 1610 |
| 2016 | 0 | 186 | 1292 | 25 | 111 | 28 | 1642 | 19 | 1661 | 1661 |
| 2017 | 0 | 128 | 1219 | 0 | 95 | 38 | 1480 | 1 | 1481 | 1481 |
| 2018 | 0 | 135 | 1220 | 0 | 12 | 33 | 1513 | 0 | 1513 | 1513 |
| 2019 | 0 | 174 | 1189 | 0 | 143 | 57 | 1562 | 0 | 1562 | 1562 |
| 2020 | 0 | 171 | 1174 | 0 | 136 | 54 | 1535 | 0 | 1535 | 1535 |
| 2021 | 0 | 166 | 987 | 0 | 165 | 54 | 1372 | 0 | 1372 | 1372 |

* French data is not available for 1999.

Historical database, FAO, EUROSTAT and ICES database, were explored trying to extend back the time-series of commercial landings. The results show that before 1950 the reported landings were anecdotal and discontinuous (Figure 7.1) and they cannot be used for SPiCT assessment.

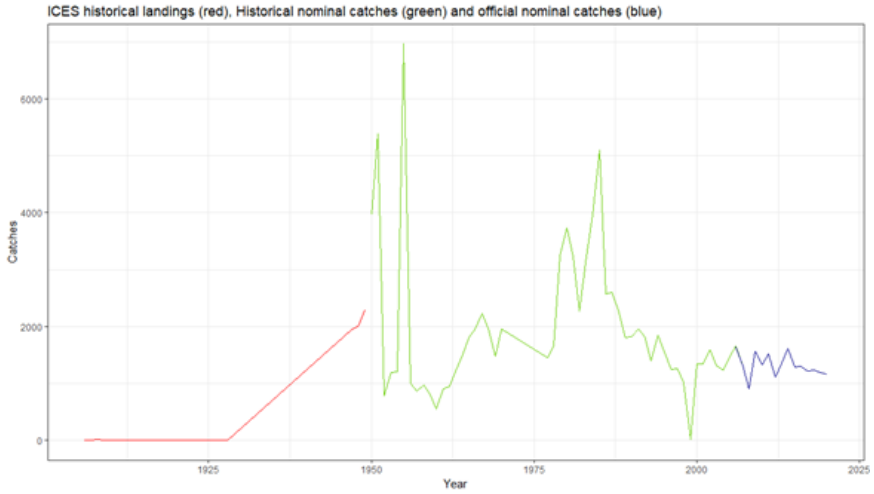


**Figure 7.1. Trends in reported commercial landings from different historical database.**

Table 7.2 and Figure 7.2 present ICES historical landings by country for pollack in ICES subareas 8 and 9a from 1950 to 1980. Values suggest misreporting for France from 1950 to 1976 and for Spain from 1971 to 1978. Therefore, we only considered years 1979 and 1980 adequate data for being used in the assessment and those values were already included in the landing considered by WGBIE2022 (Table 7.1).

**Table 7.2. Historical landings data of pollack in ICES subareas 8 and 9a by country for period 1950-80. (Source: ICES database).**

| Year | Belgium | Denmark | France | Portugal | Spain | UK - England & Wales |
|---|---|---|---|---|---|---|
| 1950 | | | | | 3966 | |
| 1951 | | | | | 5391 | |
| 1952 | | | | | 781 | |
| 1953 | | | | | 1198 | |
| 1954 | | | | | 1208 | |
| 1955 | | | | | 6962 | |
| 1956 | | | | | 1005 | |
| 1957 | | | | | 866 | |
| 1958 | | | | | 978 | |
| 1959 | | | | | 805 | |
| 1960 | | | | | 558 | |
| 1961 | | | | | 916 | |
| 1962 | | | | | 957 | |
| 1963 | | | | | 1219 | |
| 1964 | | | | | 1501 | |
| 1965 | | | | | 1808 | |
| 1966 | | | | | 1951 | |
| 1967 | | | | | 2230 | |
| 1968 | | | | | 1960 | |
| 1969 | | | | | 1484 | |
| 1970 | | | | | 1955 | |
| 1971 | | | | | | |
| 1972 | | | | | | |
| 1973 | | | | | | |
| 1974 | | | | 242 | | |
| 1975 | | | | | | |
| 1976 | 1 | | | | | |
| 1977 | 1 | | 1459 | | | |
| 1978 | 1 | | 1661 | | | |
| 1979 | | 1 | 2222 | | 1021 | 1 |
| 1980 | 1 | | 2159 | | 1576 | |

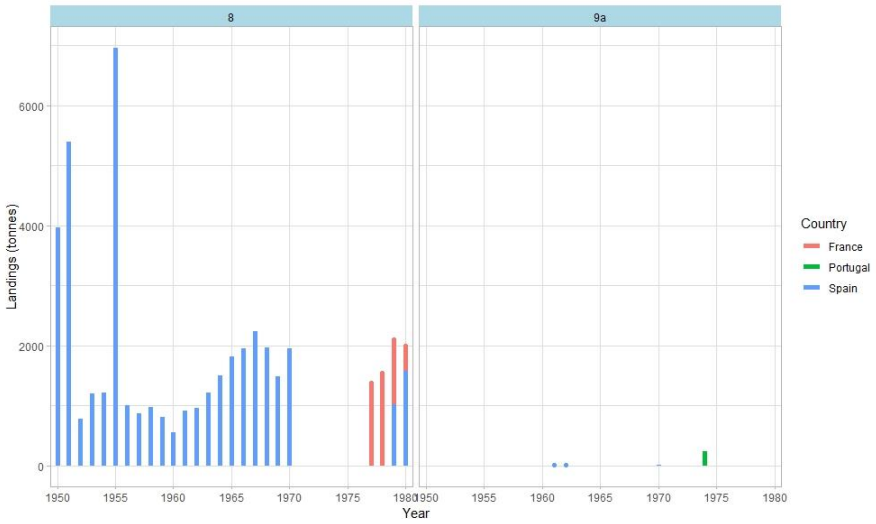


**Figure 7.2. Historical commercial landings of pollack by ICES subarea (8 and 9a) and by country (Portugal, Spain and France; ICES database).**

Therefore, the time-series of commercial landings could not be extended back and the catch period used for the SPiCT assessment was 1979-2021.

Discard data are available for the main countries and gears from 2015 to 2021 (Table 7.3). Data were extracted from InterCatch database. Discards represented an average of 2% of total commercial catches and, following the ICES guidelines, they can be considered negligible and are not used in the assessment.

**Table 7.3. Discards by country and gear. Values are in tonnes.**

| | France | | | Spain | | | Portugal |
|---|---|---|---|---|---|---|---|
| Year | Nets | Trawl | Lines | Lines | Nets | Trawl | Trawl |
| 2015 | 28.1 | 0 | 0 | 0 | 3.5 | 0 | 0 |
| 2016 | 83.1 | 5.4 | 4.3 | 0 | 0.4 | 0 | 0 |
| 2017 | 18.6 | 0 | 0 | 0 | 0 | 0 | 0 |
| 2018 | 38.7 | 0 | 0 | 0 | 0 | 2.8 | 0 |
| 2019 | 8.2 | 0 | 6.1 | 0 | 0 | 0 | 0 |
| 2020 | 8.5 | 0.0 | 0.6 | 0.0 | 0.0 | 0.0 | 0.0 |
| 2021 | 12.9 | 0 | 3.2 | 0 | 0.35 | 0 | 0 |

Although it is known that the recreational catches may be considerable, they have not been quantified (Radford et al. 2018). For this reason, it was decided to only consider commercial landings to perform the assessment.

### 7.2.2 Scientific surveys

Pollack abundance indices resulted negligible or zero in the groundfish surveys carried out in the distribution area: EVHOE, SP-NSGFS and PT-IBTS. The bottoms preferred for this species (wrecks and rocky bottoms) makes that trawl surveys are not well suited for monitoring this species.

### 7.2.3 Standardized commercial abundance index

Because of the very low or null number of individuals of pollack observed in the fishery-independent surveys in the distribution area of the stock (EVHOE, SGFS, PTGFS), it can provide a reliable biomass index for pol.27.89a. Therefore, fishery-dependent data had to be used to provide an index of exploitable biomass for this stock.

**Fleet selection**

Pollack is caught by a great diversity of métiers (Figure 7.3). However, given its biology and bathymetric distribution it is not really accessible for trawlers and only a minority of trawlers are targeting pollack. Besides, the fishing techniques of trawlers have changed over the period. The gear that might produce the best abundance index of the underlying biomass might be gillnets.

A commercial abundance index was provided using the French bottom-sets gillnetters (GNS) fleet, which represents 47% of the French landings for pollack (Figure 7.3, GNS are in green). 1155 gillnetters landed at least 1kg of pollack over the period 2000-2021.

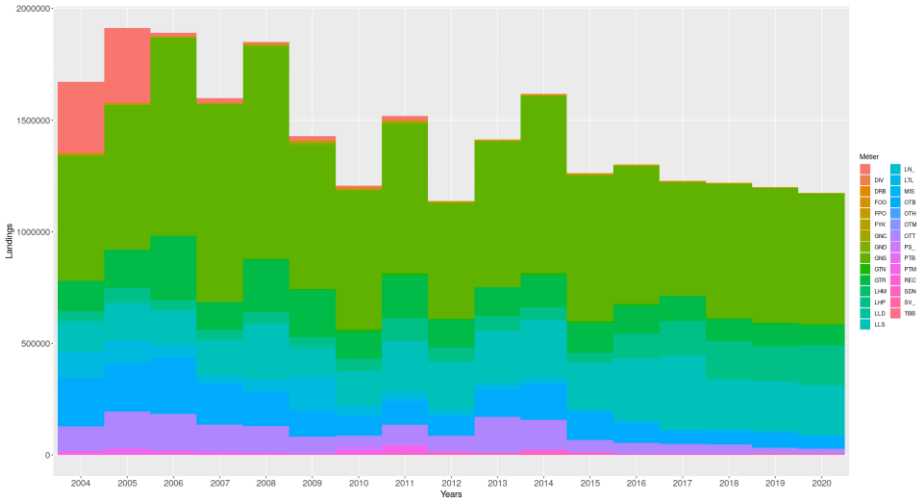


**Figure 7.3. Landings (in kg) of pollack per year and métier.**

Different filters were applied in order to select vessels catching pollack and reduce the number of vessels in the fleet of reference. The first filter concerns vessel's fishing activity [defined as years with positive landings of pollack]. Figure 7.4 represents the years of presence of vessels that have been catching pollack (at least 1 kg) during the period 2000-22. 141 vessels remain after applying a 10 years filter threshold (red line), 274 after a 5 years filter (green line) and 372 after a 3 years filter (blue line). The 5 years filter was chosen, as a compromise between the different options. It allows keeping enough vessels to constitute the data input for the CPUE models.

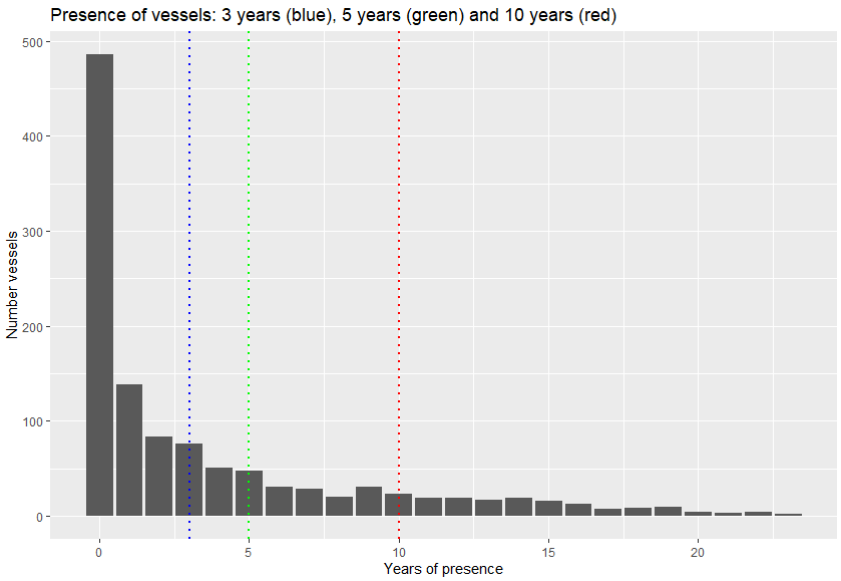


**Figure 7.4. Presence of the vessels during the 2000-2022 period.**

A selection was also made so that the vessels have been catching significant volumes of pollack per year. This selection was conducted on the vessels that were present 5 years at least during the period (*cf* previous §: 274 vessels). Figure 7.5 shows that a large part of the vessels landed limited volumes. 149 vessels remain after applying a threshold of 300 kg filter (average over the period), 113 after a 500 kg filter and 62 after a 1 tonne filter.

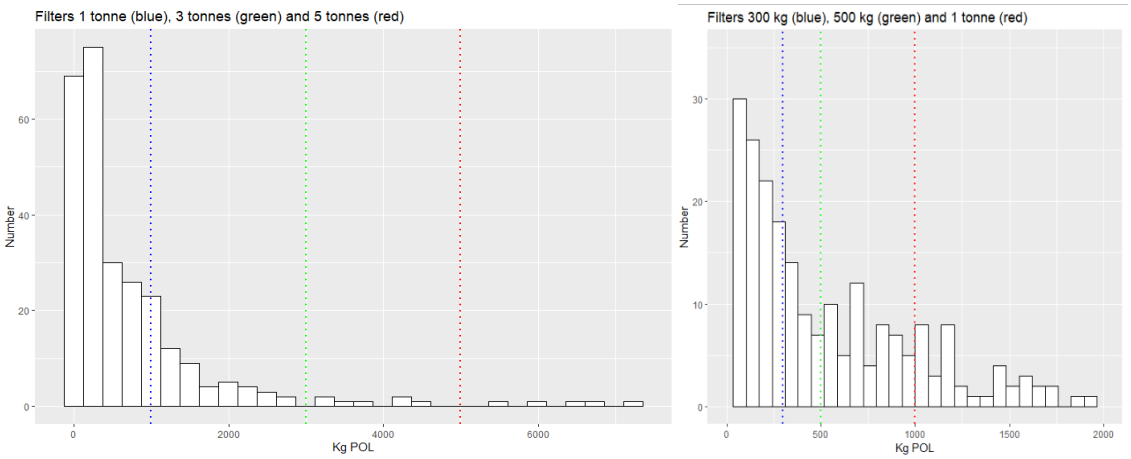


**Figure 7.5. Number of vessels and yearly average landings.**

A 500 kg filter was chosen and allows selecting vessels that landed a minimum volume of pollack per year.

### 7.2.3.1 Yearly consistency of the logbook database

As any static gear, gillnets fishing effort is usually hard to define. As an approximation, fishing time was set as the vessel time at sea.

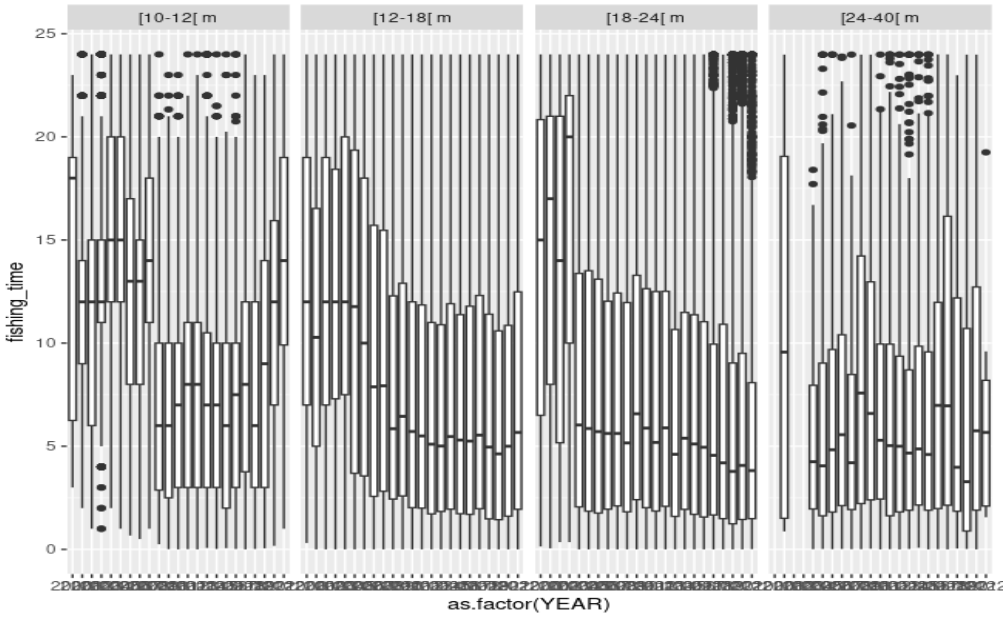


**Figure 7.6. Yearly effort distribution by vessel length class [time expressed in fishing days].**

The French database changed in 2009, which led to a change in the repositories of the effort. All declarative variables were impacted by this change in the database. Figure 7.6 shows that the effort time-series of vessel categories 10-12 m and 12-18 m have been strongly impacted by these changes and it appeared unrealistic to derive a consistent index over the whole time-series. Therefore, the data were cut in two series: from 2000 to 2009 and from 2010 to 2021.

### 7.2.3.2 Targeting covariates

Targeting behaviour can explain changes in CPUEs over time. The 10 major species that are caught with pollack are showed in Figure 7.7. Catches were normalized into relative proportions by weight and square-root transformed (Winker, 2013). To construct data input for the GAM's models, the Direct Principal Component approach was conducted. It uses directly the PC's scores of the PCA as predictor variable in the model. We retained PCs that had an eigenvalue higher than 1, in our case they were four PCs. Figure 7.8 shows the correlation graph and the correlation of variables.

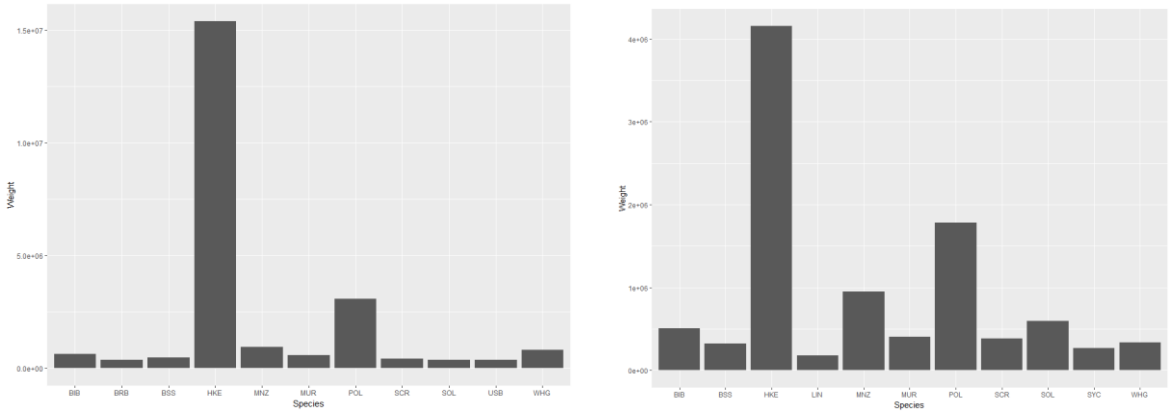


**Figure 7.7. Top 10 of species caught with pollack, for 2000-2009 (left) and 2010-2021 (right)**

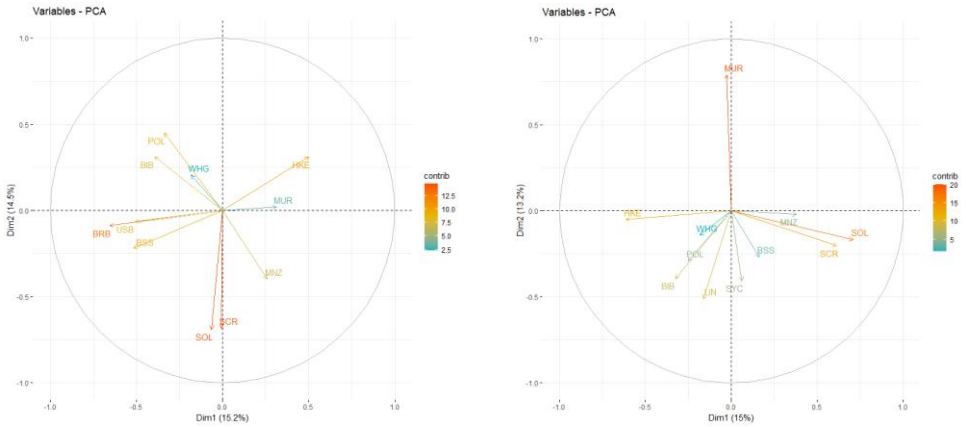


**Figure 7.8. Correlation graph and contribution of variables for 2000-2009 (left) and 2010-2021 (right).**

### 7.2.3.3 Model

The models fitting CPUE records was a GAM with a Tweedie distribution, which takes into account high frequencies of zeros in the data. A cyclic cubic regression spline was chosen to smooth the month predictor, while smoothing of other continuous variables was realized by thin plate regression spline functions. There is a random effect on vessels. Characteristics of vessels (in term of vessel length) is also included in the model. Effort was estimated using vessel time at sea and is used as an offset in the model. The PC's scores are represented by the covariates RS1, RS2, RS3 and RS4.

The final model is:

formula = "POL_weight ~ offset(log(time_sea)) + as.factor(YEAR) + s(MONTH, bs='cc', k=12) + s(carre.lon,carre.lat, k=20) + s(NAVS_COD, bs = 're') + s(RS1) + s(RS2) + s(RS3) + s(RS4) + as.factor(size_NAVS)"

model_fit <- mgcv::gam(formula = formula, data = sacrois_mod, family = tw(link="log"), method = "REML")

In order to compare the influence of adding the covariates on the predictions (especially the targeting covariate), the next five models were tested:

- "**base**": POL_weight ~ offset(log(time_sea)) + as.factor(YEAR) + s(NAVS_COD, bs = 're')
- "**mois**": POL_weight ~ offset(log(time_sea))+as.factor(YEAR)+s(MONTH, bs='cc', k=12) + s(NAVS_COD, bs = 're')
- "**space**": POL_weight ~ offset(log(time_sea))+as.factor(YEAR)+s(MONTH, bs='cc', k=12) + s(carre.lon,carre.lat, k=20) + s(NAVS_COD, bs = 're')
- "**carac**": POL_weight ~ offset(log(time_sea))+as.factor(YEAR) +s(MONTH, bs='cc', k=12) + s(carre.lon,carre.lat, k=20) +s(NAVS_COD, bs = 're')+as.factor(size_NAVS)
- "**tot**": POL_weight ~ offset(log(time_sea)) + as.factor(YEAR) + s(MONTH, bs='cc', k=12) + s(carre.lon,carre.lat, k=20) + s(NAVS_COD, bs = 're') + s(RS1) + s(RS2) + s(RS3) + s(RS4) + as.factor(size_NAVS)

Predictions were made for these five models and with the CPUE series 2000-2009 and 2010-2021 (Figure 7.9). The blue line represents the nominal CPUEs (mean of catch per year/effort). All CPUE are standardized by the mean.

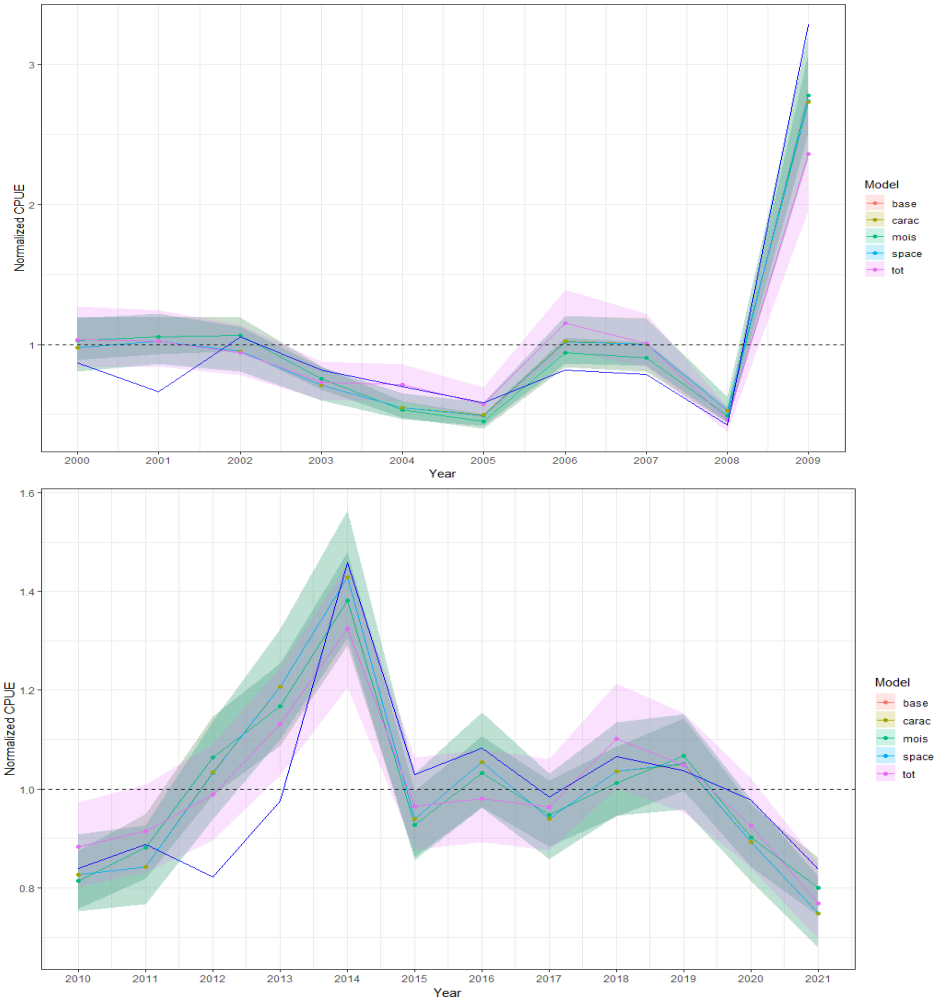


**Figure 7.9. Normalized CPUE estimated from the 5 GAM models tested for the time-series 2000-2009 (up) and 2010-21 (bottom).**

The final standardized CPUEs used in the SPiCT model are presented in Table 7.4.

**Table 7.4. Predictions of the GAM model used in the assessment of pol.27.89a.**

| Year | Predictions | Year | Predictions |
|---|---|---|---|
| 2000 | 1.03 | 2011 | 0.92 |
| 2001 | 1.02 | 2012 | 0.99 |
| 2002 | 0.94 | 2013 | 1.13 |
| 2003 | 0.73 | 2014 | 1.32 |
| 2004 | 0.71 | 2015 | 0.97 |
| 2005 | 0.57 | 2016 | 0.98 |
| 2006 | 1.15 | 2017 | 0.96 |
| 2007 | 1.00 | 2018 | 1.10 |
| 2008 | 0.46 | 2019 | 1.05 |
| 2009 | 2.36 | 2020 | 0.93 |
| 2010 | 0.88 | 2021 | 0.77 |

### 7.2.4 Length composition of landings

Length distribution of landings is available for some métiers and quarters for France (2010–2021), Spain (2015-2021) and Portugal (2019). The métiers and quarter coverage of the length sampling has changed from year-to-year, and the sampling level has been extremely low for some years. These issues reduce the representativeness and the quality of the length composition of landings. A set of length compositions of commercial landings, annual and gear-combined, for the period 2010–2021 were raised to total landings using information from ROMELIGO project (2010–2014; ICES, 2019) and from InterCatch (2015–2021; Figure 7.10).

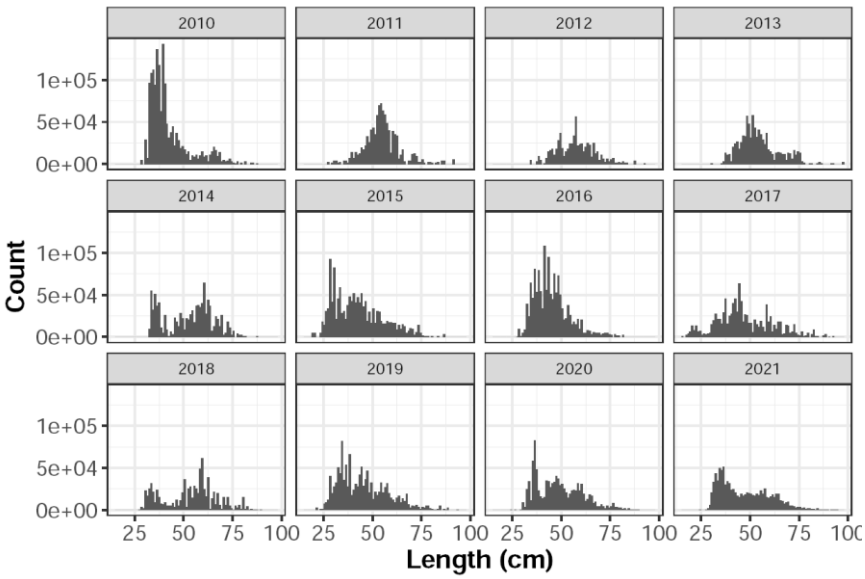


**Figure 7.10. Annual length composition of commercial landings of pol.27.89a.**

The length composition of landings was employed to estimate the length of first capture ($Lc$) of pol.27.89a following the calculation defined for Length-Based-Indicators (ICES, 2015). $Lc$ was estimated at 32.5 cm and was used as input data to calculate the $r$ priors. The $Lc$ is lower than the $Lm$ (42.3 cm), and this is related with the fact that the Minimum Recommended Conservation Size is set at 30 cm and discards of pollack are considered are considered negligible (< 5% catches).

## 7.2.5 Life-history parameters

The available data on the biology of pollack are sparse and their availability vary among stocks and ICES subareas. Life-history parameters are needed to conduct a reliable assessment, not only to incorporate the parameters in the model, but also to evaluate the plausibility of the estimated production function in production models.

The available life-history information for pollack, from literature and working documents, was reviewed. The information was selected considering the quality and extension of the scientific work and the representativeness for the Bay of Biscay and Iberian waters pollack stock (pol.27.89a). The summary of the life-history information is shown in Table 7.5. The von Bertalanffy growth parameters are available from a Bayesian analysis for Subarea 8 and from frequentist analysis for Subareas 6 and 7. The value of $Linf$ is estimated at 102.1 cm and 98.3 cm depending of the study. Related to maturity, the $Lm$ both sexes together, is at 42.3 cm, corresponding to the estimates from the microscopic study carried out in division 9a (Alonso-Fernández et al. 2013), other maturity studies in Subarea 8 confirmed this value (Léauté et al. 2018). $Lc$ and $Lmax$ were estimated in this work using the available size composition of landings for pol.27.89a. $Lc$ was estimated at 32.5 cm, well below the $Lm$ (43.2 cm), and $Lmax$ was equal to 97.5 cm.

**Table 7.5. Summary of life-history parameters selected to be used in the stock assessment of pol.27.89a. Source of the data and areas of study are indicated in the last two columns.**

| Life-history parameter | | Value (units) | Source | ICES Subarea/Division |
|---|---|---|---|---|
| $L_{inf}$ | Asymptotic length | 102.143 (cm) | Alemany (2017). Bayesian analysis. | 8 |
| | | 98.3 (cm) | Alemany (2017) | 6.7 |
| $K$ | von Bertalanffy parameter | 0.193 | Alemany (2017). Bayesian analysis. | 8 |
| | | 0.182 | Alemany (2017) | 6.7 |
| $t_0$ | von Bertalanffy parameter | -0.682 | Alemany (2017). Bayesian analysis. | 8 |
| | | -0.935 | Alemany (2017) | 6.7 |
| $L_m$ | Length-at-maturity | 42.3 (cm) | Alonso-Fernández et al (2013) | 9a |
| $t_m$ | Age-at-maturity | 3.5 (year) | Léauté et al (2018) | 8 |
| $L_{max}$ | Maximum observed length in the stock | 97.5 (cm) | Estimated from length composition (2010-2021) (this work) | 89a |
| $t_{max}$ | Maximum age | 15 (year) | Alemany (2017) | 67 |
| a | Length-weight relationship parameter | 1.09e-5 | Léauté et al (2018) | 8 |
| b | Length-weight relationship parameter | 3.044 | Léauté et al (2018) | 8 |
| $Lc$ | Length-at-50%-capture | 32.5 (cm) | Estimated from length composition (2010-2021) (this work) | 8.9a |

### 7.2.6 Estimated priors for used in the assessment

The use of sound informative priors can improve the SPiCT model fit in cases of lack of contrast in the available time-series of catch and relative abundance and will avoid a potential bias in the production function.

The initial priors on $r$ were established through a Monte-Carlo simulation which integrates stock specific life-history information and inference from life-history meta-analysis (Thorson et al. 2017). For this estimates the R package SPMpriors (github.com/henning-winker/SPMpriors) (Winker, 2020) was employed. The stock specific biological information for pol.27.89a ($Linf$=98.3 cm and $Lm$=42.3 cm) and a range for *steepness* of 0.6-0.9 were included to tune the multivariate normal (MVN) simulations. The $r$ prior derived using MVN simulations and these same data has its higher densities at lower values of $r$ with a mean value at 0.3675 and dispersion parameter equal to 0.3066 (Table 7.6). Under the Schaefer formulation these values of $r$ prior could be directly used for SPICT.

**Table 7.6. Results of the Multivariate-Normal (MVN) simulations with stock specific tuning information for pol.27.89a.**

| trait | mu.sp | cv.sp | mu.stk | cv.stk | lc.stk | uc.stk | upper.quant |
|---|---|---|---|---|---|---|---|
| Loo | 79.6805 | 0.2098 | 85.3434 | 0.1408 | 65.4653 | 111.2573 | 0.9 |
| K | 0.2068 | 0.2593 | 0.2008 | 0.2466 | 0.1448 | 0.2783 | 0.9 |
| Lm | 42.156 | 0.2328 | 44.8934 | 0.1409 | 33.4785 | 60.2005 | 0.9 |
| tm | 3.1603 | 0.3826 | 3.2526 | 0.3565 | 2.0233 | 5.2288 | 0.9 |
| tmax | 12.8543 | 0.3311 | 13.2282 | 0.3059 | 8.7576 | 19.981 | 0.9 |
| M | 0.4105 | 0.281 | 0.3998 | 0.2696 | 0.2809 | 0.5689 | 0.9 |
| h | 0.7879 | 0.2016 | 0.7795 | 0.1223 | 0.6395 | 0.88 | 0.9 |
| sigR | 0.4854 | 0.2814 | 0.4781 | 0.2699 | 0.3354 | 0.6813 | 0.9 |
| rho | 1.6177 | 0.2947 | 1.6262 | 0.2503 | 1.3559 | 1.9504 | 0.9 |
| r | 0.3842 | 0.5403 | 0.3675 | 0.3066 | 0.192 | 0.7036 | 0.9 |
| G | 7.0384 | 0.2476 | 7.2372 | 0.2328 | 5.2956 | 9.8907 | 0.9 |

For a Pella-Tomlinson production model, where the shape parameter is different from 2, the priors for *r* and shape are estimated through an Age-Structured Equilibrium Model (Winker et al. 2020) using the function *fl2asem* included in the package SPMpriors. The MVN stock parameters from *FishLife* were translated into Pella-Tomlinson stock production model priors. As the length at first capture *Lc* for the pol.27.89a, calculated in the current work, is lower than length-at-maturity, the *Lc* value was included in the configuration of the analysis. The *r* prior is defined by a central value of 0.222 and a dispersion parameter equal to 0.261 (Table 7.7). Its mean value is lower than the value corresponding to a Schaefer formulation of the surplus production model (0.367).

**Table 7.7. Mean and standard deviation (log.sd) for lognormal r prior approximations and associated input values for the inflection point Bmsy/K as determined by the shape in a Pella –Tomlinson model formulation.**

| | r | shape | Fmsy | Bmsy/K |
|---|---|---|---|---|
| mu | 0.22192684 | 0.946 | 0.23344155 | 0.35778678 |
| logsd | 0.26103633 | 0.18146549 | 0.34119912 | 0.09321143 |

## 7.3 Stock assessment

## 7.4 Input data

The input data for the model were the time-series of commercial landings for years 1979–2021 and two commercial abundance indices FR-GNS for years 2000-2009 and 2010–2021 (Figure 7.11).

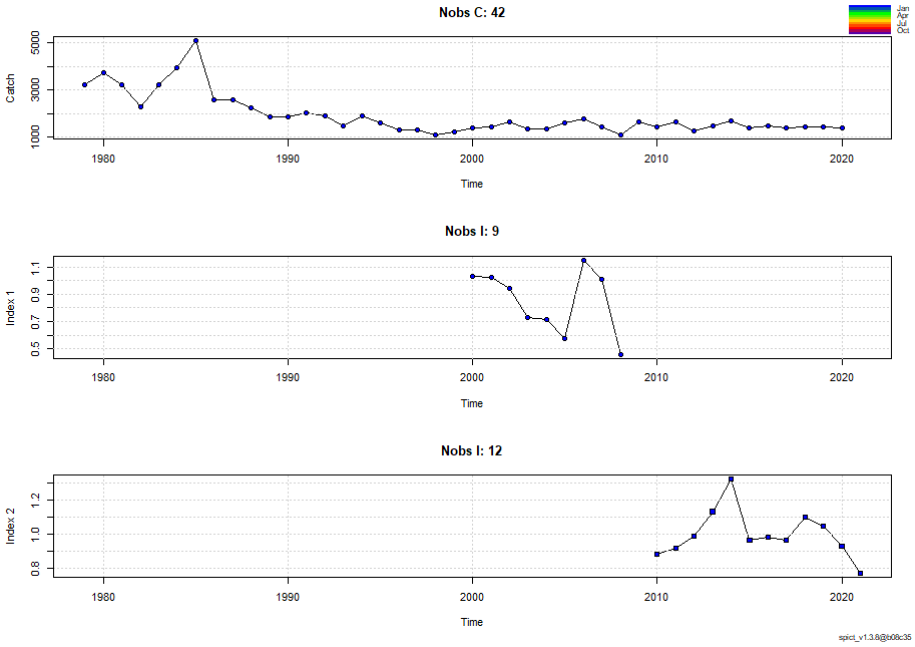


**Figure 7.11. Input data for SPiCT.**

## 7.5 Exploratory assessments

Multiple runs were built, with different priors and input data (Table 7.8). For each of the runs, convergence, as well as diagnostic figures and retrospective plots were examined.

The main problem that we encountered was the high uncertainty of the fishing mortality and the catch in the results plots. Even if diagnostics were fine in the last trials, this high uncertainty could not allow estimating correctly the parameters. The best runs (Run 7, Run 10 and Run 14.1) showed very high uncertainty on catch. The results of these runs are presented in Figures 7.12, 7.13 and 7.14.

The results of these exploratory SPiCT assessments suggested that the model does not have enough information to estimate all parameters of the model. This is likely a result of the short length of the abundance indices used (10 + 12 years) and the lack of contrast in catch series in he over-lapping period Catch-CPUE.

**Table 7.8. Summary of the definition and diagnostics test of the sxploratory runs for pol.27.89a.**

| n° run | Time series | Uncertainty | Prior logr | Prior logn | Prior logbkfrac | Prior alpha and beta | Convergence | Diagnostics | Retrospective | r estimation | K estimation | n estimation | bkfrac estimation | BMSYs | FMSYs | MSYs | B 2021 | F2021 | B2021/B MSY | F2021/F MSY |
|---|---|---|---|---|---|---|---|---|---|---|---|---|---|---|---|---|---|---|---|---|
| 1 | 1979-2020 | identical | default | default | default | default | no | / | / | / | / | / | / | / | / | / | / | / | / | / |
| 2 | 1979-2021 | identical | default | log(2), 0.00001 | default | default | no | / | / | / | / | / | / | / | / | / | / | / | / | / |
| 3 | 1979-2022 | identical | log(0.43), 0.2 | log(2), 0.00001 | default | default | yes but high uncertainty F and C | problem normality catch | ok | / | / | / | / | / | / | / | / | / | / | / |
| 4 | 1979-2023 | higher (10x) in 1999 | log(0.43), 0.2 | log(2), 0.00001 | default | default | yes but high uncertainty F and C | problem normality catch | ok | / | / | / | / | / | / | / | / | / | / | / |
| 5 | 1979-2020, 1999 removed | identical | log(0.43), 0.2 | log(2), 0.00001 | default | default | yes but high uncertainty F and C | ok | ok +/- | / | / | / | / | / | / | / | / | / | / | / |
| 6 | 1979-2020, 1999 - average 1998-2000 | identical | log(0.43), 0.2 | log(2), 0.00001 | default | default | yes but high uncertainty F and C | ok | ok | / | / | / | / | / | / | / | / | / | / | / |
| 7 | 1979-2020, 1999 - average 1998-2000 | identical | log(0.43), 0.2 | log(2), 0.00001 | log(0.3), 0.25 | default | yes but uncertainty on estimates | ok | ok | 0.47 | 3.53E+04 | 2 | 0.39 | 1.74E+04 | 0.23 | 4.00E+03 | 2.67E+04 | 0.048 | 1.54 | 0.2 |
| 8 | 1979-2020, 1999 - average 1998-2000 | identical | log(0.43), 0.2 | log(2), 0.00001 | log(0.7), 0.2 | default | yes but high uncertainty F and C | ok | ok | / | / | / | / | / | / | / | / | / | / | / |
| 9 | 1979-2020, 1999 - average 1998-2000 | identical | log(0.43), 0.2 | log(2), 0.00001 | log(0.9), 0.25 | default | yes but high uncertainty F and C | ok | ok | / | / | / | / | / | / | / | / | / | / | / |
| 10 | 1979-2020, 1999 - average 1998-2000 | identical | log(0.43), 0.2 | log(2), 0.00001 | log(0.2), 0.5 | default | yes but uncertainty on estimates | ok | ok | 0.46 | 3.46E+04 | 2 | 0.49 | 1.70E+04 | 0.23 | 3.90E+03 | 2.60E+04 | 0.049 | 1.54 | 0.21 |
| 11 | 1979-2020, 1999 - average 1998-2000 | identical | log(0.43), 0.2 | log(2), 0.5 | default | default | yes but high uncertainty F and C | ok | ok | / | / | / | / | / | / | / | / | / | / | / |
| 12 | 1979-2020, 1999 - average 1998-2000 | identical | log(0.43), 0.2 | log(2), 0.5 | log(0.2), 0.5 | default | yes but high uncertainty F and C | ok | ok | / | / | / | / | / | / | / | / | / | / | / |
| 12.1 | 1979-2020, 1999 - average 1998-2000 | identical | log(0.43), 0.2 | log(2), 0.5 | log(0.5), 0.5 | default | yes but high uncertainty F and C | ok | one retro did not converge | / | / | / | / | / | / | / | / | / | / | / |
| 12.2 | 1979-2020, 1999 - average 1998-2000 | identical | log(0.43), 0.2 | log(2), 0.5 | log(0.7), 0.5 | default | yes but high uncertainty F and C | ok | ok | / | / | / | / | / | / | / | / | / | / | / |
| 13 | 1979-2020, 1999 - average 1998-2000 | identical | log(0.43), 0.2 | log(2), 0.5 | log(0.2), 0.5 | desabled | yes but high uncertainty F and C | ok | ok | / | / | / | / | / | / | / | / | / | / | / |
| 14 | 1979-2020, 1999 - average 1998-2000 | identical | log(0.22), 0.2 | log(1.1), 0.5 | log(0.2), 0.5 | default | yes but high uncertainty F and C | ok | ok | / | / | / | / | / | / | / | / | / | / | / |
| 14.1 | 1979-2020, 1999 - average 1998-2000 | identical | log(0.22), 0.2 | log(1.1), 0.00001 | log(0.2), 0.5 | default | yes but uncertainty on estimates | ok | ok | 0.23 | 4.10E+04 | 1.1 | 0.48 | 1.58E+04 | 0.21 | 3.34E+03 | 3.00E+04 | 0.044 | 1.94 | 0.2 |
| 14.2 | 1979-2020, 1999 - average 1998-2000 | identical | log(0.22), 0.2 | log(1.1), 0.00001 | log(0.5), 0.5 | default | yes but high uncertainty F and C | ok | not OK | / | / | / | / | / | / | / | / | / | / | / |

### 7.5.1 Final assessment

No model configuration was accepted by the Workshop to use as final model assessment. Indeed, the abundance index time-series is not long, resulting from the cut of the CPUE series in two. Also, the two series of catch and abundance index do not show enough contrast to allow a good fit of the model. Finally, even when some runs showed correct diagnostics and not retrospective patterns, the estimates obtained with the model seem not to correspond to the state of the stock (high biomass and low fishing mortality).

## 7.6 Future considerations/recommendations

This stock identity of pol.27.89a is still unclear and it would need to be addressed before a future benchmark of the species.

Although it is known that recreational catches of pollack in subarea 8 and division 9a could be high, they have never been quantified. The change to an assessment and advice system that allow to manage the commercial and recreational pollack catches would require to have estimates of the recreational catches.

The available time-series of commercial landings (1979-2021) is lack of contrast, especially in the last 20 years, making very complicate to achieve a good fit of a SPiCT model. Besides, the unavailability of a fishery-independent abundance index increases the difficulty of fitting a SPiCT model.

Based on the available information of the stock (length composition of landings, an abundance index and life-history parameters), length based assessment methods can be applied to assess pol.27.89a. Therefore, the ICES technical guidelines for harvest control rules and stock assessment in categories 2 and 3 (ICES, 2022) indicates that the method 2.1. the *rfb* rule is appropriate to this stock.

## 7.7 Reviewer report

The stock is currently a category 5 stock without an index. The landings come primarily from France and Spain with minor catches from Portugal mainly gillnets and longlines and are available since 1979. Discards are considered negligible (2% of the catch). There are recreational catches, but they have not been quantified.

A new commercial abundance index was prepared and presented based on the French gillnet fleet. The total number of vessels (1155) was filtered to only include those that had a 5-year period of at least 500 kg of landings; leading to 113 vessels being included in the index.

Soak time and net length (effort) was not available, so the vessel time at sea was used. Effort was also not stored in a consistent way in the French databases before and after 2010. The inconsistency was presented to the group and the decision to split the index into two time-series 2000-2009 and 2010-2021 was it was decided to split the index in two.

A Tweedie-GAM is used to standardize the commercial CPUE. It uses an offset for effort, year as fixed effect, vessel as random effect, a cyclical spline on month, and a two-dimensional spatial spline. Targeting is dealt with using principal component analysis (PCA) that includes 10 major species caught together with pollack. All principal components that had an eigenvalue larger than one were included as covariates in the Tweedie-GAM. Pollack catches are also included in the PCA, which can be problematic because the principal components are thus not independent of the response (in worst case one of the principal components is exactly the pollock catches, and a seemingly perfect fit can be obtained).

Very little contrast in the data did not lead to an acceptable SPiCT assessment. Several runs were attempted using different assumptions (e.g. restricting or fixing shape parameters, different initial depletion assumptions), but none did lead to an acceptable assessment.

The main decision is to move the stock to category 3 and use ICES empirical rules to provide advice based on the biomass index presented along with length-based indicators and information about the growth of the stock from literature (von Bertalanffy K). The index standardization procedure was presented and deemed acceptable to be used in the rfb-rule. Length–frequency distributions from landings were also presented but not discussed. The rfb-rule is to be used for the stock but also not discussed and should be evaluated by the assessment working group or an external expert that has expertise in the ICES empirical rules.

### 7.7.1 Conclusions

Any of the SPiCT assessment model configurations tested was considered appropriate to be used as basis for providing advice for Pollack in ICES subarea 8 and division 9a.

Alternatively, the use of integrated models could be explored in future to account for the good amount of length and biological information available for this stock.

## 7.8 References

Alemany, J. 2017. Développement d'un cadre Bayésien pour l'évaluation de stocks à données limitées et élaboration de scénarios de gestion, cas particuliers de la seiche (Sepia officinalis) et du lieu jaune (Pollachius pollachius). Ph.D. Thesis. Université Caen Normandie. 262 pp.

Alonso-Fernández A., Villegas-Rios, D., Valdés-López, M., Olveira-Rodríguez, B., Saborido-Rey, F. 2013. Reproductive biology of pollack (Pollachius pollachius) from the Galician shelf (north-west Spain). Journal of the Marine Biological Association of the United Kingdom, 2013, 93(7): 1951-1963.

ICES. 2012. Report of the Working Group on Assessment of New MoU Species (WGNEW). ICES CM 2012/ACOM:20.

ICES. 2015. Report of the Fifth Workshop on the Development of Quantitative Assessment Methodologies based on Life-history Traits, Exploitation Characteristics and other Relevant Parameters for Data-Limited Stocks (WKLIFE V), 5–9 October 2015, Lisbon, Portugal. ICES CM 2015/ACOM: 56.

ICES. 2019. Working Group for the Bay of Biscay and the Iberian Waters Ecoregion (WGBIE). ICES Scientific Reports. 1:31. 692 pp. http://doi.org/10.17895/ices.pub.5299.

ICES. 2021. Benchmark Workshop on the development of MSY advice for category 3 stocks using Surplus Production Model in Continuous Time; SPiCT (WKMSYSPiCT). ICES Scientific Reports. 3:20. 317 pp. https://doi.org/10.17895/ices.pub.7919.

ICES. 2022. ICES technical guidance for harvest control rules and stock assessments for stocks in categories 2 and 3. In Report of ICES Advisory Committee, 2022. ICES Advice 2022, Section 16.4.11. https://doi.org/10.17895/ices.advice.19801564.

Léauté, J-P, Caill-Milly, N. and Lissardy, M. 2018. ROMELIGO: Improvement of the fishery knowledge of striped red mullet, whiting and pollack of the Bay of Biscay, p 532. In ICES. 2018. Report of the Working Group for the Bay of Biscay and and Iberian Waters Ecoregion (WGBIE).

Moreau J. 1964. Contribution à l'étude du lieu jaune (Gadus pollachius L.). Rev. Trav. Inst. Pêches Marit., 28(3), 238–255.

Pedersen, M.W. and Berg, C.W. 2017. A stochastic surplus production model in continuous time. Fish and Fisheries, 18: 226–243. url:https://onlinelibrary.wiley.com/doi/abs/10.1111/faf.12174, doi:10.1111/faf.12174.

Quéro J-C. and Vayne J-J. 1997. Les poissons de mer des pêches françaises. « Les encyclopédies du naturaliste ». Ed. Delachaux and Niestle, 304p.

Radford Z., Hyder K., Zarauz L., Mugerza E., Ferter K., Prellezo R., Strehlow H.V., Townhill B., Lewin W.C., Weltersbach M.S. 2018. The impact of marine recreational fishing on key fish stocks in European waters. PLoS One. 2018 Sep 12;13(9):e0201666. doi: 10.1371/journal.pone.0201666. PMID: 30208030; PMCID: PMC6135385.

Thorson, J.T. 2019. FishLife: Predict life history parameters for any fish (https://github.com/James-Thorson-NOAA/FishLife ).

Thorson, J.T., Cope, H.M., Branch, T.A and O.P. Jensen. 2012. Spawning biomass reference points for exploited marine fishes, incorporating taxonomic and body size information. *Canadian Journal of Fisheries and Aquatic Sciences,* 69: 1556–1568.

Thorson, J.T., Munch, S.B., Cope, J.M., and J. Gao. 2017. Predicting life history parameters for all fishes worldwide. *Ecological Applications*, 27(8): 2262–2276. doi/10.1002/eap.1606/full.

Winker, H. 2020. SPMpriors: SPMprior generation with FishLife. (https://github.com/HenningWinker/SPMpriors).

Winker, H., Kerwath, S. and Attwood, C. 2013. Comparison of two approaches to standardize catch-per-unit-effort for targeting behaviour in a multispecies hand-line fishery. *Fisheries Research*, 139. doi: 118-131. 10.1016/j.fishres.2012.10.014.

Winker, H., Mourato, B., Chang. Y. 2020. Unifying parameterizations between age-structured and surplus production models: an application to atlantic white marlin (Kajikia albida) with simulation testing. *Collect. Vol. Sci. Pap.* ICCAT, 76(4): 219-234.

## 7.9 Working document for pollack

# Life history information relevant for the stock assessment of pollack in Subarea 8 and Division 9a

*Paz Sampedro[1], Fanny Ouzoulias[2] and Youen Vermard[2]*

**ABSTRACT**

The available data on the biology of pollack are sparse and their availability vary among stocks and ICES subareas. Life history parameters are needed to conduct a reliable assessment, not only to incorporate the parameters in the model, but also to evaluate the plausibility of the estimated production function in production models. In this work, the life history information available in the literature and previous studies was reviewed and compiled to be used in the assessment of pollack. Besides, the use of sound informative priors can improve the SPiCT model fit in cases of lack of contrast in the available time-series of catch and relative abundance and will avoid a potential bias in the production function. Using a Monte-Carlo simulation approach life history parameters were converted into priors for parameters of surplus production models.

## 1. Life history information

The available life history information for pollack, from literature and working documents, was reviewed. The information was selected considering the quality and extension of the scientific work and the representativeness for the Bay of Biscay and Iberian waters pollack stock (pol.89a). The summary of the life history information is shown in Table 1. The von Bertalanffy growth parameters are available from a Bayesian analysis for Subarea 8 and from frequentist analysis for Subareas 6 and 7. The value of $Linf$ is estimated at 102.1 cm and 98.3 cm depending of the study. Related to maturity, the $Lm$ both sexes together, is at 42.3 cm, corresponding to the estimates from the microscopic study carried out in division 9a (Alonso-Fernández et al. 2013), other maturity studies in Subarea 8 confirmed this value (Léauté et al. 2018). $Lc$ and $Lmax$ were estimated in this work using the available size composition of landings for pol.89a. $Lc$ was estimated at 32.5 cm, well below the $Lm$ (43.2 cm), and $Lmax$ was equal to 97.5 cm.

[1] Centro Oceanográfico de A Coruña - CN IEO–CSIC- Spain

[2] IFREMER - France

**Table 1. Summary of life history parameters selected to be used in the stock assessment of pol.89a. Source and areas of study are indicated in the last two columns.**

| Life history parameter | | Value (units) | Source | ICES Subarea/ Division |
|---|---|---|---|---|
| $L_{inf}$ | Asymptotic length | 102.143 (cm) | Alemany (2017). Bayesian analysis. | 8 |
| | | 98.3 (cm) | Alemany (2017) | 6.7 |
| $K$ | Von Bertalanffy parameter | 0.193 | Alemany (2017). Bayesian analysis. | 8 |
| | | 0.182 | Alemany (2017) | 6.7 |
| $t_0$ | Von Bertalanffy parameter | -0.682 | Alemany (2017). Bayesian analysis. | 8 |
| | | -0.935 | Alemany (2017) | 6.7 |
| $L_m$ | Length-at-maturity | 42.3 (cm) | Alonso-Fernández et al (2013) | 9a |
| $t_m$ | Age-at-maturity | 3.5 (year) | Léauté et al (2018) | 8 |
| $L_{max}$ | Maximum observed length in the stock | 97.5 (cm) | Estimated from length composition (2010-2021) (this work) | 89a |
| $t_{max}$ | Maximum age | 15 (year) | Alemany (2017) | 67 |
| **a** | Length-weight relationship parameter | 1.09e-5 | Léauté et al (2018) | 8 |
| **b** | Length-weight relationship parameter | 3.044 | Léauté et al (2018) | 8 |
| $Lc$ | Length-at-50%-capture | 32.5 (cm) | Estimated from length composition (2010-2021) (this work) | 8.9a |

### 2. Length of first capture ($Lc$) and maximum observed length in the stock ($Lmax$)

Length compositions of landings are available for some *metiers* from 2010 to 2021 and they were compiled from Romeligo project (2010-2014) and InterCatch (2015-2021). The different length composition by *metier* were weighted to estimate an annual length

composition of the stock landings. The length of first capture $Lc$, the length at which 50% of fish is retained, was derived by fitting the length-based estimator to the available size data. Since 2017, the $Lc$ was estimated at 32.5 cm except in year 2020.

Table 2. Length of first capture and other length based indicators for pol.89a.

| Year | $Lc$ | $Linf$ | $Lm$ | $Lmean$ |
|---|---|---|---|---|
| 2010 | 32.5 | 98.2 | 42.3 | 42 |
| 2011 | 52.5 | 98.2 | 42.3 | 58.6 |
| 2012 | 47.5 | 98.2 | 42.3 | 58.7 |
| 2013 | 47.5 | 98.2 | 42.3 | 56.6 |
| 2014 | 32.5 | 98.2 | 42.3 | 52.8 |
| 2015 | 27.5 | 98.2 | 42.3 | 43.1 |
| 2016 | 37.5 | 98.2 | 42.3 | 46.4 |
| 2017 | 32.5 | 98.2 | 42.3 | 49.1 |
| 2018 | 32.5 | 98.2 | 42.3 | 53.4 |
| 2019 | 32.5 | 98.2 | 42.3 | 46.2 |
| 2020 | 37.5 | 98.2 | 42.3 | 50.2 |
| 2021 | 32.5 | 98.2 | 42.3 | 47.1 |

The $Lmax$ the maximum observed length in the stock, was calculated from the length composition available and it corresponds to 97.5 cm.

### 3. Generating priors for stock assessment of pollack in 8 and 9a with SPiCT

The use of informative priors on $r$ allows to fit an assessment model in situations of lack of contrast in the catch and CPUE/Survey series and also to avoid a potential bias in the production function estimate. It is also important take into account that are values from other models that might not correspond exactly to $r$ values from SPiCT. The initial priors on $r$ were established through a Monte-Carlo simulation which integrates stock specific life history information and inference from life history meta-analysis (Thorson et al. 2017) using the R package `SPMpriors` (github.com/henning-winker/SPMpriors) (Winker, 2020). The stock specific biological information for pol.89a ($Linf$=98.3 cm and $Lm$=42.3 cm) were included to tune the multivariate normal (MVN) simulations. The $r$ prior derived using MVN simulations and these same data has its higher densities at lower values of $r$ (Figure 1,2) with a mean value at 0.3675 and dispersion parameter

equal to 0.3066 (Table 3). Under the Schaefer formulation these values of $r$ prior could be directly used for SPICT.

**Table 3. Results of the Multivariate-Normal (MVN) simulations with stock specific tuning information for pol.89a.**

| trait | mu.sp | cv.sp | mu.stk | cv.stk | lc.stk | uc.stk | upper.quant |
|---|---|---|---|---|---|---|---|
| Loo | 79.6805 | 0.2098 | 85.3434 | 0.1408 | 65.4653 | 111.2573 | 0.9 |
| K | 0.2068 | 0.2593 | 0.2008 | 0.2466 | 0.1448 | 0.2783 | 0.9 |
| Lm | 42.156 | 0.2328 | 44.8934 | 0.1409 | 33.4785 | 60.2005 | 0.9 |
| tm | 3.1603 | 0.3826 | 3.2526 | 0.3565 | 2.0233 | 5.2288 | 0.9 |
| tmax | 12.8543 | 0.3311 | 13.2282 | 0.3059 | 8.7576 | 19.981 | 0.9 |
| M | 0.4105 | 0.281 | 0.3998 | 0.2696 | 0.2809 | 0.5689 | 0.9 |
| h | 0.7879 | 0.2016 | 0.7795 | 0.1223 | 0.6395 | 0.88 | 0.9 |
| sigR | 0.4854 | 0.2814 | 0.4781 | 0.2699 | 0.3354 | 0.6813 | 0.9 |
| rho | 1.6177 | 0.2947 | 1.6262 | 0.2503 | 1.3559 | 1.9504 | 0.9 |
| r | 0.3842 | 0.5403 | 0.3675 | 0.3066 | 0.192 | 0.7036 | 0.9 |
| G | 7.0384 | 0.2476 | 7.2372 | 0.2328 | 5.2956 | 9.8907 | 0.9 |

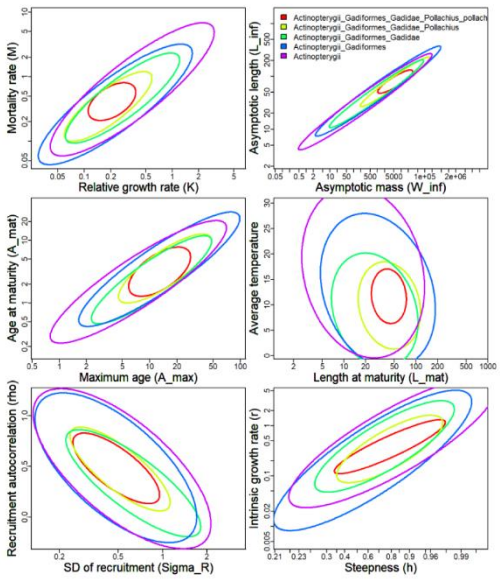


**Figure 1. Bi-variate plots of predicted value intervals for pollack, and its parent taxa, tuned to the Bay of Biscay and Iberian waters stock Linf and Lm.**

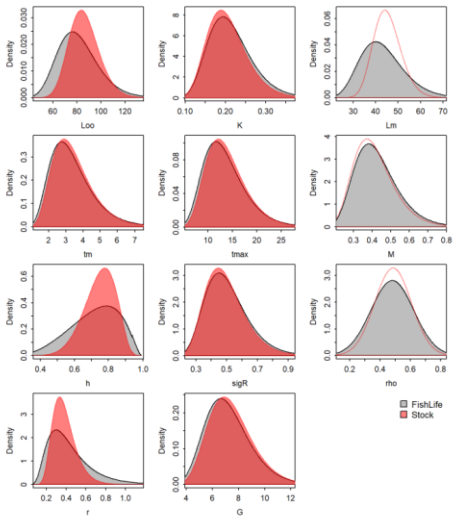


**Figure 2. FishLife and stock-specific density distributions of generated life history parameter and other quantities of interest for pol.89a.**

For a Pella-Tomlinson production model, where the shape parameter is different from 2, the priors for $r$ and shape are estimated through an Age-Structured Equilibrium Model (Winker et al. 2020) using the function *fl2asem* included in the package SPMpriors. The MVN stock parameters from FishLife were translated into Pella-Tomlinson stock production model priors. As the length at first capture $L_c$ for the pol.89a, calculated in the current work, is lower than length-at-maturity ($L_m$), the Lc value was included in the configuration of the analysis. The r prior is defined by a central value of 0.222 and a dispersion parameter equal to 0.261 (Table 4). Its mean value is lower than the value corresponding to a Schaefer formulation of the surplus production model (0.367).

**Table 4. Mean and standard deviation (log.sd) for lognormal $r$ prior approximations and associated input values for the inflection point Bmsy/K as determined by the shape in a Pella –Tomlinson model formulation.**

| | r | shape | Fmsy | Bmsy/K |
|---|---|---|---|---|
| mu | 0.22192684 | 0.946 | 0.23344155 | 0.35778678 |
| logsd | 0.26103633 | 0.18146549 | 0.34119912 | 0.09321143 |

# 8 Thornback ray in the Cantabrian Sea

## rjc.27.8c – *Raja clavata* in Division 8.c

## 8.1 Introduction

Thornback ray (*Raja clavata)* is one of the most frequent skates in the Atlantic Iberian waters. It is a coastal benthic species with a wide geographic distribution in the Northeast Atlantic and Mediterranean Sea. The species is found on different types of substrata (mud, sand and gravel bottoms) at depths ranging from shallow waters to 400 m or more but mainly from 50–200 m. In particularly in the Cantabrian Sea is the most abundant skate species.

### 8.1.1 Fishery information

Data used correspond to landings (t) of *Raja clavata* by the Spanish fleet (the main fleet) operating in this area (ICES Division 8.c; Cantabrian Sea) which represents around the 99% of landings in this area (Table 8.1). Species-specific landings are available only from 2009. Prior to 2009, landings were not reported by species and most landings of thornback ray were reported as 'skates and rays'. The most important fleet in terms of landings is the trawl fleet which accounts for around the 67% of landings, followed by gillnets (26%) and longline (6%).

### 8.1.2 Current assessment and advice

The first assessment of this stock (rjc.27.8c) was conducted in 2022. Before, the assessment of this stock was included with stock rjc.27.8abd (northern Bay of Biscay) as rjc.27.8 stock, however in 2022 (Lorance, 2022; Trenkel *et al*., 2022) the stock was split (see WKELASMO) in two components rjc.27.8abd and rjc.278c. Iberian skates (ICES areas 8.c and 9.a) are assessed since 2014 under ICES category 3 of DLS (Data Limited Stocks) using biomass indicator trends obtained from the two main surveys conducted in the area. In 2022 following ICES guidelines (ICES, 2021b) the stock was assessed applying the *rfb* rule (Rodriguez-Cabello and Velasco, 2022).

## 8.2 Input data for stock assessment

According to the recommendations made during the previous benchmark meeting two different time-series data were considered for this new assessment. One which included species-specific data for this stock both landings (t) and discards from 2009 to 2021. Another scenario corresponded to landings estimates (t) from 1996 to 2021. Prior to 2009 not landings at species level is available, Therefore, data corresponding to previous years has been estimated. Based on specific landings from 2010–2020 and on board sampling a ratio of 40% of *Rajidae* landings was attributed to thornback ray in Division 8.c. Retrospective landings prior 2009 have been calculated using this ratio (Figure 8.1).

### 8.2.1 Landings and discards (e.g.)

Data used correspond to landings (t) of *Raja clavata* by the Spanish fleet operating in this area ICES Division 8.c (Cantabrian Sea). Species-specific landings are available only from 2009. Discard estimates are also available from that period and are variable ranging from 8% to 37% (Figure 8.2). Discards estimates obtained from the National Observers Programme (PNDB).

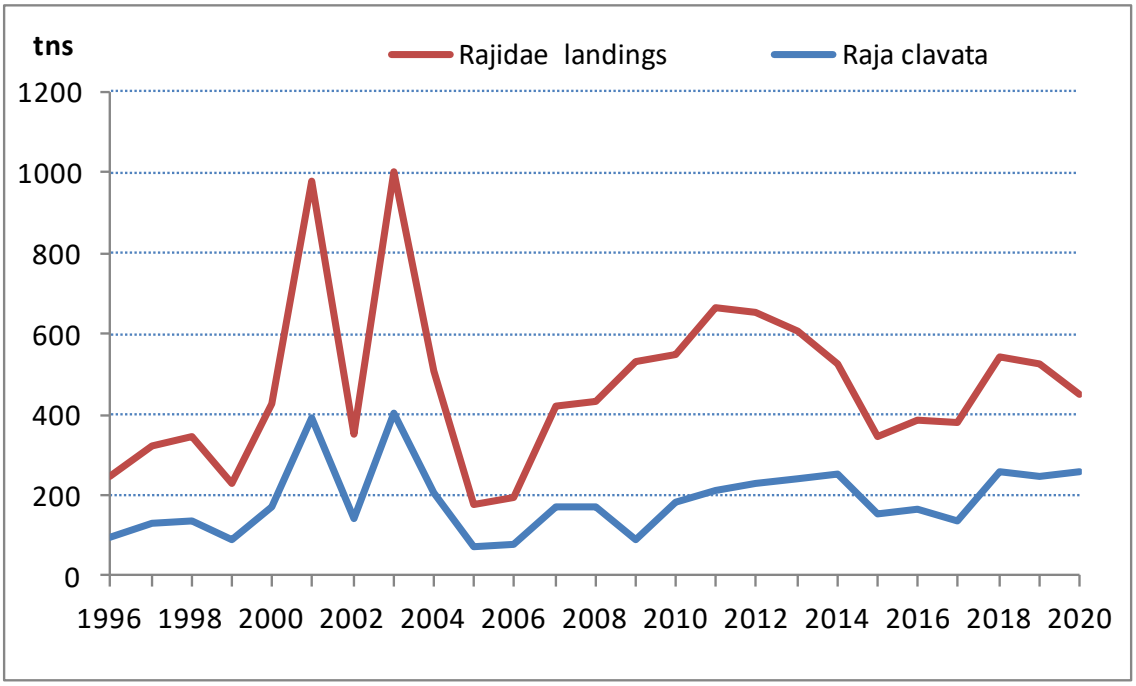


**Figure 8.1. Total landings of Rajidae species in ICES Division 8.c since 1996 and estimates of *Raja clavata* landings from 1996 to 2008.**

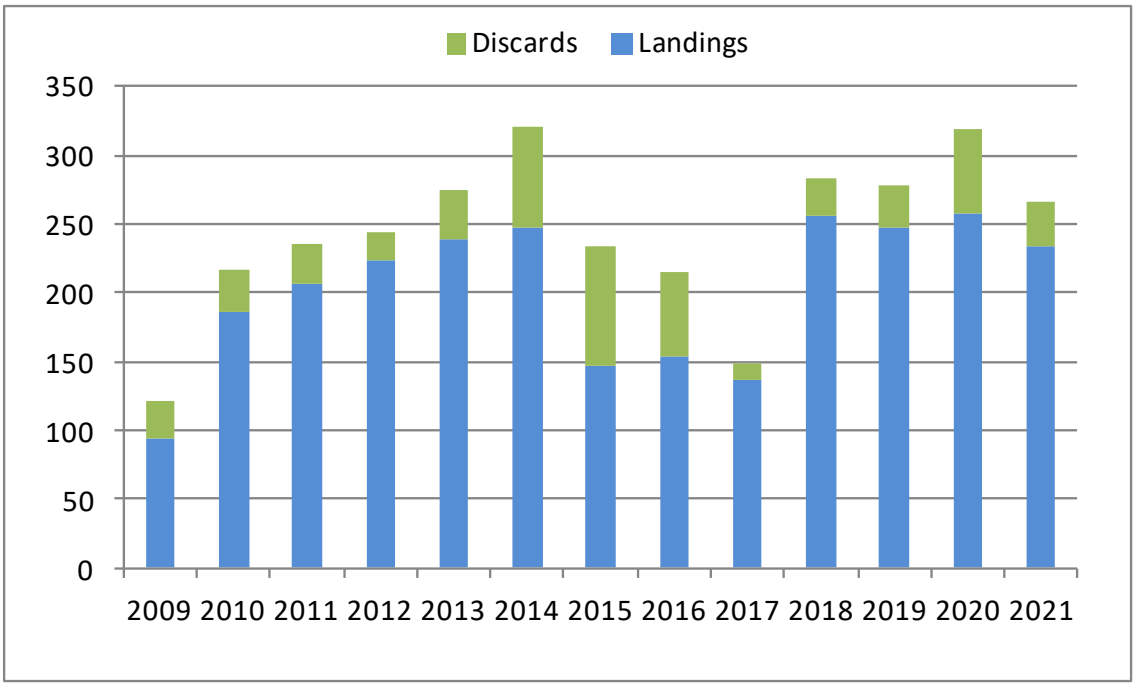


**Figure 8.2. Landings and discards of *Raja clavata* by the Spanish fleet in Division. 8.c years 2009–2021.**

**Table 8.1. Thornback ray in ICES Div 8c. ICES estimates of landings by country (in tonnes).**

| | Landings (t) | | |
|---|---|---|---|
| Year | Spain | France | Total |
| 2009 | 94.0 | 0.09 | 94 |
| 2010 | 186.0 | 0.03 | 186 |
| 2011 | 206.1 | 0.27 | 206 |
| 2012 | 223.3 | 0.45 | 224 |
| 2013 | 238.4 | 0.05 | 238 |
| 2014 | 247.9 | 0.15 | 248 |
| 2015 | 146.4 | 0.06 | 146 |
| 2016 | 154.3 | 0.12 | 154 |
| 2017 | 136.4 | 0.05 | 136 |
| 2018 | 256.0 | 0.01 | 256 |
| 2019 | 247.4 | 0.02 | 247 |
| 2020 | 257.1 | 0.02 | 257 |
| 2021 | 232.9 | 0.04 | 233 |

### 8.2.2 Biomass index

The Spanish Institute of Oceanography (IEO) carries out annual bottom-trawl surveys along the continental shelf of Galicia and Cantabrian Sea following the standard IBTS methodology for the western and southern areas (ICES, 2017). The biomass index used in this analysis corresponds to the standardized biomass index obtained from the annual bottom-trawl survey carried out in the study area *Demersales* (SpNGFS-WIBTS-Q4) in the fourth quarter. The sampling design is random stratified sampling based on 30 minutes bottom-trawl hauls with five geographical sectors and three depth strata ( > 70–120 m, 121–200 m and 201–500 m). Some extra hauls are carried out every year, if possible, to cover shallower ( < 70 m) and deeper ( > 500 m) grounds more information ICES, 2017). The catches of the additional hauls are not included in the calculations of the stratified abundance indices but the information from these depths is considered relevant to obtain more information about the depth range and distribution of the species and also used to obtain biological data (Blanco *et al*., 2021). The survey index time-series started in 1983 and is standardized from 1990. The biomass or abundance index is expressed as Kg/haul or Number/haul respectively. It represents the mean stratified catch per 30 minutes trawl following the same methodology as Cochran (1971) and Grosslein and Laurec (1982) among others.

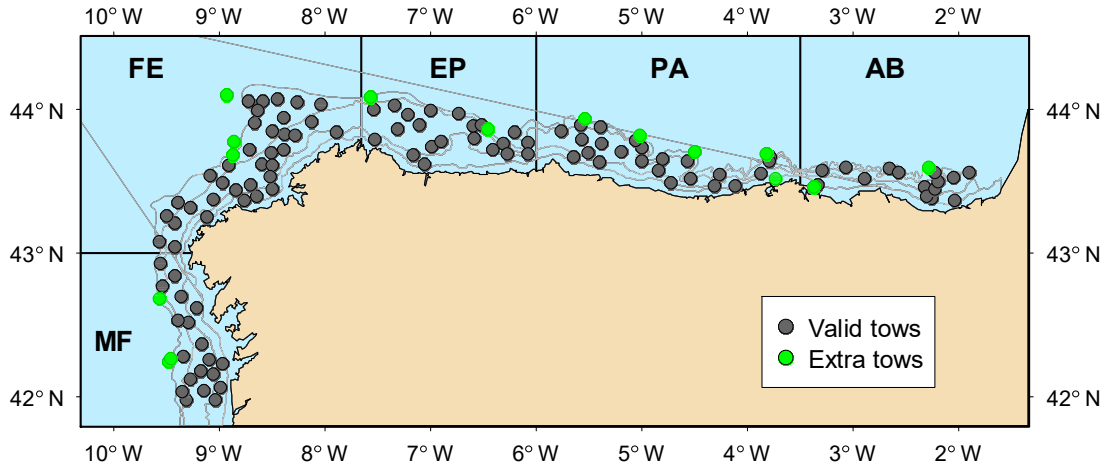


**Figure 8.3. Stratification design and hauls on the Northern Spanish shelf groundfish survey (example in 2021); Depth strata are: A) 70–120 m, B) 121–200 m and C) 200–500 m. Geographic sectors are MF: Miño-Finisterre, FE: Finisterre-Estaca, EP: Estaca-cabo Peñas, PA: Peñas-cabo Ajo, and AB: Ajo-Bidasoa.**

The equations for the whole area are as follows:

$$Mean\ stratified\ catch = \bar{Y}_{st} = \frac{1}{A}\sum A_h \bar{y}_h$$

$$Stratified\ Variance = S^2_{(\bar{Y}_{st})} = \frac{1}{A^2}\sum \frac{A_h^2 S_h^2}{n_h}$$

$$SE\ (S\tan dard\ Error) = \sqrt{S^2_{(\bar{Y}_{st})}}$$

Where,

$A$= Area total
$A_h$= Area of each strata
$\bar{Y_h}$= Mean catch in each strata

The biomass of *R. clavata*, shows an increasing trend from the beginning of the time-series with interannual fluctuations (Figure 8.4). Two changes of vessel have taken place during the last time-series of the survey. In 2013 the existing RV "*Coornide de Saavedra*" was replaced by a new one "*Miguel Oliver*". In 2021 a severe breakage of the new ship used to conduct the survey, forced to change the vessel. In both cases the gear was the same standard gear used on the survey (SPNGFS-WIBTS-Q4) however the true effect of this change in the species catchability is unknown. For this reason high uncertainty is given those years in the following SPiCT analysis.

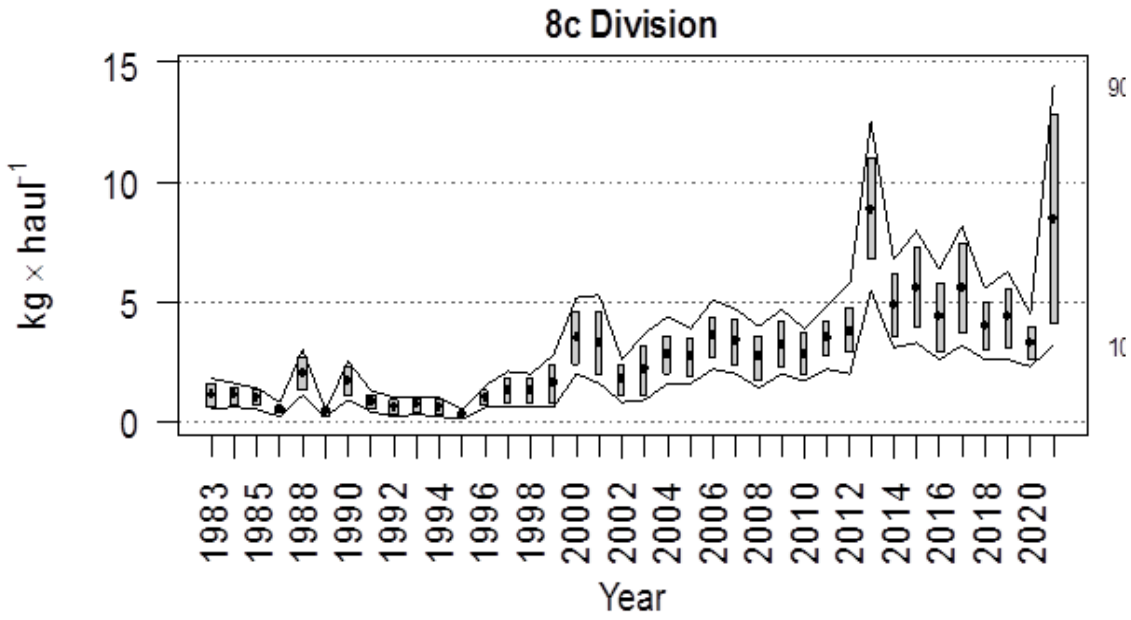


**Figure 8.4. Evolution of *R. clavata* biomass index during the North Spanish shelf bottom-trawl survey time-series in ICES Division 8.c. Boxes mark parametric standard error of the stratified biomass index. Lines mark bootstrap confidence intervals (α = 0.80, bootstrap iterations = 1000).**

**Table 8.2. Biomass index (kg/haul) and standard error (SE) obtained from North Spanish trawl survey 1990 to 2021.* Years with a change of research vessel.**

| | TOTAL | | |
|---|---|---|---|
| Year | Yst | SE | CV |
| 1990 | 1.67 | 0.60 | 0.36 |
| 1991 | 0.78 | | |
| 1992 | 0.60 | 0.30 | 0.49 |
| 1993 | 0.65 | 0.28 | 0.43 |
| 1994 | 0.62 | 0.31 | 0.5 |
| 1995 | 0.26 | 0.14 | 0.54 |
| 1996 | 1.02 | | |
| 1997 | 1.28 | 0.53 | 0.42 |
| 1998 | 1.25 | 0.51 | 0.41 |
| 1999 | 1.59 | 0.80 | 0.5 |
| 2000 | 3.48 | 1.11 | 0.32 |
| 2001 | 3.28 | 1.27 | 0.39 |
| 2002 | 1.75 | 0.65 | 0.37 |
| 2003 | 2.17 | 1.05 | 0.48 |

| | TOTAL | | |
|---|---|---|---|
| Year | Yst | SE | CV |
| 2004 | 2.81 | 0.80 | 0.28 |
| 2005 | 2.64 | 0.80 | 0.3 |
| 2006 | 3.55 | 0.84 | 0.24 |
| 2007 | 3.36 | 0.94 | 0.28 |
| 2008 | 2.64 | 0.91 | 0.34 |
| 2009 | 3.22 | 0.92 | 0.29 |
| 2010 | 2.81 | 0.82 | 0.29 |
| 2011 | 3.47 | 0.73 | 0.21 |
| 2012 | 3.82 | 0.98 | 0.26 |
| 2013* | 8.86 | 2.15 | 0.24 |
| 2014 | 4.86 | 1.28 | 0.26 |
| 2015 | 5.62 | 1.66 | 0.3 |
| 2016 | 4.33 | 1.42 | 0.33 |
| 2017 | 5.57 | 1.87 | 0.34 |
| 2018 | 3.97 | 1.00 | 0.25 |
| 2019 | 4.33 | 1.22 | 0.28 |
| 2020 | 3.28 | 0.65 | 0.2 |
| 2021* | 5.86 | 4.36 | 0.74 |

### 8.2.3 Life-history information

Thornback ray is an oviparous species which length at birth is around 11–13 cm. There are no specific biological studies conducted in this Area (8.c) however growth and maturity information is reported for other areas. Studies from Portuguese waters provided a maturity length of 78.4 for females and 67.6 cm for males and an estimated fecundity of 135 eggs per female (Serra-Pereira *et al.*, 2011). These authors also carried out a study to determine the age based on dermal denticles and provided growth parameters ($L\infty$ = 128 cm and k = 0.117 $y^{-1}$). Other maturity estimates and growth parameters are available for this species in other northern areas (for example Gallagher *et al.*, 2005; Walker, 1999; Whittamore and McCarthy, 2005).

The thornback ray length distributions obtained from research surveys ranged from 12 to 102 cm (Figure 8.5) although the bulk of individuals are within 20 to 85 cm. Maximum length recorded from commercial fishing sampling in Division 8.c is 104 cm and usually length distributions range from 30 to 90 cm for all gears combined. Thus according to the maximum observed length both from survey and commercial length data the estimated asymptotic length for this stock is 110 cm (Froese and Binohlan, 2000; Froese, 2004). Studies from other areas provided larger

asymptotic lengths for this species. Due to the fact that the landings length distribution is sex combined and average value of maturity length has been used. A summary of the life-history parameters use in the last assessment of this stock is shown in Table 8.3.

**Table 8.3. Biological parameters used for calculating the LBI parameters (rjc.27.8c).**

| Parameter | Value | Definition | Source |
|---|---|---|---|
| L∞ (cm) | 110 | Asymptotic average maximum length | $L_{inf}$ =Lobs / 0.95 (Froese, 2004) |
| $L_{mat}$ | 73.2 | Length at 50% maturity | Serra-Pereira *et al.,* 2011 |
| K | 0.117 | growth coefficient (year$^{-1}$) | Serra-Pereira *et al.,* 2008 |
| a | 0.0018 | Condition factor parameter of length-weight relationship | IEO Database |
| b | 3.33 | Slope parameter of length-weight relationship | IEO Database |
| M/K | 1.5 | ratio of natural mortality to von Bertalanffy growth rate | Jensen, 1996 |

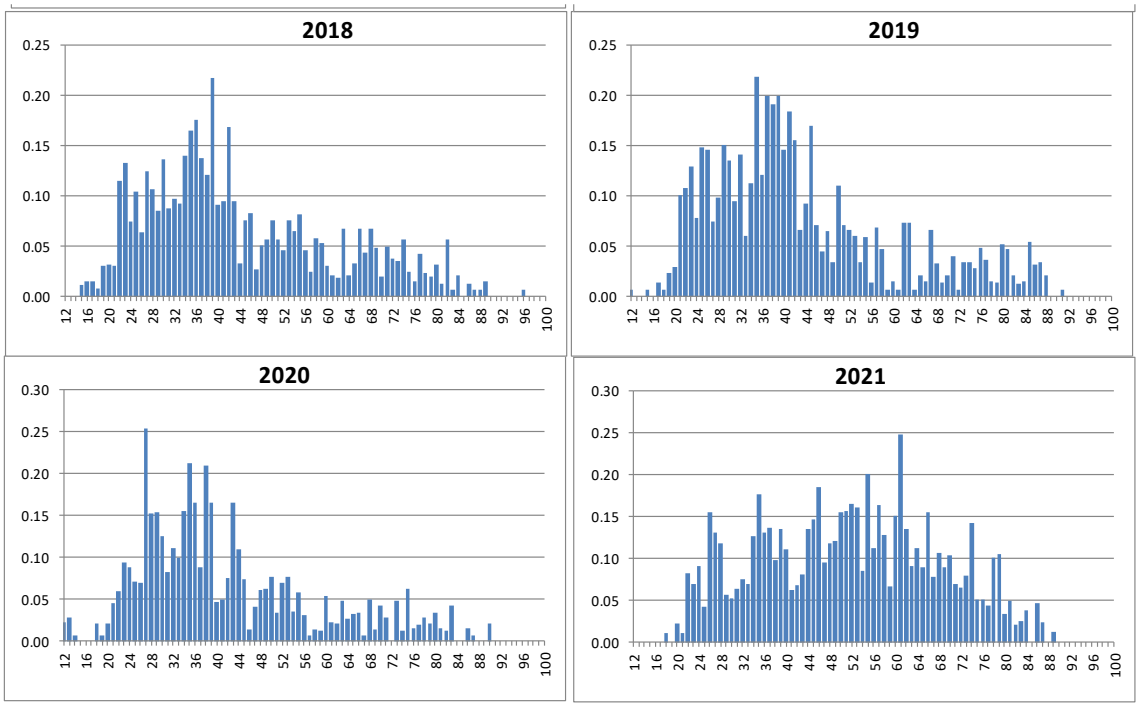


**Figure 8.5. *Raja clavata* (rjc.27.8c) Stratified length–frequency distributions derived from survey data for the last 4 years (2018–2021).**

## 8.3 Stock assessment

Following ICES guidelines (ICES, 2021b), a SPiCT model was explored and chosen for assessment of this stock. Several sensitivity runs were performed to analyse the robustness of the assessment based on different catch time-series and biomass index time-series. In addition different priors were tested particularly those relate with the shape of production curve (n) and the intrinsic growth rate (r). Besides the sensitivity of the assessment to the standard deviation of the priors mainly the intrinsic growth rate (logr), the biomass process noise (logsdb), and the index

observation noise (logsdi) was also tested. Details on these runs are presented in each of the specific sections below.

### 8.3.1 Exploratory assessments

More than 15 exploratory assessments for Thornback ray in Division 8.c were performed to analyse the robustness of the assessment to the model assumptions and settings, such as assumed prior distributions, splitting the abundance index, or assumed landings time-series. Figure 8.6 shows the final baseline assessment side by side with all sensitivity runs. While the biomass and fishing mortality on absolute scale span a wide range, on relative scale, all sensitivity runs show a similar trajectory suggesting recovering biomass from low levels in the 1990s above $B_{MSY}$ and a recent decline in biomass, while the fishing mortality is below $F_{MSY}$ since the late 1990s. Only four runs suggest that the biomass is at or below $B_{MSY}$ in the last years (Figure 8.6). In the following sections, the sensitivity runs and their results are explained in more detail.

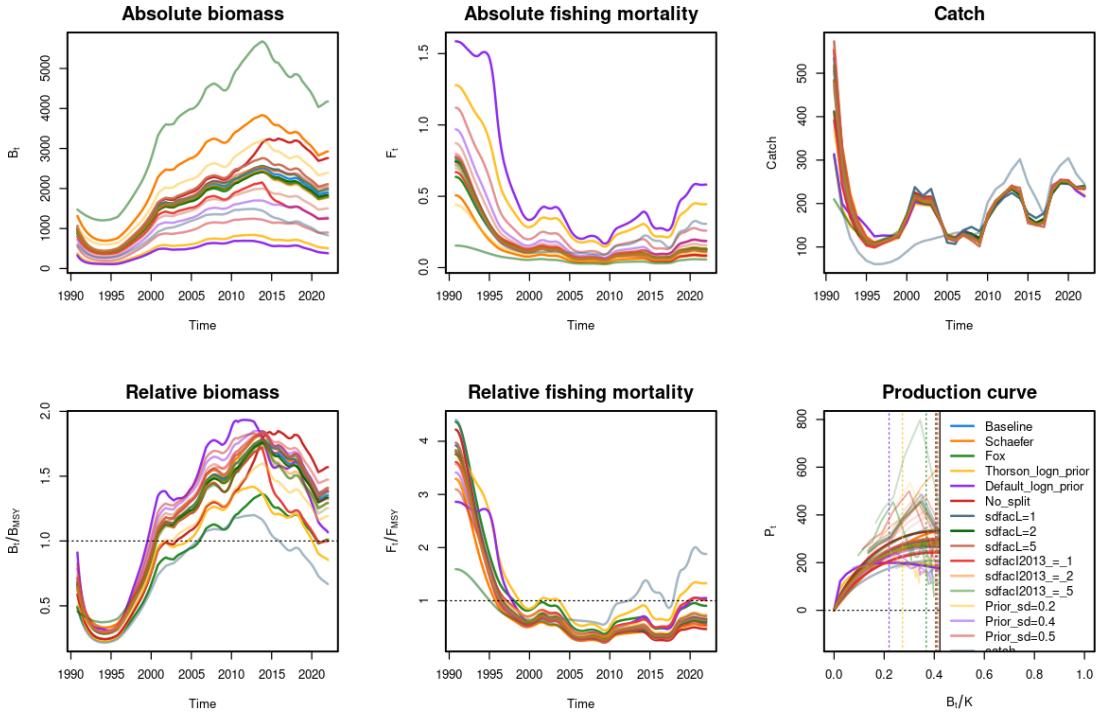


**Figure 8.6. Final assessment (Baseline) and all sensitivity runs for Thornback ray in Division 8.c (rjc.27.8c).**

#### 8.3.1.1 Sensitivity to the shape of the production curve

The sensitivity to the shape of the production curve (Gamma prior for n in the baseline assessment) was tested by four additional scenarios: (1) Fixing the production curve to n = 2 ("Schaefer"); (2) Fixing the production curve to n = 1 ("Fox"); (3) Using the corresponding prior but a assuming a lognormal distribution rather than a Gamma distribution ("Thorson_logn_prior"); (4) Using the SPiCT default prior for n ("Default_logn_prior"). Although the production curves vary, the relative results of the baseline and Schaefer model are almost identical (Figure 8.7). The default and Thorson's logn prior lead to highly left skewed production curves suggesting a lower maximum productivity at lower biomass levels. Although these runs are more conservative estimating a lower relative biomass, the Gamma prior for n was the preferable option, as it allows for more flexibility of the production curve than fixing it, while avoiding low n values below 1.

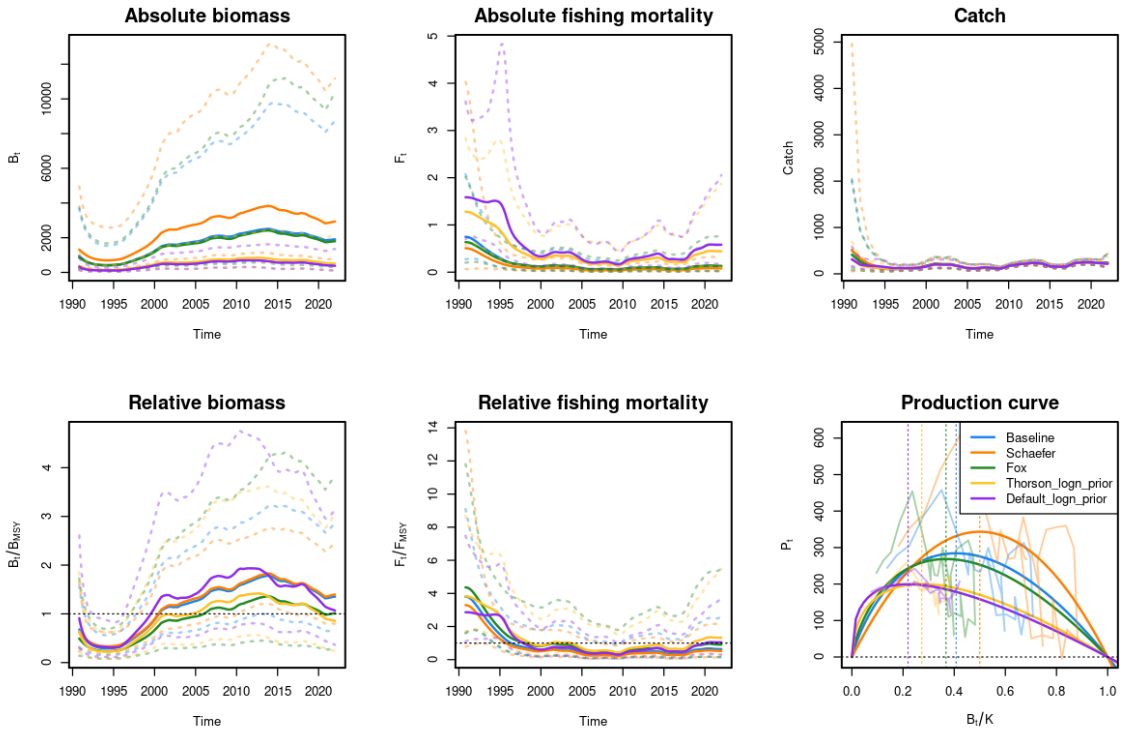


**Figure 8.7. Final assessment (Baseline) and all sensitivity runs regarding the shape of the production curve for Thornback ray in Division 8.c (rjc.27.8c).**

### 8.3.1.2 Sensitivity to splitting the abundance index

As explained above, the research vessel of the scientific survey changed in 2013 leading to the decision to split the estimated abundance index into separate indices within SPiCT for the baseline assessment. Figure 8.8 shows that splitting the index leads to a more conservative assessment estimating higher relative biomass from 2000 to 2013 but suggesting a more rapid decline in biomass since 2013.

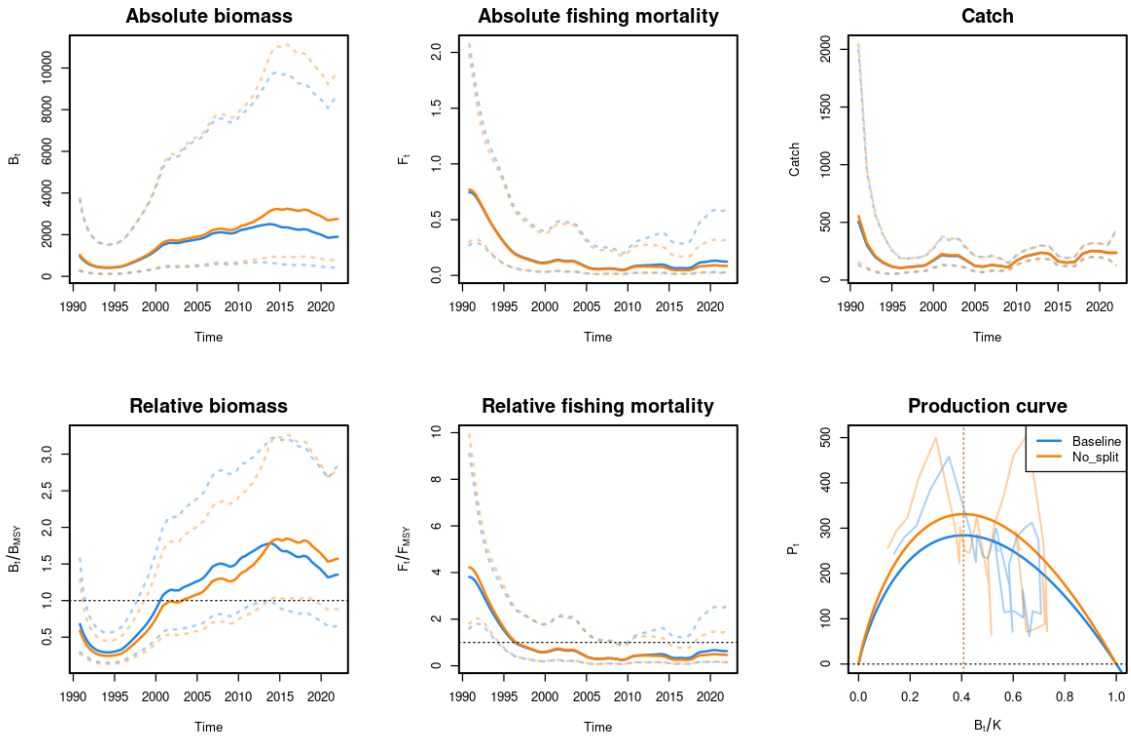


**Figure 8.8. Final assessment (Baseline) and all sensitivity runs regarding the split of the abundance index for Thornback ray in Division 8.c (rjc.27.8c).**

### 8.3.1.3 Sensitivity to uncertainty scaling

The baseline assessment assumes higher uncertainty for catches before 2009 by a factor of 3 and a higher uncertainty of the abundance index in 2013 by a factor of 3. Figure 8.9 shows that the results are not sensitive to these factors as long as the factor for the uncertainty of the abundance index in year 2013 is larger than 1. As Table 8.2 indicates the estimated CV for this year (0.24) is comparable to the years before and after (0.26), while the estimated index is more than 2 times larger than the years before and after. Although using the estimated CV as the uncertainty scaling for the index in this year gives with a more pronounced decline in biomass in the last years more conservative results, the assessment did not pass diagnostic tests (see Section 8.7). The assumption of higher than estimated uncertainty for the index in 2013 is supported by the unusually high estimated abundance in the year where the scientific survey introduced a new research vessel.

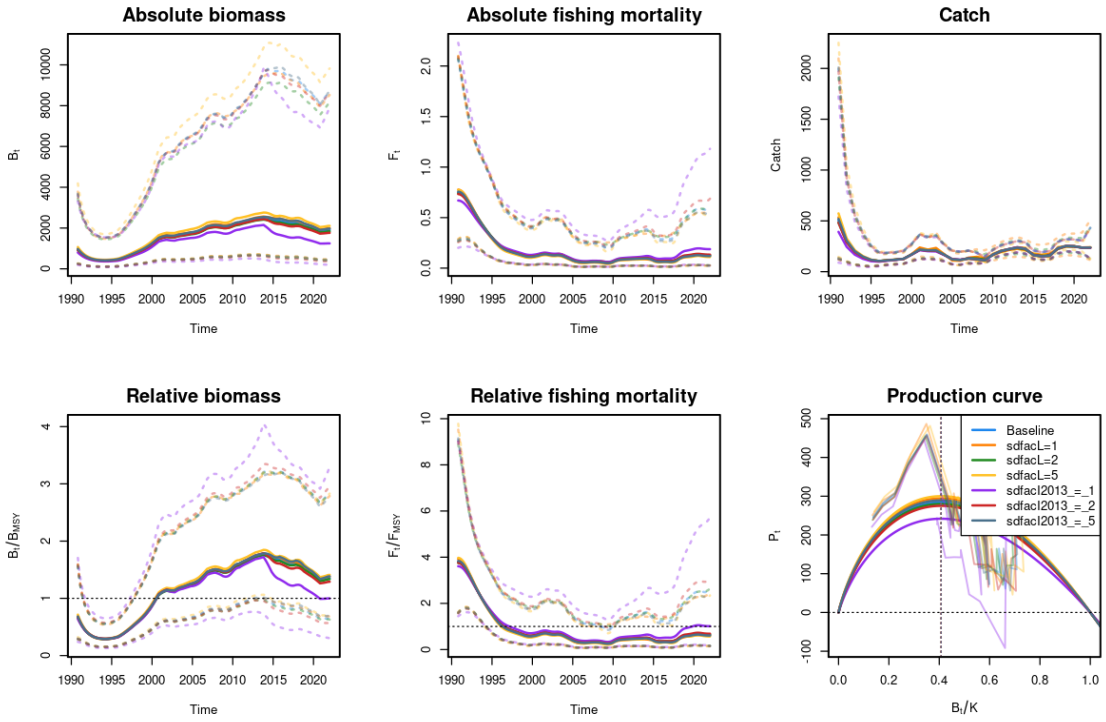


**Figure 8.9. Final assessment (Baseline) and all sensitivity runs regarding the uncertainty scaling of landings and the abundance index for Thornback ray in Division 8.c (rjc.27.8c).**

### 8.3.1.4 Sensitivity to SD of priors

The sensitivity of the assessment to the standard deviation of the priors (for the intrinsic growth rate (logr), the biomass process noise (logsdb), and the index observation noise (logsdi)) was tested by varying it from 0.2 to 0.5. The results did not vary significantly on relative terms between SD=0.3 (baseline) and larger deviations of these priors (Figure 8.10). However, assuming more informative priors (SD = 0.2), the estimated maximum productivity and absolute biomass is higher and thus the estimated relative biomass consistently lower. On the other hand, the diagnostic tests were not passed for this sensitivity run, as the jitter analysis indicated multiple local maxima and alternative parameter combinations (see Section 8.7). At the same time, less informative priors led to a larger intrinsic growth rate as in the baseline assessment and as expected (see Section 8.7). Thus, it was decided that a standard deviation of 0.3 poses a reasonable compromise.

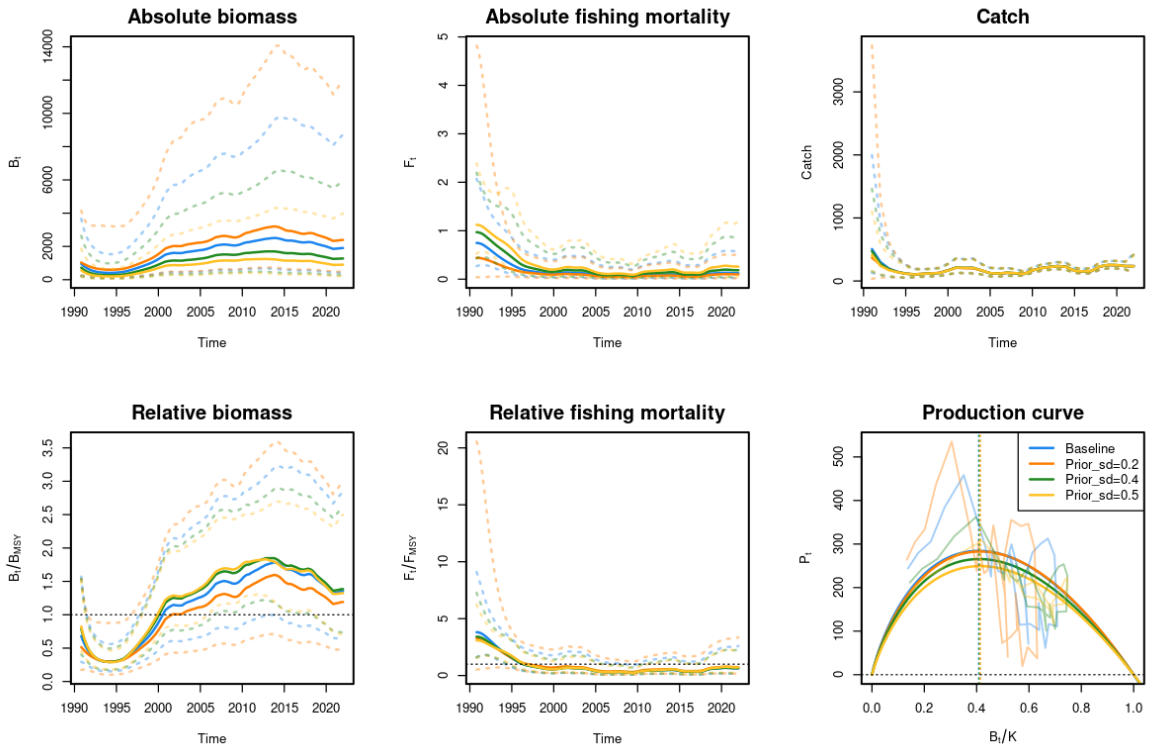


**Figure 8.10. Final assessment (Baseline) and all sensitivity runs regarding the standard deviation of the prior distributions for Thornback ray in Division 8.c (rjc.27.8c).**

### 8.3.1.5 Sensitivity to landings/catch time-series

The sensitivity of the assessment to the assumed landings/catch time-series was tested by using the shorter but more certain catch time-series (landings and discards) from 2009 to 2021 rather than the landings time-series from 1996 to 2021. Using the shorter catch time-series estimates a lower maximum productivity and thus lower absolute and relative biomass and higher fishing mortality in particular in more recent years (Figure 8.11). However, this run predicts lower overall catches than the "observed" landings for the period 1995 to 2005. Furthermore, the assessment with the shorter catch time-series does not pass the diagnostic tests (see Section 8.7).

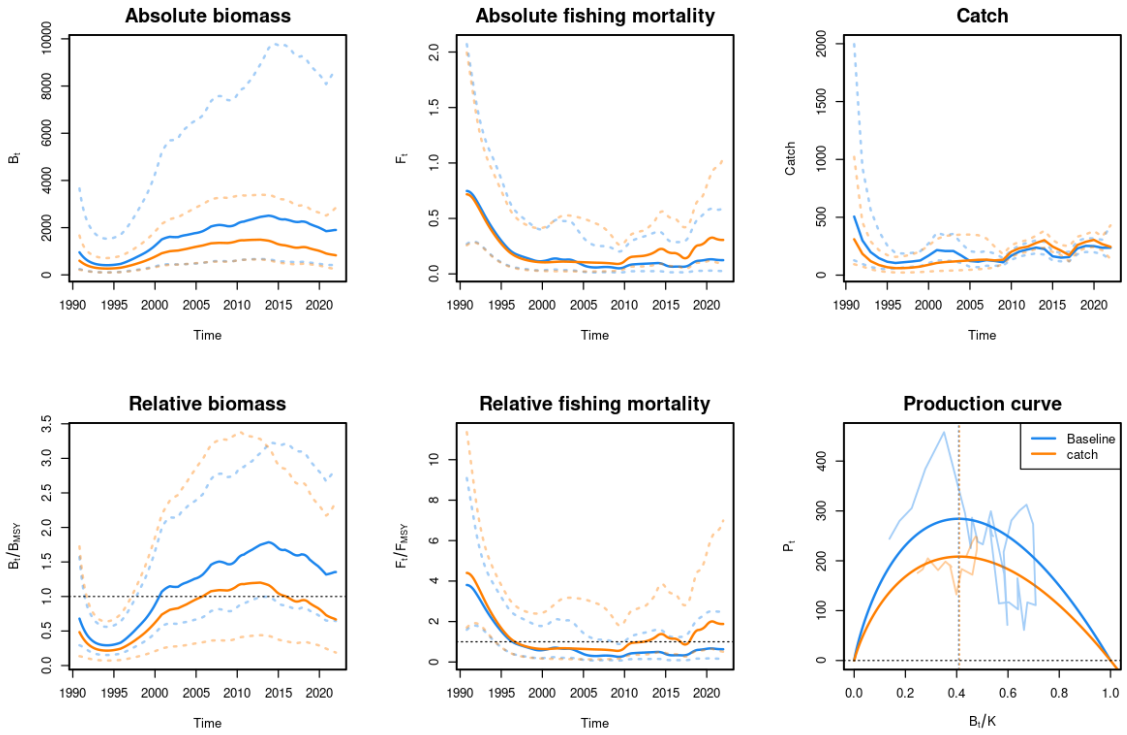


**Figure 8.11. Final assessment (Baseline) and all sensitivity runs regarding the landings/catch time-series for Thornback ray in Division 8.c (rjc.27.8c).**

### 8.3.1.6 Sensitivity to prior means

Lastly, a prior sensitivity analysis was performed by in- and decreasing one prior by +/- 25% at the time. This corresponds to following prior means and scenarios: (1) r = 0.1125 ("r_low"), (2) r = 0.1875 ("r_high"), (3) sdb = 0.11 ("sdb_low"), (4) sdb = 0.19 ("sdb_high"), (5) sdi = 0.28 and 0.25 for the two indices before and after 2013, respectively ("sdi_low"), and (6) sdi = 0.47 and 0.41 for the two indices before and after 2013, respectively ("sdi_high"). The results were not sensitive to these changes (Figure 8.12).

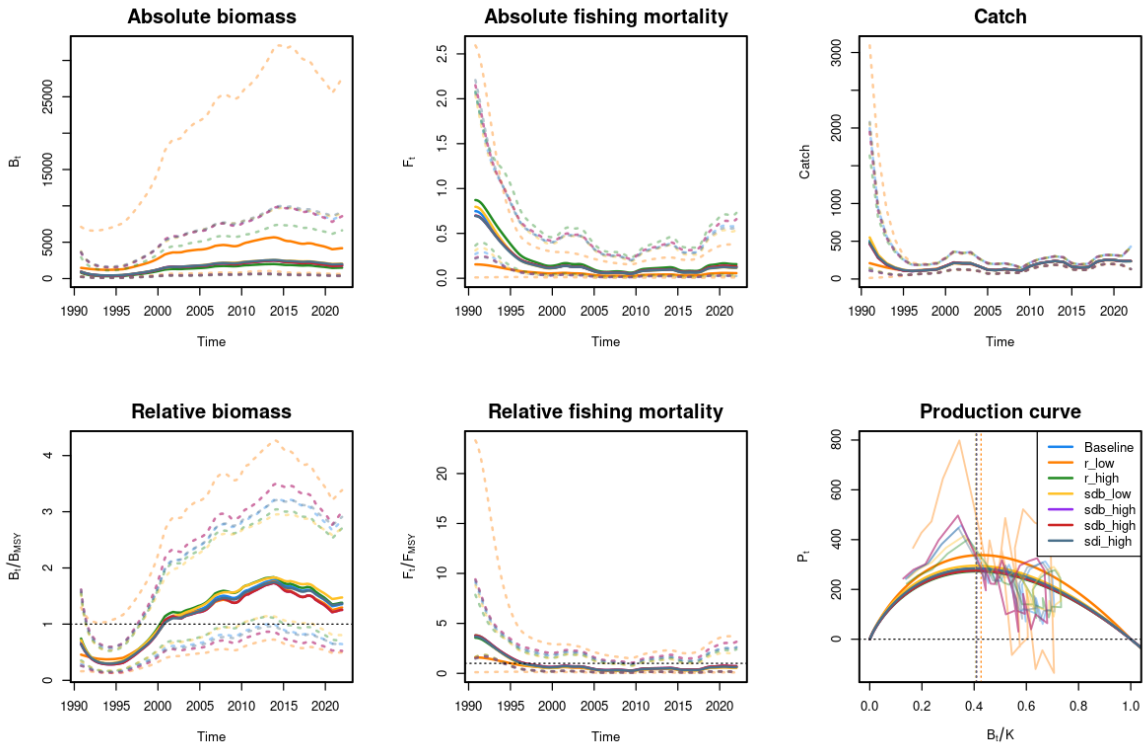


**Figure 8.12. Final assessment (Baseline) and all sensitivity runs regarding the prior means for Thornback ray in Division 8.c (rjc.27.8c).**

## 8.3.2 Final assessment

The input data for the final assessment of this stock were a landings time-series from 1996 to 2021 and an abundance index split into two separate time blocks (from 1990–2012 and 2013–2021) due to the change in research vessel in 2013 described above. The final assessment settings and priors are described in Table 8.3.

**Table 8.3. Input data and SPiCT settings for the final assessment of Thornback ray in Division 8.c (rjc.27.8c).**

| Data and Setting | Values (reference) |
|---|---|
| Data | |
| Landings | Landings from 1996 - 2021 |
| Biomass index from 1990 - 2012 | Stratified mean index based on 3 depth strata and 5 geographical sectors |
| Biomass index from 2013 - 2021 | Stratified mean index based on 3 depth strata and 5 geographical sectors |
| SPiCT settings | |
| Standard deviation scaling for the catch observations (stdevfacC) | Before 2009: 1.5, after 2009: 0.5 (difference of factor 3) |

| | |
|---|---|
| Standard deviation scaling for the index observations (stdevfacI) | Estimated values (see Table 8.2) and 3 times original value in 2013 (0.74 x 3 = 2.23) |
| Prior for shape of the production curve (n) | Gamma distribution (3.48, 6.35) corresponding to N(0.548, 0.294) for logn (based on overall average value of meta study by Thorson et al. (2012)) |
| Prior for the logarithm of the intrinsic growth rate (logr) | N(0.15, 0.3) corresponding to N(0.2, 0.3) for a Schaefer model (based on FishBase (Froese and Pauly, 2022)) |
| Prior for the logarithm of the standard deviation of the biomass process noise (logsdb) | N(0.15, 0.3) (based on meta study by Casper Berg (unpublished)) |
| Prior for the logarithm of the standard deviation of the survey index observation noise (logsdi) | N(0.37,0.3) and N(0.33,0.3) for the 2 indices (based on the mean of the estimated SD) |
| Euler discretization time-step (dteuler) | 1/16 (default) |

The landings time-series was used in the baseline assessment as the catch information is only available from 2009–2021. The higher uncertainty of the catches before 2009 was accounted for by using an uncertainty scaling of factor 3. The abundance index was split into two indices to account for the change in research vessel in the scientific survey in 2013. The higher estimated abundance in 2013 was assumed to be 3 times less certain than the estimated uncertainty suggested. A Gamma prior for the shape of the production curve corresponding to the prior for n on log scale suggested by the meta study by Thorson et al. (2012). A prior around 0.15 was assumed for the intrinsic growth rate (r). This corresponds to a prior around r = 0.2 for a Schaefer model while accounting for the shape of the production curve which changes the interpretation of r (here: using a Gamma prior corresponding to a prior around n = 1.5; see Section 8.7 for more details). The value of r = 0.2 for a Schaefer model is the suggested average intrinsic growth rate by FishBase (Froese and Pauly, 2022). A prior around 0.15 was assumed for the noise of the biomass process as suggested by a meta study performed by Casper Berg (unpublished). The prior for the observation noise for the two indices set to the estimated mean standard deviation of the two indices. The default Euler discretization time-step of 1/16 was used.

The final model converged, and the variance of all model parameters was finite. The model estimates a low biomass in the 1990s that recovered to levels above $B_{MSY}$ since 2000 but shows a decreasing trend since 2013 (Figures 8.13 and 8.14). The fishing mortality is estimated to have been high around levels of 4 times $F_{MSY}$ in the 1990, but since then decreased and remained low and below $F_{MSY}$. Estimated landings fluctuate around levels below and around $_{MSY}$ and indicate to have been much higher at the beginning of the time-series. The estimated production curve is slightly left skewed with highest productivity around 40% of the carrying capacity (K). The model parameters, estimated reference points, and stock status are shown in Table 8.4.

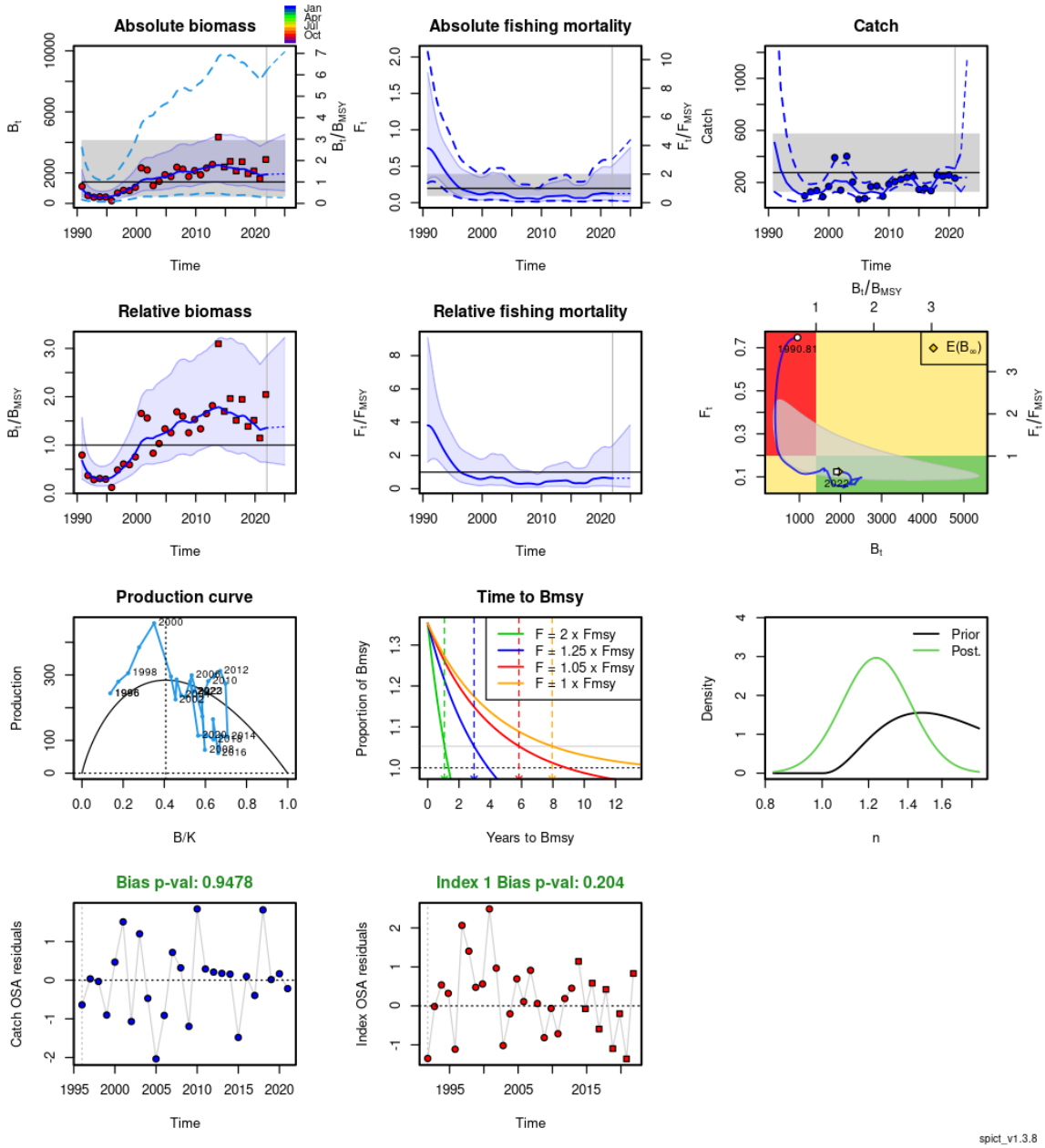


**Figure 8.13. Final assessment results for Thornback ray in Division 8.c (rjc.27.8c).**

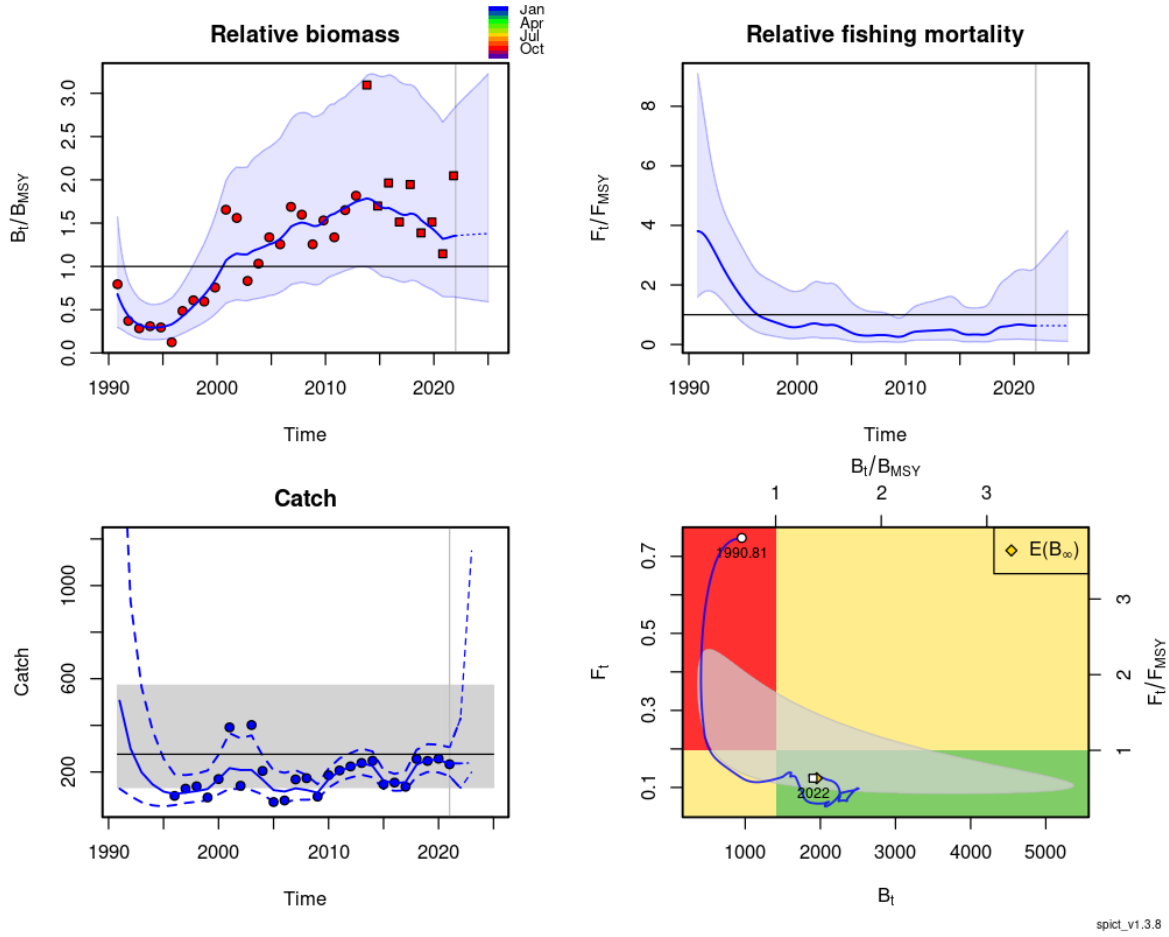


**Figure 8.14. Relative biomass and fishing mortality, landings and the Kobe plot for the final assessment of Thornback ray in Division 8.c (rjc.27.8c).**

**Table 8.4. Model parameter estimates, estimated reference points and states for the final assessment of Thornback ray in Division 8.c (rjc.27.8c).**

```
Convergence: 0  MSG: relative convergence (4)
Objective function at optimum: 47.4213373
Euler time step (years):  1/16 or 0.0625
Nobs C: 26,  Nobs I1: 23,  Nobs I2: 9

Residual diagnostics (p-values)
    shapiro   bias    acf   LBox shapiro bias acf LBox
 C   0.5815 0.9478 0.3925 0.7325       -    -   -    -
 I1  0.5799 0.2040 0.2424 0.3835       -    -   -    -
 I2  0.7997 0.8976 0.1564 0.1351       -    -   -    -
 F   0.8241 0.2878 0.0628 0.1328       -    -   .    -
 B   0.2981 0.2474 0.0506 0.2107       -    -   .    -

Priors
 logngamma  ~  dgamma[3.48, 6.346] (mean=0.548, sd=0.294)
      logr  ~  dnorm[log(0.15), 0.3^2]
    logsdb  ~  dnorm[log(0.15), 0.3^2]
   logsdi1  ~  dnorm[log(0.375), 0.3^2]
   logsdi2  ~  dnorm[log(0.327), 0.3^2]

Model parameter estimates w 95% CI
            estimate        cilow        ciupp    log.est
 alpha1    2.2804655    1.2037168 4.320387e+00  0.8243796
 alpha2    2.0801745    1.0404870 4.158751e+00  0.7324518
 beta      0.8803972    0.3694002 2.098264e+00 -0.1273822
 r         0.2440780    0.1308645 4.552347e-01 -1.4102675
 rc        0.3947735    0.2018684 7.720185e-01 -0.9294430
 rold      1.0318381    0.2307096 4.614848e+00  0.0313418
 m       284.2513093  137.1092513 5.893024e+02  5.6498587
 K      3533.4906238 1241.5074575 1.005677e+04  8.1700415
 q1        0.0014966    0.0004273 5.241000e-03 -6.5045859
 q2        0.0020370    0.0004892 8.481900e-03 -6.1962908
 n         1.2365468    0.9500740 1.609399e+00  0.2123226
 sdb       0.1295981    0.0774486 2.168620e-01 -2.0433174
 sdf       0.3319661    0.1843556 5.977660e-01 -1.1027224
 sdi1      0.2955439    0.2084345 4.190583e-01 -1.2189378
 sdi2      0.2695866    0.1716056 4.235116e-01 -1.3108656
 sdc       0.2922620    0.1838569 4.645846e-01 -1.2301045

Deterministic reference points (Drp)
           estimate       cilow        ciupp   log.est
 Bmsyd 1440.0727354 486.0435535 4266.7153353  7.272449
 Fmsyd    0.1973868   0.1009342    0.3860093 -1.622590
 MSYd   284.2513093 137.1092513  589.3023708  5.649859
Stochastic reference points (Srp)
           estimate       cilow      ciupp   log.est rel.diff.Drp
 Bmsys 1405.2039528 480.2113780 4111.93537  7.247938 -0.024814037
 Fmsys    0.1964054   0.0997056    0.38689 -1.627574 -0.004996667
 MSYs   275.9554855 133.1737362  571.82018  5.620240 -0.030062181

States w 95% CI (inp$msytype: s)
                    estimate       cilow        ciupp    log.est
 B_2021.94      1901.6329715 415.9189522 8694.5015122  7.5504683
 F_2021.94         0.1239455   0.0257604    0.5963604 -2.0879135
 B_2021.94/Bmsy    1.3532790   0.6456599    2.8364219  0.3025305
 F_2021.94/Fmsy    0.6310695   0.1545586    2.5766845 -0.4603393

Predictions w 95% CI (inp$msytype: s)
                  prediction       cilow        ciupp    log.est
 B_2025.00      1937.8286289 377.8589993 9938.0451483  7.5693234
 F_2025.00         0.1239460   0.0178075    0.8627072 -2.0879091
 B_2025.00/Bmsy    1.3790373   0.5897263    3.2247904  0.3213856
 F_2025.00/Fmsy    0.6310722   0.1032905    3.8556523 -0.4603349
 Catch_2023.00   477.8686508 198.8700605 1148.2796701  6.1693359
 E(B_inf)       1951.4105799          NA           NA  7.5763078
```

Figure 8.15 shows assumed prior and estimated posterior distributions and suggested that estimated parameters informed by available data and prior distributions (posterior are not substantial different but also not completely overlapping with prior distributions).

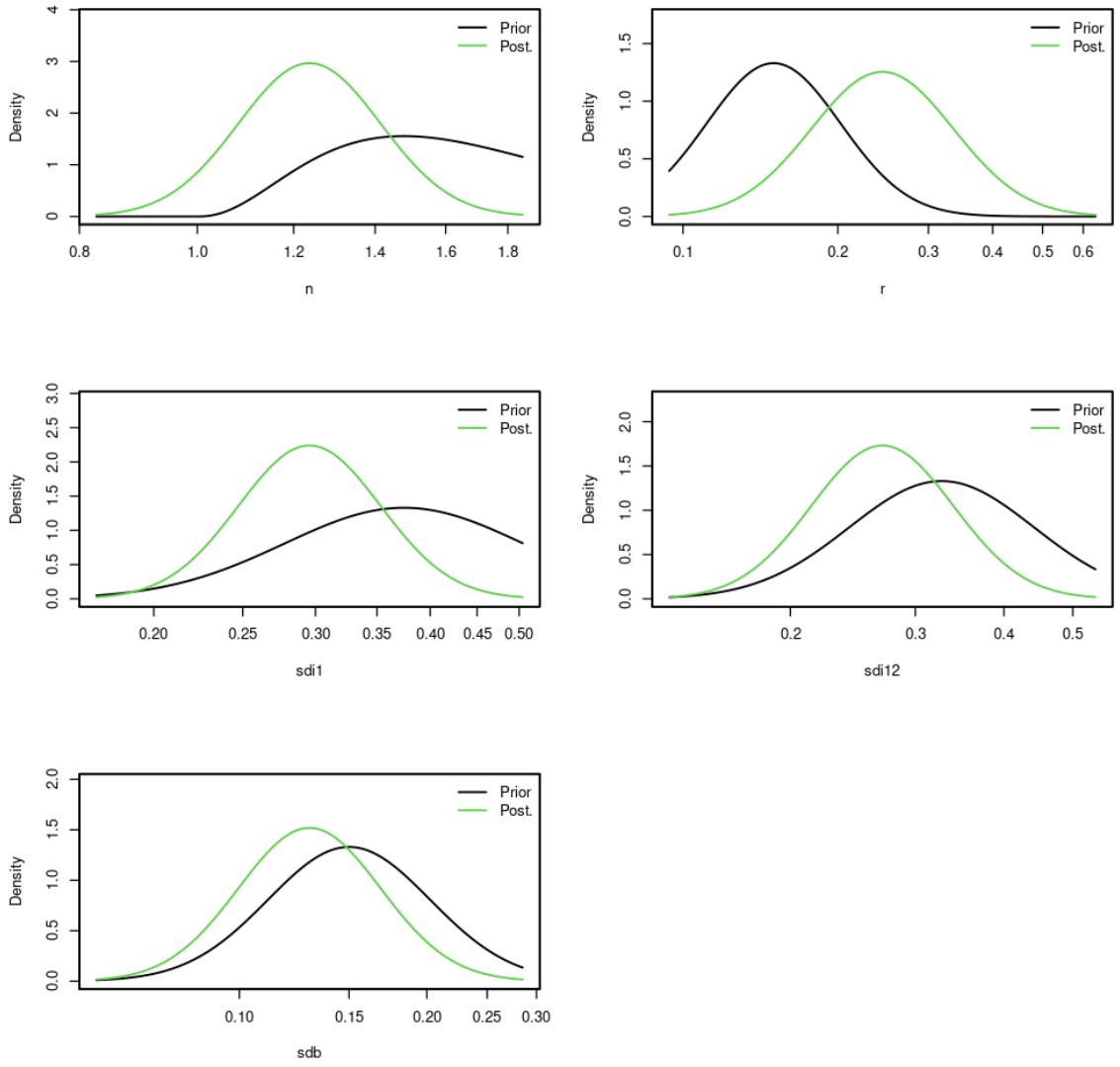


**Figure 8.15. Prior-posterior distributions for the final assessment of Thornback ray in Division 8.c (rjc.27.8c).**

The one-step-ahead observation residuals and process residuals pass the bias, autocorrelation, and normality tests (p-values < 0.05; Figures 8.16 and 8.17) and, thus, do not indicate major violation of model assumptions.

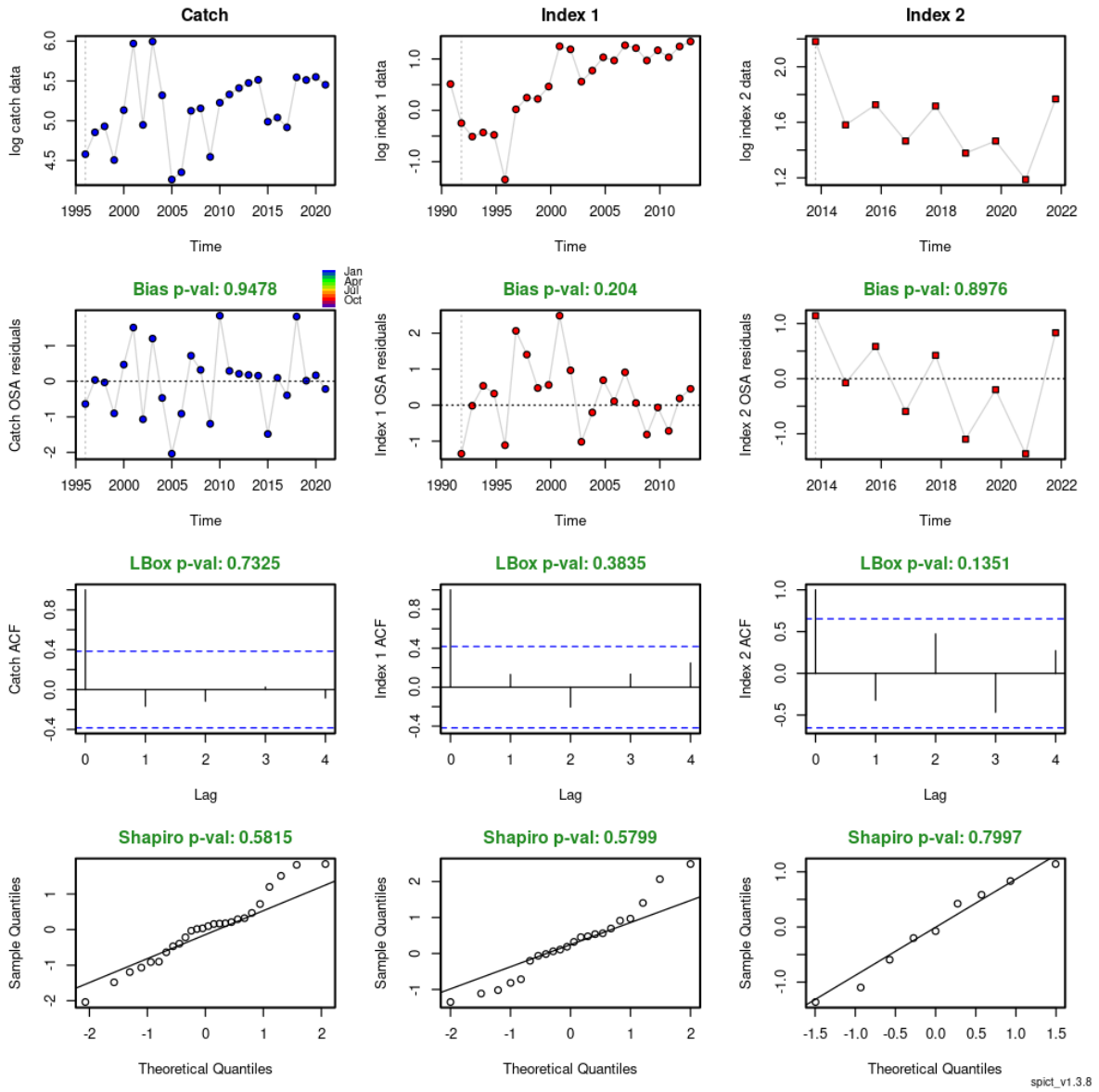


**Figure 8.16. One-step-ahead observation residuals for the final assessment of Thornback ray in Division 8.c (rjc.27.8c).**

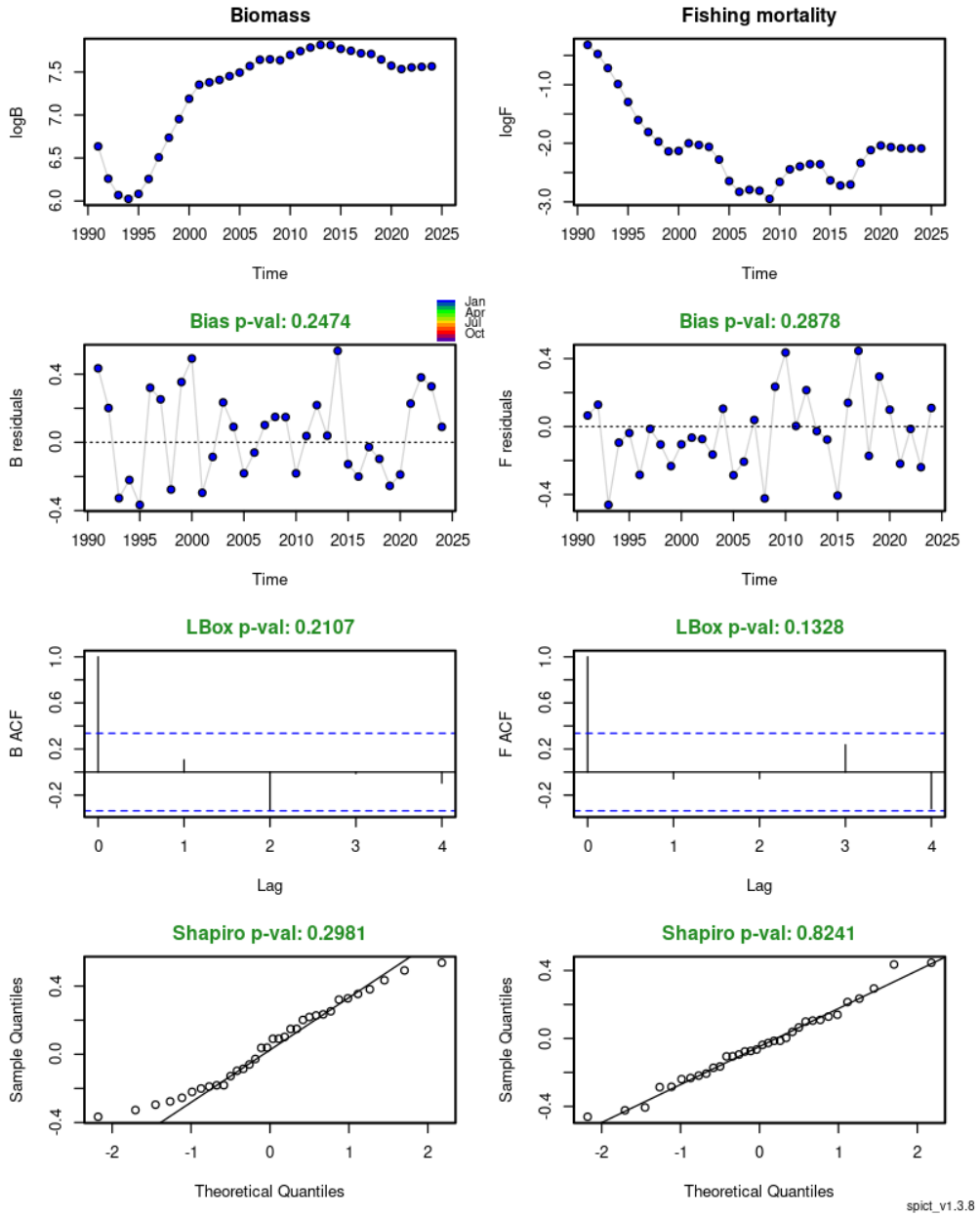


**Figure 8.17. Process residuals of the final assessment of Thornback ray in Division 8.c (rjc.27.8c).**

While the retrospective analysis with 5 peels could indicate a consistent divergence of the biomass on absolute scale, the relative biomass and fishing mortality rate do not indicate a retrospective bias (Figure 8.18). On relative scales, there is no consistent over- or underestimation visible in the graph or indicated by the Mohn's rho values (0.025 and –0.139 for the relative biomass and fishing mortality rate, respectively).

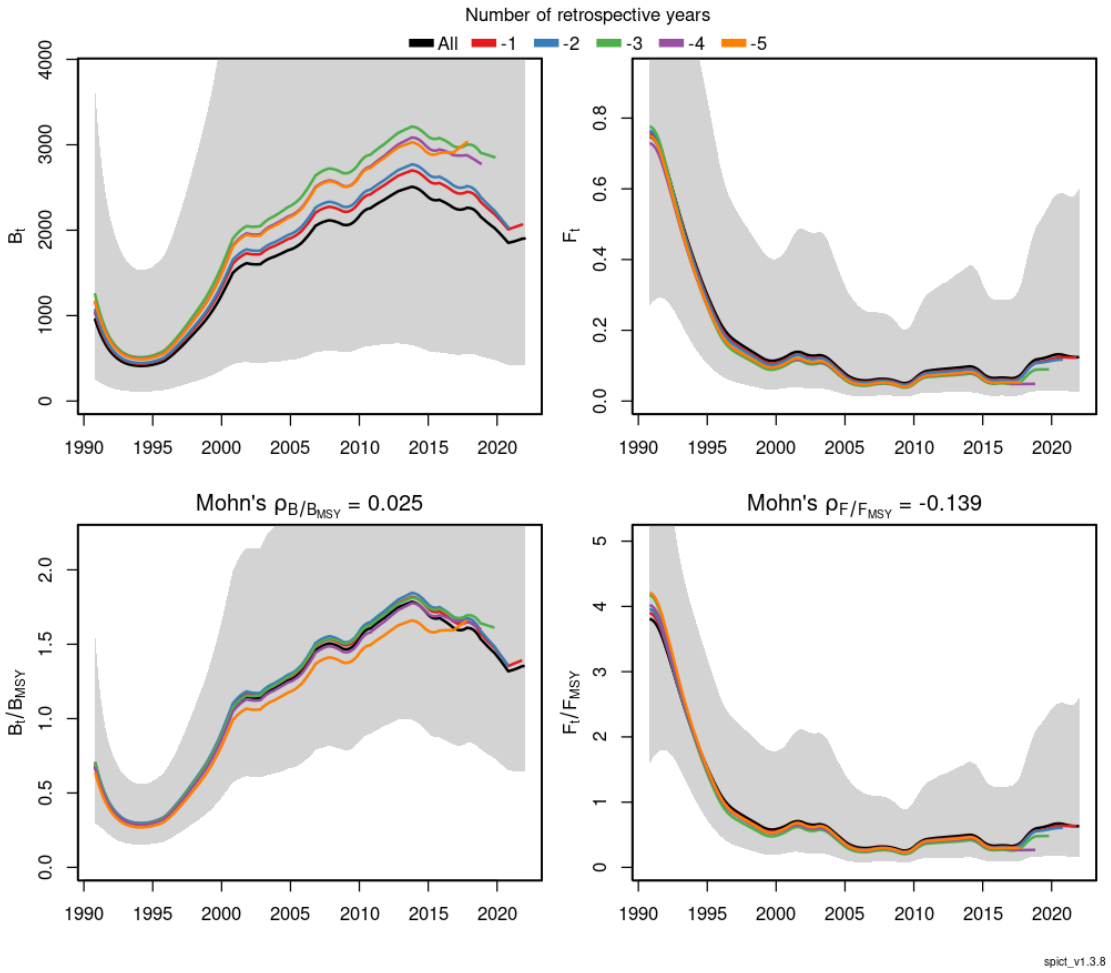


**Figure 8.18. Retrospective analysis for the final assessment of Thornback ray in Division 8.c (rjc.27.8c).**

The final assessment passes the hindcast cross validation analysis, which indicates that the final assessment model can predict the abundance index more accurately than the naïve predictor (MASE < 1; Figure 8.19).

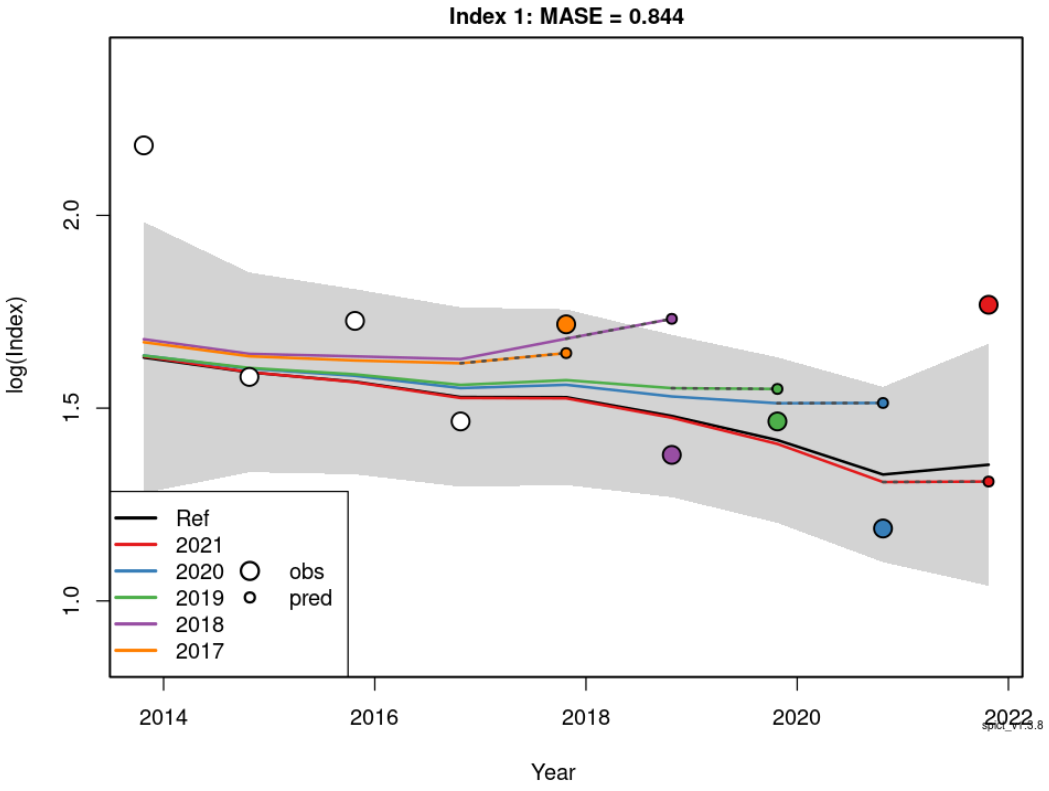


**Figure 8.19. Hindcast cross validation for the abundance index for the final assessment of Thornback ray in Division 8.c (rjc.27.8c).**

The Jitter analysis with 20 trials does not indicate multiple local optima and evenly likely parameter combinations for the final assessment (Table 8.5). The large proportion of non-converged trials can partly be explained by initial values for n below 1, which results in NaN evaluation in the optimization procedure and thus non-convergence when the Gamma prior for n is used.

**Table 8.5. Results of the jitter analysis for the final assessment of Thornback ray in Division 8.c (rjc.27.8c).**

| | Distance | m | K | q | q | n | sdb | sdf | sdi | sdi | sdc |
|---|---|---|---|---|---|---|---|---|---|---|---|
| Basevec | 0.00 | 284.25 | 3533.49 | 0 | 0 | 1.24 | 0.13 | 0.33 | 0.3 | 0.27 | 0.29 |
| Trial 1 | 0.00 | NA | NA | NA | NA | NA | NA | NA | NA | NA | NA |
| Trial 2 | 0.00 | 284.25 | 3533.49 | 0 | 0 | 1.24 | 0.13 | 0.33 | 0.3 | 0.27 | 0.29 |
| Trial 3 | 0.00 | 284.25 | 3533.49 | 0 | 0 | 1.24 | 0.13 | 0.33 | 0.3 | 0.27 | 0.29 |
| Trial 4 | 0.01 | 284.25 | 3533.48 | 0 | 0 | 1.24 | 0.13 | 0.33 | 0.3 | 0.27 | 0.29 |
| Trial 5 | 0.00 | NA | NA | NA | NA | NA | NA | NA | NA | NA | NA |
| Trial 6 | 0.00 | NA | NA | NA | NA | NA | NA | NA | NA | NA | NA |
| Trial 7 | 0.01 | 284.25 | 3533.49 | 0 | 0 | 1.24 | 0.13 | 0.33 | 0.3 | 0.27 | 0.29 |
| Trial 8 | 0.01 | 284.25 | 3533.48 | 0 | 0 | 1.24 | 0.13 | 0.33 | 0.3 | 0.27 | 0.29 |
| Trial 9 | 0.00 | NA | NA | NA | NA | NA | NA | NA | NA | NA | NA |
| Trial 10 | 0.00 | NA | NA | NA | NA | NA | NA | NA | NA | NA | NA |
| Trial 11 | 0.01 | 284.25 | 3533.48 | 0 | 0 | 1.24 | 0.13 | 0.33 | 0.3 | 0.27 | 0.29 |
| Trial 12 | 0.00 | 284.25 | 3533.49 | 0 | 0 | 1.24 | 0.13 | 0.33 | 0.3 | 0.27 | 0.29 |
| Trial 13 | 0.01 | 284.25 | 3533.48 | 0 | 0 | 1.24 | 0.13 | 0.33 | 0.3 | 0.27 | 0.29 |
| Trial 14 | 0.01 | 284.25 | 3533.48 | 0 | 0 | 1.24 | 0.13 | 0.33 | 0.3 | 0.27 | 0.29 |
| Trial 15 | 0.00 | NA | NA | NA | NA | NA | NA | NA | NA | NA | NA |
| Trial 16 | 0.01 | 284.25 | 3533.48 | 0 | 0 | 1.24 | 0.13 | 0.33 | 0.3 | 0.27 | 0.29 |
| Trial 17 | 0.01 | 284.25 | 3533.49 | 0 | 0 | 1.24 | 0.13 | 0.33 | 0.3 | 0.27 | 0.29 |
| Trial 18 | 0.01 | 284.25 | 3533.48 | 0 | 0 | 1.24 | 0.13 | 0.33 | 0.3 | 0.27 | 0.29 |
| Trial 19 | 0.01 | 284.25 | 3533.48 | 0 | 0 | 1.24 | 0.13 | 0.33 | 0.3 | 0.27 | 0.29 |
| Trial 20 | 0.00 | NA | NA | NA | NA | NA | NA | NA | NA | NA | NA |

## 8.4 Future considerations/recommendations

The neglecting of discard information available for part of the longer landings time-series is not ideal. The sensitivity analysis and exploratory runs showed that the assessment using the shorter catch time-series estimates lower productivity and, thus, worse stock status (lower $B/B_{MSY}$ and higher $F/F_{MSY}$ throughout the time-series, but in particular in recent years. This underlines the importance of revisiting available landings and discards information. Future work should be allocated to developing a model that can utilize a landings and discard time-series of different lengths as well as the reconstruction of historical landings and discards.

Furthermore, it would be valuable to include the option to share parameters between abundance indices. This is particularly relevant to cases such as here when a longer time-series is split into time blocks. It would be relevant to be able to assume a share the catchability but estimate separate variance parameters or share a common variance but estimate separate catchabilities between abundance indices.

It should be emphasized that the any catch advice based on the final model corresponds to the landings rather than the catches (landings + discards).

## 8.5 Reviewer report

Thornback ray is currently a category 3 stock and suitable for trend-based advice. Information about the landings of Thornback ray in Division 8.c are available from 1996 onward. Discard information is only available from 2009 onward with fluctuating levels between 9% and 37% with an average discard ratio of 17%. Landings before 2009 are likely more uncertain as no species-specific information is available (no species disaggregation).

The abundance index was calculated using a stratified mean approach with 5 sectors and 3 depth strata based on the groundfish trawl survey "demersales". The uncertainty associated with the

index is available as the standard deviation of the estimated positive catch rates on natural scale. In two years, no uncertainty information is available. From 2013 onward, a newer vessel was used for the survey. In 2021, the survey vessel broke down and the survey was continued with an older vessel.

The SPiCT assessment of Thornback ray in Division 8.c is considered suitable for providing management advice. The assessment passes all diagnostic checks and is robust over a wide range of tested alternative scenarios. The accepted SPiCT assessment uses the longer landings time-series from 1996 onward with higher uncertainty before 2009 and the abundance index split into two indices in 2013 with a higher uncertainty in 2013. Furthermore, the assessment includes a Gamma prior for the shape of the production curve based on the meta study by Thorson et al. (2012), a prior for the intrinsic rate of population growth around 0.2 based on FishBase, a prior for the biomass process noise around 0.15 based on a meta study (Berg (unpublished)), and a prior for the observation uncertainty of the indices around the average standard deviation of the estimated uncertainty of the stratified mean index calculation. The estimated perception of the stock was not sensitive to the assumed prior distributions.

The SPiCT assessment uses landings as input and, therefore, the short-term-forecast is in terms of landings. The advice TAC can be given in terms of landings as presented below, or an assumption needs to be made about the discard rate in order to estimate corresponding catch advice. Several possible biennial TACs based on a range of catch fractiles are presented in the report. Due to following reasons, it should be considered to follow a more risk averse and precautionary approach by for example basing the recommended TAC on a lower fractile (e.g. 15th percentile; cp Figure 8.20 for the catch advice for 2023 and 2024) for the catch distribution than the general 35th percentile: (i) Elasmobranchs are sensitive species due to lower fertility and less understood stock recruitment relationships, (ii) the model and any advice based on the model is based on landings and does not consider potentially changing discard rates, (iii) the advice is biennial and conservation measures are likely slower, and (iv) the assessment is based on a single abundance index, which suggests a continuously increasing abundance of Thornback ray in Division 8.c. This trend should be confirmed by other information and a spatio-temporal model of the survey data. To derive the annual landings advice, the catch in the management table (Figure 8.20) has to be divided by 2, for instance when using the 'ices_c15' rule the landings advice would be 228.1 tonnes for each of the years 2023 and 2024.

```
SPiCT timeline:

      Observations             Intermediate             Management
    1990.81 - 2022.00        2022.00 - 2023.00       2023.00 - 2025.00
  |----------------------| ----------------------| ----------------------|

Management evaluation: 2025.00

Predicted catch for management period and states at management evaluation time:

                   C B/Bmsy F/Fmsy
1. No fishing    0.5   1.69   0.00
2. fmsy        712.2   1.22   1.00
3. hockeyStick 712.2   1.22   1.00
4. ices_c35    604.5   1.30   0.82
5. ices_c30    569.8   1.32   0.77
6. ices_c25    534.5   1.34   0.72
7. ices_c20    497.8   1.37   0.66
8. ices_c15    458.2   1.39   0.60
9. ices_c10    412.8   1.42   0.54
10. ices_c05   353.7   1.46   0.45
```

**Figure 8.20. Catch advice for various harvest control rules for a two-year management interval (2023 and 2024) and relative states in 2025 for the final SPiCT assessment of Thornback ray in Division 8.c (rjc.27.8c).**

### 8.5.1 Conclusions

The SPiCT assessment model of Thornback ray in Division 8.c is considered suitable for providing management advice.

## 8.6 References


Blanco, M. Fernández-Zapico, O. Ruiz-Pico, S., Velasco, F., Rodríguez-Cabello, C., Preciado, I.,.Punzón, A. González-Irusta, JM., Velasco, E. 2021. Results on main elasmobranch species captured in the bottom-trawl surveys on the Northern Spanish Shelf. Working Document presented at WGEF, 14–23 June 2022. Lisbon. 42 pp. (WGEF_2022_WD_07).

Cochran, W.G., 1971. Muestreo estratificado aleatorio. Muestreo sistematico. In ''Técnicas de muestreo''. Ed. By Continental S. A. Mex. 127–297.

Froese, R., Binohlan, C. 2000. Empirical relationships to estimate asymptotic length, length at first maturity and length at maximum yield-per-recruit in fishes, with a simple method to evaluate length frequency data.

Froese, R. 2004. Keep it simple: three indicators to deal with overfishing. Fish and Fisheries, 5 (1), 86–91. https://doi.org/10.1111/j.1467-2979.2004.00144.x

Froese, R., Pauly D. Editors. 2022. FishBase. World Wide Web electronic publication. www.fishbase.org

Gallagher, M.J., Nolan, C.P., Jeal, F. 2005. Age, growth and maturity of the commercial ray species from the Irish Sea. J. Northw. Atl. Fish. Sci., 35: 47–66. http://dx.doi.org/10.2960/J.v35.m527

Grosslein, M.D. and Laurec, A., 1982. Bottom-trawl surveys design, operation and analysis. CECAF/ECAF Series 81/22 (En). https://www.fao.org/publications/card/en/c/d6b9c05d-9944-5acc-8926-8b8fb3829721/

ICES.2017. Manual of the IBTS North Eastern Atlantic Surveys. Series of ICES Survey Protocols SISP 15. 92 pp. http://doi.org/10.17895/ices.pub.3519

ICES. 2021a. Benchmark Workshop on the development of MSY advice for category 3 stocks using Surplus Production Model in Continuous Time; SPiCT (WKMSYSPiCT). ICES Scientific Reports. 3:20. 317 pp. https://doi.org/10.17895/ices.pub.7919

ICES 2021b. Tenth Workshop on the Development of Quantitative Assessment Methodologies based on LIFE-history traits, exploitation characteristics, and other relevant parameters for data-limited stocks (WKLIFE X). ICES Scientific Reports. 2:98. 72 pp. http://doi.org/10.17895/ices.pub.5985

Lorance, P. 2022. Stock distribution of Thornback ray (Raja clavata) in Subarea 8, Bay of Biscay. Working document presented at ICES WKELASMO 2022.

Rodríguez-Cabello, C., Velasco, F. 2022. Assessment of *Raja clavata* stock in ICES Division 8c (rjc.27.8c) applying the rfb rule. Working Document presented at WGEF, 14–23 June 2022. Lisbon. 8 pp. (WGEF_2022_WD_14).

Serra-Pereira, B., Figueiredo, I., Farias, I., Moura, T., Gordo, L.S. 2008. Description of dermal denticles from the caudal region of *Raja clavata* and their use for the estimation of age and growth. ICES Journal of Marine Science, 65: 1701–1709.

Serra-Pereira, B., Figueiredo, I., Gordo, L. 2011. Maturation, fecundity, and spawning strategy of the thornback ray, *Raja clavata*: do reproductive characteristics vary regionally? Marine Biology, 158: 2187–2197.

Thorson, J.T., Cope, J.M., Branch, T.A. and Jensen, O.P., 2012. Spawning biomass reference points for exploited marine fishes, incorporating taxonomic and body size information. Canadian Journal of Fisheries and Aquatic Sciences, 69(9), pp.1556–1568. https://doi.org/10.1139/f2012-077

Trenkel, V.M., Charrier, G., Lorance, P., Bravington, M.V. 2022. Close-kin mark–recapture abundance estimation: practical insights and lessons learned. ICES Journal of Marine Science, 2022 https://doi.org/10.1093/icesjms/fsac002.

Walker, P. 1999. Fleeting images—dynamics of North Sea ray populations. PhD thesis, Faculty of Biology, University of Amsterdam. 145 pp.

Whittamore, J. M., McCarthy, I. D. 2005. The population biology of the thornback ray, Raja clavata in Caernarfon Bay, north Wales. Journal of the Marine Biological Association of the UK, 85: 1089–1091.

# 8.7 Working document for thornback ray in the Cantabrian Sea (Division 8.c; rjc.27.8c)

## 8.7.1 WD Annex 1: Age-structured rebuilding simulation evaluation for Thornback Ray with SPiCT

*Author: Henning Winker (GFCM)*

# Age-structured rebuilding simulation evaluation for Thornback Ray with Spict

Henning Winker (GFCM)

12 January, 2023

## Contents

**1 Packages and installations** 1
1.1 Installations . . . 2

**2 Life history parameters** 3

**3 SPMpriors with FishLife** 3

**4 Leslie matrix with stock-specitic direct input** 6

**5 Setting up a generic OM for Thornback Skate** 7
5.1 Estimating priors from FLStock and SRR . . . 8
5.2 Simulating stock dynamics with evolutionary F-trajectories . . . 10

**6 Simulation testing with Spict** 15

**7 Spict estimation scenarios** 15
7.1 Quick simulation performance comparison . . . 20
7.2 Dome shaped survey index . . . 24

```
## Warning: package 'knitr' was built under R version 4.2.2
```

## 1 Packages and installations

The following R packages are used

For generic life history parameters

- FishLife
- SPMpriors
- JABBA

As generic FLStock stock constructors

- FLCore
- FLife
- FLBRP
- FLRef

Surplus production model fitting

- spict

Note that several updates and new functions were pushed to **FLRef** on 10th of Jan of 2023, which are required to implement the below R code.

### 1.1 Installations

```
install.packages("ggplot2")
install.packages("devtools")
install.packages("TMB", type = "source")
devtools::install_github("DTUAqua/spict/spict")
devtools::install_github("james-thorson/FishLife")
devtools::install_github("henning-winker/SPMpriors")
# FLR
devtools::install_github("flr/FLCore")
devtools::install_github("flr/ggplotFL")
devtools::install_github("flr/FLBRP")
devtools::install_github("flr/FLasher")
devtools::install_github("flr/mse")
devtools::install_github("flr/FLSRTMB")
devtools::install_github("flr/FLife")
devtools::install_github("henning-winker/FLRef")
devtools::install_github("JABBAmodel/JABBA")
```

Load packages

```
# Load
library(ggplot2)
library(spict)
library(FishLife)
library(SPMpriors)
library(FLCore)
library(ggplotFL)
library(FLRef)
library(FLife)
library(JABBA)
library(ggpubr)
```

## 2 Life history parameters

Regional life history parameters of bll.27.3a47de for females were assumed assumed as follows:

```
# Taken from Great North Sea
linf = 155
k = 0.129
t0 = -1
a50 = 5.5
a = 0.00001
b = 3.04
tmax = 20

# check vbgf
La = data.frame(age=0:tmax,La=vonbert(linf,k,t0,age=0:tmax))
La
      age        La
   1    0  18.75904
   2    1  35.24774
   3    2  49.74088
   4    3  62.47997
   5    4  73.67731
   6    5  83.51947
   7    6  92.17047
   8    7  99.77448
   9    8 106.45821
   10   9 112.33303
   11  10 117.49684
   12  11 122.03570
   13  12 126.02524
   14  13 129.53194
   15  14 132.61424
   16  15 135.32350
   17  16 137.70487
   18  17 139.79803
   19  18 141.63786
   20  19 143.25503
   21  20 144.67648
```

An instantaneous rate of natural mortality was estimated using Then based on the maximum age estimates `tmax1 = 22` and `tmax2 = 12`

```
M = 4.899*tmax^-.916
M
   [1] 0.3150387
```

## 3 SPMpriors with FishLife

SPMpriors enables to compute two types of priors based on: (1) a Leslie Matrix approach (2) an Age-Structured Equilibrium Model

The first approach is suitable for Schaefer model formulation of the production function, whereas the second approach requires a Pella-Tomlinson production. Note that a current issue with SPMpriors is that using

several traits will cancel each other out. It is therefore suggested to use only one key trait, e.g. either `tmax` or `Loo`, but not both togher.

In this example `tmax` is used, steepness for (here `h`) is restricted by uniform distribution to a typically considered range for rays and sharks `h = c(0.3,0.7)`.

First the Leslie prior option for a Schaefer model is explored.

```
fl1 = SPMpriors::flmvn_traits(
  Genus="Raja",Species="clavata",
  h=c(0.3,0.7),tmax=c(tmax,0.3),Plot=TRUE)
   Closest match: Elasmobranchii_Rajiformes_Rajidae_Raja_clavata
```

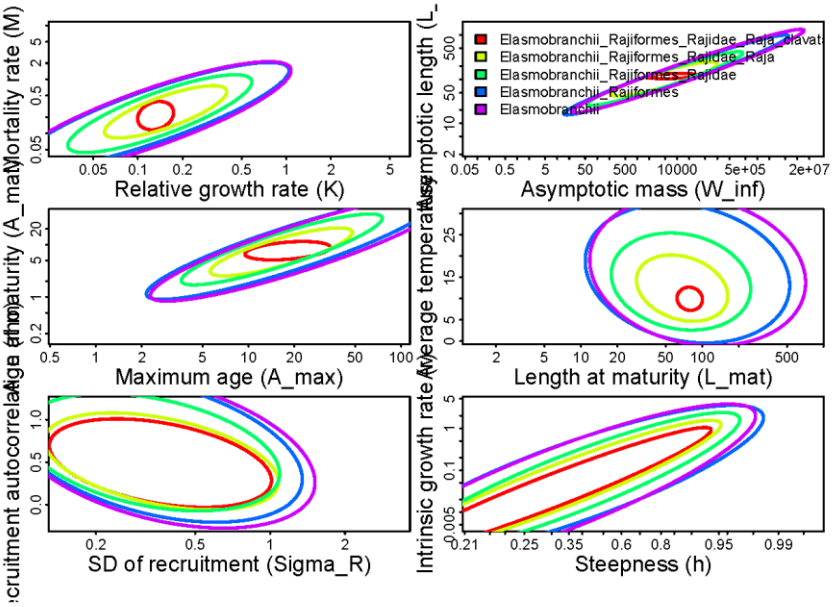

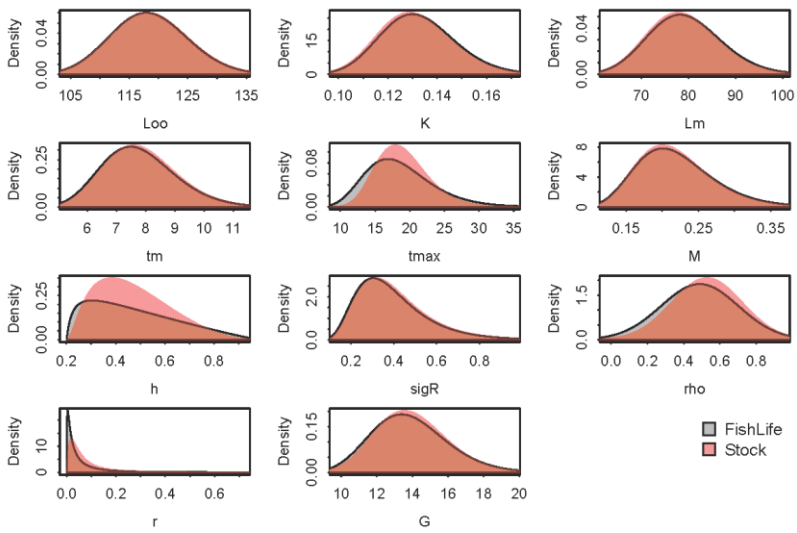


```
# this is because tmax1 is outside global range
nrow(fl1$mvnstk)
   [1] 88924
lh1 = fl1$traits
# Global FishLife
r.sp = lh1[lh1$trait=="r","mu.sp"]
# Tuned to tmax=20 and h = 0.3-0.6
r1 = lh1[lh1$trait=="r","mu.stk"]

# Global Fish Life
r.sp
   [1] 0.0326
# tuned
r1
   [1] 0.0526
```

```
# Assume Lc at 20 cm
asem1 = fl2asem(fl1,Lc=50,t0=t0,aW=1000*a,bW=b)
   Warning in (rshape)^(-1/(rshape - 1)) - bmsyk: longer object length is not a
   multiple of shorter object length

   Warning in (rshape)^(-1/(rshape - 1)) - bmsyk: longer object length is not a
   multiple of shorter object length

asem1
         r    shape fmsy bmsyk
```

```
   mu    NA 0.101000   NA     0
   logsd NA 1.222429   NA   NaN
```

In this cases shape of the production function is larger closer to a Schaefer production function.

## 4 Leslie matrix with stock-specitic direct input

The recent version of the JABBA package provides a Leslie matrix function for use stock specific estimates to get an expected value for $r$.

The first step is build a jbio object and then pass this object to compute $r$ (and Generation time) with jbleslie(). Here both the steepness and the fecundity function are explored.

```
# steepness from FishLife
lh1[lh1=="h","mu.sp"]
   [1] 0.3039
lh1[lh1=="h","mu.stk"]
   [1] 0.384

s= lh1[lh1=="h","mu.stk"]


# Steepness
bio1 = jbio(amax=tmax,nsexes=2,Loo=linf,k=k,t0=t0,aW=1000*a,bW=b,
     mat=c(a50,a50*1.2,1),M=c(M),h=s)

# fecundity assumed 100 eggs per female
bio2 = jbio(amax=tmax,nsexes = 2,
            Loo=linf,k=k,t0=t0,aW=1000*a,bW=b,
            mat=c(a50,a50*1.2,1),M=c(M),fec=100)

bio.fec = jbio(amin = 0,amax = 20,Loo = c(154.7),
               k=c(0.129),t0=c(-1),aW=0.01,bW=3.04,
               mat=c(5.5,6,1),M=c(0.26),fec=32,empty=FALSE)
jbleslie(bio.fec)
   $r
   [1] 0.06880519

   $gt
   [1] 9.253241

r2 = jbleslie(bio1)$r
r3 = jbleslie(bio2)$r

# FishLife
r1
   [1] 0.0526
# Leslie Steepness
r2
   [1] 0.1602492
# Leslie Fecundity
r3
```

```
   [1] 0.1314549
# Mean
mean(c(r1,r2,r3))
   [1] 0.114768
```

The $r$ estimates are fairly consistent between a steepness assumption of `{r} round(s,2)` and the fecundity of 100 eggs per female, but notably higher than the global FishLife estimate.

## 5 Setting up a generic OM for Thornback Skate

The `FLife` function `lhPar()` is populated with some of basic life history estimates for growth,length-weight, maturity based on regional information and steepness from FishLife/SPMpriors.

```
par=lhPar(FLPar(linf=linf,k=k,t0=t0,
            a=a,b=b,a50 =a50,
            s=s,m1=M))
```

The `FLife` function `lhEql` is then used as a constructer for a basic `FLBRP()` object.

```
eql=lhEql(par,range = c(min = 0, max = tmax, minfbar = 3, maxfbar = tmax, plusgroup=tmax))
```

Now further manipulations can be made, such as adjusting the inbuilt Gislason $M$ to a scaled Lorenzen $M$ and specifying a new maturity ogive.

```
# M
m(eql)[] = Mlorenzen(stock.wt(eql),Mref=M,Aref=2)

mat50 = a50
mat95 = a50*1.2
mat(eql) = newselex(mat(eql),FLPar(S50=mat50,mat95=mat95,Smax=1000,Dcv=0.5,Dmin=0.1))
```

It is important to then update the stock recruitment the stock recruitment relationship for a given steepness $s$ value if key biological parameters are modified.

```
# check srr parameters
params(eql)
   An object of class "FLPar"
   params
     a   b
   525 670
   units:  NA
# update SRR given s after modifying m
eql = updsr(eql,s=s)
params(eql)
   An object of class "FLPar"
   params
       a     b
    90.4 669.6
   units:  NA
```

After making all the desired modifications the time horizon can be adjusted with `fbar` range. Here a time horizon from 1981-2020 is chosen.

```
# change time horizon with a fixed intial f0
f0 = 0.02
fbar(eql) = FLQuant(f0,dimnames=list(year=1946:2022))
```

Now `FLBRP` can be directly converted into an `FLStock` and the stock recruitment relationship can be extracted.

```
stk = as(eql,"FLStock")
units(stk) = standardUnits(stk) # assign units
sr = as(as(eql,"predictModel"),"FLSR")
```

Once the stock is constructed further manipulations are straight forward, such as specifying fishing selectivity using the 5-parameter selectivity function `newselex`

A new selectivity can be set by adjusting the `harvest` slot. If some dome-shaping is desired, $Smax$ has to be smaller then the plus group, $Dcv$ governs the slope of the half-normal and $Dmin$ governs the hight at the right end tail.

```
# catch before maturity
S50 = 2.5 # selectivity < age-2
S95 = 3.5
# No Doming
Smax = 100
Dcv = 0.5
Dmin = 0.2

harvest(stk) =  f0*newselex(
  harvest(stk),FLPar(S50=S50,S95=S95,
    Smax=Smax,Dcv=Dcv,Dmin=Dmin))
```

The so generated age-structured relationships for weight-at-age, maturity-at-age, natural mortality and selective are shown in Fig. 1.

```
ggplot(FLQuants(stk,"m","catch.sel","mat","catch.wt"))+
  geom_line(aes(age,data))+
  facet_wrap(~qname,scale="free")+theme_bw()
```

### 5.1 Estimating priors from FLStock and SRR

First, it is straight forward to compute the intrinsic rate of population increase from a Leslie for a specified steepness value. However, this $r$ estimate ignores selectivity and should only be used in the context of a Schaefer model with $F_{MSY} = r/2$.

```
r.leslie = mean(productivity(stk,s=s)$r)
r.leslie
   [1] 0.1057303
# Fmsy
r.leslie/2
   [1] 0.05286516
```

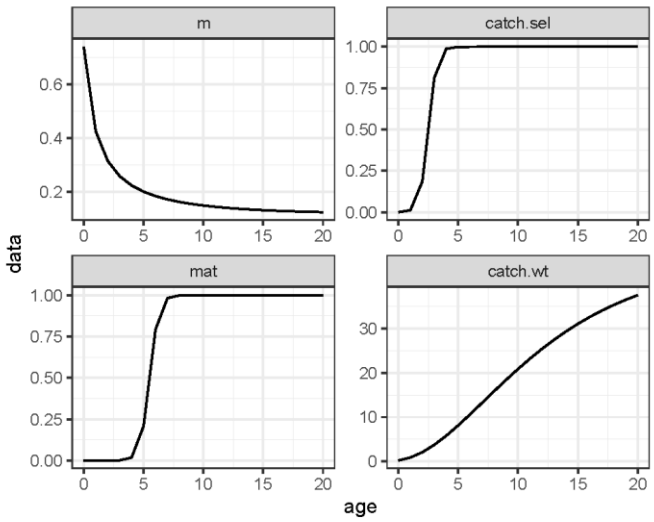


Figure 1: Specified biological and selectivtiy function for natural mortality, selectivity, maturity and somatic growth in weight-at-age

An alternative is to estimate $r$ and the shape parameter $n$ as function $MSY$, $VB_{MSY}$ and $VB_0$ from an age-structured equilibrium model (ASEM), where $BB$ denotes that the vulnarable (or exploitable) biomass as function of selectivity. The basic relationships for $r$ and $n$ can then be approximated as follows:

$$F_{MSY} = \frac{MSY}{VB_{MSY}}$$

$$\frac{VB_{MSY}}{EB_0} = n^{(-\frac{1}{n-1})}$$

$$r = F_{MSY}\frac{n-1}{1-n^{-1}}$$

To compute the expected values for $r$ and $n$ (here denoted as $m$), requires the stock biology and selectivity together with the SRR as input.

```
brp = FLBRP(stk,sr)
r.pella = asem2spm(brp)

r.pella[1:4]
   An object of class "FLPar"
   params
        r      m  BmsyK   Fmsy
   0.0508 1.4034 0.4317 0.0362
   units:  NA
```

The surplus production curves are plotted as function of the vulnerable biomass `vb` and spawning biomass `ssb` in Fig. 2, together with approximated curves of the 3-parameter Pella-Tomlinson function.

```
ggpubr::ggarrange(
plotpf(brp,rel=F),
plotpf(brp,rel=T),common.legend = T
)
```

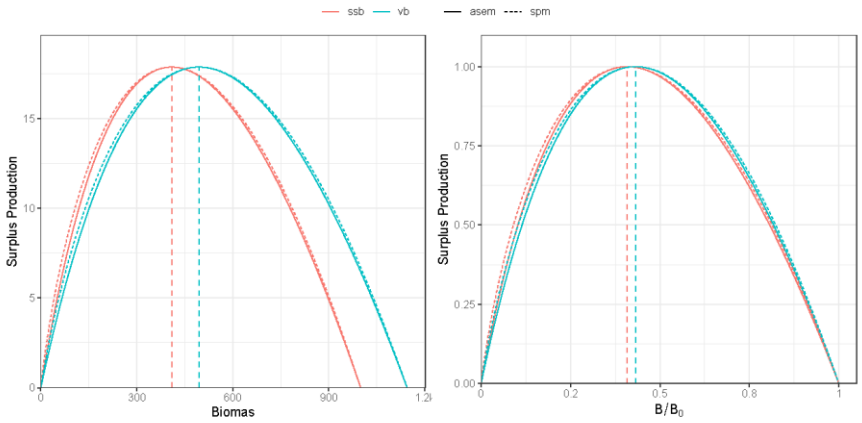


Figure 2: Specified biological and selectivtiy function for natural mortality, selectivity, maturity and somatic growth in weight-at-age

### 5.2 Simulating stock dynamics with evolutionary F-trajectories

The operating model is assumed to represent the "true" age-structured stock dynamics for evaluating the estimation accuracy of Spict. The "true" MSY based reference points can be easily added to the `FLStock` by extending it to `FLStockR`.

```
# Estimate refpts
brp = computeFbrp(stk,sr,proxy="msy",blim=0.3,type="btgt")
   Computing Fmsy with Btgt = Bmsy

    Blim = 0.3 with Btgt corresponding to Fmsy
stk = FLStockR(stk)
stk@refpts = Fbrp(brp)
# check
stk@refpts
   An object of class "FLPar"
   params
       Fmsy     Btgt     Blim     Flim      Yeq       B0       R0
   3.68e-02 4.09e+02 1.23e+02 6.72e-02 1.79e+01 1.00e+03 5.41e+01
   units:  NA
```

```
ploteq(brp)
```

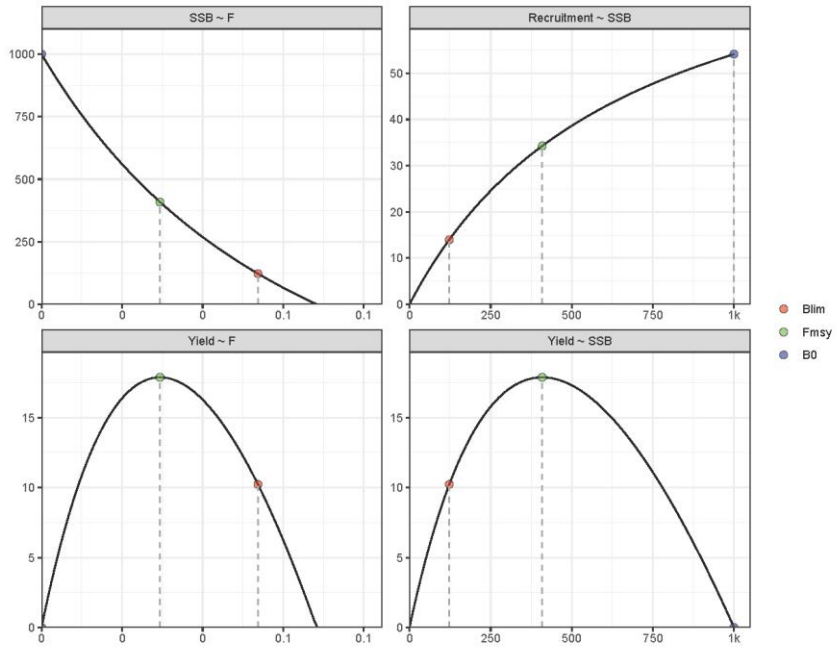


Figure 3: Equilibrium curves Recruitment, SSB, F and Landings and estimated MSY-based reference points for the thornback ray OM

**FLRef** provides generic functions to create F-trajectory for generating a wider range of plausible states for the OM, including **rffwd** and **fudc**. Here, the **fudc** function is used for illustration, which generates and up-down-constant F-pattern with the option to add random noise.

```
its = 100
# propagate desired iterations
stki <- propagate(stk, its)
# Create F-pattern up-down-constant
fmsy = Fbrp(brp)["Fmsy"]
f = fudc(stk,fhi=3.5,flo=0.1,fref=fmsy,sigmaF=0)
fy = fudc(stki,fhi=3.5,flo=0.1,fref=fmsy,sigmaF=0.25)
plot(f,fy,iter(fy,1),iter(fy,2),
     iter(fy,3),iter(fy,5),iter(fy,6))+
  ylab("F")+theme_bw()+theme(legend.position = "none")
   Warning: Ignoring unknown parameters: linewidth
```

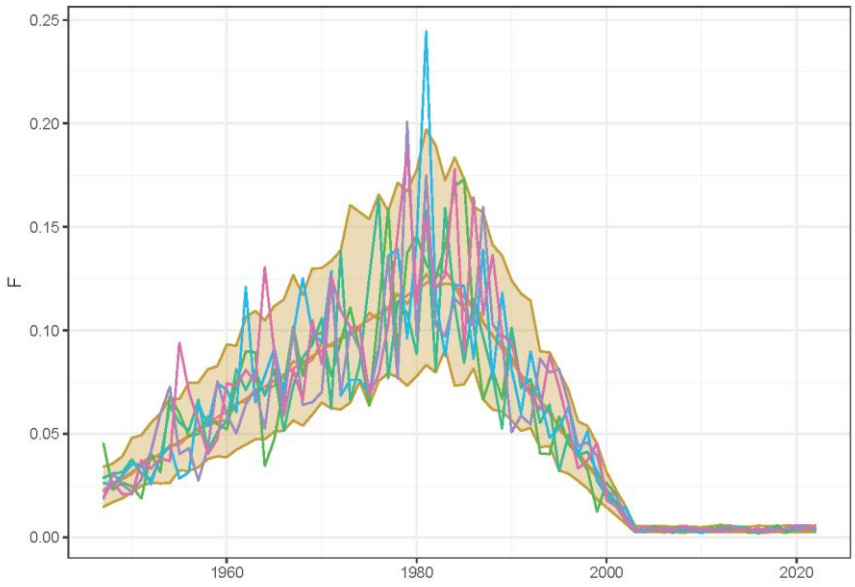


Figure 4: Simulated up-down-constant F-pattern without and with random noise for 5 random iterations

The stock dynamics can then be forecasted by adding random recruitment.

```
set.seed(123)
its = 100
# Random recruitment deviations with sigR = 0.5 and AR1 rho = 0.5 (high corr)
rec_devs = ar1rlnorm(0.5, 1946:2022, its, 0, 0.5)
# project Fs over om horizon
om <- ffwd(stki,sr,
             fbar=fy, # add F here
             deviances=rec_devs)
om@refpts = stk@refpts
```

```
plotAdvice(om)+geom_vline(xintercept = 1990,linetype=2)
```

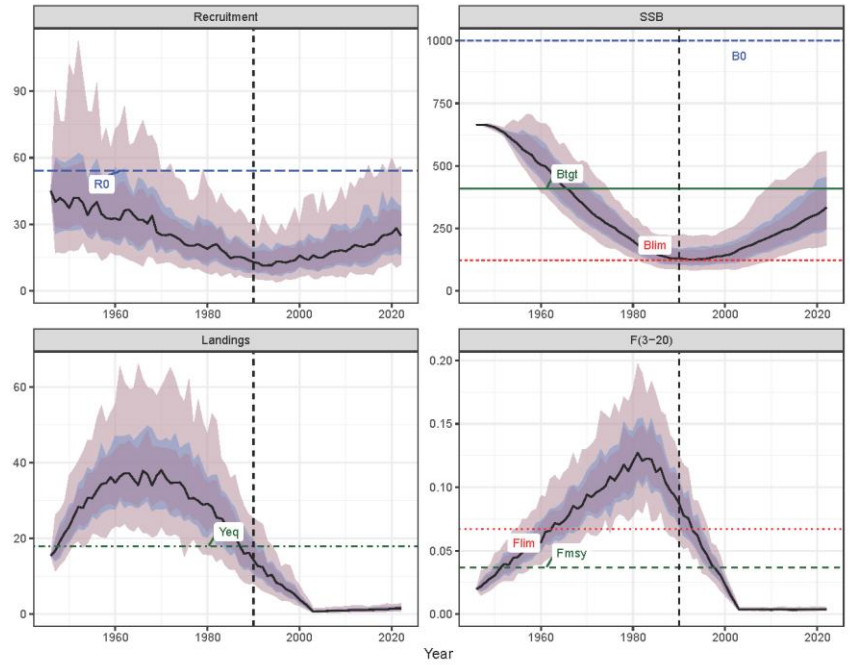


Figure 5: Simulated population dynamics compared to reference points from the off-the-shelf OM for thornback ray based on 100 iterations

The last step is to generate the observed survey index using the `FLRef` function `bioidx.sim()`. By default, the index assumes the same fishing selectivity in the stock object (but see `?bioidx.sim`. In this case, a moderate observation error of `sigma=0.3` is assumed and the catchability coefficient $q$ that scales the exploitable biomass to the index is set as `q = 0.001`. The index is assumed to start in 1999.

```
idx = window(bioidx.sim(om,sigma=0.3,q=0.001),start=1990)
```

```
flqs= FLQuants("B/Bmsy"=ssb(om)/om@refpts["Btgt"],
               "F/Fmsy"=fbar(om)/om@refpts["Fmsy"],
               "Catch/MSY"=catch(om)/om@refpts["Yeq"]
               ,Index=idx@index%/%yearMeans(idx@index))

ggplot(iter(flqs,1:20))+
  geom_line(aes(year,data,col=ac(iter)),alpha=0.5)+
  theme_bw()+facet_wrap(~qname)+
  theme(legend.position = "none")+geom_hline(yintercept = 1,linetype=2)+
  scale_color_manual(values=c(rainbow(20)))+
  geom_vline(xintercept = 1990,linetype=2)
```

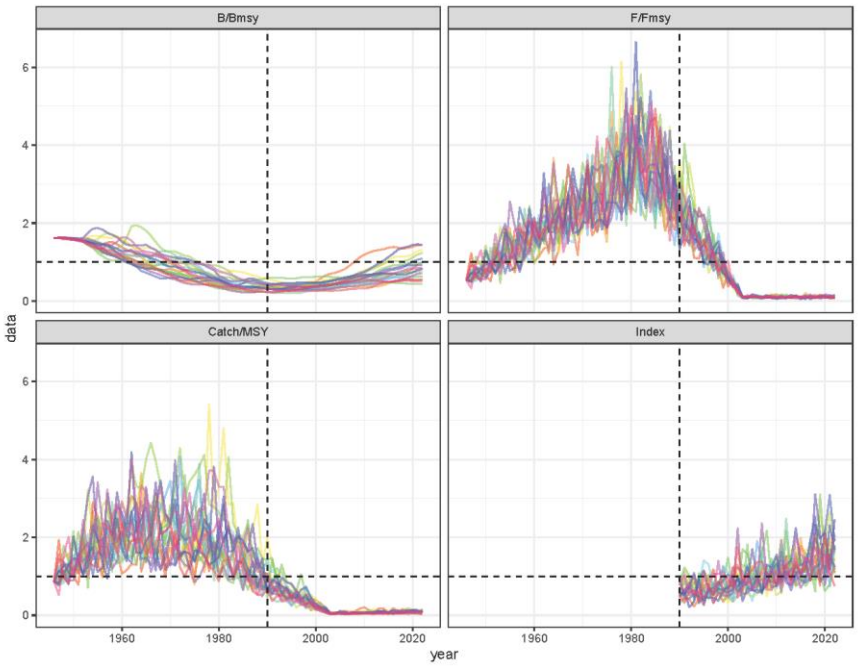


Figure 6: Individual iterations of simulated trajectories of $B/B_{MSY}$, $F/F_{MSY}$, $Catch/MSY$ and the normalized CPUE indices from the off-the-shelf OM for thornback ray shown for the first 20 iterations

## 6 Simulation testing with Spict

## 7 Spict estimation scenarios

```
#' spict.simplify
#'
#' Function to simplify spict to make it fast and robust as an MP
#'
#' @param inp spict input time series
#' @param r.pr lognormal r prior, untransformed mean,log.sd, phase
#' @param bk.pr lognormal initial depletion prior
#' @param shape.pr lognormal prior for shape
#' @param pe lognormal prior of process error on biomass
#' @param fdevs lognormal F penalty
#' @param ce lognorlam Catch penalty
#' @param dteuler time step resolution
spict.simplify = function(inp,r.pr=c(0.2,0.5,1),# r prior
                          bk.pr=c(0.8,0.3,1), # bk prior
                          shape.pr=c(2,0.01,1),
                          pe=c(1,0.3,1),
                          fdevs=c(4,0.5,1),
                          ce=c(0.1,0.1,1),
                          dteuler=1){

  inp$dteuler=dteuler
  inp$priors$logbkfrac <- c(log(bk.pr[1])-bk.pr[2]^2/2,bk.pr[2],bk.pr[3]) # this is  the bk prior
  inp$priors$logalpha <- c(0,0,0) # deactivate ratio of proc to obs error
  inp$priors$logbeta <- c(0,0,0) # deactivate catch to f devs
  inp$priors$logsdb <- c(log(pe[1])-0.5*pe[2]^2, pe[2], pe[3]) # process error
  inp$priors$logsdf <- c(log(fdevs[1])-0.5*fdevs[2]^2, fdevs[[2]], fdevs[3])
  inp$priors$logsdc <- c(log(ce)[1]-0.5*ce[2]^2, ce[2], ce[3]) #
  inp$priors$logn <- c(log(shape.pr[1]),shape.pr[2],shape.pr[3]) # Reduce shape CV
  inp$priors$logr <- c(log(r.pr[1])-0.5*r.pr[2]^2,r.pr[2],r.pr[3]) # r piror
  return(inp)

}
```

The three Schaefer model scenarios explored were:

(1) `r.est` estimate $r$ without constraints
(2) `r.low` r prior with low $r = 0.1$ with a $CV = 0.4$

(3) `r.high` r prior with low $r = 0.1$ with a $CV = 0.4$

All model scenarios assumed a `bkfrac` prior with a mean of 0.2 and CV of 0.3 to cover the range of states in the OM.

```
runi <- function(om,idx,it,dteuler=1/4){
# index
dfi =as.data.frame(iter(window(idx@index,start=1990),it))
```

```
# catch
# Short
dfc = as.data.frame(iter(window(om@catch,start=2009),it))
# Create Spict Default input
inp = list(obsC=dfc$data,timeC=dfc$year,
           obsI=dfi$data,timeI=dfi$year)

inp$dteuler = dteuler
# low r prior Schaefer
inp$priors$logn = c(log(2),0.01,1)
inp$priors$logbkfrac = c(log(0.2),0.3,1)
#r = 0.1
inp.lo = spict.simplify(inp,r.pr=c(0.1,0.4,1),# r prior
                        bk.pr=c(0.2,0.3,1), # bk prior
                        shape.pr=c(2,0.01,1),
                        pe=c(0.07,0.3,1),dteuler=dteuler)

#r = 0.2
inp.hi = spict.simplify(inp,r.pr=c(0.2,0.4,1),# r prior
                        bk.pr=c(0.2,0.3,1), # bk prior
                        shape.pr=c(2,0.01,1),
                        pe=c(0.07,0.3,1),dteuler=dteuler)

# make list of spict fits
fits = list(
  r.est= fit.spict(inp),
  r.low=fit.spict(inp.lo),
  r.high=fit.spict(inp.hi)
)
# convert spict in FLStockR
res = FLStocks(lapply(fits,function(x){
 run = spict2FLStockR(x,rel=T)
 run@refpts = rbind(run@refpts,FLPar(r=x$report$Fmsy*2))
 run
}))
# cut forecast
res = window(res,end=2022)
# Add om for comparison
flom = stock2ratios(iter(om,it))
res = FLStocks(c(om=flom,res))

return(res)
}
```

```
res = runi(om,idx,it=1,dteuler=1/4)

plot(res,metrics=list("B/Bmsy"=ssb,"F/Fmsy"=fbar,Catch=landings))+
  geom_hline(yintercept = 1,linetype=2)+theme_bw()
```

```
res = runi(om,idx,it=10,dteuler=1/4)

plot(res,metrics=list("B/Bmsy"=ssb,"F/Fmsy"=fbar,Catch=landings))+
```

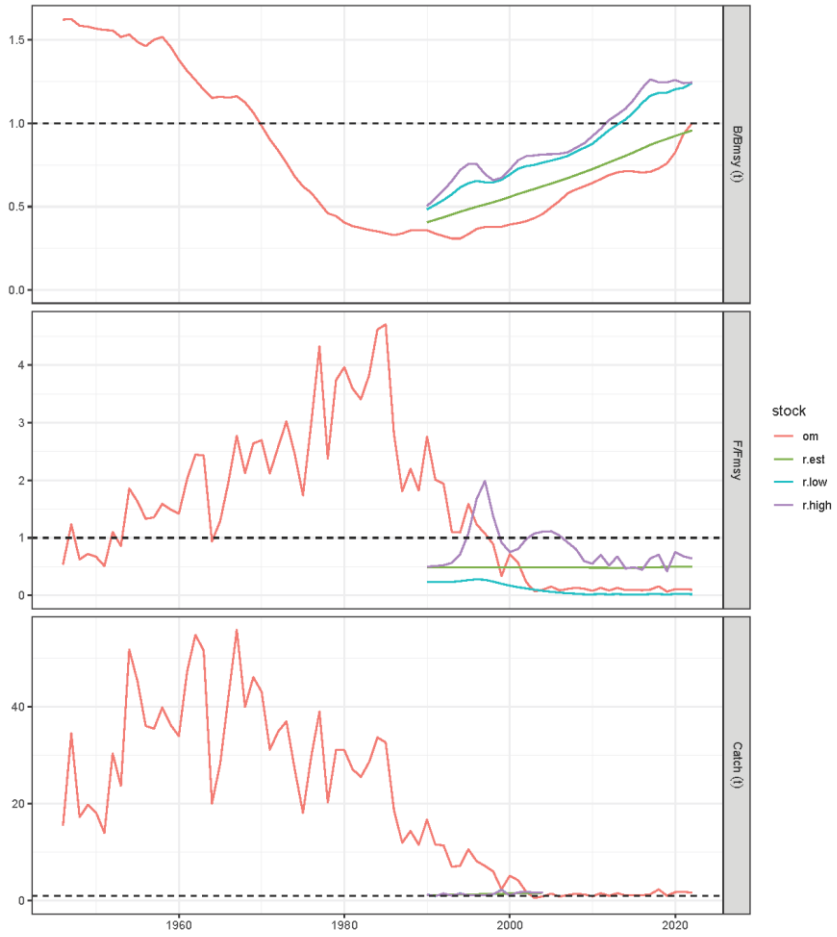


Figure 7: OM and estimated trajectories of $B/B_{MSY}$ and $F/F_{MSY}$ for the first iteration

```
geom_hline(yintercept = 1,linetype=2)+theme_bw()
```

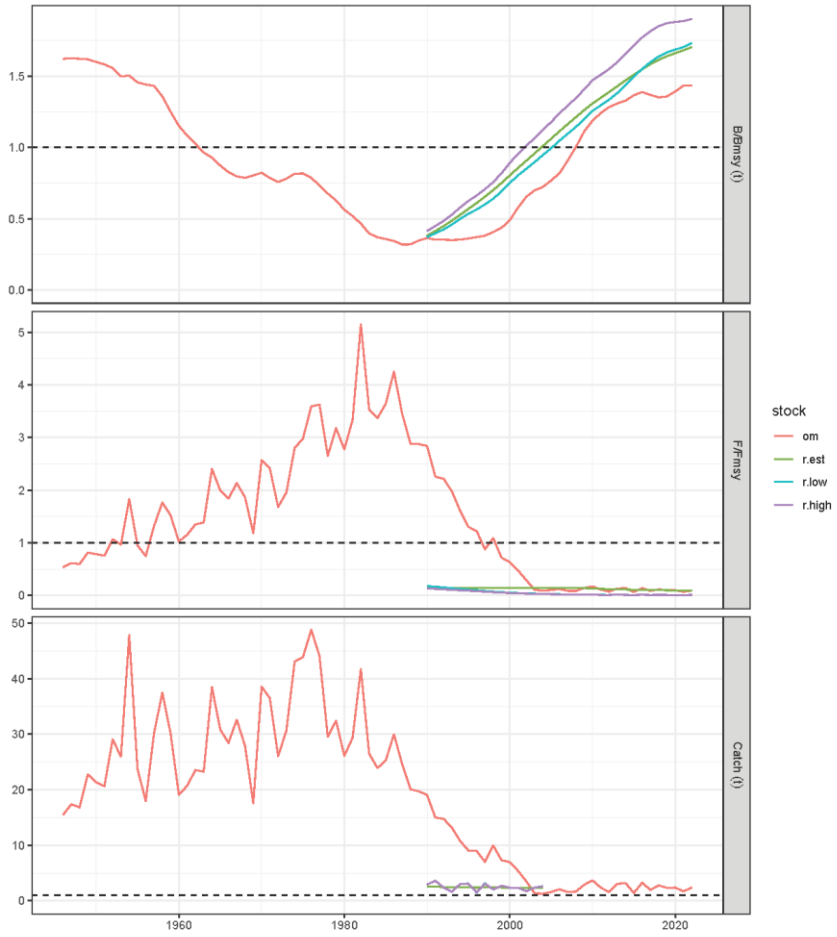


Figure 8: OM and estimated trajectories of $B/B_{MSY}$ and $F/F_{MSY}$ for iteration 10

### 7.1 Quick simulation performance comparison

```
sims = runi(om,idx,it=1,dteuler = 1)
sims =FLStocks(lapply(sims,function(x)propagate(x,its)))

for(i in 2:its){
  out=runi(om,idx,it=i,dteuler=1)
  for(j in 1:length(out)){
    iter(sims[[j]],i) = out[[j]]
    iter(sims[[j]]@refpts,i) = out[[j]]@refpts
    }}

sims= FLStocks(Map(function(x,y){
  x@name=y
  x},x=sims,y=as.list(names(sims))))
```

```
plot(sims,metrics=list("B/Bmsy"=ssb,"F/Fmsy"=fbar))+
  geom_hline(yintercept = 1,linetype=2)+theme_bw()
```

Several runs failed to converge the hessian, but these failed runs were not quantified removed for this initial evaluation.

By making use of `FLQuants` in is reasonably straight forward compute some estimation error with respect to the "true" value of $B_{MSY}$ and $F_{MSY}$ for the terminal year 2022.

```
simt= window(sims,start=2020,end=2020)
bias.b = FLQuants(lapply(simt[2:4],function(x){
  log(ssb(x))-log(window(ssb(simt$om)))
}))
bias.f = FLQuants(lapply(simt[2:4],function(x){
  log(fbar(x))-log(window(fbar(simt$om)))
}))

out = rbind(
  data.frame(as.data.frame(bias.b),what="BBmsy"),
  data.frame(as.data.frame(bias.f),what="FFmsy")
)
```

```
ggplot(out,aes(x=qname,data,fill=qname))+
  geom_boxplot(outlier.shape = NA)+
  facet_wrap(~what)+
  geom_hline(yintercept = 0,col=2)+theme_bw()+
  xlab("Scenario")+ylab("Error")+ylim(-2,2)
```

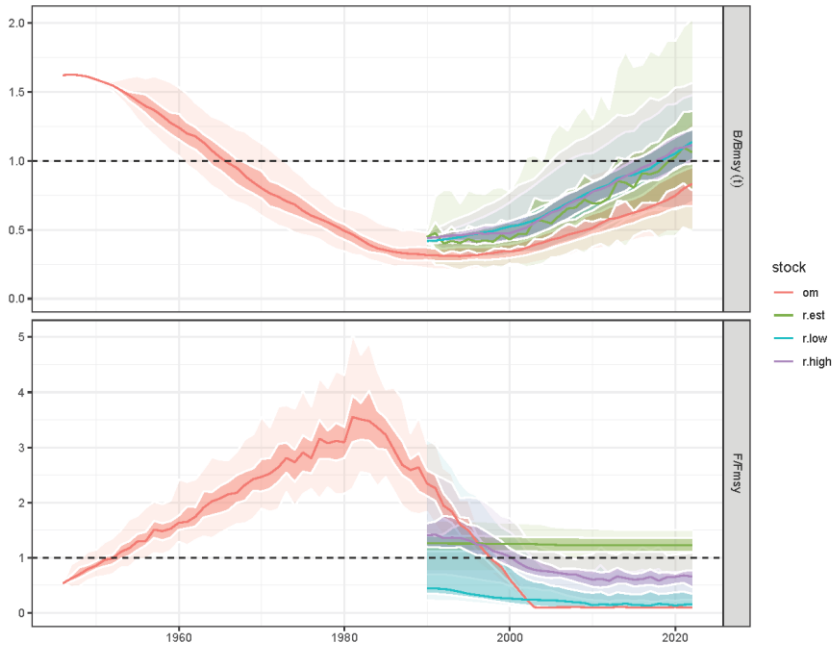


Figure 9: OM and estimated trajectories of $B/B_{MSY}$ and $F/F_{MSY}$ for 100 iterations

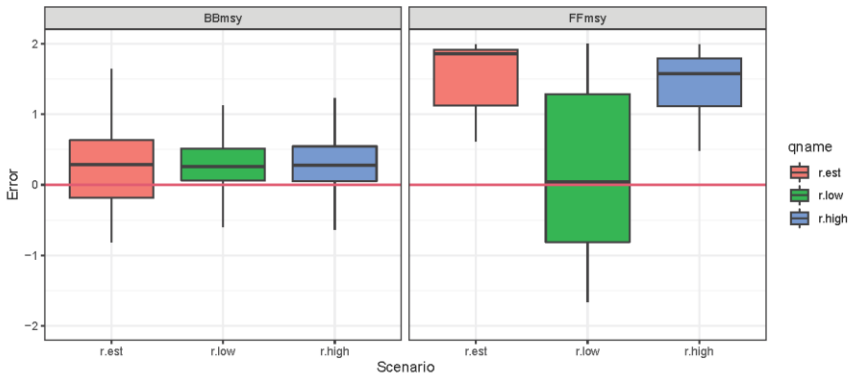


Figure 10: Boxplot showing estimation errors of $log(B/B_{MSY})$ and $log(F/F_{MSY})$ for 2022 with respect to the true quantities of the OM

All Spict scenarios showed fairly strong positive bias about the perception of stock status. The Fox models show the largest bias although the production is closer to the "true" age-structured dynamics of the OM and the Fmsy estimate is the same for prior means. One possible explanation the distortion between vulnerable biomass (vb) and ssb, where vb is linear proportional to ssb. However, this distortion appears minimal given the assumed maturity (for ssb) and selectivity (for vb) interacting with growth, natural mortality and the SRR (Figures 11). Another possible explanation is that the positive is caused by not capturing the interaction between the recruitment and age-structured lag-effects which may drive the population dynamics during the rebuilding phase, which coincides here with the observation period for the survey index.

Estimation of $r$ without strong prior constraints drives $r > 1$ up outside the known biological limits of the OM (Fig 12).

```
asem.vb = asem2spm(brp,quant="vb")

df1 = data.frame(as.data.frame(iterMedians(vb(om))/asem.vb["Bmsy"]),qname="vb")
df2 = data.frame(as.data.frame(iterMedians(ssb(om))/stk@refpts[2]),qname="ssb")
df = rbind(df1,df2)

ggplot(df,aes(year,data,color=qname))+geom_line()+
  theme_bw()+ylab(expression(B/B[MSY]))+geom_hline(yintercept = 1,linetype=2)+
  theme(legend.title = element_blank())
```

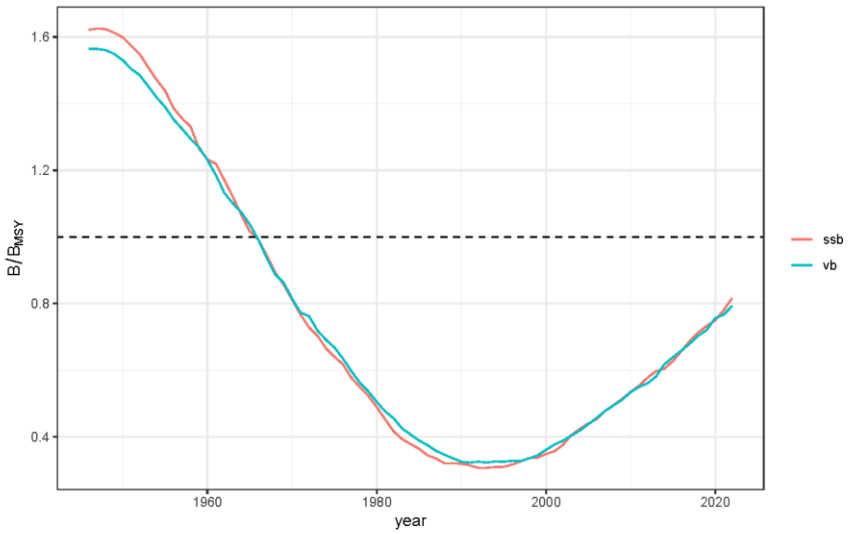


Figure 11: Median trajectories of $VB/VB_{MSY}$ and $SB/SB_{MSY}$ for 100 OM iteratsions

```
rs = do.call(rbind,lapply(sims[-1],function(x){
  data.frame(as.data.frame(x@refpts["r"]),run=x@name)
}))
```

```
ggplot(rs,aes(x=run,data,fill=run))+
  geom_boxplot(outlier.shape = NA)+theme_bw()+
  xlab("Scenario")+ylab("r")+ylim(0,2.5)
```

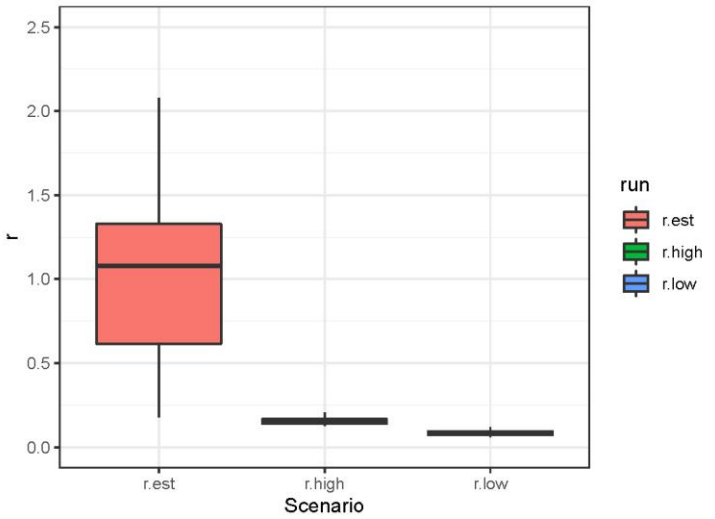


Figure 12: Comparison of estimated $r$ and estimates by constraint by low and high priors

### 7.2 Dome shaped survey index

Introducing dome shaping into the survey index can be done with `newselex`

```
survey.sel = newselex(harvest(stk),FLPar(S50=S50,S95=S95,
    Smax=6,Dcv=Dcv,Dmin=0.05))
ggplot(survey.sel)+geom_line(aes(age,data))+
  ylab("Selectivity")+xlab("Age")+theme_bw()
```

\begin{figure}

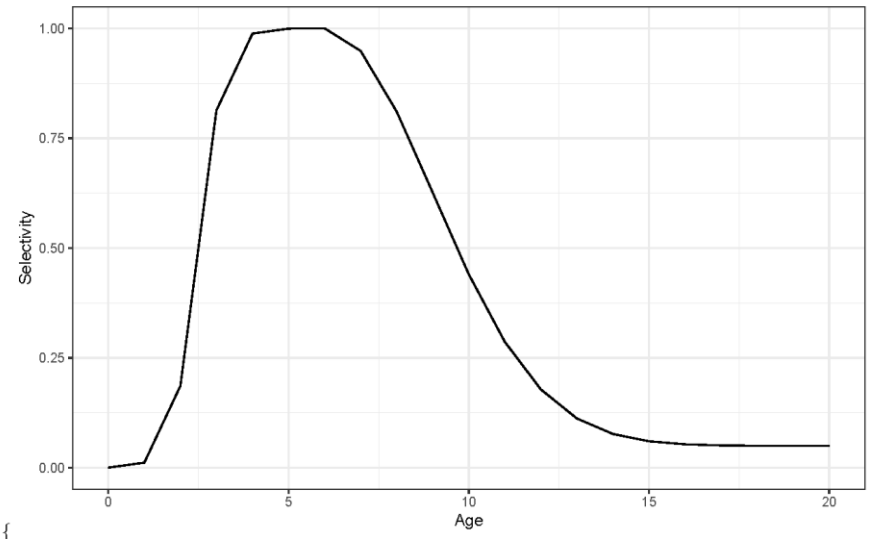


{

}

\caption{Median Trajectories of $VB/VB_{MSY}$ and $SB/SB_{MSY} for 100 OM iteratsions} \end{figure}

Next a new survey can be generated with this selectivity.

```
idx2 = window(bioidx.sim(om,sel=survey.sel,sigma=0.3,q=0.001),start=1990)
```

```
flqs= FLQuants("B/Bmsy"=ssb(om)/om@refpts["Btgt"],
               "F/Fmsy"=fbar(om)/om@refpts["Fmsy"],
               "Catch/MSY"=catch(om)/om@refpts["Yeq"]
               ,Index=idx2@index%/%yearMeans(idx2@index))

ggplot(iter(flqs,1:20))+
  geom_line(aes(year,data,col=ac(iter)),alpha=0.5)+
  theme_bw()+facet_wrap(~qname)+
  theme(legend.position = "none")+geom_hline(yintercept = 1,linetype=2)+
```

```
  scale_color_manual(values=c(rainbow(20)))+
  geom_vline(xintercept = 1990,linetype=2)
```

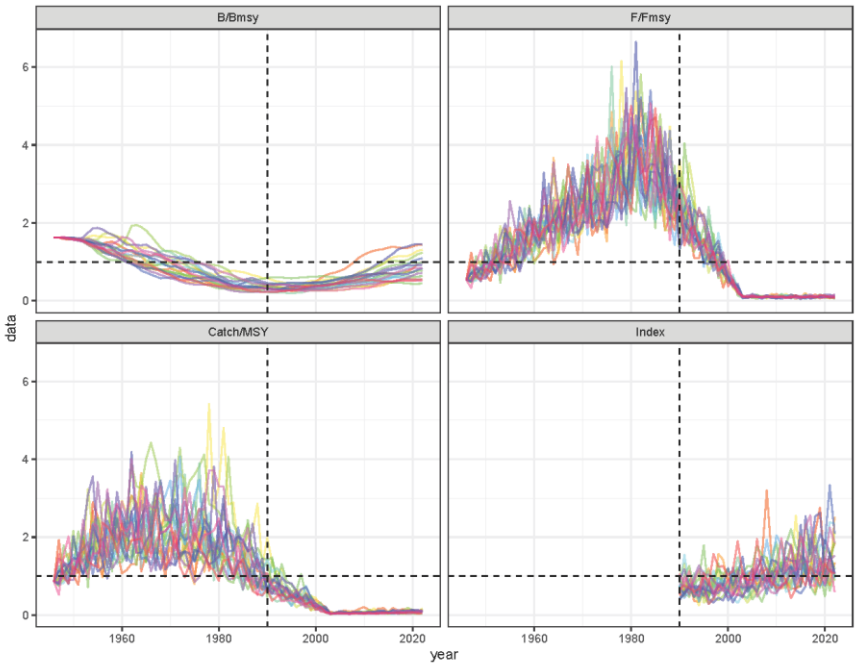


Figure 13: Individual iterations of simulated trajectories of $B/B_{MSY}$, $F/F_{MSY}$, $Catch/MSY$ and the normalized CPUE indices with dome-shaped selectivity from the off-the-shelf OM for thornback skate shown for the first 20 iterations

```
res = runi(om,idx2,it=1,dteuler=1/4)

plot(res,metrics=list("B/Bmsy"=ssb,"F/Fmsy"=fbar,Catch=landings))+
  geom_hline(yintercept = 1,linetype=2)+theme_bw()
```

```
res = runi(om,idx2,it=10,dteuler=1/4)

plot(res,metrics=list("B/Bmsy"=ssb,"F/Fmsy"=fbar,Catch=landings))+
  geom_hline(yintercept = 1,linetype=2)+theme_bw()
```

Rerun simulation with new index that has a dome-shaped selection pattern.

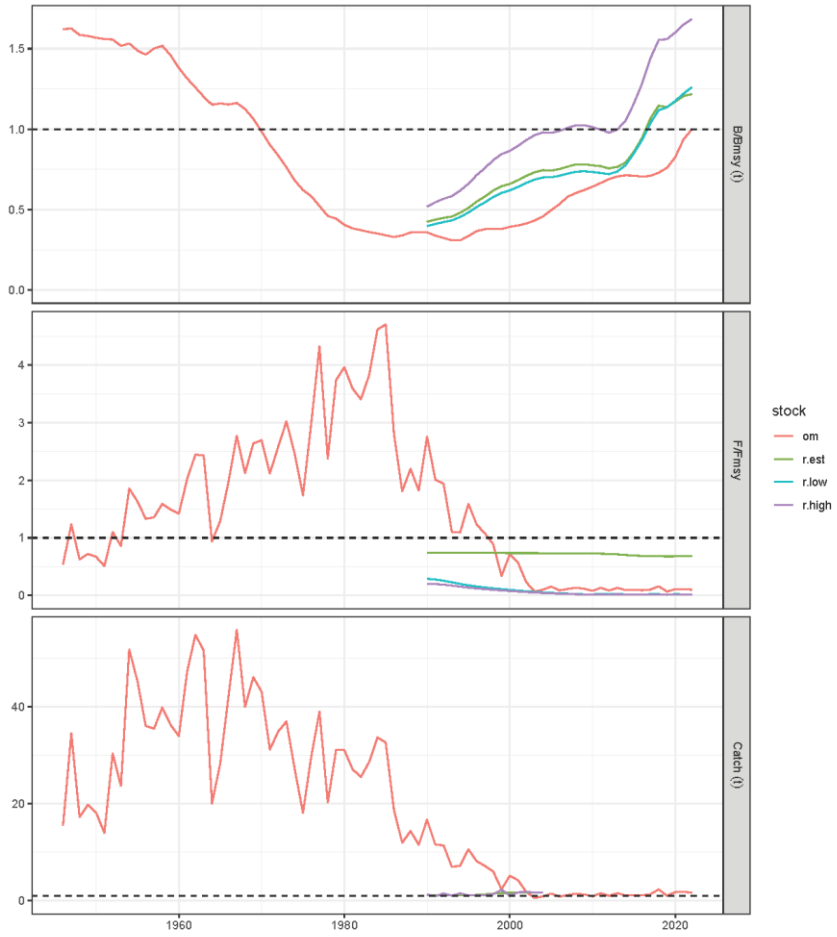


Figure 14: OM and estimated trajectories of $B/B_{MSY}$ and $F/F_{MSY}$ for iteration 1

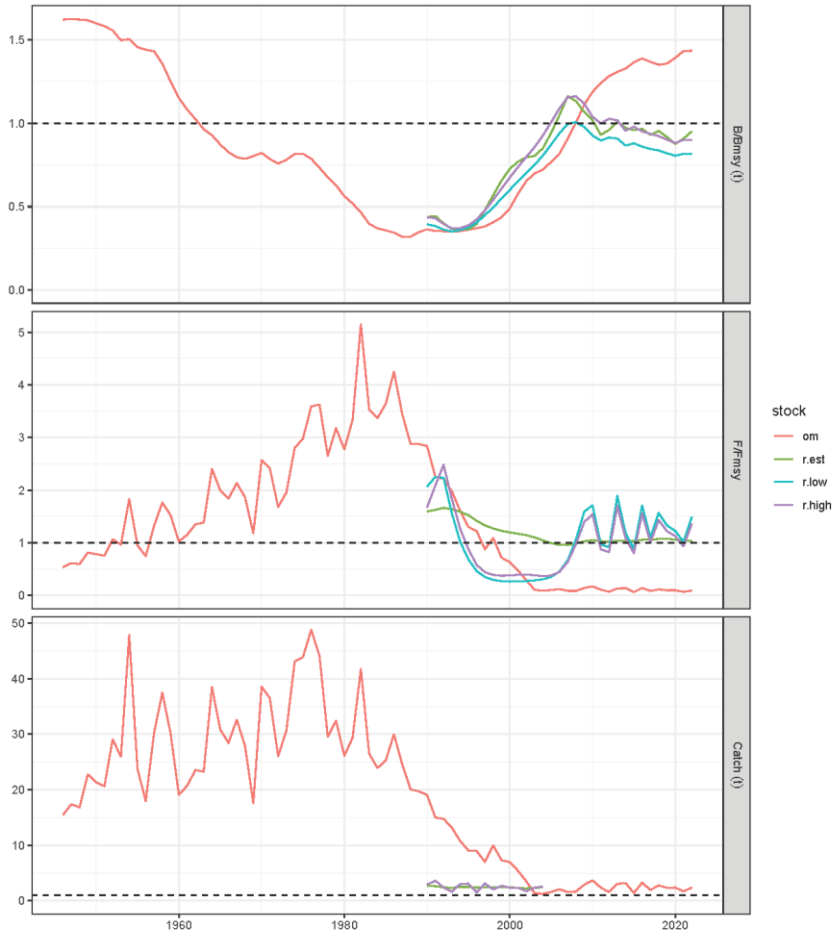


Figure 15: OM and estimated trajectories of $B/B_{MSY}$ and $F/F_{MSY}$ for iteration 10

```
sims2 = runi(om,idx2,it=1,dteuler = 1)
sims2 =FLStocks(lapply(sims2,function(x)propagate(x,its)))

for(i in 2:its){
  out=runi(om,idx2,it=i,dteuler=1)
  for(j in 1:length(out)){
    iter(sims2[[j]],i) = out[[j]]
    iter(sims2[[j]]@refpts,i) = out[[j]]@refpts
    }}

sims2= FLStocks(Map(function(x,y){
  x@name=y
  x},x=sims2,y=as.list(names(sims))))
```

```
plot(sims2,metrics=list("B/Bmsy"=ssb,"F/Fmsy"=fbar))+
  geom_hline(yintercept = 1,linetype=2)+theme_bw()
```

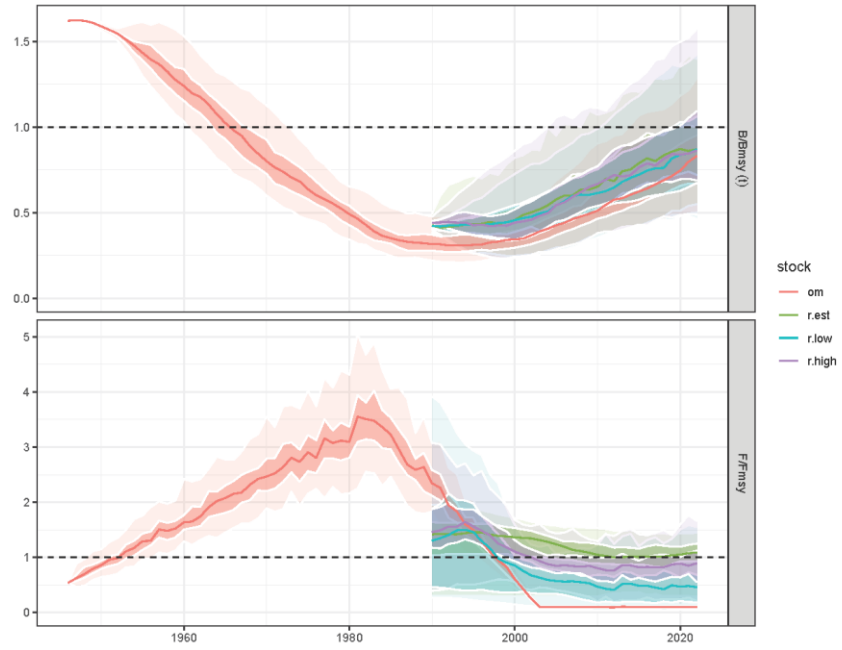


Figure 16: OM and estimated trajectories of $B/B_{MSY}$ and $F/F_{MSY}$ for 100 iterations

```
simt= window(sims2,start=2020,end=2020)
bias.b = FLQuants(lapply(simt[2:4],function(x){
  log(ssb(x))-log(window(ssb(simt$om)))
}))
bias.f = FLQuants(lapply(simt[2:4],function(x){
  log(fbar(x))-log(window(fbar(simt$om)))
}))

out = rbind(
  data.frame(as.data.frame(bias.b),what="BBmsy"),
  data.frame(as.data.frame(bias.f),what="FFmsy")
)
```

```
ggplot(out,aes(x=qname,data,fill=qname))+
  geom_boxplot(outlier.shape = NA)+
  facet_wrap(~what)+
  geom_hline(yintercept = 0,col=2)+theme_bw()+
  xlab("Scenario")+ylab("Error")+ylim(-2,2)
```

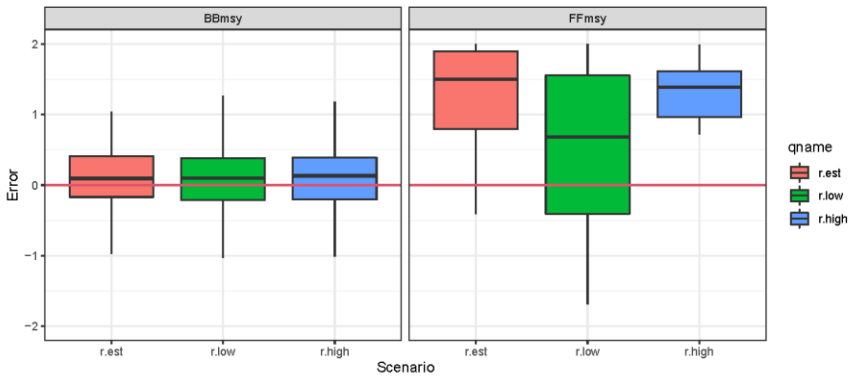


Figure 17: Boxplot showing estimation errors of $log(B/B_{MSY})$ and $log(F/F_{MSY})$ for 2022 with respect to the true quantities of the OM and dome-shaped selectivity in the survey index

```
rs = do.call(rbind,lapply(sims2[-1],function(x){
  data.frame(as.data.frame(x@refpts["r"]),run=x@name)
}))

ggplot(rs,aes(x=run,data,fill=run))+
  geom_boxplot(outlier.shape = NA)+theme_bw()+
  xlab("Scenario")+ylab("r")+ylim(0,2.5)
```

# 9 Bay of Biscay and Atlantic Iberian waters whiting

## whg.27.89a – *Merlangius merlangus* in Subarea 8 and Division 9.a

## 9.1 Introduction

Whiting (*Merlangius merlangus*) is distributed over the whole Northeast Atlantic (southeastern Barents Sea and Iceland to Portugal, also in the Black Sea, Aegean Sea, Adriatic Sea and adjacent areas) it is rare in the northwestern Mediterranean.

It is generally found from 30–100 m over sandy/muddy grounds and feed on shrimps, crabs, molluscs, small fish, polychaetes and cephalopods. Juveniles are found close inshore and migrate to the open sea only after the first year of life. Eggs are pelagic.

Genetic studies suggest NE Atlantic whiting, including northern North Sea is quite genetically homogeneous. In contrast potentially low levels of structuring has been suggested between this NE stock and that in the southern Bay of Biscay as well as within the Irish Sea and particularly the North Sea (Charrier, Coombs, McQuinn, and Laroche, 2007).

Whg.27.89a is caught in mixed demersal fisheries primarily by France and Spain (Figure 9.1 and Table 9.1). More than 95% of the total landings are realized by French fleets. In 2020 38% of the landings were realized using demersal trawls, 27 using lines, 16% gillnets, 15% demersal seines and 4% other gears.

There are concerns about the reliability of the French data from 2008–2009, which appear to be incomplete. There is some misidentification of whiting in the Portuguese markets with pollack due to the common names used for both stocks. This resulted in most pollack landings being recorded as whiting from 2004 onwards. Based on this information, pollack landings were deducted from the whiting landings during this period and were then considered as unallocated (Table 9.1). Sampling data since 2012 indicate that Portuguese landings of whiting and pollack from Division 9.a consisted of 2% whiting and 98% pollack (EC, 2015); whiting landed by Portuguese vessels makes up an insignificant proportion of the total whiting landings in this area.

Whiting belonged to a category 5 stock. Precautionary approach was conducted for whiting and ICES advised that catches in each of the years 2019, 2020, 2021, and 2022 should be no more than 2276 t.

## 9.2 Input data for stock assessment

### 9.2.1 Commercial catches and discards

InterCatch data were processed to compute landings and discards estimates (Table 9.1). Whiting is mostly caught by France (Figure 9.1).

**Table 9.1. Landings (in tonnes) per country and year.**

| Year | Belgium | France | Portugal | Spain | Total | Unallocated | ICES estimation | Discards | TAC |
|---|---|---|---|---|---|---|---|---|---|
| 1994 | | 3496 | 15 | 136 | 3647 | 0 | 3647 | 0 | |
| 1995 | | 2645 | 2 | 1 | 2648 | 0 | 2648 | 0 | |

| Year | Belgium | France | Portugal | Spain | Total | Unallocated | ICES estimation | Discards | TAC |
|---|---|---|---|---|---|---|---|---|---|
| 1996 | | 1544 | 4 | 13 | 1561 | 0 | 1561 | 0 | |
| 1997 | | 1895 | 3 | 47 | 1945 | 0 | 1945 | 0 | |
| 1998 | | 1750 | 3 | 105 | 1858 | 0 | 1858 | 0 | |
| 1999 | | | 1 | 211 | 212 | 0 | 212 | 0 | |
| 2000 | 2 | 1106 | 2 | 338 | 1448 | 0 | 1448 | 0 | 7000 |
| 2001 | 3 | 1989 | 1 | 288 | 2281 | 0 | 2281 | 0 | 5600 |
| 2002 | 3 | 1970 | 1 | 230 | 2204 | 0 | 2204 | 0 | 5600 |
| 2003 | 1 | 2275 | 4 | 171 | 2451 | 0 | 2451 | 0 | 5600 |
| 2004 | | 1965 | 77 | 249 | 2291 | –70 | 2221 | 0 | 4500 |
| 2005 | 3 | 1662 | 2 | 416 | 2083 | –2 | 2081 | 0 | 3600 |
| 2006 | 2 | 1420 | 7 | 433 | 1862 | –6 | 1856 | 0 | 3600 |
| 2007 | 4 | 1617 | 107 | 296 | 2024 | −104 | 1920 | 0 | 3600 |
| 2008 | 1 | 772 | 98 | 187 | 1058 | −93 | 965 | 0 | 3600 |
| 2009 | 2 | 1303 | 114 | 54 | 1473 | −111 | 1362 | 0 | 3600 |
| 2010 | 3 | 2234 | 114 | 101 | 2452 | −110 | 2342 | 0 | 3240 |
| 2011 | 1 | 2029 | 105 | 108 | 2243 | −102 | 2141 | 0 | 3175 |
| 2012 | 3 | 1791 | 90 | 110 | 1994 | −87 | 1907 | 0 | 3175 |
| 2014 | 1 | 1579 | 65 | 55 | 1700 | −49 | 1651 | 0 | 3175 |
| 2015 | 2 | 2138 | 38 | 56 | 2234 | −35 | 2199 | 0 | 3175 |
| 2016 | 1 | 2441 | 20 | 40 | 2502 | 23 | 2525 | 926.78 | 2540 |
| 2017 | 0 | 1871 | 18 | 20 | 1909 | 16 | 1925 | 937.8 | 2540 |
| 2018 | 2 | 1523 | 14 | | 1539 | | 1539 | 655.5 | 2540 |
| 2019 | 1 | 1348 | | 13 | 1362 | 34 | 1396 | 535 | 2276 |
| 2020 | 1 | 1094 | | 1 | 1096 | 25 | 1121 | 299 | 2276 |
| 2021 | 1 | 1229 | | 15 | 1271 | 26 | 1271 | 629 | 2276 |

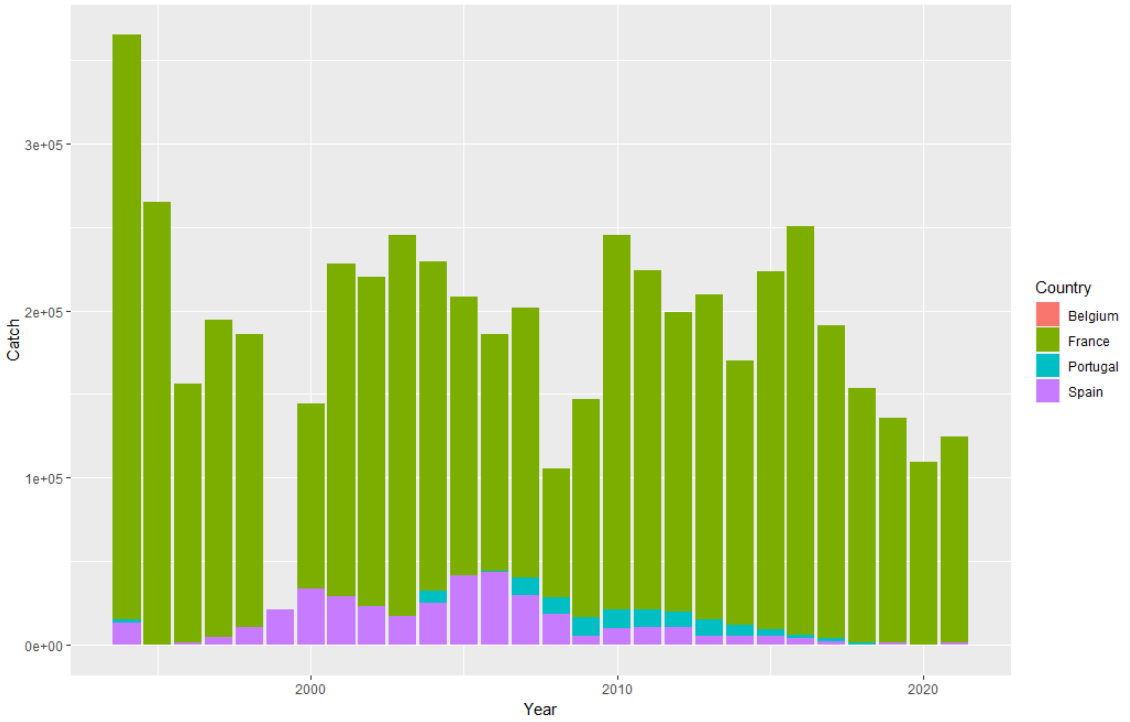


**Figure 9.1. Landings per country.**

Discard is known to happen in the different fleets catching whiting in this area. Discard rate is estimated around 0.2 to 0.3 (Table 9.2).

**Table 9.2. Whiting landings and discards after raising procedures (in tonnes).**

| Year | Landings (Imported) | Discards (Imported) | Discards (raised) | Total Discards | Overall Discard Rate |
|---|---|---|---|---|---|
| 2016 | 2525.00 | 828.40 | 98.38 | 926.78 | 0.268 |
| 2017 | 1925.00 | 617.60 | 320.20 | 937.80 | 0.328 |
| 2018 | 1565.00 | 376.00 | 279.50 | 655.50 | 0.295 |
| 2019 | 1396.00 | 243.90 | 291.20 | 535.10 | 0.280 |
| 2020 | 1122.00 | 92.50 | 206.20 | 298.70 | 0.210 |

## 9.2.2 Length structure

Length distribution is available for some métiers for France (2016–2021). Total length structure was raised using the available strata in InterCatch for the period 2016–2021 (Figure 9.2).

Due to the low sampling level in 2020, discard length structure is much noisier than in the previous years. However, landings length structures are of similar quality compared to previous years.

The length composition of landings was employed to estimate the length of first capture ($L_c$) of pol.27.89a following the calculation defined for Length-Based-Indicators (ICES, 2015). $L_c$ was estimated at 28.7 cm and was used as input data to calculate the r priors. The $L_c$ is higher than the $L_{mat}$ used for LBI (26 cm) and this is related with the fact that the Minimum Conservation Reference Size is at the level of $L_{mat}$ (27 cm)

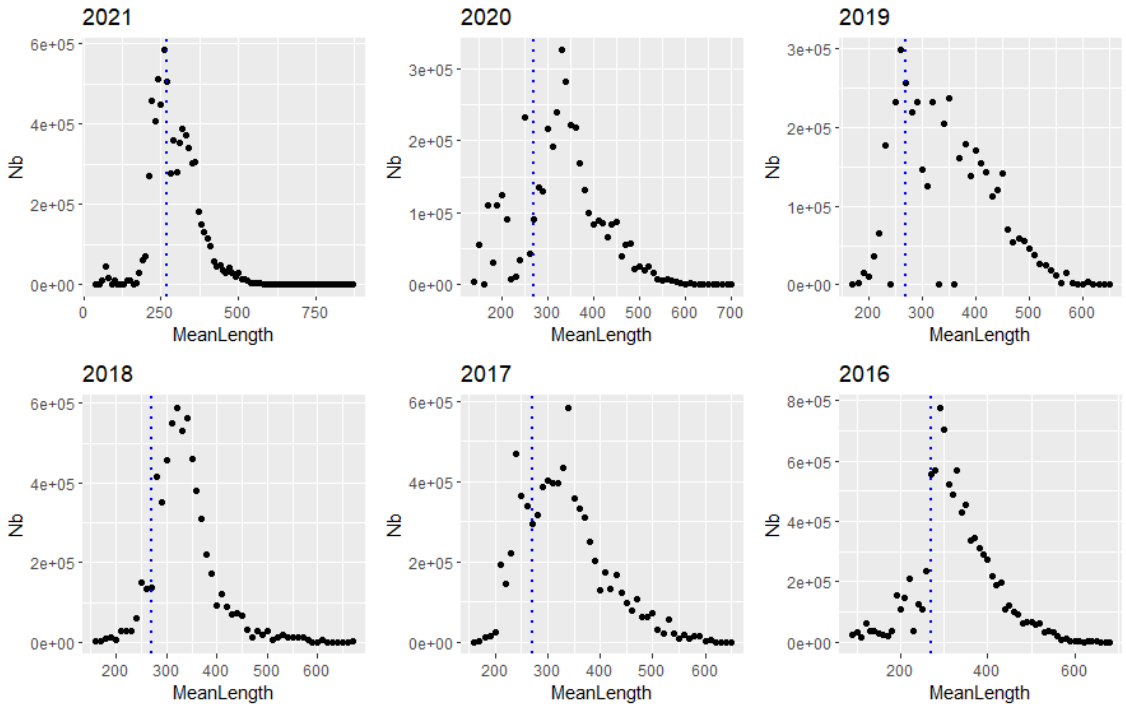


**Figure 9.2. Length structures of the landings from 2016 to 2021.**

## 9.2.3 Scientific survey

Whiting are present in the French (EVHOE-WIBTS-Q4 (G9527) from the Bay of Biscay. This species is at the southern extent of its range in the Bay of Biscay and Iberian Peninsula (Figure 9.3)

This survey was not used to provide biomass index because of discrepancies between survey length structures and commercial catches length structures. Length structures from the survey are shown in Figure 9.4.

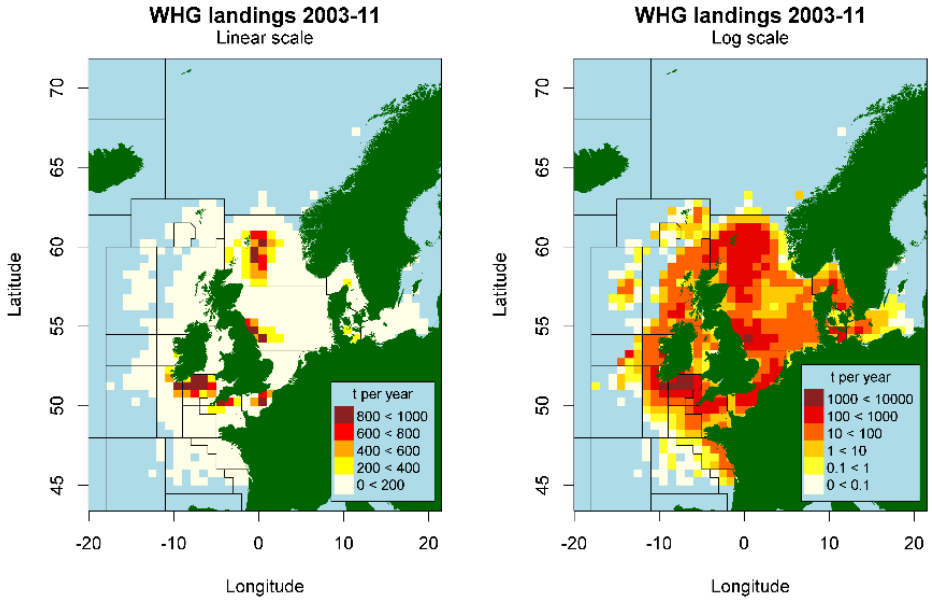


**Figure 9.3. Spatial distribution of whiting landings.**

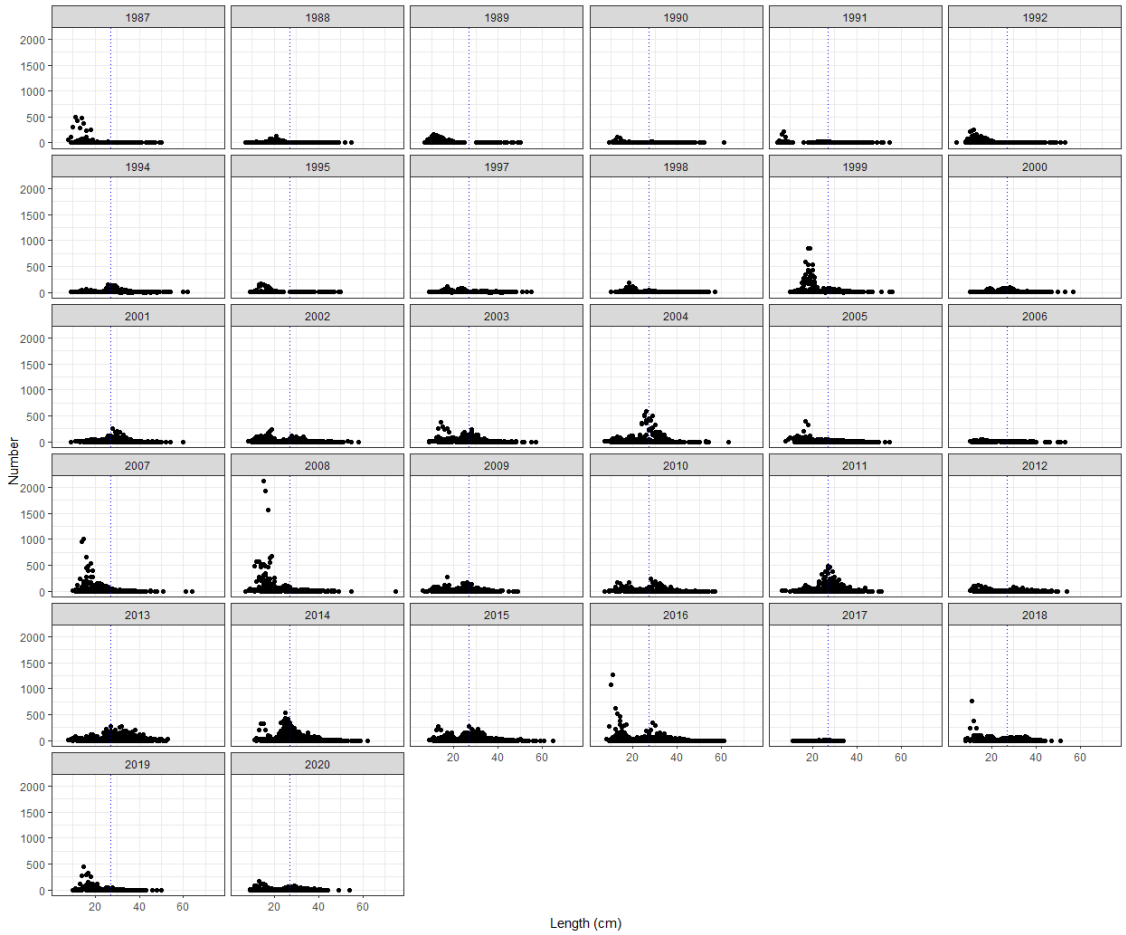


**Figure 9.4. Whiting Length structures (EVHOE).**

## 9.2.4 Standardized commercial abundance index

### 9.2.4.1 Fleet selection

Whiting is caught by a diversity of gears (Figure 9.5).

A commercial abundance index was provided using the French bottom-otter trawlers (OTB) fleet, which represents 30% of the French landings for whiting (Figure 9.5, OTB are in blue). 1176 trawlers landed at least 1 kg of whiting over the period 2000–2021.

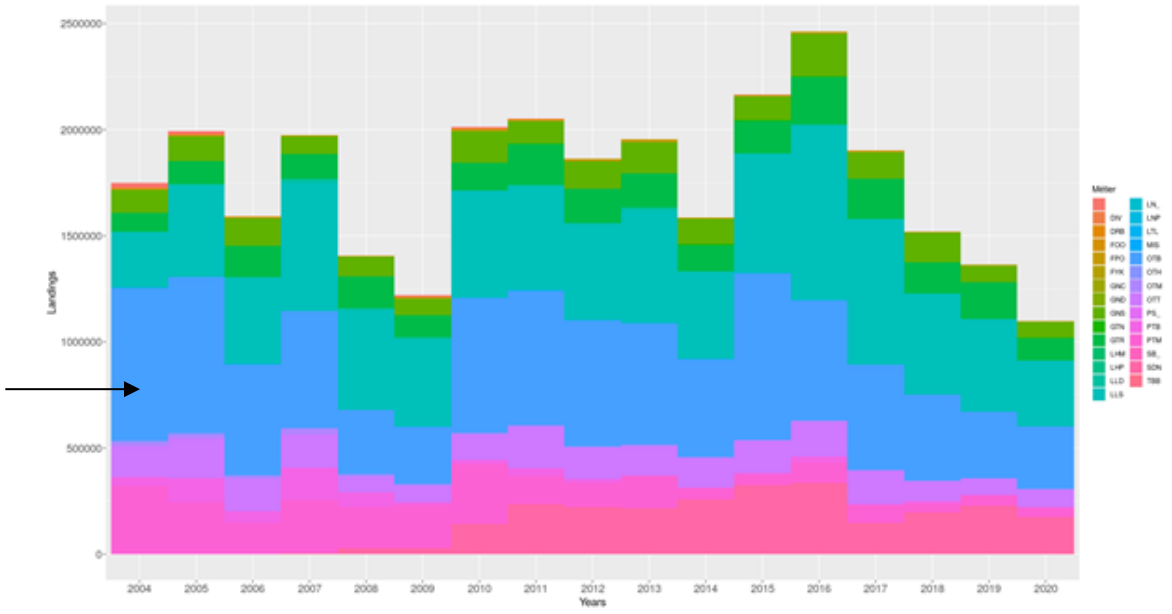


**Figure 9.5. Landings of whiting per year and per métier.**

Different filters were applied in order to select vessels catching whiting and reduce the number of vessels in the reference fleet.

The first filter concerns vessel's fishing activity [defined as years with positive landings of pollack]. Figure 9.6 represents the years of presence of vessels that have been catching whiting (at least 1 kg) during the period 2000–2022. 218 vessels remain after applying a 10 years filter threshold (red line), 400 after a 5 years filter (green line) and 536 after a 3 years filter (blue line). The 5 years filter was chosen, as a compromise between the different options. It allows keeping enough vessels to constitute the data input for the CPUE models.

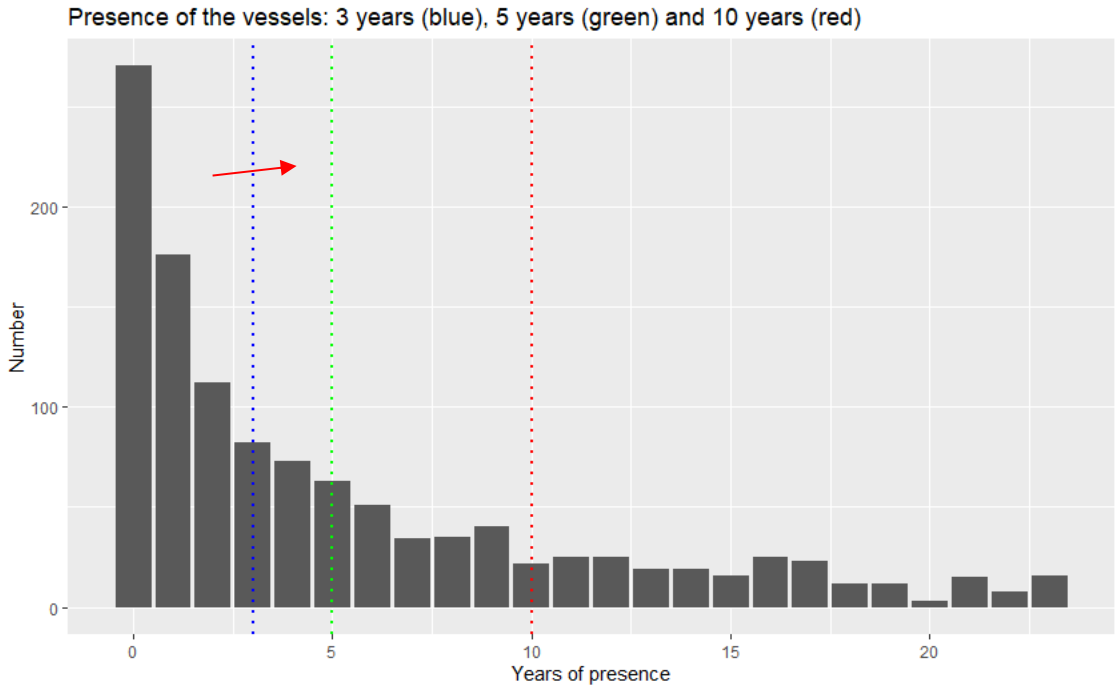


**Figure 9.6. Presence of the vessels during the 2000–2022 period.**

A selection was also made so that the vessels have been catching significant volumes of whiting per year. This selection was conducted on the vessels that were present 5 years at least during

the period (*cf* previous §: 400 vessels). Figure 9.7 shows that a large part of the vessels land limited volumes. 137 vessels remain after applying a threshold of 1 tonne filter (average over the period), 14 after a 3 tonnes filter and 5 after a 5 tonnes filter.

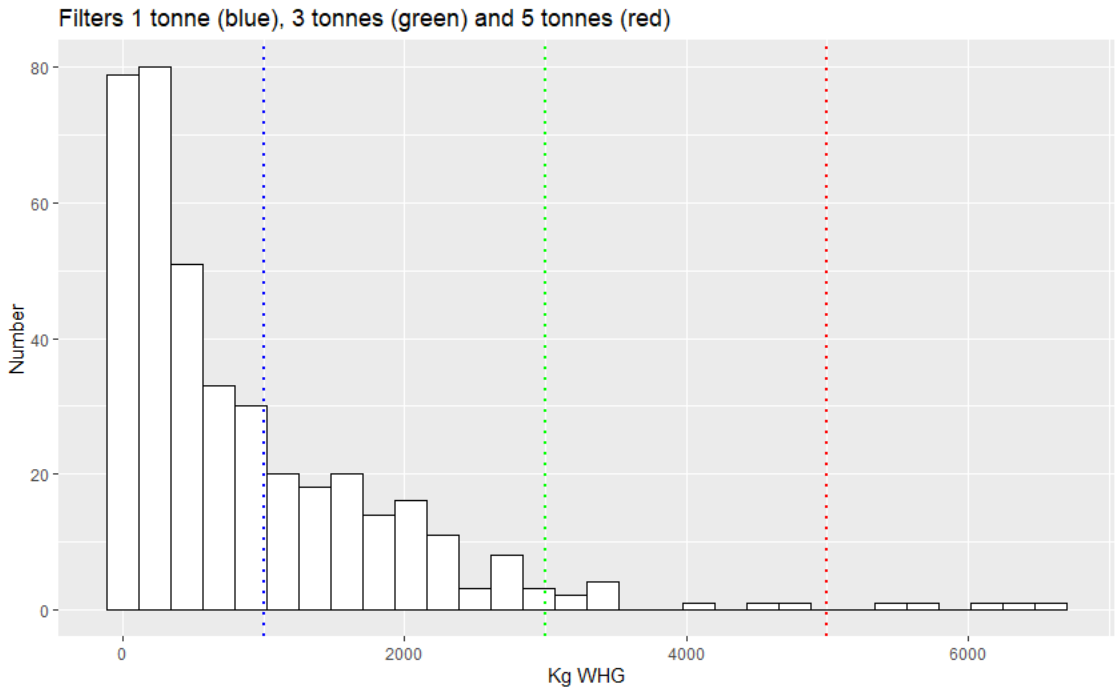


**Figure 9.7. Number of vessels and yearly average landings**

A 1 tonne filter was chosen and allows selecting vessels that landed a minimum volume of whiting per year.

### 9.2.4.2 Yearly consistency of the logbook database

The French database changed in 2009, which led to a change in the repositories of the effort.

All declarative variables were impacted by this change in the database. Figure 9.8 shows that 10–12 and 12–18 m vessel length categories effort time-series have been strongly impacted by these changes and it appeared unrealistic to derive a consistent index over the whole time-series.

Therefore, the data were cut in two distinct series: 2000–2009 and 2010–2021.

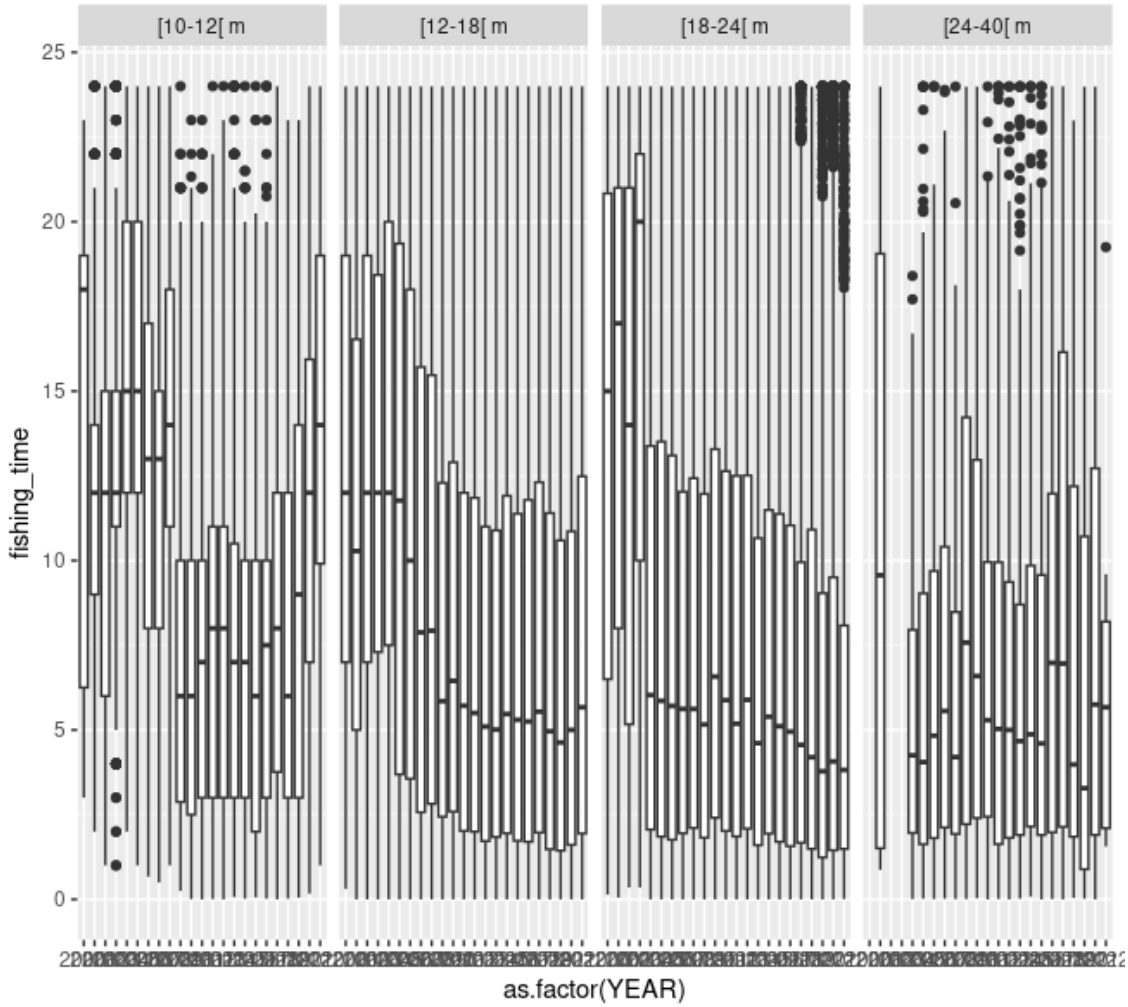


**Figure 9.8. Yearly effort distribution by vessel length class [time expressed in fishing days]**

### 9.2.4.3 Targeting covariates

Targeting behaviour can explain changes in CPUEs over time.

The 10 major species that are caught with whiting are in Figure 9.9. Catches were normalized into relative proportions by weight and square root transformed (Winker, 2013). To construct data input for the GAM's models, the Direct Principal Component approach was conducted. It directly uses the PC's scores of the PCA as predictor variable in the model. We retained PCs that had an Eigenvalue superior to 1, in our case four PCs. Figure 9.10 shows the correlation graph and the correlation of variables.

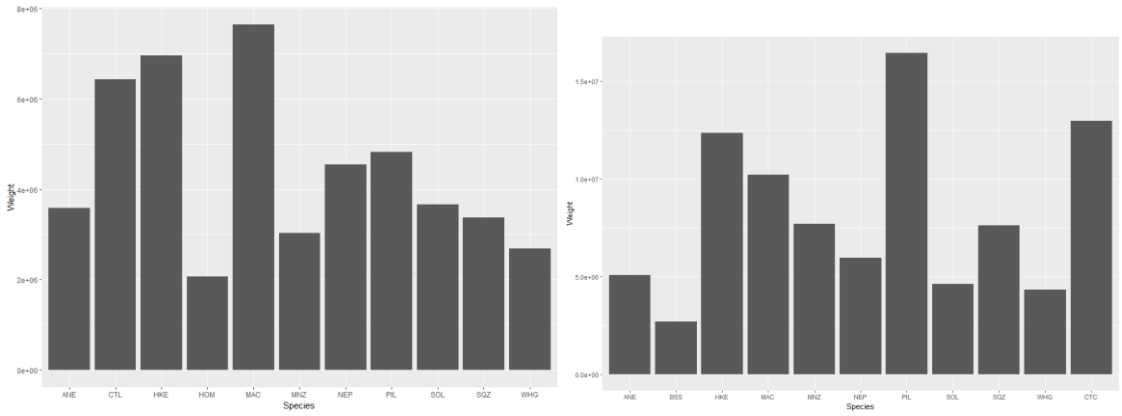


**Figure 9.9. 10 major species caught with whiting, for 2000–2009 (left) and 2010–2021 (right).**

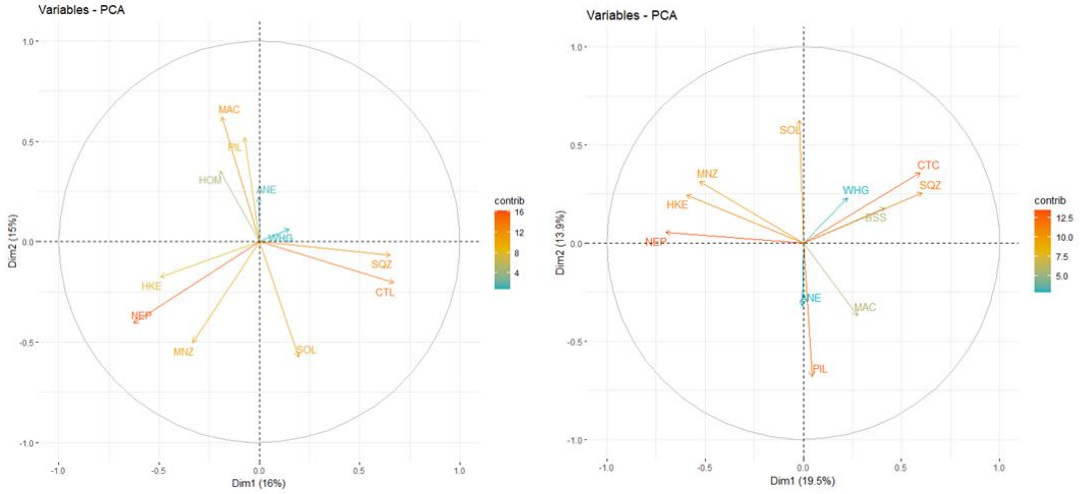


**Figure 9.9. Correlation graph and contribution of variables, for 2000–2009 (left) and 2010–2021 (right)**

### 9.2.4.4 Model

The models fitting CPUE records is a GAM with a Tweedie distribution, which takes into account high frequencies of zeros in the data. A cyclic cubic regression spline was chosen to smooth the month predictor, while smoothing of other continuous variables was realized by thin plate regression spline functions. There is a random effect on vessels. Characteristics of vessels (in term of size) is also included in the model. Effort were estimated using vessel fishing time and is used as an offset in the model. The PC's scores are represented by the covariates RS1, RS2, RS3 and RS4.

The final model is:

> formula = *"WHG_weight ~ offset(log(fishing_time)) + as.factor(YEAR) + s(MONTH, bs='cc', k=12) + s(carre.lon,carre.lat, k=20) + s(NAVS_COD, bs = 're') + s(RS1) + s(RS2) + s(RS3) + s(RS4) + as.factor(size_NAVS)"*
>
> *model_fit <- mgcv::gam(formula = formula, data = sacrois_mod, family = tw(link="log"), method = "REML")*

In order to compare the influence of adding the covariates on the predictions (especially the targeting covariate), five models were tested:

- "**base**": WHG_weight ~ offset(log(time_sea)) + as.factor(YEAR) + s(NAVS_COD, bs = 're')
- "**mois**": WHG_weight ~ offset(log(time_sea)) + as.factor(YEAR) + s(MONTH, bs='cc', k=12) + s(NAVS_COD, bs = 're')

- "**space**": WHG_weight ~ offset(log(time_sea)) + as.factor(YEAR) + s(MONTH, bs='cc', k=12) + s(carre.lon,carre.lat, k=20) + s(NAVS_COD, bs = 're')
- "**carac**": WHG_weight ~ offset(log(time_sea)) + as.factor(YEAR) + s(MONTH, bs='cc', k=12) + s(carre.lon,carre.lat, k=20) + s(NAVS_COD, bs = 're') + as.factor(size_NAVS)
- "**tot**": WHG_weight ~ offset(log(time_sea)) + as.factor(YEAR) + s(MONTH, bs='cc', k=12) + s(carre.lon,carre.lat, k=20) + s(NAVS_COD, bs = 're') + s(RS1) + s(RS2) + s(RS3) + s(RS4) + as.factor(size_NAVS)

Predictions were made for these five models and with the CPUE series 2000–2009 and 2010–2021(Figure 9.11). The blue line represents the nominal CPUEs (mean of catch per year/effort).

All CPUE are standardized by the mean.


**Figure 9.11. Predictions of the GAM model.**

The final CPUEs used in the SPiCT model are presented in Table 9.2.

**Table 9.2. Predictions of the GAM model.**

| Year | Predictions | Year | Predictions |
|---|---|---|---|
| 2000 | 1.25 | 2011 | 1.30 |
| 2001 | 1.52 | 2012 | 1.26 |
| 2002 | 1.30 | 2013 | 1.04 |
| 2003 | 1.11 | 2014 | 0.99 |
| 2004 | 1.27 | 2015 | 1.35 |
| 2005 | 0.76 | 2016 | 1.27 |
| 2006 | 0.88 | 2017 | 0.81 |
| 2007 | 0.71 | 2018 | 0.74 |
| 2008 | 0.45 | 2019 | 0.74 |
| 2009 | 0.75 | 2020 | 0.56 |
| 2010 | 1.09 | 2021 | 0.85 |

## 9.3 Stock assessment

The stock assessment was performed using the software SPiCT v1.3.8 (Pedersen and Berg, 2017) available at https://github.com/DTUAqua/spict.

**Input data**

Historical catches are reported by ICES (Figure 9.12).

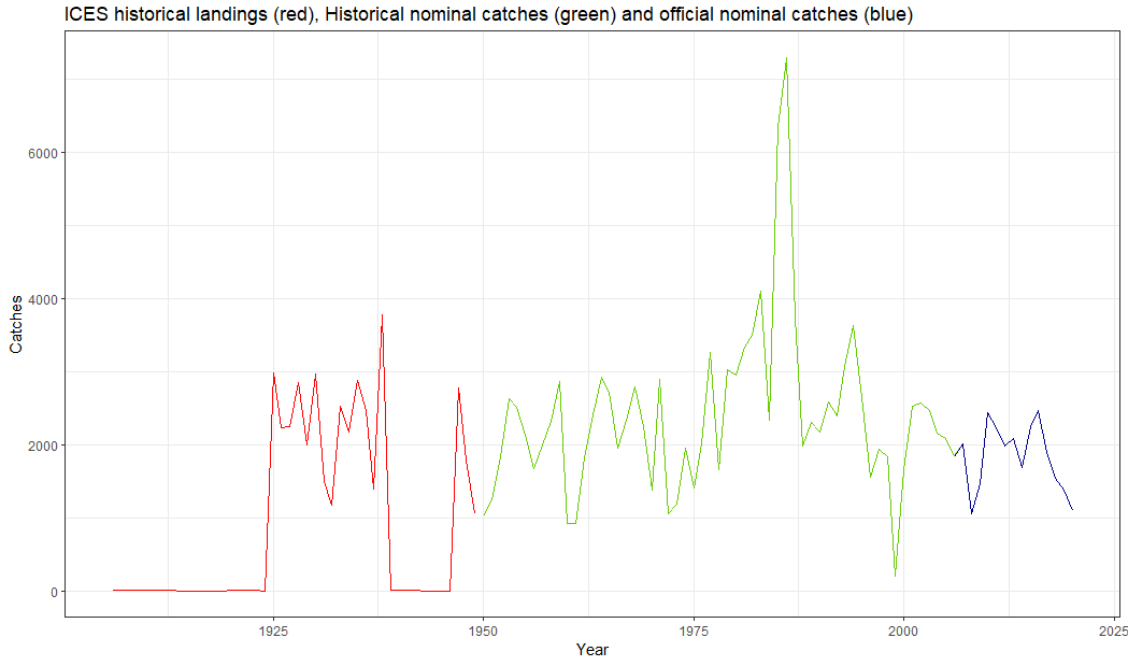


**Figure 9.12. Historical ICES landings.**

Figures 9.13 and 9.14 represent ICES catch by country.

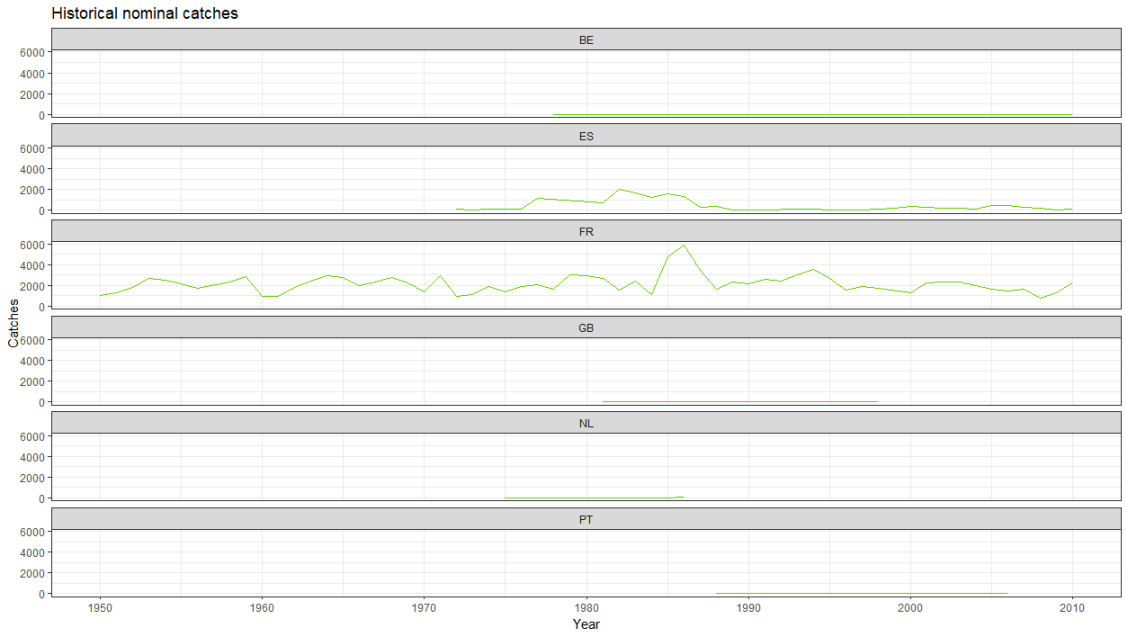


**Figure 9.13. Historical nominal ICES landings.**

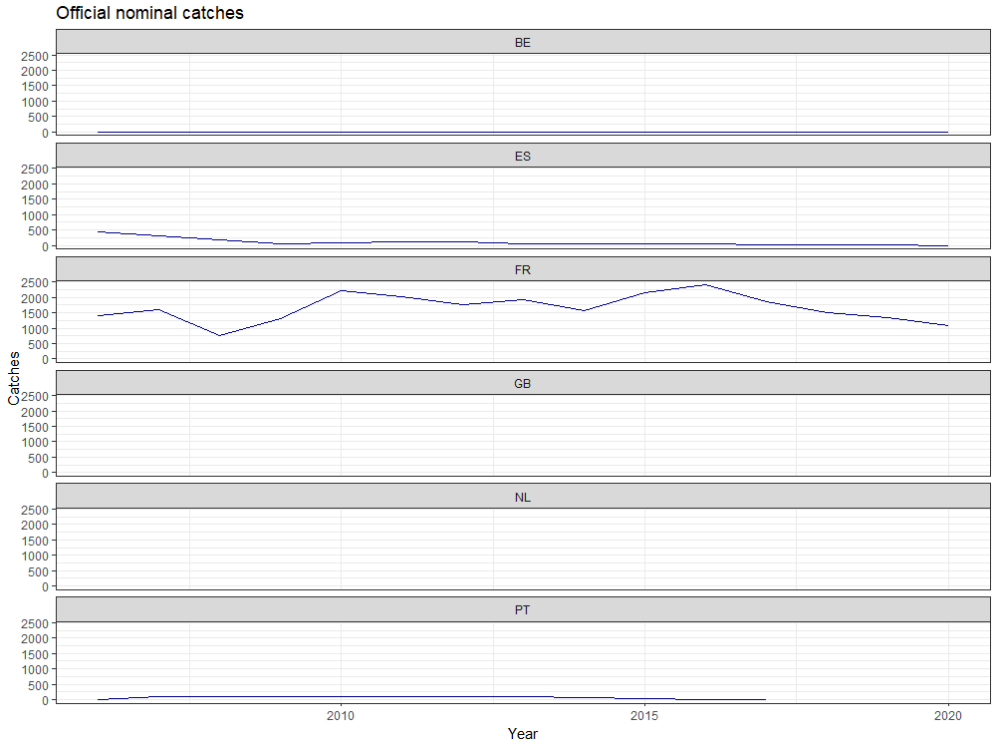


**Figure 9.14. Official nominal ICES landings.**

We started the historical series in 1975. Resulting from a change in the French database, the CPUE derived from commercial catch is uncertain in 2009. Therefore, a missing value was applied at this year. Also, 1999 shows very low catches comparing to the other years: in the last runs, we finally chose to set the value as the mean between 1998 and 2000.

The input data for the model were the time-series of commercial landings for years 1975–2021 and two commercial abundance indices FR-OTB for years 2000–2009 and 2010–2021 (Figure 9.15).

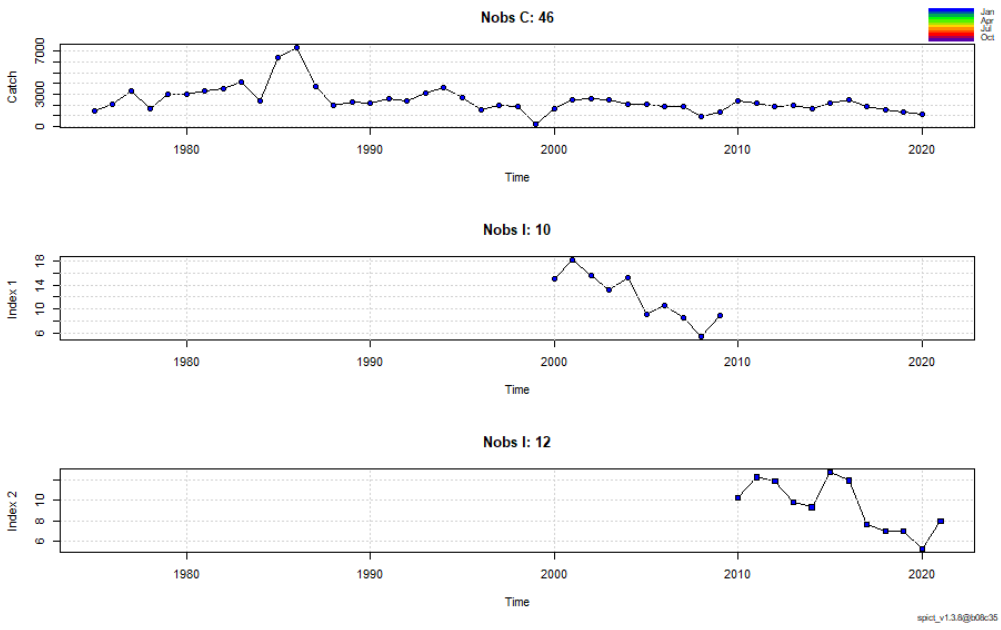


**Figure 9.15. Input data for SPiCT.**

### Prior distributions

Different priors were applied in order to achieve convergence: prior on the intrinsic growth *r*, the initial depletion level *bkfrac* and the parameter of the production curve *n*.

Prior distribution of r was estimated based on knowledge of historical stock exploitation and the species biology. Two approaches were followed to obtained r priors. The first one uses a prior obtained from *FishLife* (Thorson, 2019). This gave a r-prior of mean 0.40 (Figure 9.16 and Table 9.3).

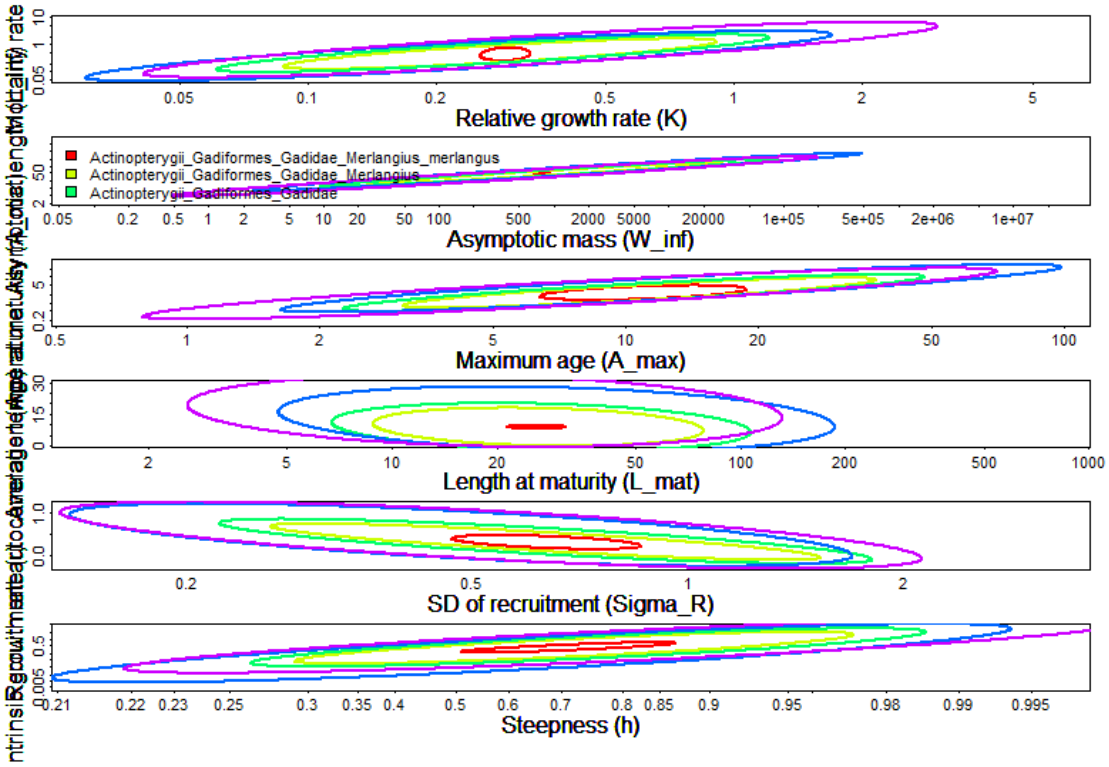


**Figure 9.16. Life-history parameters of whiting using the package *FishLife*.**

**Table 9.3. Estimations of the life-history parameters for whiting from *FishLife*.**

| Parameter | Estimation |
|---|---|
| $L_{inf}$ | 3.80 |
| K | −1.24 |
| $W_{infinity}$ | 6.66 |
| $t_{max}$ | 2.40 |
| $t_m$ | 0.86 |
| M | −0.84 |
| $L_m$ | 3.26 |

In the second approach, the package *SPMpriors* was used (Winker, 2020), in a situation where $n = 1$ (Fox model). Estimations of $L_{inf}$ and $L_m$ were needed and found on *FishBase*. That gave Linf = 41.3 cm and Lm = 28.2. The results of the priors obtained with the package *SPMpriors* are in Table 9.4.

**Table 9.4. Priors obtained with *SPMpriors.***

| Parameter | mu | logsd |
|---|---|---|
| r | 0.30 | 0.2 |
| shape | 0.81 | 0.16 |
| $f_{MSY}$ | 0.36 | 0.29 |
| $b_{msyk}$ | 0.33 | 0.09 |

Many different priors of the initial depletions were tried, and the sensibility of the results to this choice checked. It is likely that whiting was at a high level of exploitation at the beginning of the chronological series, suggesting that *bkfrac* should be high (low *logbkfrac*).

There were two different choices for the shape parameter of the production curve $n$, Fox ($n = 1$) or Schaeffer ($n = 2$), and different standard deviations.

### 9.3.1 Exploratory assessments

Multiple runs were built, with different priors and input data. For each of the runs, convergence, as well as diagnostic figures and retrospective plots were examined (Table 9.5). Model assumptions were checked using the checklist outlined in the SPiCT guidelines.

The main problem that we encountered was the high uncertainty of the fishing mortality and the catch in the results plots. This high uncertainty could not allow estimating correctly the parameters. In the only case where the uncertainty was not too high, retrospective patterns were not accepted. The best runs (n° 7, 11 and 13) showed very high uncertainty on catch or bad retrospective patterns. The results of these runs are presented in Figures 9.17, 9.18, and 9.19.

The results of these exploratory SPiCT assessments suggested that the model does not have enough information to estimate all parameters of the model. This is likely a result of the short time-series of the abundance index (15 years) and the lack of contrast in catch series in the overlapping period catch-CPUE.

| N° | Time series | Uncertainty | Prior logr | Prior logn | Prior logbkfrac | Prior alpha and beta | Convergence | Diagnostics | Retrospective | r estimation | K estimation | n estimation | bkfrac estimation | BMSYs | FMSYs | MSYs | B 2021 | F2021 | B2021/BMSY | F2021/FMSY |
|---|---|---|---|---|---|---|---|---|---|---|---|---|---|---|---|---|---|---|---|---|
| 1 | 1975-2020 | identical | default | default | default | default | yes | OK | only one retro converged | / | / | / | / | / | / | / | / | / | / | / |
| 2 | 1975-2020 | identical | default | log(2), 0,000001 | default | default | yes but very uncertainty on F | problem normality catch and bias 1st index | only two retro converged | / | / | / | / | / | / | / | / | / | / | / |
| 3 | 1975-2020 | identical | log(0,40), 0,2 | log(2), 0,000001 | default | default | yes but very uncertainty on F and C | problem normality catch | Not ok | / | / | / | / | / | / | / | / | / | / | / |
| 4 | 1975-2020 | higher (10x) in 1999 | log(0,40), 0,2 | log(2), 0,000001 | default | default | yes | problem bias 1st index | Not ok | / | / | / | / | / | / | / | / | / | / | / |
| 5 | 1975-2020, 1999 = average 1998-2000 | identical | log(0,40), 0,2 | log(2), 0,000001 | default | default | yes | problem bias 1st index | Not ok | / | / | / | / | / | / | / | / | / | / | / |
| 6 | 1975-2020, 1999 = average 1998-2000 | identical | log(0,40), 0,2 | log(2), 0,000001 | log(0,3), 0,2 | default | yes | problem bias 1st index | Not ok | / | / | / | / | / | / | / | / | / | / | / |
| 7 | 1975-2020, 1999 = average 1998-2000 | identical | log(0,40), 0,2 | log(2), 0,000001 | log(0,7), 0,2 | default | yes | OK | Not ok | / | / | / | / | / | / | / | / | / | / | / |
| 8 | 1975-2020, 1999 = average 1998-2000 | identical | log(0,40), 0,2 | log(2), 0,000001 | log(0,9), 0,2 | default | yes | OK | Not ok | / | / | | / | / | / | / | / | / | / | / |
| 9 | 1975-2020, 1999 = average 1998-2000 | identical | log(0,40), 0,2 | log(2), 0,000001 | log(0,2), 0,5 | default | yes | problem bias 1st index | Not ok | / | / | / | / | / | / | / | / | / | / | / |
| 9.1 | 1975-2020, 1999 = average 1998-2000 | identical | log(0,40), 0,2 | log(2), 0,000001 | log(0,5), 0,5 | default | yes | problem bias 1st index | Not ok | / | / | / | / | / | / | / | / | / | / | / |
| 9.2 | 1975-2020, 1999 = average 1998-2001 | identical | log(0,40), 0,2 | log(2), 0,000001 | log(0,7), 0,5 | default | yes | problem bias 1st index | Not ok | / | / | / | / | / | / | / | / | / | / | / |
| 10 | 1975-2020, 1999 = average 1998-2000 | identical | log(0,40), 0,2 | log(2), 0,5 | default | default | yes but very uncertainty on F and C | OK | OK +/- | / | / | / | / | / | / | / | / | / | / | / |
| 11 | 1975-2020, 1999 = average 1998-2000 | identical | log(0,40), 0,2 | log(2), 0,5 | log(0,2), 0,5 | default | yes but very uncertainty on F and C | OK | OK | 0,43 | 5,23E+04 | 1,44 | 0,24 | 2,11E+04 | 0,29 | 6,04E+03 | 3,08E+04 | 0,05 | 1,45 | 0,17 |
| 12 | 1975-2020, 1999 = average 1998-2000 | identical | log(0,40), 0,2 | log(2), 0,5 | log(0,2), 0,5 | desabled | yes | OK | not OK | / | / | | / | / | / | / | / | / | / | / |
| 13 | 1975-2020, 1999 = average 1998-2001 | identical | log(0,30), 0,2 | log(1.1), 0,000001 | log(0,2), 0,5 | default | yes but very uncertainty on F and C | OK | OK | 0,32 | 4,74E+04 | 1,1 | 0,24 | 1,70E+04 | 0,29 | 4,91E+03 | 2,38E+04 | 0,064 | 1,4 | 0,22 |
| 13.1 | 1975-2020, 1999 = average 1998-2001 | identical | log(0,30), 0,2 | log(1.1), 0,000001 | log(0,5), 0,5 | default | yes but very uncertainty on F and C | OK | not OK | / | / | / | / | / | / | / | / | / | / | / |
| 13.2 | 1975-2020, 1999 = average 1998-2001 | identical | log(0,30), 0,2 | log(1.1), 0,000001 | log(0,7), 0,5 | default | yes but very uncertainty on F and C | OK | not OK | / | / | / | / | / | / | / | / | / | / | / |

Run n°7

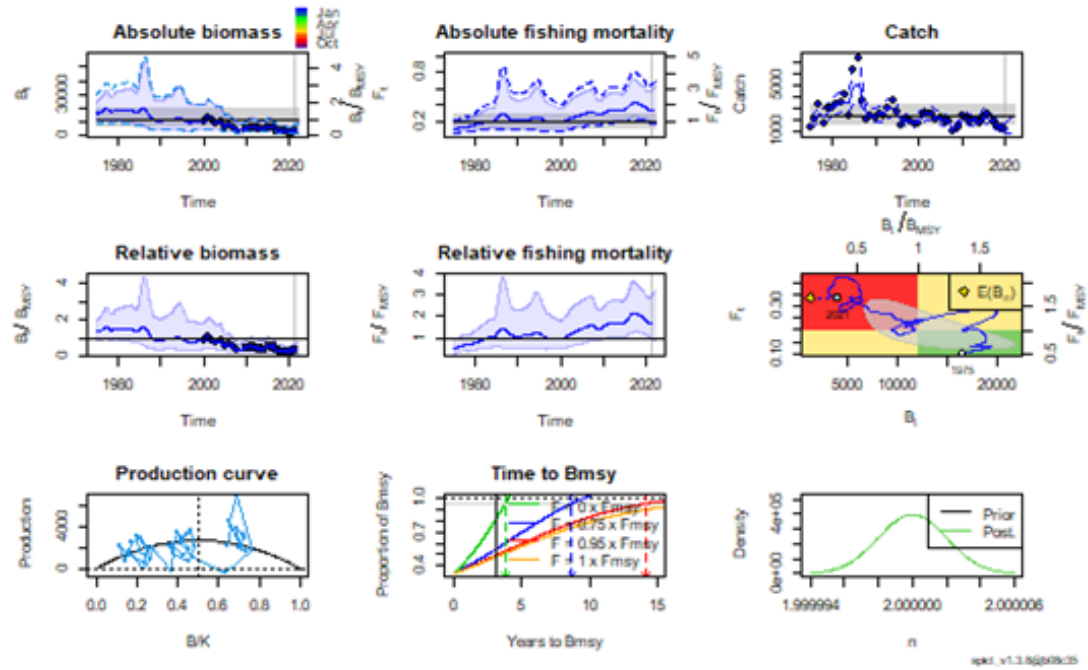
Absolute biomass
Absolute fishing mortality
Catch
Relative biomass
Relative fishing mortality
Production curve
Time to Bmsy
Time
B/K
Years to Bmsy
Prior
Post.

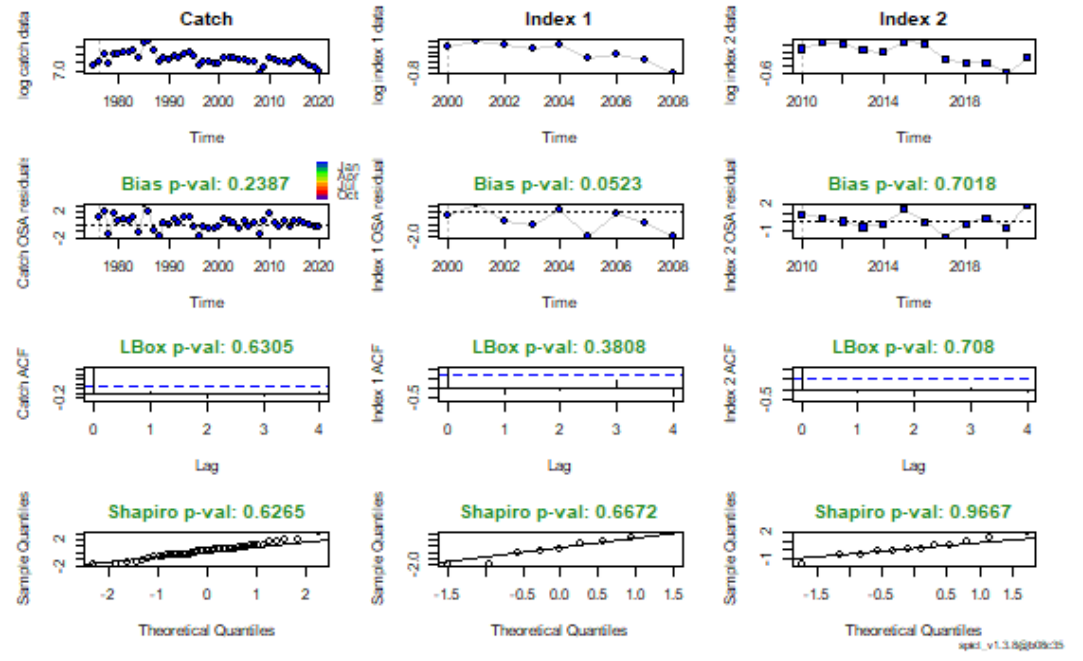
Catch
Index 1
Index 2
Bias p-val: 0.2387
Bias p-val: 0.0523
Bias p-val: 0.7018
LBox p-val: 0.6305
LBox p-val: 0.3808
LBox p-val: 0.708
Shapiro p-val: 0.6265
Shapiro p-val: 0.6672
Shapiro p-val: 0.9667
Time
Lag
Theoretical Quantiles

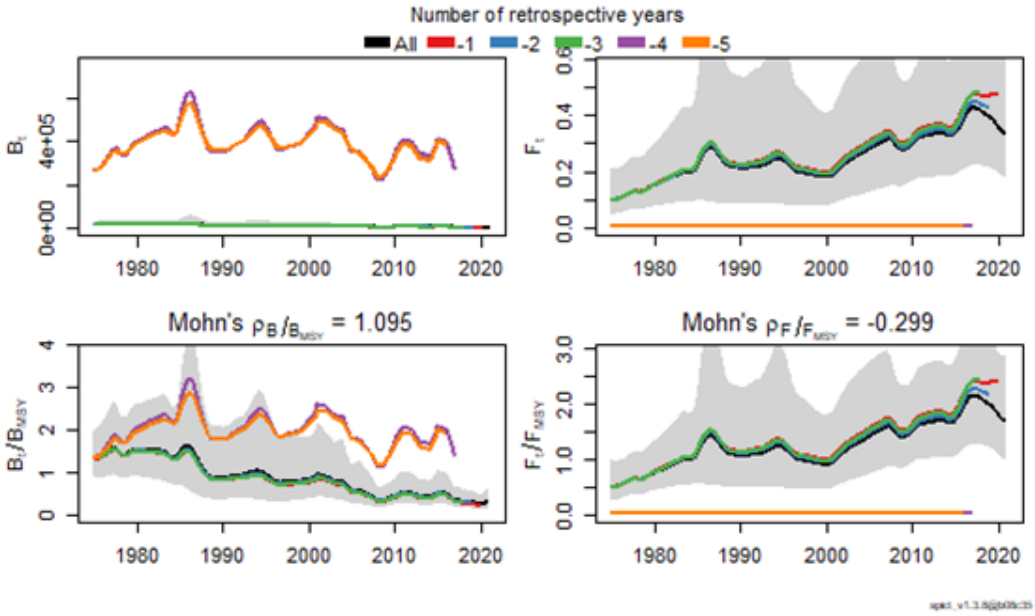


**Figure 17. Main results, diagnostics and retrospective patterns for run n°7.**

Run n°11

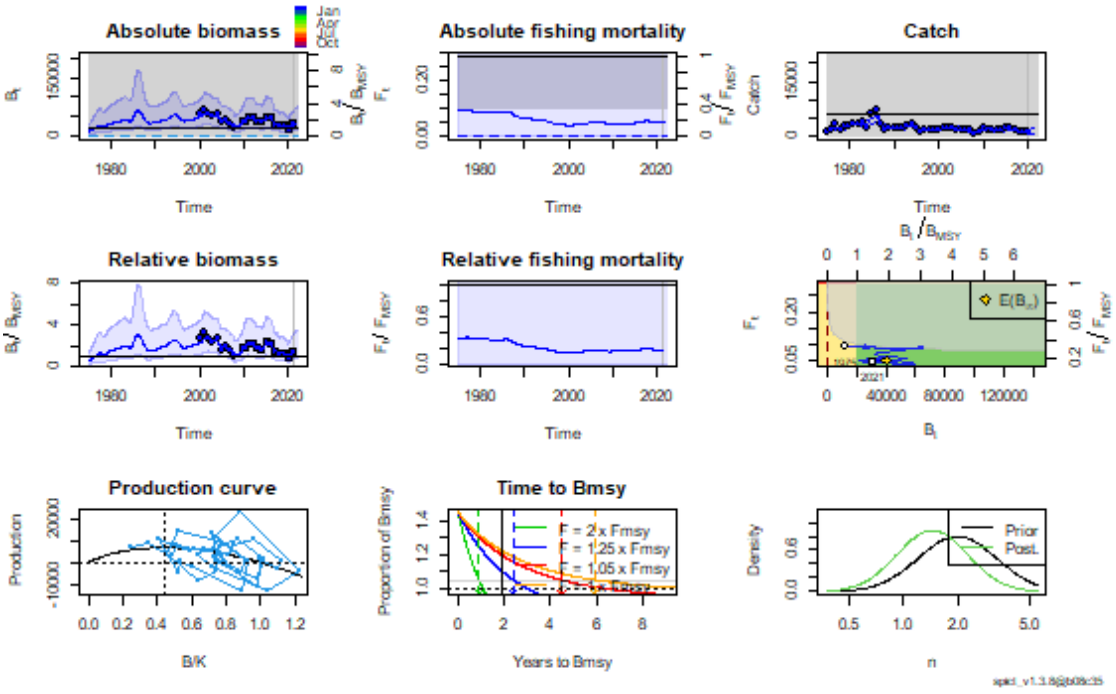

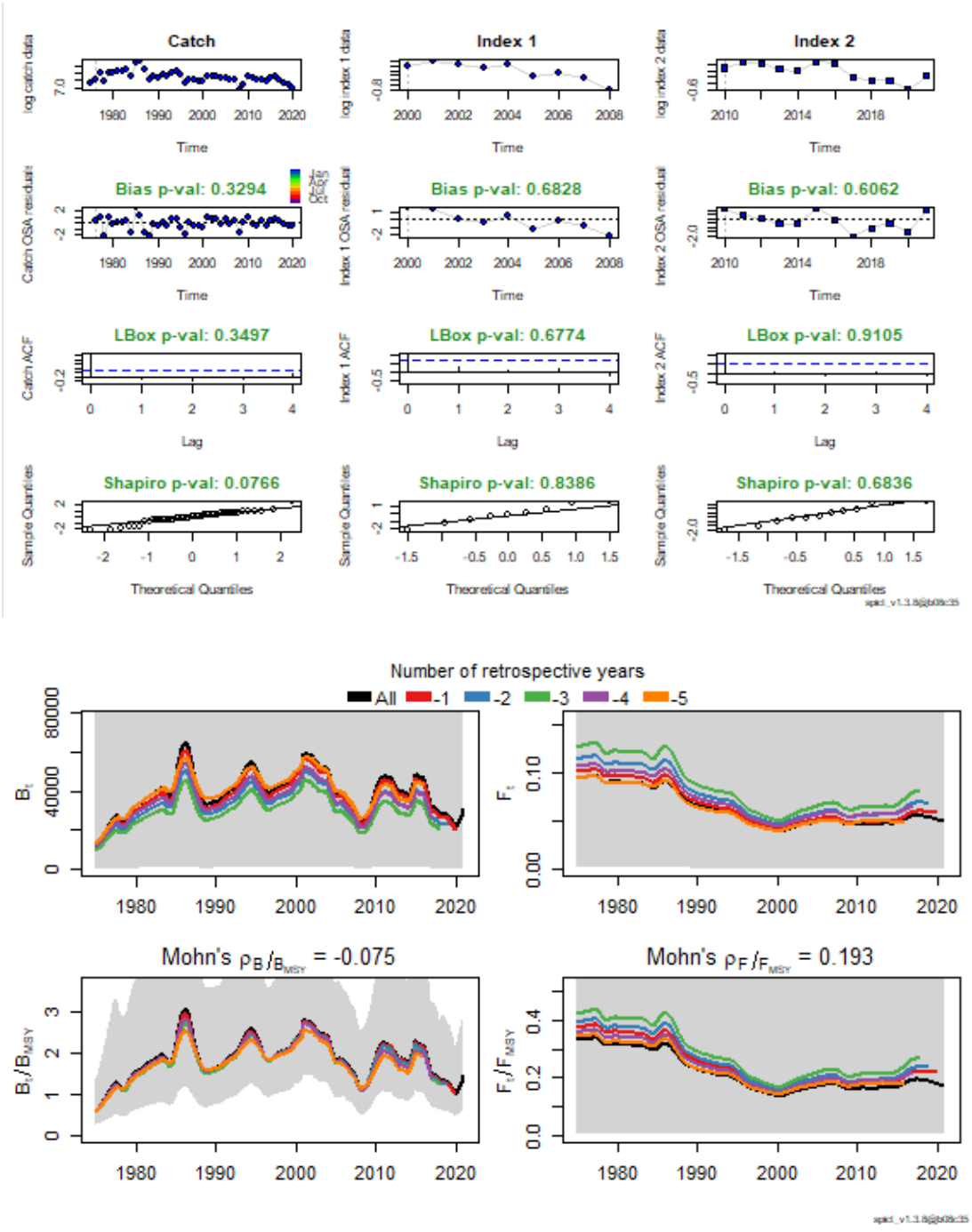


**Figure 9.18. Main results, diagnostics and retrospective patterns for run n°11.**

n°13

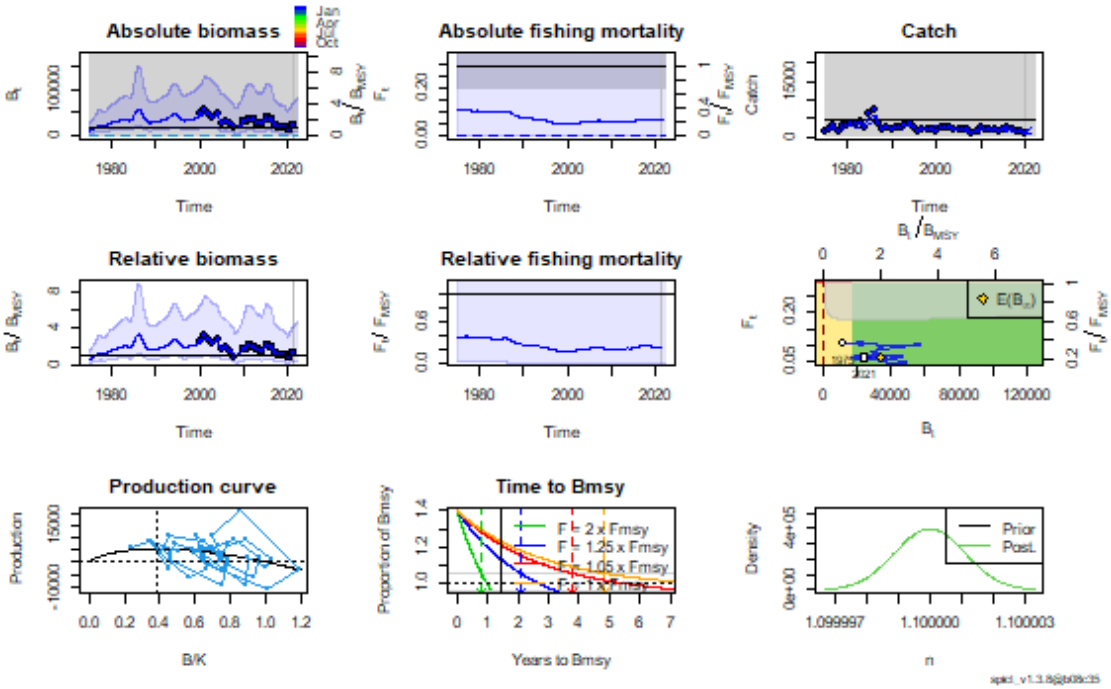
Absolute biomass
Absolute fishing mortality
Catch
Relative biomass
Relative fishing mortality
Production curve
Time to Bmsy
Time
B/K
Years to Bmsy
Prior
Post.
F = 2 x Fmsy
F = 1.25 x Fmsy
F = 1.05 x Fmsy

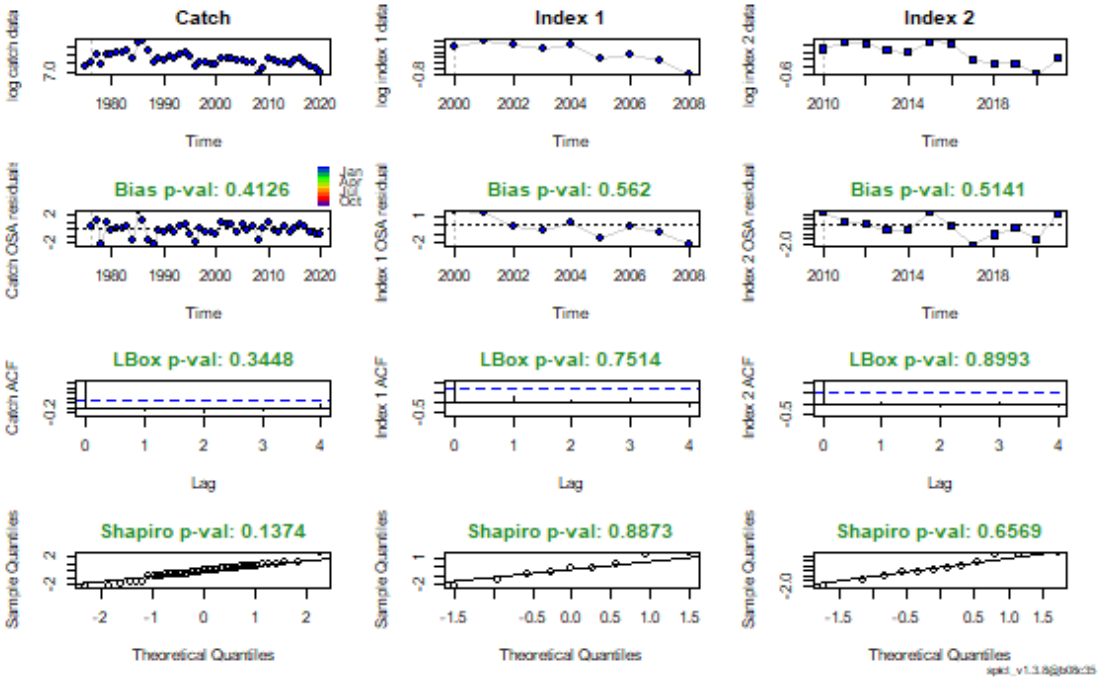
Catch
Index 1
Index 2
Bias p-val: 0.4126
Bias p-val: 0.562
Bias p-val: 0.5141
LBox p-val: 0.3448
LBox p-val: 0.7514
LBox p-val: 0.8993
Shapiro p-val: 0.1374
Shapiro p-val: 0.8873
Shapiro p-val: 0.6569
Time
Lag
Theoretical Quantiles

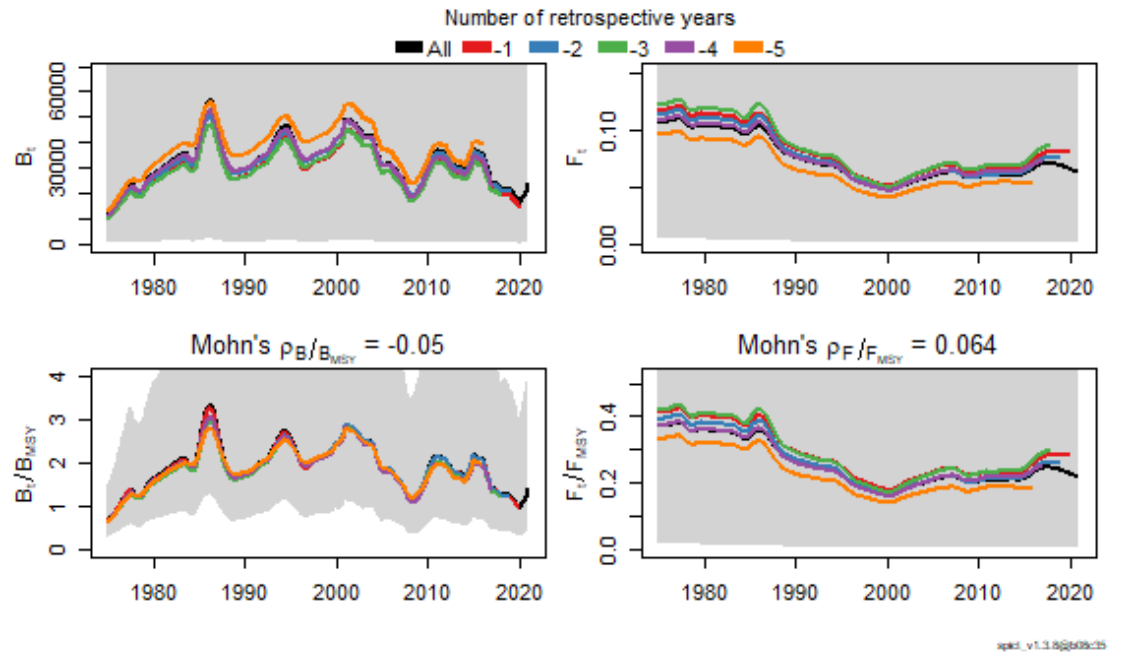


**Figure 9.19. Main results, diagnostics and retrospective patterns for run n°13.**

## 9.4 Final assessment

No model configuration was accepted by the Workshop to use as final model assessment. Indeed, the abundance index time-series is not long, resulting from the cut of the CPUE series in two. Also, the two series of catch and abundance indices do not show contrast. As a result, uncertainty on catch or fishing mortality was too high and did not allow to obtain proper estimations.

## 9.5 Future considerations/recommendations

No model configuration was accepted by the Workshop to use as final model assessment.

Category 3 assessment was proposed for that stock, using the biomass index derived from otter trawlers.

Given that landing length structures are available, length/age structured models could be tested for that stock as well as two stage model using EVOHE as an index of recruitment and the commercial CPUE as a biomass index.

## 9.6 Reviewers report

A new commercial CPUE index is presented in the report but was not discussed during the benchmark meeting. It uses the same methodology as pollack in areas 8 and 9.a with similar decisions made by the stock responsible group, i.e. about filtering the vessels that are included in the calculation of the index, the splitting of time-series into two periods due to changes in French databases and using a PCA to deal with targeting.

The assessment of whiting in areas 8 and 9.a was not presented to the group as the efforts of the stock responsible group were put towards the assessment of pol.27.89. There are some SPiCT

runs presented in the report and it seems that there is insufficient contrast in the data to support a SPiCT assessment at the moment.

The final decision is to use the new commercial CPUE index along with available length distributions as input to ICES category 3 empirical rules. Nevertheless, since the data were not discussed during the benchmark, a further external review is needed that will look at the input data and the implementation of the advice rule.

## 9.7 Conclusions

Any of the SPiCT configuration tested was considered suitable to provide advice for whiting in ICES areas 8 and 9.a.

## 9.8 References

Charrier, G; Coombs, SH; McQuinn, IH; Laroche, J. 2007 Genetic structure of whiting (Merlangius merlangus) in the north east Atlantic and adjacent waters. Marine Ecology Progress Series, 330. 201–211.

ICES. 2021. Benchmark Workshop on the development of MSY advice for category 3 stocks using Sur-plus Production Model in Continuous Time; SPiCT (WKMSYSPiCT). ICES Scientific Reports. 3:20. 317 pp. https://doi.org/10.17895/ices.pub.7919

Thorson, J.T. 2019. FishLife: Predict life history parameters for any fish (https://github.com/James-Thorson-NOAA/FishLife).

# Annex 1: List of participants

| Name | Institute | Country of institute | E-mail |
|---|---|---|---|
| Alexandros Kokkalis (reviewer) | DTU Aqua | Denmark | alko@aqua.dtu.dk |
| Andrew Campbell | Marine Institute | Ireland | andrew.campbell@marine.ie |
| Bart Vanelslander | ILVO | Belgium | bart.vanelslander@ilvo.vlaanderen.be |
| Casper Berg (reviewer) | DTU Aqua | Denmark | cbe@aqua.dtu.dk |
| Cristina Rodríguez-Cabello | IEO | Spain | cristina.cabello@ieo.csic.es |
| Damien Villagra Villanueva | ILVO | Belgium | damian.villagra@ilvo.vlaanderen.be |
| Edward Farrell | KFO | Ireland | edward@kfo.ie |
| Fanny Ouzoulias | Ifremer | France | fanny.ouzoulias@agrocampus-ouest.fr |
| Henning Winker (chair) | GFCM | Italy | henning.winker@gmail.com |
| Klaas Sys | ILVO | Belgium | klaas.sys@ilvo.vlaanderen.be |
| Loïc Baulier | Ifremer | France | loic.baulier@ifremer.fr |
| Massimiliano Cardinale (chair) | SLU Aqua | Sweden | massimiliano.cardinale@slu.se |
| Mickael Drogou | Ifremer | France | mickael.drogou@ifremer.fr |
| Paul Bouch | Marine Institute | Ireland | paul.bouch@marine.ie |
| Paz Sampedro | IEO | Spain | paz.sampedro@ieo.csic.es |
| Raphael Girardin | Ifremer | France | raphael.girardin@ifremer.fr |
| Roxanne Duncan | Marine Institute | Ireland | roxanne.duncan@Marine.ie |
| Tobias Mildenberger (reviewer) | DTU Aqua | Denmark | tobm@aqua.dtu.dk |
| Lies Vansteenbrugge | ILVO | Belgium | lies.vansteenbrugge@ilvo.vlaanderen.be |
| Wendell Medeiros-Leal | University of the Azores | Spain | wendellmedeirosleal@gmail.com |
| Youen Vermard | Ifremer | France | youen.vermard@ifremer.fr |

# Annex 2: Resolutions

**Approved August 2022**

**WKBMSYSPICT2 – Benchmark workshop 2 on development of MSY advice using SPiCT**

2022/WK/FRSG52 The **Benchmark workshop 2 on development of MSY advice using SPiCT** (WKBMSYSPiCT3), chaired by Massimiliano Cardinale, Sweden, and Henning Winker, FAO-GFCM, and attended by invited external experts Casper Berg, Denmark, Alexandros Kokkalis, Denmark, and Tobias Mildenberger, Denmark, will be established and meet online for two days in September 2022 (7–8 September) for model learning sessions with SPiCT developers; 11–13 October 2022 for a data workshop; and 9–13 January 2023 for the final assessment workshop. WKMSYSPiCT2 will evaluate the appropriateness of data and the use of the Surplus Production in Continuous Time (SPiCT) to provide MSY advice for selected stocks. The specific ToRs for this benchmark workshop are:

a) Collate necessary data and information for the application of SPiCT for the stocks listed in Annex 1 before the data workshop;

b) Review the available data and make recommendations on the most appropriate series to be used for SPiCT and potential improvements to eliminate biases;

c) Apply the SPiCT methodology and determine the appropriateness of the data and the methodology to determine stock status for each of the stocks listed using the guidance developed following WKLIFEVII, WKLIFEVIII, WKLIFEIX, and ICES 2022[1];

d) For stocks where the methodology is appropriate, determine the methods to derive the parameters for the catch forecast using the harvest control rule for providing MSY advice using SPiCT;

e) Prepare the Stock Annex for those stocks where SPiCT is considered appropriate for providing MSY advice;

f) Provide recommendations for improving the guidance and training for the application of SPiCT and for deriving MSY advice.

WKBMSYSPiCT2 will report by 20 January 2023 for the attention of ACOM.

**Supporting information**

| | |
|---|---|
| Priority | Very high. ICES provides advice on more than 260 stocks and more than 60% of these stocks are in categories 3–6 where currently MSY advice is not provided. With the development of approaches to provide MSY advice for category 3–4, these approaches must be implemented as soon as possible. |
| Scientific justification and relation to action plan | Following on a request from the European Commission through DG MARE, to improve the scientific assessment of some category 3–6 stocks, ICES has held a series of workshops (WKLIFE) to develop methodologies that would allow to provide MSY advice (see WKLIFEIX).<br>Currently, ICES provides advice for category 3–6 stocks with the precautionary approach. To provide MSY advice for many of these stocks, ICES through WKLIFEVII, WKLIFEVIII and WKLIFEIX has developed a coherent framework for category 3-4 stocks where available data would permit the use of SPiCT . |

[1] ICES. 2022. ICES technical guidance for harvest control rules and stock assessments for stocks in categories 2 and 3. In Report of ICES Advisory Committee, 2022. ICES Advice 2022, Section 16.4.11. https://doi.org/10.17895/ices.advice.19801564

| | |
|---|---|
| | The purpose of the workshop is to conduct a benchmark peer review of the application of the SPiCT approach to provide MSY advice for selected stocks. The selected stocks to be considered in this benchmark was determined based on the availability of appropriate data and capacity.<br>In addition to producing the Stock Annex for stocks where the method is appropriate, the workshop will serve to provide recommendations to improve the guidance for the method as well as potential training. |

**Annex 1: List of ICES stocks to be examined during WKBMSYSPICT2[2].**

| | |
|---|---|
| bll.27.3a47de | Brill (*Scophthalmus rhombus*) in Subarea 4 and divisions 3.a and 7.d-e (North Sea, Skagerrak and Kattegat, English Channel) |
| boc.27.6-8 | Boarfish *(Capros aper)* in subareas 6-8 (Celtic Seas, English Channel, and Bay of Biscay) |
| bll.27.3a47de | Striped red mullet (*Mullus surmuletus*) in Subarea 4 and divisions 7.d and 3.a (North Sea, eastern English Channel, Skagerrak and Kattegat) |
| ple.27.89a | Plaice (*Pleuronectes platessa*) in Subarea 8 and Division 9.a (Bay of Biscay and Atlantic Iberian waters) |
| pol.27.67 | Pollack (*Pollachius pollachius*) in subareas 6-7 (Celtic Seas and the English Channel) |
| pol.27.89a | Pollack (*Pollachius pollachius*) in Subarea 8 and Division 9.a (Bay of Biscay and Atlantic Iberian waters) |
| rjc.27.8c | Thornback ray (*Raja clavata*) in Division 8.c (Cantabrian Sea) |
| whg.27.3a | Whiting (*Merlangius merlangus*) in Division 3.a (Skagerrak and Kattegat) |
| whg.27.89 | Whiting (*Merlangius merlangus*) in Subarea 8 and Division 9.a (Bay of Biscay and Atlantic Iberian waters) |

[2] Note: final stock list for WKBMSYSPICT2 is subject to change depending on progress with SPiCT.

# Annex 3: Other working documents

| WD # | WD Title | Authors |
|---|---|---|
| 01 | SPiCT FLR toolbox for simulation testing and tuning | Henning Winker (GFCM) |
| 02 | Data preparation guidelines for WKBMSYSPICT benchmarks 2023 | Henning Winker (GFCM) and Massimiliano Cardinale (SLU) |

# Spict FLR toolbox for simulation testing and tuning

Henning Winker (GFCM)

09 January, 2023

## Contents

**1 Background** 1

**2 Population parameters** 2

**3 Packages and installations** 2

3.1 Installations . . . 3

**4 Setting up a generic OM for Pollock** 3

4.1 Life history paramters . . . 3

4.2 Estimating priors from FLStock and SRR . . . 6

4.3 Simulating stock dynamics with evolutionary F-trajectories . . . 7

**5 Simulation testing with Spict** 11

**6 Spict estimation scenarios** 11

6.1 Quick performance comparison . . . 13

**7 Supplement I: spict.simplify** 15

```
## Warning: package 'knitr' was built under R version 4.2.2
```

## 1 Background

This document provides a first overview of the FLR toolbox that currently underdevelopment to facilitate the analysis of stock productivity, reference point estimation and simulation testing of biomass dynamics models, such as Spict. The idea is to provide the tools to rapidly create minimal realistic "off the shelf" Operating Model that parameterized with the best available information about the biology and fishing and survey selectivity. These OM can then employed to emulate the data structure and characteristics (e.g. observation errors) that is available for the assessment. This enables, for example, to: (1) explore and optimise the Spict settings given the emergent data and biological properties for given stock, (2) to evaluate if the value in information of the available is sufficient for reliable stock estimation or (3) to explore potential directional bias.

## 2 Population parameters

Life history information is important for evaluating the plausible of the estimated production function by SPICT. Further, if there is a lack of contrast of contrast in the available time-series of catch and relative abundance, formulating informative priors for r using, e.g. `FishLife` (Thorson, 2020) may be warranted. Additional tools to update the initial $r$ priors from `FishLife` with stock specific biological and selectivity information are provided in the R package `SPMprior` available on github.com/henning-winker/SPMpriors.

Surplus production models, such as SPICT, are age- and size aggregated models that approximate changes in biomass as a function of the biomass of the preceding year, the surplus production in biomass and the removal by the fishery in the form of catch. Somatic growth, reproduction, natural mortality and associated density-dependent processes are inseparably captured in the estimated surplus production function that is governed by three parameters: (1) the intrinsic rate of population increase $r$ (2) the shape parameter $m$ and (3) the unfished equilibrium biomass $k$. However, there is a direct link between age-structured stock parameters and the expected surplus production function, so that stock parameters describing length-at-age ($L_a$), weight-at-age ($w_a$), maturity-at-age ($mat_a$) and selectivity-at-age ($s_a$), natural mortality $M$ and the steepness parameter $h$ of the of the assumed Beverton and Holt SSR can be used to approximate the surplus production (Winker et al., 2021).

In addition, distortions between the survey or CPUE index and the spawning stock biomass can lead to systematic bias in the productivity estimates, which may be partially corrected for by using more informative priors on $r$. For example, if length at first capture $L_c$ is smaller than length-at-maturity ($L_m$), the exploitable biomass $EB$ can be behave hyperstable relative to $SSB$, and thus disguise true magnitude of reduction of the stock's productivity as a function of $SSB$ (Winker et al., 2019, 2021).

Where possible, it is therefore recommended to compile available life history information and initial selectivity estimates (e.g. $L_c$) for both the fishery and survey to parameterize the OMs with the best available information. These may include the following parameters.

- $L_{max}$ maximum observed length in the stock
- $L_{oo}$ Asymptotic length
- $K$ Brody coefficient
- $t_0$ theoretical age at zero length
- $L_m$ length-at-maturity
- $t_m$ age-at-maturity
- $t_{max}$ maximum age
- $M$ natural mortality
- $a$, $b$ parameter of the length-weight relationship
- $L_c$ length-at-50%-capture

## 3 Packages and installations

The following R packages are used

For generic life history parameters

- FishLife
- SPMpriors

As generic FLStock stock constructors

- FLCore
- FLife

- FLBRP
- FLRef

Surplus production model fitting

- spict

### 3.1 Installations

```
install.packages("ggplot2")
install.packages("devtools")
install.packages("TMB", type = "source")
devtools::install_github("DTUAqua/spict/spict")
devtools::install_github("james-thorson/FishLife")
devtools::install_github("henning-winker/SPMpriors")
# FLR
devtools::install_github("flr/FLCore")
devtools::install_github("flr/ggplotFL")
devtools::install_github("flr/FLBRP")
devtools::install_github("flr/FLasher")
devtools::install_github("flr/mse")
devtools::install_github("flr/FLSRTMB")
devtools::install_github("flr/FLife")
devtools::install_github("henning-winker/FLRef")
```

Load packages

```
# Load
library(ggplot2)
library(spict)
library(FishLife)
library(SPMpriors)
library(FLCore)
library(ggplotFL)
library(FLRef)
library(FLife)
```

## 4 Setting up a generic OM for Pollock

### 4.1 Life history paramters

First, extract life history parameters from `FishLife` with '`SPMpriors`.

Here, Pollack (*Pollachius pollachius*) is chosen as first example

```
lh = SPMpriors::flmvn_traits(
  Genus="Pollachius",Species="pollachius",
  h=c(0.6,0.9),Plot=FALSE)$traits
   Closest match: Actinopterygii_Gadiformes_Gadidae_Pollachius_pollachius
```

```
lh
      trait   mu.sp  cv.sp  mu.stk cv.stk  lc.stk   uc.stk upper.quant
   1    Loo 79.6805 0.2094 79.7985 0.2078 61.2119 104.0287         0.9
   2      K  0.2068 0.2599  0.2074 0.2556  0.1496   0.2874         0.9
   3     Lm 42.1560 0.2320 42.3263 0.2183 31.5641  56.7581         0.9
   4     tm  3.1603 0.3843  3.1631 0.3827  1.9676   5.0850         0.9
   5   tmax 12.8543 0.3299 12.9014 0.3219  8.5413  19.4873         0.9
   6      M  0.4105 0.2804  0.4100 0.2797  0.2881   0.5834         0.9
   7      h  0.7879 0.2018  0.7820 0.1234  0.6400   0.8829         0.9
   8   sigR  0.4854 0.2820  0.4875 0.2708  0.3421   0.6948         0.9
   9    rho  1.6177 0.2955  1.6119 0.2559  1.3440   1.9333         0.9
   10     r  0.3842 0.5399  0.3781 0.3281  0.1975   0.7237         0.9
   11     G  7.0384 0.2476  7.0408 0.2474  5.1519   9.6223         0.9
```

The next the **FLife** function **lhPar()** is populated with some of basic life history estimates for growth,length-weight, maturity based on regional information and steepness from FishLife/SPMpriors.

```
s = lh[7,"mu.stk"]
tmax = 15
M = 4.899*tmax^-.916 # (Then)
par=lhPar(FLPar(linf=98.3,k=0.182,t0=-0.935,
            a=0.001*1.13e-2,b=2.8,a50=3.5,
            s=s,m1=M))
```

The **FLife** function **lhEql** is then used as a constructer for a basic **FLBRP()** object.

```
eql=lhEql(par,range = c(min = 1, max = tmax, minfbar = 1, maxfbar = tmax, plusgroup=tmax))

class(eql)
   [1] "FLBRP"
   attr(,"package")
   [1] "FLBRP"
```

Now further manipulations can be made, such as adjusting the inbuilt Gislason $M$ to a scaled Lorenzen $M$ and adjusting time horizon with the desired **fbar** range

```
# M
m(eql)[] = Mlorenzen(stock.wt(eql),Mref=M)

# change time horizon with a fixed intial f0
f0 = 0.01
fbar(eql) = FLQuant(rep(f0,70),dimnames=list(year=1951:2020))
```

Now **FLBRP** can can be readily converted into an **FLStock** and the stock recruitment relationship can be extracted.

```
stk = as(eql,"FLStock")
units(stk) = standardUnits(stk) # assign units
sr = as(as(eql,"predictModel"),"FLSR")
```

Once the stock is contructed further manipulations are straight forward. For example, **FLRef** provides the 5-parameter selectivity function **newselex** as a flexible option to specify alternatively shaped maturity ogives and selectivity functions, comprising the following components:

1. A *logistic* describing the ascending limb of the selectivity curve

$$S_a = \frac{1}{1 + exp(-log(19)\frac{a - S_{50}}{S_{95} - S_{50}})}$$

where $S_{50}$ and $S_{95}$ are the ages where $S_a$ corresponds to 0.5 and 0.95.

2. An adjustable *halfnormal* decribing the descending

$$S_a = -(D_{min} - 1)\frac{dnorm(age, S_{max}, S_{max}D_{cv})}{max(dnorm(S_{max}, S_{max}D_{cv}))} + 1$$

where *dnorm* denotes a normal probability density distribution, S_{max} corresponds to the mean of the normal distribution where $S_a$ peaks, $D_{cv}$ determines the slope of the descending limb with the standardeviation of the normal give by the product $S_{max}D_{cv}$, and $D_{min}$ determines the mimimum the descending slope (height).

The expected $S_a$ is then defined as a peace-wise function of the form:

$$S_a = \begin{cases} g(logistic) & \text{if } age < S_a \\ g(halfnormal) & \text{if } age \geq S_a \end{cases}$$

For example, a maturity ogive can be specified by setting $S50$ to the age at 50% maturity and $S95$ to the age at 95% maturity, while the other 3 parameters have no influence as long as $Smax$ is larger than the plus group.

```
mat50 = 3.5
mat95 = mat50*1.5
mat(stk) = newselex(mat(stk),FLPar(S50=mat50,mat95=mat95,Smax=1000,Dcv=0.5,Dmin=0.1))
```

A new selectivity can be set by adjusting the **harvest** slot. If some dome-shaping is desired, $Smax$ has to be smaller then the plus group, $Dcv$ governs the slope of the half-normal and $Dmin$ governs the hight at the right end tail.

```
# catch before maturity
S50 = 0.5*mat50 # selectivity < age-2
S95 = mat50*0.9
# Some Doming
Smax = S50*4
Dcv = 0.5
Dmin = 0.2

harvest(stk) =  f0*newselex(harvest(stk),FLPar(S50=S50,S95=S95,
                Smax=Smax,Dcv=Dcv,Dmin=Dmin))
```

The so generated age-structured relationships for weight-at-age, maturity-at-age, natural mortality and selective are shown in Fig. 1.

```
ggplot(FLQuants(stk,"m","catch.sel","mat","catch.wt"))+
  geom_line(aes(age,data))+
  facet_wrap(~qname,scale="free")+theme_bw()
```

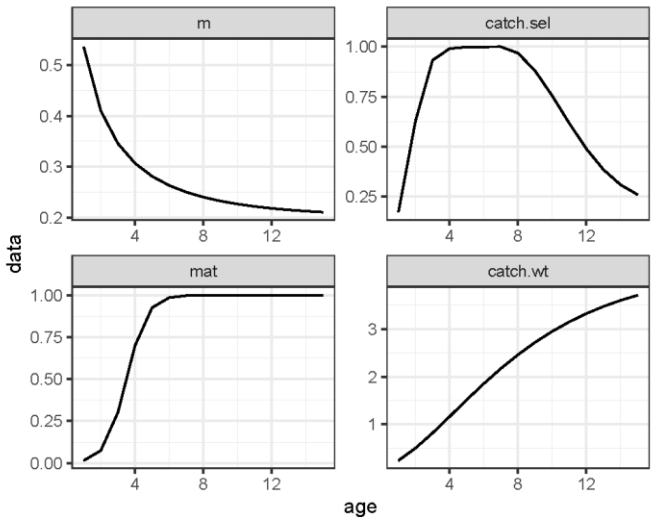


Figure 1: Specified biological and selectivtiy function for natural mortality, selectivity, maturity and somatic growth in weight-at-age

### 4.2 Estimating priors from FLStock and SRR

First, it is straight forward to compute the intrinsic rate of population increase from a Leslie for a specified steepness value. However, this $r$ estimate ignores selectivity and should only be used in the context of a Schaefer model with $F_{MSY} = r/2$.

```
r.leslie = mean(productivity(stk,s=s)$r)
r.leslie
   [1] 0.4415887
# Fmsy
r.leslie/2
   [1] 0.2207944
```

An alternative is to estimate $r$ and the shape parameter $n$ as function $MSY$, $EB_{MSY}$ and $EB_0$ from an age-structured equilibrium model (ASEM), where $EB$ denotes that the exploitable biomass as function of selectivity. The basic relationships for $r$ and $n$ can then be approximated as follows:

$$F_{MSY} = \frac{MSY}{EB_{MSY}}$$

$$\frac{EB_{MSY}}{EB_0} = n^{(-\frac{1}{n-1})}$$

$$r = F_{MSY}\frac{n-1}{1-n^{-1}}$$

To compute the expected values for $r$ and $n$ (here denoted as $m$), requires the stock biology and selectivity together with the SRR as input.

```
r.pella = asem2spm(stk,sr)

r.pella
   An object of class "FLPar"
   params
       r     m BmsyK  Fmsy
   0.217 0.923 0.353 0.235
   units:  NA
```

In this case the shape of the production more closely approximates a Fox model ($n = 0.37$)m, but the $F_{MSY}$ is broadly comparible the Leslie matrix estimate for a Schaefer model.

### 4.3 Simulating stock dynamics with evolutionary F-trajectories

The operating model is assumed to represent the "true" age-structured stock dynamics for evaluating the estimation accuracy of Spict. The "true" MSY based reference points can be easily added to the `FLStock` by extending it to `FLStockR`.

```
# Estimate refpts
brp = computeFbrp(stk,sr,proxy="msy",blim=0.1,type="b0")
   Computing Fmsy with Btgt = Bmsy

     Blim = 0.1B0
stk = FLStockR(stk)
stk@refpts = Fbrp(brp)
# check
stk@refpts
   An object of class "FLPar"
   params
       Fmsy     Btgt     Blim     Flim      Yeq       B0       R0
      0.177  261.793  112.931    0.295   87.208 1129.310  471.943
   units:  NA
```

```
ploteq(brp)
```

`FLRef` provides `rffwd` as an extension of the `FLCore` F-projection function`ffwd`, which enables to setup a control object for generating randomized evolutionary F-trajectories (Thorson et al. 2016). The parameters required are: (1) $Feq$ which sets the terminal depletion level baseline relative to $SB_0$, `Frate` which is determines the turn-over time of the `F-evalution`, `Fsigma` determines the annual variation in F and `SB0` is reference biomass level that is typically specified as $SSB_0$.

```
its = 100 # iterations
b0 = an(refpts(eql)["virgin","ssb"]) # SSB0 for brp

control = FLPar(Feq=0.15,Frate=0.08,Fsigma=0.15,SB0=b0,
                minyear=dims(stk)$minyear+1,
                maxyear=dims(stk)$maxyear,its=its)
```

The stock dynamics are forecasted with random recruitment under and evolving F-trajectory.

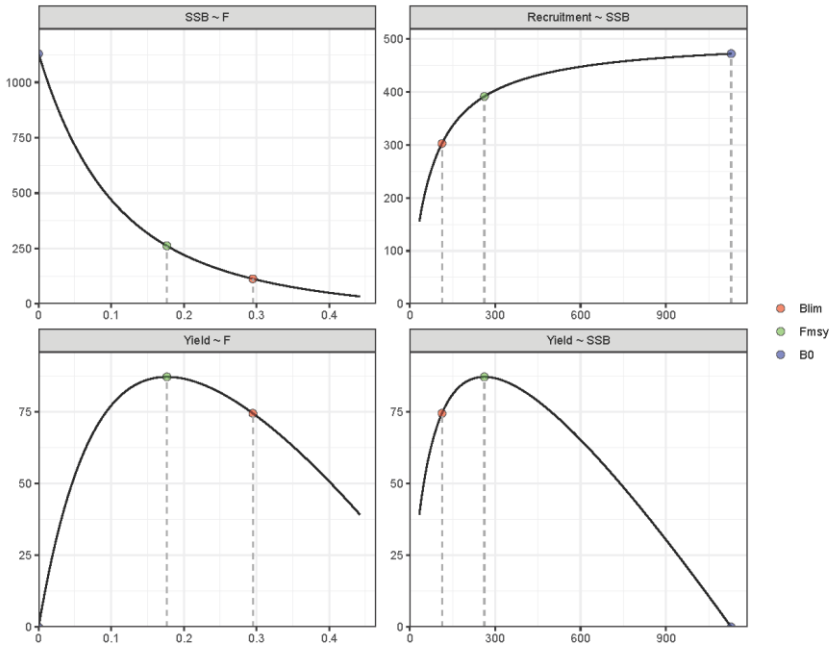


Figure 2: Equilibrium curves Recruitment, SSB, F and Landings and estimated MSY-based reference points for the pollock OM

```
set.seed(123)
# Random recruitment deviations with sigR = 0.5 and AR1 rho = 0.3
rec_devs = ar1rlnorm(0.3, 1951:2020, its, 0, 0.5)
# propagate desired iterations
stki <- propagate(stk, its)
# create OM
om <- rffwd(stki,sr,
            control=control,
            deviances=rec_devs)
om@refpts = stk@refpts
```

```
plotAdvice(om)
```

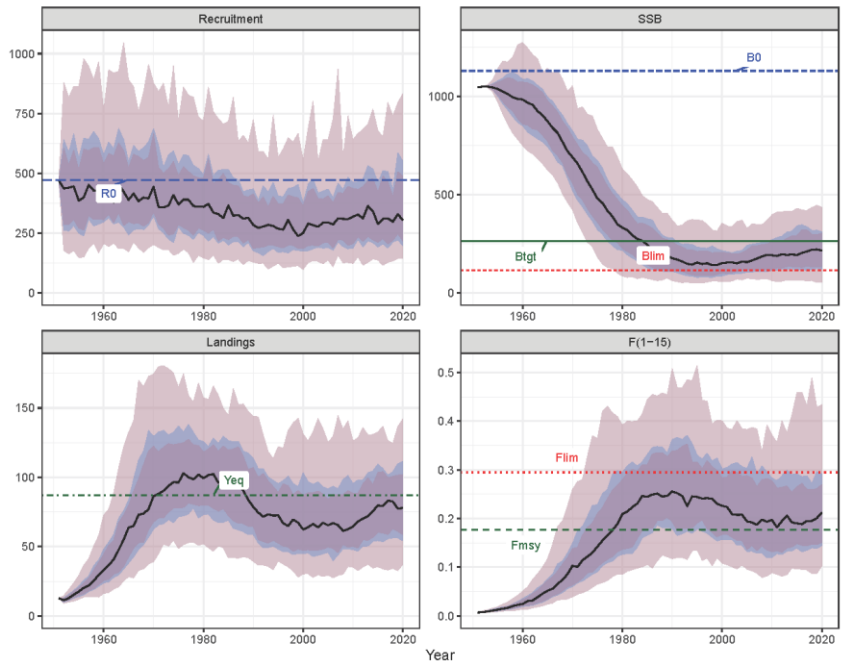


Figure 3: Simulated population dynamics compared to reference points from the off-the-shelf OM for pollock based on 100 iterations

The last step is to generate the observed CPUE index using the `FLRef` function `bioidx.sim()`. By default, the index assumes the same fishing selectivity in the stock object. In this case, a moderate observation error of `sigma=0.25` is assumed and the catchability coefficient $q$ that scales the exploitable biomass to the index is set as `q = 0.001`. The CPUE index is assumed to start in 1985.

```
idx = window(bioidx.sim(om,sigma=0.25,q=0.001),start=1985)
```

```
flqs= FLQuants("B/Bmsy"=ssb(om)/om@refpts["Btgt"],
               "F/Fmsy"=fbar(om)/om@refpts["Fmsy"],
               "Catch/MSY"=catch(om)/om@refpts["Yeq"]
               ,Index=idx@index%/%yearMeans(idx@index))

ggplot(iter(flqs,1:20))+
  geom_line(aes(year,data,col=ac(iter)),alpha=0.5)+
  theme_bw()+facet_wrap(~qname)+
  theme(legend.position = "none")+geom_hline(yintercept = 1,linetype=2)+
  scale_color_manual(values=c(rainbow(20)))+
  ggtitle("Pollack")
```

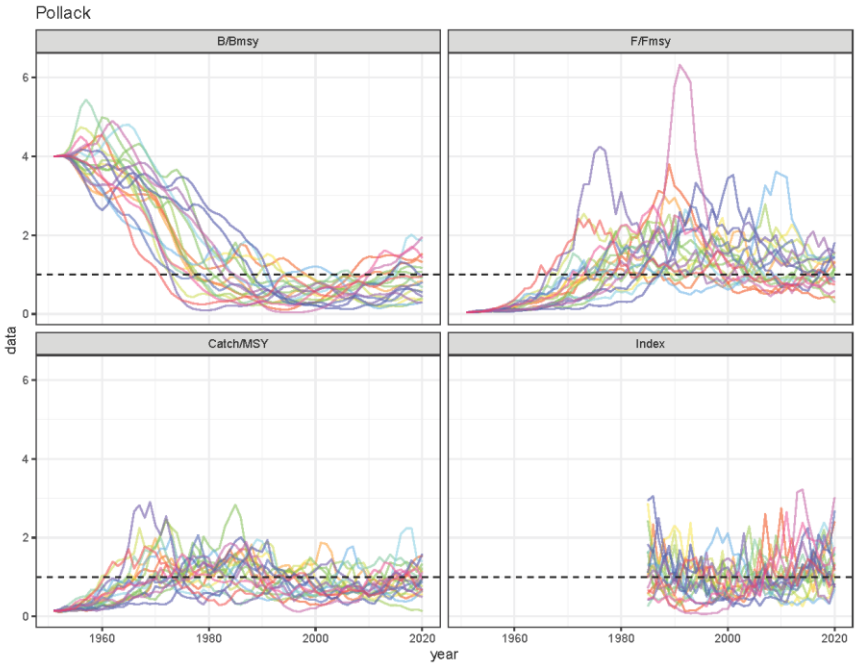


Figure 4: Individual iterations of simulated trajectories of $B/B_{MSY}$, $F/F_{MSY}$, $Catch/MSY$ and the normalized CPUE indices from the off-the-shelf OM for pollock shown for the first 20 iterations

## 5 Simulation testing with Spict

## 6 Spict estimation scenarios

Initial trials indicated that the default settings are not suitable to fit Spict with historical catch data that are longer than the index. Therefore, the catch time series input also started 1985. The scenarios explored for illustration are:

(1) Default Spict setting
(2) Schaefer model with Leslie matrix $r$ prior
(3) Pella-Tomlinson model with ASEM priors for $r$ and shape $m$

Below a simple wrapper function is presented that:

- Fits the 3 Spict scenarios
- Applies `spict2FLStockR` to convert Spict fits into simplified `FLStock` objects
- Apply `stock2ratios` to convert OM into a simplified `FLStock` object
- Combines all into a `FLStocks` object output

```
runi <- function(om,idx,it,dteuler=1/4){
# index
dfi =as.data.frame(iter(window(idx@index,start=1985),it))
# catch
dfc = as.data.frame(iter(window(om@catch,start=1985),it))
# Create Spict Default input
inp = list(obsC=dfc$data,timeC=dfc$year,
            obsI=dfi$data,timeI=dfi$year)
inp$dteuler = dteuler
# input with Schaefer prior
inps= inp
inps$priors$logn= c(log(2),0.01,1)
inps$priors$logr= c(log(r.leslie[[1]])-0.5*0.5^2,0.5,1)
# input pella-tomlinson asem priors
inpp= inp
inpp$priors$logn= c(an(r.pella["m"])-0.5*0.3^2,0.3,1)
inps$priors$logr= c(an(r.pella["r"])-0.5*0.3^2,0.3,1)

# make list of spict fits
fits = list(
  Default=fit.spict(inp),
  Schaefer=fit.spict(inps),
  Pella=fit.spict(inpp)
)
# convert spict in FLStockR
res = FLStocks(lapply(fits,function(x){
 spict2FLStockR(x,rel=T)
}))
# cut forecast
res = window(res,end=2020)
# Add om for comparison
flom = stock2ratios(iter(om,it))
```

```
res = FLStocks(c(om=flom,res))
return(res)
}
```

```
res = runi(om,idx,it=1,dteuler=1/4)

plot(res,metrics=list("B/Bmsy"=ssb,"F/Fmsy"=fbar))+
  geom_hline(yintercept = 1,linetype=2)+theme_bw()
```

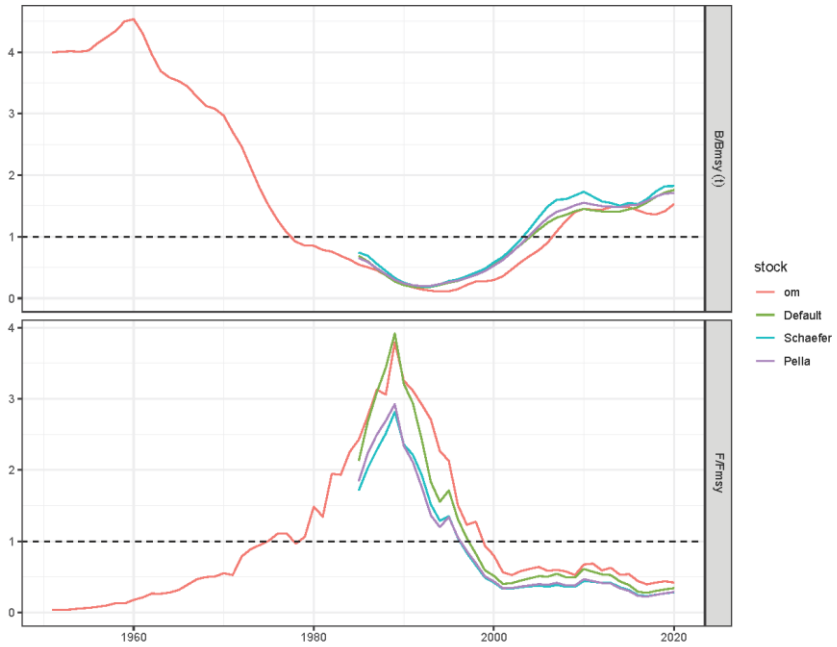


Figure 5: OM and estimated trajectories of $B/B_{MSY}$ and $F/F_{MSY}$ for the first iteration

```
sims = runi(om,idx,it=1,dteuler = 1)
sims =FLStocks(lapply(sims,function(x)propagate(x,its)))

for(i in 2:its){
  out=runi(om,idx,it=i,dteuler=1)
  for(j in 1:length(out)) iter(sims[[j]],i) = out[[j]]}

sims= FLStocks(Map(function(x,y){
  x@name=y
```

```
  x},x=sims,y=as.list(names(sims))))
```

```
plot(sims,metrics=list("B/Bmsy"=ssb,"F/Fmsy"=fbar))+
  geom_hline(yintercept = 1,linetype=2)+theme_bw()
```

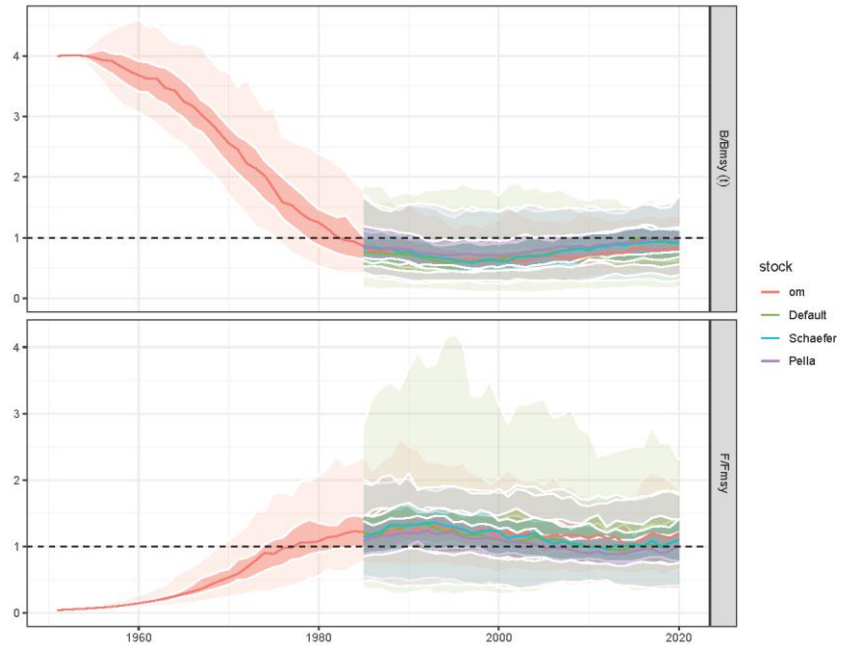


Figure 6: OM and estimated trajectories of $B/B_{MSY}$ and $F/F_{MSY}$ for 100 iterations

### 6.1 Quick performance comparison

By making use of `FLQuants` in is reasonably straight forward compute some estimation error with respect to the "true" value of $B_{MSY}$ and $F_{MSY}$ for the terminal year 2020.

```
bias.b = FLQuants(lapply(sims[2:4],function(x){
  log(ssb(x))-log(window(ssb(sims$om),start=1985))
}))
bias.f = FLQuants(lapply(sims[2:4],function(x){
  log(fbar(x))-log(window(fbar(sims$om),start=1985))
}))
```

```
out = rbind(
  data.frame(as.data.frame(bias.b),what="BBmsy"),
  data.frame(as.data.frame(bias.f),what="FFmsy")
)
```

Figure 7 indicates that scenario 2 and 3, which used moderately informative prior can somewhat improve the overall accuracy of the stock status estimate.

```
ggplot(out)+geom_boxplot(aes(x=qname,data,fill=qname))+
  facet_wrap(~what)+
  geom_hline(yintercept = 0,col=2)+theme_bw()+
  xlab("Scenario")+ylab("Error")
```

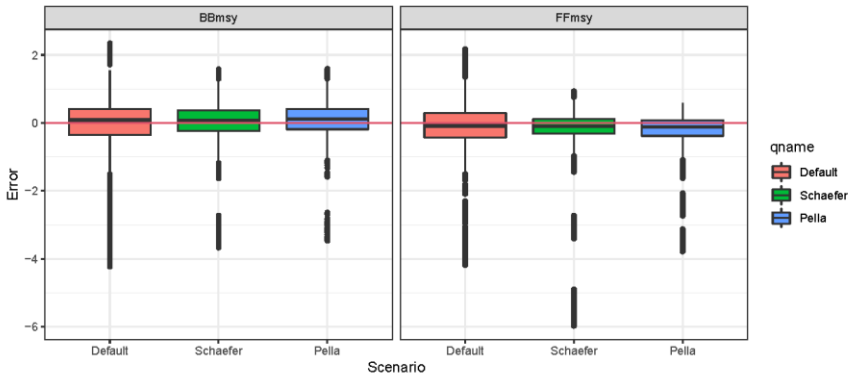


Figure 7: Boxplot showing estimation errors of $log(B/B_{MSY})$ and $log(F/F_{MSY})$ for 2020 with respect to the true quantities of the OM

## 7 Supplement I: spict.simplify

```
#' spict.simplify
#'
#' Function to simplify spict to make it fast and robust as an MP
#'
#' @param inp spict input time series
#' @param r.pr lognormal r prior, untransformed mean,log.sd, phase
#' @param bk.pr lognormal initial depletion prior
#' @param shape.pr lognormal prior for shape
#' @param proc.pr lognormal prior of process error on biomass
#' @param fdevs lognormal F penalty
#' @param cdevs lognorlam Catch penalty
#' @paran dteuler time step resolution
spict.simplify = function(inp,r.pr=c(0.2,0.5,1),# r prior
                          bk.pr=c(0.8,0.3,1), # bk prior
                          shape.pr=c(2,0.01,1),proc.pr=c(0.07,0.3,1),
                    fdevs=c(3,0.5,1),cdevs=c(0.05,0.1,1),dteuler=1){

  inp$dteuler=dteuler
  inp$priors$logbkfrac <- c(log(bk.pr[1])-bk.pr[2]^2/2,bk.pr[2],bk.pr[3]) # this is the bk prior
  inp$priors$logalpha <- c(0,0,0) # deactivate ratio of proc to obs error
  inp$priors$logbeta <- c(0,0,0) # deactivate catch to f devs
  inp$priors$logsdb <- c(log(proc.pr[1]), proc.pr[2], proc.pr[3]) # process error
  inp$priors$logsdf <- c(log(fdevs[1]), fdevs[[2]], fdevs[3]) # F random walk
  inp$priors$logsdc <- c(log(0.05), 0.1, 1) # Control catch error sd
  inp$priors$logn <- c(log(shape.pr[1]),shape.pr[2],shape.pr[3]) # Reduce shape CV
  inp$priors$logr <- c(log(r.pr[1]),r.pr[2],r.pr[3]) # r piror
  return(inp)

}
```

```
# index
dfi =as.data.frame(iter(window(idx@index,start=1985),1))
# long catch time series
dfc = as.data.frame(iter(window(om@catch,start=1951),1))
inp = list(obsC=dfc$data,timeC=dfc$year,
           obsI=dfi$data,timeI=dfi$year)

r.prior = c(r.pella[[1]]-0.5*0.3^2,0.3,1)
n.prior = c(r.pella[[2]]-0.5*0.3^2,0.3,1)

simp = spict.simplify(inp,r.pr=r.prior,# r prior
                          bk.pr=c(0.9,0.3,1), # b/k prior
                          shape.pr=n.prior,proc.pr=c(0.07,0.3,1))

fit = fit.spict(simp)
```

```
plot2(fit)
```

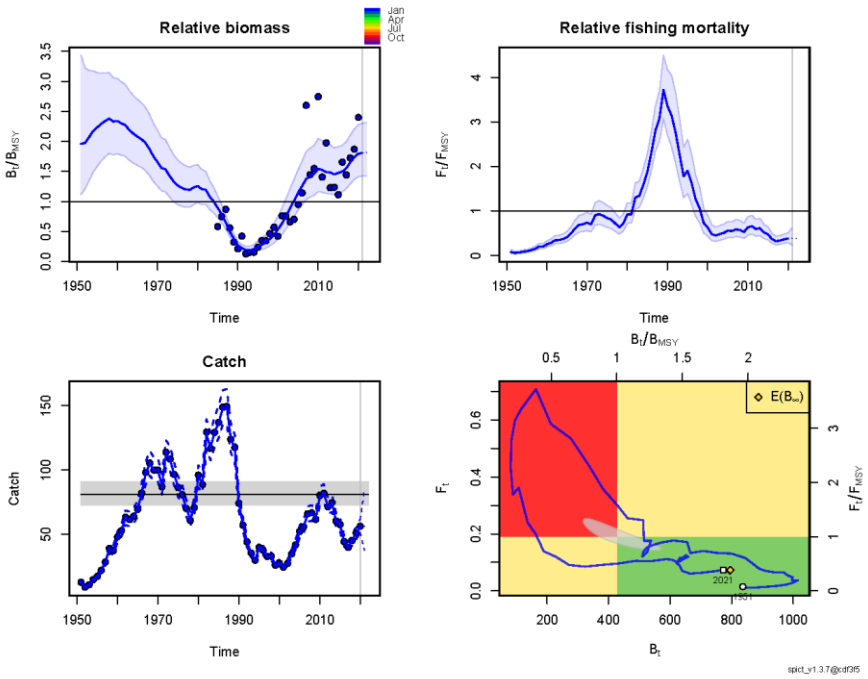


Figure 8: Spict fit with spict.simplify

# Data preparation guidelines for WKBMSYSPICT benchmarks 2023

Henning Winker (GFCM) and Massimiliano Cardinale (SLU)

15 November, 2022

## Table of Contents

1 Background ..... 1
2 Catch data ..... 1
3 Population parameters ..... 2
4 Size composition data ..... 3
5 Fisheries-dependent CPUE Standardization Guidelines ..... 3
5.1 Simulation dataset ..... 3
5.2 Targeting covariates ..... 9
5.3 Final GAMM model evaluation ..... 20
6 References ..... 26

## 1 Background

This document provides some initial guidance for preparing the data and compiling additional biological information and auxiliary data for WKBMSYSPICT in 2023.

## 2 Catch data

Historical catches should ideally encompass earlier periods with relatively low exploitation and ideally the start of the fishery. ICES historical database is available under the ICES website. A script and the original database is also available under WKMSYSPICT1 SharePoint and can be provided if requested by the Chairs to the stock assessors and meeting participants. In cases where historical landing statistics cannot be recovered, anecdotal information can still be helpful to corroborate model runs and justify choices of initial $b/k$ priors. This is recalling the guidelines put forward by WKMSYSPICT 2001, which recommended that when historical catches are not available the b/k ratio prior should be set to at 0.5 or lower with moderate to small CVs (i.e., 0.2–0.5). In these cases, it is generally recommended to evaluate the fits, retrospective pattern and ideally the prediction skill of additional sensitivity runs (e.g., $b/k$ = 0.3, 0.5, 0.8). It is important to note that there is a much higher risk to long-term yields and stock biomass when specifying positively biased

catch levels than the equivalent negative bias (Hordyk et al., 2019). Thus, catch statistics that are uncertain but most likely underestimated are still useful for model development and should be tested and eventually used in the final model.

## 3 Population parameters

Life history information is important for evaluating the plausible of the estimated production function by SPICT. Further, if there is a lack of contrast in the available time-series of catch and relative abundance, formulating informative priors for r using, e.g. `FishLife` (Thorson, 2020) may be warranted. Additional tools to update the initial $r$ priors from `FishLife` with stock specific biological and selectivity information are provided in the R package `SPMprior` available on github.com/henning-winker/SPMpriors.

Surplus production models, such as SPICT, are age- and size aggregated models that approximate changes in biomass as a function of the biomass of the preceding year, the surplus production in biomass and the removal by the fishery in the form of catch. Somatic growth, reproduction, natural mortality and associated density-dependent processes are inseparably captured in the estimated surplus production function that is governed by three parameters: (1) the intrinsic rate of population increase $r$ (2) the shape parameter $m$ and (3) the unfished equilibrium biomass $k$. However, there is a direct link between age-structured stock parameters and the expected surplus production function, so that stock parameters describing length-at-age ($L_a$), weight-at-age ($w_a$), maturity-at-age ($mat_a$) and selectivity-at-age ($s_a$), natural mortality $M$ and the steepness parameter $h$ of the of the assumed Beverton and Holt SSR can be used to approximate the surplus production (Winker et al., 2020a).

In addition, distortions between the survey or CPUE index and the spawning stock biomass can lead to systematic bias in the productivity estimates, which may be partially corrected for by using more informative priors on $r$. For example, if length at first capture $L_c$ is smaller than length-at-maturity ($L_m$), the exploitable biomass $EB$ can be behave hyperstable relative to $SSB$, and thus disguise true magnitude of reduction of the stock's productivity as a function of $SSB$ (Winker et al., 2020a, 2020b).

Where possible, it is therefore recommended to compile available life history information and initial selectivity estimates (e.g. $L_c$) for both the fishery and survey to aid the benchmark review process. These should include the following parameters.

- $L_{max}$ maximum observed length in the stock
- $L_{oo}$ Asymptotic length
- $K$ Brody coefficient
- $t_0$ theoretical age at zero length
- $L_m$ length-at-maturity
- $t_m$ age-at-maturity
- $t_{max}$ maximum age
- $M$ natural mortality

- $a$, $b$ parameter of the length-weight relationship
- $L_c$ length-at-50%-capture

## 4 Size composition data

Size composition data are available for several stocks under assessment. At a first instance these data provide information about selectivity, which is important for evaluation of the assessment (see above). However, together with life history parameters size composition can also provide important information about scales of biomass and fishing mortality (i.e. $Z = M + F$). The new version of the github repository `SS-DL` (https://github.com/shcaba/SS-DL-tool) provides an efficient way to fit basic Stock Synthesis models to size, index and catch data for the purpose of additional evaluations. This may be particularly useful for stocks where there is doubt about the status estimates due to a lack of contrast and conflicts with the perceived exploitation history.

To provide the options of conducting additional analyses for evaluation purposes, it therefore requested to prepare catch by fleet, indices and size composition data using the example format for ICES monkfish that is provided in the form of the following csv file on the SharePoint folder `/Data`|:

- mon89.catch.csv
- mon89.idx.csv
- mon89.lfd.csv

## 5 Fisheries-dependent CPUE Standardization Guidelines

The following section builds on a simulated CPUE dataset to provide additional guidance on options available for the standardization of fisheries dependent CPUE indices as well as on the presentation of results.

CPUE is standardized using Generalized Additive Mixed Models (GAMMs), which included the covariates year, spatial position and vessel as random effect. In an attempt to account for variation in targeting, the following two approaches are illustrated: (1) deriving a factor for targeting from a cluster analysis of the catch composition (He et al. 1997), and (2) using the direct Principle Component (DPC) approach, which involves the principle components (PC) of the decomposed catch composition as predictor variable (Winker et al. 2013; Winker et al. 2014).

### 5.1 Simulation dataset

The CPUE data are generated using spatial simulator (Ono et al. 2015; Thorson et al. 2016). A detailed description of the method is provided in Appendix A of Thorson et al. (2016) and source code is available at the accompanying GitHub page (https://github.com/James-Thorson/spatial_DFA). However, for the purpose of this example GAMM application the original code was slightly modified as illustrated below.

The example data CPUEsim.rdata are available on the ICES SharePoint and can be load by:

```
load("CPUEsim.rdata",verbose=T)
   Loading objects:
     Data
```

Next load a couple of R packages

```
# Load
library(mgcv)
library(ggplot2)
library("ggfortify")
library("nFactors")
library("cluster")
library(reshape2)
```

...and define some ggplot options

```
d = Data$Data
sc <- scale_x_continuous(breaks=seq(min(d$year)+1, max(d$year), 2))
th <- theme(axis.text.x  = element_text(angle=90, vjust=0.5),
            panel.grid.minor = element_blank())
jet.colors <- colorRampPalette(c("#00007F", "blue", "#007FFF", "cyan", "#7FFF
7F", "yellow", "#FF7F00", "red", "#7F0000"))
```

In a first step the simulator generates a bathymetry profile across a 50 x 50 grid using random gaussian fields (Fig. 1)

```
Data$Plots[[1]]
```

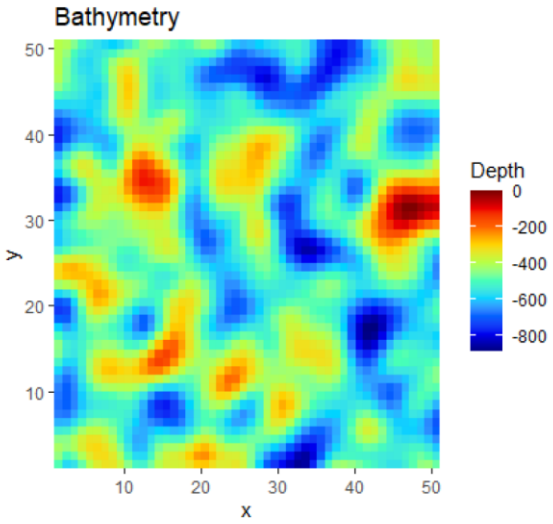


***Fig. 1:*** *Simulated bathymetry profile*

A specific depth profile is then assigned to each of four species as function of a preferred mean depth $\mu_p$ and a depth range $\sigma_p$, such that:

- Species 1: $\mu_p = 220$ and $\sigma_p = 0.5$
- Species 2: $\mu_p = 550$ and $\sigma_p = 0.5$
- Species 3: $\mu_p = 250$ and $\sigma_p = 0.3$
- Species 4: $\mu_p = 1000$ and $\sigma_p = 0.5$

Therefore, Species 1 and 3 have similar depth distributions, but Species 3 sits slight deeper and has a narrower depth range. Species 2 and Species 4 occur in increasing depth (Fig. 2).

```
   ggplot() +
   geom_raster(data = Data$Biomass.XY, aes(x = x, y = y, fill = log(Density+
1)))+
  facet_wrap(~variable)+
  scale_fill_gradientn(colors = (jet.colors(10))) +
      coord_quickmap(xlim = c(0.5,NA), ylim=c(0.5,NA),expand = FALSE)+
  ggtitle("True spatial densisities")
```

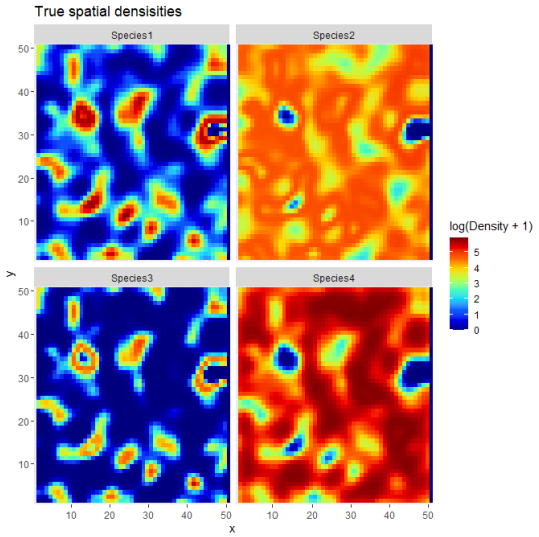


***Fig. 2:*** *Simulated spatial densities (kg/km²) for four species*

The underlying population dynamics are simulated over 30 years and are governed by a Schaefer model as a function of $r$ and $k$, such as:

- Species 1: $k = 0.3$ and $k = 320000$
- Species 2: $r = 0.17$ and $k = 420000$
- Species 3: $r = 0.12$ and $k = 56000$
- Species 4: $r = 0.08$ and $k = 540000$

There are 30 vessels operating with a mean catchability $q$, but variations among vessels is associated with CV = 0.2 to emulate a random vessel effect. CPUE data per species are generated from a Tweedie distribution with relative high over-dispersion. The mean of the distribution is a function of the density in the grid. Highest CPUE observations occur for Species 4 and lowest for Species 3. The resulting frequencies of CPUE observations are shown in Figure 3.

```
ggplot(data=Data$Data)+geom_histogram(aes(x=CPUE),bins=80,fill="grey",col=1)+
  facet_wrap(~Sp, scales = "free")+theme_bw()+xlab("CPUE")+ylab("Frequency")
```

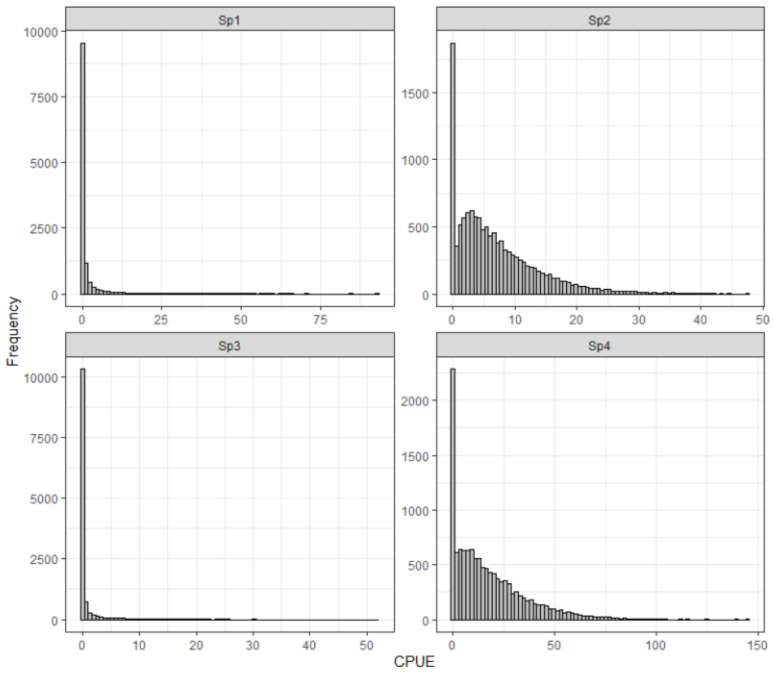


***Fig. 3:*** *Frequency distribution of simulated CPUE data by species*

To explicitly introduce systematic species targeting effects, directed fishing effort at specific depth profile governed through profit optimization given specifies specific densities and fish prices, where the latter changed systematically for the time-blocks of 1-10, 11-20 and 21-30 years. For example, the shallow water Species 1 is most valuable in first decade, but then its price drops to about a third for the year 11-30, whereas the deepwater Species 4, shows the reverse trend of sequentially increasing fish prices over the three decades. As a result of these so induced systematic changes in targeting, the nominal CPUE is severely biased compared to the "True" trend in biomass (Fig. 4).

```
Data$Plots$CPUE
```

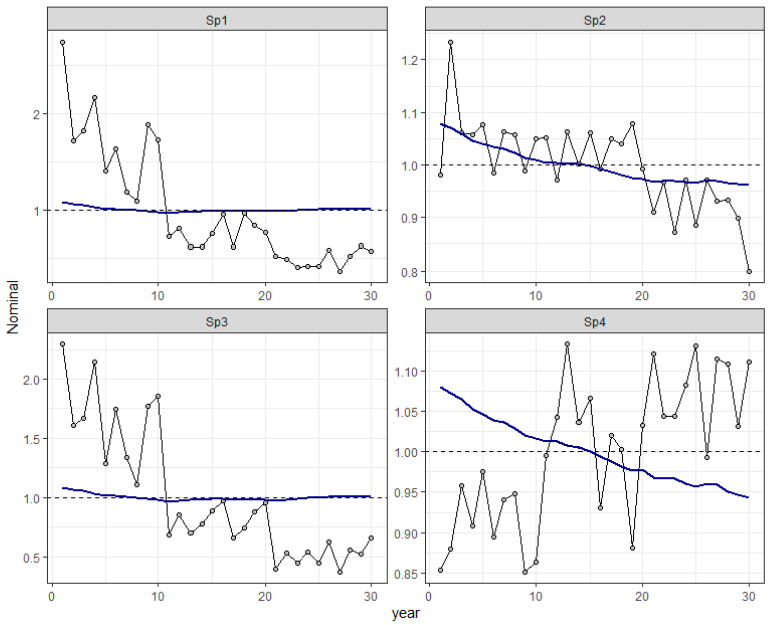


***Fig. 4:*** *Comparisons between the normalized nominal CPUE (grey points) and the True biomass trend*

## 5.2 Targeting covariates

Clustering of the catch composition data was conducted by applying the CLARA (Clustering Large Applications) clustering technique. To obtain the input data matrix for the cluster analysis, the $CPUE_{i,j}$ matrix of record $i$ and species $j$ is first decomposed into its Principal Components (PCs) using Principal Component Analysis (PCA). This is down-weight the influence of the abundance signal of the species of interest and thereby minimising issues with non-independence between the response and the predictor variable for targeting.

For this purpose, the data matrix comprising the $CPUEi, j$ records for all reported species are extracted from the dataset and normalized into relative proportions by weight to eliminate the influence of catch volume, fourth-root transformed and PCA-transformed.

```
# Flip species column
nsp = length(unique(Data$Data$Sp))
d =  data.frame(ID = rep(1:(nrow(Data$Data)/nsp),nsp),Data$Data)
d= reshape2::dcast(d,ID+year+vessel+X+Y+Xobs+Yobs+depth~Sp,value.var = "CPUE"
,fun.aggregate = mean)

# Create dataset with species columns
spd = d[,paste0("Sp",1:nsp)]
spd$sums = apply(spd,1,sum)
d = d[spd$sums>0,]
spd = spd[spd$sums>0,1:nsp]


# create data for PCA input
pca_dat <- sqrt(sqrt(spd/apply(spd,1,sum)))


#run PCA
names(pca_dat)
   [1] "Sp1" "Sp2" "Sp3" "Sp4"
pca<-prcomp(pca_dat, scale=T)


# Predict PCs for each observations
pr_pca <- predict(pca,pca_dat)
pcs <- data.frame(pr_pca[,1:(ncol(pr_pca))])
```

A drawback of the remaining non-independence between response and the decomposed species composition matrix is that model selection criteria (e.g. AIC, BIC) are unlikely to be appropriate since they select too many non-meaningful targeting signatures, leading to confounding and over-precision in the abundance trend (Winker et al., 2014). As an alternative for selecting the number of meaningful clusters, an approach based on the selection of non-trivial PCs through non-graphical solutions for Catell's Scree test in association with the Kaiser-Guttman rule (Eigenvalue > 1), called Optimal Coordinate test, is followed here, which is available in the R package 'nFactors' (Raiche and Magis 2010).

The optimal number of clusters considered is then taken as the number of retained PCs plus one (Winker et al. 2014).

```
# get Eigenvalue
eig = summary(pca)$sdev^2


# run Optimal Coordinates test
OCtest = nScree(eig)
npc = as.numeric(OCtest$Components[1])
ncl = npc+1

# clus_dat <- pca_dat
cl_sel = clara(pca_dat, ncl,sample=100,sampsize=250,pamLike = TRUE)
pcs$FT = as.matrix(cl_sel$cluster)[,1]
pca_dat$FT = factor(pcs$FT)
```

The results suggest that only the first two PCs are non-trivial and correspondingly three clusters were selected as optimal for the CLARA clustering (Fig. 5).

```
autoplot(pca,data = pca_dat,x=1,y=2,colour="FT",
             loadings = TRUE, loadings.colour = 'blue',
             loadings.label = TRUE,  loadings.label.size = 5)+theme_bw()
```

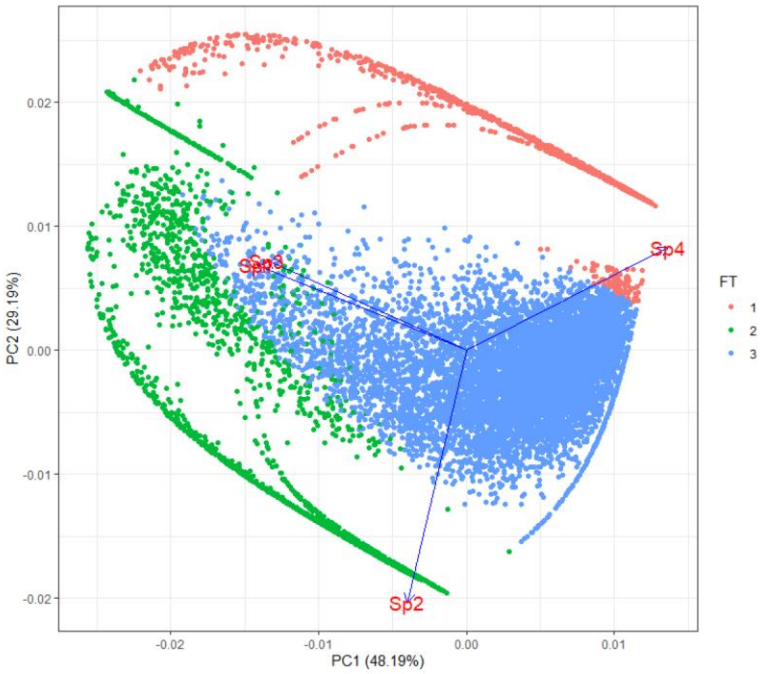


***Fig. 5:*** *Graphical representation of the three clusters that characterise the different fishing tactics projected over the first two Principal Components (PCs), where only PC1 was determined to be non-trivial.*

Subsequently, the identified cluster for each catch composition record is aligned with the original dataset and treated as categorical variable (FT).

```
d = data.frame(d,pcs)
```

It can help to show how the percentage of records within each cluster has evolved over time to evaluate if there is evidence for systematic changes in targeting (Fig. 6).

```
# Check cluster composition here
sp.comp = aggregate(as.matrix(spd)~FT,d,sum)
sp.prop = round(sp.comp[,2:ncol(sp.comp)]/apply(sp.comp[,2:ncol(sp.comp)],1,s
um)*100,1)
```

```
# Group composition
sp.prop
      Sp1  Sp2  Sp3  Sp4
   1  5.4  0.1  2.7 91.8
   2 34.2 50.0 13.6  2.3
   3  1.9 26.7  0.9 70.5
nspec = ncol(sp.prop)
tactics = 1:nrow(sp.prop)
col.sp = NULL
FT.sp = NULL


# Find the dominant species per cluster
d$Tactic = paste0("Tactic",d$FT)


ggplot(d,aes(year,fill=Tactic))+geom_bar(position="fill")+theme_bw()+
  sc+th+ylab("Proportion")
```

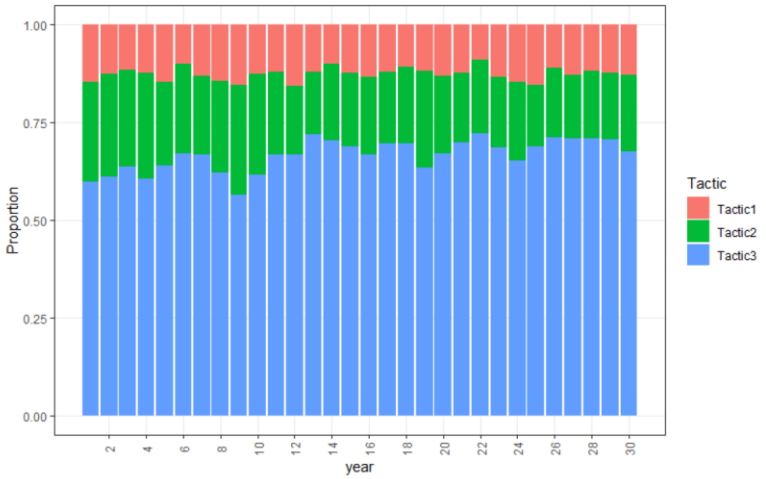


***Fig. 6:*** *Annual change in proportions of clusters as a latent predictor for Fishing Tactic (FT)*

Another way of visualization is to plot that clusters and PCs spatially. In the case of the clusters (Fig. 7), the most frequently occurring cluster is depicted in each grid cell, whereas for the PCs the average PC scores are plotted for each cell (Fig. 8). This also highlights that clustering implicitly assume that fishing tactics originate from discrete process, whereas the PCs also permit a continuous transition in fishing tactics.

```
xyf  =reshape2::dcast(aggregate(FT~X+Y+Tactic,d,length),X+Y~Tactic,fun.aggreg
```

```
ate = sum)
   Using FT as value column: use value.var to override.
xyf$FT = factor(apply(xyf[,-c(1:2)],1,which.max))

ggplot() +
  geom_raster(data = xyf, aes(x = X, y = Y, fill = FT)) +
  scale_fill_discrete() +
  coord_quickmap(xlim = c(1,NA), ylim=c(1,NA),expand = FALSE)+ggtitle("Cluste
r")
```

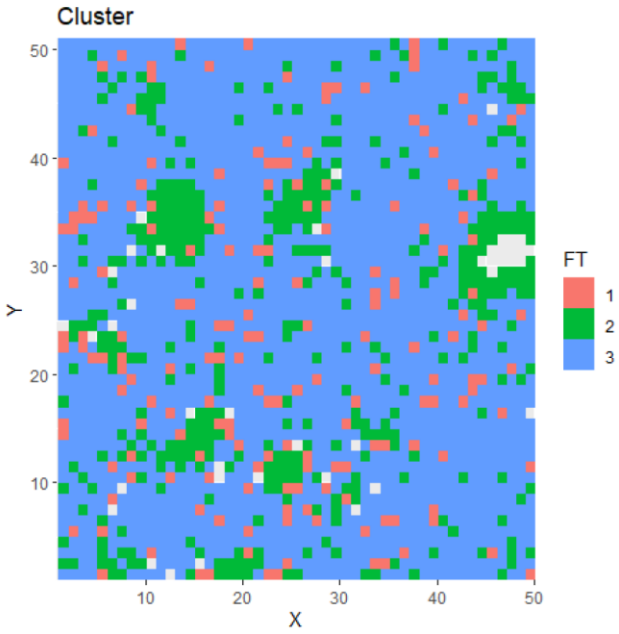


***Fig. 7:*** *Spatial distribution of most frequently assigned clusters across grid cells.*

```
xypc = reshape2::melt(aggregate(cbind(PC1,PC2)~X+Y,d,mean), id.vars = c("X",
"Y"))
ggplot() +
  geom_raster(data = xypc, aes(x = X, y = Y, fill =value)) + facet_wrap(~vari
able)+
  scale_fill_gradientn(colors = (jet.colors(10))) +
  coord_quickmap(xlim = c(1,NA), ylim=c(1,NA),expand = FALSE)+ggtitle("Princi
ple Components")
```

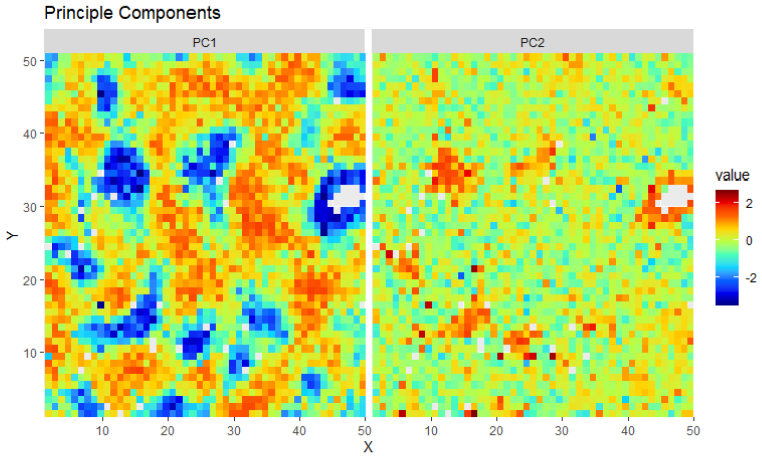


***Fig. 8:*** *Spatial distribution average Principle Component scores across grid cells.*

To create additional realism, the reported spatial scale is assumed to be at a coarser spatial resolution in the form of the midpoints of a 5x5 grid ($X_{obs}$, $Y_{obs}$) than true underlying spatial processes that are simulated at a 1x1 resolution ($X$,$Y$).

The CPUE records are fitted by assuming Tweedie distribution. The Tweedie distribution belongs to the family of exponential dispersion models and is characterized by a two-parameter power mean-variance function of the form $Var(Y) = \phi\mu p$, where $\phi$ is the dispersion parameter, $\mu$ is the mean and $p$ is the power parameter (Candy 2004, Dunn and Smyth 2005). Here, we considered the case of $1 < p < 2$, which represents the special case of a Poisson ($p = 1$) and gamma ($p = 2$) mixed distribution with an added mass at 0. This makes it possible to accommodate high frequencies of zeros in combination with right-skewed continuous numbers in a natural way when modelling CPUE data (Winker et al. 2014).

The full GAMMs evaluated were:

1. Base: $CPUE = exp(\beta_0 + Year + \alpha_V)$
2. Spatial: $CPUE = exp(\beta_0 + Year + s_1(X_{obs}, Y_{obs}) + \alpha_V)$
3. DPC: $CPUE = exp(\beta_0 + Year + s_1(X_{obs}, Y_{obs}) + s_2(PC1) + s_2(PC1) + \alpha_V)$
4. Cluster: $CPUE = exp(\beta_0 + Year + s_1(X_{obs}, Y_{obs}) + FT + \alpha_V)$

where $s_1()$ denotes thin plate spline interaction of the reported midpoints of coarser 5x5 spatial resolution, $X_{obs}$ and $Y_{obs}$, $s_2()$ is a thin plate smoothing function for the first and second principle component, $FT$ is the vector of cluster numbers treated as categorical variable, and $\alpha_V$ is the random effect for Vessel $V$ (Helser et al. 2004). Note that for convenience, no spatial-temporal interaction using, e.g. a tensor product,

$te(X_{obs}, Y_{obs}, Year)$, is considered here for illustration. However, R code to set up the correspondingly more complex prediction datasets can be provided on request.

As it is not possible to estimate the optimal power parameter $p$ internally within GAMMs, $p$ was first optimized within a fixed effect GAM, which did not include vessel as random effect. The so estimated $p$ parameters can then be input into the GAMM as fixed parameter (see code under 5.4).

First fixed effect structure is defined.

```
models = c("Base","Spatial","DPC","Cluster")

mods = list(
  Base = formula(y~as.factor(year)),
  Spatial = formula(y~as.factor(year)+s(Xobs,Yobs,k=8)),
  DPC = formula(y~as.factor(year)+s(Xobs,Yobs,k=8)+s(PC1,k=3)+s(PC2,k=3)),
  Cluster = formula(y~as.factor(year)+s(Xobs,Yobs,k=8)+as.factor(FT))
)
```

Then loop over all models by species

```
gams = popt = gamms =  list()
for(i in 1:nsp){
d$y = d[,paste0("Sp",i)]
  gams[[i]] = lapply(mods,function(x){
  gam(x,data=d,family=tw())
})
names(gams[[i]]) = models
popt[[i]] = do.call(c,lapply(gams[[i]],function(x){as.numeric(gsub(")","",str
split(x$family[[1]], "=")[[1]][2]))}))
}
names(gams) = paste0("Sp",1:4)
```

Next create the prediction dataset and predict the expected CPUE and standard error for all candidate models by species. For comparisons, all estimated CPUE indices are standardized by their means.

```
pdat = data.frame(year=sort(unique(d$year)),Xobs=25,Yobs=25,FT=1,PC1=0,PC2=0)

idx = NULL

for(i in 1:nsp){
pr = do.call(rbind,Map(function(x,y){
  p <- predict(x,pdat,type="link",se=T)
  df = data.frame(year=pdat$year,Model=y,mu=exp(p$fit),se=p$se.fit)
  df$mu= df$mu/mean(df$mu) # normalize
  df$lci = exp(log(df$mu)-1.96*df$se)
```

```
  df$uci = exp(log(df$mu)+1.96*df$se)
  df$lci = df$lci/mean(df$mu)
  df$uci = df$uci/mean(df$mu)
  df
},x=gams[[i]],y=models))
idx = rbind(idx,data.frame(pr,Sp=paste0("Sp",i)))
}
rownames(idx) = 1:nrow(idx)
idx$Model = factor(idx$Model,levels=models)
```

A comparison between the standardized indices and the "True" biomass trend from the simulation model are shown in Fig. 9. The results show that the DPC approach produces in this case trend least biased trends in relative abundance. For Species 4, the DPC even reversed the increasing CPUE index of the Base model and correctly predicts an approximately unbiased declining trend. The Cluster approach was able to partially correct for the targeting induced bias but was notably less efficient than the DPC. The spatial information at the reported coarse 5x5 resolution was ineffective to account for targeting.

```
dt = Data$Biomass
dt$Model = "True" # True biomass trend
ggplot(idx,aes(year,mu,color=Model))+facet_wrap(~Sp,scales = "free")+
  geom_ribbon(aes(ymin = lci, ymax = uci,fill=Model),alpha=0.2,col=0)+
  geom_line()+geom_point()+geom_hline(yintercept = 1,linetype=2)+sc+th+
  ylab("Normalized CPUE")+xlab("Year")+theme_bw()+geom_line(data=dt,aes(year,
True),size=1)
```

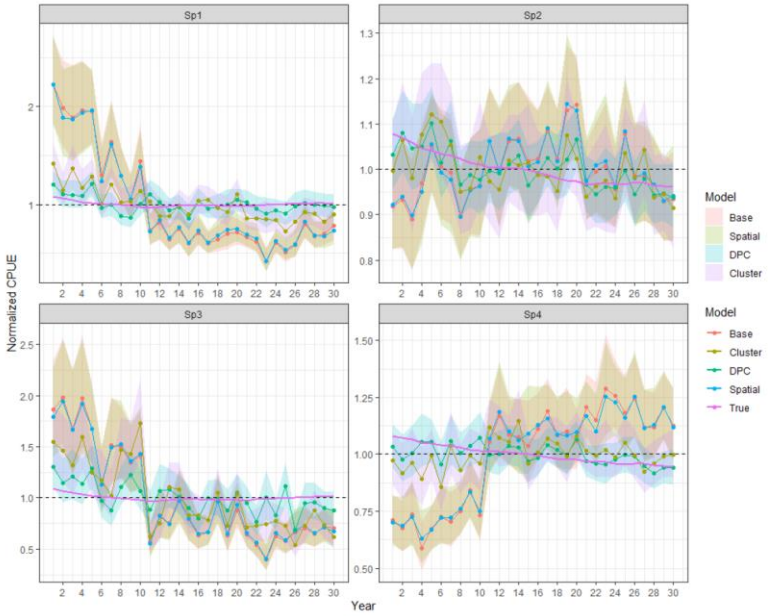


***Fig. 9:*** *Spatial distribution average Principle Component scores across grid cells.*

The following code generates prediction data for comparing the expected spatial CPUE distribution by species between the Spatial and DPC GAMs.

```
spdat = d
spdat$year=max(spdat$year)
spdat$xy = paste0(spdat$X,".",spdat$X)
spdat$Xobs=spdat$X
spdat$Yobs=spdat$Y
spdat = aggregate(cbind(PC1,PC2)~year+Xobs+Yobs+X+Y, spdat,mean)
spidx = NULL
for(i in 1:nsp){
  pr = do.call(rbind,Map(function(x,y){
    p <- predict(x,spdat,type="link",se=T)
    df = data.frame(spdat,Model=y,CPUE=exp(p$fit)/mean(exp(p$fit)),se=p$se.fi
t)
    df
  },x=gams[[i]][3],y=models[3]))
  spidx = rbind(spidx,data.frame(pr,Sp=paste0("Sp",i)))
}
rownames(spidx) = 1:nrow(spidx)
```

```
# Spatial only
spoidx = NULL
for(i in 1:nsp){
  pr = do.call(rbind,Map(function(x,y){
    p <- predict(x,spdat,type="link",se=T)
    df = data.frame(spdat,Model=y,CPUE=exp(p$fit)/mean(exp(p$fit)),se=p$se.fi
t)
  },x=gams[[i]][2],y=models[2]))
  spoidx = rbind(spoidx,data.frame(pr,Sp=paste0("Sp",i)))
}
rownames(spoidx) = 1:nrow(spoidx)
```

The predicted CPUE based on the Spatial GAM alone shows relatively coarse spatial structuring (Fig. 10), whereas the DPC GAM with the additional information of Principle scores from the species composition more closely resembles the patchiness of fine scale spatial distribution (Fig. 11) when compared to the "True" densities in Fig. 2.

```
  ggplot() +
  geom_raster(data = spoidx, aes(x = X, y = Y, fill = log(CPUE+1))) + facet_w
rap(~Sp)+
  scale_fill_gradientn(colors = (jet.colors(10))) +
  coord_quickmap(xlim = c(0.5,NA), ylim=c(0.5,NA),expand = FALSE)+ggtitle("Pr
edicted Spatial Distribution: Spatial Only")
```

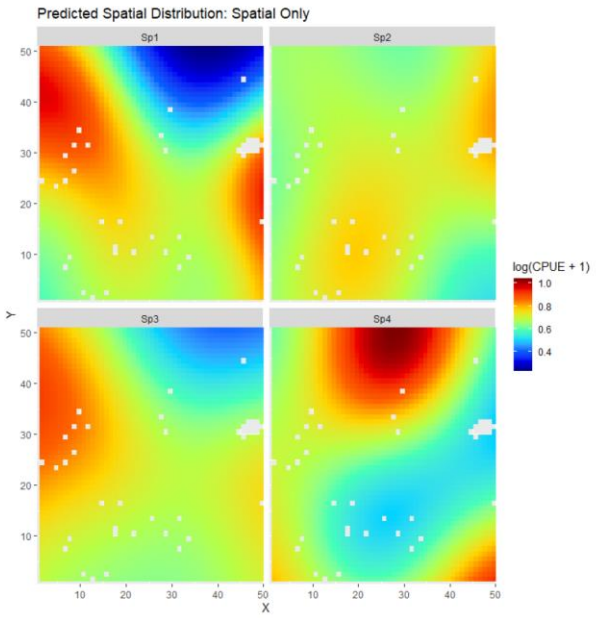


***Fig. 10:*** *Spatial distribution average Principle Component scores across grid cells.*

```
ggplot() +
  geom_raster(data = spidx, aes(x = X, y = Y, fill = log(CPUE+1))) + facet_wr
ap(~Sp)+
  scale_fill_gradientn(colors = (jet.colors(10))) +
  coord_quickmap(xlim = c(0.5,NA), ylim=c(0.5,NA),expand = FALSE)+ggtitle("Pr
edicted Spatial Distribution: Spatial + DPC")
```

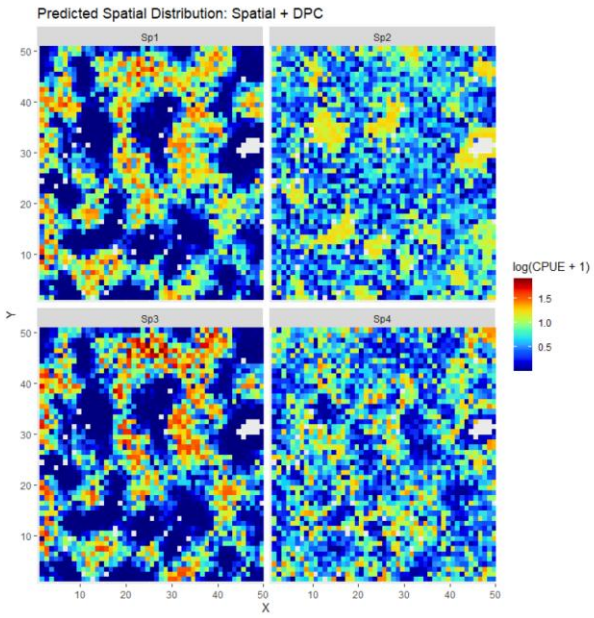


***Fig. 12:*** *Spatial distribution average Principle Component scores across grid cells.*

## 5.3 Final GAMM model evaluation

Subsequently, the DPC is selected for evaluations using a GAMM with random vessel effects.

```
# Select Best Model to include random vessel effect: Here DPC
smod = 3


# fit tweedie GAMMs with random vessel effect for the 4 Species
gamms= NULL
for(i in 1:nsp){
  d$y = d[,paste0("Sp",i)]
  gamms[[i]] = Map(function(x,y){
    gamm(x,data=d,family=Tweedie(p=y),random=list(vessel=~1),method="REML")
  },x=mods[smod],y=popt[[i]][smod]) # change selmod
  names(gamms[[i]]) = models[smod]
}
names(gamms) = paste0("Sp",1:4)
```

The following R code provides an example on how to compute the "influence" that each explanatory variable has on the unstandardized CPUE in each year as recommended by Bentley et al. (2012). Predictor variables with coefficients of high magnitude do not necessarily have great influence. For a variable to have great influence, there must be changes in the relative distribution of that variable among years to impact on the estimated year-effect of interest. Influence can be directly computed from the estimated coefficients (see Bentley et al. 2012) or perhaps more conveniently by predicting the coefficient effect for each observation, while controlling the remainder of variables (see below).

```
# Partial influence
yrs= unique(d$year)
pid = d
pid$year = max(pid$year)
pid$vessel = pid$vessel[1]


# Spatial
pid.xy = pid
pid.xy$PC1=0
pid.xy$PC2=0


# PC1
pid.pc1 = pid
pid.pc1$PC2 = 0
pid.pc1$Xobs = median(pid$Xobs)
pid.pc1$Yobs = median(pid$Yobs)


# PC2
pid.pc2 = pid
pid.pc2$PC1 = 0
pid.pc2$Xobs = median(pid$Xobs)
pid.pc2$Yobs = median(pid$Yobs)

deltas = NULL
for(i in 1:nsp){
  prid.xy = predict(gamms[[i]][[1]]$gam,pid.xy)
  prid.pc1 = predict(gamms[[i]][[1]]$gam,pid.pc1)
  prid.pc2 = predict(gamms[[i]][[1]]$gam,pid.pc2)
  p.xy = mean(prid.xy)
  p.pc1 = mean(prid.pc1)
  p.pc2 = mean(prid.pc2)

  delta =do.call(rbind,lapply(yrs,function(x){
  rbind(
  data.frame(year = x,Species=paste0("Sp",i),variable="Spatial",
  delta  = exp(sum(prid.xy[d$year==x]-p.xy)/length(prid.xy[d$year==x]))),
  data.frame(year = x,Species=paste0("Sp",i),variable="PC1",
```

```
            delta  = exp(sum(prid.pc1[d$year==x]-p.pc1)/length(prid.pc2[d$ye
ar==x]))),
  data.frame(year = x,Species=paste0("Sp",i),variable="PC2",
            delta  = exp(sum(prid.pc2[d$year==x]-p.pc2)/length(prid.pc2[d$ye
ar==x]))
  )
}))
deltas = rbind(deltas,delta)
}
deltas$variable = factor(deltas$variable,levels=unique(deltas$variable))
```

The influence plots indicate that $s_2$(PC1) has by the strongest influence on the estimated year-effect for all species (Fig. 13).

```
ggplot(deltas)+
  geom_line(aes(year,delta,color=variable),size=0.9)+
  facet_wrap(~Species)+geom_hline(yintercept = 1)+
  theme_bw()+sc+th+ylab("Influence")+xlab("Year")
```

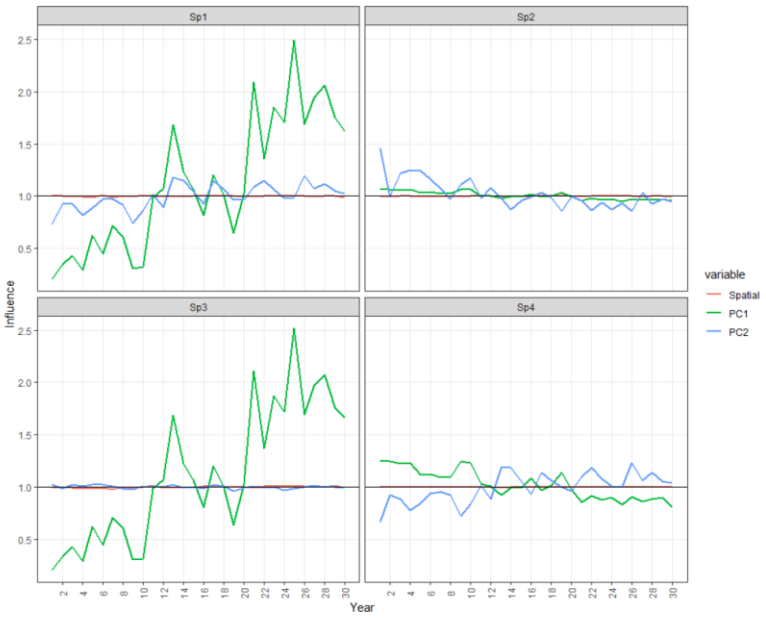


***Fig. 13:*** *Annual influence values for each fixed effect term in the final DPC-GAMM model.*

Random effects can be extracted using the following R code and are illustrated in Fig. 14.

```
# Extract Random Effect for DPC model
RE = NULL
for(i in 1:nsp){
re = as.numeric(summary(gamms[[i]][[1]]$lme)$coefficient$random$vessel)
re = data.frame(Vessel=1:length(re),Effect=re)
nB = nrow(re)
SD = data.frame(lci=c(-1*(sd(re$Effect))),uci=c(1*(sd(re$Effect))))
CI = data.frame(lsd=c(-1*(sd(re$Effect)*1.96)),usd=c(1*(sd(re$Effect)*1.96)))
re = data.frame(re,SD,CI,Sp=paste0("Sp",i))
RE = rbind(RE,re)
}
```

The results indicate that "True" standard deviation of 0.2 (red dashed lines) for the simulated vessel effect is generally adequately estimated (dark grey shaded area), with exception for the least abundant Species 3 (Fig. 14).

```
ggplot(RE,aes(Vessel,Effect))+facet_wrap(~Sp)+theme_bw()+geom_point()+ylab("R
andom Effect")+
  geom_ribbon(aes(ymin = lci, ymax = uci),alpha=0.4,col="lightgrey")+
  geom_ribbon(aes(ymin = lsd, ymax = usd),alpha=0.4,col="grey")+
  scale_x_continuous(breaks=c(0,seq(1,nB, 2)))+geom_hline(yintercept = 0)+
  geom_hline(yintercept = c(-0.2,0.2),linetype=2,color="red")
```

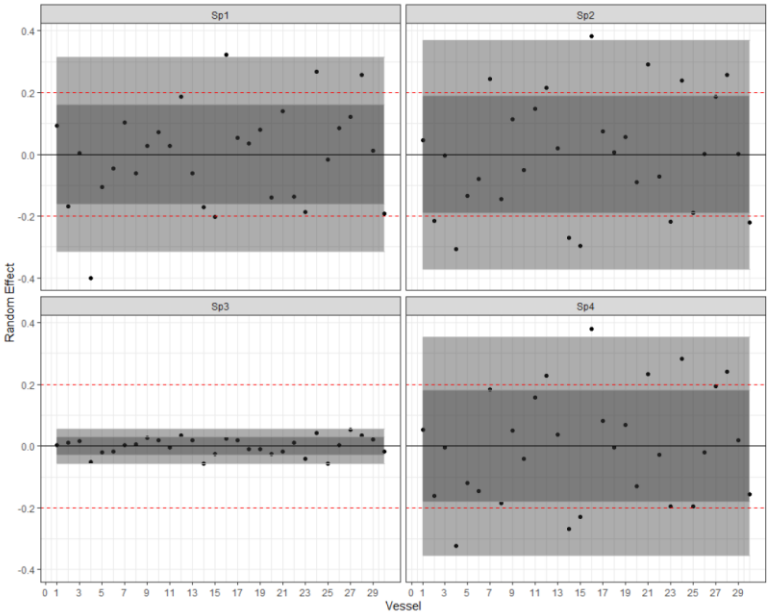


***Fig. 14:*** *Random effects coefficients (dots) illustrating the deviation from the mean of zero across the 30 vessels in the simulated dataset. The dark grey shaded are denote the estimated standardization from the mean, the light grey the 95% CIs and the dashed red lines the True standardization of the random vessel effect*

```
# Final standardized Indexx
stidx = NULL
for(i in 1:nsp){
  pr = do.call(rbind,Map(function(x,y){
    p <- predict(x$gam,pdat,type="link",se=T)
    df = data.frame(year=pdat$year,Model=y,mu=exp(p$fit),se=p$se.fit)
    df$mu= df$mu/mean(df$mu) # normalize
    df$lci = exp(log(df$mu)-1.96*df$se)
    df$uci = exp(log(df$mu)+1.96*df$se)
    df$lci = df$lci/mean(df$mu)
    df$uci = df$uci/mean(df$mu)
    df
  },x=gamms[[i]],y=models[smod]))
  stidx = rbind(stidx,data.frame(pr,Sp=paste0("Sp",i)))
}
rownames(idx) = 1:nrow(idx)
```

Finally, a dataset of standardized GAMM-DPC CPUE indices in computed for the four species and compared to the "True" simulated biomass trend (Fig. 15).

```
dt = Data$Biomass
dt$Model = "True"
ggplot(stidx,aes(year,mu))+facet_wrap(~Sp,scales = "free")+
  geom_ribbon(aes(ymin = lci, ymax = uci),fill="grey",alpha=0.9,col=0)+
  geom_line()+geom_point()+geom_hline(yintercept = 1,linetype=2)+sc+th+
  ylab("Normalized CPUE")+xlab("Year")+theme_bw()+geom_line(data=dt,aes(year,
True),size=1,color="blue")
```

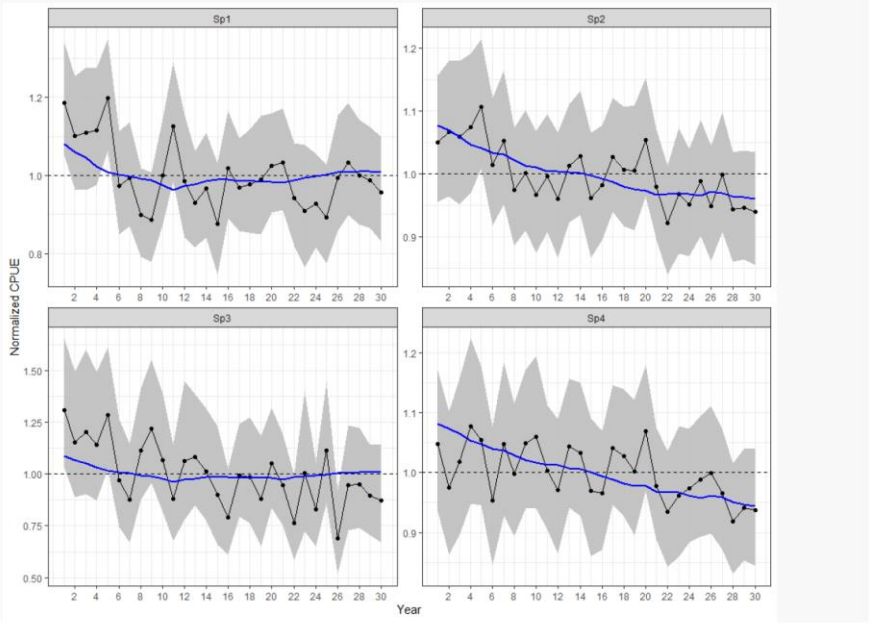


***Fig. 15:*** *Standardized CPUE indices for four species using the DPC-GAMM model (black dots) with 95% CIs. The blue solid line shows the True biomass trend as generated by the simulation models*

## 6 References

He, X., Bigelow, K. A., and Boggs, C. H. 1997. Cluster analysis of longline sets and fishing strategies within the Hawaii-based fishery. Fisheries Research, 31: 147–158.

Helser, T., Punt, A. E., and Methot, R. D. 2004. A generalized linear mixed model analysis of a multi-vessel fishery resource survey. Fisheries Research, 70: 251–264.

Hordyk, A. R., Huynh, Q. C., and Carruthers, T. R. 2019. Misspecification in stock assessments: Common uncertainties and asymmetric risks. Fish and Fisheries, 20: 888–902.

Ono, K., Punt, A. E., and Hilborn, R. 2015. Think outside the grids: An objective approach to define spatial strata for catch and effort analysis. Fisheries Research, 170: 89–101.

Raiche, G., Magis, D., 2010. nFactors: Parallel Analysis and Non Graphical Solutions to the Cattell Scree Test. R Package Version 2.3.3.

Thorson, J.T.; Fonner, R.; Haltuch, M.A.; Ono, K.; Winker, H. 2016. Accounting for spatiotemporal variation and fisher targeting when estimating abundance from multispecies fishery data. Canadian Journal of Fisheries and Aquatic Sciences. 73:1-14.

Thorson, J. T. 2020. Predicting recruitment density dependence and intrinsic growth rate for all fishes worldwide using a data-integrated life-history model. Fish and Fisheries, 21: 237–251. John Wiley & Sons, Ltd. https://doi.org/10.1111/faf.12427.

Winker, H., Kerwath, S. E., and Attwood, C. G. 2013. Comparison of two approaches to standardize catch-per-unit-effort for targeting behaviour in a multispecies hand-line fishery. Fisheries Research, 139: 118–131.

Winker, H., Kerwath, S. E., and Attwood, C. G. 2014. Proof of concept for a novel procedure to standardize multispecies catch and effort data. Fisheries Research, 155: 149–159.

Winker, H., Carvalho, F., Thorson, J.T., Kell, L.T., Parker, D., Kapur, M., Sharma, R., Booth, A.J., Kerwath, S.E., 2020a. JABBA-Select: Incorporating life history and fisheries' selectivity into surplus production models. Fish. Res. 222, https://doi.org/10.1016/j.fishres.2019.105355.

Winker, H., Mourato, B., Chang, Y., 2020b. Unifying parameterizations between age-structured and surplus production models: An application to Atlantic white marlin (*Kajika albida*) with simulation testing. Col. Vol. Sci. Pap. ICCAT 76, 219–234.

# Annex 4: Stock Annex updates

| Stock code | Stock description | DOI |
|---|---|---|
| bll.27.3a47de | Brill (*Scophthalmus rhombus*) in Subarea 4 and divisions 3.a and 7.d-e (North Sea, Skagerrak and Kattegat, English Channel) | https://doi.org/10.17895/ices.pub.24913293 |
| boc.27.6-8 | Boarfish *(Capros aper)* in subareas 6-8 (Celtic Seas, English Channel, and Bay of Biscay) | https://doi.org/10.17895/ices.pub.24922122 |
| bll.27.3a47de | Striped red mullet (*Mullus surmuletus*) in Subarea 4 and divisions 7.d and 3.a (North Sea, eastern English Channel, Skagerrak and Kattegat) | https://doi.org/10.17895/ices.pub.24922125 |
| ple.27.89a | Plaice (*Pleuronectes platessa*) in Subarea 8 and Division 9.a (Bay of Biscay and Atlantic Iberian waters) | https://doi.org/10.17895/ices.pub.24922128 |
| pol.27.67 | Pollack (*Pollachius pollachius*) in subareas 6-7 (Celtic Seas and the English Channel) | https://doi.org/10.17895/ices.pub.24922131 |
| pol.27.89a | Pollack (*Pollachius pollachius*) in Subarea 8 and Division 9.a (Bay of Biscay and Atlantic Iberian waters) | https://doi.org/10.17895/ices.pub.24922134 |
| rjc.27.8c | Thornback ray (*Raja clavata*) in Division 8.c (Cantabrian Sea) | https://doi.org/10.17895/ices.pub.24922137 |
| whg.27.89a | Whiting (*Merlangius merlangus*) in Subarea 8 and Division 9.a (Bay of Biscay and Atlantic Iberian waters) | https://doi.org/10.17895/ices.pub.24922140 |